AD 678759

48

HUDSON LABORATORIES of Columbia University

145 Palisade Street, Dobbs Ferry, N.Y. 10522

TECHNICAL REPORT No. 150

THE HUDSON LABORATORIES RAY TRACING PROGRAM

by

H. Davis

H. Fleming

W. A. Hardy

R. Miningham

S. Rosenbaum

June 1968

Document cleared for public release and sale; its distribution is unlimited.

Contract Nonr-266(84)

360

CU-178-68-ONR-266-Phys.

Hudson Laboratories
of
Columbia University
Dobbs Ferry, New York 10522

Technical Report No. 150

THE HUDSON LABORATORIES RAY TRACING PROGRAM

by

H. Davis, H. Fleming, W. A. Hardy,

R. Miningham, and S. Rosenbaum

UNCLASSIFIED

June 1968

This report consists
of 363 pages.

Copy No.
of 145 copies.

This work was supported by the Office of Naval Research under Contract Nonr-266(84). Reproduction in whole or in part is permitted for any purpose of the United States Government.

ABSTRACT

A series of computer programs has been developed for the calculation of the acoustical field in long-range, low-frequency underwater sound propagation in the deep ocean. The programs involve the extraction of data inputs from available data banks, the calculation of ray trajectories, and intensity calculations that are based on the mapping of ray densities into the far acoustical field. This report outlines the methods used in the calculations and provides incidental commentary on the results of the program and its application to underwater sound propagation.

CONTENTS

LIST OF FIGURES

CHAPTER I

INTRODUCTION

1.1. Objectives

The results of a number of experiments in low-frequency, long-range underwater sound propagation have shown that bottom interactions as well as changes in the velocity profiles with range will play important roles in determining the efficiency of the acoustical transmission between an underwater source and its receiver. To include these effects in the analysis of experimental data, Hudson Laboratories has developed a ray tracing program which is especially adapted to multipath long-range acoustical propagation – oriented toward ranges of several hundred to several thousand miles – with the point of view that the program should be:

i) at least semi-quantitative with respect to the prediction of acoustical transmission losses,

ii) a flexible research tool that can be used in connection with the analysis of results from specific experiments to choose parameters needed for the prediction of intensity, and

iii) as complete as possible in terms of assimilating and organizing for convenience a variety of data inputs and presenting computed results to the scientist for his interpretation.

This complete ray tracing program, or, more accurately, the system of programs that has been developed (Fig. 1) is discussed in this report with the motives that led to the selection of certain techniques.

The work can be divided in a natural manner into three major groupings:

1.2. Data Inputs

1.3. Ray Tracing

1.4. Intensity Calculations

and these groups are also consecutive steps in the data flow. The over-all program can be illustrated in terms of representative outputs for each group above, which will also serve as an introduction to the details of, and a summary of, the present program.

1.2. Data Inputs

Figure 2 indicates a great circle path from 30°N, 20°W to 50°N, 25°W over which it is desired to obtain data for predicting the transmission loss. Coordinates for this track, or for tracks specified by an initial position and bearing, are computed so that the path can be plotted on standard bathymetric charts to obtain a bottom profile. Figure 3 is an example of the track coordinates printed at 25-mile increments.

If no special velocimetric data are available for this path, e.g., data from a particular experiment, or if given data are to be checked against standard data for the area, the magnetic tape files of the National Oceanographic Data Center (NODC) can be searched for data of given months for sound velocity profiles that possess depths equal to or greater than a Maximum Depth of Observation (MDO), and which lie within a specified range or zone width from the given track. Figure 4 gives the identification numbers of all velocity profiles catalogued by NODC for the months 10, 11, 12 with an MDO greater than 1500 meters and which lie within 50 miles of the track of Fig. 1.

All the velocity profiles selected as pertinent to a given track from any input data source are converted to a standard form for editorial review before insertion into the ray tracing program. Stations given in terms of temperature, salinity, and depth are converted to sound velocity and depth entries by use of Wilson's equation.[1] Also, if the MDO of a station is less than a maximum bottom depth for the ray tracing, an inverse solution is made of Wilson's equation to determine the water temperature at the MDO and the profile is extrapolated to greater depths by assuming that the water temperature is constant and the sound velocity is a function of pressure only. Figure 5 shows the standard form used for the profiles. A four-point fit of entered data points is used to determine the sound velocity at 20-meter intervals to 2000 meters and at 100-meter intervals to the greatest depths. The MDO of the profile of Fig. 5 was 5277 meters and the entered velocity represented a water temperature of 1.818° for an assumed salinity of 35.0‰. Insofar as the roughly 1.8° temperature is typical of deep water in the geographical area of the profile, this velocity profile and its extrapolation were accepted as valid for inclusion into the ray tracing program.

[1] References are compiled at the end of each chapter.

Any number of velocity profiles can be inserted into the program to construct the total velocity field; additionally, and provided that profiles can be obtained at the beginning and end of the acoustical path, a number of shallower profiles, e.g., BT or X-BT casts, can be inserted to fill in important detail relating to the surface or near-surface velocity structure. This process is described in detail later in this report (Chapter II). The net result is the construction of a set of velocity profiles ordered in range over the acoustical path which constitutes the velocity field for the subsequent ray tracing. Accompanying this data is a bottom contour, i.e., a set of bottom depth vs range entries.

The variation of the velocity profiles with range can be inspected in detail by plotting the difference between successive entries with respect to a standard, usually the initial, velocity profile entry. This is shown in Fig. 6. The multiplot not only indicates typical local variations among the set of profiles but shows the manner in which the velocity profile structure, e.g., the profile shape and the depth of the sound channel, changes over the acoustical path. These changes represent propagation through different ocean regions such as those defined by the major oceanic currents. The changes permit profound modification of the acoustical field via interactions such as the trapping or ejection of rays from surface or secondary sound channels.

A control form, "Ray Trace Data Search Specifications," is shown in Fig. 7 and this is used to initiate data selection from available data banks.

1.3. Ray Tracing

Figure 8 gives the control form for the "Ray Trace Program Operating Specifications." The form is used to specify the initial conditions for the ray tracing iteration and also to select parameters that control the accuracy and computational speed of the program. For a given source depth and initial angle the ray is traced in the velocity field and in conjunction with the bottom profile prepared previously. Usually a range of initial angles is specified together with an angular increment and the ray trace is repeated for each increment until the entire angular spectrum has been traced.

Figure 9 indicates a printout that is available for each ray traced. Range, depth, angle, travel time, and height above bottom are printed on the bottom, and the top plot depicts the progress of the ray between the surface and the bottom. Printout intervals, typically 1.0 or 2.0 miles, are selected and extra printouts are given at each turning point and surface or bottom hit.

An objective of the program is to determine the principal arrival structure that constitutes far field illumination. The angular increments are chosen small enough so that, insofar as possible, each arrival is well defined. In practical situations this usually requires from one hundred to two hundred rays or more. Summary information of the total field is obtained by compiling the data from the individual ray tracings on an output tape to produce multiplot data or data for the intensity calculations discussed in Chapter IV. Figures 10a through 10d indicate the build-up of the total field by the various rays from the source. To reduce confusion in this representation of the field patterns, each plot is limited to a maximum number of 30 rays.

More specific data are given in the Ray Depth Distribution Plot of Fig. 11. These plots can be obtained at every range that is also a printout interval of the ray trace program. The sequence of the plot is in terms of the angular increments used in the ray trace and the asterisks show the depth of that ray at the selected range. A ray will be oscillating in depth about that range (Fig. 9) and the maximum and minimum depths of the oscillations that occur about the printout range are indicated by the plus and minus signs in Fig. 11a. The extreme right-hand side of the figure plots the travel time for each ray.

It is clear that if a vertical line is drawn in Fig. 11, representing a given depth between the surface and the bottom, the line will intersect certain families of rays and each intersection will give a different arrival that can contribute to the acoustic field. In this figure the shallower angles correspond to sound duct propagation and the steeper angles represent RSR and bottom bounce propagation.

1.4. Intensity Calculations

Figure 12 is the control form for the "Ray Trace Intensity Calculations" and indicates a number of parameters that are included in the calculation such as wavelength, attenuation functions, source and receiver directivity functions, etc. These are described in Chapter IV. It is a feature of the calculations that intensity is determined as a probability distribution that is obtained by mapping the arrival structure depicted in Fig. 11 across the ocean depth at a given range. This permits a calculation of the intensity at a given range and depth, and therefore the transmission loss. It also determines the distribution of intensity in depth as the sound propagates between the confining sea surface and bottom planes of the ocean.

All such calculations are subject to uncertainties in the input data and must be interpreted as averages over "representative" data. Additional averaging is necessary to account for the fluctuations that are due to multipath structure. In a coarse differentiation corresponding to limiting physical situations, the intensity calculations have been classified into three types, only two of which, types II and III, are considered for long-range propagation.

The Type II intensity calculation is applicable where the depth distribution of acoustical intensity will change with range. Figure 13 shows a printout that gives the transmission loss calculated at twelve depths and for nineteen equally spaced range intervals, usually two-mile increments, that are centered on a given range. These data could be used, for example, to construct the predicted transmission loss to a given receiver from a source that is towed in range at a specified depth. Successive outputs of the type of Fig. 13 can be continuously plotted to give the transmission loss as a function of range in the form of Fig. 14.

When the input data becomes uncertain, and at very long ranges such that convergence zone structure is "washed out," it becomes preferable not to predict the range-dependent Type II transmission losses but instead to average these over a large range interval that would correspond to a convergence zone. For this limit of averaging a Type III transmission loss is calculated with the printout shown in Fig. 15. The calculation is based on a representative range R and takes the form of a depth distribution of transmission loss in which every ray that is traced can make a contribution provided the ray has not suffered so great an attenuation prior to range R that it has been terminated earlier in the program.

It is not the function of this report to undertake detailed comparisons of the data computed by these programs with specific experimental results. However, as an indication of the ability of the program to predict acoustical transmission using realistic oceanographic environmental data, the predicted curve of Fig. 14 may be compared with Fig. 16 which gives a transmission loss measured by A. N. Guthrie and J. D. Shaffer during a summer 1967 tow of a 13.33 Hz projector over the Hatteras Plain. Velocity profile input data were obtained at approximately 30-mile intervals using Sippican X-BT casts to 750 meters and deep velocimeter casts were obtained at the end points of the tow. The bottom profile was taken from the PFR records of the towing ship (USNS J. W. Gibbs). The transmission was monitored from the USNS Mizar by a sonobuoy-suspended hydrophone at a depth of 100 meters. The depth of the towed projector was 30 meters.

The velocimeter casts indicated a strong thermocline to the surface from a depth of 150 meters with a roughly isothermal layer of about 200 to 250 meters below the thermocline. The latter layer strongly affected the transmission, acting as a partial sound channel. The experimental data, obtained from digitized records, are based on an intensity average taken over a 2-mile range interval.

The agreement between experiment and theory is partially fortuitous because:

i) application of ray theory to the very low 13.33 Hz frequency is questionable, and

ii) the bottom reflectivity loss function used in the calculation is an extrapolated estimate.

Nonetheless, this and other comparisons that have been made with experiments are highly encouraging; they also indicate that the details of the transmission loss vs range plots are highly sensitive to specific features of the input data, e.g., horizontal gradients and certain types of bottom features, and that these must be included in any realistic predictive model.

The examples of Figs. 1 through 15 serve as an introduction to the program. They indicate the computational volume that is required to obtain a reasonably complete description of a sound field that may contain twenty to thirty arrivals or more, and also to estimate the distribution of these arrivals with depth at given ranges. With the GE-235 computer available to the Laboratories, a program extending to a 1000-mile range that computes 200 rays will require about 10 to 15 hours for the ray tracing itself plus about two hours for associated plots and intensity calculations. With a modern higher speed computer and, admittedly, with technical improvements in programming it is estimated that the computational time could be cut to one-fiftieth to one-hundredth of the present running time. Features of the present program that are discussed in detail in subsequent chapters of this report include:

i) a capacity for the inclusion of mixtures of all types of velocity profiles, e.g., surface BT casts, deep Nansen casts, etc., to obtain as precise a construction of the velocity field as the data permits,

ii) the inclusion of horizontal gradients, earth's curvature corrections, and available bottom data in a straightforward manner,

iii) a capability for "trading-off" computational accuracy in terms of shorter computer running times according to the nature and reliability of the input data and the type of calculation desired.

Separate experimental studies in long-range acoustical propagation (not reported here) have shown that the horizontal gradients and at least a limited number of bottom interactions must be included to obtain agreement between predictive models for the sound transmission and experimental data, especially at low acoustical frequencies. As a generalization, the bottom interactions that are most important for long-range propagation are of three types:

i) the terrain local to a source that can either augment the ray field by slope-aided rays that propagate to the far field or can attenuate the field by obstructing many rays that could otherwise propagate,

ii) prominent rises, e.g., seamounts or ridges, at intermediate ranges that obstruct the ducting of the sound energy, and

iii) terrain at the farthest ranges that can obstruct the sound by additional terrain shadowing or, conversely, can create "hot spots" due to favorable slopes.

The sound paths and bottom interactions shown in Fig. 17 are typical of physical conditions that prevail in the real ocean and represent the type of propagation toward which the present program is directed. The source is located on a bank at range zero. The sound energy spreads hemispherically, neglecting bottom propagation, to a near range, R_1, but during this propagation the steep rays interact strongly with the bottom so that only a fraction η of the source power radiates outwardly beyond R_1 and the fraction $(1-\eta)$ is lost to the bottom. The propagation to range R_1 acts like a filter that eliminates all but the shallow angles. If the bottom is deep between ranges R_1 and a further range R_2, almost all of the η fraction of the source power propagates as cylindrical spreading with very little decrease in the value of η. An intervening obstruction at range R_2 will cause a further filtering of the ducted energy and will produce a distinct decrease in η to a value η' after which the power will again spread cylindrically with a nearly constant fraction η'. Finally, if there is an interaction with the bottom at range R_3, there will be a further attenuation in the power; however, low-angle reflections from a slope at R_3 can give an increase in the intensity observed at certain depths at the range of R_3.

The frequent observations of nearly ideal cylindrical spreading from intermediate to long ranges give such a model a strong empiric basis as, at least, a good approximation for cylindrically spreading waves. Also, the fractions η can be measured in given ocean regions if the total intensity that propagates throughout the full depth of the ocean can be measured.

The present program attempts a predictive model of such acoustical transmission with special concentration on:

i) the intensity distribution in depth and as a function of range of source and receiver,

ii) prediction of the loss fraction η as a function of the depth of the source, the prevailing bathymetry, and the dominant velocity field,

iii) the effect of changing velocity profiles which, by their change through ocean regions, contract or expand the duct that controls the cylindrical spreading of the sound field.

Reference for Chapter I

1. W. D. Wilson; J. Acoust. Soc. Am. 23, 10, 1357 (1960).

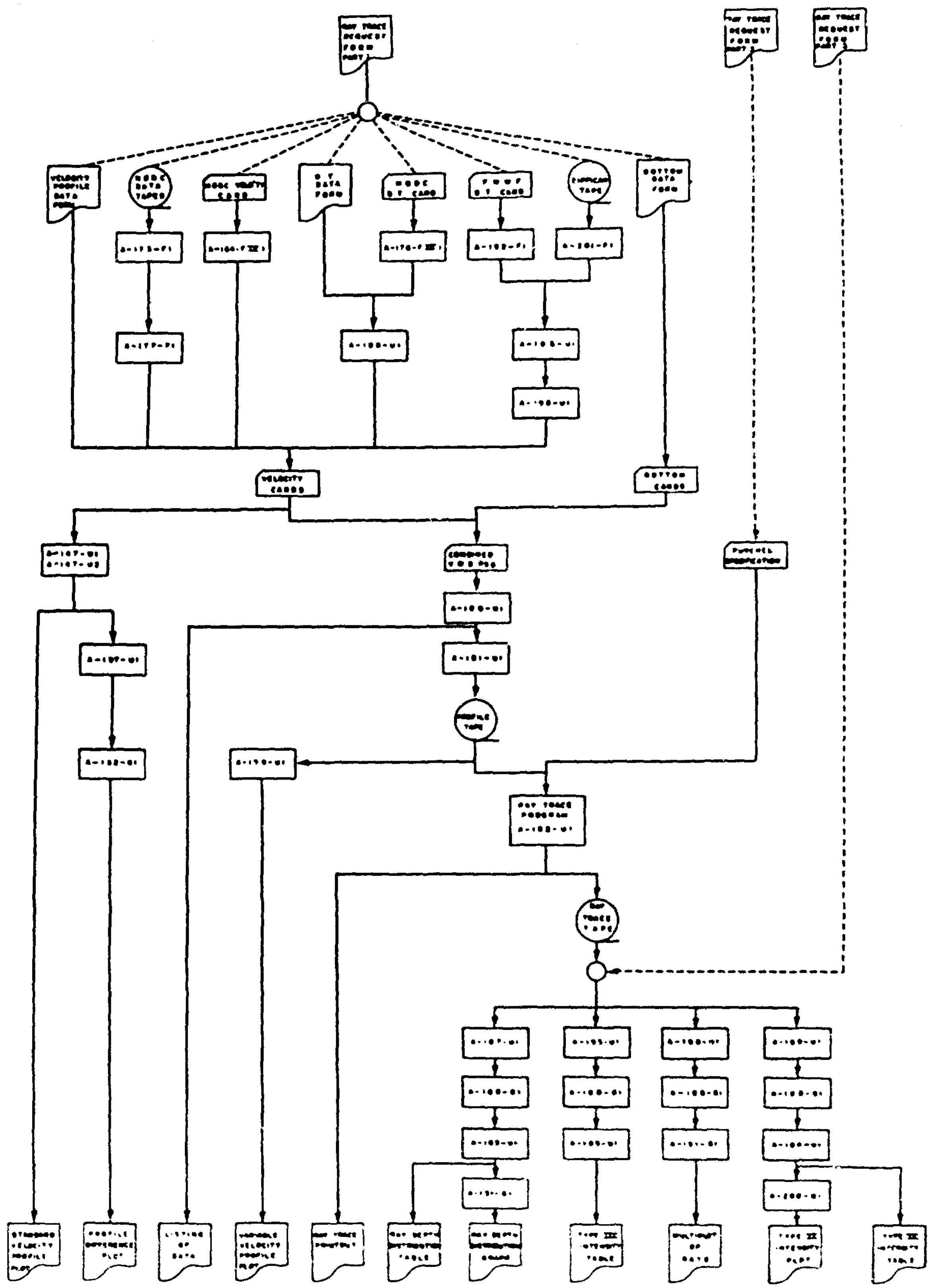

Fig. 1. Ray trace data flow diagram.

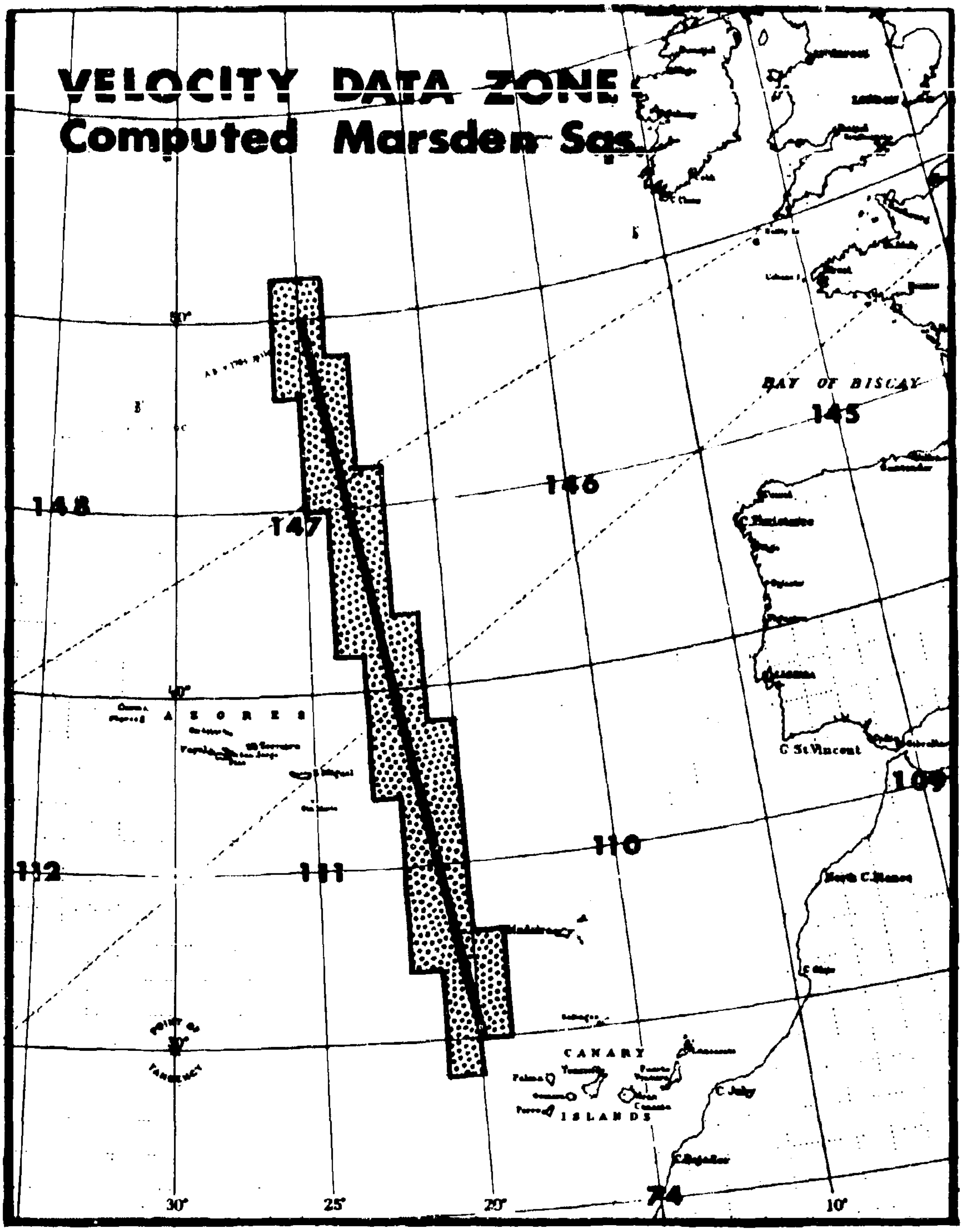

Fig. 2. The ray path between 30°N, 20°W and 50°N, 25°W drawn on a great circle chart. Marsden squares were computed by program A-173-F1.

DATA SEARCH PROGRAM (A-173-F1) - R D MININGHAM
GREAT CIRCLE BEARINGS AND DISTANCES

COMPUTED ON CLARKE 1866 SPHEROID- DISTANCE IN MILES

MAJOR RADIUS = 3443,955907 MINOR RADIUS = 3432,280990

FROM LATITUDE	LONGITUDE	TO LATITUDE	LONGITUDE	DISTANCE	BEARING
30 0 0,	20 0 0,	50 0 0,	25 0 0,	1220,3400	350,6805

RANGE	LATITUDE	LONGITUDE	BEARING TO FINAL POINT
25,0	30 24 40,16	20 4 41,42	350,6902
50,0	30 49 20,14	20 9 25,19	350,6110
75,0	31 13 59,96	20 14 11,38	350,5711
100,0	31 38 39,61	20 19 0,03	350,5303
125,0	32 3 19,08	20 23 51,21	350,4887
150,0	32 27 58,37	20 28 44,99	350,4462
175,0	32 52 37,47	20 33 41,43	350,4029
200,0	33 17 16,38	20 38 40,59	350,3586
225,0	33 41 55,09	20 43 42,55	350,3135
250,0	34 6 33,60	20 48 47,38	350,2674
275,0	34 31 11,91	20 53 55,14	350,2204
300,0	34 55 50,01	20 59 5,91	350,1725
325,0	35 20 27,88	21 4 19,78	350,1235
350,0	35 45 5,54	21 9 36,80	350,0736
375,0	36 9 42,97	21 14 57,08	350,0227
400,0	36 34 20,16	21 20 20,68	349,9707
425,0	36 58 57,12	21 25 47,70	349,9177
450,0	37 23 33,83	21 31 18,22	349,8636
475,0	37 48 10,28	21 36 52,33	349,8084
500,0	38 12 46,48	21 42 30,12	349,7521
525,0	38 37 22,42	21 48 11,70	349,6947
550,0	39 1 58,08	21 53 57,15	349,6361
575,0	39 26 33,46	21 59 46,57	349,5763
600,0	39 51 8,56	22 5 40,08	349,5153
625,0	40 15 43,36	22 11 37,78	349,4531
650,0	40 40 17,86	22 17 39,78	349,3896
675,0	41 4 52,06	22 23 46,19	349,3249
700,0	41 29 25,93	22 29 57,14	349,2588
725,0	41 53 59,48	22 36 12,73	349,1914
750,0	42 18 32,70	22 42 33,10	349,1227
775,0	42 43 5,57	22 48 58,37	349,0526
800,0	43 7 38,09	22 55 28,68	348,9811
825,0	43 32 10,25	23 2 4,16	348,9082
850,0	43 56 42,04	23 8 44,95	348,8338
875,0	44 21 13,44	23 15 31,19	348,7580
900,0	44 45 44,45	23 22 23,05	348,6807
925,0	45 10 15,07	23 29 20,66	348,6019
950,0	45 34 45,26	23 36 24,19	348,5216
975,0	45 59 15,04	23 43 33,79	348,4399
1000,0	46 23 44,38	23 50 49,64	348,3567
1025,0	46 48 13,28	23 58 11,90	348,2721
1050,0	47 12 41,73	24 5 40,74	348,1862
1075,0	47 37 9,71	24 13 16,34	348,0992
1100,0	48 1 37,21	24 20 58,86	348,0114
1125,0	48 26 4,23	24 28 48,47	347,9233
1150,0	48 50 30,76	24 36 45,31	347,6362
1175,0	49 14 56,80	24 44 49,50	347,7535
1200,0	49 39 22,38	24 53 0,98	347,6905

Fig. 3. Great circle computed along ray path at 25 n.m. increments.

VELOCITY DATA SEARCH PROGRAM - R.D. MININGHAM (A-173-F1)
SPECIFICATIONS- MDO= 1500
MONTHS= OCT, NOV, AND DECEMBER
MAXIMUM RANGE FROM RAY PATH= 50,0

TEST RUN

MARSDEN SQ	IDENTIFICATION	DEPTH METERS	MONTH	YEAR	LATITUDE DEG	LATITUDE MIN	LONGITUDE DEG	LONGITUDE MIN	DISTANCE FROM ORIGIN (NM)	DISTANCE FROM RAY PATH
11100	80043,	4000	10	21	30	17,0	20	44,0	41,75	-30,47
11110	2090075,	4800	12	61	31	21,0	20	9,0	81,18	5,54
11120	6220096,	4600	12	57	32	16,0	20	12,0	136,08	12,02
11182	7150010,	2800	10	55	38	44,0	22	40,0	539,52	-38,55
11191	5780028,	3600	10	56	39	40,0	21	43,0	565,18	15,33
14701	9610041,	3300	10	58	40	47,0	21	48,0	651,95	23,57
14702	6230029,	4000	10	57	40	14,0	22	41,0	626,98	-22,27
14703	9610042,	1600	10	58	40	32,0	23	2,0	648,23	-34,57
14723	8770011,	1900	10	59	42	21,0	23	23,0	757,79	-28,73
14732	9610037,	3800	10	58	43	49,0	22	37,0	837,31	21,38
14743	9610036,	1500	10	58	44	36,0	23	27,0	890,14	-4,90
14754	9610035,	2500	10	58	45	25,0	24	18,0	945,95	-30,24
18304	9610111,	2100	12	58	50	1,0	24	25,0	1216,68	23,15

Fig. 4. References to velocity profiles stored on NODC tapes. Selection was made by program A-173-F1 according to the indicated criteria.

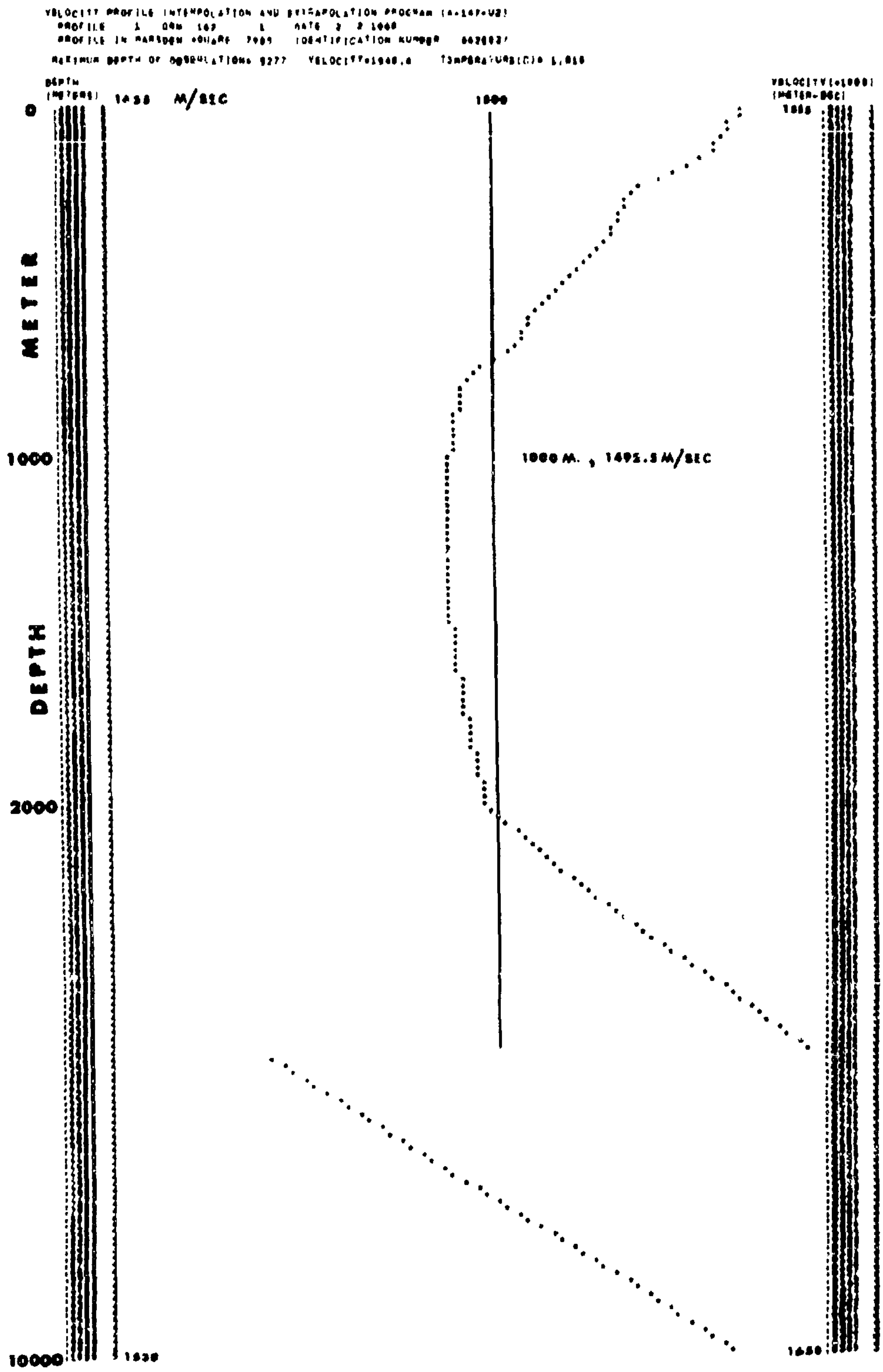

Fig 5. Velocity profile plotted in a standard format. This profile was extrapolated from a depth of 5277 meters.

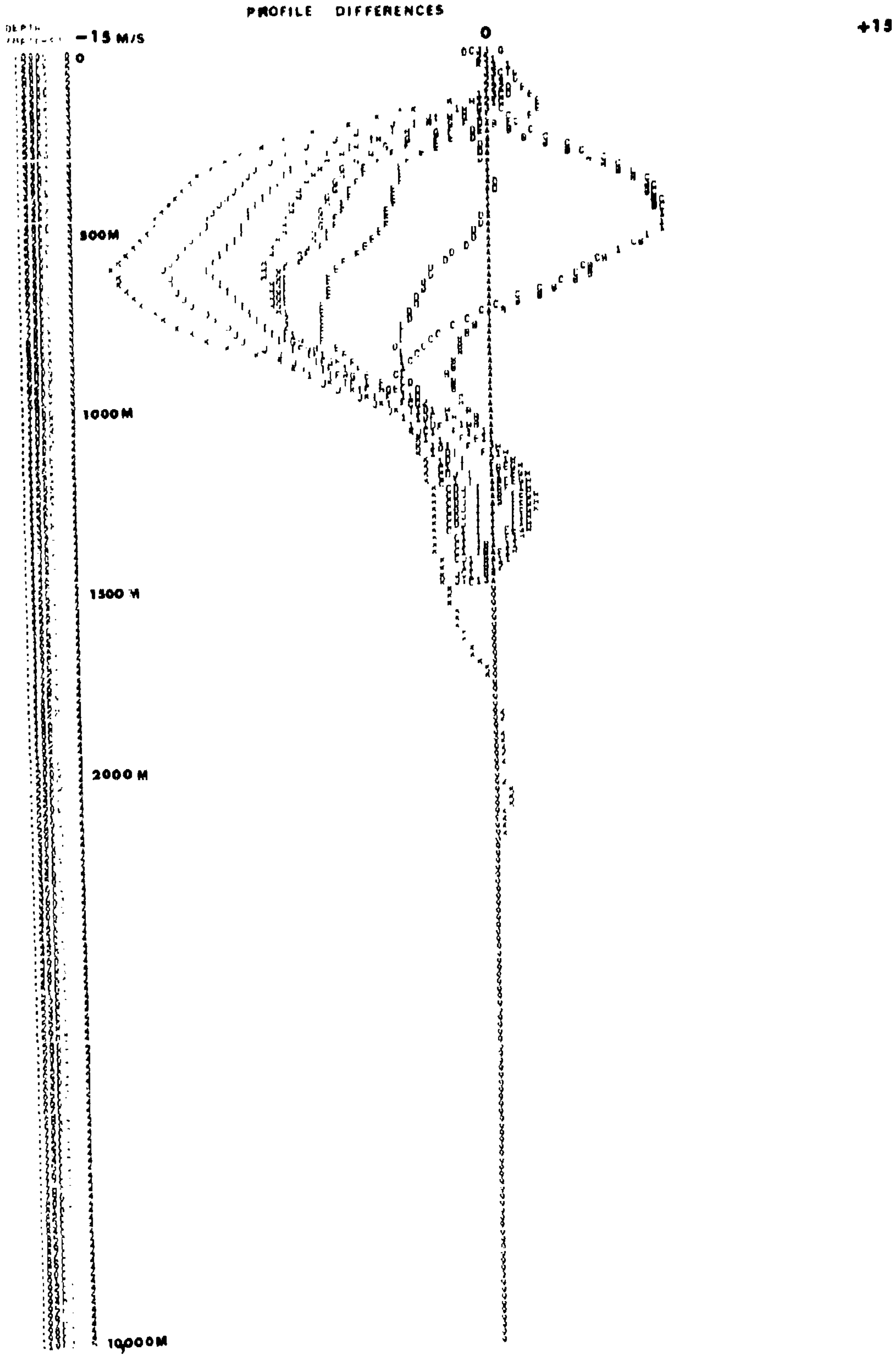

Fig. 6. A multiplot of the profile differences of 10 profiles (B-K) as compared to profile A.

HUDSON LABORATORIES OF COLUMBIA UNIVERSITY
ANALYSIS DEPARTMENT DATA FLOW SYSTEM
SENIOR SCIENTIST RAY TRACE REQUEST FORM- PART 1

Ray trace number ________RT______ Date ____________________

Senior scientist ________________________ Operation____________________

RAY TRACE DATA SEARCH SPECIFICATIONS

1. Ray path (answer either a or b)

a. Begining position: (origin) Latitude ____________ deg min sec Longitude ____________ deg min sec.

Ending position: Latitude ____________ deg min sec Longitude ____________ deg min sec.

b. Begining position: (origin) Latitude ____________ deg min sec Longitude ____________ deg min sec.

Initial bearing (deg):____________________.

Final range (n.m.):____________________.

Ray path printout increment (n.m.):____________________.

2. Maximum width of velocity data zone (n.m.):________________.

3. Acceptable months for velocity data:________________________________.

4. Acceptable years for velocity data:________________________________.

5. Minimum acceptable sample depth for published velocity data:__________.

6. Bottom contour increment (fathoms):____________________.

7. Indicate below experimental velocity and bottom data that are to be used; indicate operation numbers, dates, locations, etc.

Fig. 7. Ray trace request form used to specify the data that are to be used in the Ray Trace Program.

HUDSON LABORATORIES OF COLUMBIA UNIVERSITY
ANALYSIS DEPARTMENT DATA FLOW SYSTEM
SENIOR SCIENTIST RAY TRACE REQUEST FORM- PART 2

Ray trace number ______RT______ Date ______________

Senior Scientist ____________________ Operation ______________

RAY TRACE OPERATING SPECIFICATIONS

1. Initial depth of ray (at range 0):

   a. Give depth from surface (meters): ______________, or

   b. Check if on bottom: ______________.

2. Maximum iteration increment (meters): ______________.

3. Minimum iteration increment (meters): ______________.

4. Required accuracy for predicting velocity field, ϵ (m/sec): ________.

5. Maximum number of allowed surface hits: ______________.

6. Maximum number of allowed bottom hits: ______________.

7. Maximum allowed grazing angle (degrees): ______________.

8. Final range of ray trace (nautical miles): ______________.

9. Printout increment (nautical miles): ______________.

10. Initial angles to be traced (degrees): from ______ to ______ by ______

____

11. Check for earth's curvature correction: YES ________, NO ________.

12. Depth for the extrapolating parameter beta (meters): ______________.

13. Other information: ______________________________

Fig. 8. Ray trace request form used to specify parameters used in the Ray Trace Program.

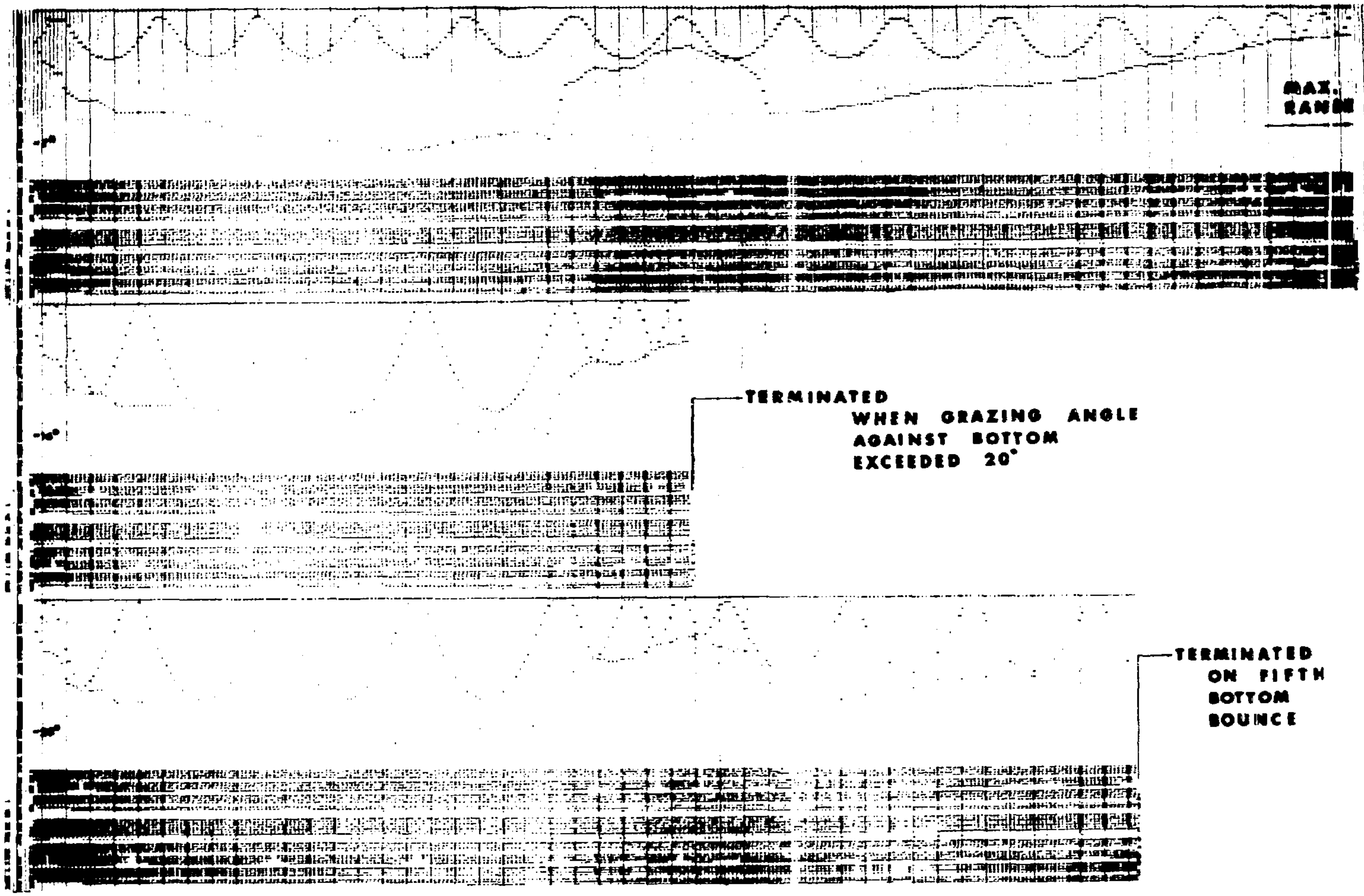

Fig. 9. Printouts of the RayTrace Program showing plot of the bottom and ray path. Digital values are printed along with the plot at 1-n.m. increments.

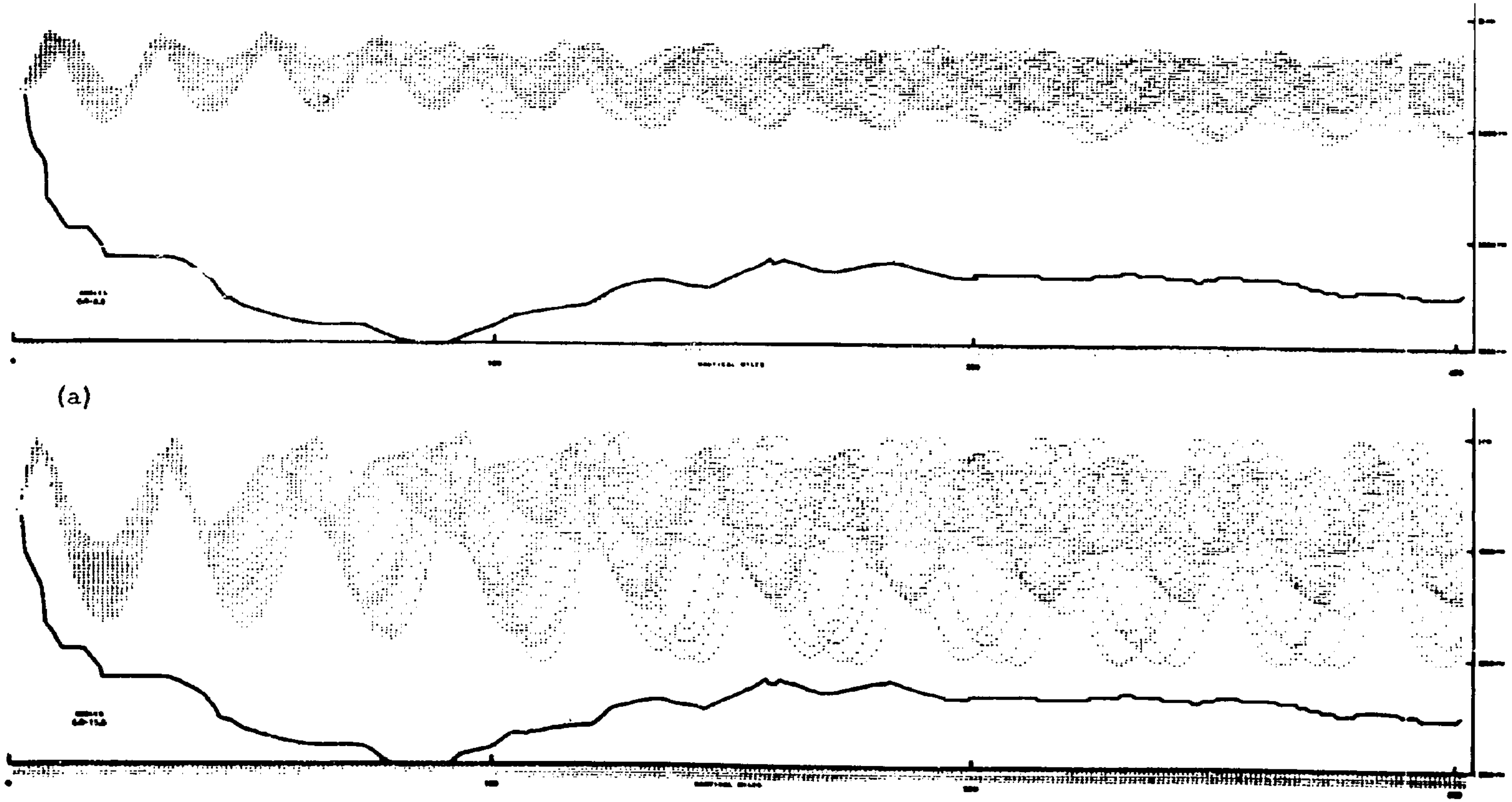

(a)

(b)

Fig. 10 (a-d). Multiplot of ray paths. Thirty rays are plotted in each figure.

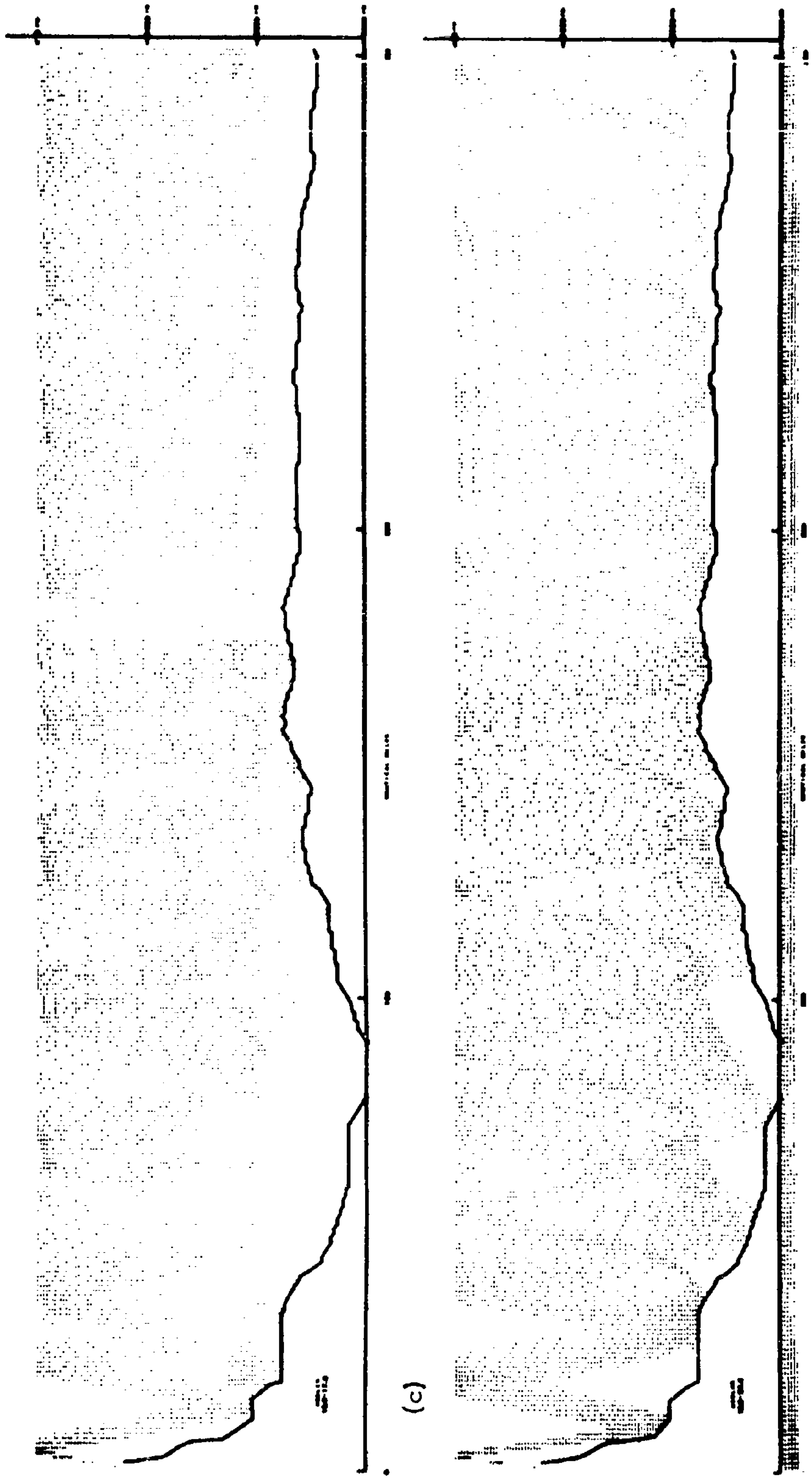

Fig. 10 (c and d).

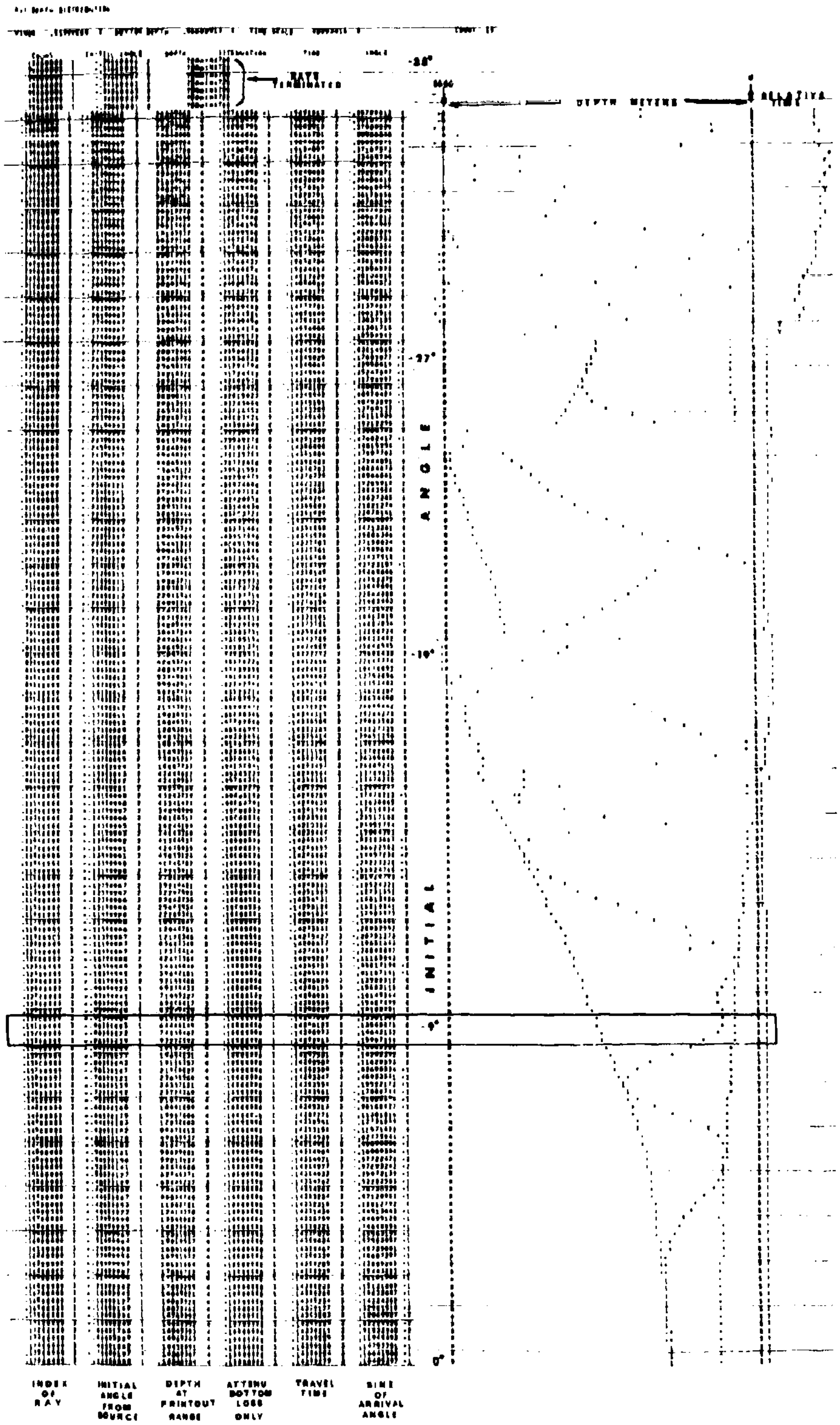

Fig. 11. Ray depth distribution plot at a range of 115 n.m.

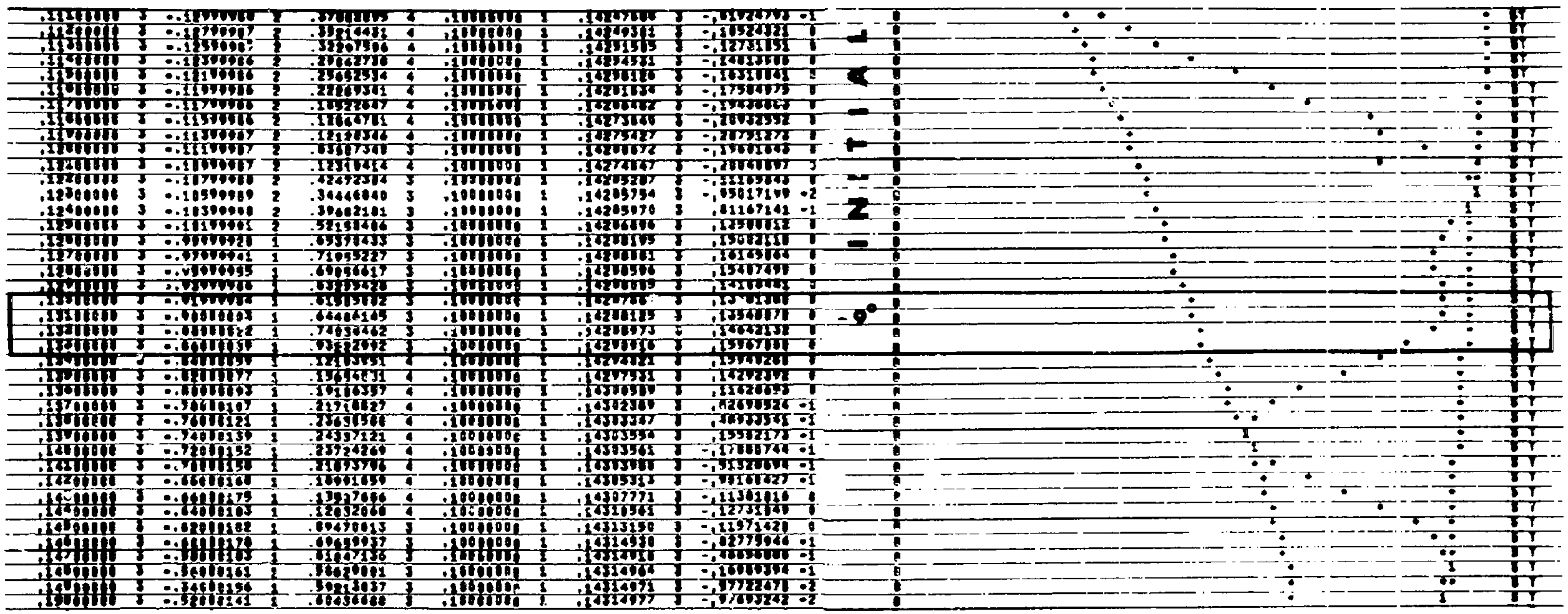

Fig. 11a. Enlarged section of Fig. 11. The maximum and minimum depths of the oscillations about the printout range are indicated by the plus and minus signs. The depth of the ray at the printout range is indicated by an asterisk. "S" indicates the surface and "B" indicates the bottom.

HUDSON LABORATORIES OF COLUMBIA UNIVERSITY
ANALYSIS DEPARTMENT DATA FLOW SYSTEM
SENIOR SCIENTIST RAY TRACE REQUEST FORM - PART 3

Ray Trace Number ______ RT ______ Date ______________

Senior Scientist ______________ Operation ______________

ANALYSIS SPECIFICATIONS

I. MULTIPLOTS (limit of 30 rays per plot)

1. Angles to be plotted (degrees):

a. from ______ to ______ c. from ______ to ______

b. from ______ to ______ d. from ______ to ______

II. RAY DEPTH DISTRIBUTION PLOT

1. Bottom loss (answer a or b):

a. α (fractional) = $C\exp - \left[(A\varphi)^2 + \frac{B(\sin \varphi)^2 \sigma^2}{\lambda} \right]$

Sigma Table	
Range Interval	Sigma
zero to ______ (n.m.)	______
to ______	______
to ______	______
to ______	______

C = ______________

B = ______________ meters

λ = ______________ meters

A = ______________

b. Specify function with three parameters:

____

2. Surface loss:

a. $\beta = 1$, or

b. Specify function: β = ______________

3. Center ranges for calculation:

a. Ranges (nautical miles): ______________

____

b. or, specify initial range with distribution every ______ nautical mile. Initial range: ______________.

Fig. 12 (a-c). Ray trace request form used for specifying data reduction procedures that are to be used on the output of the Ray Trace Program.

III. TYPE II INTENSITY CALCULATION

1. Ranges (nautical miles):

a. Initial range __________ with calculation every ______________ n.m.

b. or, specify ranges ____

2. Depths for calculation (meters): ______________________________

3. Wavelengths for calculation (meters): __________________________

4. Bottom loss:

a. Check if same as for Ray Depth Distribution Plot _________ or,

b. Specify function with three parameters: ________________________

____

5. Surface loss

a. Check if same as for Ray Depth Distribution Plot: ________ or,

b. Specify function with three parameters: ________________________

____

6. Source Directivity Function

a. $f = 1$, or

b. $f = 4 \sin^2 \left(\frac{2\pi}{\lambda} z \sin \varphi \right)$, $0 \leq z \leq r\lambda$, r (integer) __________ or,

c. Specify function: ____

7. Receiver Directivity Function

a. $g = 1$, or

b. $g = 4 \sin^2 \left(\frac{2\pi}{\lambda} z \sin \varphi \right)$, $0 \leq z \leq r'\lambda$, r' (integer) __________ or,

c. Specify function: ____

8. Distribution Density Function

a. $w(z-z_j) = \frac{P}{\pi z_B} \frac{1}{1 + (P(z-z_j)/z_B)^2}$ P = __________ or,

b. $w(z-z_j) = \frac{P}{\sqrt{\pi}\, z_B} \mathrm{EXP} \left[\frac{P(z-z_j)}{z_B} \right]^2$ P = __________

9. N = number of rays ($180^\circ/\Delta\varphi$) ______________________.

Fig. 12 (b).

IV. TYPE III INTENSITY CALCULATION

1. N = number of rays ($180^{\circ}/\Delta\varphi$) ______________.

2. M = number of depth intervals ______________(integer).

3. Wavelengths (meters):____

4. Center ranges for calculation (n.m.)________________________________

____

5. Loss and directivity functions:

a. Check if same as for Type II Intensity Calculation ________ or,

b. Specify functions:____

____

____

V. OTHER INSTRUCTIONS

____

____

____

____

____

____

____

Fig. 12 (c).

TYPE II INTENSITY CALCULATION (A 184 U1) 2
CENTER RANGE .12800000 3 NAUTICAL MILES
WAVELENGTH .50000000 2 SMOOTHING FACTOR .25000000 2 NO ANGLES .15000000 3

RANGE	R-18	R-16	R-14	R-12	R-10	R-8	R-6	R-4	R-2	R
BOTTOM	5157.7	5163.2	5164.9	5165.4	5166.0	5169.2	5177.3	5185.3	5193.4	5195.3
DEPTH										
0	.000	.000	.000	.000	.000	.000	.000	.000	.000	.000
20	-108.350	-134.520	-103.293	-108.696	-108.489	-101.747	-114.098	-107.735	-107.020	-103.949
25	-104.331	-102.578	-100.431	-104.751	-106.058	-99.893	-112.942	-107.911	-105.259	-103.144
30	-102.672	-101.625	-90.911	-103.700	-105.234	-98.440	-111.174	-104.201	-103.903	-101.947
35	-101.208	-90.758	-98.711	-101.934	-104.107	-97.290	-109.784	-103.400	-102.057	-100.450
40	-100.092	-98.704	-97.734	-102.857	-103.210	-96.363	-106.007	-102.541	-102.052	-99.408
500	-91.610	-92.915	-94.272	-95.940	-96.259	-98.289	-97.439	-101.110	-101.373	-92.275
1000	-97.203	-98.339	-96.921	-94.989	-99.348	-101.047	-102.525	-107.280	-100.032	-97.773
1500	-95.501	-96.063	-97.919	-94.553	-98.759	-101.133	-102.933	-99.076	-89.467	-97.783
2000	-93.104	-95.749	-94.134	-94.803	-99.324	-100.035	-100.482	-90.471	-87.260	-89.449
2500	-92.117	-94.048	-95.374	-90.422	-97.714	-97.970	-100.047	-87.498	-87.774	-91.147
3000	-91.271	-91.800	-93.013	-95.788	-98.190	-96.491	-87.014	-86.605	-89.057	-93.579
4000	-87.806	-90.879	-93.149	-90.102	[illegible]	-94.363	-100.754	-99.205	-101.751	-99.596

RANGE	R+2	R+4	R+6	R+8	R+10	R+12	R+14	R+16	R+18
BOTTOM	5196.9	5198.5	5200.9	5204.1	5207.4	5210.3	5210.6	5211.4	5211.9
0	.000	.000	.000	.000	.000	.000	.000	.000	.000
20	-94.183	-89.754	-92.342	-98.160	-101.322	-101.509	-10[illegible].417	-103.803	-103.997
25	-93.188	-87.804	-90.401	-96.200	-99.289	-99.578	-102.318	-101.945	-101.393
30	-90.497	-85.239	-88.845	-94.020	-97.824	-98.031	-103.567	-100.403	-100.479
35	-89.207	-84.931	-87.565	-93.308	-96.219	-96.755	-102.115	-99.120	-99.244
40	-88.144	-83.934	-86.495	-92.197	-95.000	-95.003	-100.334	-98.051	-98.231
500	-85.875	-87.170	-84.773	-89.534	-90.969	-91.307	-93.587	-94.299	-94.749
1000	-89.807	-93.187	-89.447	-87.991	-93.210	-94.884	-94.291	-98.437	-97.575
1500	-91.330	-95.549	-98.719	-87.288	-91.920	-94.555	-95.051	-98.330	-97.493
2000	-93.511	-97.204	-98.754	-90.014	-87.154	-93.236	-96.759	-94.131	-97.979
2500	-98.141	-97.522	-98.362	-99.060	-88.265	-90.207	-94.114	-94.853	-95.115
3000	-95.598	-94.157	-97.977	-97.901	-96.381	-85.036	-91.517	-93.036	-93.772
5000	-101.520	-100.[illegible]	-99.884	-101.432	-100.680	-99.390	-98.924	-99.365	-98.556

TYPE II INTENSITY CALCULATION (A 184 U1) 2
CENTER RANGE .12800000 3 NAUTICAL MILES
WAVELENGTH .15000000 2 SMOOTHING FACTOR .25000000 2 NO ANGLES .15000000 3

RANGE	R-18	R-16	R-14	R-12	R-10	R-8	R-6	R-4	R-2	R
BOTTOM	5157.7	5163.2	5164.9	5165.4	5166.0	5169.2	5177.3	5185.3	5193.4	5195.3
DEPTH										
0	.000	.000	.000	.000	.000	.000	.000	.000	.000	.000
20	-95.290	-96.842	-94.380	-95.884	-98.085	-95.980	-102.179	-96.925	-96.227	-96.817
25	-95.520	-94.068	-94.574	-95.400	-98.052	-95.669	-101.308	-100.341	-99.278	-99.402
30	-95.496	-95.427	-94.812	-95.885	-99.145	-98.337	-100.158	-102.352	-103.869	-104.238
35	-95.348	-95.207	-94.317	-95.452	-96.719	-96.975	-99.157	-99.823	-99.847	-100.840
40	-95.412	-95.135	-94.703	-95.339	-96.572	-96.829	-99.016	-99.001	-99.720	-100.701
500	-92.927	-92.501	-93.491	-94.157	-94.547	-94.027	-92.024	-93.792	-94.532	-93.739
1000	-97.297	-98.701	-96.159	-97.982	-99.008	-97.770	-102.865	-101.196	-98.043	-92.194
1500	-97.827	-98.693	-99.111	-99.501	-96.539	-98.487	-99.674	-98.279	-93.205	-92.734
2000	-95.150	-96.143	-99.181	-96.179	-99.144	-99.123	-98.300	-97.778	-92.428	-93.270
2500	-95.825	-97.374	-95.059	-96.883	-98.575	-98.986	-99.596	-92.301	-92.307	-93.559
3000	-94.728	-93.892	-95.165	-97.580	-96.034	-96.142	-92.295	-91.577	-92.383	-98.335
5000	-97.815	-97.358	-94.531	-92.713	-93.228	-95.237	-99.252	-98.409	-100.598	-99.372

RANGE	R+2	R+4	R+6	R+8	R+10	R+12	R+14	R+16	R+18
BOTTOM	5196.9	5199.5	5200.9	5204.1	5207.4	5210.3	5210.6	5211.4	5211.9
0	.000	.000	.000	.000	.000	.000	.000	.000	.000
20	-90.214	-86.382	-88.201	-92.535	-94.028	-93.794	-99.775	-96.000	-92.869
25	-92.664	-85.753	-87.811	-92.064	-93.150	-93.529	-98.277	-95.270	-92.800
30	-90.339	-85.304	-88.027	-91.816	-92.503	-93.567	-97.032	-95.237	-96.758
35	-94.817	-89.587	-92.018	-94.395	-95.450	-95.014	-97.801	-96.710	-97.139
40	-94.487	-89.019	-91.918	-94.000	-95.343	-95.717	-97.654	-96.407	-96.998
500	-90.466	-91.505	-89.443	-93.479	-94.615	-94.247	-95.278	-94.815	-94.997
1000	-93.556	-95.774	-94.147	-92.505	-96.137	-97.822	-95.769	-99.031	-96.372
1500	-94.528	-95.642	-100.997	-92.176	-95.690	-97.684	-97.684	-99.085	-97.539
2000	-95.058	-98.360	-95.127	-94.302	-91.902	-96.819	-97.597	-96.100	-98.910
2500	-96.770	-98.752	-97.696	-97.445	-92.457	-93.816	-96.721	-97.513	-97.750
3000	-95.964	-95.415	-95.799	-96.923	-95.299	-90.118	-94.867	-96.463	-94.963
5000	-100.015	-98.994	-98.803	-98.788	-98.540	-98.399	-98.232	-99.315	-98.769

Fig. 13. Type II intensity calculation printout.

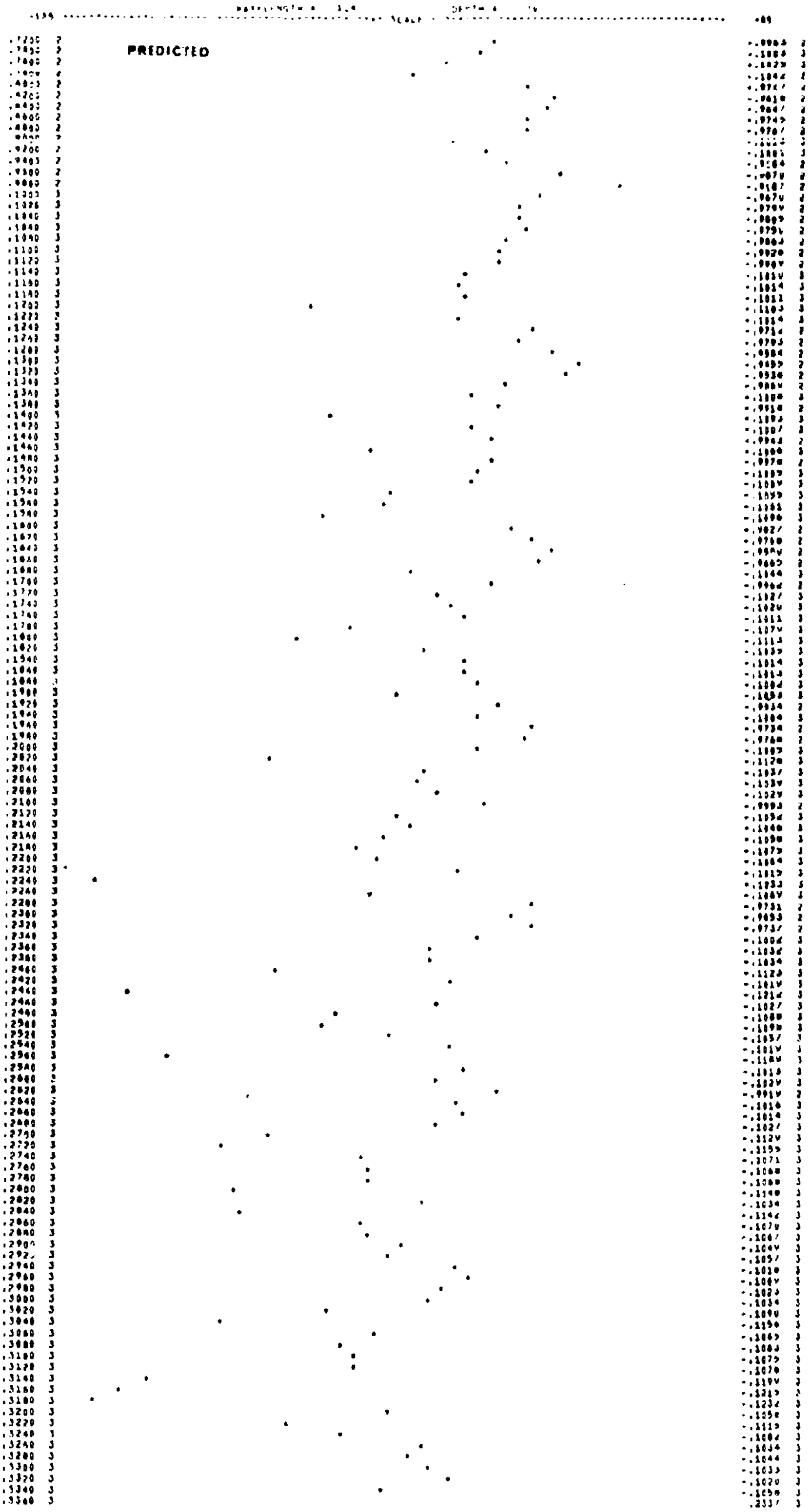

Fig. 14. Transmission loss curve calculated from ray tracings based on data taken in Hudson Laboratories Operation 251.

```
TYPE 111 INTENSITY CALCULATION

RANGE      300.0  NAUTICAL MILES                                          1 RANGE OF    1 WAVELENGTH
BOTTOM DEPTH   5276.4 METERS          DEPTH INTERVALS M= 25

NUMBER OF ANGLES
 .15000000  3

WAVELENGTH    114.0 METERS
```

COUNT	DEPTH		TRANSMISSION	LOSS
1	.21105574	3	-.91979623	2
2	.42211148	3	-.96742446	2
3	.63316722	3	-.97295497	2
4	.84422297	3	-.98329795	2
5	.10552787	4	-.98878165	2
6	.12663345	4	-.99053935	2
7	.14773902	4	-.99079693	2
8	.16884459	4	-.99001902	2
9	.18995017	4	-.98865658	2
10	.21105574	4	-.98713711	2
11	.23216131	4	-.98560860	2
12	.25326689	4	-.98404223	2
13	.27437246	4	-.98215823	2
14	.29547804	4	-.97973651	2
15	.31658361	4	-.97655462	2
16	.33768918	4	-.97223693	2
17	.35879476	4	-.96575223	2
18	.37990033	4	-.95633123	2
19	.40100591	4	-.96321212	2
20	.42211148	4	-.96104540	2
21	.44321706	4	-.96064752	2
22	.46432263	4	-.96329827	2
23	.48542821	4	-.97026654	2
24	.50653378	4	-.97830883	2
25	.52763935	4	-.98273667	2

Fig. 15. Type III intensity calculation printout.

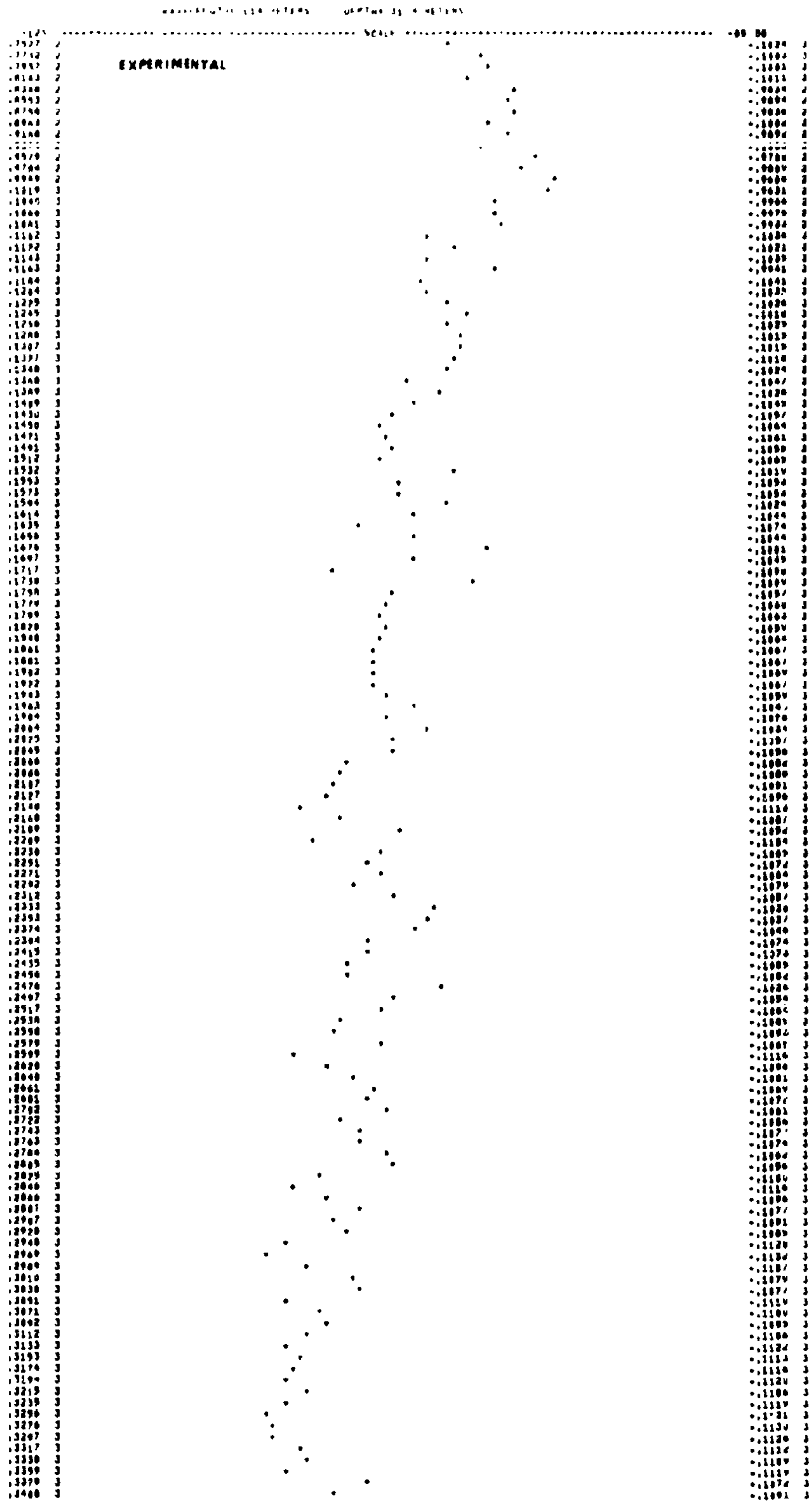

Fig. 16. Experimental transmission loss curve for Operation 251.

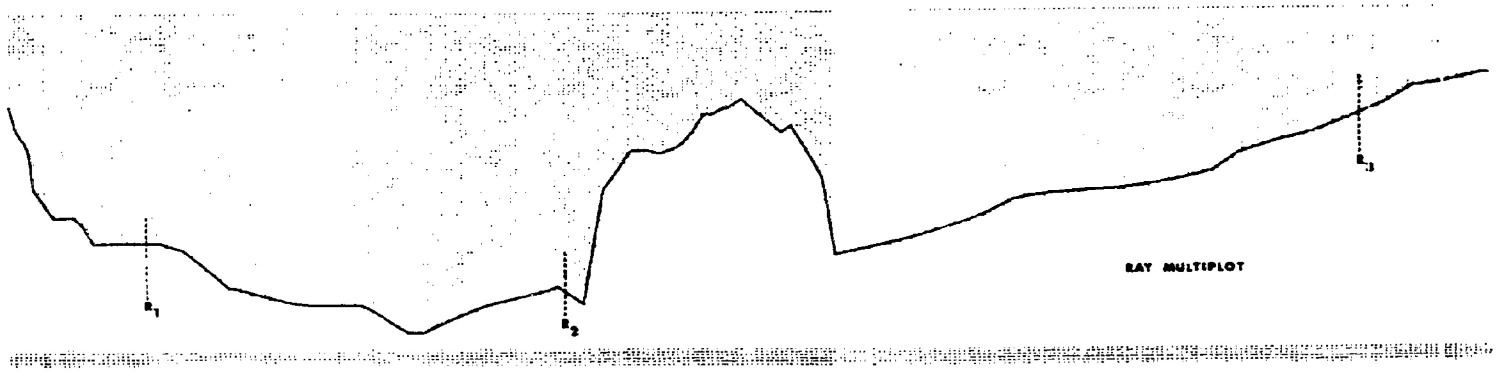

Fig. 17. Multiplot of ray paths over a 300-mile range.

CHAPTER II

DATA INPUTS AND PROGRAM ORGANIZATION

2. 1. Introduction

This chapter of the report is concerned with the selection and preparation of data inputs which are used to construct the velocity field and bottom profiles for the Ray Trace Program. In application, the program must be able to accept data from many different sources, and for this reason it was necessary to develop a series of programs into a data flow system. The specific programming details of the system are not given in this chapter, but only the basic principles upon which the system was designed.

2. 2. Data Flow System

Over-all objectives in the data flow system have been on:

1) Flexibility
2) Speed of data assembly
3) Error detection
4) Documentation

2. 2. 1. Flexibility

Applications of the ray-tracing program have ranged from time calculations over a short path with data printouts every tenth of a nautical mile, to estimates of transmission loss using relatively crude input data with data printouts at widely separated ranges. The source of the data varies from program to program and all data must be reduced to common formats. The data flow system has been designed to accommodate as many types of inputs as possible.

2. 2. 2. Speed In Data Assembly

Speed in assembling data is accomplished by having the computer do most of the necessary reduction procedures. The output of one program is the input to another program and thus, once having entered the system, there should be no further need to manipulate data by hand. Time is also saved by having the computer print out a variety of visual displays and plots of data, which are formated for use in reports. A number of forms (data reduction sheets) have also been developed to effect with ease the initial entrance of data which are not on a medium that is readable by the computer, i.e., card or tape, into the system. Data from any source can be written on forms and punched on cards for special entries.

2.2.3. Error Detection

Every program checks data for consistency and physical impossibilities, e.g., successive range entries must increase in magnitude and it is impossible to have negative depths. This eliminates gross accidental errors in the final data package but final validation depends on editorial review by a scientist as to the acceptability of the input data.

2.2.4. Documentation

Every reduction procedure that is performed on the data is documented by printouts which are labeled to allow cross referencing of its information with the original source or other data reduction printouts. Many of the printouts are self-explanatory and can be copied for use in reports without long explanations.

2.3. Program Management

The first stage of the data flow system funnels data from the various sources into one package (a card deck) for the ray calculations. The second stage calculates the ray paths, and the third stage analyzes data based on the ray paths to give intensity calculations, distribution plots, etc. The three stages of the data flow system are directed by the scientist with the use of three forms. The intent of these forms is as follows.

(1) Data search specifications, Fig. 7. This form specifies the acoustical path and its length, requests searches for velocity field and bathymetric data, references actual experimental data that would be applicable, and indicates the accuracy that is required for the data inputs.

(2) Program operating specifications, Fig. 8. This form details the functions and the parameters that are to be used in the Ray Trace Program. Program accuracy is implicitly controlled by specifications on this form, e.g., the maximum iteration increment, the required accuracy for predicting the velocity field, and the number and initial angles of rays used in estimating a ray probability distribution.

(3) Analysis specifications, Fig. 12. This form controls the selection of various printout or plot options that are available and also specifies physical data such as bottom attenuation functions or directivity functions. The more commonly used ray trace analysis routines have been programmed and are immediately available. They are:

a) Type II Intensity Calculation

b) Type III Intensity Calculation

c) Ray Depth Distribution Plot

d) Multi-Plot of Rays

e) Transmission Loss vs Range.

At this stage, the scientist may also request a special program to be written which would analyze the results of the Ray Trace Program in some unique manner.

The description and the effects of various parameters used in the forms can be found in the appropriate chapters of this report. This chapter specifies the use of the first form and affords some information on the second, Figs. 7 and 8. The flow diagram in Fig. 1 shows the data processing channels of the data flow system and provides an outline for this chapter.

2.4. Ray Path Specifications

A ray trace path may be specified as:

(1) Between two positions each located by their latitude and longitude, or

(2) An initial position, initial bearing, and a final range.

In either event, track information is developed at specified range intervals along a great circle as in Fig. 18.

2.5. Sources of Sound Velocity Profile Data

Primarily, the sound velocity profile data that are used to construct the velocity field will come from three sources:

(1) National Oceanographic Data Center. NODC has compiled physical and chemical data from more than 300,000 oceanographic stations located throughout the world. Hudson Laboratories has references to all these stations and the data for the majority of them. Velocity

profiles are immediately available for the Pacific Ocean and for much of the Atlantic (Fig. 19) and information for the other areas can be obtained on short order. For reference, the geographic distribution of velocity profiles in the North Atlantic that are deeper than 1,950 meters is shown in Fig. 20, and Fig. 21 shows the distribution in the month of December.

(2) Published Data from other than NODC. The Hudson Laboratories library receives "data publications" from many oceanographic institutions during a year. All the publications that contain information on the temperature, salinity, or sound structure of an area are indexed with respect to geographical location. Atlases, technical reports, and any other published information which could be helpful in the construction of the velocity field are also indexed in this manner.

(3) Hudson Laboratories Experiments. Experiments that include velocimeter, X-BT, or BT data taken along the total length of the acoustical path will allow the construction of the best possible velocity field. Even a partial experimental coverage of the path is a help in the selection of the most appropriate information from published data. Experimental data can be combined with published velocity profiles with prudence; i.e., one can take the upper portion of the profile as that of a shallow BT cast but use published data to represent more stable, deeper profiles.

2.6. Selection of Velocity Profile Data

The data flow system is grouped into sub-systems. Some of these assist in the selection of velocity data from large sources such as NODC and the Hudson Laboratories library where it would be difficult to retrieve information without a predefined procedure. The major criteria for selection are:

(1) Proximity to a designated ray path

(2) Month or season

(3) Maximum Depth of Observation (MDO).

2.6.1. Proximity

There is a maximum distance from a ray path such that velocity profiles which lie within the area determined by the ray path and a data zone width are considered acceptable. This area is called the "velocity profile data zone." The NODC Data Search Procedure (Fig. 22) generates this zone by first computing the great circle between the beginning and end point of the ray path (Fig. 18) and then computing Marsden Squares (1 degree areas) that lie in its path and on each side of it, out to the designated maximum distance (Fig. 23).

2.6.2. Season

Profiles are also classified and searched for according to months to permit the selection of profiles which will reflect seasonal characteristics of an area (Fig. 24).

2.6.3. Maximum Depth of Observation

A minimum of two deep profiles are needed to construct the velocity field. They are used at the beginning and at the end of the ray path and should have a maximum depth of observation (MDO) for which the water temperature and salinity have become constant.

After a general selection of profiles has been made, it is the responsibility of the scientist to investigate each profile's finer characteristics, e.g., the year in which the profile was taken, the institution which conducted the survey, the shape of the profile relative to other data being used in the program, and other factors which would determine its application for use in the Ray Trace Program. This final selection constitutes a data-editing review.

2.7. <u>Velocity Field Construction Program</u>

Velocity profiles are entered in the Velocity Field Construction (VFC) program in order of increasing range from the beginning position of the ray path to the end position. Only data in the form "depth vs velocity" are used in the program; therefore, it is necessary to convert information that exists as pressure, temperature, and salinity combinations to this form. This conversion is usually done prior to the running of the program by a sub-system of the data flow system.

The first step in constructing the velocity field is to extrapolate all of the entered profiles to a depth equal to the deepest bottom point along the ray path. Two types of profiles are recognized for this procedure and are treated differently. Profiles are tagged "deep" or "shallow" before they enter the VFC program and are distinguished by the following definitions:

(1) Deep profiles have a MDO at a depth where, with further increase in depth, significant changes in temperature and salinity would not be expected; thus the velocity at greater depths can be extrapolated as a function of pressure alone.

(2) Shallow profiles have a MDO at a depth where, with further increase in depth, changes in temperature and salinity could be expected, and these changes must be included in the calculation of velocities at greater depths (Fig. 25).

2.7.1. Profile Extrapolation

Deep profiles are extrapolated by first calculating the temperature at its MDO and then using this temperature in Wilson's equations to calculate velocities at greater depths. The salinity is considered constant at 35 ‰ and the temperature is calculated by using the depth and velocity at the MDO in an inverse solution of Wilson's equations, Fig. 26.

A procedure is available for extrapolating shallow profiles if they have two bracketing deep profiles, i.e., a deep profile at a range greater than the shallow profile, and a deep profile at a range less than the shallow profile. At great depths the velocity values of the shallow profile are calculated by linear interpolation with respect to range between the two deep profiles. Although the linear interpolated values may be a satisfactory representation of the true velocity structure at great depths, these values will usually not match the MDO of the shallow profile. For this reason, an adjustment is made between the MDO of the shallow profile and a much deeper depth to insure that the interpolated profiles will be continuous. The depth β is chosen as the (arbitrary) depth at which linear interpolation between the deep profiles is permissible, Figs. 25 and 27.

Figure 27 is a schematic illustrating the extrapolation procedures for deep and shallow profiles. Parts of the schematic have been exaggerated for the purpose of clarity and it should not be considered to represent proper proportion. The interpolation and extrapolation formulas are given in Fig. 25 and an example of extrapolated profiles is given in Table 5.3.1.

2.7.2. Curvature and Gradient Data

The second step in the Velocity Field Construction Program is the calculation of curvature and gradient parameters for all the depths of a profile where there is a value for the velocity that is either given as input data or calculated by one of the foregoing extrapolation procedures. A modified 4-point interpolation is used between listed points on the profile; thus, the vertical velocity structure can be completely defined at the range of the given profile. The formulas for calculating the curvature and gradient are given in Fig. 28. The modified 4-point interpolation procedure, also known as the "Special 4-point fit," is a weighted average of two 3-point parabolic fits.

Only the curvature and gradient parameters at data points are calculated in the VFC program and entered on the data input tape. The interpolation of velocities and derivatives, vertically and horizontally, is done directly in the Ray Trace Program (Chapter III), using the expansions of Fig. 28 in depth and linearly interpolating all the parameters in range between the ranges of successive velocity profile entries. The result of this field composition is the set $v(R, z)$, $Z(R, z)$, $D(R, z)$, and $G(R, z)$ defined continuously over the range R and the ocean depth z, and these are used in a Taylor expansion of the velocity from any point as discussed in Chapter III, Eq. (3).

2.8. "Four-Point" Fits

There are, of course, many types of 4-point fits for estimation of the trend of a function between discretely entered data points. The selection of the special 4-point fit used in the present program was guided by its relative simplicity and by the fact that it gave a smoother approximation than alternative fits which could permit very large local curvatures. To illustrate this, Fig. 29 gives a comparison of the effect of a single displacement from an otherwise constant function according to fits obtained by:

i) linear interpolation

ii) Lagrange 4-point

iii) Bedford Institute 4-point

iv) Special 4-point.

The Bedford Institute method has been tested and adjusted for optimum agreement with experimental data. See Fig. 30 for formulas

2.9. Sources of Bottom Data

The horizontal bottom profile along the ray path has proved to be an important factor in ray trace programs. Geological features such as seamounts or banks can totally obstruct, partially attenuate, or redirect rays as they travel along paths determined by the velocity field.

Primarily the data for constructing the bottom profile will come from two sources:

(1) Published charts. The USN Oceanographic Office has published BC (bottom contour) charts that cover most of the world's oceans. Foreign countries, e.g., Russia, Germany, Great Britain, etc., also publish charts with bottom contours. Charts depicting the detailed structure of a small area are often found in technical reports.

(2) Research Experiments. As was true with velocity data, the best source of bottom data comes from bathymetric surveys along the ray trace path.

2.9.1. Bottom Profile Construction

The Ray Trace Program presently reads bottom data in the form of range vs depth, which is usually obtained in the following manner:

(1) The ray path is plotted on the appropriate BC charts, and then

(2) The distance from the beginning position of the ray path to each of the contours that cross the ray path is calculated. This distance can be computed by having a printout of the great circle (Fig. 18) which lists: range vs geographic position, at small increments (25 miles or less) along the ray path. The ranges for contours between the listed positions can then be read graphically from the BC chart.

Contours are usually read at 100-fathom intervals, but the selection of a smaller or larger interval may be necessary to emphasize special features.

The Ray Trace Program linearly interpolates between input points to provide a continuous trace of the bottom. This fit has proved reliable for most ray traces; however, it is occasionally desirable to have a smoother representation of the bottom. This can be obtained by using a 3- or 4-point fit, prior to running the Ray Trace Program, to generate additional points between those originally listed. This procedure should be adopted with caution and used only in an area where one has an intimate knowledge of the geology and feels that the smoother bottom is closer to the actual situation then the linearly interpolated bottom with discontinuous slopes.

2.10. Inputs to the Ray Trace Program

At this point in the data flow system the velocity and bottom data can be combined into a data package for the Ray Trace Program. Associated with this package must be operating instructions, which are taken from the Ray Trace Request Form - Part 2 (Fig. 8), and provide the following information to the program:

(1) Initial depth of the rays to be traced. This is in reality the depth of the sonic source or receiver at range zero.

(2) The initial angles to be traced. Each angle in the program is traced separately from range zero.

(3) Final range of the ray trace.

(4) Printout increment. Information concerning the position and angle of the ray is printed at any desired increment (usually 1 or 2 n. m.) along the ray path.

(5) Iteration parameters. The rays are traced through the velocity field by computing the position of the ray every few meters. The increment at which the ray path is computed is variable and depends on the iteration parameters selected (Chapter III - 3.3). These parameters control the accuracy with which the ray path is

predicted; the smaller the iteration increment, the better the prediction but consequently the longer the computing time. All ray traces do not require the same accuracy. A balance must be considered between the prediction of the ray path and the accuracy of the data; using very small iteration increments will not improve the quality of the input data used for the velocity field or the bottom.

(6) Physical parameters. The Ray Trace Program accounts for energy losses due to bulk absorption, bottom hits, and surface hits. The attenuation functions that are used to compute the losses are specified as inputs. The computing of a ray path is terminated when the accumulated loss of a ray meets a specified maximum. The details of these procedures are described in Chapter IV.

The operating instructions for the Ray Trace Program are entered separately from the data package. Thus, it is possible to run different ray traces, i.e., different specifications, on the same data.

2.11. Outputs of the Ray Trace Program

The outputs of the Ray Trace Program are a printout and a magnetic tape with numerical values, at the specified printout intervals for the:

(1) depth of the ray,

(2) angle of the ray from the horizontal,

(3) accumulated travel time of the ray, and

(4) the distance to the bottom from the depth of the ray (bottom difference).

In addition to the record of this information at the specified interval, the program prints the same data when the ray hits the bottom, hits the surface, or the angle of the ray is zero. A plot of the bottom, the surface, and the path of the ray accompanies the numerical values on the printout.

Analysis of the ray trace can be made directly from the printout or by other computer programs that are capable of reading the Ray Trace Program's output tape. As has been previously mentioned, there are standard analysis routines that have been programmed, but the scientist is at liberty to develop other analysis procedures for his specific purpose.

2.12. Conclusion

It has been the intent of this chapter to give the reader an over-all viewpoint of the Ray Trace Program, and concepts rather than operational details have been presented. Parenthetical cross references to other chapters were given to direct the reader to a more detailed explanation of the topics being discussed. The Ray Trace Program has been defined as a series of programs and procedures, organized into a data flow system for advantages in speed, accuracy, and flexibility in data processing. It is believed that through this approach, the Ray Trace Program will have its greatest effectiveness as a tool for the acoustical scientist.

VELOCITY DATA SEARCH PROGRAM
GREAT CIRCLE BEARINGS AND DISTANCES - R.D. MININGHAM (A-173-F1)

COMPUTED ON CLARK 1866 SPHEROID - DISTANCE IN N. M.

MAJOR RADIUS = 3443.955997 MINOR RADIUS = 3432.280998

TEST RUN

FROM LATITUDE	LONGITUDE	TO LATITUDE	LONGITUDE	DISTANCE	BEARING
20 0 0.	65 0 0.	30 0 0.	70 0 0.	657.0359	336.5216

RANGE	LATITUDE	LONGITUDE	BEARING TO FINAL POINT
25.0	20 22 55.50	65 10 37.52	336.4655
50.0	20 45 50.41	65 21 18.07	336.4082
75.0	21 8 44.70	65 32 1.74	336.3496
100.0	21 31 38.38	65 42 48.59	336.2896
125.0	21 54 31.42	65 53 38.70	336.2286
150.0	22 17 23.80	66 4 32.16	336.1660
175.0	22 40 15.52	66 15 29.03	336.1032
200.0	23 3 6.56	66 26 29.39	336.0387
225.0	23 25 56.91	66 37 33.32	335.9730
250.0	23 48 46.54	66 48 40.90	335.9062
275.0	24 11 35.46	66 59 52.21	335.8382
300.0	24 34 23.64	67 11 7.32	335.7693
325.0	24 57 11.07	67 22 26.32	335.6993
350.0	25 19 57.73	67 33 49.28	335.6285
375.0	25 42 43.62	67 45 16.27	335.5566
400.0	26 5 28.73	67 56 47.39	335.4844
425.0	26 28 13.04	68 8 22.68	335.4116
450.0	26 50 56.55	68 20 2.24	335.3386
475.0	27 13 39.25	68 31 46.11	335.2656
500.0	27 36 21.14	68 43 34.35	335.1930
525.0	27 59 2.23	68 55 27.00	335.1231
550.0	28 21 42.54	69 7 24.08	335.0558
575.0	28 44 22.09	69 19 25.55	334.9945
600.0	29 7 0.95	69 31 31.32	334.9460
625.0	29 29 39.26	69 43 41.10	334.9319
650.0	29 52 17.41	69 55 54.01	335.1647

Fig. 18. Great Circle computed along ray path at 25 n.m. increments.

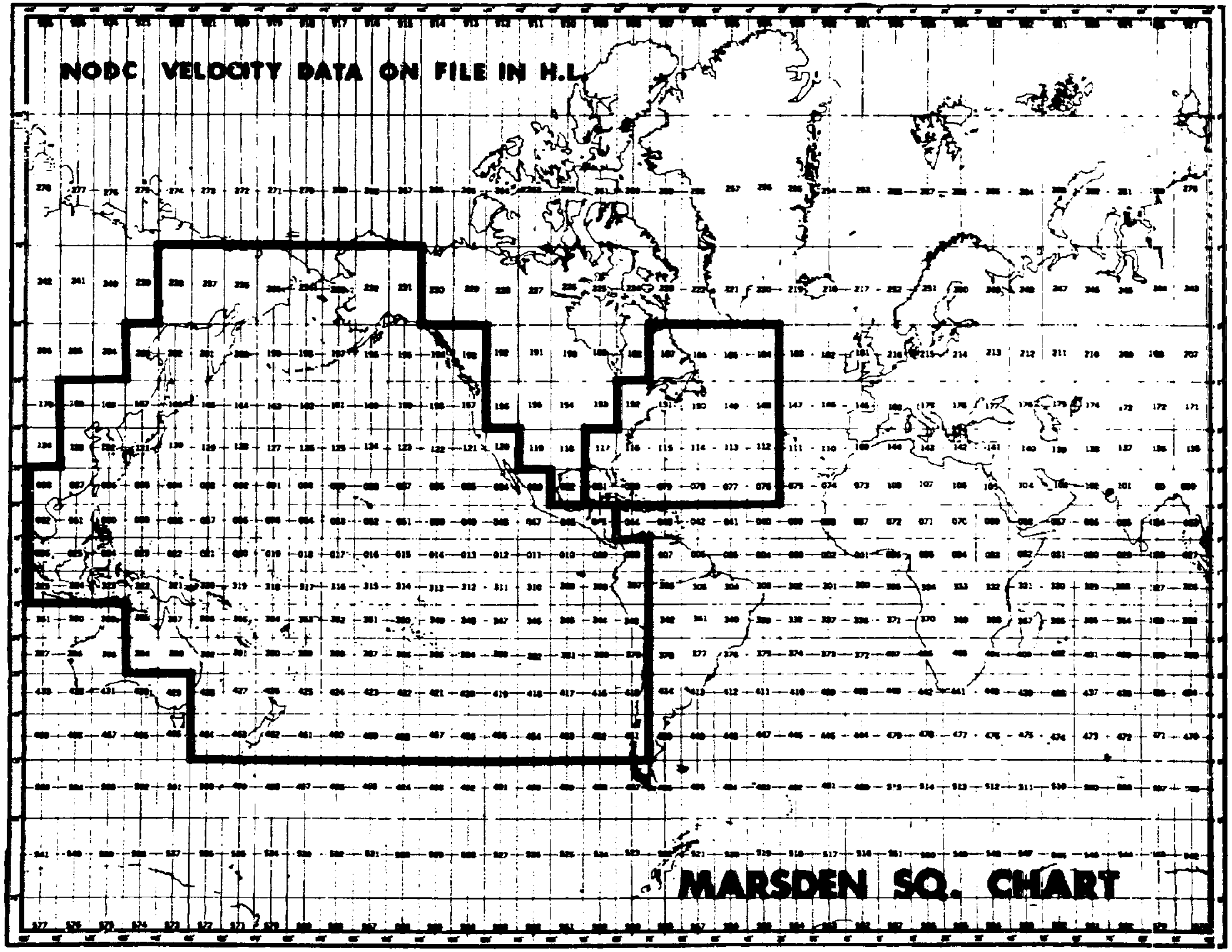

Fig. 19. NODC Velocity Data available at Hudson Laboratories shown on a Marsden Square chart.

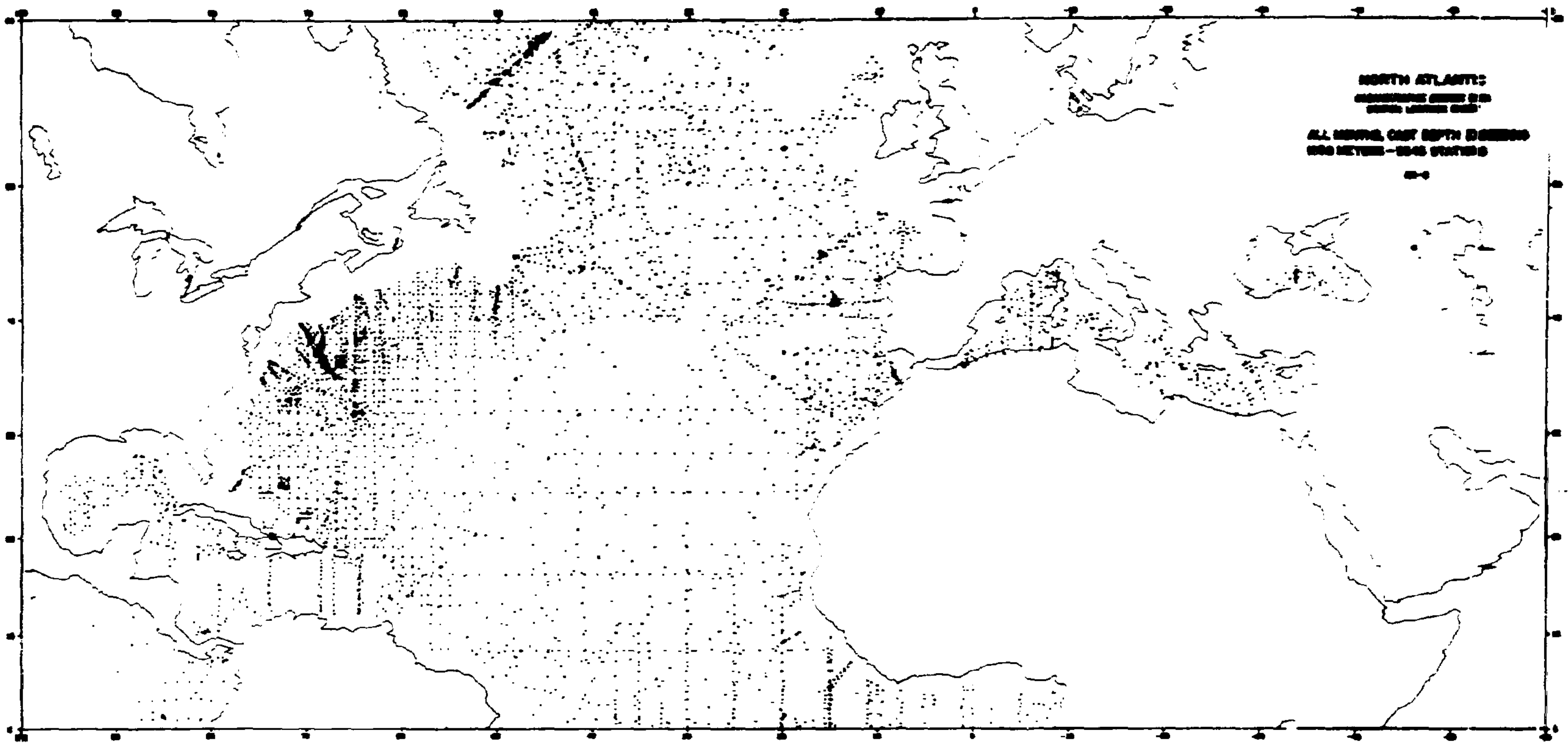

Fig. 20. Geographic distribution of velocity profiles in the North Atlantic exceeding 1900 meters.

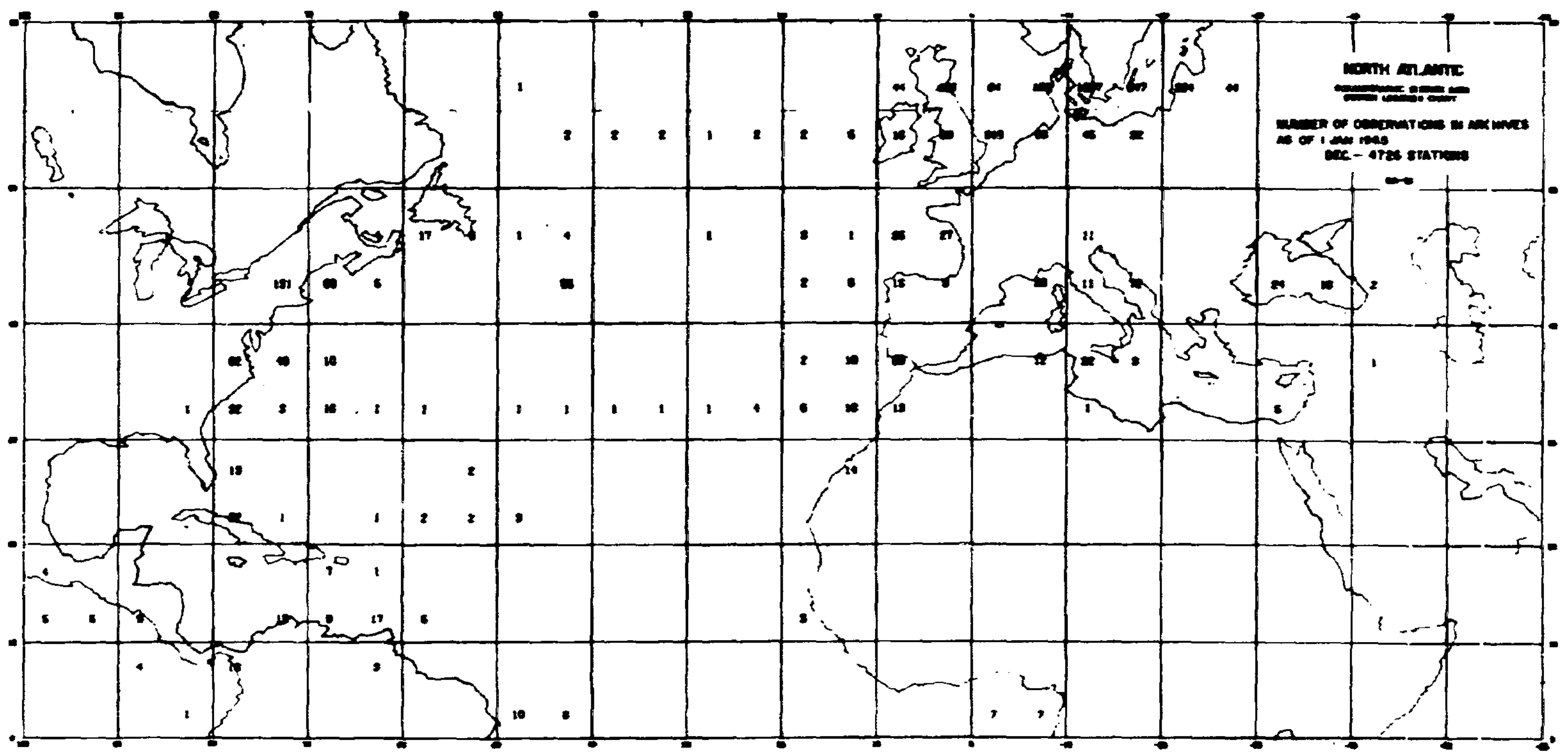

Fig. 21. Geographic distribution of velocity profiles available in the North Atlantic for the month of December.

HUDSON LABORATORIES OF COLUMBIA UNIVERSITY
ANALYSIS DEPARTMENT DATA FLOW SYSTEM
RAY TRACE VELOCITY DATA SEARCH PROCEDURE

Ray trace data search specifications:

1. Begining and ending position of ray path.
2. Ray path printout increment.
3. Maximum width of data zone.
4. Acceptable months for data.
5. Acceptable years for data.
6. Minimum acceptable sample depth for data.

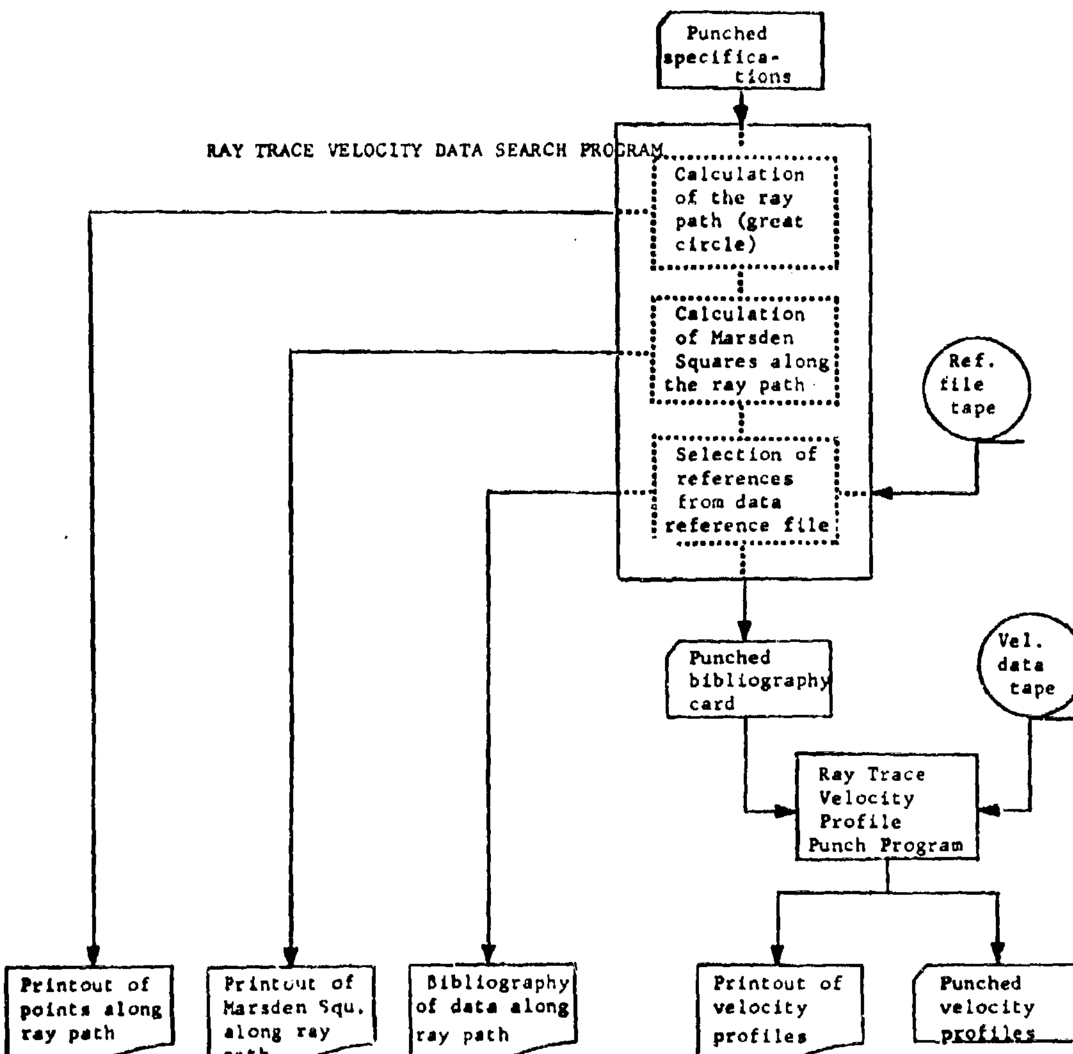

Fig. 22. Flow chart of the Ray Trace Velocity Data Search Procedure which extracts velocity profiles from NODC data tapes.

```
MARSDEN SQUARES     [illegible]ST RUN
 4395
 4396
 7904
 7905
 7906
 7914
 7915
 7916
 7917
 7924
 7925
 7926
 7927
 7935
 7936
 7937
 7938
 7945
 7946
 7947
 7948
 7956
 7957
 7958
 7959
 7966
 7967
 7968
 7969
 7977
 7978
 7979
 7987
 7988
 7989
 7998
 7999
 8070
 8080
 8090
 8091
11508
11509
11600
```

Fig. 23. List of Marsden Squares calculated along a ray path; sample output of Ray Trace Velocity Data Search Procedure.

```
VELOCITY DATA SEARCH PROGRAM - R.D. MININGHAM (A-173-F1)
  SPECIFICATIONS- MDO= 1500
                  MONTHS=   June
                  MAXIMUM RANGE FROM RAY PATH=  50,0

  TEST RUN
```

	MARSDEN SQ	IDENTIFICATION	DEPTH METERS	MONTH	YEAR	LATITUDE DEG	LATITUDE MIN	LONGITUDE DEG	LONGITUDE MIN	DISTANCE FROM ORIGIN (NM)	DISTANCE FROM RAY PATH
A	7905	6620027,	5300	6	60	20	0,	65	0,	0,21	-0,01
B	7916	6620026,	5100	6	60	21	0,	66	0,	82,13	-27,01
C	7937	5660020,	3300	6	54	23	40,0	67	38,0	263,92	-44,02
D	7947	5660021,	3300	6	54	24	36,0	67	22,0	304,90	-8,03
	7957	5660022,	3400	6	54	25	35,0	67	6,0	323,54	29,57
	8090	5660175,	5000	6	55	29	32,0	70	32,0	645,03	-35,06
E	11509	5660174,	5300	6	55	30	0,	69	30,0	646,25	24,09
F	11600	6460071,	4900	6	58	30	17,0	70	26,0	662,22	-11,01

Fig. 24. References to velocity profiles along a ray path for the month of June. Output of Ray Trace Velocity Data Search Procedure.

EXTRAPOLATION OF SHALLOW PROFILES BY INTERPOLATING BETWEEN TWO DEEP PROFILES

$v^S(z)$ = VELOCITY AT DEPTH z OF THE SHALLOW PROFILE.

$v^S(MDO)$ = VELOCITY AT DEPTH MDO OF THE SHALLOW PROFILE.

$v_i^D(Z)$ = VELOCITY AT DEPTH z OF A DEEP PROFILE AT RANGE i.

$v_{i+1}^D(z)$ = VELOCITY AT DEPTH z OF A DEEP PROFILE AT RANGE i+1.

R^S = RANGE OF THE SHALLOW PROFILE WITH $R_i^D \leq R^S < R_{R_{i+1}}^D$.

β = AN ARBITRARY DEPTH PARAMETER.

FOR MDO<z<β.

$$v^S(z) = v_i^D(z) + \frac{R^S - R_i^D}{R_{i+1}^D - R_i^D}\left[v_{i+1}^D(z) - v_i^D(z) \right] +$$

$$\frac{\beta - z}{\beta - MDO}\left[v^S(MDO) - v_i^D(MDO) \right] -$$

$$\left(\frac{\beta - z}{\beta - MDO} \right)\left(\frac{R^S - R_i^D}{R_{i+1}^D - R_i^D} \right)\left[v_{i+1}^D(MDO) - v_i^D(MDO) \right] .$$

FOR $\beta \leq z$.

$$v^S(z) = v_i^D(z) + \frac{R^S - R_i^D}{R_{i+1}^D - R_i^D}\left[v_{i+1}^D(z) - v_i^D(z) \right] .$$

Fig. 25. Formulas for the interpolation and extrapolation of shallow profiles by interpolating between two deep profiles.

VELOCITY CALCULATIONS GIVEN TEMPERATURE - WILSONS EQUATIONS

GIVEN DEPTH (z) IN METERS CALCULATE PRESSURE (P) IN KG/CM^2

FOR $z \leq 200$ METERS

$\alpha = -3.54428T-12$, $\beta = 9.961477T-4$, $z = -z$

$P_{PSI} = ((-\beta + (\beta^2 - 4\alpha z)^{1/2})/(2\alpha))/689.47$

FOR $z > 200$ METERS

$\alpha = -2.62085T-12$, $\beta = 9.94765T-4$, $\eta = 2.40443T-1$, $z = -z$

$P_{PSI} = ((-\beta + (\beta^2 - 4\alpha(\eta + z))^{1/2})/(2\alpha))/689.47$

FOR ALL DEPTHS

$P_{KG/CM(2)} = P_{PSI}(0.0703) + 1.0332$

WILSONS EQUATIONS P=PRESURE KG/CM^2 S=SALINITY 0-00 T=TEMPERATURE DEG. C.

$\Delta VT = 4.6233T - 5.4585(10^{-2})T^2 + 2.822(10^{-4})T^3 - 5.07(10^{-7})T^4.$

$\Delta VP = 1.60518(10^{-1})P + 1.0279(10^{-5})P^2 + 3.451(10^{-9})P^3 - 3.503(10^{-12})P^4.$

$\Delta VS = \underline{1.391(S-35) - 7.8(10^{-2})(S-35)^2}.$

$\Delta VSTP = \underline{(S-35)(-1.197(10^{-2})T + 2.61(10^{-4})P - 1.96(10^{-7})P^2 - 2.09(10^{-6})PT)} +$
$P(-2.796(10^{-4})T + 1.3302(10^{-5})T^2 - 6.644(10^{-8})T^3) + P^2(-2.391(10^{-7})T +$
$9.286(10^{-10})T^2) - 1.745(10^{-10})P^3T.$

$v = 1449.22 + \Delta VT + \Delta VP + \Delta VS + \Delta VSTP.$

TEMPERATURE CALCULATIONS GIVEN VELOCITY (ITERATIVE METHOD)

GIVEN v_{MDO} , P_{MDO} CALCULATE T_{MDO}

(1) ASSUME T=10

(2) CALCULATE WITH WILSONS EQUATIONS v_{T} (USING T AND S=35

NOTE THE UNDERLINED PORTIONS OF WILSONS EQUATIONS ARE EQUAL TO ZERO WHEN THE SALINITY IS 35.

(3) IF $v_T = v_{MDO}$ THEN $T_{MDO} = T$ OTHERWISE CONTINUE.

(4) $\Delta v = v_{MDO} - v_T$

(5) $\Delta T = \Delta v/4$

(6) $T = T + \Delta T$ AND GO TO STATEMENT 2.

TEST ACCURACY TO 2 DECIMAL PLACES.

Fig. 26. Wilson's Equation for calculating velocities.

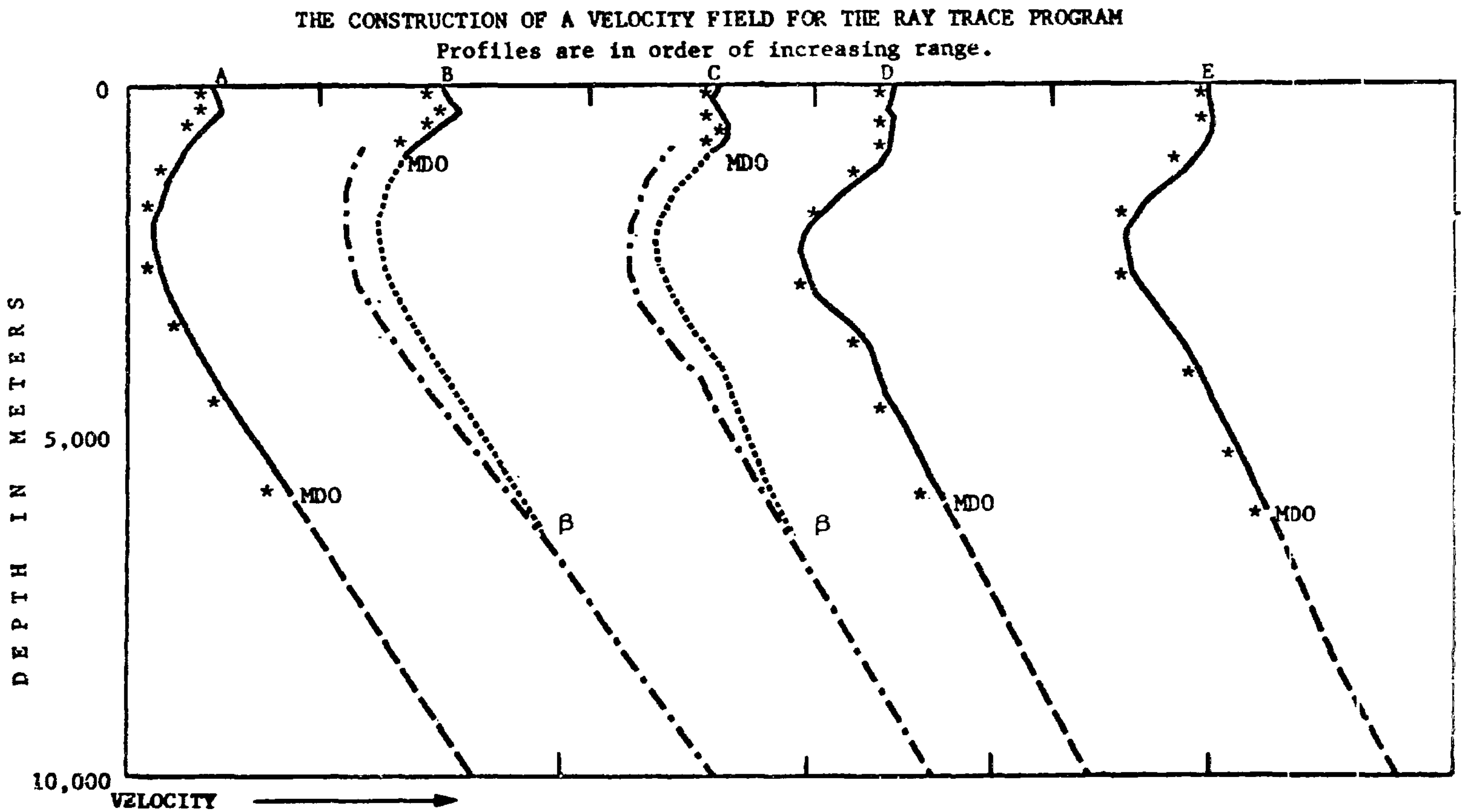

* Input data value (depths at which the velocity was observed).
——— Input data interpolated with a four point fit.
— — — Deep profile extrapolated by using Wilson's equations with a constant temperature.
—·—·— Shallow profile extrapolated with linearly interpolated values between two deep profiles.
······· Shallow profile adjusted for profile continuity between depths MDO and β .
β Depth parameter for shallow profiles
MDO Maximum Depth of Observation. NOTE: Earth's curvature correction is added to velocity.

Fig. 27. Schematic representation of the extrapolation procedures for deep and shallow profiles.

SPECIAL FOUR POINT FIT

CALCULATION OF CURVATURE (Z_i) AND GRADIENT (D_i) AT z_i.

$$Z_i = \frac{(v_{i+1}-v_i)(z_{i-1}-z_i)^2-(v_{i-1}-v_i)(z_{i+1}-z_i)^2}{(z_{i+1}-z_i)(z_{i-1}-z_i)(z_{i+1}-z_{i-1})}$$

$$D_i = 2\,\frac{(v_{i+1}-v_i)(z_{i-1}-z_i)-(v_{i-1}-v_i)(z_{i+1}-z_i)}{(z_{i+1}-z_i)(z_{i-1}-z_i)(z_{i+1}-z_{i-1})}$$

FOR $z_i \le z \le z_{i+1}$

$$v_i^{\alpha} = v_i+Z_i(z-z_i)+D_i\frac{(z-z_i)^2}{2}$$

$$v_{i+1}^{\alpha} = v_{i+1}+Z_{i+1}(z-z_{i+1})+D_{i+1}\frac{(z-z_{i+1})^2}{2}$$

$$v(z) = \frac{z-z_i}{z_{i+1}-z_i}\,v_{i+1}^{\alpha}+\frac{z_{i+1}-z}{z_{i+1}-z_i}\,v_i^{\alpha}$$

$$Z = \frac{v_{i+1}^{\alpha}-v_i^{\alpha}}{z_{i+1}-z_i} + \frac{z-z_i}{z_{i+1}-z_i}\left[Z_{i+1}+D_{i+1}(z-z_{i+1})\right] + \frac{z_{i+1}-z}{z_{i+1}-z_i}\left[Z_i+D_i(z-z_i)\right].$$

$$D = \frac{2(Z_{i+1}-Z_i+D_{i+1}(z-z_{i+1})-D_i(z-z_i))+(D_{i+1}(z-z_i)+D_i(z_{i+1}-z))}{(z_{i+1}-z_i)}.$$

EARTH'S CURVATURE CORRECTION (BREKHOVSKIKH, L.M. - WAVES IN LAYERED MEDIA)

$v_i = v_i\left(1+\frac{z_i}{\alpha}\right)$. $\alpha = 6.37\times 10^6$ METERS.

Fig. 28. Formulas for calculating curvature and gradient.

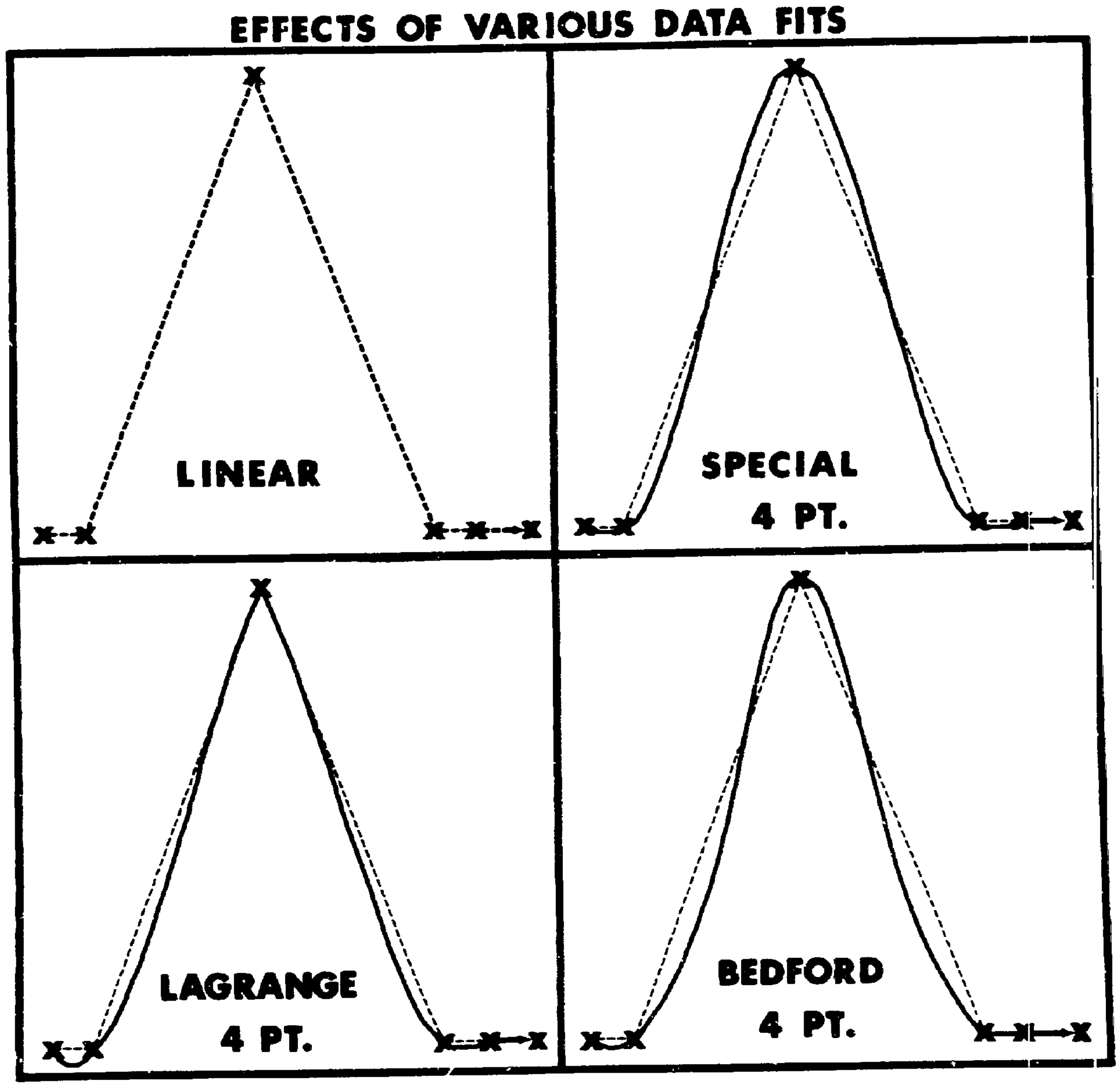

Fig. 29. Plot of the effects of various data fits.

LAGRANGE FIT

N= NUMBER OF POINTS FITTED

$$v(z) = \sum_{i=1}^{N} (v(z)_i \left(\prod_{j=1}^{i-1} \frac{(z-z_j)}{(z_i-z_j)} \prod_{j=i+1}^{N} \frac{(z-z_j)}{(z_i-z_j)} \right)).$$

BEDFORD INSTITUTE FOUR POINT FIT (REPORT NO. BIO 66-3)

v_{P1}= PARABOLA FITTED TO (1),(2), AND (3).

v_{P2}= PARABOLA FITTED TO (2),(3), AND (4).

$$v_A = \frac{(v_2-v_3)(z-z_2)}{(z_2-z_3)} + v_2$$ LINEAR INTERPOLATED VALUE BETWEEN (2) AND (3).

$$v_B = \frac{(v_2-v_1)(z-z_2)}{(z_2-z_1)} + v_2$$ LINEAR EXTRAPOLATED VALUE USING (1) AND (2).

$$v_C = \frac{(v_4-v_3)(z-z_3)}{(z_4-z_3)} + v_3$$ LINEAR EXTRAPOLATED VALUE USING (3) AND (4).

$$v_R = \frac{1}{2} \left(v_A + \frac{(v_A-v_B)^2 v_C + (v_A-v_C)^2 v_B}{(v_A-v_B)^2 + (v_A-v_C)^2} \right)$$ REFERENCE CURVE

$$v(z) = \frac{|v_R-v_{P1}| + |v_R-v_{P2}| \, v_{P1}}{|v_R-v_{P1}| + |v_R-v_{P2}|}$$

Fig. 30. Formulas for Lagrange and Bedford Institute method of fits.

CHAPTER III

RAY TRACING

3.1. Introduction

A number of references discuss the ray approximation to a spreading wavefront and the conditions under which it will be valid.[1, 2]

The two primary limitations are:

i) there shall be no abrupt changes in the spatial derivatives of the velocity field over a distance that is comparable to a wavelength, and

ii) the space rate of change of the amplitudes of the waves must be small enough so that the waves can be described by "local plane waves."

In practical terms condition i), above, will be satisfied in the ocean except for very low frequencies and at the boundaries of the medium, and condition ii) will be satisfied except at source points and at ray crossing points where the rays focus or form caustics. In the latter regions the field amplitudes must be determined by wave solutions but, provided that condition i) remains valid, the ray solutions can be continued through the crossing regions and into the far field without ambiguity. (This is further discussed in the Appendix.)

3.2. Development of Solution

3.2.1. Ray Equation

In ray tracing the propagation is represented by the geometrical spreading of the wavefronts from the source, and the latter are described by their orthogonal trajectories or ray paths. It is assumed that everywhere in the ocean the velocity field is known and given by $v(\vec{r})$, i.e., as a scalar function of the position vector $\vec{r}$ in the medium. If the vector $\vec{A}$ specifies the ray path and ds is a differential increment along the path the ray equation is[3]

$$\frac{d}{ds}\left[\frac{1}{v(\vec{r})}\ \frac{d\vec{A}}{ds}\right] = \text{grad}\left[\frac{1}{v(\vec{r})}\right] \qquad \text{(III. 1)}$$

The ray tracing solution to (III. 1) is determined by an initial position $\vec{r}_o$ and an initial direction $\hat{r}_s$ from this origin which is considered a source point. The geometrical acoustical field due to the source is given by the mapping into the far field of all the rays considered as functions of $\hat{r}_s$. Thus, the ray solution is given by a continuous function of position

$$\vec{A} = \vec{A}\left(\vec{r}_0 , \hat{r}_s\right) \tag{III. 2}$$

3. 2. 2. Expansion of Velocity Field

In applying (III. 1) to the practical case of cylindrical spreading, it is convenient to use the coordinates of range R and depth z measuring these from the origin and the sea surface, respectively, and to measure the ray angle from the horizontal, θ , with a positive angle pointing to deeper depths. At any point $\left(R_i , z_i\right)$ in the medium the velocity field program of Chapter II gives not only the value of the velocity at that point, $v_i = v\left(\vec{r}_i\right)$, but also the vertical and horizontal gradients as well as the vertical curvature of the velocity field. Thus, if a ray has been followed to $\left(R_i , z_i\right)$ the velocity at a neighboring point $\left(R_{i+1} , z_{i+1}\right)$ can be approximated by

$$v_{i+1}\left(R_{i+1} , z_{i+1}\right) = v_i\left(R_i , z_i\right) + Z_i\left(z_{i+1} - z_i\right) + G_i\left(R_{i+1} - R_i\right) + D_i\frac{\left(z_{i+1} - z_i\right)^2}{2} \tag{III. 3}$$

In (III. 3) Z_i is the vertical gradient, G_i is the horizontal gradient, and D_i is the vertical curvature of the velocity field, all evaluated at position $\left(R_i , z_i\right)$. A ray at this point and with a ray direction θ_i can be iterated to a further position by use of the velocity field expansion parameters of (III. 3) and in terms of an iteration parameter. In the present work the arc length of the ray has been used for the iteration parameter in preference to other parameters such as an increment in range or in depth. However, two comments must be made before Eq. (III. 1) is expressed in a form suitable for solution by computer iteration.

3. 2. 3. A Semi-Invariant for the Iteration

It is well known that if the medium is purely horizontally stratified, i. e., with no horizontal gradients G_i , a simple invariant exists for each ray path. This is

$$c = \frac{\cos\theta}{v} = \text{constant for } G = 0 \quad . \qquad \text{(III. 4)}$$

Equation (III. 4) has greatest application to predicting the depth of turning points of the ray and thus the amplitude of the vertical oscillation of the ray about a sound channel as a function of an initial ray angle and the sound velocity at the origin of the ray, i. e., the depths z_t at which $\cos\theta = 1 = \cos\theta_o\, v\left(z_t\right)/v\left(z_o\right)$. In the ocean the average horizontal gradients of the sound velocity field are weaker than the vertical gradients - this does not mean that they can be completely ignored - and it is permissible to regard c of (III. 4) as a semi-invariant, i. e., changing only slightly during an interation from c_i to c_{i+1} . A detailed expansion of c_i in terms of an arc length increment Δ from $\left(R_i\, ,\, z_i\right)$ gives

$$c_{i+1} = c_i - c_i^2\, G_i\left(1 + \tan^2\theta_i\right)\Delta + c_i^3\, G_i\, Z_i \tan\theta_i\left(1 + \tan^2\theta_i\right)\Delta^2 + \ldots \quad . \qquad \text{(III. 5)}$$

In the program (III. 5) is carried as a parallel iteration with those giving the spatial coordinates (R, z) and is also used to define the cosine of the ray angle at each iteration in the form

$$\cos\theta_{i+1} = v_{i+1}\, c_{i+1} \quad . \qquad \text{(III. 6)}$$

Besides the use of the cosine of the ray angle, the iteration expansion also requires the sine and tangent functions of the angle. If these are obtained in every iteration by inverse trigonometric solutions or, for example, by $\sin\theta = \pm\sqrt{1 - \cos^2\theta}$, the high order expansions used in the machine programs by such functions represent a penalty in terms of machine accuracy and, especially, in terms of machine computation time. To avoid these limitations the trial $\sin\theta$ is calculated by a separate iteration expansion that involves only machine multiplications and additions.

$$\begin{aligned}\left(\sin\theta_{i+1}\right)_t = {} & \sin\theta_i - c_i^2\, v_i\left(Z_i - G_i \tan\theta_i\right)\Delta \\ & - c_i^2\left(Z_i^2 \sin\theta_i + Z_i\, G_i \cos\theta_i + v_i\, D_i \sin\theta_i\right)\frac{\Delta^2}{2} \qquad \text{(III. 7)} \\ & - c_i^2\left[3\, Z_i\, D_i \sin^2\theta_i - c_i\, Z_i \cos\theta_i\left(Z_i^2 + v_i\, D_i\right)\right]\frac{\Delta^3}{6}\end{aligned}$$

and the trial sine of (III. 7) is further corrected to agree with (III. 6) by*

$$\sin\theta_{i+1} = \left(\sin\theta_{i+1}\right)_t \qquad \text{for } \left(\sin\theta_{i+1}\right)_t \leq .01$$

$$= \frac{1}{2}\left[\frac{1-\cos^2\theta_{i+1}}{\left(\sin\theta_{i+1}\right)_t} + \left(\sin\theta_{i+1}\right)_t\right] \qquad \text{for } \left(\sin\theta_{i+1}\right)_t > .01 \quad . \tag{III. 8}$$

The tangent of the angle is given by

$$\tan\theta_{i+1} = \frac{\sin\theta_{i+1}}{\cos\theta_{i+1}} \quad . \tag{III. 9}$$

The development of the trigonometric functions of the ray angle via Eqs. (III. 5) through (III. 9) possesses the following advantages:

i) accuracy throughout the entire iteration to an extent determined by the accuracy of the corrections of (III. 5) to the semi-invariant of (III. 4),

ii) adjustment of the ray angle at any position to a value determined by the velocity field program at that point,

iii) speed of computation. (The coefficients of the arc length and its powers in (III. 7) are also required in (III. 11) so that this computation is not wasted.)

3.2.4. Range, Depth, and Time Iterations

From the above (III. 1) can be developed to give the increment in range and depth for travel over an arc length Δ .

$$\begin{aligned} R_{i+1} = {} & R_i + \cos\theta_i\,\Delta + c_i\left(Z_i \sin\theta_i - G_i \sin\theta_i \tan\theta_i\right)\frac{\Delta^2}{2} \\ & + c_i\left[D_i \sin^2\theta_i - c_i^2\, v_i\, Z_i\left(Z_i - G_i \tan\theta_i\right)\right]\frac{\Delta^3}{6} \\ & - c_i^3\, Z_i\left(4\, v_i\, D_i \sin\theta_i + Z_i\, G_i \cos\theta_i + Z_i^2 \sin\theta_i\right)\frac{\Delta^4}{24} \end{aligned} \tag{III. 10}$$

* (III. 8) comes from the condition that $\cos^2\theta + \sin^2\theta = 1$ and, if $\sin\theta = (\sin\theta)_t + \sigma$, by assuming that $1 \gg \sigma \gg \sigma^2$.

$$z_{i+1} = z_i + \sin\theta_i\,\Delta - c_i^2 v_i\left(Z_i - G_i \tan\theta_i\right)\frac{\Delta^2}{2}$$

$$- c_i^2\left(Z_i^2 \sin\theta_i + Z_i G_i \cos\theta_i + v_i D_i \sin\theta_i\right)\frac{\Delta^3}{6} \qquad \text{(III. 11)}$$

$$- c_i^2\left[3 Z_i D_i \sin^2\theta_i - c_i Z_i \cos\theta_i\left(Z_i^2 + v_i D_i\right)\right]\frac{\Delta^4}{24} \quad .$$

A similar derivation can be used for the travel time of the ray

$$T = \int_0^{\overline{A}} \frac{ds}{v(\vec{r})} \qquad \text{(III. 12)}$$

or, as an iteration,

$$T_{i+1} = T_i + \frac{\Delta}{v_i}\left[1 - c_i\left(Z_i \tan\theta_i + G_i\right)\frac{\Delta}{2} + c_i^2\left(Z_i^2 - v_i D_i \tan\theta_i^2 + \right.\right.$$

$$\left.\left. 2 Z_i^2 \tan\theta_i^2 + 2 Z_i G_i \tan\theta_i + 2 G_i^2\right)\frac{\Delta^2}{6}\right] \quad . \qquad \text{(III. 13)}$$

The accuracy of the above iterations is discussed in Chapter V, with respect to smooth velocity profiles that are characteristic of theoretical models with known ray solutions. Over all, the results indicate that these expressions permit the use of very large Δ increments that approach 1000 meters per iteration. Associated with large Δ values, of course, is a reduction in the computation time that is required per increment. In ray tracing in the ocean the rays spend most time in the deeper regions where the vertical gradients are small and are nearly constant and this encourages the use of large Δ values for efficient utilization of the computer.

3. 3. Adaptive Controls of Iteration Interval

In surface waters generally and wherever velocimetry casts have been taken with small depth intervals to show detailed structure in a velocity profile, the approximation (III. 3) breaks down and may become unreliable over vertical distances of the order of tens of meters, or less. Such data, for example, can show vertical gradients that approach unity (meters/sec/meter), or 0. 1 (meters/sec/meters^2) vertical curvature, and with these coefficients both (III. 3) and all the iteration expansions become invalid unless Δ is kept small. It is to be noted, on the other hand, that if data have been taken at widely spaced depths, as may be typical of older data taken by Nansen casts, the 4-point fit used to obtain a continuous representation of the velocity profile (Chapter II) will effect an automatic smoothing of the data to yield gradients and curvatures that can be several orders of magnitud smaller than the values indicated above.

Under these circumstances the selection of Δ as an input parameter is conditioned by the nature of the input data and Δ becomes limited by the largest gradient and curvature values that can be expected as these are determined by the tabulations of the input data listings. As an alternative to the use of a small fixed Δ for the entire ray path, the present program establishes a series of control tests for the purposes of adapting Δ to control the accuracy of the calculation with respect to specific structure of the velocity field at any one point and to determine the interval over which the expansion (III. 3) will predict the field in the neighborhood of a given point.

3.3.1 Sine Increment Test

After any iteration to a given point, the velocity field program is entered to determine the velocity v_i and the parameters c_i, Z_i, D_i, and G_i at that point. From these, and from (III. 6) and (III. 9), a tentative calculation is made with (III. 7) to obtain the sine of the ray angle that would result from an iteration over the maximum Δ that is set into the program. A new iteration interval Δ'_1 is then selected that is the least of

i) Δ , or

$$\text{ii)} \quad \sqrt{\frac{S}{\left|\left(\sin \theta_{i+1}\right)_t - \sin \theta_i\right|}}\ \Delta \qquad \text{(III. 14a)}$$

where S is an input parameter, typically 0.01 to 0.1. Equation (III. 14a) cuts back Δ to a value such that the change of the sine of the ray angle in the next iteration is of order S .

The use of the square root in (III. 14a) assumes that the change in the sine of the ray angle for the iteration Δ exceeds S primarily because of the magnitude of the coefficients of the terms Δ^2 and Δ^3 in (III. 7). The assumption is based on the maximum magnitude of the vertical curvature that is typical of many velocity profiles, approaching 0.1 meter/sec/meter^2, and because the curvature exceeds the gradient term in the iteration expansions by the ratio $v_i D_i / Z_i^2$. Thus, the overwhelming necessity for the cutback in Δ is due to profiles with high curvature.

The test of (III. 14a) is by itself not a sufficient test for the accuracy of the sine iteration of (III. 7), for it may happen that the higher order terms of the expansion are large but accidentally cancel each other. In order to catch such accidents (III. 14a), resulting in Δ'_1, is followed by a further test that cuts back Δ'_1 to a value Δ_1 such that Δ_1 is <u>the least of</u>

i) Δ'_1, or

ii) $$\sqrt{\frac{S}{\left| c^2 Z_i D_i \left(\Delta'_1\right)^3 \right|}} \qquad \text{(III. 14b)}$$

The criterion for (III. 14b) is effectively six times the Δ term of highest power in the expansion (III. 7); the accuracy of the sine increment is controlled such that the contribution of this term is less than $S/6$.

Equations (III. 14), admittedly, will not limit the change in the sine of the ray angle to a value that is less than S in the circumstance that the curvature is small and the vertical gradient is (uniformly) large. In this event it would be preferable to truncate Δ by a linear difference ratio rather than the square root ratio in (III. 14) and to accept the increase in computer running time that the stronger cutback would represent. This has not been considered necessary for the following reasons:

i) (III. 14) will effect a partial reduction in Δ so that the accuracy of the sine iteration is at least improved by the test.

ii) The testing of the program discussed in Chapter V shows that the iteration expansions are highly accurate for profiles with large gradients but small curvatures.

iii) Partial compensation for errors that may originate through the use of large Δ increments in high-gradient regions and which are not bounded by (III. 14) will be made by the semi-invariant corrections expressed by (III. 5) through (III. 8).

iv) High-gradient regions in the velocity profile structure are usually associated with high-curvature regions that fluctuate in sign. Thus, the particular problem considered here tends to arise accidentally at depths for which the small curvature is due to a transition of the curvature from one algebraic sign to another. In this event Δ_1 will be still further truncated by the velocity field accuracy test discussed below.

3.3.2. Velocity Field Accuracy Test

A further cutback will be required in Δ_1 in high gradient-curvature layers if the velocity field expansion of (III. 3) fails to predict the velocity established by the field construction program at distances Δ_1 from a given point. This problem is sensed in the present program by testing for the accuracy of (III. 3) and by adapting the increment Δ_1 to a value such that (III. 3) is satisfied with an accuracy parameter ε. The steps for this test are:

i) At a point $\left(R_i, z_i\right)$ and for a ray angle θ_i (III. 10) and (III. 11) are calculated for Δ_1 to obtain the range and depth increments projected for the next iteration.

ii) The increments of i), above, are used in (III. 3) to determine a trial velocity $\left(v_{i+1}\right)_t$ at the point $\left(R_{i+1}, z_{i+1}\right)_t$.

iii) The velocity field program is entered to determine the value of the velocity given by the input data to the program at the new point calculated in ii), above, giving $\left(v_{i+1}\right)_f$.

iv) A new iteration interval Δ_2 is chosen for the iteration from $\left(R_i, z_i\right)$ such that it is <u>the least of</u>

a) Δ_1 ; or

b) $$\varepsilon \frac{\Delta_1}{\left|\left(v_{i+1}\right)_f - \left(v_{i+1}\right)_t\right|} \quad . \qquad \text{(III. 15)}$$

Of course, if iv-a), above, is satisfied, the point $\left(R_{i+1}, z_{i+1}\right)$ calculated in ii), above, can be used directly for advancing the ray without the re-iteration over Δ_2 demanded by iv).

3. 3. 3. Minimum Increment Size

Each velocity profile in the program can be entered without restriction on the depth interval between successive entries (a maximum limit of 375 entries is set by memory capacity, however) to allow flexibility for expressing detailed profile structure. If the entries are dense in a given layer and a large Δ_1 is attempted, the velocity field accuracy test permits the extension of the iteration to a depth beyond the range of the field expansion contained in a given 4-point fit that is used to express profile continuity. To ensure that the iteration does not pass over the intervening profile structure too rapidly, the truncation of Δ_1 by (III. 15) has been made linear in this test in contrast to the square root contraction of the sine increment test of (III. 14). This has been done as a safeguard even though the dominant requirement for an ε -truncation of Δ_1 is due to the curvature terms.

The linear reduction, however, can greatly increase computer running time when the profiles include sharp breaks in the velocity gradients that must be defined by profile entries taken for small depth intervals. The bilinear profile used in the program testing gives a dramatic example of this, as shown in Chapter V. Such a "kink" in a profile is very unlikely in nature and in any event is smoothed by the 4-point fit used in the program over the interval of the depth entries by which such a feature is defined. Realistic profiles are well represented, within a measurement accuracy of 0. 4 meter/sec, by entries at intervals of 10 to 20 meters.

By construction, therefore, the expansion of the velocity field of (III. 3) will be accurate over an iteration interval that is of the order of the minimum depth interval of the data entries, and it becomes wasteful to permit the velocity field accuracy test to cut back Δ_1 to a value less than this minimum increment Δ_m . Δ_m is used in the program as an input parameter determined prior to ray tracing by inspection of the input velocity field data.

3. 3. 4. Turning Point Contraction

It has been straightforward to apply a further test that becomes effectiv^ near turning points of the ray, especially as these occur in high · lient-curvature layers of the sound velocity profiles. It consists of a reduction of Δ_2 to Δ_m when $c_i\left(v_{i+1}\right)_f \geq 1$ and this restriction acts as a safeguard to prevent the cosine of the ray angle from exceeding unity.

3. 4. Error Estimates

The use of the adaptive iteration intervals together with the choice of the maximum iteration interval Δ initially set into the program provides a close control of program accuracy that can be balanced against computer running time. Specific examples are discussed in Chapter V, "Program Accuracy." Because the depth amplitudes of the rays are controlled by the semi-invariant of Eqs. (III. 5) and (III. 6), the primary effect of adjustments of Δ , S , Δ_m , and ϵ is on the range accuracy, i. e., on the range at which a given ray crosses a specific depth or has a turning point with ray angle zero.

This behavior is entirely analogous with the range uncertainty that can be estimated for theoretical models of the velocity field with respect to small perturbations of the field that correspond to a velocity uncertainty.[4] There will also be a "phase uncertainty" of the rays due to the variation of the travel time that will correspond to the range uncertainty. With respect to physical applications, the variation of a calculated range with different choices of ϵ in (III. 15) can be considered a measure of the sensitivity of the ray calculation to the accuracy of the input data of the velocity field. For example, if the input velocity profiles have an accuracy of 0. 5 meter/sec the use of an ε of 0.1 meter/sec may give a more precise formal result for the given input data than a calculation using an ε of 0.5 meter/sec, but it is questionable whether the difference is physically meaningful. Also, the increased accuracy that will be obtained with the smaller ε will require a longer computer running time.

A precise error analysis of the effect of the adaptive iteration interval will depend critically on the details of the given velocity field. For the sound structure of the ocean the error will arise chiefly in the failure of the Taylor expansion of (III. 3) to account for detail in the vertical sound velocity profiles.* As a rough estimate, assume that the error in (III. 3) arises from neglect of an nth order term in the expansion, i. e., the error δv_i can be represented by

$$\delta v_i \approx E_i \frac{(z_{i+1} - z_i)^n}{n!} \tag{III. 16}$$

where E is the nth derivative of the profile with respect to z . (n must be ≥ 3 .) The error in a range iteration, δR_i , will be of the form

$$\delta R_i \approx c_i E_i \sin^n \theta_i \frac{\Delta^{n+1}}{(n+1)!} \quad . \tag{III. 17}$$

Note that the linear form of the adaptive iteration interval correction given by (III. 15) will over-compensate the (n + 1)th order correction of (III. 17) if δv_i is greater than ε , so that the maximum error will occur if the difference between the velocity predicted by (III. 3) and the value entered into the velocity field is ε itself. The error due to (III. 16) will thus have the maximum value in any iteration of

$$\delta R_i \approx \frac{c_i \Delta}{n} \varepsilon \tag{III. 18}$$

---

* It is certainly true that the average horizontal gradient of the ocean is much smaller than the average vertical gradient. If, however, the model velocity field is constructed with distinct thermal "patches," local horizontal gradients could become important. In practice, however, the velocity field is nearly always measured by velocity depth profiles taken many miles apart so that horizontal gradients are small just because of the scale of the measurement process.

and the average error per iteration will be less than this. Further, the errors in (III. 17) due to (III. 15) will tend to occur with different algebraic signs as the ray is traced over its full range - if the errors tend to cancel, and cancel randomly, the net fractional error in range δR will be, under these assumptions,

$$\frac{\delta R}{R} \approx \frac{c_i \epsilon}{n} \sqrt{\frac{\Delta}{R}} \approx \frac{1}{n}\left(\frac{\epsilon}{v}\right)\sqrt{\frac{\Delta}{R}} \quad . \tag{III. 19}$$

It is to be emphasized that estimates such as those of (III. 18) and (III. 19) are themselves first-order approximations, and cannot be applied for large Δ or ϵ, i.e., for iteration intervals such that the error δv_i of (III. 16) becomes comparable to the velocity change predicted by (III. 3). However, and apart from exceptional and special velocity fields, it is reasonable to conclude from (III. 18) that for nominal values of the expansion parameters the maximum fractional error in range will be the fraction $\epsilon / n v$ and may be much less than this when (III. 19) applies.

3.5. Printouts

The use of the flexible iteration interval measured along the ray paths is disadvantageous with respect to two other requirements of the ray tracing program. These are: i) the need for printouts of the ray path at specified range intervals, and ii) the determination of the range and depth at which surface or bottom hits may occur. To accommodate these requirements a set of controlling tests is carried during the ray tracing so that the iteration interval Δ can be further adapted to predict just the value that will advance the ray to a specific point.

The procedure is simplest for the printout points. For these a ray is continued until the range accumulated in iteration would exceed an incremented printout interval such as every mile. At this stage of the program the last iteration has satisfied all other tests such as those of the adaptive iteration intervals given by tests (III. 14) and (III. 15). If R^p is the printout range and the iteration changes in range by (III. 10) from R_i to R_{i+1}, a new iteration increment is defined by the approximate linearly projected value

$$\Delta^p = \frac{R^p - R_i}{\cos \theta_i} \quad \text{for} \quad R_{i+1} \geq R^p \geq R_i \tag{III. 20}$$

and equations (III. 7) through (III. 13) are used for the Δ^p iteration to printout

i) range,

ii) depth,

iii) sine of the ray angle,

iv) travel time, and

v) height of the ray from the bottom.

Because (III. 20) is only an approximation, the printouts are themselves approximations; the error involved is easily monitored for it leads to a range printout such as 156.00011 instead of the 156.00000 mile integer value at a specified printout range. The error of the example is typical only when Δ increments of 500 meters or more are used. If higher accuracy printout data are required, it is easily achieved by using appropriately smaller Δ values. In any event, the error is only in the printout data and is not accumulated over the history of the ray.

In addition to the printouts at specified range intervals, the ray position is printed at ray turning points at which the ray angle is zero. The procedure is similar to that just described for the range printouts except that the iteration interval is linearly interpolated over the sine of the ray angle when the sine changes sign.

Printouts are also provided when the ray strikes the sea surface or bottom. At the sea surface the ray is reflected specularly by changing the sign of the sine of the incident angle, but at the bottom the ray is reflected specularly with respect to the bottom slope and this also changes the semi-invariant c_i of (III. 5). These reflections interrupt the ray in its transit and their positions must be computed as accurately as possible. A quadratic solution is used to determine the iteration interval Δ such that the ray is advanced to the specific point of contact and further tests are used to insure that the proper quadratic solution is chosen.

·though the procedures are straightforward they are extensive and w.. ıot be described here in detail. Some of the tests guard against the possibility that for a large iteration interval and a nearly grazing ray near a surface, the projected ray position by itself might indicate an apparent miss of the surface due to a curvature of the ray which causes it to be re-entrant. Additional problems arise at the bottom because of the bottom slope. The tests for the reflections are graded in application so that they are not applied except as they are keyed into the program by the ray proximity to the reflecting surface. For example, a sufficient initial test is whether the initial ray position for an iteration is within an iteration interval Δ of the sea surface or the minimum entered bottom depth.

3.6. Ray Magnification Function

The ray tracing solution, Eq. (III. 2), for the propagation in the inhomogeneous medium is obtained by computer printout of the range and depth positions of the set of rays which are distinguished by the initial directions of the rays from the origin. For cylindrical spreading it is convenient to use a linear parameter τ to specify the initial angle through the relationship $\tau = r_s \theta$ where θ is the initial angle and r_s is a standard radius from the origin that is conventionally taken as one yard.

Formally, the solution (III. 2) will permit continuous derivatives among the variables, R, z, and τ. In particular, the derivative

$$M(R, z, \tau) = \left.\frac{dz}{d\tau}\right|_R \qquad \text{(III. 21)}$$

represents the magnification of the arc length $d\tau$ that is projected to form the depth interval dz at range R and is termed the magnification function of ray τ. It expresses the mapping characteristic of the ray tracing solution that is also represented by the concept of ray tubes (or ray shells for cylindrical spreading) with these determined as the volume between differentially spaced rays from the source. In a nonhomogeneous medium the different tubes will bend due to refraction and their cross sections will expand or contract as they propagate into the far field. The mapping of the rays is not unique, however, for entirely different elements $d\tau$ may be projected into a common depth interval dz at range R. In underwater acoustics the τ- values projected into a common depth interval are termed different "arrivals" because a receiver at that position will detect a single source impulse as a set of time-separated signals with delays representing the different travel times for the different paths that connect the source and receiver. It may also happen that there are some depth intervals which are not mapped by any $d\tau$ because no rays exist that connect such positions with the origin; such regions constitute "shadow zones."

3.7. Ray Depth Distribution Plots

Although the ray paths of individual τ rays can be obtained by computer printout (Fig. 9) a summary of the contribution of all the rays is contained in the ray depth distribution plots in which at a given range successive depths are plotted as functions of rays with incremented initial angles. Plots of this type, representing differing physical situations, are shown in Figs. 11, 31, and 32. The slopes of these plots, if the slopes can be identified, give the magnification function $M(R, z, \tau)$ of (III.21). Each intersection of the curve with a given depth identifies an arrival or possible ray path for acoustical transmission that can also be identified by the travel time plotted on the right-hand side of the figures. Finally, and as a guide for estimating the effectiveness of the rays, an attenuation value, determined by the sea surface and the bottom reflections undergone by the ray in its travel to the given range, is listed in the data printout of the plot. Rays which have been attenuated by these mechanisms to more than a preset level are excluded from the plots.

Each of the ray depth distribution plots of the figures shows a distinctive pattern that represents the action of the inhomogeneous velocity field and its boundaries on the initially spherical wave that starts from the origin and propagates to the given range. Also, the depth amplitude of the oscillation of the rays about the sound channel that is plotted shows the depth interval that would be illuminated by the individual arrivals. It is important to note that small changes of the velocity field usually produce only a minor effect on the depth amplitudes but shift or "snake" the curve to alter the identification of the initial angle of an arrival that reaches a given depth interval at the given range. A partial summary of the type of information available from these plots and comments on such data are:

i) Identification of the range of initial angles from the source that can couple to a given depth interval. For example, in Fig. 11, for angles less than about -12°, there is no effective coupling to a region at or near the sea surface.

ii) Well-defined, differentiable arrivals, i.e., those for which the magnification function (III.21) can be calculated, can occur at near to intermediate ranges, e.g., Figs. 11 and 32, but these are observed only for rays which have undergone bottom interactions when the bottom is especially smooth (as it was for the bottom of the Hatteras Plain used for the data of Fig. 14).

iii) Even if a group of rays has undergone no surface or bottom reflections, it is often found that there may be abrupt jumps in the depths of successive rays so that differentiation in the sense of (III.21) is impossible, at least on the scale of the initial angle increments used to obtain the plot. Such behavior originates in special details of the velocity profiles used to construct the velocity field, e.g., in regions with different slopes particularly in or near the surface thermocline.

iv) The effects of ii) and iii), above, can be traced to their origins by consulting the individual ray printouts to identify the special features of the velocity profiles or bottom structure that are responsible. One of the principal effects of the horizontal gradients or, more specifically, the effect of mixing velocity profiles with differing structures, is to increase the breakup of the arrival structure with increasing range. A dramatic example of this occurs when rays become trapped in or are ejected from a surface sound channel, an effect that would not be possible if an average profile, i.e., a stratified medium, were used for the total velocity field.

When a ray depth distribution plot shows smooth behavior, indicating a well-defined arrival structure, the ray tracing calculations will provide a clear and direct representation of the acoustic field; indeed, if this occurs it is also an indication that the data inputs for the physical parameters that control the propagation are favorable in the sense that the velocity field is simple in structure and an ocean bottom, if it is important, is also well defined and smooth. On the other hand, if the plots show breakup of the arrival structure when the incremented initial angles differ by fractions of a degree, it must be concluded that the computation is expressing the fact that the data inputs themselves represent a complex physical environment.

Much of the experience of Hudson Laboratories in long-range, low-frequency underwater sound propagation indicates that the data demand the inclusion of the effects of the "irregular" arrivals, for frequently they will carry a major fraction of the acoustic energy. They are especially important when there are shadow zones that cannot be illuminated except by bottom reflections, or for the study of the effects of bottom terrain on the modulation of the acoustic field that passes over it, or for the changes in the vertical intensity distribution of the field in propagation across water masses with distinct structural differences in their velocity profiles. Acoustical data of this type can be related to specific environmental features and the latter cannot be approximated by representative or smoothed data inputs.

In the next chapter, on intensity calculations, a method will be presented for using all of the ray arrivals by interpreting their mapping property as a probability distribution in the far acoustical field. The probability interpretation is especially useful because it can combine the uncertainties that are necessarily present in the input oceanographic data with more fundamental theoretical limitations in the techniques for computing wave fields in inhomogeneous media with irregular boundaries. For example, and from the standpoint of ray theory, the following comments are pertinent:

1) If rays have been traced for a set of incremented initial angles with separation $\Delta\theta_s$ and it is found that the arrival structure "breaks up," it is clearly possible to repeat the calculations for initial angle increments $\Delta\theta'_s$ with $\Delta\theta'_s \ll \Delta\theta_s$. This fills in the detail of the arrival structure and permits evaluation of the magnification function of (III.21) by the limiting process

$$M(R, z, \tau) = \lim_{\Delta\theta'_s \to 0} \left(\frac{z_{\theta'_s + \Delta\theta'_s} - z_{\theta'_s}}{r_s \Delta\theta'_s} \right)_R \qquad \text{(III. 22)}$$

2) The requirement for accuracy in ray tracing is not primarily towards specifying the range and depth positions of rays with given initial angles - in any event such data are exceptionally sensitive at long ranges to variations in the input field data. It is necessary, however, that the relative positions of closely spaced rays be computed accurately if the $M(R, z, \tau)$ of (III. 22) is to represent the spreading of a propagating ray tube.

3) A limit on the accuracy with which (III. 22) can be computed will be set by the buildup of machine errors as a given ray is iterated. If such errors are serious the magnification function defined by (III. 22) will not be uniform over a set of differentially incremented initial angles.

4) The accuracy requirement of 3), above, is usually a trivial limitation, however. In every detailed examination that has been made of ray tracings in which the magnification function shows abrupt or erratic changes in slope the cause of such behavior has been traced to structure of the input environmental data. Apart from bottom interactions and shadow zone boundaries, the usual origin of the change is due to a change in slope (not an abrupt change, for the velocity field construction program produces profiles which are continuous in both the velocity and its vertical gradient) in the upper thermocline. The effect is increased over a range of initial angles when a number of profiles with differing thermocline structure are used to form the velocity field.

An example of this can be observed in the ray depth distribution plot of Fig. 32 for the very shallow angles from the 100-meter deep ray trace origin. These rays were injected into an approximately isovelocity region below an upper thermocline. The detailed field, obtained by use of the Sippican X-BT casts, usually showed a slight positive thermocline below the main thermocline but some of the casts showed a slight negative thermocline. Several of the shallow angle rays actually skipped a convergence zone or two due to trapping in this region and before being refracted downward when they came into a positive thermocline. This behavior, of course, is highly sensitive with respect to small variations in the input data and would depend, for example, on whether velocity profiles taken at night were mixed with velocity profiles taken during the day.

5) The use of highly detailed input data for the velocity profiles, e.g., the use of the X-BT casts with readout at 5- or 10-meter intervals as compared to data based on much larger readout intervals from Nansen casts, produces a "graininess" or fluctuation in the magnification functions which increases with range and which is not due to machine error but reflects the nature of the input data. It is expected that in acoustical propagation these effects are equivalent to the type of fluctuations that are ascribed to microstructure.

6) Not only are the effects of 4) and 5), above, sensitive to detailed structure of the environmental data but it becomes physically meaningless, at least on the basis of ray tracing, to compute rays with very small initial angle increments for the purpose of defining a magnification function that is continuous for differentially incremented initial angles, even when machine errors can be neglected. Both for refraction through small depth intervals and for bottom reflection from small bottom segments a limit will be reached that is set by diffraction spreading. If a magnification function is smoothly defined, in the sense indicated above, it represents a well-defined spreading wavefront; in contrast, an aberrant magnification function that can be identified with a single arrival represents wavefront warpage. In both ray and wave optics the effect of distorted wavefronts is to produce a lack of resolution and a spreading of energy about an average or central position. This, it must be assumed, is given by the trajectory of the central ray.

References for Chapter III

1. Physics of Sound in the Sea, Summary Technical Report of NDRC, Division 6, Volume 8; Washington, D. C. (1946).
2. C. B. Officer, Introduction to the Theory of Sound Transmission with Application to the Ocean, McGraw Hill Book Co., N. Y. (1958).
3. M. Born and E. Wolf, Principles of Optics, Pergamon Press, N. Y. (1959).
4. I. Tolstoy and C. S. Clay, Ocean Acoustics, McGraw Hill Book Co., N. Y. (1966).

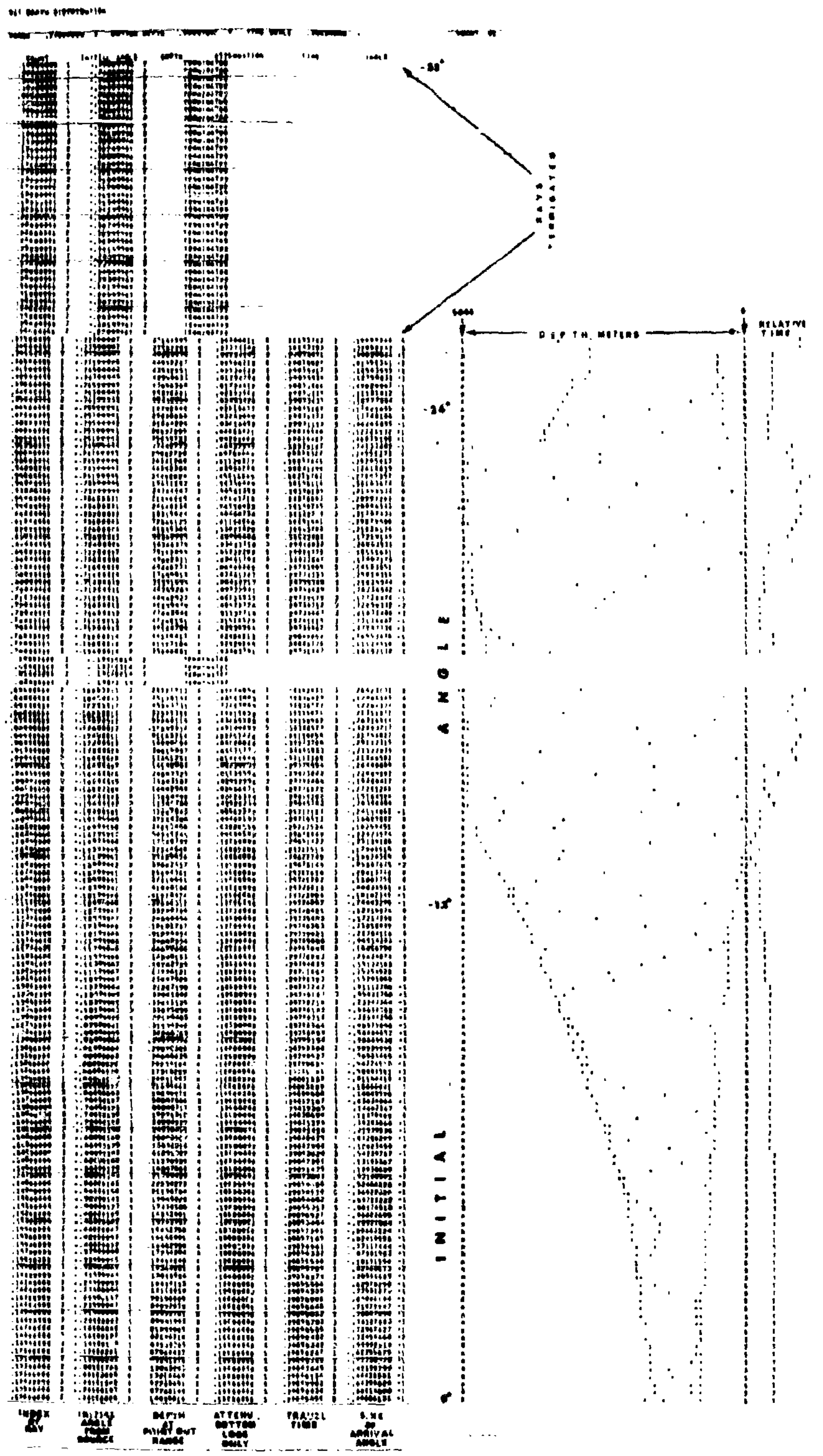

Fig. 31. Ray depth distribution plot at 225-mile range. This figure is based on the same ray tracing and environmental field used in Fig. 10. It is to be compared with Fig. 11 which is the ray depth distribution plot at 115-mile range. Although the depth amplitudes of the rays as a function of initial angle are comparable, note that the number of arrivals has greatly increased and that the magnification function (III.21) has become more difficult to define.

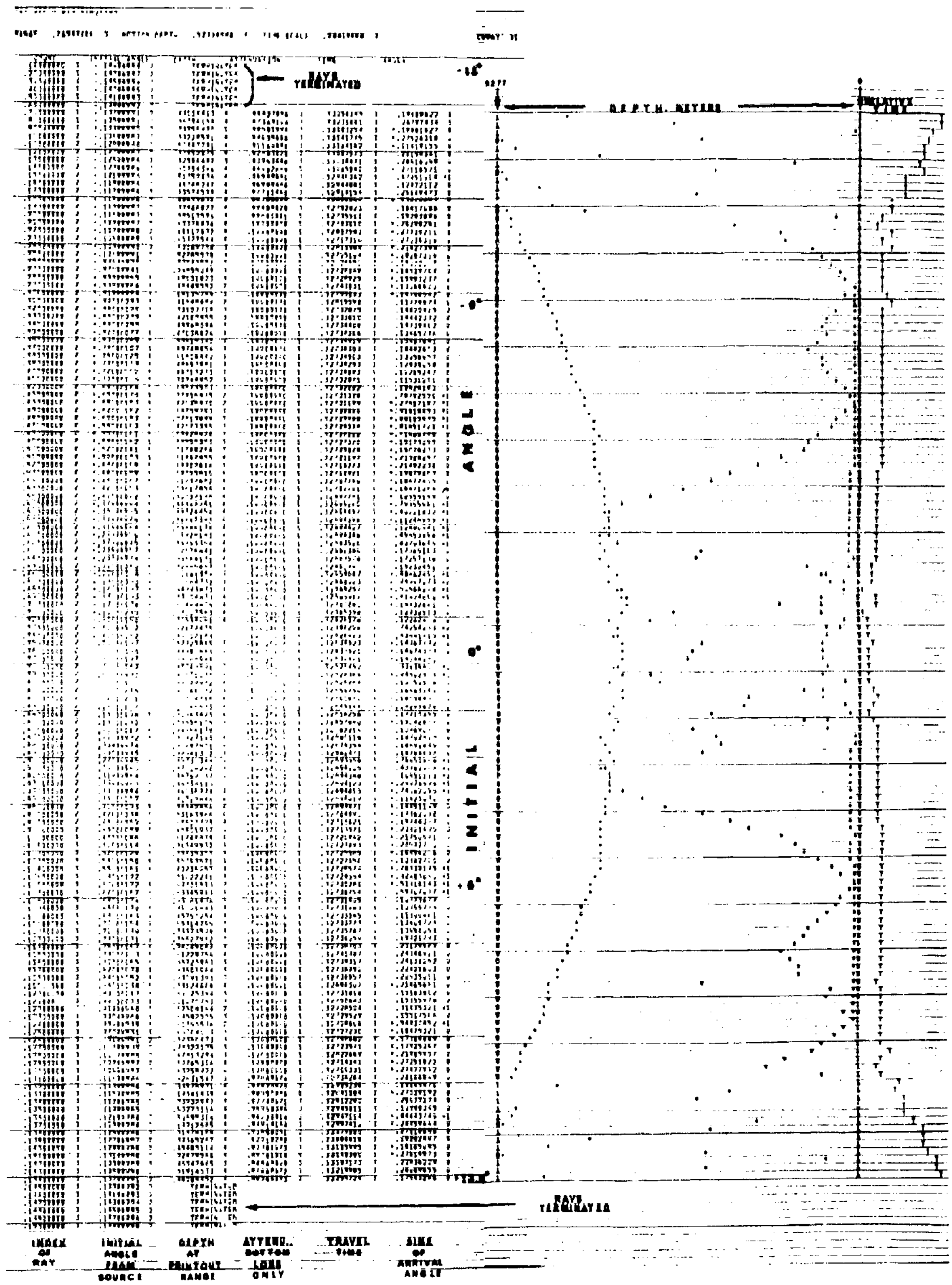

Fig. 32. Ray depth distribution plot at 240-mile range. This figure is based on ray tracing for the A. N. Guthrie and J. D. Shaffer experiment described in Introduction. Depth distribution plot shows that transmission can be described in terms of three regimes ordered with respect to initial angles of the rays: 1) angles < -10° and > 10° for which the transmission involves bottom reflections, 2) angular range from -10° to -3° and from 3° to 10° for which a well-defined arrival structure exists, and 3) the angular range from -3° to 3°, representing rays shallowly injected into a variable isothermal region, for which no well-defined arrival structure exists.

CHAPTER IV

TRANSMISSION LOSS

4.1. Preliminary Observations

The objective of this chapter is to use the ray tracing solution, Eq. (III.2), obtained from the computer printouts, to calculate the intensity in the far acoustical field. First, however, it will be convenient to review briefly certain concepts which are conventional and which will be used in the computations.

4.1.1. Transmission Loss

The intensity in the acoustical field is normalized with respect to source power and is expressed as a transmission loss measured in decibels,

$$\text{T.L.} = 10 \log_{10} \frac{I_d}{I_{yd}} \qquad \text{(IV.1)}$$

where I_d is the intensity measured at a given position in the field and I_{yd} is the intensity produced by the (point) source at a distance of one yard. Alternatively, the average sound pressure P_d that is measured can be used to express the transmission loss by

$$\text{T.L.} = 20 \log_{10} \frac{P_d}{P_{yd}} \qquad \text{(IV.2)}$$

$$= 20 \log_{10} P_d - 71.6 - 10 \log W \quad . \qquad \text{(IV.3)}$$

In (IV.3) the acoustical pressure produced by a source of power W watts at a distance of one yard has been expressed in dynes/cm^2 and these are, then, the units to be used for the detected pressure, P_d . In both (IV.2) and (IV.3) the nearly unit factor $\left[(\rho v)_{yd}/(\rho v)_d\right]$, the ratio of the acoustical impedances at the source and detector, respectively, has been dropped.

4.1.2. Spreading Loss

The contraction, or expansion, of a differential ray tube from a source that propagates through the medium will lead to a "spreading loss." For cylindrical spreading, and neglecting any other attenuation or absorption than that due to the geometrical divergence of the ray tube, it is straightforward to show that the intensity of a single arrival at position (R, z) will be given by[1]

$$I_d = I_{yd} \frac{\cos \theta_o}{\cos \theta} \frac{1}{M(R, z, \tau)} \frac{r_{yd}}{R} \quad . \qquad \text{(IV. 4)}$$

In (IV.4) r_{yd} is the standard distance of one yard, θ is the arrival angle of the ray at the point (R, z) , θ_o is the initial angle of the ray, and $M(R, z, \tau)$ is the magnification factor of Eq. (III.21); also, $\tau = r_{yd}\theta_o$.

4.1.3. Reciprocity Theorem

Insofar as the rays traced from an origin represent the acoustical field spreading outwards, it is natural to consider the source of the sound at the origin and the resultant field as that which would be measured by a probing hydrophone. In many experiments the receiver is fixed and it is the source that is used as the probe, e.g., a towed projector from a ship. In fact, and thanks to a reciprocity theorem, the same calculation can be used for both types of measurement procedures.[2]

The reciprocity theorem, valid for a stable medium, and scalar wave fields, states that it is possible to interchange the positions of the source and receiver in the medium without alteration of the transmission loss. This is related, of course, to the fact that ray paths are reversible and the spreading loss between the two positions is, to first order, independent of the choice of either as an origin.

4.1.4. Multipath Interference

The extrinsic variable of the acoustic field is the instantaneous pressure. Within the ray approximation, and thus away from diffraction determined regions such as turning points, the net pressure can be expressed as the sum of local plane waves each of which represents an independent arrival, i.e.,

$$P(R', z') = \sum_j A_j \, e^{-i\left(\omega_j t - kR' \cos \theta_j - kz' \sin \theta_j + \phi_j\right)} \quad . \qquad \text{(IV. 5)}$$

R′ and z′ are the coordinates of a point in the field near a reference point (R_o, z_o) and are used here to express the displacements $(R - R_o)$ and $(z - z_o)$ in range and depth, respectively. At the reference point the individual arrivals have amplitudes A_j, ray angle θ_j, relative phases ϕ_j, and frequencies ω_j. $k = 2\pi/\lambda$ is the wave number and is (2π times) the reciprocal wavelength. From (IV. 5) it is clear that the instantaneous pressure may have any magnitude from 0 to the sum of the component amplitudes and the precise value will depend on the relative phases. Also, in the region of (R_o, z_o) there will be an interference structure that depends upon the arrival angles.

The average intensity in the region of the reference point will be

$$\langle I \rangle = \frac{\langle PP^* \rangle}{\rho v}$$

$$= \frac{1}{\rho v T} \int_{t-\frac{T}{2}}^{t+\frac{T}{2}} \frac{1}{\mathcal{R}\mathcal{Z}} \int_{R_o-\mathcal{R}/2}^{R_o+\mathcal{R}/2} \int_{z_o-\mathcal{Z}/2}^{z_o+\mathcal{Z}/2} PP^* \, dt\, dR'\, dz' \qquad \text{(IV. 6)}$$

where a time average is taken over a duration T and a space average is taken over the interval of dimensions $\mathcal{R}$ and $\mathcal{Z}$. Substitution of (IV. 5) into (IV. 6) leads to an average intensity and fluctuations around this average

$$\rho v \langle I \rangle = \frac{1}{2} \sum_j \langle A_j^2 \rangle + \frac{2}{T\mathcal{R}\mathcal{Z}} \int_T \int_{\mathcal{R}} \int_{\mathcal{Z}} dt\, dR\, dz \left\{ \sum_j \sum_{j \neq \kappa} A_j A_\kappa \cos\Big[(\omega_j - \omega_\kappa) t - kR(\cos\theta_j - \cos\theta_\kappa) - kz(\sin\theta_j - \sin\theta_\kappa) + \phi_j - \phi_\kappa \Big] \right\} . \qquad \text{(IV. 7)}$$

The single sum represents the sum of the intensities of the individual arrivals,

$$\langle I \rangle = \sum_j I_j \qquad \text{(IV. 8)}$$

and the double sum of (IV. 7) gives the fluctuations of intensity that define the interference structure about (R_o, z_o).

If the velocity field is stable, a definite meaning can be given to the phases ϕ_j, calculating these in terms of the travel time to (R_o, z_o) and the additional phase corrections discussed in the Appendix, and the interfering terms in (IV.7) are then determined from the ray tracing. In long-range propagation, however, the phases become unpredictable, not in a formal sense, for they are readily calculated in the model velocity field, but with respect to uncertainties in measurement as well as the inevitable changes in the velocity field with time that occur in the real ocean. Indeed, in the limit of many contributory arrivals that possess random phase differences the interference terms of (IV.7) will cancel each other and the double sum will tend to vanish.

Unfortunately, it is an experimental observation from transmission measurements in the real ocean that the fluctuations of the signal do not average to an rms level that is small compared to the mean value of (IV.8). This partly indicates that the effective number of arrivals is not large, but it can also indicate that the arrival amplitudes A_j are not approximately equal, reflecting an attenuation that depends upon the paths of the arrivals.

It is possible, however, to obtain a phase independent intensity by carrying out the time and space averaging integrals of (IV.7), leading to (IV.8). It is this approach that is taken in the present work with the consequence that the transmission loss that is computed for (IV.1) via (IV.8) must be understood to apply not to instantaneous experimental measurements but to data that have been averaged over a sufficient scale so that the limit (IV.8) is approached. This will occur for:

1. A time average of period T such that $1/T$ is small compared to a frequency spread that can exist for the different arrivals or for which T is large with respect to a time required for changes in the velocity field of the ocean that randomize the phase differences in (IV.7).
2. A range average over the interval R with R sufficiently large so that the oscillations of the integrand minimize the contribution of this integral with respect to the average intensity given by (IV.8). A rough condition for this is

$$\mathcal{R} > \frac{\lambda}{\cos\theta_j - \cos\theta_\kappa} \qquad \text{(IV.9)}$$

3. A depth average similar to that of 2), above, and under the condition

$$\mathcal{J} > \frac{\lambda}{\sin\theta_j - \sin\theta_K} \quad . \tag{IV.10}$$

This development of the effects of multipath interference is schematic and has suppressed certain details. Among these are:

1. The fact that the A_j wave amplitudes are themselves space dependent, and this should be included in the integral of (IV.7).
2. The neglect of diffraction effects. These will be particularly important near depths which are turning points for the arrivals that are defined by the ray depth distribution plots, for at these points the magnification function vanishes. Also, at these points the wave amplitudes will show their greatest spatial dependence.
3. Even if the diffraction effects are ignored, the condition (IV. 9) will not be appropriate for small ray angles - for these the cosines of (IV. 9) will be nearly unity and the denominator of (IV. 9) will tend to vanish. Thus, at long wavelengths, it will again be necessary to consider the spatial dependence of the wave amplitudes to choose the scale of $\mathcal{R}$ such that (IV. 8) is truly a phase independent limit of (IV. 7). Similar remarks apply to the interval $\mathcal{J}$; however, note that for small angle arrivals the ratio $\mathcal{J}/\mathcal{R}$ goes as $\left(\theta_j + \theta_K\right)/2$ indicating that the depth interval gives more rapid averaging than the range interval.

Despite these limitations, which are also cautions against applying rigid or arbitrary definitions for the scale of $\mathcal{R}$ and $\mathcal{J}$, the discussion does clarify the distinctions between experimental tests of transmission loss that depend on broadband sources or cw projectors. For the former, e.g., shots or air guns, the definition of transmission loss, (IV. 1), can be modified by considering all quantities as spectral densities leading, in particular, to the frequency dependent transmission loss spectrum. This is valuable physical data. It is also simpler to calculate this as an average over a large bandwidth because (IV.8) is then a good approximation, due to the cancellations in (IV.7), over the frequency bandwidth. Finally, impulse sources are especially useful if arrival structure can be distinguished as distinct time-delayed impulses in the received signals.

CW experiments, on the other hand, are notorious for the large interference fluctuations that are consistently measured in long-range propagation experiments. It is, however, simpler to make these measurements, using narrow band filters for detection, and a detailed continuous record is obtained that does reveal the extent and the dominant periods of the multipath interference. Also, the moving source (or hydrophone) that probes the field enables a spatial average to be taken in terms of the probe velocity and the data time series.

4.2. Loss and Weighting Functions

No general-purpose descriptive model of propagation, such as the present program, can expect to deal comprehensively with detailed physical effects, especially those that require intensive, specialized data specification. Examples would include the effects of specific local bottom profiles and their composition and sub-structure on individual acoustical reflections or the dependence of surface scattering amplitudes on the windrow density of the sea surface. This is not to say that such effects are not important, but rather emphasizes practical limitations that must be accepted in treatments of long-range propagation. The constraints occur because: i) it is nearly impossible (or at least extremely rare) that these types of detailed environmental data will be available for an acoustical experiment over, say, a path of 100 miles or more, and ii) programs and sub-programs that utilize such data inputs become increasingly complex.

The approach of the present work is intermediate. On the one hand the interpretation of the acoustical field will be given in terms of probability functions, to be defined later, with the anticipation that if the physical effects can be described statistically they can be included in the program in a natural way. On the other hand specific interactions, especially those due to acoustical interactions with the ocean boundaries that represent loss or scattering, are included on the assumption that they can be described by a few representative parameters. The principal interactions of this type that are used in the program are given below - their approximate character will be apparent.

4.2.1. Bottom Reflectivity

It is assumed that a ray incident against a bottom with a grazing angle χ relative to the bottom will suffer a fractional attenuation

$$a_b = a_b\left(C, \lambda, \chi, \sigma_b\right) \qquad \text{(IV.11)}$$

which is written as a function of certain constants, C, and the parameters of wavelength, λ, grazing angle against the bottom χ, and a coefficient σ_b. The subscript b indicates a particular bottom hit - for B bottom hits the total fractional attenuation is

$$a = \prod_{b=1}^{B} a_b \qquad \text{(IV.12)}$$

A functional description of a_b can be given with respect to well-known models such as the Rayleigh reflection law, which is wavelength independent, or as a scattering law from a rough bottom with variance σ_b. Experiments in special areas can be cited for the support of either of these models but, and particularly for long wavelengths, the bulk of published data gives very little guide towards the choice of a representative function for a_b or for adjusting such a function in terms of the geological structure of a region, assuming this is known.

In the present program a_b can be specified by a scientist who has a preference for a given function, or, preferably, who chooses a function that gives a good average fit to experimental data appropriate to the region of the ray tracing. Geological variations can be approximated by tabulation of σ_b as a function of range.

Three a_b functions have been used as approximations in lieu of more specific data:

1. A "square" but lossy critical angle, i.e.,

$$\alpha_b = k \quad \text{for} \quad 0 \leq k \leq 1 \quad \text{and} \quad 0 \leq \chi \leq \chi_c$$

$$= 0 \quad \text{for} \quad \chi_c < \chi \quad . \tag{IV.13}$$

Typical values that have been used would be

$$k = 1/2 \quad \text{and} \quad \chi_c = 20°$$

2. A roughness approximation

$$\alpha_b = A \exp -\left[\left(C_1\chi\right)^2 + C_2 \frac{\sin^2\chi}{\lambda} \sigma_b^2\right] \tag{IV.14}$$

Again, typical values are $A = 0.7$, $C_1 = 0.725$, and $C_2 = 18.364$. The choice in (IV.14) of a dependence of $1/\lambda$ rather than the $(1/\lambda)^2$ dependence that would be predicted on a pure roughness model has been guided by the experiments of Bucker et al.[3]

3. Termination of a ray after B bottom hits. This approximation can be used with either of 1) or 2), above. It has the practical advantage that it can be used directly in the ray tracing program to stop rays and to save machine running time that would be wasted on rays that continually strike the bottom.

4.2.2. Surface Reflectivity

A fractional attenuation for surface reflectivity can be used that is similar to α_b for bottom reflectivity, i.e.,

$$\beta_s = \beta_s\left(C, \lambda, \chi, \sigma_s\right) \tag{IV.15}$$

where the subscript s indicates a particular surface hit and the total attenuation of a ray striking the surface S times is given by

$$\beta = \prod_{s=1}^{S} \beta_s \qquad \text{(IV.16)}$$

For surface reflections, however, an optimum choice can be made using the function

$$\beta_s = 1 - .0234 \left(\frac{f}{1000}\right)^{3/2} \left(\frac{\sigma_s}{3.28}\right)^{3/2} \qquad \text{(IV.17)}$$

as given by Marsh.[4] In (IV.17) σ_s is the mean wave height and f is the frequency in Hz. It is clear from (IV.17) that for acoustical frequencies of the order of several hundred cycles or less the surface reflectivity loss can be neglected $\left(\beta_s = 1\right)$.

4.2.3. Volume Attenuation

Volume, or bulk, attenuation is expressed by a fractional attenuation

$$r = e^{-\delta R} \qquad \text{(IV.18)}$$

for a ray at range R and for an absorption coefficient δ . The frequency dependence of δ , as a low-frequency limit, has been taken as

$$\delta = \frac{9.5 \times 10^{-3}}{\lambda^2} \qquad \text{(IV.19)}$$

where λ is given in meters and R in (IV.18) is in nautical miles. (IV.19) is the low-frequency approximation of the plane wave attenuation coefficient given by Marsh and Shulkin.[5]

Equations (IV.18) and (IV.19) represent the extension to low frequencies of data taken at higher frequencies under conditions such that δ represents bulk absorption in the medium. A number of other expressions have been determined from transmission measurements in the ocean and which are derived, primarily, as factors modifying a sonar type equation in the regime of cylindrical spreading. Insofar as these experiments do not distinguish additional loss mechanisms that may occur, especially those due to bottom or surface losses, the averaged attenuation factors from the transmission measurements should not be used in a program that enters the different types of losses explicitly.

It is fortunate that for frequencies of several hundred cycles or less the available experimental evidence indicates that the attenuation introduced by scattering mechanisms in the ocean is small, i.e., of the order of (IV.19), approaching (IV.19) as a limit. Unfortunately there is little direct evidence to support this conclusion, but it may be inferred because:

i) scattering will introduce loss either by the interaction itself or by conversion of acoustical energy into directions that will be steeply incident against the bottom and the energy will be absorbed there, and

ii) the experimental volume absorption reported for measurements of transmission in the sound channel, i.e., SOFAR propagation, is small. Sheehy and Halley,[6] for example, give

$$\alpha = 2.1 \times 10^{-6} f^{3/2} \text{ dB/n. mile} \quad , \tag{IV.20}$$

a loss of 2 dB over a range of 1000 miles at 100 Hz.

In the present program (IV.20) could be used in place of (IV.19). However, the surface and bottom losses and the uncertainties in the α_b and β_s functions that describe these losses can be expected to dominate the weak absorption expressed by (IV.18) or (IV.20).

4.2.4. Directivity Functions

If the apparatus used as source or receiver in an acoustical experiment is directional, it is straightforward to assign weights to the individual rays according to a directivity factor that describes the dependence of the radiated power on an angle relative to a fixed direction. If a bottom-mounted source or hydrophone is used as a ray origin it becomes directional even though the components may themselves be isotropic. This is easily accounted for by tracing only rays that propagate into the water, i.e., all initial angles are taken upward (and thus are negative), and the rays that would require propagation through the bottom are ignored.

If the source and receiver are not located on a boundary but are near a reflecting surface the response of the element will be directional because of the interference patterns that are termed the "Lloyd Mirror effect."[7]

It is to be emphasized that a ray is not a physical entity but a representation of a local plane wave - a ray arrival implies an extended wave surface that propagates in the ray direction. When the source and/or receiver are near a boundary surface, one part of the wave will arrive directly at the element and another section of the wave will arrive by a reflected path. Inasmuch as the net path differences are small and occur in the immediate region of the element and the reflection, the phase difference of the two arrivals must be accounted for. This leads to a modulation of the intensity that depends on the angle of arrival and is given by the directivity function

$$g(z, \lambda, \theta) = 4 \sin^2\left[\frac{2\pi z}{\lambda} \sin\theta\right] \qquad \text{(IV. 21)}$$

for complete reflection from the sea surface. z is the depth of the source or receiver, λ is the wavelength, and θ is the arrival angle. If the directivity patterns of (IV. 21) are plotted for various values of the parameter $(z/\lambda) = r$, then $g(z, \lambda, \theta)$ is small for all θ for r approximately zero but becomes highly rosetted for values of r of order two or greater.

The meaning of (IV. 21) becomes unclear, however, as r is extended beyond values of two or three. For shallow angles that carry most of the acoustical energy in long-range propagation and for large r the use of (IV. 21) implies that the effective region of reflection occurs at a large range from the arrival point. In turn the phase relationships between the two arrivals become increasingly less predictable at the same time that the directivity factor is becoming increasingly sensitive to small angular displacements. (IV. 21) has been truncated in the present program for these reasons to have the form

$$g(z, \lambda, \theta) = 4 \sin^2\left[\frac{2\pi z}{\lambda} \sin\theta\right] \qquad 0 \le z \le r\lambda$$

$$= 1 \qquad r\lambda < z \qquad \text{(IV. 22)}$$

r is a program input parameter.

(IV. 22) accounts for the major wavelength dependence of the transmission losses that are computed when the program is applied to shallow sources and/or receivers.

Figure 13 shows a printout of an intensity calculation that is described in Chapter IV-4.4.1. From this data a number of plots can be obtained giving transmission loss as a function of range for designated wavelengths and depths. One of these is shown in Fig. 14 as a prediction of the experimental data shown in Fig. 16. Figures 33 and 34 are taken from the same intensity calculation: Fig. 33 shows the transmission loss for wavelengths 15, 50, and 114 meters for a source at a depth of 500 meters and Fig. 34 shows the transmission loss for the same wavelengths for a source depth of 5000 meters. (In the calculations the receiver was fixed at a depth of 100 meters and the source was towed. See Chapter IV-4.1.2.)

The directivity function of (IV.22) was applied to the 100-meter receiver, the origin of the ray traces, for the wavelengths of 50 and 114 meters. It was applied to the towed source at 30 meters depth for all the wavelengths. For the receiver the 50-meter wavelength gives a maximum power at the horizontal angle of $\pm 7.2°$ and this couples to a well-defined arrival structure. At 114 meters, however, the angle is $\pm 16.6°$, so that most power becomes lost in bottom interactions. The lobe maxima for the 30-meter deep source and wavelengths 15 and 50 meters are $\pm 7.2°$ and $\pm 24.7°$, respectively, and at 114 meters wavelength the full maximum is not attained even for 90° rays. For the depths of Figs. 33 and 34 no source directivity functions were applied.

The plots of these figures show the emphasis given to convergence zone structure by the 50-meter wavelength not only because the $\pm 7.2°$ lobes provide strong illumination in favorable ray directions but because the lobe minimum at $\pm 14.5°$ suppresses the contributions from the bottom interactions.

A modification similar to (IV. 22) should be applied to a hydrophone that is mounted near, but not on, the bottom. This has not been attempted in the present program because an adequate approximation to (IV. 22) would require that the complex (magnitude and phase) bottom reflection coefficient be known.

4.3. Intensity Calculations

The ray tracing solution, Chapter III, together with the loss factors and weighting functions of Chapter IV-4.2, allows an estimate to be made of the power flow from the source that can propagate to increasing ranges. Close to the origin all the rays must be evaluated, i.e., rays with initial angles from +90° to -90°, but most of these will strike the bottom at steep angles and will be strongly attenuated. The effective power flow is limited to the regime of rays that illuminate a relatively shallow solid angle - this is described as a transition from spherical to cylindrical spreading.

The detailed bathymetry local to a source can profoundly influence this transition, as has been indicated in the multiplots of Figs. 10 and 17. It is a good approximation to assume that the sound velocity structure near the origin will be stable so that if the bathymetry in this region is well defined and the loss factors α_b correspond to experiment, the fraction of the source power that is effectively radiated into the far field can be determined with fair precision.

The present chapter gives a description of how the detail obtained in the ray tracing solutions can be used not only to determine the fractional power from the source but to construct vertical distributions of the sound intensity as a function of range. The intensities are readily converted into transmission loss values through (IV.1). The derivations given represent the calculation of a phase-independent intensity, as discussed in Chapter IV-1.4, and it is again emphasized that the results apply as spatial and/or time averages of the more complex multipath interferences.

4.3.1. Addition of Arrival Structure

The intensity of a single arrival will be the product of the spreading loss (IV.4) and the factors of Chapter IV-2, i.e.,

$$I\left(R, z, \tau, v_i\right) = \Phi\left(R, z, \tau, v_i\right) \frac{1}{M\left(R, z, \tau, v_i\right)} \qquad \text{(IV. 23)}$$

$$\Phi\left(R, z, \tau, v_i\right) = I_{yd} \frac{r_{yd} \cos\theta_o}{R \cos\theta} \alpha \beta \gamma g_o g_d \qquad \text{(IV. 24)}$$

The notation of (IV. 23) and (IV. 24) has been extended, principally by the symbolic use of v_i to represent the model velocity field and other environmental data inputs which are necessary to construct a given ray tracing solution. τ designates the individual rays from the origin and (R, z) is the position in the field at which the intensity is evaluated. g_o is the directivity factor that may apply to the rays from the origin of the ray tracing, g_d is the detector directivity factor at (R, z), and all the factors α, β, γ, g_o, and g_d will depend on the ray parameters and the history of the ray as it propagates from the origin to (R, z). $\phi\left(R, z, \tau, v_i\right)$ is to be considered a weighting function for each ray; the function also depends on the wavelength but this has not been indicated explicitly in the notation.

The phase-independent intensity is given by (IV. 8) as the sum of the arrival intensities. This is represented by

$$I\left(R, z, v_i\right) = \int_{\tau} \Phi\left(R, z, \tau, v_i\right) \frac{\delta\left[\tau - \tau\left(R, z, v_i\right)\right]}{M\left(R, z, \tau, v_i\right)} d\tau \qquad \text{(IV. 25)}$$

The δ-function in (IV. 25) is the conventional sifting operator with the properties

$$F(x) = \int F(x') \, \delta(x-x') \, dx' \qquad \text{(IV. 26)}$$

$$1 = \int \delta \, (x-x') \, dx' \qquad \text{(IV. 27)}$$

and, as used in (IV. 25), it expresses the stipulation that the only contribution to the integral comes from those arrivals whose initial τ-directions give rays that pass through (R, z). The function $\tau = \tau\left(R, z, v_i\right)$ indicates that at range R and for the field v_i the τ-directions that arrive at depth z have been identified by use of the ray depth distribution plots such as those of Figs. 11, 31, and 32.

The notation of (IV. 23) and elsewhere is appropriate for continuous functions – indeed, if the velocity field and the bottom profiles possess continuous derivatives, the ray tracing solution will be a continuous function. Technically, however, this function is approximated in the computer solution by printouts at discrete (R, z) positions for increment τ-directions.

The application of (IV.25), using the computer solutions, is represented graphically in the lower part of Fig. 35. Rays with initial angles $\theta_1, \ldots, \theta_{16}$ have been traced to range R and produce a map of the rays to the depths $z_1, \ldots, z_{16}$. Three cycles of the depth distribution have been indicated in Fig. 35 and each cycle represents a single arrival. To determine the summed intensity at a depth z_R, a vertical line is constructed in Fig. 35 which selects the three initial angles that would map to the depth z_R at range R.

The (Stiltjes) integral in (IV.25) measures the contribution of each arrival as a product of $\Phi\left(R, z, \tau, v_i\right)$ and $1/M\left(R, z, \tau, v_i\right)$. The former depends on the history of the ray and the latter is calculated by (III.22 of Chapter III) as a limiting ratio of $\Delta z/\Delta\tau\rfloor_{z_R}$, provided this ratio can be defined. The existence of the limit is assumed in Fig. 35 and is also implied by the assumption of a well-defined arrival structure.

The ray depth distribution plots of Figs. 11, 31, and 32 indicate that, for increasing range and as a function of the detailed structure of the input velocity field and bottom profiles, the function $\tau\left(R, z, v_i\right)$ becomes increasingly erratic and random, at least on the scale of the initial angle increments used for these plots. The comments on this behavior given at the end of Chapter III suggest that when this occurs it reflects a complex physical environment; also, if the functions are "filled in" by more detailed computation, it is just this structure which is most sensitive to small variations of the input model.

The transition to random arrivals is indicated at the top of Fig. 35 for which the depths calculated for successively incremented initial angles near θ_N do not form a continuous pattern and do not permit the magnification function to be calculated. The ray theory states that the flux $I_{yd}\, d\tau$ is transformed to the flux $I_d\, dz$ but does not indicate the degree to which the flux is spread over the depth of the ocean at range R.

In short, if (IV. 25) is followed as a prescription for calculating intensity, it leads to ambiguities which can be resolved only by additional computation that is very likely to be physically meaningless. It is clearly advantageous to rederive (IV. 25) to a form in which all the calculated arrivals are treated on an equal basis and which emphasizes properties of the ray solution that are not sensitive to the detailed structure of the data inputs. An example of such a property is the depth amplitude of the oscillation of the rays about the sound channel which is shown by the + and - limits on the ray depth distribution plots. It may happen that changes in the velocity field v_i will change the labelling of specific initial rays which can couple to a position (R, z), i.e., a translation of the function $\tau\left(R, z, v_i\right)$, but will not produce significant changes in the computed sound intensity.

4.3.2. Ray Probability Density

The δ-function of (IV. 25) identifies the initial τ-directions that couple to (R, z) by performing a sifting operation – it is the limiting form of a probability distribution in which τ is considered a function of the variables $\left(R, z, v_i\right)$ and a strict functional dependence exists between τ and these variables due to the ray tracing solution. Specifically, it is possible to make the correspondence

$$\delta\left[\tau - \tau\left(R, z, v_i\right)\right] \rightarrow w\left(\tau \mid R, z, v_i\right) \qquad \text{(IV. 28)}$$

in which $w\left(\tau \mid R, z, v_i\right)$ is the conditional probability density that the ray tracing solution in the model field v_i will yield a ray with an initial direction specified by τ that maps to the position (R, z).

The general expression of possible relationships between the variables will be given by the joint probability density $w\left(R, z, \tau, v_i\right)$ with the normalization

$$\int_R \int_z \int_\tau \int_{v_i} w\left(R, z, \tau, v_i\right) dR\, dz\, d\tau\, dv_i = 1 \quad . \qquad \text{(IV.29)}$$

A number of marginal distribution densities can be derived from the joint distribution density and further simplifications can be made by choosing products for which the distribution densities are independent. For example, the two-dimensional density $w(\tau, v_i)$ can be factored as $w(\tau)\, w(v_i)$ because the choice of initial ray directions will not depend on the probability of different types of velocity fields.

Of the four variables of the joint distribution, two may be specified and these will be chosen as the position (R, z). It follows that the greatest interest is on the conditional distribution density $w(z, \tau, v_i | R)$, i.e., the density of z, τ, and v_i at a fixed range R, and this is related to the joint distribution by

$$w(z, \tau, v_i | R) = \frac{w(R, z, \tau, v_i)}{w(R)} \quad . \qquad \text{(IV.30)}$$

The conditional density of (IV.30) can be factored as

$$w(z, \tau, v_i | R) = w(z | R, \tau, v_i)\, w(\tau)\, w(v_i) \quad . \qquad \text{(IV.31)}$$

Also, by definition of the magnification factor,

$$M(R, z, \tau, v_i) = \left.\frac{dz}{d\tau}\right]_{R, z, \tau, v_i} \qquad \text{(IV.32)}$$

it follows that

$$w(z | R, \tau, v_i) = \frac{w(\tau | R, z, v_i)}{M(R, z, \tau, v_i)} \quad . \qquad \text{(IV.33)}$$

When all of these operations are combined in the integral of (IV.25) together with the replacement (IV.28), the intensity in the model velocity field v_i becomes

$$I(R, z, v_i) = \int_{\tau} \phi(R, z, \tau, v_i)\, \frac{w(z, \tau, v_i | R)}{w(\tau)\, w(v_i)}\, d\tau \quad . \qquad \text{(IV.34)}$$

The intensity that would be measured at (R, z) as an average over all possible velocity fields is obtained by multiplying (IV. 34) by $w(v_i)$ and taking the average distribution

$$I(R, z) = \int_{\tau} \int_{v_i} \phi \, (R, z, \tau, v_i) \, \frac{w(z, \tau, v_i \,|\, R)}{w(\tau)} \, d\tau \, d v_i \qquad \text{(IV.35)}$$

Equation (IV. 35) is the basic result of this chapter. Its significance becomes clear if it is assumed that the velocity field is single valued and is given by v_s . The integral over $d v_i$ in (IV. 35) decreases the order of the marginal density of the integrand and the weighting function $\phi \, (R, z, \tau, v_s)$ is a constant for the integration.

$$I(R, z, v_s) = \int_{\tau} \Phi \, (R, z, \tau, v_s) \, \frac{w(z, \tau \,|\, R, v_s)}{w(\tau)} \, d\tau \qquad \text{(IV. 36)}$$

The integral over τ in (IV. 36) further reduces the order of the density function to give a probability density that depends on depth alone; specifically, (IV. 36) shows that <u>the acoustical intensity at position (R, z) is the weighted probability density by which the arrival structure is mapped from the origin into the depth of the ocean at range R</u> . The weighting function is

$$\frac{\Phi \, (R, z, \tau, v_s)}{w(\tau)} \quad . \qquad \text{(IV. 37)}$$

When uniform increments are chosen for τ , $w(\tau)$ is uniform in the interval $-\frac{\pi r_{yd}}{2} \leq \tau \leq \frac{\pi r_{yd}}{2}$ and

$$w(\tau) = \frac{1}{\pi r_{yd}} \qquad \text{(IV. 38)}$$

For a stable velocity field (IV. 36) can, of course, be returned to the original form (IV. 25) by reintroducing the magnification functions. (IV. 36), however, is the more general form for the mapping operation that is implied by ray tracing and furthermore (IV. 36) permits a standard statistical interpretation independently of the determination of the magnification functions. The immediate advantages of this method are:

i) When a large number of rays are traced the entire arrival structure that can contribute to the field is included.

ii) Even though the magnification functions become erratic, (IV.36) is fully equivalent to (IV.25) provided that the resultant field distribution can be considered stationary.

iii) When small changes of the velocity field are considered, (IV.35) indicates that the variables z and τ at range R are no longer related by a set of single-valued functions but must be interpreted as distributions.

iv) The calculation of (IV.36) is a straightforward computer sort program in which the rays that are labeled by their initial angles are reordered in terms of their depths at a given range.

v) It is at least useful that this interpretation of the intensity is in a direct correspondence with the density of the rays that are printed out as multiplot distributions, e.g., Figs. 10 and 17.

4.4. Types of Intensity Distributions

In the general expression for the average intensity in the field, (IV.35), the single symbol v_i is used to differentiate among velocity fields. Such notation is highly simplified and unspecific with respect to the complex time-dependent temperature and salinity changes that will occur in the ocean. The application of (IV.35) is, of course, straightforward in principle but becomes unrealistic in practical application. It requires that a nearly continuous sampling be made of the velocity field over a long period of time, that the ray tracing calculations be made for each velocity field measurement, and these data are then to be further averaged over all velocity fields for comparison with experimental acoustical data that are taken simultaneously with the velocity data and are averaged over the same time period. The procedure would be significant only if all other input data, e.g., bottom losses, absorption, etc., were known with sufficient precision so that the method would constitute a true test of the averaging procedures.

Instead, most calculations are made on the basis of a model velocity field which, it is hoped, is at least representative of the field at the time of an experiment. Very little is known, at least for long-range acoustical propagation, of measures of the extent to which changes of the velocity field will modify the transmission loss between a given source and receiver. It has been emphasized in preceding chapters of this report that representative environmental data inputs for a given ray tracing lead to complex arrival structure: it is a pragmatic conclusion that although the replacement of a given velocity field by a "smoothed" average field may greatly simplify the calculated arrival structure, it does not follow that the resultant acoustical field is itself representative. A more formal statement of this conclusion is obtained by noting that the weighting and probability density functions in the integral of (IV. 35) are not separable except under special assumptions.

In the present chapter intensity calculations are made or are indicated for three different assumptions. As classifications, these are:

Type	Applicable Range	Velocity Field	Intensity
I	Short	Stable	Requires calculation of relative phase of arrivals via (IV. 7) or method of Appendix
II	Intermediate	"Stable"	Range dependent intensity following (IV. 36)
III	Long	Stable in profile structure	Averaged in range over, roughly, a convergence zone interval. No resolvable arrival structure.

The Type I calculation is a limiting case that will not be typical of long-range propagation for it assumes that the velocity field will be so stable that the relative phases of arrivals are also stable. The Type II and Type III calculations are discussed subsequently.

4.4.1. Type II Intensity Calculation

At a given range R and for a velocity field v_s, the computer solution does not give a continuous functional relationship between τ and the depth z, but a set of printout data that is incremented in τ. The integral (IV.36) is to be replaced by the finite sum

$$I(R, z, v_s) \rightarrow \sum_j \Phi(R, z, \tau_j, v_s) \frac{w(z, \tau_j | R, v_s)}{w(\tau_j)} \Delta\tau_j \qquad \text{(IV.39)}$$

The assumption of a "stable" velocity field v_s demands that there be a specific z_j depth for each τ_j-ray. What is required, however, is an estimation of the continuous function of depth $I(R, z, v_s)$ that is obtained from the discretely sampled input data points, the z_j. A standard procedure for this uses sampling functions. The depth density function of (IV.39) is expanded as

$$w(z, \tau_j | R, v_s) = w\left[(z - z_j) | \tau_j, R, v_s\right] w(\tau_j) \qquad \text{(IV.40)}$$

where $w\left[(z - z_j) | \tau_j, R, v_s\right]$ is the conditional density for displacements of z from the depths z_j for given values of the other parameters. At this stage it is simpler to drop the explicit labeling of these parameters and to write $w(z - z_j)$ without ambiguity. The interval $\Delta\tau_j$ is selected in terms of an angular input in the ray tracing program. If N rays are traced that are equally spaced over the range of τ,

$$\Delta\tau_j = \frac{\pi r_{yd}}{N} \qquad \text{(IV.41)}$$

and (IV.39) becomes

$$I(R, z, v_s) = \frac{\pi r_{yd}}{N} \sum_j \Phi(R, z, \tau_j, v_s) w(z - z_j) \qquad \text{(IV.42)}$$

For normalization in depth from the surface to the bottom depth z_B, it is necessary that

$$\int_0^{z_B} w(z - z_j)\, dz = 1 \quad \text{for all } z_j \qquad \text{(IV.43)}$$

A number of sampling functions can be used for the smooth estimations of $I(R, z, v_s)$, e.g., histogram plots, $(\sin x)/x$, triangles, etc. Their selection is arbitrary in the limit of large N. In the present program two functions are immediately available:

$$w_L = \frac{p}{\pi z_B} \frac{1}{1 + \left[\frac{(z - z_j) p}{z_B}\right]^2} \qquad \text{(Lorentz)} \qquad \text{(IV. 44)}$$

$$w_G = \frac{2p}{\sqrt{\pi}\, z_B} \exp - \left[\frac{(z - z_j) p}{z_B}\right]^2 \qquad \text{(Gauss)} \qquad \text{(IV. 45)}$$

In (IV. 44) and (IV. 45) the choice of a small constant p represents a large uncertainty in the depth of a given arrival, but the choice of too large a value for p will isolate the distribution of $I(R, z, v_s)$ to the neighborhood of individual arrivals. From statistical considerations that are based on the reliability of sampled estimates p should be of the order of $N^{1/3}$ to $N^{1/2}$ with the larger number being applicable when the intensity distribution can be assumed to be a smooth and uniformly sampled function of depth.

As an example of the use of (IV. 44) and (IV. 45), a fictitious output data tape from the ray tracing program was prepared with depth entries given by

$$z_j = 5000 - 2500 \sin \frac{\pi}{2J} j \quad ; \quad -J \le j \le J \quad , \qquad j\text{ , } J \text{ integer} \quad . \qquad \text{(IV. 46)}$$

In the limit of very large J the theoretical distribution density for the input data of (IV. 46) is given by

$$w(z) = \frac{1}{\pi} \frac{1}{\sqrt{(2500)^2 - (5000 - z)^2}} \quad ; \quad 2500 \le z \le 7500$$

$$= 0 \quad ; \quad |5000 - z| > 2500 \quad . \qquad \text{(IV. 47)}$$

Figure 36 indicates the smoothing effected by the two sampling functions when $J = 15$, i.e., 6° increments in (IV. 46), and for the coarse parameter $p = 5$ and for the finer resolution of $p = 25$. The bottom depth z_B was taken to be 10,000 (meters). Figure 36 clearly indicates the effect of the much longer "tail" of the Lorentz function.

(IV. 42) has been derived on the assumption of a stable velocity field and the choice of $w(z - z_j)$ was made on the basis of sampling theory. An alternative and less restrictive derivation of (IV. 42) is obtained by the direct assumption that the average effect of variations of the velocity field in (IV. 35) leads to the density function of (IV. 40) and thus to (IV. 42). This interpretation demands that the representative field of the calculation, v_s, is the average velocity field. Also, the choice of a particular $w(z - z_j)$ density is no longer arbitrary but must be guided by oceanographic experience.

The construction of the intensity distribution by use of density functions also serves for the averaging of the acoustical field in the neighborhood of foci or caustics. When the arrival structure is well defined in the ray depth distribution plots there will be certain depths at which the magnification function, $dz/d\tau$, becomes zero - in fact, as discussed in the Appendix, the intensity at these depths will be finite and will be spatially spread by diffraction effects. The latter will be more typically represented by the Gaussian density function of (IV. 45) which has, very roughly, the shape of the fall off of intensity in a Fresnel shadow. Although the turning points of the ray depth distribution plots require no special treatment in the present program, following (IV. 42), they are, of course, regions of high intensity because of the high probability of τ-arrivals in these regions. However, the "spreading" factor, p, of (IV. 44) or (IV. 45) is to be limited to a maximum upper value when used to express diffraction spreading.

It is an obvious defect of the Type II calculation that the distribution densities $w(z - z_j)$ are used for three quite independent reasons, i.e.,

i) for velocity field averaging,

ii) for estimating the smoothed intensity distribution based on N data points, and

iii) for averaging diffraction-limited fields.

Another important factor that effectively limits the Type II calculation is the long running time requirement for the ray tracing program on our present computer and the implied pressures, economic and operational, for reducing the number of rays traced, N, to a minimum. Some relief in this direction is obtained by tracing only the shallower angle rays on the assumption that steeper rays are so severely attenuated that they are ineffective; this must be tested by monitoring the attenuation factors that apply to the steeper initial angles.

In view of these problems and the data uncertainties themselves, it is recommended that the Type II intensity calculation be deliberately "over-averaged" by the choice of a small p in (IV.44) or (IV.45) with a value not to exceed 20. This choice, at present, is arbitrary; it also implies that the number of rays that are traced be of order 200.

Finally, it is emphasized that the Type II calculation is based on specific assumptions, i.e., (IV.40), and the type of field chosen, the depths of the source and receiver, the degree of bottom scattering, the presence of horizontal gradients, etc. It would not be expected that the Type II assumptions would apply to a low-frequency, shallow source in a thermocline that shows a strong diurnal variation for in this physical situation the range period of the rays that cycle about the sound channel would depend strongly on the surface thermocline. On the other hand, if the source is at or near the sound channel axis the shallow rays from the source will not be affected by the thermocline, the steep rays will be only partially affected, and only the rays that make nearly grazing angles with the surface will be sensitive to the thermocline variations. If, indeed, a given physical situation can be as clearly defined as in this example, it becomes appropriate to introduce further refinements such as making the density width parameter p a function of τ. Generally, however, decisions of this type are possible only after detailed examination of the ray depth distribution plots and when specific features of the plots can be traced to environmentally sensitive sections of the input data.

4.4.2. Type III Intensity Calculation

When a ray is traced to long ranges, it will continue to show an oscillation about the sound channel and can be characterized by the depth amplitude of this oscillation and the range period. Also, there will be a ray angle at any given depth due to the cycling of the ray. The precise (R, z) position due to a given τ-initial direction becomes increasingly uncertain with range, however. This would be expected because of the sensitivity of the range periods to details of the velocity profile structure and is also evidenced by the scatter of the arrival positions for small angular increments of the initial ray angles.

The Type III intensity calculations provide an estimate of the acoustical power that is spreading cylindrically by assuming that each ray, modified by the weighting function $\phi(R, z, \tau, v_s)$, delivers its fraction of the source power through a cylindrical shell at an average range R_o. The power carried by the ray has a distribution that is characteristic of the depth amplitude and ray angle of the oscillating ray but the ray position in range is assumed to be completely uncertain.

To express this assumption it is convenient to return to the joint distribution $w(R, z, \tau, v_i)$ of (IV. 29) and, using (IV. 30), to expand the averaging of (IV. 35) to express the range average,

$$\overline{I(R_o, z)} = \frac{1}{\mathcal{R}} \int_{R_o - \frac{\mathcal{R}}{2}}^{R_o + \frac{\mathcal{R}}{2}} \int_{\tau} \int_{v_i} \phi(R, z, \tau, v_i) \frac{w(R, z, \tau, v_i)}{w(\tau)\, w(R)} \, dR \, d\tau \, dv_i \quad . \text{(IV. 48)}$$

The bar over the intensity in (IV. 48) shows the range averaging over an interval $\mathcal{R}$. The assumption of the Type III calculation consists in replacing (IV. 48) by

$$\overline{I(R_o, z)} = \int_{\tau} \phi(R_o, z, \tau, v_s) \frac{\overline{w(z, \tau \mid R, v_s)}}{w(\tau)} \, d\tau \qquad \text{(IV. 49)}$$

where the bar over $\overline{w(z, \tau \mid R, v_s)}$ indicates a similar range average, and it is also assumed that the model or representative field v_s is suitable as an average field for the calculation.

Analogously to (IV. 47) the range-averaged density of (IV. 49) can be estimated as

$$\overline{w(z, \tau \mid R, v_s)} = \frac{1}{\Delta\tau} \frac{w(\tau)}{\tan\theta} Q(z) \qquad \text{(IV. 50)}$$

with Q(z) defined by

$$Q(z) = 0 \;, \quad 0 \leq z < z_- \;, \text{ and}$$

$$z_+ < z \leq z_B$$

$$Q(z) = 1 \;, \quad z_- \leq z \leq z_+ \qquad \text{(IV. 51)}$$

In (IV. 50) and (IV. 51) z_- is the minimum depth of oscillation of the ray τ z_+ is the maximum depth of the oscillation, and the range interval between these two depths is given by $\Delta\tau$. z_- and z_+ are to bracket the center range R_o . Q(z) expresses the probability that the ray does not carry (appreciable) energy outside the depth interval in which it oscillates. It follows that

$$\overline{I(R_o, z)} = \int_\tau \phi\,(R_o, z, \tau, v_s)\, Q(z) \frac{d\tau}{\Delta\tau \tan\theta} \qquad \text{(IV. 52)}$$

In (IV. 52) $Q(z)/(\Delta\tau \tan\theta)$ plays the role of the density $w(z, \tau \mid R, v_s)$ of (IV. 36).

The form of the density function of (IV. 52) has the defect that near turning points where $\tan\theta$ vanishes there will be an infinite contribution over an infinitesimal depth interval, and the accidental selection of such a depth would give a contribution that would dominate all other arrivals. To provide averaging over a depth interval it may be noted that $\tan\theta = dz/dR$ and M depth intervals can be selected, each of depth Δz with

$$\Delta z = \frac{z_B}{M} \qquad \text{(IV. 53)}$$

This averaging yields

$$I_{III}(R_o, z_m) = \frac{1}{\Delta z} \int_{z_{m-1}}^{z_m} \overline{I(R_o, z)}\, dz \qquad \text{(IV. 54)}$$

$$= \frac{1}{\Delta z} \int_{\tau} \int_{z_{m-1}}^{z_m} \phi(R_o, z, \tau, v_s)\, Q(z) \frac{dr}{\Delta \tau}\, dR \qquad \text{(IV. 55)}$$

$$= \frac{1}{\Delta z} \int_{\tau} \overline{\phi(R_o, z_m, \tau, v_s)}\, Q(z) \frac{\Delta R_m}{\Delta \tau}\, d\tau \ . \qquad \text{(IV. 56)}$$

In (IV. 56) the attenuation, spreading, and directivity functions constituting ϕ have been expressed as an average value in the depth interval given by z_m and the change in range of the ray through the depth interval from z_{m-1} to z_m has been expressed by ΔR_m . It is straightforward to show that the integral of (IV. 56) over the full depth of the ocean represents the net power that propagates cylindrically at the range R_o .

In the present program the form of (IV. 56) presents a minor difficulty in its demand for the range intervals ΔR_m at which the ray crosses preset depths. (The output of the ray tracing program consists of printouts of the depths at which the ray crosses given ranges.) To obtain the ΔR_m and also the angles θ at the center of each depth interval, interpolations are used and the result is then summed over τ .

The Type III assumptions will be most applicable when the velocity field is stable at the origin of the ray tracing and the prevailing bathymetry is well defined in that region. This implies that the field distribution and its angular aperture are well defined as the sound spreads from the source region at, for example, the range R_1 of Fig. 17. Subsequently and at much greater ranges the field is averaged by (IV. 56); but the function $\overline{\phi(R, z_m, \tau, v_s)}$ still involves functions, especially the bottom attenuation α_b , that are evaluated at the precise positions that are calculated by the specific ray tracing solutions in the representative field v_s .

If the bottom is deep and relatively smooth from the range R_1 to the range at which the intensity is determined by the Type III calculation, the ϕ-functions will be good approximations even with respect to averages over different types of velocity fields v_i ; however, this may not be true if there is a strong perturbation of the ray solution at an intermediate range, e.g., the seamount structure in Fig. 17. If the Type III calculation is applied to a further range after the seamount obstruction, it is necessary to assume:

i) the velocity field from R_1 to R_2 in Fig. 17 is stable and the seamount bathymetry and the bottom attenuation functions are known so that the field distribution and aperture after the seamount have been well calculated by the ray tracing, or

ii) the averaging procedure expressed by (IV.49) applies over the entire ray path; also, the net interaction with the seamount calculated in the model field v_s is an adequate average even though there may be detailed changes that can occur if v_s is allowed to vary. That is, arrivals which may have missed the seamount entirely in one velocity field will interact with it in another field and conversely, but on the average the net attenuation of the spreading sound energy will not be greatly affected.

The classification of the intensity calculations and the procedures for calculating these are based on explicit assumptions as to the behavior of the field under averaging of environmental input parameters and for given input conditions such as the source and receiver depths. If the origin of the ray trace is in the upper thermocline and this is expected to show strong variation over short periods of time, it is not expected that the Type II calculations will apply although the Type III calculation may apply if surface attenuation can be neglected and for large bottom slopes near the origin. Usually, however, the combination of a near-surface source in a changing thermocline will strongly affect the proportion of rays which are bottom attenuated - for example, for the seamount obstruction of Fig. 17 and for a surface source the density of the rays that pass over the obstruction can be visualized as moving up and down following the changes of the thermocline. This simple example emphasizes that if either a Type II or Type III calculation is made for comparison with experiment, it is essential that the model velocity field v_m used in the calculation be the average field.

Guides as to the sensitivity of the ray distributions with respect to the environmental conditions can be obtained from the ray depth distribution plots and, as required, from the individual ray tracing printouts. These data can indicate optimum density functions for the intensity calculations. If neither the Type II or Type III calculations can be expected to apply, it is at least useful to attempt two independent calculations that are based on extremes of the velocity field that can be expected to occur, and to compare the transmission loss values that are given by each field.

References for Chapter IV

1. Physics of Sound in the Sea, Summary Technical Report of NDRC, Division 6, Volume 8; Washington, D. C. (1946).
2. Ibid.
3. H. P. Bucker, J. A. Whitney, G. S. Yee, and R. R. Gardiner, J. Acoust. Soc. Am. 37, 1037 (1965). The specific form of the bottom reflectivity function (IV.14) was kindly suggested to us by Dr. Norman Lord of Hudson Laboratories as a result of his study of a number of bottom reflectivity experiments that have been reported.
4. H. W. Marsh, J. Acoust. Soc. Am. 35, 240 (1963).
5. M. Shulkin and H. W. Marsh, J. Brit. IRE, 25, 493 (1963).
6. M. J. Sheehy and R. Halley, J. Acoust. Soc. Am. 29, 464 (1957).
7. Physics of Sound in the Sea, loc. cit.

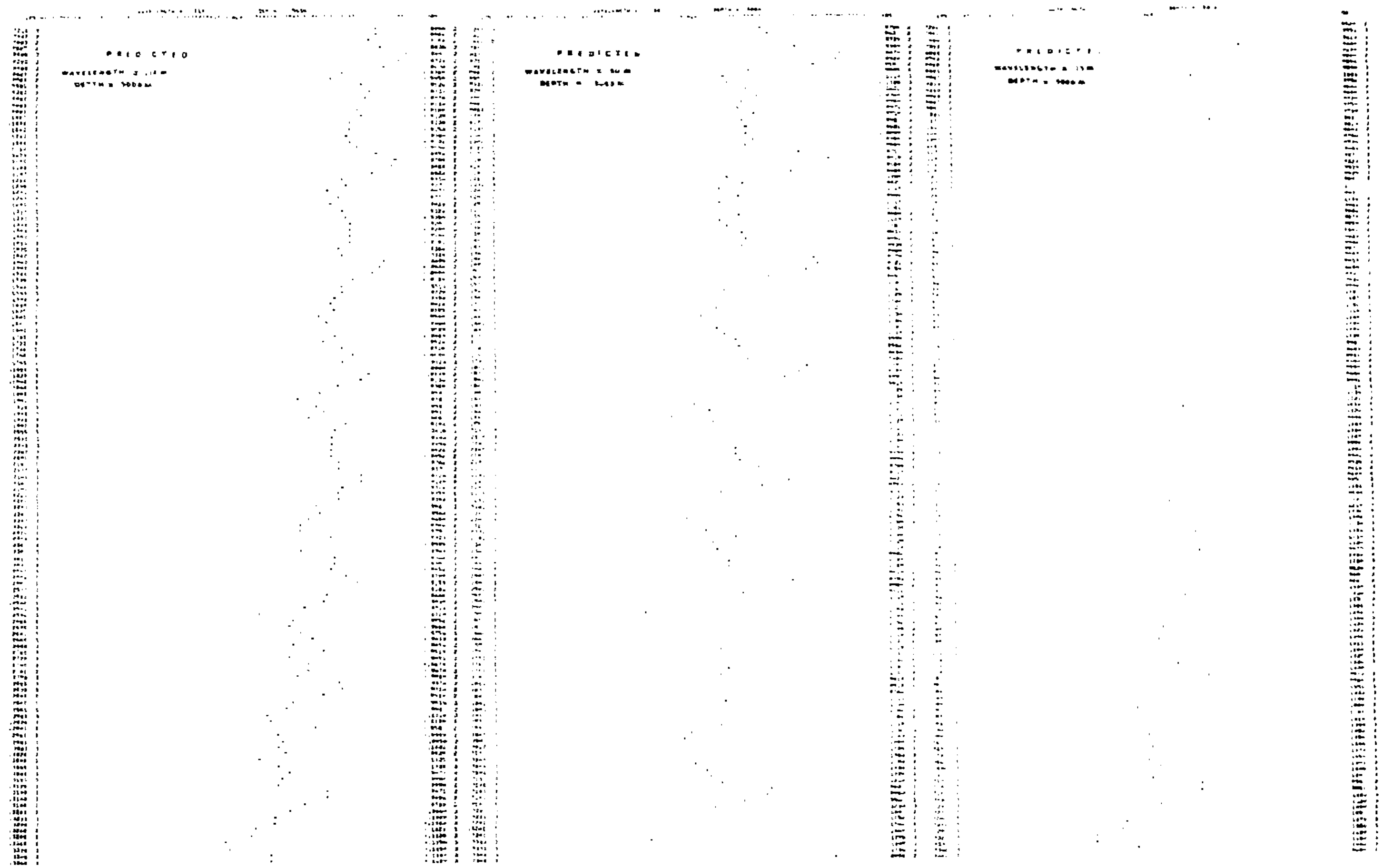

Fig. 33. Computed transmission losses as a function of range for A. N. Guthrie and J. D. Shaffer environmental data, but for hypothetical source at depth of 500 meters.

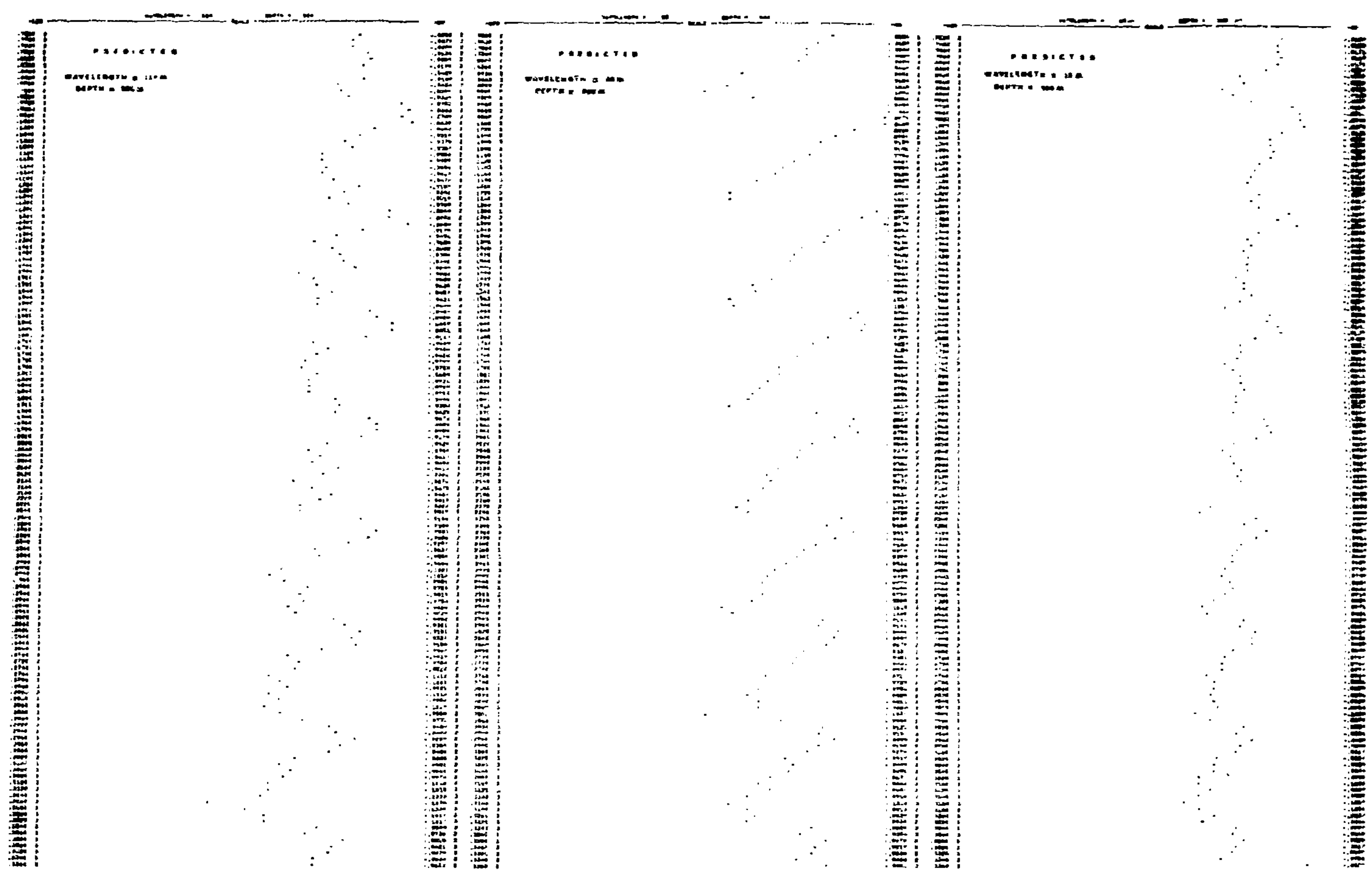

Fig. 34. Computed transmission losses as a function of range for A. N. Guthrie and J. D. Shaffer environmental data, but for source depth of 5000 meters.

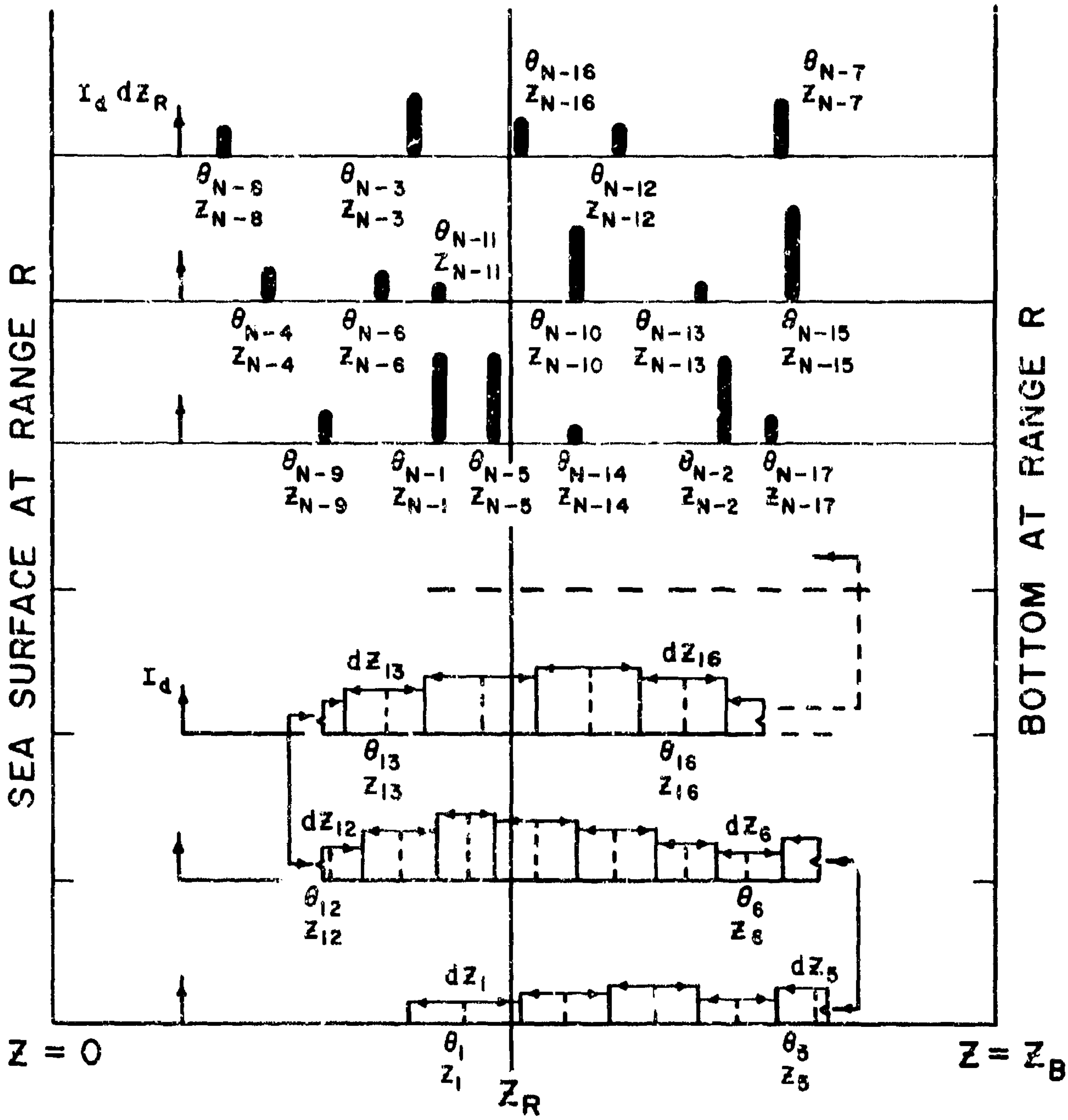

Fig. 35. Distributions of ray arrivals.

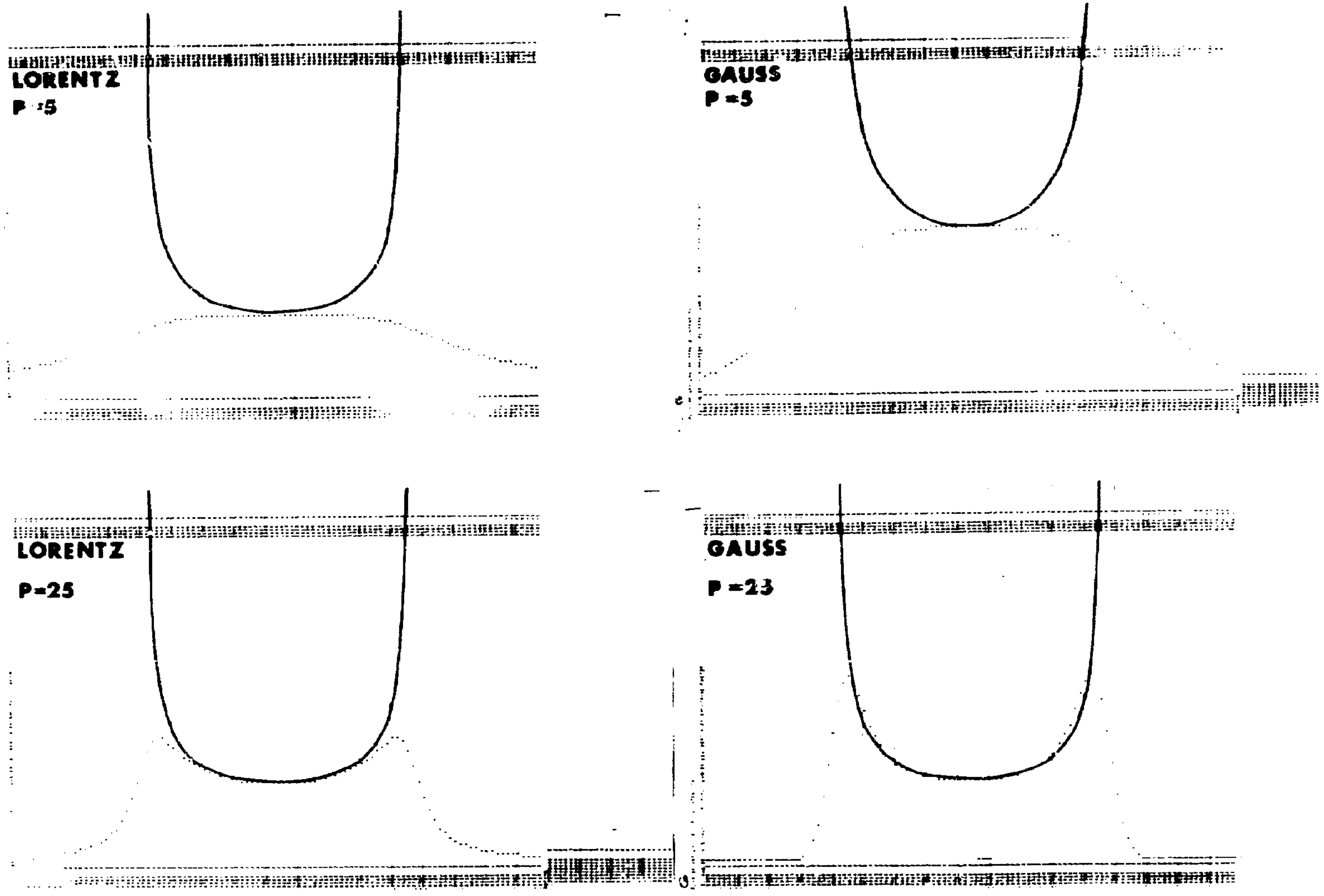

Fig. 36. Effect of various types of sampling functions used to determine continuous functions based on sampled data. Solid curve represents Eq. (IV.47). Computer plot gives distribution determined from data inputs of (IV.46) with $J = 15$ and with use of functions (IV.44) or (IV.45). The vertical scale of distribution for Gaussian sampling function with $p = 5$ is twice that of all other figures.

CHAPTER V

PROGRAM ACCURACY

5.1. Program Control Parameters

It has been emphasized in the preceding Chapters that accuracy in a ray tracing calculation is necessary to determine the depth distribution of intensity of the acoustical field, especially the accuracy that expresses the ability of the program to deal with and compute ray paths in the regions of high gradients and curvatures that are typical of the near sea surface structure of the velocity profiles. This is true whether the intensity is calculated for single arrivals through the magnification factor (equivalent to spreading loss) of (III.21) or through the averaging procedures of Chapter IV which do not require direct determination of the magnification factor. On the other hand, it has also been emphasized that as the program complexity and computer running time are increased together, as these are required for accurate expression of the detailed structure, one is calculating the effect of just that detail which is most sensitive to changes of the field in the ocean and which is, therefore, increasingly less likely to represent the actual field at the time of a given experiment. Finally, the problem is complicated by a conclusion of Chapter IV, i.e., it is not a valid procedure to average the environmental data inputs by smoothing these for this process leads to regular arrival structure that does not show the "breakup" that is found in the calculations that are based on more realistic velocity profile structure.

The basic ray tracing program, outlined in Chapter III, uses control parameters that adapt the iteration increment to follow the velocity field structure. For very accurate work the maximum iteration increment can always be made small and the control parameters made "tight." More important, however, is the degree to which the maximum iteration interval can be made very large, conserving computer running time, but calculational accuracy is kept within set limits by adjustment of the adaptive iteration controls. In terms of the constrictions discussed in the previous paragraph these limits must also be appraised as to whether they are physically meaningful.

To a certain extent the action and interaction of the controls can be followed by program testing on smooth, simple velocity fields with known theoretical ray solutions. Practical specification of the control parameters, however, must follow from tests on real velocity profiles which contain the maximum gradients and curvatures that can be expected in the ocean.

The input parameters which control the accuracy are summarized below:

i) Maximum Iteration Increment (Δ).
Roughly, the running time of the program over a given range is inversely proportional to Δ. If Δ is too large, however, every iteration will be contracted by one or another of the subsequent tests and this will reverse the trend and lead to longer computer running times. Also, the use of large Δ values even for initial tests in high Z_i and D_i regions leads to breakdown of the iteration expansions to such a degree that the subsequent Δ contractions based on the tests are not properly defined.

ii) Sine Incremental Test (S Test).
This test examines the effect of a tentative iteration of magnitude Δ that depends on the Z_i, D_i, and G_i gradients and curvatures at a given point as these are determined by the velocity field construction program. If this leads to a change in the sine of the ray angle by an amount greater than S, then Δ is contracted to a new Δ_1 as given by (III. 14).

iii) Velocity Field Accuracy Test (ϵ Test).
The velocity predicted by the Z_i, D_i, and G_i field expansion parameters for a tentative iteration of magnitude Δ_1 is compared with the velocity at the same point which is set by the velocity field construction program. If these disagree by an amount greater than ϵ then the iteration of Δ_1 is further contracted to Δ_2 by the use of (III. 15).

iv) Minimum Increment (Δ_m) .

A minimum increment can be set into the program and is to be of the order of the minimum depth interval between velocity profile entries. Use of Δ_m avoids too large a contraction of Δ_2 by the ϵ test or S test.

In addition to the above parameters that are entered explicitly, the program implicitly includes the semi-invariant control of (III. 6) and (III. 7).

5.2 Test Procedures

A number of elementary program tests were made as the program developed, primarily to check the operational sequences, indexing of entries, and gross programming errors. Such tests included isovelocity profiles, earth curvature corrections, boundary location and ray reflection calculations, etc., and need not be reported here. Attention is instead concentrated on ray tracing in those velocity fields which reveal the effect of the program control parameters on the accuracy of the ray tracing. The following models have been chosen for this:

I. Hyperbolic Cosine Profile

II. Bilinear Profile

III. Real Velocity Field

IV. Reversibility Test in Real Velocity Field

The results of the above tests are presented as data printouts with the following formats:

A. Computer plot of the profile (or profiles).

B. Tabulation of specific data inputs with the gradient and curvature values of the profiles at these points. These are the data that are used directly in the ray tracing program.

C. A summary output derived from the ray trace output tape consisting of printouts giving the range, depth, travel time, and sine of the ray angle at turning points of the ray and at surface and bottom reflections. The program control parameters and the computer running time are also given with the printouts.

5.3. Hyperbolic Cosine Profile

$$v(z) = 1500 \cosh 3 \times 10^{-4} (z-3000) \quad . \qquad (V.1)$$

This is a smooth profile for which the gradient and curvature increase uniformly and continuously on either side of the center depth, 3000 meters. The 4-point fit that is based on data points entered every 50 meters gives an excellent representation of the profile shape and the ε-test does not produce truncation of Δ unless ε is made very small and for very large Δ. The results of this test primarily indicate the accuracy of the basic iteration expansions in smooth profile regions as well as the effect of the S-test.

Figure 37 is a computer plot of the hyperbolic profile. In the depth region of 3000 meters the shape is roughly that of the axis of a sound channel but the continuously increasing curvature together with the large factor multiplying the depth dependence in (V. 1), i.e., 3×10^{-4}/meter, produce unrealistically large values of the sound velocity at depth intervals greater than 500 meters from the axis. The data inputs, based on a 3-point fit about each entered point, are given in Table 5.3.1 (these inputs are converted into a 4-point fit in the ray trace program as discussed in Chapter II). The curvature, coefficient D in the Table, is small as compared with the curvature of realistic sound velocity profiles (compare with Chapter V-5.5), but the gradients, coefficient Z, are comparable in the depth intervals from 1000 to 2000 meters and from 4000 to 5000 meters.

Summaries of thirteen ray tracing calculations in the hyperbolic cosine field over a range of 300 miles are shown in Tables 5.3.2.1 through 5.3.2.13, giving only the calculated turning points. A large, upwardly directed, initial angle of -30° was selected to emphasize the high gradient regions of the profile but, for this test, to avoid surface or bottom hits. For the highest accuracy parameters of Table 5.3.2.1 and Table 5.3.2.13, the results are exactly those that would be predicted by formal solutions.[1] Attention is called to the fact that although there is some shift in the range of the turning points for larger values of the control parameters, the effect of the semi-invariant control is to maintain nearly precise values for the depth amplitudes of the cycling rays. Note also that due to the presentation based on turning points the variations in the travel time that occur among the printouts must be normalized with respect to the range deviations of the turning points.

The principal conclusion that can be drawn from the data of Tables 5.3.2.1 - 5.3.2.13 is that for the arc length increment, Δ, of 500 meters or less there is negligible error in the iterations. For values of Δ of 1000 meters or more the accuracy becomes controlled by the sine increment test. By inspection of the discrepancies in the ranges of the turning points for Δ increments of 1000 meters or more with respect to the accurate solutions obtained by the Δ increments of 250 meters it can be concluded that:

i. Agreement would have been improved by the use of maximum sine increments that were considerably less than the minimum value of 0.020 used in Tables 5.3.2.1-5.3.2.13.

ii. It is a defect of the simple form of the sine increment test given by (III.14) that is does not contract the iteration if there is little net change in the sine of the ray angle. This permits errors to grow in the range and depth coordinates of the ray when there are large Δ increments with small change in the ray angle, e.g., for the rays that cross the axis. This is the principal reason why the results of Tables 5.3.2.6, 5.3.2.7, and 5.3.2.12 have not converged to the more accurate values of Table 5.3.2.13.

It is clear from the results that increased accuracy requires greater computer running time, although there is an advantage in using large Δ increments in association with a strong control obtained through the sine increment test if rather nominal discrepancies can be tolerated. However, this is a feature of the smooth form of the hyperbolic cosine profile and is not necessarily true for more complex velocity profile types.

DEEP PROFILE AT RANGE 306.000 MILES TEMP AT OBSERVED MAXIMUM DEPTH 6,650 DEG CENTIGRADE

VELOCITY VS DEPTH

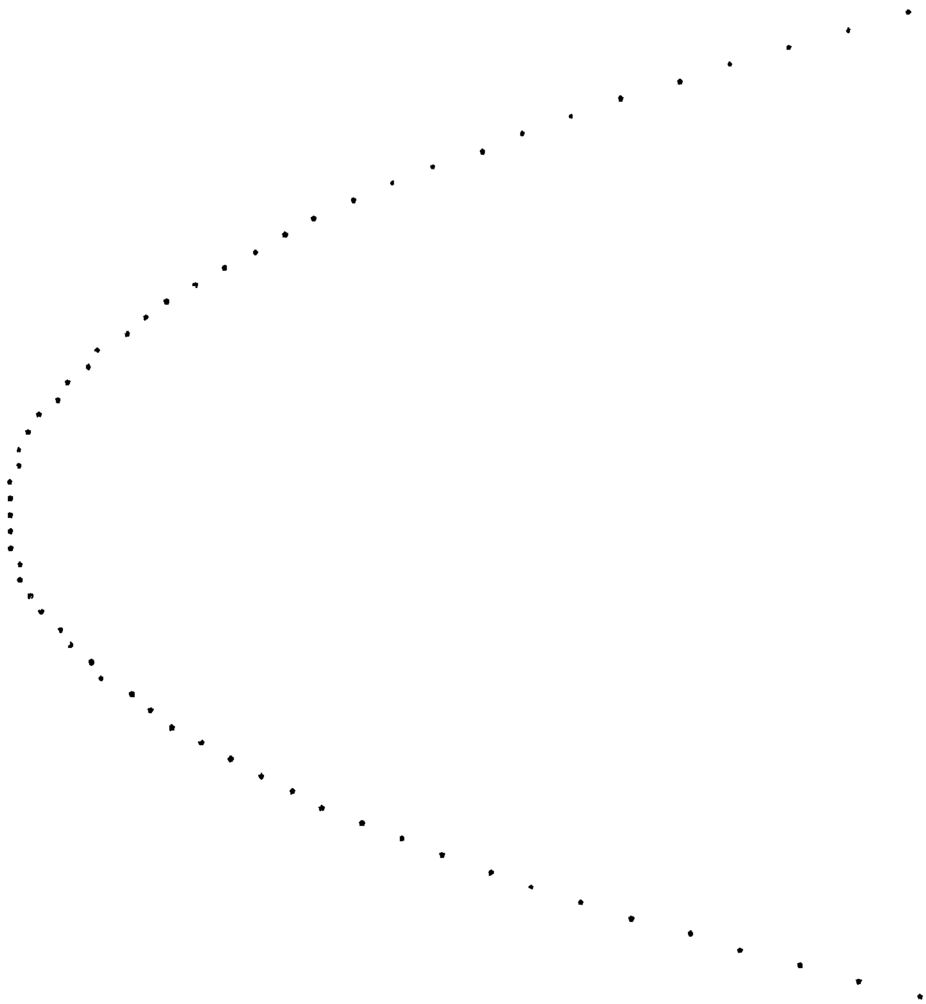

.0000	0	.2150	4
.1000	3	.2104	4
.2000	3	.2061	4
.3000	3	.2020	4
.4000	3	.1980	4
.5000	3	.1942	4
.6000	3	.1906	4
.7000	3	.1871	4
.8000	3	.1839	4
.9000	3	.1808	4
.1000	4	.1778	4
.1100	4	.1750	4
.1200	4	.1724	4
.1300	4	.1699	4
.1400	4	.1676	4
.1500	4	.1654	4
.1600	4	.1634	4
.1700	4	.1616	4
.1800	4	.1598	4
.1900	4	.1582	4
.2000	4	.1568	4
.2100	4	.1555	4
.2200	4	.1543	4
.2300	4	.1533	4
.2400	4	.1524	4
.2500	4	.1517	4
.2600	4	.1511	4
.2700	4	.1506	4
.2800	4	.1503	4
.2900	4	.1501	4
.3000	4	.1500	4
.3100	4	.1501	4
.3200	4	.1503	4
.3300	4	.1506	4
.3400	4	.1511	4
.3500	4	.1517	4
.3600	4	.1524	4
.3700	4	.1533	4
.3800	4	.1543	4
.3900	4	.1555	4
.4000	4	.1568	4
.4100	4	.1582	4
.4200	4	.1598	4
.4300	4	.1616	4
.4400	4	.1634	4
.4500	4	.1654	4
.4600	4	.1676	4
.4700	4	.1699	4
.4800	4	.1724	4
.4900	4	.1750	4
.5000	4	.1778	4
.5100	4	.1808	4
.5200	4	.1839	4
.5300	4	.1871	4
.5400	4	.1906	4
.5500	4	.1942	4
.5600	4	.1980	4
.5700	4	.2020	4
.5800	4	.2061	4
.5900	4	.2104	4
.6000	4	.2150	4

Fig. 37.

DATE 18 3 1968 [illegible]

DEEP PROFILE AT RANGE 336.000 MILES   TEMP AT OBSERVED MAXIMUM DEPTH [illegible] DEG CENTIGRADE

TABLE OF VALUES OF OBSERVED POINTS

DEPTH-METERS	VELOCITY-M/SEC	COEFFICIENT Z		COEFFICIENT G	
.000	2149.6299	-.46189823	0	.19141983	-3
50.000	2126.7739	-.45232769	0	.19141983	-3
100.000	2104.3968	-.44280743	0	.18939973	-3
150.000	2082.4932	-.43338669	0	.18742961	-3
200.000	2061.0501	-.42406357	0	.18549999	-3
250.000	2040.0848	-.41483980	0	.18361987	-3
300.000	2019.5749	-.40570141	0	.18175964	-3
350.000	1999.5167	-.39665031	0	.17996449	-3
400.000	1979.9007	-.38770439	0	.17819916	-3
450.000	1960.7462	-.37883779	0	.17647171	-3
500.000	1942.0249	-.37005640	0	.17478409	-3
550.000	1923.7406	-.36135030	0	.17313995	-3
600.000	1905.8891	-.35274151	0	.17153168	-3
650.000	1888.4664	-.34420481	0	.16996841	-3
700.000	1871.4687	-.33574390	0	.16843567	-3
750.000	1854.8920	-.32735990	0	.16694031	-3
800.000	1838.7327	-.31904869	0	.16549429	-3
850.000	1822.9872	-.31080959	0	.16407165	-3
900.000	1807.6518	-.30264350	0	.16269426	-3
950.000	1792.7231	-.29453960	0	.16134336	-3
1000.000	1778.1970	-.28658490	0	.16004486	-3
1050.000	1764.0726	-.27853460	0	.15876694	-3
1100.000	1750.3444	-.27062780	0	.15753708	-3
1150.000	1737.0099	-.26278628	0	.15633163	-3
1200.000	1724.0663	-.25499281	0	.15516730	-3
1250.000	1711.5186	-.24726261	0	.15404053	-3
1300.000	1699.3401	-.23958799	0	.15294418	-3
1350.000	1687.5518	-.23196739	0	.15187988	-3
1400.000	1676.1433	-.22439898	0	.15085963	-3
1450.000	1665.1120	-.21688091	0	.14985962	-3
1500.000	1654.4552	-.20941181	0	.14890442	-3
1550.000	1644.1780	-.20199969	0	.14798958	-3
1600.000	1634.2963	-.19461309	0	.14708420	-3
1650.000	1624.7895	-.18728031	0	.14622803	-3
1700.000	1615.5287	-.17998960	0	.14540274	-3
1750.000	1606.7105	-.17273949	0	.14460449	-3
1800.000	1598.2543	-.16552020	0	.14384009	-3
1850.000	1590.1977	-.15835411	0	.14311076	-3
1900.000	1582.4158	-.15121560	0	.14242020	-3
1950.000	1575.0361	-.14411119	0	.14175964	-3
2000.000	1568.0078	-.13703920	0	.14112015	-3
2050.000	1561.3327	-.12999889	0	.14052429	-3
2100.000	1555.0079	-.12298623	0	.13995132	-3
2150.000	1549.0336	-.11602201	0	.13941698	-3
2200.000	1543.4077	-.10904390	0	.13890742	-3
2250.000	1538.1292	-.10211031	0	.13843613	-3
2300.000	1533.1967	-.95149004	-1	.13799418	-3
2350.000	1528.6092	-.88318498	-1	.13757246	-3
2400.000	1524.3657	-.81441193	-1	.13719948	-3
2450.000	1520.4651	-.74590111	-1	.13684407	-3
2500.000	1516.9067	-.67795898	-1	.13652496	-3
2550.000	1513.6895	-.60836985	-1	.13623123	-3
2600.000	1510.8130	-.54131718	-1	.13597946	-3
2650.000	1508.2763	-.47338688	-1	.13574926	-3
2700.000	1506.0791	-.40356103	-1	.13555149	-3
2750.000	1504.2207	-.33702982	-1	.13537970	-3
2800.000	1502.7088	-.27017212	-1	.13524788	-3
2850.000	1501.5190	-.20297606	-1	.13513641	-3
2900.000	1500.6750	-.13502598	-1	.13506493	-3
2950.000	1500.1687	-.67904003	-2	.13502049	-3
3000.000	1500.0000	.00000000	0	[illegible]	-3
3050.000	1500.1687	.67904003	-2	.13502049	-3
3100.000	1500.6750	.13502598	-1	.13506493	-3
3150.000	1501.5190	.20297606	-1	.13513641	-3
3200.000	1502.7088	.27017212	-1	.13524788	-3
3250.000	1504.2207	.33702982	-1	.13537970	-3
3300.000	1506.0791	.40356103	-1	.13555149	-3
3350.000	1508.2763	.47338688	-1	.13574926	-3
3400.000	1510.8130	.54131718	-1	.13597946	-3
3450.000	1513.6895	.60836985	-1	.13623123	-3
3500.000	1516.9067	.67795898	-1	.13652496	-3
3550.000	1520.4651	.74590111	-1	.13684407	-3
3600.000	1524.3657	.81441193	-1	.13719948	-3
3650.000	1528.6092	.88318498	-1	.13757246	-3
3700.000	1533.1967	.95149004	-1	.13799418	-3
3750.000	1538.1292	.10211031	0	.13843613	-3
3800.000	1543.4077	.10904390	0	.13890742	-3
3850.000	1549.0336	.11602201	0	.13941698	-3
3900.000	1555.0079	.12298623	0	.13995132	-3
3950.000	1561.3327	.12999889	0	.14052429	-3
4000.000	1568.0078	.13703920	0	.14112015	-3
4050.000	1575.0361	.14411119	0	.14175964	-3
4100.000	1582.4158	.15121560	0	.14242020	-3
4150.000	1590.1977	.15835411	0	.14311076	-3
4200.000	1598.2543	.16552020	0	.14384009	-3
4250.000	1606.7105	.17273949	0	.14460449	-3
4300.000	1615.5287	.17998960	0	.14540274	-3
4350.000	1624.7895	.18728031	0	.14622803	-3
4400.000	1634.2963	.19461309	0	.14708420	-3
4450.000	1644.1780	.20199969	0	.14798958	-3
4500.000	1654.4552	.20941181	0	.14890442	-3
4550.000	1665.1120	.21688091	0	.14985962	-3
4600.000	1676.1433	.22439898	0	.15085963	-3
4650.000	1687.5518	.23196739	0	.15187988	-3
4700.000	1699.3401	.23958799	0	.15294418	-3
4750.000	1711.5186	.24726261	0	.15404053	-3
4800.000	1724.0663	.25499281	0	.15516730	-3
4850.000	1737.0099	.26278628	0	.15633163	-3
4900.000	[illegible]	.27062780	0	.15753708	-3
4950.000	1764.0726	.27853460	0	.15876694	-3
5000.000	1778.1970	.28658490	0	.16004486	-3
5050.000	1792.7231	.29453960	0	.16134336	-3
5100.000	1807.6518	.30264350	0	.16269426	-3
5150.000	1822.9872	.31080959	0	.16407165	-3
5200.000	1838.7327	.31904869	0	.16549429	-3
5250.000	1854.8920	.32735990	0	.16694031	-3
5300.000	1871.4687	.33574390	0	.16843567	-3
5350.000	1888.4664	.34420481	0	.16996841	-3
5400.000	1905.8891	.35274151	0	.17153168	-3
5450.000	1923.7406	.36135030	0	.17313995	-3
5500.000	1942.0249	.37005640	0	.17478409	-3
5550.000	1960.7462	.37883779	0	.17647171	-3
5600.000	1979.9007	.38770439	0	.17819916	-3
5650.000	1999.5167	.39665031	0	.17996449	-3
5700.000	2019.5749	.40570141	0	.18175964	-3
5750.000	2040.0848	.41483980	0	.18361987	-3
5800.000	2061.0501	.42406357	0	.18549999	-3
5850.000	2082.4932	.43338669	0	.18742961	-3
5900.000	2104.3968	.44280743	0	.18939973	-3
5950.000	2126.7739	.45232769	0	.19141983	-3
6000.000	2149.6299	.40617284	0	-.19176946	-2
7000.000	1600.0000	-.15064219	1	-.19176946	-2

TABLE OF VALUES OF EXTRAPOLATED POINTS

DEPTH-METERS	VELOCITY-M/SEC	Z COEFFICIENT	G COEFFICIENT

Table 8.3.

RAY TRACE ANALYSIS PROGRAM- R D MININGHAM - (A-201-01)
RAY NUMBER= 1 INITIAL ANGLE= -30.000 DEGREES

COSH

LIST OF TURNING POINTS 1.0472 sec/mile TOTAL TIME 5:10

NUMBER	RANGE NM	DEPTH M	SINE	SECONDS
1	2,8272	1168,9793	,00000000	3,4906
2	8,4816	4831,0207	,00000000	10,4720
3	14,1361	1168,9793	,00000000	17,4533
4	19,7905	4831,0207	,00000000	24,4346
5	25,4449	1168,9793	,00000000	31,4160
6	31,0993	4831,0207	,00000000	38,3973
7	36,7538	1168,9793	,00000000	45,3786
8	42,4082	4831,0207	,00000000	52,3599
9	48,0626	1168,9793	,00000000	59,3413
10	53,7170	4831,0207	,00000000	66,3226
11	59,3714	1168,9793	,00000000	73,3039
12	65,0258	4831,0207	,00000000	80,2852
13	70,6802	1168,9793	,00000000	87,2665
14	76,3347	4831,0207	,00000000	94,2478
15	81,9891	1168,9793	,00000000	101,2292
16	87,6435	4831,0207	,00000000	108,2105
17	93,2979	1168,9793	,00000000	115,1918
18	98,9523	4831,0207	,00000000	122,1731
19	104,6067	1168,9793	,00000000	129,1544
20	110,2612	4831,0207	,00000000	136,1358
21	115,9156	1168,9793	,00000000	143,1171
22	121,5700	4831,0207	,00000000	150,0984
23	127,2244	1168,9793	,00000000	157,0797
24	132,8788	4831,0207	,00000000	164,0611
25	138,5333	1168,9793	,00000000	171,0424
26	144,1877	4831,0207	,00000000	178,0237
27	149,8421	1168,9793	,00000000	185,0050
28	155,4965	4831,0207	,00000000	191,9864
29	161,1509	1168,9793	,00000000	198,9677
30	166,8053	4831,0207	,00000000	205,9490
31	172,4597	1168,9793	,00000000	212,9303
32	178,1141	4831,0207	,00000000	219,9116
33	183,7685	1168,9793	,00000000	226,8929
34	189,4229	4831,0207	,00000000	233,8742
35	195,0773	1168,9793	,00000000	240,8556
36	200,7317	4831,0207	,00000000	247,8369
37	206,3862	1168,9793	,00000000	254,8182
38	212,0406	4831,0207	,00000000	261,7995
39	217,6950	1168,9793	,00000000	268,7808
40	223,3494	4831,0207	,00000000	275,7621
41	229,0038	1168,9793	,00000000	282,7435
42	234,6582	4831,0207	,00000000	289,7248
43	240,3126	1168,9793	,00000000	296,7061
44	245,9671	4831,0207	,00000000	303,6874
45	251,6215	1168,9793	,00000000	310,6687
46	257,2759	4831,0207	,00000000	317,6500
47	262,9303	1168,9793	,00000000	324,6314
48	268,5847	4831,0207	,00000000	331,6127
49	274,2391	1168,9793	,00000000	338,5940
50	279,8935	4831,0207	,00000000	345,5753
51	285,5479	1168,9793	,00000000	352,5566
52	291,2023	4831,0207	,00000000	359,5379
53	296,8567	1168,9793	,00000000	366,5192

NGLE DEG=-30,000 EPSILON= ,5000 DELTA= 250 MIN DELTA=100 SIN TEST= ,100

Table 5.3.2.1

RAY TRACE ANALYSIS PROGRAM- R D MILINGHAM - (A-201-01)
RAY NUMBER= 2 INITIAL ANGLE= -30,000 DEGREES COSH

LIST OF TURNING POINTS 0.5574 sec/mile TOTAL TIME 2:45

NUMBER	RANGE NM	DEPTH M	SINE	SECONDS
1	2,8273	1168,9793	,00000000	3,4906
2	8,4815	4831,0207	,00000000	10,4718
3	14,1362	1168,9793	,00000000	17,4534
4	19,7905	4831,0207	,00000000	24,4345
5	25,4452	1168,9793	,00000000	31,4161
6	31,0994	4831,0207	,00000000	38,3973
7	36,7541	1168,9796	,00000000	45,3788
8	42,4084	4831,0207	,00000000	52,3600
9	48,0629	1168,9796	,00000000	59,3415
10	53,7173	4831,0207	,00000000	66,3228
11	59,3717	1168,9795	,00000000	73,3041
12	65,0262	4831,0207	,00000000	80,2855
13	70,6806	1168,9795	,00000000	87,2668
14	76,3351	4831,0207	,00000000	94,2482
15	81,9894	1168,9794	,00000000	101,2294
16	87,6440	4831,0207	,00000000	108,2109
17	93,2982	1168,9794	,00000000	115,1921
18	98,9529	4831,0207	,00000000	122,1737
19	104,6072	1168,9794	,00000000	129,1548
20	110,2619	4831,0207	,00000000	136,1365
21	115,9161	1168,9794	,00000000	143,1176
22	121,5708	4831,0207	,00000000	150,0992
23	127,2250	1168,9793	,00000000	157,0803
24	132,8797	4831,0207	,00000000	164,0619
25	138,5339	1168,9793	,00000000	171,0431
26	144,1886	4831,0207	,00000000	178,0247
27	149,8429	1168,9793	,00000000	185,0058
28	155,4975	4831,0204	,00000000	191,9874
29	161,1518	1168,9793	,00000000	198,9686
30	166,8064	4831,0204	,00000000	205,9501
31	172,4607	1168,9793	,00000000	212,9313
32	178,1152	4831,0205	,00000000	219,9127
33	183,7696	1168,9793	,00000000	226,8940
34	189,4240	4831,0205	,00000000	233,8753
35	195,0785	1168,9793	,00000000	240,8567
36	200,7328	4831,0206	,00000000	247,8379
37	206,3874	1168,9793	,00000000	254,8194
38	212,0416	4831,0206	,00000000	261,8006
39	217,6963	1168,9793	,00000000	268,7822
40	223,3505	4831,0206	,00000000	275,7633
41	229,0052	1168,9793	,00000000	282,7449
42	234,6595	4831,0206	,00000000	289,7261
43	240,3141	1168,9793	,00000000	296,7077
44	245,9684	4831,0206	,00000000	303,6888
45	251,6230	1168,9793	,00000000	310,6704
46	257,2773	4831,0207	,00000000	317,6515
47	262,9320	1168,9793	,00000000	324,6331
48	268,5862	4831,0207	,00000000	331,6143
49	274,2408	1168,9796	,00000000	338,5958
50	279,8951	4831,0207	,00000000	345,5770
51	285,5497	1168,9796	,00000000	352,5585
52	291,2040	4831,0207	,00000000	359,5397
53	296,8585	1168,9795	,00000000	366,5211

ANGLE DEG=-30,000 EPSILON= ,5000 DELTA= 500 MIN DELTA=100 SIN TEST= ,100

Table 5.3.2.2

RAY TRACE ANALYSIS PROGRAM- R D MININGHAM - (A-201-01)
RAY NUMBER= 3 INITIAL ANGLE= -30,000 DEGREES

COSH

LIST OF TURNING POINTS 0.3209 sec/mile TOTAL TIME 1:35

NUMBER	RANGE NM	DEPTH M	SINE	SECONDS
1	2,8271	1168,9876	,00000000	3,4896
2	8,4818	4831,0120	,00000000	10,4712
3	14,1364	1168,9884	,00000000	17,4529
4	19,7911	4831,0113	,00000000	24,4345
5	25,4461	1168,9793	,00000000	31,4166
6	31,1011	4831,0207	,00000000	38,3986
7	36,7561	1168,9793	,00000000	45,3807
8	42,4112	4831,0206	,00000000	52,3627
9	48,0661	1168,9794	,00000000	59,3447
10	53,7210	4831,0206	,00000000	66,3266
11	59,3759	1168,9794	,00000000	73,3085
12	65,0307	4831,0206	,00000000	80,2904
13	70,6855	1168,9794	,00000000	87,2722
14	76,3402	4831,0206	,00000000	94,2539
15	81,9949	1168,9794	,00000000	101,2356
16	87,6498	4831,0207	,00000000	108,2176
17	93,3048	1168,9793	,00000000	115,1996
18	98,9598	4831,0207	,00000000	122,1816
19	104,6148	1168,9793	,00000000	129,1636
20	110,2697	4831,0207	,00000000	136,1456
21	115,9247	1168,9793	,00000000	143,1276
22	121,5797	4831,0207	,00000000	150,1096
23	127,2346	1168,9793	,00000000	157,0915
24	132,8895	4831,0207	,00000000	164,0735
25	138,5444	1168,9793	,00000000	171,0555
26	144,1994	4831,0207	,00000000	178,0374
27	149,8543	1168,9793	,00000000	185,0193
28	155,5092	4831,0207	,00000000	192,0013
29	161,1641	1168,9793	,00000000	198,9832
30	166,8189	4831,0207	,00000000	205,9651
31	172,4738	1168,9793	,00000000	212,9470
32	178,1287	4831,0207	,00000000	219,9289
33	183,7835	1168,9793	,00000000	226,9108
34	189,4384	4831,0207	,00000000	233,8927
35	195,0933	1168,9793	,00000000	240,8746
36	200,7482	4831,0207	,00000000	247,8565
37	206,4031	1168,9793	,00000000	254,8385
38	212,0579	4831,0207	,00000000	261,8204
39	217,7128	1168,9793	,00000000	268,8023
40	223,3677	4831,0207	,00000000	275,7842
41	229,0226	1168,9793	,00000000	282,7661
42	234,6774	4831,0207	,00000000	289,7480
43	240,3323	1168,9793	,00000000	296,7299
44	245,9872	4831,0207	,00000000	303,7118
45	251,6420	1168,9793	,00000000	310,6937
46	257,2969	4831,0207	,00000000	317,6756
47	262,9518	1168,9793	,00000000	324,6575
48	268,6067	4831,0207	,00000000	331,6394
49	274,2615	1168,9793	,00000000	338,6213
50	279,9164	4831,0207	,00000000	345,6031
51	285,5713	1168,9793	,00000000	352,5850
52	291,2261	4831,0207	,00000000	359,5669
53	296,8810	1168,9793	,00000000	366,5488

ANGLE DEG=-30,000 EPSILON= ,5000 DELTA=1000 MIN DELTA=100 SIN TEST= ,100

Table 5.3.2.3

RAY TRACE ANALYSIS PROGRAM- R D MININGHAM - (A-201-01)
RAY NUMBER= 4 INITIAL ANGLE= -30,000 DEGREES

LIST OF TURNING POINTS 0.2533 sec/mile TOTAL TIME 1:15

NUMBER	RANGE NM	DEPTH M	SINE	SECONDS
1	2,8258	1168,9950	,00000000	3,4850
2	8,4827	4831,0205	,00000000	10,4694
3	14,1410	1168,9793	,00000000	17,4545
4	19,7941	4831,0133	,00000000	24,4355
5	25,4493	1168,9958	,00000000	31,4176
6	31,1038	4831,0086	,00000000	38,3990
7	36,7613	1168,9795	,00000000	45,3838
8	42,4191	4831,0206	,00000000	52,3684
9	48,0715	1169,0285	,00000000	59,3476
10	53,7251	4830,9637	,00000000	66,3261
11	59,3787	1169,0301	,00000000	73,3068
12	65,0362	4831,0225	,00000000	80,2896
13	70,6933	1168,9780	,00000000	87,2723
14	76,3487	4831,0212	,00000000	94,2539
15	82,0028	1168,9853	,00000000	101,2350
16	87,6626	4831,0213	,00000000	108,2211
17	93,3148	1168,9934	,00000000	115,1984
18	98,9701	4831,0075	,00000000	122,1787
19	104,6254	1168,9963	,00000000	129,1611
20	110,2825	4831,0208	,00000000	136,1454
21	115,9366	1168,9905	,00000000	143,1269
22	121,5954	4831,0212	,00000000	150,1127
23	127,2534	1168,9782	,00000000	157,0967
24	132,9069	4831,0141	,00000000	164,0786
25	138,5619	1168,9890	,00000000	171,0605
26	144,2191	4831,0205	,00000000	178,0451
27	149,8780	1168,9789	,00000000	185,0304
28	155,5302	4831,0071	,00000000	192,0077
29	161,1853	1168,9932	,00000000	198,9880
30	166,8455	4831,0224	,00000000	205,9737
31	172,4982	1168,9977	,00000000	212,9525
32	178,1527	4831,0081	,00000000	219,9341
33	183,8083	1169,0320	,00000000	226,9163
34	189,4661	4831,0212	,00000000	233,9013
35	195,1242	1168,9779	,00000000	240,8854
36	200,7814	4831,0222	,00000000	247,8679
37	206,4342	1168,9865	,00000000	254,8473
38	212,0899	4831,0134	,00000000	261,8299
39	217,7466	1168,9847	,00000000	268,8143
40	223,4035	4831,0210	,00000000	275,7987
41	229,0609	1168,9789	,00000000	282,7833
42	234,7148	4830,9678	,00000000	289,7629
43	240,3713	1168,9791	,00000000	296,7469
44	246,0280	4831,0208	,00000000	303,7310
45	251,6817	1168,9931	,00000000	310,7102
46	257,3368	4830,9699	,00000000	317,6902
47	262,9932	1168,9792	,00000000	324,6719
48	268,6492	4831,0215	,00000000	331,6539
49	274,3019	1169,0301	,00000000	338,6337
50	279,9593	4831,0224	,00000000	345,6165
51	285,6151	1168,9786	,00000000	352,5985
52	291,2682	4831,0037	,00000000	359,5770
53	296,9258	1168,9791	,00000000	366,5617

ANGLE DEG=-30,000 EPSILON= ,5000 DELTA=2000 MIN DELTA=100 SIN TEST= ,100

Table 5.3.2.4

RAY TRACE ANALYSIS PROGRAM- R D MINNINGHAM - (A-201-01)
RAY NUMBER= 5 INITIAL ANGLE= -30,000 DEGREES

COSH

LIST OF TURNING POINTS 0.2693 sec/mile TOTAL TIME 1:20

NUMBER	RANGE NM	DEPTH M	SINE	SECONDS
1	2,8231	1169,0449	,00000000	3,4825
2	8,4759	4830,9707	,00000000	10,4601
3	14,1428	1168,9785	,00000000	17,4533
4	19,7941	4831,0120	,00000000	24,4302
5	25,4493	1169,1772	,00000000	31,4112
6	31,1136	4831,0235	,00000000	38,3992
7	36,7623	1169,0400	,00000000	45,3741
8	42,4152	4830,9674	,00000000	52,3510
9	48,0838	1168,9769	,00000000	59,3408
10	53,7479	4831,0243	,00000000	66,3276
11	59,3971	1168,9963	,00000000	73,3027
12	65,0659	4831,0236	,00000000	80,2952
13	70,7306	1168,9734	,00000000	87,2816
14	76,3819	4831,0109	,00000000	94,2591
15	82,0501	1168,9753	,00000000	101,2507
16	87,7101	4831,0256	,00000000	108,2392
17	93,3564	1169,0506	,00000000	115,2144
18	99,0259	4831,0212	,00000000	122,2041
19	104,6736	1169,0385	,00000000	129,1780
20	110,3414	4831,0223	,00000000	136,1704
21	116,0034	1168,9785	,00000000	143,1598
22	121,6527	4830,9421	,00000000	150,1353
23	127,3162	1168,9776	,00000000	157,1253
24	132,9714	4831,0167	,00000000	164,1049
25	138,6373	1168,9790	,00000000	171,0937
26	144,3018	4831,0282	,00000000	178,0796
27	149,9506	1169,1448	,00000000	185,0557
28	155,5974	4830,8590	,00000000	192,0290
29	161,2462	1168,9876	,00000000	199,0010
30	166,8985	4830,8613	,00000000	205,9786
31	172,5468	1168,9915	,00000000	212,9506
32	178,2060	4831,0227	,00000000	219,9356
33	183,8564	1169,0597	,00000000	226,9122
34	189,5215	4831,0221	,00000000	233,9021
35	195,1844	1168,9779	,00000000	240,8913
36	200,8342	4831,0077	,00000000	247,8679
37	206,4899	1168,9882	,00000000	254,8477
38	212,1436	4831,0030	,00000000	261,8263
39	217,8108	1168,9785	,00000000	268,8197
40	223,4742	4831,0220	,00000000	275,8094
41	229,1301	1168,9786	,00000000	282,7926
42	234,7935	4831,0220	,00000000	289,7823
43	240,4444	1168,9881	,00000000	296,7589
44	246,0968	4830,9504	,00000000	303,7365
45	251,7574	1168,9761	,00000000	310,7197
46	257,4090	4830,8335	,00000000	317,6973
47	263,0653	1168,9832	,00000000	324,6777
48	268,7321	4831,0258	,00000000	331,6655
49	274,3825	1169,1649	,00000000	338,6434
50	280,0486	4831,0239	,00000000	345,6309
51	285,7074	1168,9775	,00000000	352,6138
52	291,3712	4831,0244	,00000000	359,6021
53	297,0244	1168,9840	,00000000	366,5807

ANGLE DEG=-30,000 EPSILON= ,5000 DELTA=3000 MIN DELTA=100 SIN TEST= ,100

Table 5.3.2.5

RAY TRACE ANALYSIS PROGRAM- R D MININGHAM - (A-201-01)
RAY NUMBER= 6 INITIAL ANGLE= -30,000 DEGREES

COSH

LIST OF TURNING POINTS 0.5574 sec/mile TOTAL TIME 2:45

NUMBER	RANGE NM	DEPTH M	SINE	SECONDS
1	2,8272	1168,9793	,00000000	3,4904
2	8,4817	4831,0207	,00000000	10,4720
3	14,1362	1168,9793	,00000000	17,4536
4	19,7908	4831,0207	,00000000	24,4351
5	25,4453	1168,9793	,00000000	31,4167
6	31,0997	4831,0207	,00000000	38,3982
7	36,7543	1168,9793	,00000000	45,3798
8	42,4088	4831,0207	,00000000	52,3614
9	48,0634	1168,9793	,00000000	59,3429
10	53,7179	4831,0206	,00000000	66,3245
11	59,3724	1168,9793	,00000000	73,3060
12	65,0269	4831,0207	,00000000	80,2876
13	70,6814	1168,9793	,00000000	87,2692
14	76,3360	4831,0207	,00000000	94,2508
15	81,9905	1168,9793	,00000000	101,2323
16	87,6450	4831,0207	,00000000	108,2139
17	93,2995	1168,9793	,00000000	115,1954
18	98,9541	4831,0207	,00000000	122,1770
19	104,6086	1168,9793	,00000000	129,1586
20	110,2631	4831,0206	,00000000	136,1402
21	115,9176	1168,9793	,00000000	143,1217
22	121,5722	4831,0207	,00000000	150,1033
23	127,2267	1168,9793	,00000000	157,0848
24	132,8813	4831,0207	,00000000	164,0664
25	138,5357	1168,9794	,00000000	171,0480
26	144,1902	4831,0207	,00000000	178,0295
27	149,8448	1168,9793	,00000000	185,0111
28	155,4993	4831,0207	,00000000	191,9927
29	161,1539	1168,9793	,00000000	198,9742
30	166,8083	4831,0206	,00000000	205,9558
31	172,4628	1168,9793	,00000000	212,9373
32	178,1174	4831,0207	,00000000	219,9189
33	183,7719	1168,9793	,00000000	226,9005
34	189,4265	4831,0207	,00000000	233,8821
35	195,0809	1168,9794	,00000000	240,8636
36	200,7354	4831,0207	,00000000	247,8451
37	206,3900	1168,9793	,00000000	254,8267
38	212,0445	4831,0207	,00000000	261,8083
39	217,6991	1168,9793	,00000000	268,7899
40	223,3536	4831,0206	,00000000	275,7714
41	229,0080	1168,9793	,00000000	282,7530
42	234,6626	4831,0207	,00000000	289,7345
43	240,3171	1168,9793	,00000000	296,7161
44	245,9717	4831,0207	,00000000	303,6977
45	251,6262	1168,9794	,00000000	310,6792
46	257,2806	4831,0207	,00000000	317,6608
47	262,9352	1168,9793	,00000000	324,6424
48	268,5897	4831,0207	,00000000	331,6239
49	274,2443	1168,9793	,00000000	338,6055
50	279,8988	4831,0206	,00000000	345,5871
51	285,5533	1168,9793	,00000000	352,5686
52	291,2078	4831,0207	,00000000	359,5502
53	296,8623	1168,9793	,00000000	366,5317

ANGLE DEG=-30,000 EPSILON= ,5000 DELTA=1000 MIN DELTA=100 SIN TEST= ,020

Table 5.3.2.6

RAY TRACE ANALYSIS PROGRAM- R D MININGHAM - (A-201-01)
RAY NUMBER= 7 INITIAL ANGLE= -30,000 DEGREES

COSH

LIST OF TURNING POINTS 0.3547 sec/mile TOTAL TIME 1:45

NUMBER	RANGE NM	DEPTH M	SINE	SECONDS
1	2,8271	1168,9793	,00000000	3,4900
2	8,4819	4831,0202	,00000000	10,4729
3	14,1370	1168,9798	,00000000	17,4566
4	19,7923	4831,0202	,00000000	24,4404
5	25,4475	1168,9798	,00000000	31,4242
6	31,1027	4831,0202	,00000000	38,4080
7	36,7579	1168,9798	,00000000	45,3918
8	42,4131	4831,0202	,00000000	52,3756
9	48,0683	1168,9798	,00000000	59,3595
10	53,7236	4831,0202	,00000000	66,3433
11	59,3788	1168,9798	,00000000	73,3271
12	65,0340	4831,0202	,00000000	80,3109
13	70,6892	1168,9798	,00000000	87,2947
14	76,3444	4831,0202	,00000000	94,2785
15	81,9997	1168,9798	,00000000	101,2623
16	87,6549	4831,0202	,00000000	108,2462
17	93,3101	1168,9798	,00000000	115,2300
18	98,9653	4831,0202	,00000000	122,2138
19	104,6205	1168,9798	,00000000	129,1976
20	110,2758	4831,0202	,00000000	136,1814
21	115,9310	1168,9798	,00000000	143,1652
22	121,5862	4831,0202	,00000000	150,1490
23	127,2414	1168,9798	,00000000	157,1328
24	132,8966	4831,0202	,00000000	164,1167
25	138,5518	1168,9798	,00000000	171,1005
26	144,2071	4831,0202	,00000000	178,0843
27	149,8623	1168,9798	,00000000	185,0681
28	155,5175	4831,0202	,00000000	192,0519
29	161,1727	1168,9798	,00000000	199,0357
30	166,8279	4831,0202	,00000000	206,0195
31	172,4831	1168,9798	,00000000	213,0033
32	178,1384	4831,0202	,00000000	219,9871
33	183,7936	1168,9798	,00000000	226,9710
34	189,4488	4831,0202	,00000000	233,9548
35	195,1040	1168,9798	,00000000	240,9386
36	200,7592	4831,0202	,00000000	247,9224
37	206,4144	1168,9798	,00000000	254,9062
38	212,0697	4831,0202	,00000000	261,8900
39	217,7249	1168,9798	,00000000	268,8738
40	223,3801	4831,0202	,00000000	275,8576
41	229,0353	1168,9798	,00000000	282,8414
42	234,6905	4831,0202	,00000000	289,8252
43	240,3457	1168,9798	,00000000	296,8091
44	246,0010	4831,0202	,00000000	303,7929
45	251,6562	1168,9798	,00000000	310,7767
46	257,3114	4831,0202	,00000000	317,7605
47	262,9666	1168,9798	,00000000	324,7443
48	268,6218	4831,0202	,00000000	331,7281
49	274,2770	1168,9798	,00000000	338,7119
50	279,9323	4831,0202	,00000000	345,6957
51	285,5875	1168,9798	,00000000	352,6795
52	291,2427	4831,0202	,00000000	359,6633
53	296,8979	1168,9798	,00000000	366,6471

ANGLE DEG=-30,000 EPSILON= ,5000 DELTA=3000 MIN DELTA=100 SIN TEST= ,020

Table 5.3.2.7

RAY TRACE ANALYSIS PROGRAM- R D MININGHAM - (A-201-01)
RAY NUMBER= 8 INITIAL ANGLE= -30,000 DEGREES

COSH

LIST OF TURNING POINTS 0.3547 sec/mile TOTAL TIME 1:45

NUMBER	RANGE NM	DEPTH M	SINE	SECONDS
1	2,8271	1168,9876	,00000000	3,4896
2	8,4818	4831,0120	,00000000	10,4712
3	14,1364	1168,9884	,00000000	17,4529
4	19,7911	4831,0113	,00000000	24,4345
5	25,4461	1168,9793	,00000000	31,4166
6	31,1011	4831,0207	,00000000	38,3986
7	36,7561	1168,9793	,00000000	45,3807
8	42,4112	4831,0206	,00000000	52,3627
9	48,0661	1168,9794	,00000000	59,3447
10	53,7210	4831,0206	,00000000	66,3266
11	59,3759	1168,9794	,00000000	73,3085
12	65,0307	4831,0206	,00000000	80,2904
13	70,6855	1168,9794	,00000000	87,2722
14	76,3402	4831,0206	,00000000	94,2539
15	81,9949	1168,9794	,00000000	101,2356
16	87,6498	4831,0207	,00000000	108,2176
17	93,3048	1168,9793	,00000000	115,1996
18	98,9598	4831,0207	,00000000	122,1816
19	104,6148	1168,9793	,00000000	129,1636
20	110,2697	4831,0207	,00000000	136,1456
21	115,9247	1168,9793	,00000000	143,1276
22	121,5797	4831,0207	,00000000	150,1096
23	127,2346	1168,9793	,00000000	157,0915
24	132,8895	4831,0207	,00000000	164,0735
25	138,5444	1168,9793	,00000000	171,0555
26	144,1994	4831,0207	,00000000	178,0374
27	149,8543	1168,9793	,00000000	185,0193
28	155,5092	4831,0207	,00000000	192,0013
29	161,1641	1168,9793	,00000000	198,9832
30	166,8189	4831,0207	,00000000	205,9651
31	172,4738	1168,9793	,00000000	212,9470
32	178,1287	4831,0207	,00000000	219,9289
33	183,7835	1168,9793	,00000000	226,9108
34	189,4384	4831,0207	,00000000	233,8927
35	195,0933	1168,9793	,00000000	240,8746
36	200,7482	4831,0207	,00000000	247,8565
37	206,4031	1168,9793	,00000000	254,8385
38	212,0579	4831,0207	,00000000	261,8204
39	217,7128	1168,9793	,00000000	268,8023
40	223,3677	4831,0207	,00000000	275,7842
41	229,0226	1168,9793	,00000000	282,7661
42	234,6774	4831,0207	,00000000	289,7480
43	240,3323	1168,9793	,00000000	296,7299
44	245,9872	4831,0207	,00000000	303,7118
45	251,6420	1168,9793	,00000000	310,6937
46	257,2969	4831,0207	,00000000	317,6756
47	262,9518	1168,9793	,00000000	324,6575
48	268,6067	4831,0207	,00000000	331,6394
49	274,2615	1168,9793	,00000000	338,6213
50	279,9164	4831,0207	,00000000	345,6031
51	285,5713	1168,9793	,00000000	352,5850
52	291,2261	4831,0207	,00000000	359,5669
53	296,8810	1168,9793	,00000000	366,5488

ANGLE DEG=-30,000 EPSILON=2,0000 DELTA=1000 MIN DELTA=100 SIN TEST= ,100

Table 5.3.2.8

RAY TRACE ANALYSIS PROGRAM. R D MININGHAM - (A-201-01)
RAY NUMBER= 9 INITIAL ANGLE= -30,000 DEGREES

LIST OF TURNING POINTS 0.5574 sec/mile COSH TOTAL TIME 2:45

NUMBER	RANGE NM	DEPTH M	SINE	SECONDS
1	2,8272	1168,9793	,00000000	3,4904
2	8,4817	4831,0207	,00000000	10,4720
3	14,1362	1168,9793	,00000000	17,4536
4	19,7908	4831,0207	,00000000	24,4351
5	25,4453	1168,9793	,00000000	31,4167
6	31,0997	4831,0207	,00000000	38,3982
7	36,7543	1168,9793	,00000000	45,3798
8	42,4088	4831,0207	,00000000	52,3614
9	48,0634	1168,9793	,00000000	59,3429
10	53,7179	4831,0206	,00000000	66,3245
11	59,3724	1168,9793	,00000000	73,3060
12	65,0269	4831,0207	,00000000	80,2876
13	70,6814	1168,9793	,00000000	87,2692
14	76,3360	4831,0207	,00000000	94,2508
15	81,9905	1168,9793	,00000000	101,2323
16	87,6450	4831,0207	,00000000	108,2139
17	93,2995	1168,9793	,00000000	115,1954
18	98,9541	4831,0207	,00000000	122,1770
19	104,6086	1168,9793	,00000000	129,1586
20	110,2631	4831,0206	,00000000	136,1402
21	115,9176	1168,9793	,00000000	143,1217
22	121,5722	4831,0207	,00000000	150,1033
23	127,2267	1168,9793	,00000000	157,0848
24	132,8813	4831,0207	,00000000	164,0664
25	138,5357	1168,9794	,00000000	171,0480
26	144,1902	4831,0207	,00000000	178,0295
27	149,8448	1168,9793	,00000000	185,0111
28	155,4993	4831,0207	,00000000	191,9927
29	161,1539	1168,9793	,00000000	198,9742
30	166,8083	4831,0206	,00000000	205,9558
31	172,4628	1168,9793	,00000000	212,9373
32	178,1174	4831,0207	,00000000	219,9189
33	183,7719	1168,9793	,00000000	226,9005
34	189,4265	4831,0207	,00000000	233,8821
35	195,0809	1168,9794	,00000000	240,8636
36	200,7354	4831,0207	,00000000	247,8451
37	206,3900	1168,9793	,00000000	254,8267
38	212,0445	4831,0207	,00000000	261,8083
39	217,6991	1168,9793	,00000000	268,7899
40	223,3536	4831,0206	,00000000	275,7714
41	229,0080	1168,9793	,00000000	282,7530
42	234,6626	4831,0207	,00000000	289,7345
43	240,3171	1168,9793	,00000000	296,7161
44	245,9717	4831,0207	,00000000	303,6977
45	251,6262	1168,9794	,00000000	310,6792
46	257,2806	4831,0207	,00000000	317,6608
47	262,9352	1168,9793	,00000000	324,6424
48	268,5897	4831,0207	,00000000	331,6239
49	274,2443	1168,9793	,00000000	338,6055
50	279,8988	4831,0206	,00000000	345,5871
51	285,5533	1168,9793	,00000000	352,5686
52	291,2078	4831,0207	,00000000	359,5502
53	296,8623	1168,9793	,00000000	366,5317

ANGLE DEG=-30,000 EPSILON=2,0000 DELTA=1000 MIN DELTA=100 SIN TEST= ,020

Table 5.3.2.9

RAY TRACE ANALYSIS PROGRAM. R D MININGHAM - (A-201-01)
RAY NUMBER= 10 INITIAL ANGLE= -30,000 DEGREES

COSH

LIST OF TURNING POINTS 0.1851 sec/mile TOTAL TIME 0:55

NUMBER	RANGE NM	DEPTH M	SINE	SECONDS
1	2,8349	1168,9743	,00000000	3,4906
2	8,4998	4831,0257	,00000000	10,4835
3	14,1648	1168,9743	,00000000	17,4764
4	19,8297	4831,0257	,00000000	24,4693
5	25,4947	1168,9743	,00000000	31,4622
6	31,1596	4831,0257	,00000000	38,4551
7	36,8245	1168,9743	,00000000	45,4480
8	42,4895	4831,0257	,00000000	52,4409
9	48,1544	1168,9743	,00000000	59,4338
10	53,8194	4831,0257	,00000000	66,4267
11	59,4843	1168,9743	,00000000	73,4196
12	65,1493	4831,0257	,00000000	80,4125
13	70,8142	1168,9743	,00000000	87,4054
14	76,4791	4831,0257	,00000000	94,3983
15	82,1441	1168,9743	,00000000	101,3912
16	87,8090	4831,0257	,00000000	108,3841
17	93,4740	1168,9743	,00000000	115,3770
18	99,1389	4831,0257	,00000000	122,3699
19	104,8039	1168,9743	,00000000	129,3628
20	110,4688	4831,0257	,00000000	136,3557
21	116,1337	1168,9743	,00000000	143,3486
22	121,7987	4831,0257	,00000000	150,3415
23	127,4636	1168,9743	,00000000	157,3344
24	133,1286	4831,0257	,00000000	164,3273
25	138,7935	1168,9743	,00000000	171,3202
26	144,4584	4831,0257	,00000000	178,3131
27	150,1234	1168,9743	,00000000	185,3060
28	155,7883	4831,0257	,00000000	192,2989
29	161,4533	1168,9743	,00000000	199,2918
30	167,1182	4831,0257	,00000000	206,2847
31	172,7832	1168,9743	,00000000	213,2776
32	178,4481	4831,0257	,00000000	220,2705
33	184,1130	1168,9743	,00000000	227,2634
34	189,7780	4831,0257	,00000000	234,2563
35	195,4429	1168,9743	,00000000	241,2492
36	201,1079	4831,0257	,00000000	248,2421
37	206,7728	1168,9743	,00000000	255,2350
38	212,4377	4831,0257	,00000000	262,2279
39	218,1027	1168,9743	,00000000	269,2208
40	223,7676	4831,0257	,00000000	276,2137
41	229,4326	1168,9743	,00000000	283,2066
42	235,0975	4831,0257	,00000000	290,1995
43	240,7624	1168,9743	,00000000	297,1924
44	246,4274	4831,0257	,00000000	304,1853
45	252,0923	1168,9743	,00000000	311,1782
46	257,7573	4831,0257	,00000000	318,1711
47	263,4222	1168,9743	,00000000	325,1640
48	269,0872	4831,0257	,00000000	332,1569
49	274,7521	1168,9743	,00000000	339,1498
50	280,4170	4831,0257	,00000000	346,1427
51	286,0820	1168,9743	,00000000	353,1356
52	291,7469	4831,0257	,00000000	360,1285
53	297,4119	1168,9743	,00000000	367,1214

ANGLE DEG=-30,000 EPSILON=2,0000 DELTA=3000 MIN DELTA=100 SIN TEST= .100

Table 5.3.2.10

RAY TRACE ANALYSIS PROGRAM- R D MININGHAM - (A-201-01)
RAY NUMBER= 11 INITIAL ANGLE= -30,000 DEGREES

LIST OF TURNING POINTS 0.3209 sec/mile TOTAL COSH TIME 1:35

NUMBER	RANGE NM	DEPTH M	SINE	SECONDS
1	2,8271	1168,9793	,00000000	3,4900
2	8,4819	4831,0202	,00000000	10,4729
3	14,1370	1168,9798	,00000000	17,4566
4	19,7923	4831,0202	,00000000	24,4404
5	25,4475	1168,9798	,00000000	31,4242
6	31,1027	4831,0202	,00000000	38,4080
7	36,7579	1168,9798	,00000000	45,3918
8	42,4131	4831,0202	,00000000	52,3756
9	48,0683	1168,9798	,00000000	59,3595
10	53,7236	4831,0202	,00000000	66,3433
11	59,3788	1168,9798	,00000000	73,3271
12	65,0340	4831,0202	,00000000	80,3109
13	70,6892	1168,9798	,00000000	87,2947
14	76,3444	4831,0202	,00000000	94,2785
15	81,9997	1168,9798	,00000000	101,2623
16	87,6549	4831,0202	,00000000	108,2462
17	93,3101	1168,9798	,00000000	115,2300
18	98,9653	4831,0202	,00000000	122,2138
19	104,6205	1168,9798	,00000000	129,1976
20	110,2758	4831,0202	,00000000	136,1814
21	115,9310	1168,9798	,00000000	143,1652
22	121,5862	4831,0202	,00000000	150,1490
23	127,2414	1168,9798	,00000000	157,1328
24	132,8966	4831,0202	,00000000	164,1167
25	138,5518	1168,9798	,00000000	171,1005
26	144,2071	4831,0202	,00000000	178,0843
27	149,8623	1168,9798	,00000000	185,0681
28	155,5175	4831,0202	,00000000	192,0519
29	161,1727	1168,9798	,00000000	199,0357
30	166,8279	4831,0202	,00000000	206,0195
31	172,4831	1168,9798	,00000000	213,0033
32	178,1384	4831,0202	,00000000	219,9871
33	183,7936	1168,9798	,00000000	226,9710
34	189,4488	4831,0202	,00000000	233,9548
35	195,1040	1168,9798	,00000000	240,9386
36	200,7592	4831,0202	,00000000	247,9224
37	206,4144	1168,9798	,00000000	254,9062
38	212,0697	4831,0202	,00000000	261,8900
39	217,7249	1168,9798	,00000000	268,8738
40	223,3801	4831,0202	,00000000	275,8576
41	229,0353	1168,9798	,00000000	282,8414
42	234,6905	4831,0202	,00000000	289,8252
43	240,3457	1168,9798	,00000000	296,8091
44	246,0010	4831,0202	,00000000	303,7929
45	251,6562	1168,9798	,00000000	310,7767
46	257,3114	4831,0202	,00000000	317,7605
47	262,9666	1168,9798	,00000000	324,7443
48	268,6218	4831,0202	,00000000	331,7281
49	274,2770	1168,9798	,00000000	338,7119
50	279,9323	4831,0202	,00000000	345,6957
51	285,5875	1168,9798	,00000000	352,6795
52	291,2427	4831,0202	,00000000	359,6633
53	296,8979	1168,9798	,00000000	366,6471

ANGLE DEG=-30,000 EPSILON=2,0000 DELTA=3000 MIN DELTA=100 SIN TEST= ,020

Table 5.3.2.11

RAY TRACE ANALYSIS PROGRAM- R D MININGHAM - (A-201-U1)
RAY NUMBER= 12 INITIAL ANGLE= -30,000 DEGREES

COSH

LIST OF TURNING POINTS 0.5574 sec/mile TOTAL TIME 2:45

NUMBER	RANGE NM	DEPTH M	SINE	SECONDS
1	2,8272	1168,9793	,00000000	3,4904
2	8,4817	4831,0207	,00000000	10,4720
3	14,1362	1168,9793	,00000000	17,4536
4	19,7908	4831,0207	,00000000	24,4351
5	25,4453	1168,9793	,00000000	31,4167
6	31,0998	4831,0207	,00000000	38,3982
7	36,7542	1168,9793	,00000000	45,3797
8	42,4088	4831,0207	,00000000	52,3613
9	48,0633	1168,9793	,00000000	59,3429
10	53,7178	4831,0206	,00000000	66,3244
11	59,3723	1168,9793	,00000000	73,3059
12	65,0268	4831,0207	,00000000	80,2874
13	70,6813	1168,9793	,00000000	87,2690
14	76,3358	4831,0207	,00000000	94,2506
15	81,9903	1168,9793	,00000000	101,2321
16	87,6448	4831,0207	,00000000	108,2137
17	93,2993	1168,9793	,00000000	115,1952
18	98,9538	4831,0207	,00000000	122,1767
19	104,6084	1168,9793	,00000000	129,1583
20	110,2629	4831,0207	,00000000	136,1399
21	115,9174	1168,9793	,00000000	143,1214
22	121,5719	4831,0206	,00000000	150,1029
23	127,2264	1168,9794	,00000000	157,0844
24	132,8809	4831,0206	,00000000	164,0659
25	138,5354	1168,9793	,00000000	171,0474
26	144,1898	4831,0207	,00000000	178,0289
27	149,8443	1168,9793	,00000000	185,0104
28	155,4989	4831,0207	,00000000	191,9919
29	161,1534	1168,9793	,00000000	198,9735
30	166,8079	4831,0207	,00000000	205,9551
31	172,4625	1168,9794	,00000000	212,9366
32	178,1169	4831,0207	,00000000	219,9181
33	183,7714	1168,9793	,00000000	226,8997
34	189,4259	4831,0207	,00000000	233,8812
35	195,0804	1168,9793	,00000000	240,8628
36	200,7350	4831,0207	,00000000	247,8444
37	206,3894	1168,9793	,00000000	254,8259
38	212,0439	4831,0207	,00000000	261,8074
39	217,6984	1168,9793	,00000000	268,7889
40	223,3529	4831,0207	,00000000	275,7705
41	229,0075	1168,9793	,00000000	282,7520
42	234,6620	4831,0206	,00000000	289,7336
43	240,3164	1168,9793	,00000000	296,7151
44	245,9709	4831,0207	,00000000	303,6966
45	251,6255	1168,9793	,00000000	310,6782
46	257,2800	4831,0207	,00000000	317,6598
47	262,9345	1168,9794	,00000000	324,6413
48	268,5889	4831,0207	,00000000	331,6228
49	274,2434	1168,9793	,00000000	338,6043
50	279,8979	4831,0207	,00000000	345,5859
51	285,5525	1168,9793	,00000000	352,5675
52	291,2070	4831,0206	,00000000	359,5490
53	296,8614	1168,9793	.00000000	366,5305

ANGLE DEG=-30,000 EPSILON= ,1000 DELTA=1000 MIN DELTA= 20 SIN TEST= ,020

Table 5.3.2.12

RAY TRACE ANALYSIS PROGRAM- R D MININGHAM - (A-201-U1)
RAY NUMBER= 13 INITIAL ANGLE= -30,000 DEGREES

LIST OF TURNING POINTS 1.1993 sec/mile TOTAL COSH TIME 5:55

NUMBER	RANGE NM	DEPTH M	SINE	SECONDS
1	2,8272	1168,9793	,00000000	3,4906
2	8,4816	4831,0207	,00000000	10,4720
3	14,1361	1168,9793	,00000000	17,4533
4	19,7905	4831,0207	,00000000	24,4346
5	25,4449	1168,9793	,00000000	31,4159
6	31,0993	4831,0207	,00000000	38,3973
7	36,7537	1168,9793	,00000000	45,3786
8	42,4081	4831,0207	,00000000	52,3599
9	48,0626	1168,9793	,00000000	59,3412
10	53,7170	4831,0207	,00000000	66,3226
11	59,3714	1168,9793	,00000000	73,3039
12	65,0258	4831,0207	,00000000	80,2852
13	70,6802	1168,9793	,00000000	87,2665
14	76,3347	4831,0207	,00000000	94,2479
15	81,9891	1168,9793	,00000000	101,2292
16	87,6435	4831,0207	,00000000	108,[illegible]05
17	93,2979	1168,9793	,00000000	115,1918
18	98,9523	4831,0207	,00000000	122,1731
19	104,6067	1168,9793	,00000000	129,1545
20	110,2611	4831,0207	,00000000	136,1358
21	115,9156	1168,9793	,00000000	143,1171
22	121,5700	4831,0207	,00000000	150,0984
23	127,2244	1168,9793	,00000000	157,0797
24	132,8788	4831,0207	,00000000	164,0610
25	138,5332	1168,9793	,00000000	171,0424
26	144,1876	4831,0207	,00000000	178,0237
27	149,8420	1168,9793	,00000000	185,0050
28	155,4964	4831,0207	,00000000	191,9863
29	161,1509	1168,9793	,00000000	198,9676
30	166,8053	4831,0207	,00000000	205,9490
31	172,4597	1168,9793	,00000000	212,9303
32	178,1141	4831,0207	,00000000	219,9116
33	183,7685	1168,9793	,00000000	226,8929
34	189,4229	4831,0207	,00000000	233,8742
35	195,0773	1168,9793	,00000000	240,8555
36	200,7317	4831,0207	,00000000	247,8369
37	206,3861	1168,9793	,00000000	254,8182
38	212,0405	4831,0207	,00000000	261,7995
39	217,6949	1168,9793	,00000000	268,7808
40	223,3493	4831,0207	,00000000	275,7621
41	229,0038	1168,9793	,00000000	282,7434
42	234,6582	4831,0207	,00000000	289,7247
43	240,3126	1168,9793	,00000000	296,7060
44	245,9670	4831,0207	,00000000	303,6874
45	251,6214	1168,9793	,00000000	310,6687
46	257,2758	4831,0207	,00000000	317,6500
47	262,9302	1168,9793	,00000000	324,6313
48	268,5846	4831,0207	,00000000	331,6126
49	274,2390	1168,9793	,00000000	338,5939
50	279,8934	4831,0207	,00000000	345,5752
51	285,5478	1168,9793	,00000000	352,5565
52	291,2022	4831,0207	,00000000	359,5378
53	296,8566	1168,9793	,00000000	366,5192

ANGLE DEG=-30,000 EPSILON= ,1000 DELTA= 250 MIN DELTA= 20 SIN TEST= ,020

Table 5.3.2.13

5.4. Bilinear Profile

The bilinear velocity profile, shown in Fig. 38, is a symmetrical profile composed of two constant gradient regions It is formally defined by

$$
\begin{aligned}
v(z) &= 1500 - 0.05\,(z-3000) \;; \quad z < 3000 \\
v(z) &= 1500 \;; \quad z = 3000 \\
v(z) &= 1500 + 0.05\,(z-3000) \;; \quad z > 3000
\end{aligned}
\qquad (V.2)
$$

This profile is easily represented in the ray tracing program by the use of a limited number of data inputs in the constant gradient regions, but the gradient discontinuity at the depth of 3000 meters can only be approximated. The present program interpolates between discretely entered data inputs to produce a smoothed representation of the profile that also possesses continuous gradients. As a stratagem, therefore, the break in the gradient was confined to a depth interval of $\pm$ 0.50 meter about the axis of the profile by defining the profile in terms of the data inputs of Table 5.4.1. The 3-point fit applied to each data entry gives a curvature, coefficient D, of 0.20 at the axis - the 4-point fit used in the ray tracing program increases this curvature to the value 0.40 at the axis but the curvature decreases to zero at the depths 3000 $\pm$ 0.50 meters.

With the exception of the region of the gradient discontinuity and for transitions across it, the velocity field is exactly predicted by the velocity field expansion. Also, and because of the vanishing curvature in the constant gradient regions, the iteration equations will be highly accurate. It follows that the principal result of the tests of the ray tracing program in the bilinear field will be to test the ability of the ε-test to sense and correct for the gradient discontinuity at 3000 meters. Similarly, the use of large minimum iteration intervals, Δ_m, will blur the effects of the transition of the rays across the axis of the profile insofar as they are projected for the arc length Δ_m by an expansion that is valid on only one side of the axis.

The test results are shown for a -15° ray with origin at the axis of the profile and for a 300-mile ray trace in Tables 5.4.2.1 through 5.4.2.11. Again, only the turning point data are presented. As with the hyperbolic cosine velocity field the turning point depths are calculated with excellent precision for all of the control parameters. It is to be noted that the running time of the program <u>increases</u> with Δ for fixed values of the other control parameters, indicating that the ε-test is not only limiting the iteration interval but that an increase in Δ produces an unnecessary truncation over a greater fraction of the arc length of the ray. In contrast, increasing Δ_m drastically drops the computer running time although it does this at the cost of lower accuracy in the results.

The data of Tables 5.4.2.7 and 5.4.2.11 are especially interesting. For these, Δ_m was increased to 100 meters. Because the curvature at the origin of the ray was 0.40, the first iteration of the ray was so large that it reversed the sign of the sine of the initial ray angle, producing the apparent turning point at the range 0.0427 miles. Subsequently, the semi-invariant test of (III.8) compensated for this error but the residual effect of this initial "jog" of the ray shortened the range of the first turning point by 0.16 mile. In the subsequent iterations the terminal point of each iteration never fell so close to the axis that a further false turning point of this type could occur. These data demonstrate not only that the parameter Δ_m must be carefully selected with respect to the properties of the input data but also shows the net effect that can be expected when a serious breakdown of the control tests occurs. Note that the semi-invariant test was able, during the first one-quarter cycle of the ray, to reduce the error to 0.16 mile - had there been no correction of this type the test results would have been absurd.

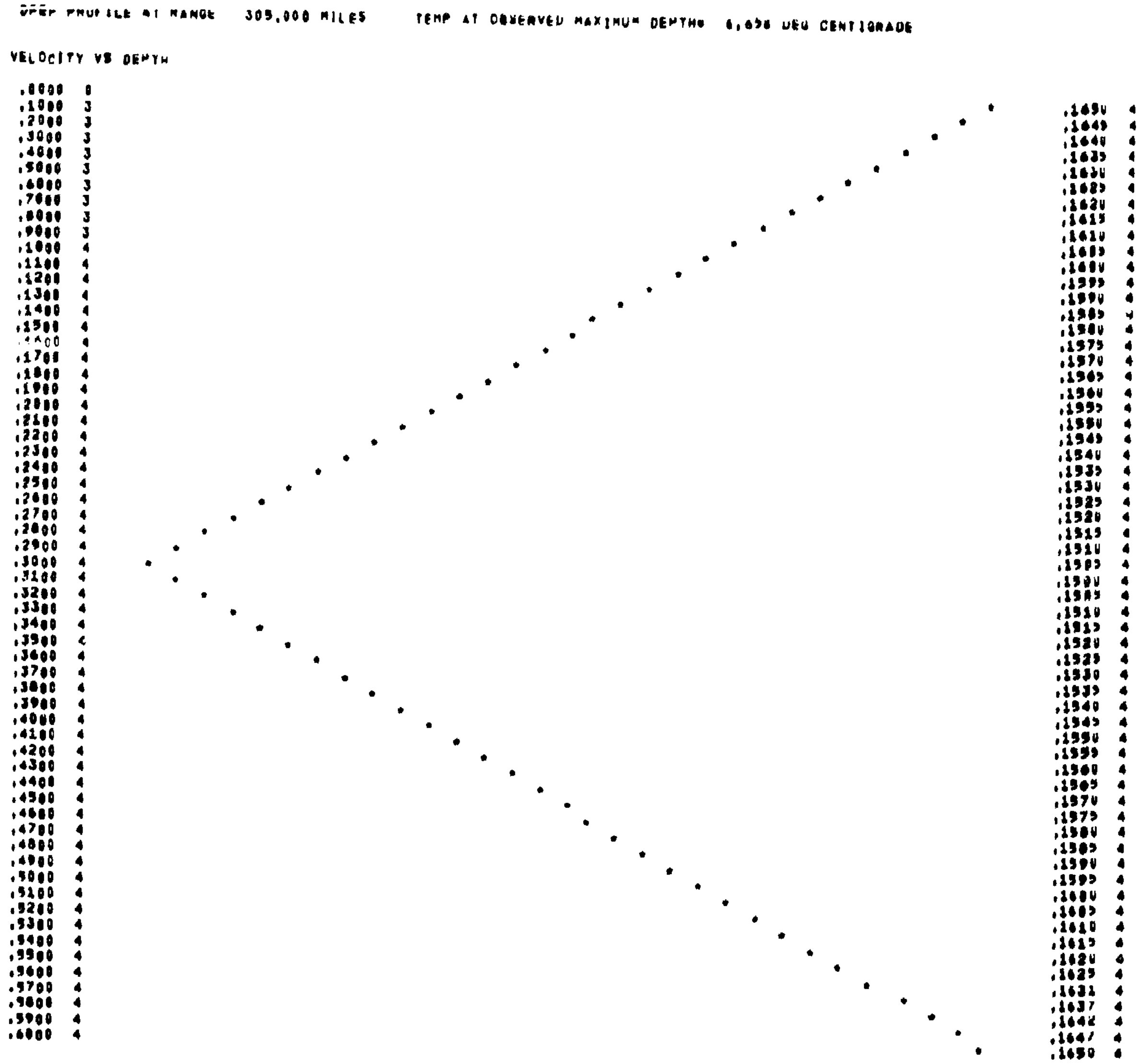
SVP PROFILE AT RANGE 305,000 MILES
TEMP AT OBSERVED MAXIMUM DEPTH 6,698 DEG CENTIGRADE
VELOCITY VS DEPTH

Fig. 38.

DATE 18 3 1968 ID NUMBER 63 SET 3

DEEP PROFILE AT RANGE 305,000 MILES TEMP AT OBSERVED MAXIMUM DEPTH= 6,658 DEG CENTIGRADE

TABLE OF VALUES OF OBSERVED POINTS

DEPTH-METERS	VELOCITY-M/SEC	COEFFICIENT Z	COEFFICIENT D
.000	1650,0000	-.50000000 -1	.00000000 0
500.000	1625,0000	-.50000000 -1	.00000000 0
1000.000	1600,0000	-.50000000 -1	.00000000 0
1500.000	1575,0000	-.50000000 -1	.00000000 0
2000.000	1550,0000	-.50000000 -1	.00000000 0
2500.000	1525,0000	-.50000000 -1	.00000000 0
2900.000	1505,0000	-.50000000 -1	.00000000 0
2950.000	1502,5000	-.50000016 -1	-.64675804 -9
2998.000	1500,1000	-.49999245 -1	.32772313 -7
2998.500	1500,0750	-.49999237 -1	.00000000 0
2999.000	1500,0500	-.49999237 -1	.00000000 0
2999.500	1500,0250	-.49999237 -1	.00000000 0
3000.000	1500,0000	.00000000 0	.19999695 0
3000.500	1500,0250	.49999237 -1	.00000000 0
3001.000	1500,0500	.49999237 -1	.00000000 0
3001.500	1500,0750	.49999237 -1	.00000000 0
3002.000	1500,1000	.49999245 -1	.32772313 -7
3050.000	1502,5000	.50000016 -1	-.64675804 -9
3100.000	1505,0000	.50000000 -1	.00000000 0
3500.000	1525,0000	.50000000 -1	.00000000 0
4000.000	1550,0000	.50000000 -1	.00000000 0
4500.000	1575,0000	.50000000 -1	.00000000 0
5000.000	1600,0000	.50000000 -1	.00000000 0
5500.000	1625,0000	.50000000 -1	.00000000 0
6000.000	1650,0000	.16666667 -1	-.13333333 -3
7000.000	1600,0000	-.11666667 0	-.13333333 -3

TABLE OF VALUES OF EXTRAPOLATED POINTS

DEPTH-METERS	VELOCITY-M/SEC	Z COEFFICIENT	D COEFFICIENT

RAY TRACE ANALYSIS PROGRAM- R D MINIGHAM - (A-201-01)
RAY NUMBER= 1 INITIAL ANGLE= -15.000 DEGREES

BILINEAR

LIST OF TURNING POINTS 0.5166 sec/mile TOTAL TIME 2:35

NUMBER	RANGE NM	DEPTH M	SINE	SECONDS
1	4.3404	1941.7145	.00000000	5.2968
2	13.0213	4058.2855	.00000000	15.8905
3	21.7021	1941.7144	.00000000	26.4842
4	30.3830	4058.2855	.00000000	37.0779
5	39.0639	1941.7145	.00000000	47.6716
6	47.7447	4058.2855	.00000000	58.2653
7	56.4256	1941.7145	.00000000	68.8590
8	65.1064	4058.2855	.00000000	79.4527
9	73.7873	1941.7145	.00000000	90.0463
10	82.4681	4058.2855	.00000000	100.6400
11	91.1490	1941.7145	.00000000	111.2337
12	99.8298	4058.2855	.00000000	121.8274
13	108.5107	1941.7145	.00000000	132.4211
14	117.1915	4058.2855	.00000000	143.0148
15	125.8724	1941.7145	.00000000	153.6084
16	134.5532	4058.2855	.00000000	164.2021
17	143.2341	1941.7145	.00000000	174.7958
18	151.9149	4058.2855	.00000000	185.3895
19	160.5957	1941.7146	.00000000	195.9831
20	169.2766	4058.2855	.00000000	206.5768
21	177.9574	1941.7145	.00000000	217.1705
22	186.6383	4058.2855	.00000000	227.7642
23	195.3191	1941.7145	.00000000	238.3579
24	203.9999	4058.2855	.00000000	248.9516
25	212.6808	1941.7145	.00000000	259.5452
26	221.3616	4058.2855	.00000000	270.1389
27	230.0425	1941.7145	.00000000	280.7326
28	238.7233	4058.2855	.00000000	291.3262
29	247.4042	1941.7145	.00000000	301.9199
30	256.0850	4058.2855	.00000000	312.5136
31	264.7658	1941.7145	.00000000	323.1073
32	273.4467	4058.2854	.00000000	333.7009
33	282.1275	1941.7145	.00000000	344.2946
34	290.8083	4058.2855	.00000000	354.8883
35	299.4892	1941.7145	.00000000	365.4819

LIST OF BOTTOM HITS

NO BOTTOM HITS

LIST OF SURFACE HITS

NO SURFACE HITS

DEPTH M=3000.0000 EPSILON= .1000 DELTA= 250 MIN DELTA= 4 SIN TEST= .020

Table 5.4.2.1

RAY TRACE ANALYSIS PROGRAM- R D MIMINGHAM - (A-201-01)
RAY NUMBER= 2 INITIAL ANGLE= -15.000 DEGREES

BILINEAR

LIST OF TURNING POINTS **0.6333 sec/mile** **TOTAL TIME 3810**

NUMBER	RANGE NM	DEPTH M	SINE	SECONDS
1	4.3404	1941.7145	.00000000	5.2968
2	13.0213	4058.2855	.00000000	15.8905
3	21.7021	1941.7145	.00000000	26.4842
4	30.3830	4058.2855	.00000000	37.0779
5	39.0639	1941.7145	.00000000	47.6716
6	47.7447	4058.2854	.00000000	58.2653
7	56.4256	1941.7146	.00000000	68.8590
8	65.1064	4058.2854	.00000000	79.4526
9	73.7873	1941.7145	.00000000	90.0463
10	82.4681	4058.2855	.00000000	100.6400
11	91.1490	1941.7145	.00000000	111.2337
12	99.8298	4058.2855	.00000000	121.8274
13	108.5107	1941.7145	.00000000	132.4211
14	117.1915	4058.2855	.00000000	143.0148
15	125.8724	1941.7144	.00000000	153.6084
16	134.5532	4058.2855	.00000000	164.2021
17	143.2341	1941.7144	.00000000	174.7958
18	151.9149	4058.2855	.00000000	185.3895
19	160.5957	1941.7145	.00000000	195.9832
20	169.2766	4058.2855	.00000000	206.5768
21	177.9574	1941.7145	.00000000	217.1705
22	186.6382	4058.2855	.00000000	227.7642
23	195.3191	1941.7145	.00000000	238.3579
24	203.9999	4058.2855	.00000000	248.9516
25	212.6807	1941.7145	.00000000	259.5452
26	221.3616	4058.2855	.00000000	270.1389
27	230.0424	1941.7145	.00000000	280.7326
28	238.7232	4058.2855	.00000000	291.3263
29	247.4041	1941.7145	.00000000	301.9199
30	256.0849	4058.2855	.00000000	312.5136
31	264.7657	1941.7145	.00000000	323.1073
32	273.4466	4058.2855	.00000000	333.7009
33	282.1274	1941.7145	.00000000	344.2946
34	290.8082	4058.2855	.00000000	354.8883
35	299.4890	1941.7145	.00000000	365.4819

LIST OF BOTTOM HITS

NO BOTTOM HITS

LIST OF SURFACE HITS

NO SURFACE HITS

DEPTH M=3000.0000 EPSILON= .1000 DELTA= 500 MIN DELTA= 4 SIN TEST= .020

Table 5.4.2.2

RAY TRACE ANALYSIS PROGRAM- R D MININGHAM - (A-201-01)
RAY NUMBER= 3 INITIAL ANGLE= -15.000 DEGREES

BILINEAR

LIST OF TURNING POINTS 0.7833 sec/mile TOTAL TIME 3:55

NUMBER	RANGE NM	DEPTH M	SINE	SECONDS
1	4.3404	1941,7144	,00000000	5,2969
2	13,0213	4058,2855	,00000000	15,8905
3	21,7022	1941,7145	,00000000	26,4842
4	30,3830	4058,2855	,00000000	37,0779
5	39,0639	1941,7145	,00000000	47,6716
6	47,7447	4058,2855	,00000000	58,2653
7	56,4256	1941,7144	,00000000	68,8590
8	65,1064	4058,2855	,00000000	79,4527
9	73,7873	1941,7145	,00000000	90,0464
10	82,4681	4058,2855	,00000000	100,6400
11	91,1490	1941,7145	,00000000	111,2337
12	99,8298	4058,2855	,00000000	121,8274
13	108,5107	1941,7145	,00000000	132,4211
14	117.1915	4058,2855	,00000000	143,0148
15	125,8724	1941,7145	,00000000	153,6085
16	134,5532	4058,2855	,00000000	164,2021
17	143,2341	1941,7145	,00000000	174,7958
18	151,9149	4058,2855	,00000000	185,3895
19	160,5957	1941,7145	,00000000	195,9832
20	169,2765	4058,2855	,00000000	206,5768
21	177,9574	1941,7145	,00000000	217,1705
22	186.6382	4058,2855	,00000000	227,7642
23	195,3190	1941,7145	,00000000	238,3579
24	203,9998	4058,2856	,00000000	248,9516
25	212.6807	1941,7144	,00000000	259,5452
26	221,3615	4058,2855	,00000000	270,1389
27	230,0423	1941,7145	,00000000	280,7326
28	238,7232	4058,2856	,00000000	291,3262
29	247.4040	1941,7145	,00000000	301,9199
30	256,0848	4058,2855	,00000000	312,5136
31	264,7656	1941,7145	,00000000	323,1072
32	273,4465	4058,2855	,00000000	333,7009
33	282,1273	1941,7145	,00000000	344,2946
34	290,8081	4058,2855	,00000000	354,8882
35	299,4889	1941,7145	,00000000	365,4819

LIST OF BOTTOM HITS

NO BOTTOM HITS

LIST OF SURFACE HITS

NO SURFACE HITS

DEPTH M=3000,0000 EPSILON= ,1000 DELTA=1000 MIN DELTA= 4 SIN TEST= ,020

Table 5.4.2.3

RAY TRACE ANALYSIS PROGRAM• R D MININGHAM - (A-201-01)
RAY NUMBER= 4 INITIAL ANGLE= -15,000 DEGREES **BILINEAR**

LIST OF TURNING POINTS **0.9666 sec/mile** **TOTAL TIME 4:50**

NUMBER	RANGE NM	DEPTH M	SINE	SECONDS
1	4,3404	1941,7144	,00000000	5.2969
2	13,0213	4058,2855	,00000000	15,8906
3	21,7022	1941,7145	,00000000	26,4843
4	30,3830	4058,2855	,00000000	37.0779
5	39,0639	1941,7145	,00000000	47,6716
6	47,7447	4058,2855	,00000000	58.2653
7	56,4256	1941,7145	,00000000	68,8590
8	65,1064	4058,2854	,00000000	79,4527
9	73,7873	1941,7145	,00000000	90,0464
10	82,4681	4058,2855	,00000000	100.6401
11	91,1489	1941,7145	,00000000	111,2337
12	99,8298	4058,2855	,00000000	121.8274
13	108.5106	1941.7145	,00000000	132,4211
14	117,1915	4058,2855	,00000000	143,0148
15	125,8723	1941,7145	,00000000	153,6084
16	134,5531	4058,2855	,00000000	164,2021
17	143,2340	1941,7145	,00000000	174,7958
18	151,9148	4058,2855	,00000000	185,3895
19	160,5956	1941,7145	,00000000	195.9831
20	169,2764	4058,2855	,00000000	206,5768
21	177,9572	1941,7145	,00000000	217,1705
22	186,6381	4058,2855	,00000000	227,7642
23	195,3189	1941,7145	,00000000	238,3578
24	203,9997	4058,2855	,00000000	248,9515
25	212,6805	1941,7145	,00000000	259,5452
26	221,3613	4058,2855	,00000000	270,1389
27	230,0421	1941,7145	,00000000	280,7325
28	238,7230	4058,2854	,00000000	291,3262
29	247,4038	1941,7145	,00000000	301,9198
30	256,0846	4058,2854	,00000000	312,5135
31	264,7654	1941,7146	,00000000	323,1071
32	273,4462	4058,2855	,00000000	333,7008
33	282,1270	1941,7145	,00000000	344,2945
34	290,8078	4058,2854	,00000000	354,8881
35	299,4885	1941,7145	,00000000	365,4818

LIST OF BOTTOM HITS

NO BOTTOM HITS

LIST OF SURFACE HITS

NO SURFACE HITS

DEPTH M=3000,0000 EPSILON= ,1000 DELTA=2000 MIN DELTA= 4 SIN TEST= ,020

Table 5.4.2.4

RAY TRACE ANALYSIS PROGRAM- R D MIGHINGHAM - (A-201-01)
RAY NUMBER= 5 INITIAL ANGLE= -15.000 DEGREES

BILINEAR

LIST OF TURNING POINTS 0.3000 sec/mile TOTAL TIME 1:30

NUMBER	RANGE NM	DEPTH M	SINE	SECONDS
1	4.3394	1941.7145	.00000000	5.2954
2	13.0202	4058.2855	.00000000	15.8891
3	21.7011	1941.7145	.00000000	26.4828
4	30.3819	4058.2855	.00000000	37.0765
5	39.0618	1941.7144	.00000000	47.6689
6	47.7427	4058.2855	.00000000	58.2626
7	56.4234	1941.7144	.00000000	68.8561
8	65.1043	4058.2855	.00000000	79.4498
9	73.7843	1941.7145	.00000000	90.0424
10	82.4651	4058.2855	.00000000	100.6360
11	91.1457	1941.7145	.00000000	111.2293
12	99.8265	4058.2855	.00000000	121.8230
13	108.5064	1941.7145	.00000000	132.4154
14	117.1873	4058.2856	.00000000	143.0091
15	125.8681	1941.7145	.00000000	153.6027
16	134.5489	4058.2855	.00000000	164.1964
17	143.2289	1941.7145	.00000000	174.7889
18	151.9098	4058.2855	.00000000	185.3826
19	160.5903	1941.7145	.00000000	195.9758
20	169.2711	4058.2855	.00000000	206.5695
21	177.9511	1941.7145	.00000000	217.1620
22	186.6319	4058.2855	.00000000	227.7557
23	195.3127	1941.7145	.00000000	238.3492
24	203.9935	4058.2855	.00000000	248.9429
25	212.6735	1941.7145	.00000000	259.5354
26	221.3544	4058.2855	.00000000	270.1291
27	230.0349	1941.7145	.00000000	280.7223
28	238.7157	4058.2855	.00000000	291.3160
29	247.3956	1941.7144	.00000000	301.9085
30	256.0765	4058.2855	.00000000	312.5021
31	264.7573	1941.7145	.00000000	323.0957
32	273.4361	4058.2855	.00000000	333.6894
33	282.1181	1941.7144	.00000000	344.2819
34	290.7989	4058.2855	.00000000	354.8756
35	299.4795	1941.7146	.00000000	365.4688

LIST OF BOTTOM HITS

NO BOTTOM HITS

LIST OF SURFACE HITS

NO SURFACE HITS

DEPTH M=3000.0000 EPSILON= .1000 DELTA=1000 MIN DELTA= 25 SIN TEST= .020

Table 5.4.2.5

RAY TRACE ANALYSIS PROGRAM- R D MIGGINGHAM - (A-201-01)
RAY NUMBER= 6 INITIAL ANGLE= -15.000 DEGREES

BILINEAR

LIST OF TURNING POINTS **0.3166 sec/mile** **TOTAL TIME 1:35**

NUMBER	RANGE NM	DEPTH M	SINE	SECONDS
1	4,3387	1941,7144	,00000000	5.2946
2	13,0196	4058,2855	,00000000	15,8883
3	21,7004	1941,7145	,00000000	26.4820
4	30,3813	4058,2855	.00000000	37,0757
5	39.0621	1941.7145	,00000000	47.6694
6	47,7430	4058.2855	,00000000	58.2630
7	56.4238	1941.7145	,00000000	68.8567
8	65,1047	4058,2855	,00000000	79,4504
9	73.7855	1941,7145	,00000000	90.0441
10	82,4663	4058,2855	,00000000	100.6377
11	91.1471	1941.7145	,00000000	111.2314
12	99,8280	4058,2855	,00000000	121.8250
13	108,5084	1941,7145	,00000000	132.4181
14	117,1892	4058.2855	,00000000	143.0118
15	125,8701	1941,7145	,00000000	153,6055
16	134,5509	4058,2855	,00000000	164,1992
17	143,2318	1941,7145	,00000000	174,7928
18	151,9126	4058,2855	,00000000	185,3865
19	160,5935	1941,7145	,00000000	195,9802
20	169,2743	4058,2855	,00000000	206.5739
21	177,9551	1941,7145	,00000000	217,1676
22	186,6360	4058,2854	,00000000	227.7612
23	195,3168	1941,7145	,00000000	238.3549
24	203,9976	4058,2855	,00000000	248,9485
25	212,6784	1941,7146	,00000000	259,5422
26	221,3590	4058.2855	,00000000	270.1355
27	230,0395	1941.7145	,00000000	280.7288
28	238,7204	4058,2855	,00000000	291,3225
29	247,4012	1941,7146	,00000000	301.9162
30	256,0821	4058,2854	,00000000	312.5099
31	264,7629	1941,7145	,00000000	323,1035
32	273,4438	4058,2855	,00000000	333.6972
33	282,1246	1941.7145	,00000000	344,2909
34	290,8054	4058,2855	,00000000	354.8846
35	299,4863	1941,7145	,00000000	365.4782

LIST OF BOTTOM HITS

NO BOTTOM HITS

LIST OF SURFACE HITS

NO SURFACE HITS

DEPTH M=3000,0000 EPSILON= ,1000 DELTA=2000 MIN DELTA= 25 SIN TEST= ,020

Table 5.4.2.6

TRACE ANALYSIS PROGRAM- R D MININGHAM - (A-201-01)
NUMBER= 7 INITIAL ANGLE= -15,000 DEGREES

BILINEAR

OF TURNING POINTS 0.2333 sec/mile

TOTAL TIME 1:10

NUMBER	RANGE NM	DEPTH M	SINE	SECONDS
1	,0427	2984,7695	,00000000	,0526
2	4,1785	4058,2856	,00000000	5,0894
3	12,8586	1941,7145	,00000000	15,6822
4	21,5388	4058,2855	,00000000	26,2752
5	30,2192	1941,7145	,00000000	36,8684
6	38,8998	4058,2855	,00000000	47,4617
7	47,5804	1941,7145	,00000000	58,0552
8	56,2612	4058,2855	,00000000	68,6488
9	64,9420	1941,7145	,00000000	79,2424
10	73,6229	4058,2855	,00000000	89,8361
11	82,3029	1941,7145	,00000000	100,4289
12	90,9832	4058,2855	,00000000	111.0219
13	99,6636	1941,7145	.00000000	121,6151
14	108,3441	4058,2854	,00000000	132,2084
15	117,0248	1941,7145	,00000000	142,8019
16	125,7055	4058,2855	,00000000	153,3954
17	134,3863	1941,7145	.00000000	163,9891
18	143,0672	4058,2855	,00000000	174.5827
19	151,7052	1941,7145	,00000000	185,1235
20	160,3857	4058,2855	,00000000	195,7168
21	169,0663	1941,7145	,00000000	206.3102
22	177,7470	4058,2855	,00000000	216,9038
23	186,4278	1941,7145	,00000000	227,4974
24	195,1086	4058,2855	,00000000	238,0911
25	203,7895	1941,7145	,00000000	248,6847
26	212,4697	4058,2855	,00000000	259,2777
27	221,1501	1941,7145	,00000000	269,8708
28	229,8306	4058,2855	,00000000	280,4641
29	238,5112	1941,7145	,00000000	291,0575
30	247,1919	4058,2854	,00000000	301,6511
31	255,8727	1941,7145	,00000000	312,2447
32	264,5535	4058,2855	,00000000	322,8384
33	273,2176	1941,7145	,00000000	333,4116
34	281,8985	4058,2855	,00000000	344,0052
35	290,5793	1941,7144	,00000000	354,5989
36	299,2594	4058,2855	,00000000	365,1918

OF BOTTOM HITS

0 BOTTOM HITS

OF SURFACE HITS

0 SURFACE HITS

M=3000,0000 EPSILON= ,1000 DELTA=1000 MIN DELTA=100 SIN TEST= ,020

Table 5.4.2.7

RAY TRACE ANALYSIS PROGRAM• R D MINIGHAM - (A-201-01)
RAY NUMBER= 8 INITIAL ANGLE= -15,000 DEGREES

BILINEAR

LIST OF TURNING POINTS **0.3000 sec/mile** **TOTAL TIME 1:30**

NUMBER	RANGE NM	DEPTH M	SINE	SECONDS
1	4,3403	1941,7145	,00000000	5.2966
2	13,0211	4058,2855	,00000000	15,8903
3	21,7019	1941,7144	,00000000	26.4839
4	30,3828	4058,2855	,00000000	37,0776
5	39,0636	1941,7146	,00000000	47,6713
6	47,7444	4058,2855	,00000000	58,2649
7	56,4253	1941,7145	,00000000	68,8586
8	65,1061	4058,2855	,00000000	79,4522
9	73,7869	1941,7145	,00000000	90,0459
10	82,4677	4058,2854	,00000000	100,6395
11	91,1486	1941,7145	,00000000	111,2332
12	99,8294	4058,2855	,00000000	121,8269
13	108,5102	1941,7145	,00000000	132,4205
14	117,1911	4058,2855	,00000000	143,0142
15	125,8719	1941,7145	,00000000	153,6078
16	134,5527	4058,2855	,00000000	164,2015
17	143,2335	1941,7145	,00000000	174,7951
18	151,9144	4058,2855	,00000000	185,3888
19	160,5952	1941,7144	,00000000	195,9824
20	169,2760	4058,2855	,00000000	206,5761
21	177,9568	1941,7146	,00000000	217,1697
22	186,6376	4058,2855	,00000000	227,7634
23	195,3185	1941,7145	,00000000	238,3570
24	203,9993	4058,2855	,00000000	248,9507
25	212,6801	1941,7145	,00000000	259,5444
26	221,3609	4058,2855	,00000000	270,1380
27	230,0417	1941,7145	,00000000	280,7316
28	238,7226	4058,2855	,00000000	291,3253
29	247,4034	1941,7145	,00000000	301,9189
30	256,0842	4058,2855	,00000000	312,5126
31	264,7650	1941,7145	,00000000	323,1062
32	273,4458	4058,2854	,00000000	333,6999
33	282,1267	1941,7145	,00000000	344,2935
34	290,8075	4058,2855	,00000000	354,8872
35	299,4883	1941,7145	,00000000	365,4808

LIST OF BOTTOM HITS

NO BOTTOM HITS

LIST OF SURFACE HITS

NO SURFACE HITS

DEPTH M=3000,0000 EPSILON=1,0000 DELTA= 500 MIN DELTA= 20 SIN TEST= .020

Table 5.4.2.8

RAY TRACE ANALYSIS PROGRAM- R D MIDDINGHAM - (A-201-01)
RAY NUMBER= 9 INITIAL ANGLE= -15.000 DEGREES

BILINEAR

LIST OF TURNING POINTS **0.2500 sec/mile** **TOTAL TIME 1:15**

NUMBER	RANGE NM	DEPTH M	SINE	SECONDS
1	4,3401	1941.7145	,00000000	5,2963
2	13,0209	4058,2855	,00000000	15,8900
3	21,7017	1941,7144	,00000000	26,4837
4	30,3826	4058,2855	,00000000	37,0774
5	39,0635	1941,7145	,00000000	47,6711
6	47,7443	4058,2856	,00000000	58,2647
7	56,4252	1941,7144	,00000000	68,8584
8	65,1060	4058,2855	,00000000	79,4521
9	73,7869	1941,7144	,00000000	90,0458
10	82.4677	4058.2855	,00000000	100.6395
11	91,1486	1941,7145	,00000000	111,2332
12	99,8294	4058,2855	,00000000	121,8268
13	108,5103	1941,7145	,00000000	132.4205
14	117,1911	4058,2855	,00000000	143,0142
15	125,8720	1941,7145	,00000000	153,6079
16	134,5528	4058,2855	,00000000	164,2015
17	143,2336	1941,7145	,00000000	174,7952
18	151,9145	4058,2855	.00000000	185,3889
19	160,5953	1941,7145	,00000000	195,9826
20	169,2762	4058,2855	,00000000	206,5763
21	177,9570	1941,7145	,00000000	217,1699
22	186,6379	4058,2855	,00000000	227,7636
23	195,3187	1941,7145	,00000000	238,3573
24	203,9996	4058,2855	,00000000	248,9510
25	212,6804	1941,7145	,00000000	259,5447
26	221,3613	4058,2854	,00000000	270,1383
27	230,0421	1941,7145	,00000000	280,7320
28	238,7230	4058,2854	,00000000	291,3257
29	247,4038	1941,7145	,00000000	301,9194
30	256,0846	4058,2855	,00000000	312,5130
31	264,7655	1941,7145	,00000000	323,1067
32	273,4463	4058,2854	,00000000	333,7004
33	282,1272	1941,7145	,00000000	344,2940
34	290,8080	4058,2855	,00000000	354,8877
35	299,4889	1941,7145	,00000000	365,4814

LIST OF BOTTOM HITS

NO BOTTOM HITS

LIST OF SURFACE HITS

NO SURFACE HITS

DEPTH M=3000,0000 EPSILON=1,0000 DELTA=1000 MIN DELTA= 20 SIN TEST= ,020

Table 5.4.2.9

RAY TRACE ANALYSIS PROGRAM- R D MILLINGHAM - (A-201-01)
RAY NUMBER= 10 INITIAL ANGLE= -15.000 DEGREES

BILINEAR

LIST OF TURNING POINTS **0.2166 sec/mile** **TOTAL TIME 1:05**

NUMBER	RANGE NM	DEPTH M	SINE	SECONDS
1	4.3398	1941,7145	.00000000	5.2960
2	13,0206	4058,2855	.00000000	15,8897
3	21,7014	1941,7145	,00000000	26.4832
4	30,3822	4058,2855	,00000000	37.0769
5	39,0630	1941,7145	,00000000	47,6705
6	47,7438	4058,2855	,00000000	58,2641
7	56,4246	1941,7146	,00000000	68.8578
8	65,1054	4058.2854	.00000000	79.4514
9	73,7863	1941,7145	,00000000	90,0451
10	82,4671	4058,2855	.00000000	100,6387
11	91,1478	1941,7145	,00000000	111,2323
12	99,8287	4058.2855	.00000000	121.8260
13	108,5094	1941.7145	,00000000	132.4195
14	117,1903	4058,2855	,00000000	143,0132
15	125,8711	1941,7145	,00000000	153.6068
16	134,5518	4058.2855	,00000000	164.2004
17	143.2327	1941,7146	,00000000	174.7941
18	151.9134	4058.2855	,00000000	185.3877
19	160,5943	1941,7145	,00000000	195.9814
20	169.2751	4058,2855	.00000000	206.5750
21	177,9558	1941,7146	.00000000	217.1685
22	186,6367	4058,2855	.00000000	227.7622
23	195,3174	1941.7145	,00000000	238,3558
24	203,9983	4058,2855	,00000000	248.9495
25	212,6791	1941,7145	,00000000	259.5431
26	221,3598	4058,2855	,00000000	270,1367
27	230,0407	1941,7145	,00000000	280,7304
28	238,7214	4058,2854	,00000000	291,3239
29	247,4023	1941,7145	,00000000	301.9176
30	256,0831	4058,2855	,00000000	312.5112
31	264,7638	1941.7146	.00000000	323.1048
32	273,4447	4058,2855	,00000000	333,6985
33	282,1254	1941,7145	,00000000	344,2920
34	290,8063	4058.2854	.00000000	354.8857
35	299,4871	1941,7145	,00000000	365,4793

LIST OF BOTTOM HITS

NO BOTTOM HITS

LIST OF SURFACE HITS

NO SURFACE HITS

DEPTH M=3000,0000 EPSILON=1,0000 DELTA=2000 MIN DELTA= 20 SIN TEST= .020

Table 5.4.2.10

RAY TRACE ANALYSIS PROGRAM- R D HIGINGHAM - (A-201-01)
RAY NUMBER= 11 INITIAL ANGLE= -15,000 DEGREES

BILINEAR

LIST OF TURNING POINTS 0.2000 **sec/mile** **TOTAL TIME 1:00**

NUMBER	RANGE NM	DEPTH M	SINE	SECONDS
1	.0427	2984,7695	,00000000	,0526
2	4,1785	4058,2856	,00000000	5,0894
3	12,8585	1941.7145	.00000000	15.6822
4	21,5367	4058.2855	,00000000	26.2728
5	30,2175	1941,7145	.00000000	36.8664
6	38,8960	4058,2855	,00000000	47.4575
7	47,5768	1941,7145	,00000000	58.0511
8	56,2554	4058,2855	,00000000	68,6422
9	64,9362	1941,7145	,00000000	79,2359
10	73,6148	4058,2855	.00000000	89.8269
11	82,2956	1941,7145	,00000000	100,4206
12	90,9741	4058,2855	,00000000	111,0117
13	99,6549	1941,7145	,00000000	121.6053
14	108,3335	4058,2855	,00000000	132,1964
15	117,0143	1941.7145	,00000000	142,7900
16	125,6929	4058,2855	,00000000	153,3811
17	134,3737	1941,7145	,00000000	163,9747
18	143.0522	4058,2655	,00000000	174.5658
19	151.7330	1941,7145	,00000000	185,1594
20	160,4116	4058.2855	,00000000	195,7505
21	169,0924	1941,7145	.00000000	206,3441
22	177,7709	4058.2855	.00000000	216,9352
23	186,4518	1941,7145	,00000000	227,5288
24	195.1303	4058.2855	.00000000	238,1199
25	203.8111	1941.7145	.00000000	248,7136
26	212,4897	4058,2855	.00000000	259,3046
27	221.1705	1941.7145	.00000000	269.8983
28	229,8490	4058,2855	,00000000	280,4893
29	238.5298	1941,7145	.00000000	291.0830
30	247.2084	4058.2854	,00000000	301,6741
31	255.8892	1941,7145	,00000000	312,2677
32	264,5677	4058,2855	.00000000	322,8588
33	273,2486	1941,7145	,00000000	333,4524
34	281.9271	4058.2855	,00000000	344,0435
35	290.6079	1941.7145	.00000000	354.6371
36	299,2865	4058,2854	,00000000	365,2282

LIST OF BOTTOM HITS

NO BOTTOM HITS

LIST OF SURFACE HITS

NO SURFACE HITS

DEPTH M=3000.0000 EPSILON=5,0000 DELTA=1000 MIN DELTA=100 SIN TEST= ,020

Table 5.4.2.11

5.5. Real Velocity Field

In 1967 Hudson Laboratories conducted an experiment during which Sippican X BT casts were taken to a depth of 750 meters (T-7 probes) at regular range intervals. These data, together with several deep velocimeter casts, were used to construct the total velocity field consisting of the profiles shown in Figs. 39 through 58 and the tabulated data of Tables 5.5.1.1 through 5.5.1.20. Additionally, bottom depth entries were made at intervals of one mile or less over the total range of 350 miles. Type II intensity calculations (Chapter IV) were made on the basis of 251 rays that were traced in the velocity field. Ray calculations for two of the initial angles are presented in this Chapter. The origin of the rays was at 2331.7 meters depth.

5.5.1. The 14.80° Ray

The 14.80° ray propagated in either an RSR mode or through multiple surface and bottom reflections depending on the bottom contour. The ray was terminated at about 250.6 miles as a result of striking the side of a steep seamount. The results of the calculations for eleven sets of control parameters are shown in Tables 5.5.2.1 through 5.5.2.11. The most accurate values are those of Table 5.5.2.1. Summary comments of these data are:

i. The drop in computer running time for an increase in Δ_m from 25 to 100 meters shows that the control parameters sensing the detail in the velocity profiles were reducing the iteration increment to less than 100 meters over a large fraction of the ray path, even when the maximum iteration increment was limited to 250 meters.

ii. The increase in running time when the S-test parameter was raised from 0.020 to 0.100 indicates that the subsequent ε-test is required to produce greater truncation of the iteration increment when it is not pre-limited by the S-test.

iii. Some increase in the computer running time over that of the previous two tests is due to the requirement that the tape readers that provide the velocity profile data into active memory must take extra time to read-in the consecutive velocity profiles as their ranges are crossed by the advancing ray. This implies that the time required per ray mile will increase with the number of vertical profile entries used to define the sound velocity field.

iv. The reasonable agreement between tests for which the S-test control was 0.020 and those for which it was 0.100 indicate that the iteration increments are not being limited by the accuracy of the iteration expansion as much as they are by the ε-test, insofar as these effects are separable. That is, the truncation of Δ is primarily due to the limiting of Δ as the ray attempts to follow the detailed structure of the velocity field.

v. The data of Table 5.5.2.10, for which ε was increased from 0.40 to 1.00, is in rough agreement with the more accurate data of Table 5.5.2.1 at the final range of the bottom hit at 250.6 miles. However, the fluctuations of the preceding turning point ranges, or the ranges of the preceding surface and bottom hits, with respect to Table 5.5.2.1, are noticeably greater than are the comparable data of Table 5.5.2.3, for which ε was 0.40. This indicates a general tendency for the errors in the ray positions to tend to cancel as the rays pass through velocity profiles with sharply changing curvatures, viz Chapter III-3.4. In this sense the use of a large ε can be considered as a rough averaging procedure for a profile's detailed structure; the semi-invariant test assists and controls this process by correcting the ray angle at each iteration to be in agreement with the given velocity field. At turning points of the ray, however, the semi-invariant test becomes less effective. Formally precise results in these regions require that ε be made small, as will be apparent in the discussion of the 12.80° ray.

5.5.2. The 12.80° Ray

The 12.80° ray did not make surface or bottom hits in its transit, but did cycle across the full depth of the ocean with an upper turning point approximately 60 meters below the sea surface. The path of this ray, therefore, was especially sensitive to the fluctuations in the upper water structure.

The comments given for the 14.80° ray will also apply to the 12.80° ray, except that the variations of the turning point ranges as a function of the control parameters are greater for the 12.80° ray.

The comments given at the end of Chapter III emphasize that if the vertical profiles of the velocity field are complex, in the sense that the gradients and curvatures change rapidly as a function of depth, there will be significant wavefront distortion and this will appear as an aberration of the plot of the ray depth distribution at a given range. More precisely, the range period of the cycling ray will depend upon the specific structure of the velocity field over the path of the ray and this will lead to fluctuations of the magnification factor that is defined for rays with nearly infinitesimal increments in their initial angles. In long-range propagation one must expect not only the major caustics and foci that are obtained from smoothed data inputs that represent long-term averages of the velocity field but at any one time there will be many secondary caustics that can be regarded as being due to the wavefront aberration. These effects increase with range and they are one reason why the present program computes intensity as a weighted average of many rays, as has been discussed in Chapter IV.

The 12.80° ray is presented here as an excellent example of the difficulties that are implicit in the entire method of ray tracing in inhomogeneous media. The shallow turning point of this ray, at 261 miles, occurred at a depth that was just above a very shallow secondary sound channel - this channel was, in fact, introduced by the velocity field construction program as it attempted to smooth the transition across an abrupt change in slope of the temperature of the thermocline. Additionally, the channel was not present in the velocity profile that was entered at the range 243 miles but was found in the profile at 263 miles; the physical existence of the channel, at the time the ship transited these ranges, was further indicated at the subsequent profile range of 273 miles where it appeared somewhat more strongly and at a slightly deeper depth.

In short, the shallow turning-point depth of the 12.80° ray was just above the weak sound channel. As indicated by the most accurate ray tracing summaries of Tables 5.5.3.1 - 5.5.3.11, the ray was able to continue turning and proceeded to deeper depths. The results of Tables 5.5.3.6, 7, 9 were obtained for less stringent values of the control parameters and for these the ray became trapped for several oscillations in the slight secondary channel. It is to be noted that this trapping could have been obtained for a very slight change in the initial ray angle and for the most accurate ray tracing; conversely, Table 5.5.3.9 shows that relaxation of the ε-test to allow an uncertainty of 1.0 meter/sec also permitted the trapping to occur. Whether this type of trapping actually did occur in the experiment would require analysis of the measurement accuracy of the velocity profile structure and would also require detailed interpretation of the experimental results. This question is less important than the general result of the ray tracing program that the set of rays with turning points in this region showed a marked distortion in the ray magnification function for these rays. In any event, and for low acoustical frequencies with wavelengths of the order of tens of meters, the limited depth interval of only a few meters of the sound channel of this example could be expected to have only a minor physical effect on an extended wavefront.

It has been remarked that the variation in the ranges of the turning points as a function of the control parameters was more marked for the 12.80° ray than for the 14.80° ray, primarily because the steeper angle of the latter ray made it less sensitive to the detail of the upper thermocline structure than was the case for the rays with turning points in this region. However, the precision of the most accurate ray tracing of the 12.80° ray, Table 5.5.3.1, was confirmed independently by the reversibility test presented in the next section.

DEEP PROFILE AT RANGE .000 MILES TEMP AT OBSERVED MAXIMUM DEPTH= 2.209 DEG CENTIGRADE

VELOCITY VS DEPTH

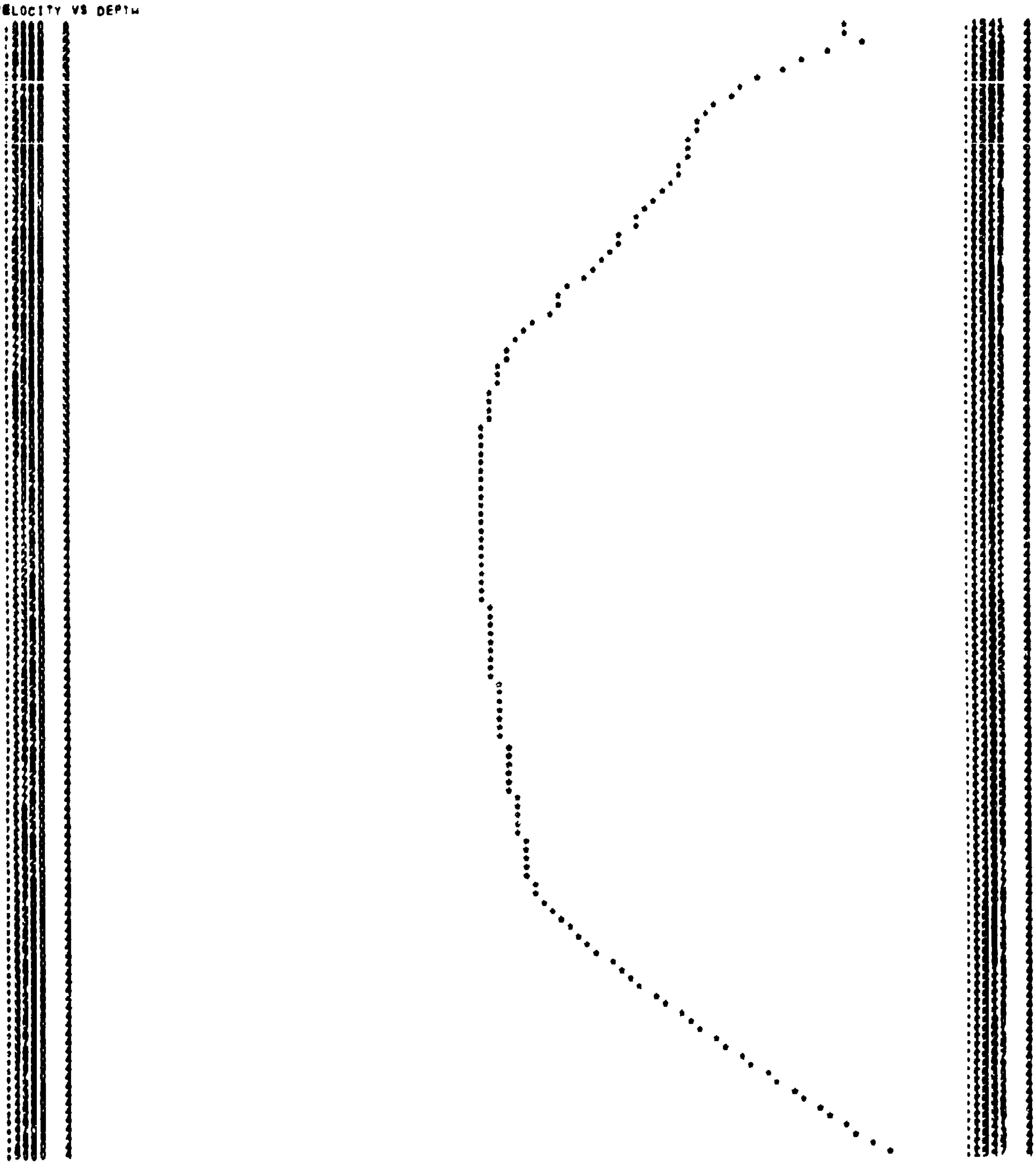

Fig. 39.

SHALLOW PROFILE AT RANGE 50.200 MILES

VELOCITY VS DEPTH

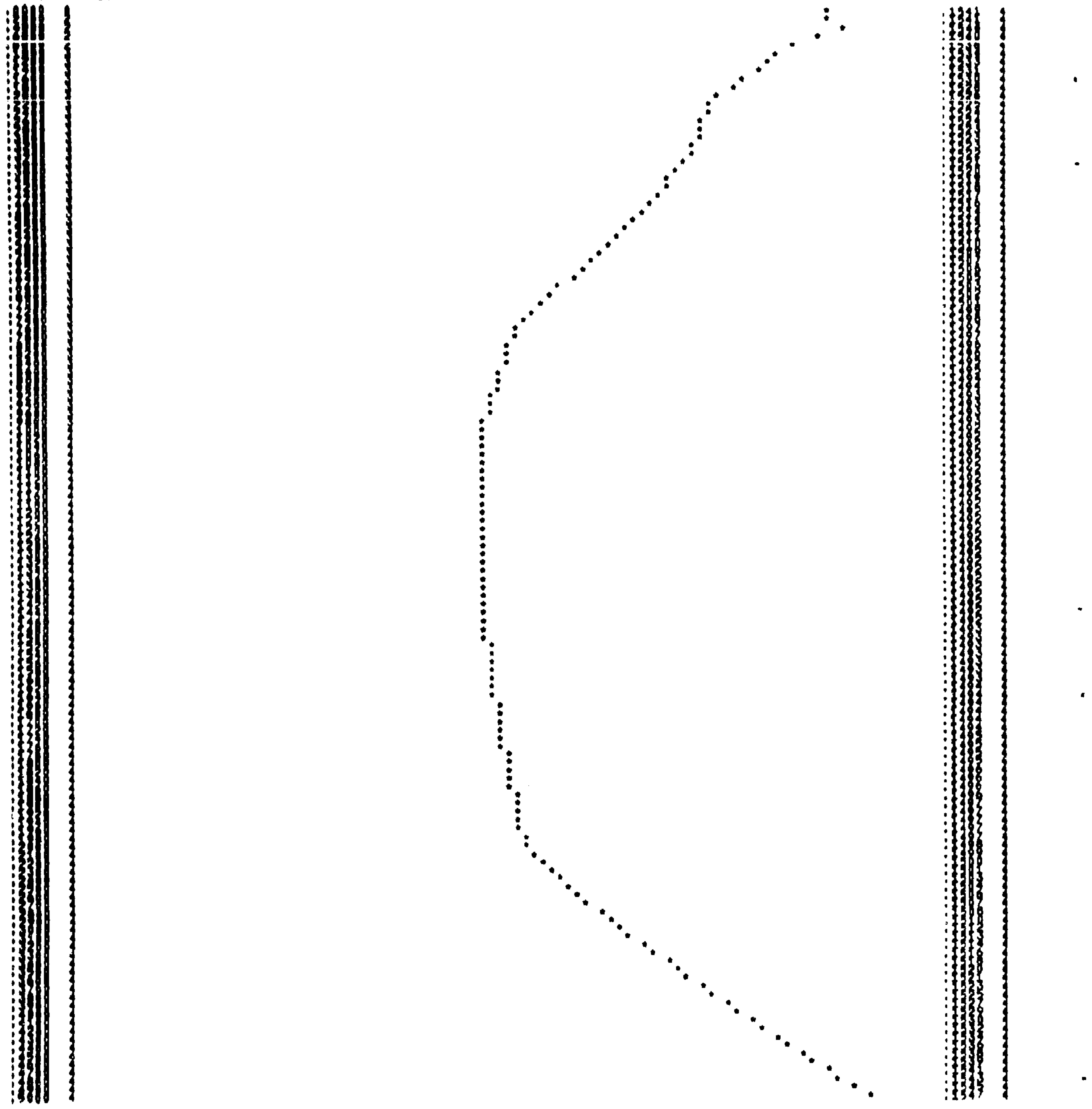

Fig. 40.

SHALLOW PROFILE AT RANGE 74.400 MILES

VELOCITY VS DEPTH

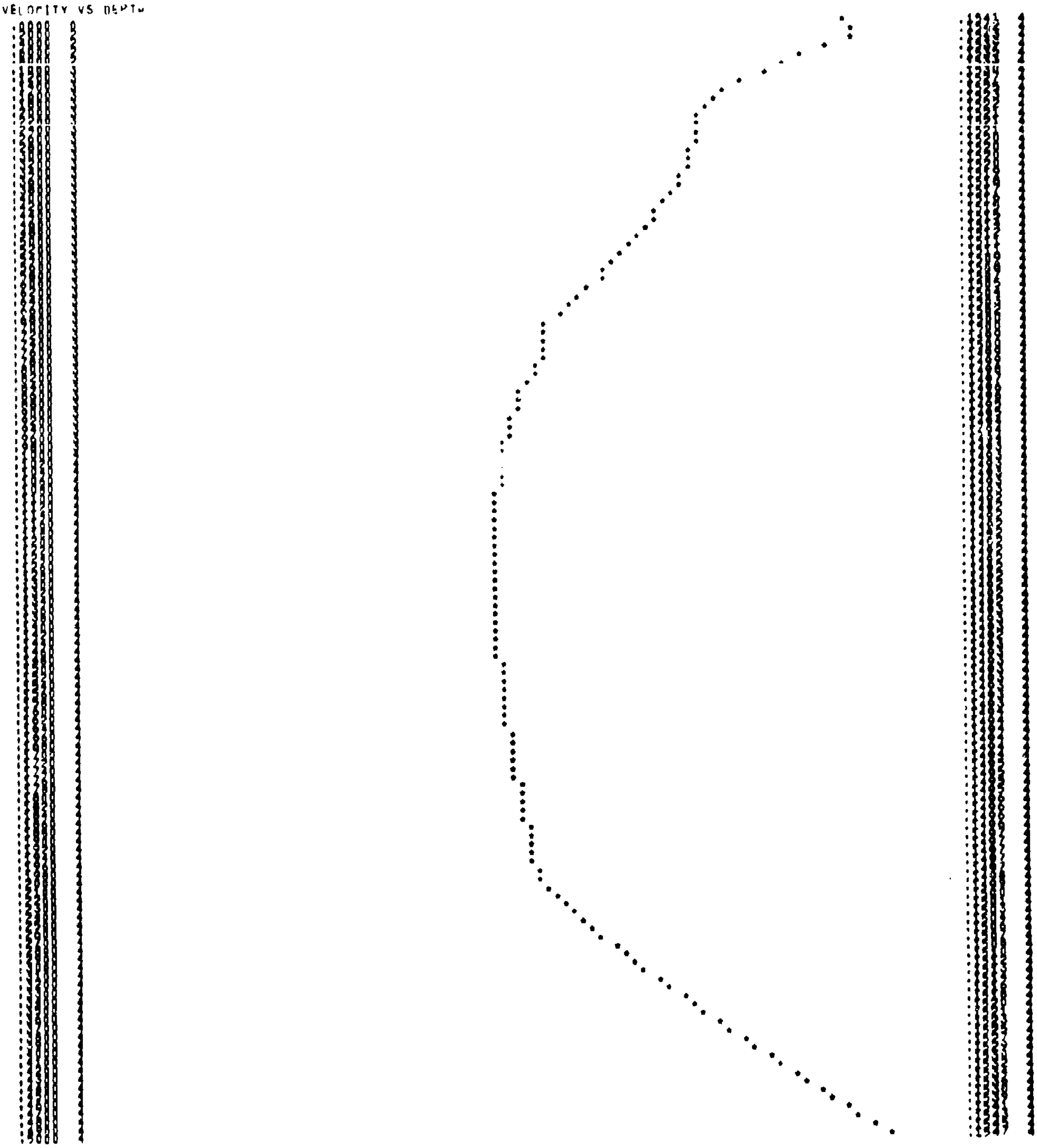

Fig. 41.

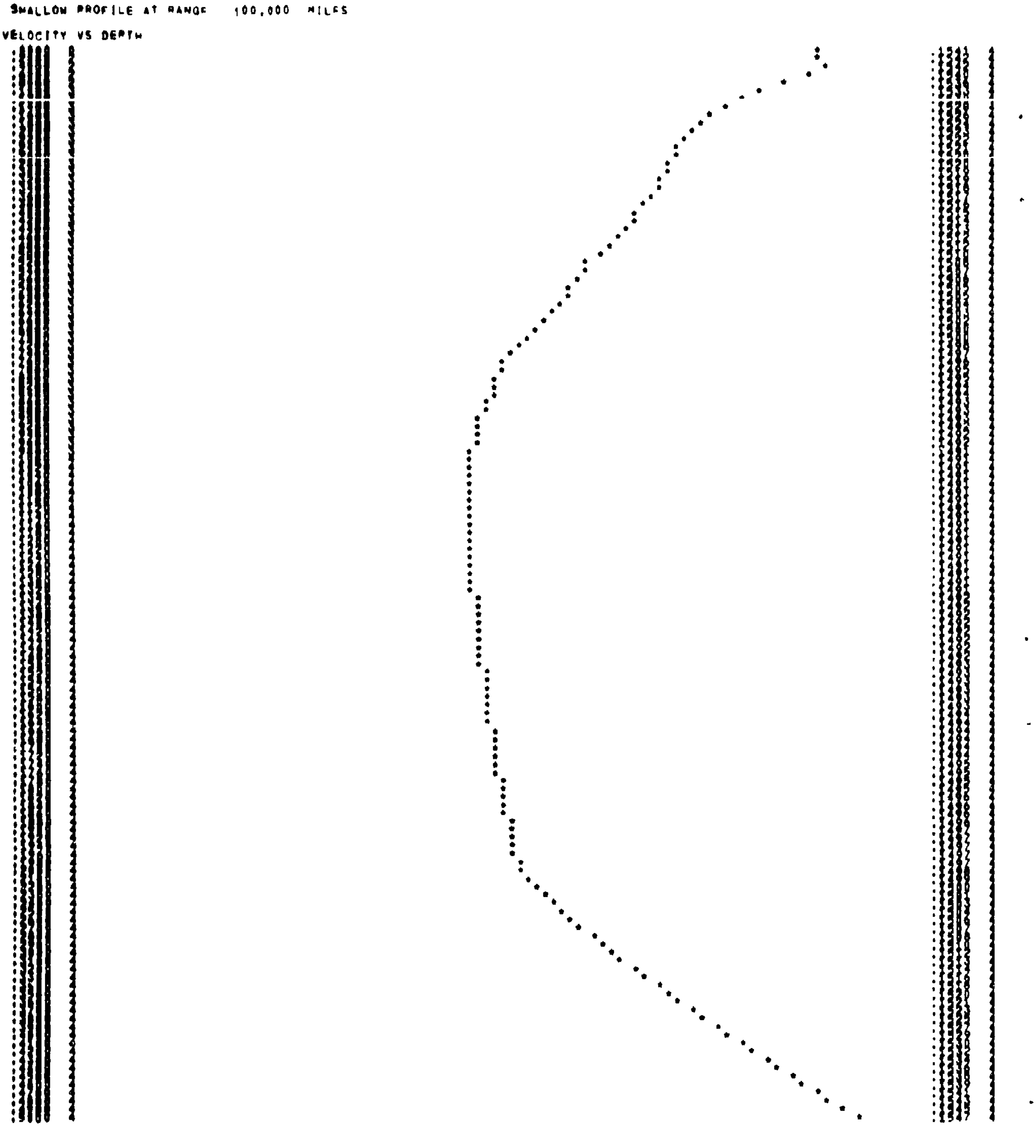

Fig. 42.

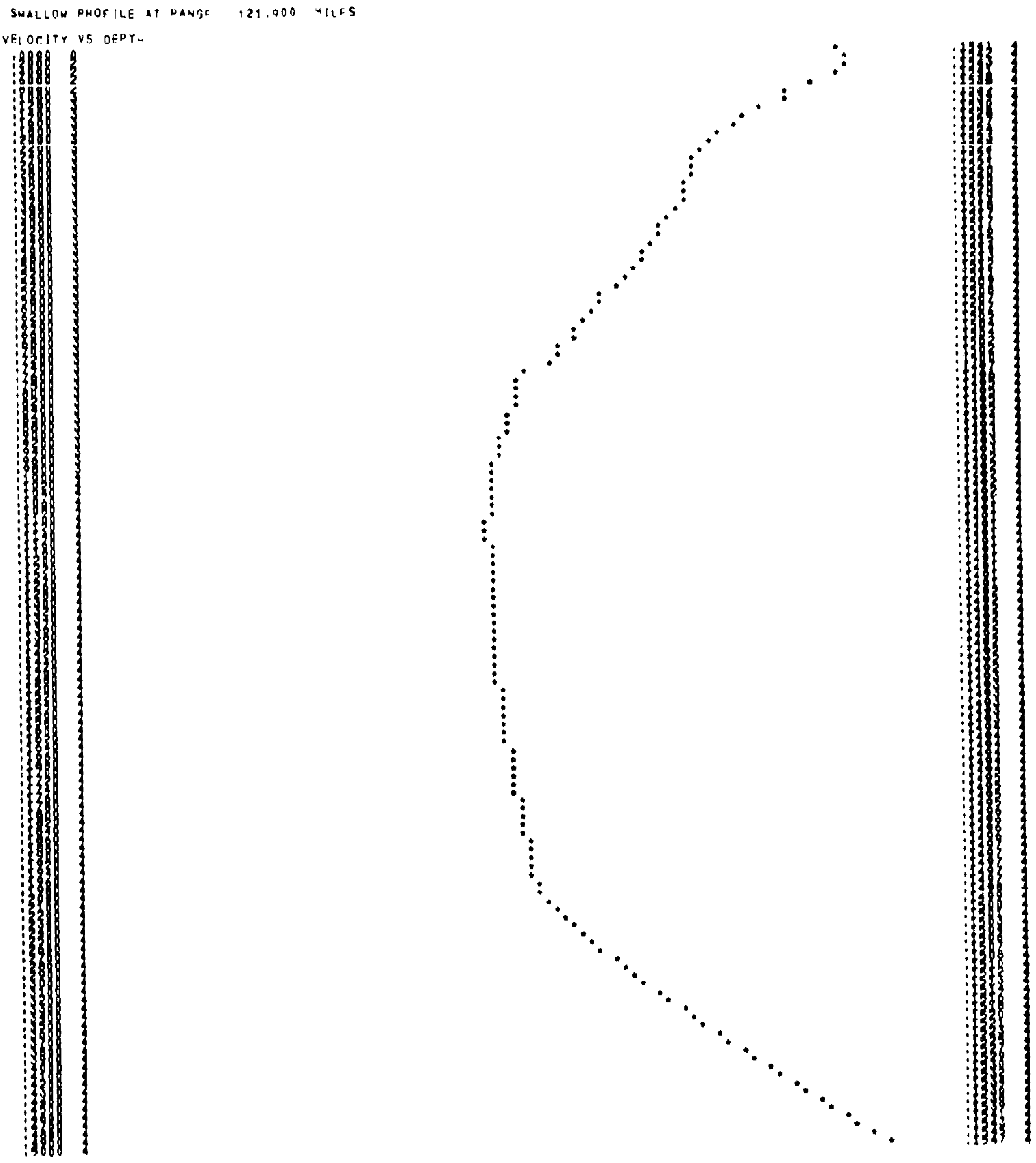

Fig. 43.

SHALLOW PROFILE AT RANGE 144.43 MILES

VELOCITY VS DEPTH

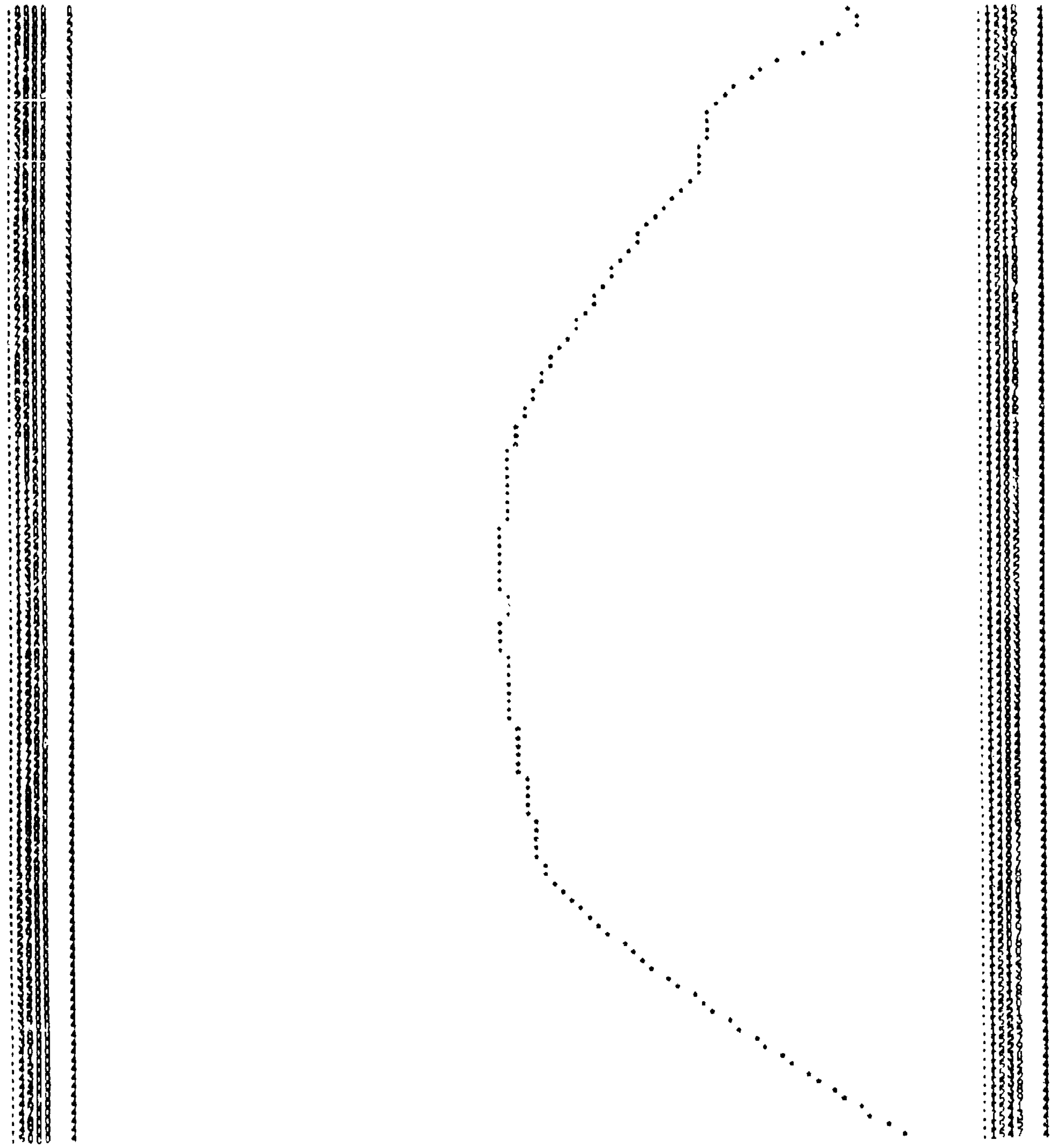

Fig. 44.

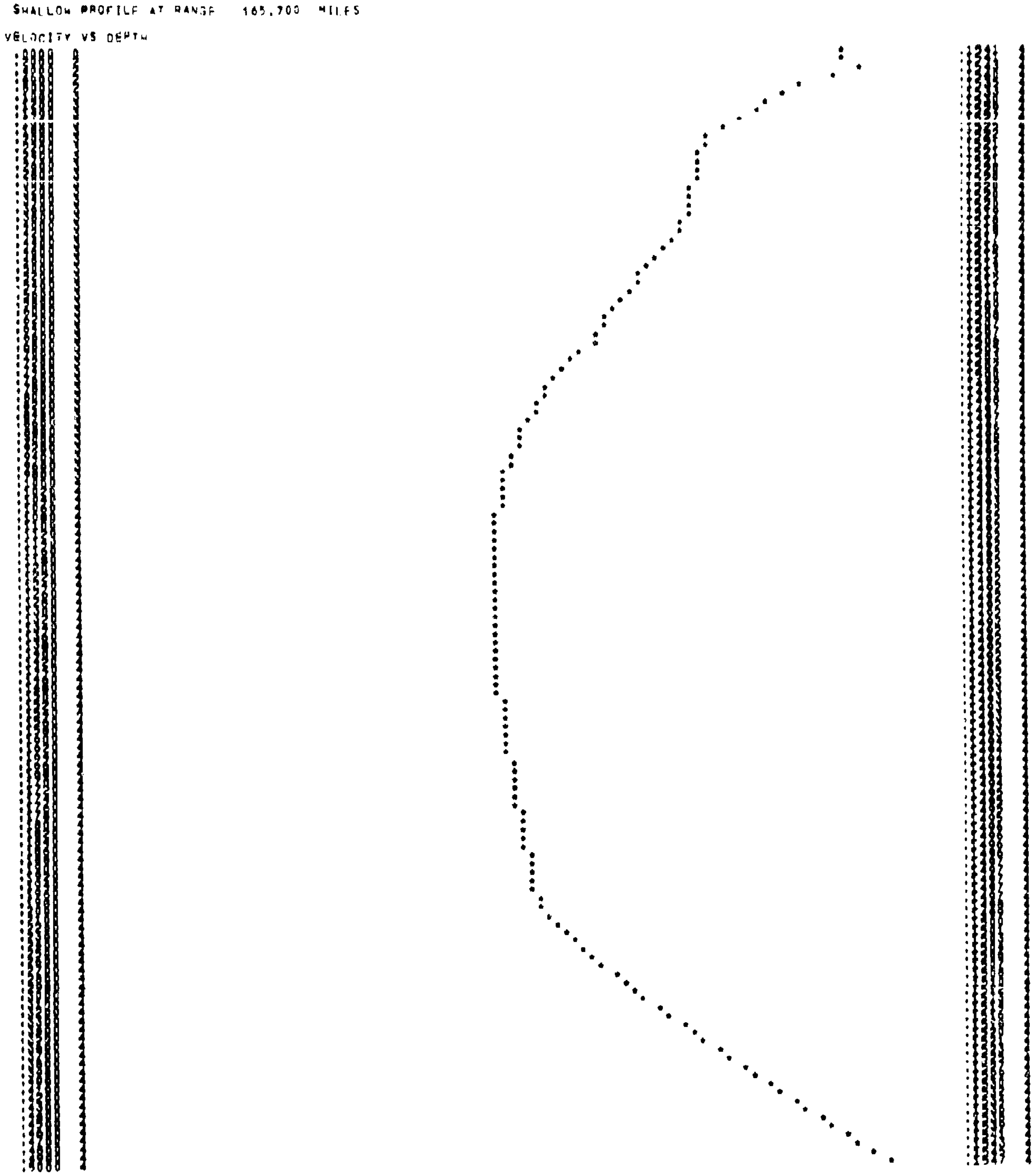

Fig. 45.

SHALLOW PROFILE AT RANGE 175.000 MILES

VELOCITY VS DEPTH

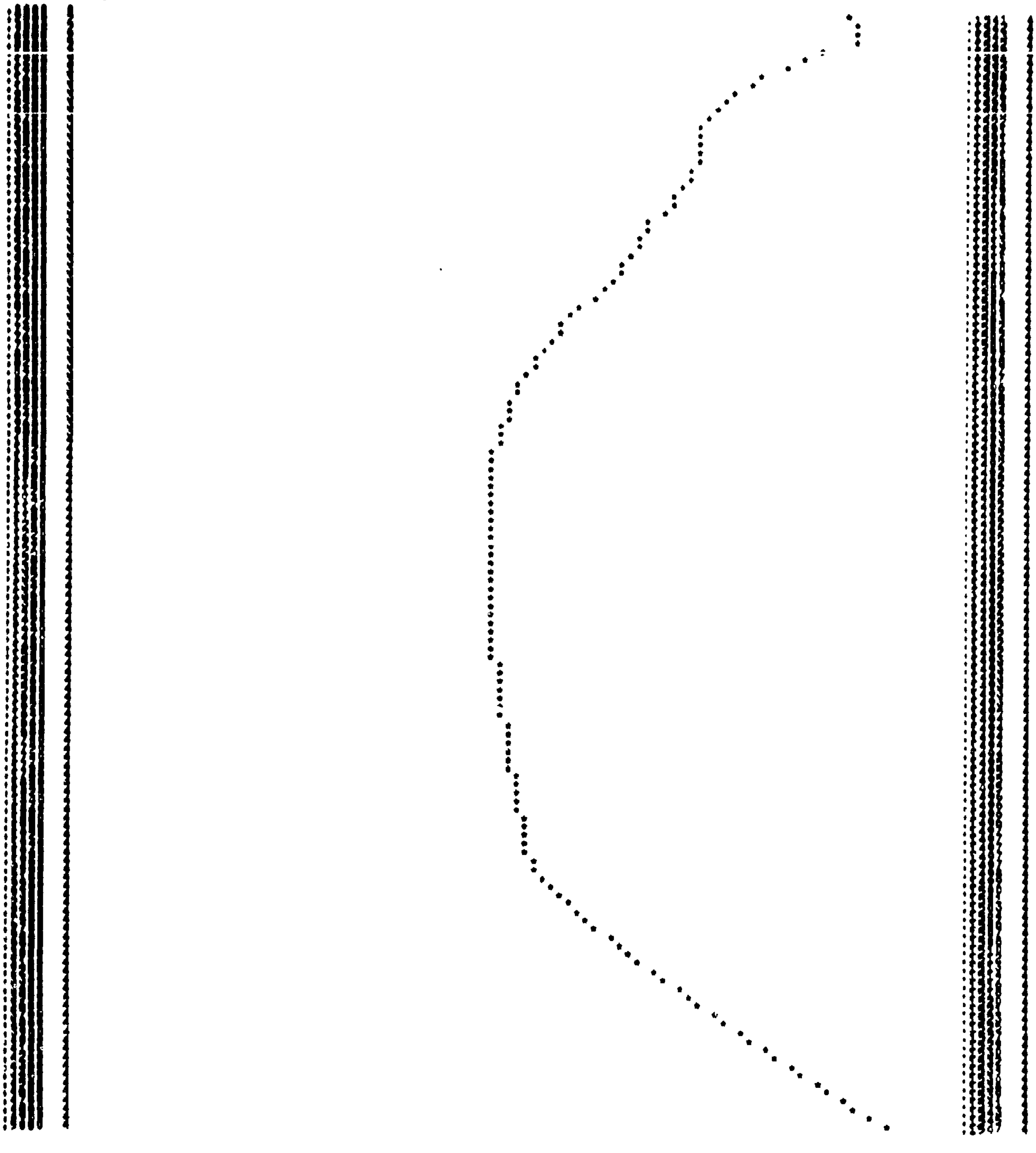

Fig. 46.

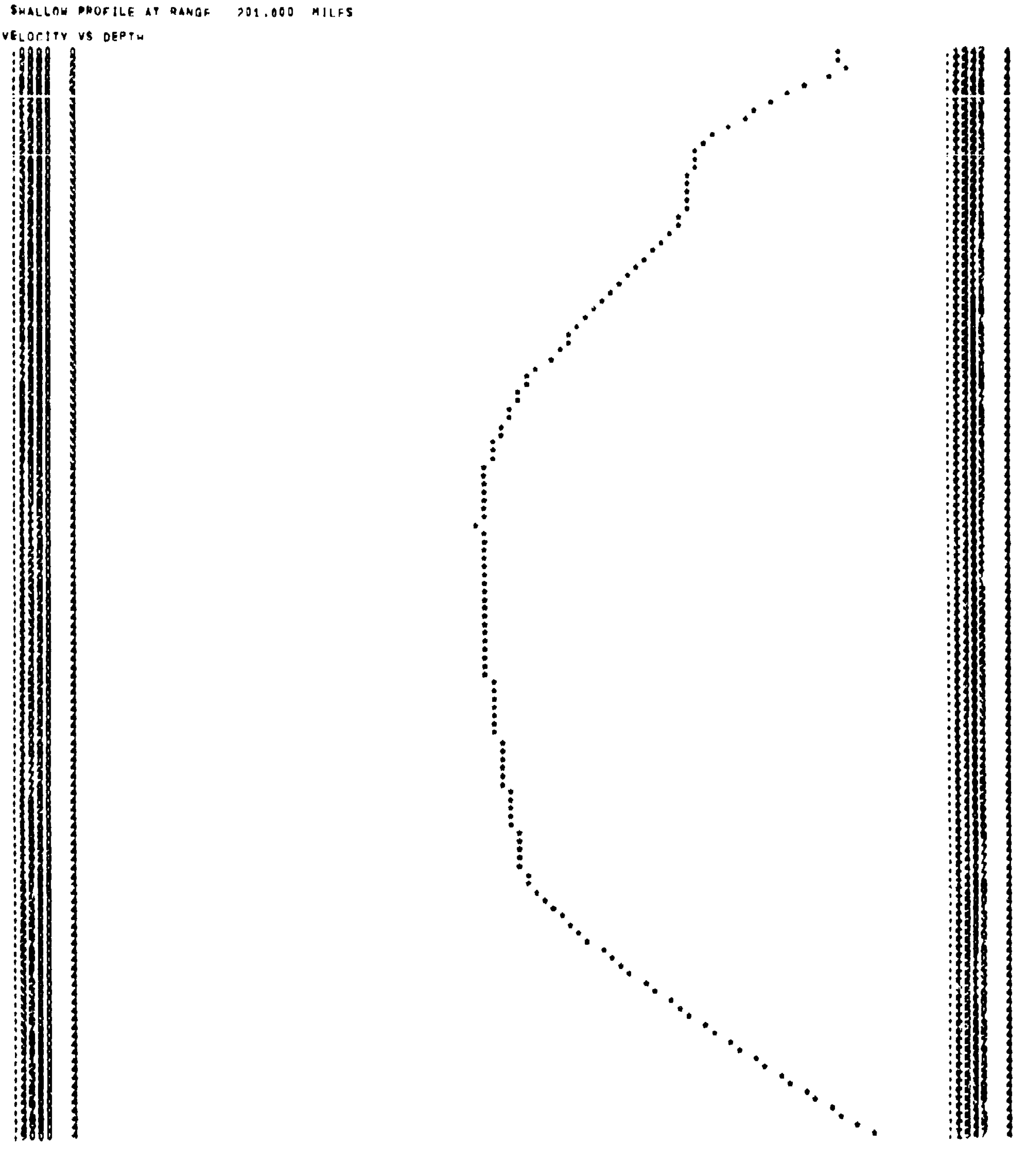

Fig. 47.

SHALLOW PROFILE AT RANGE 219.300 MILES

VELOCITY VS DEPTH

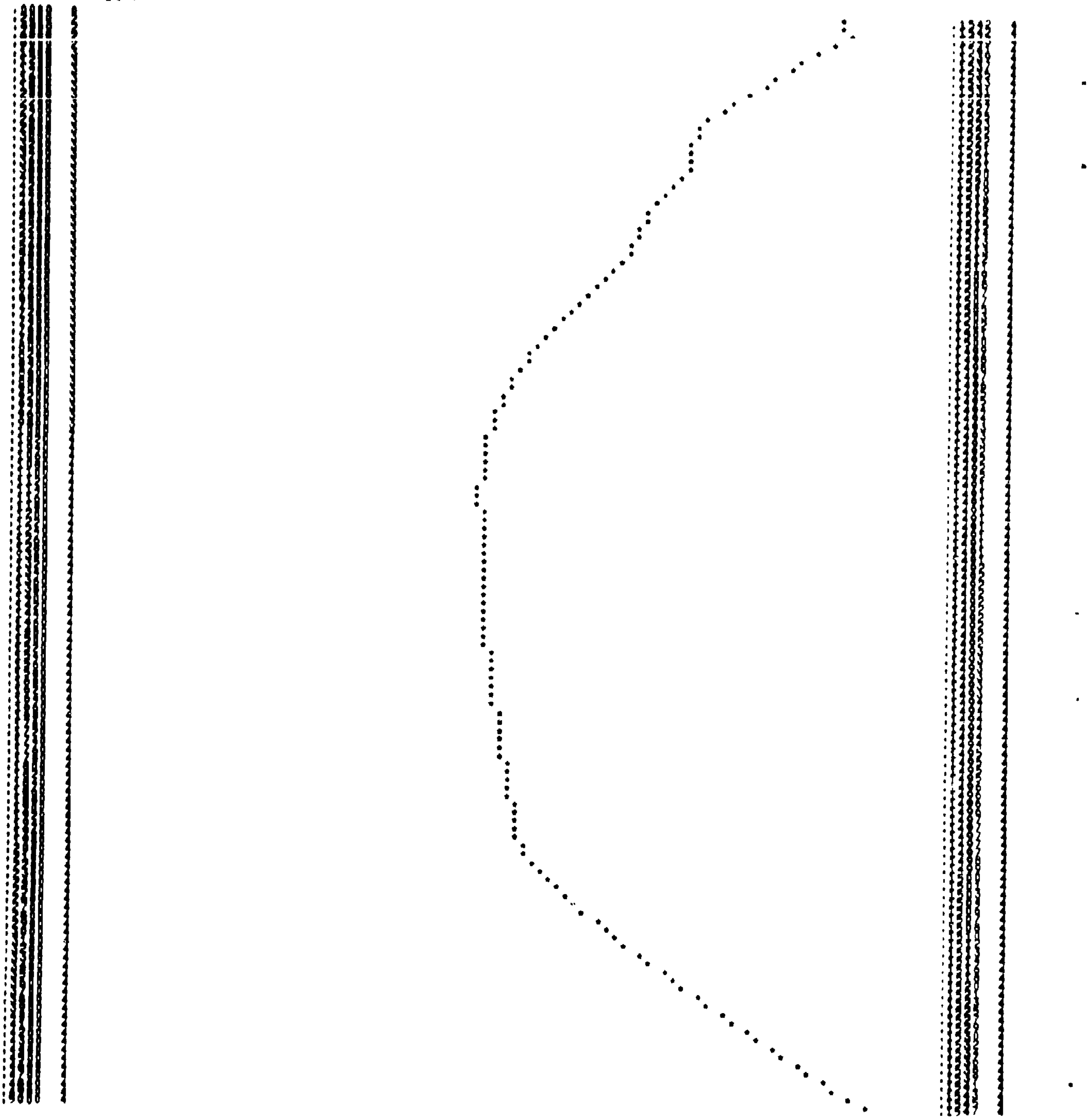

Fig. 48.

SHALLOW PROFILE AT RANGE 234,000 MILES

VELOCITY VS DEPTH

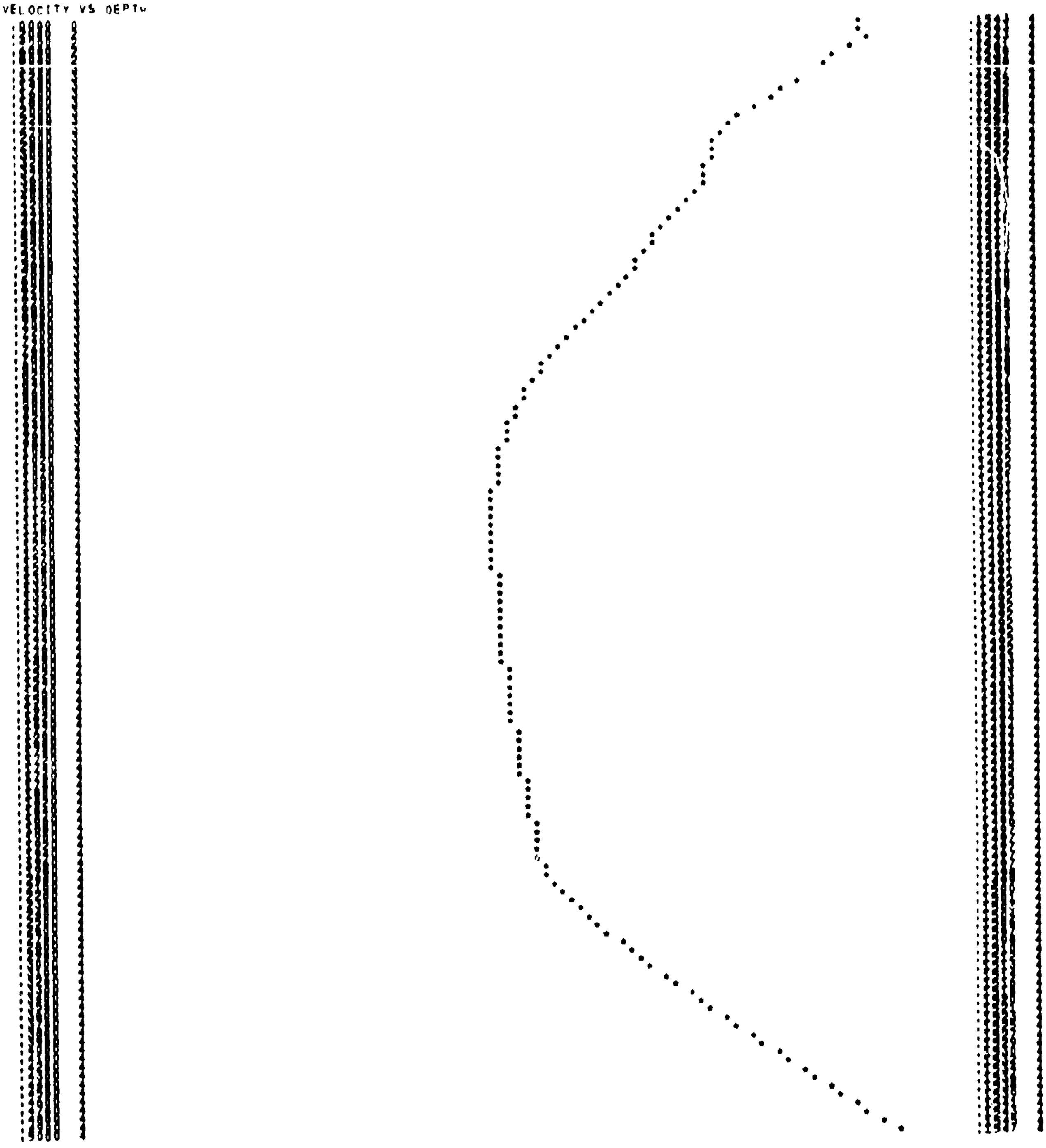

Fig. 49.

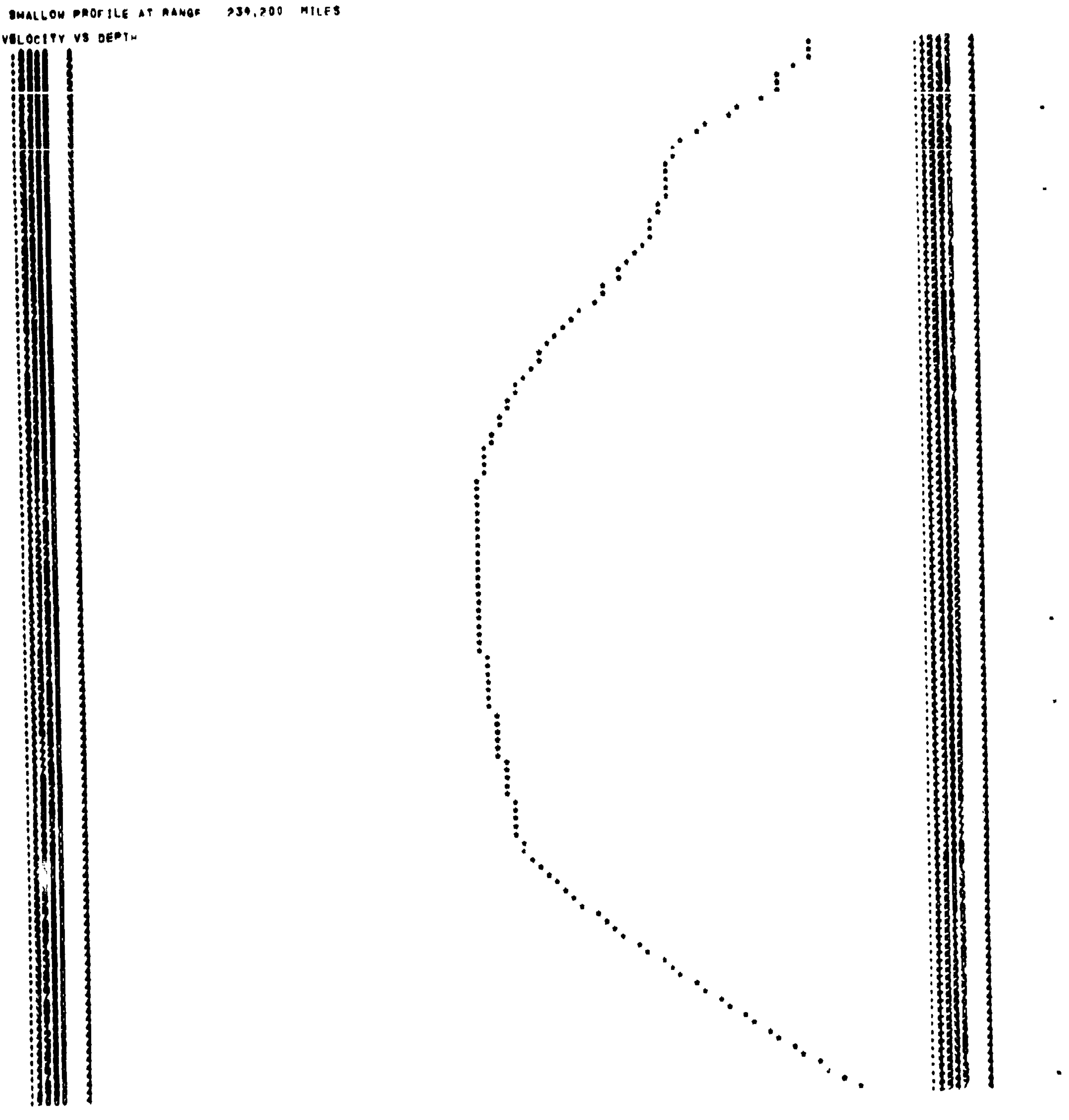

Fig. 50.

SHALLOW PROFILE AT RANGE 248.900 MILES

VELOCITY VS DEPTH

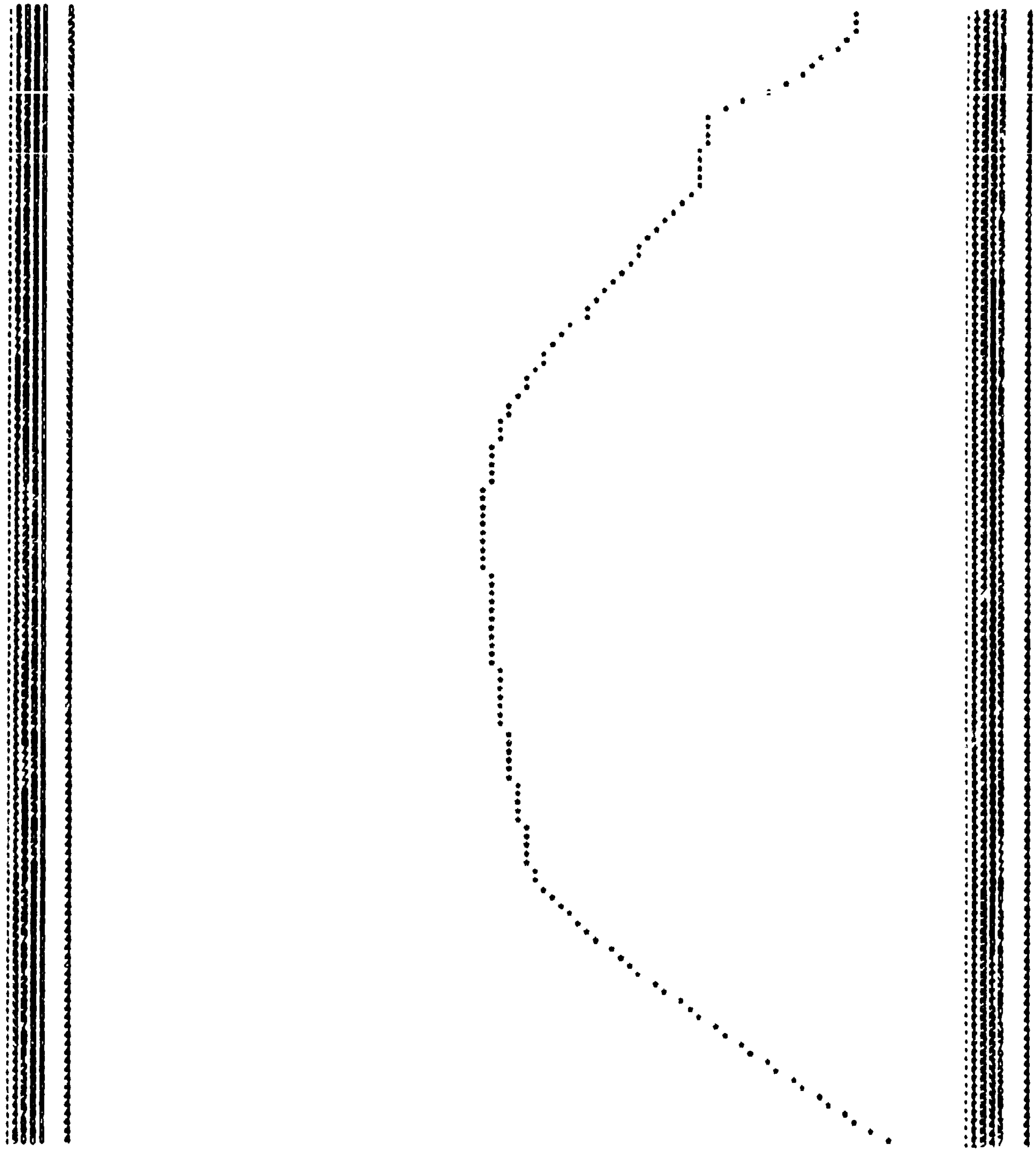

Fig. 51.

SHALLOW PROFILE AT RANGE 263.700 MILES

VELOCITY VS DEPTH

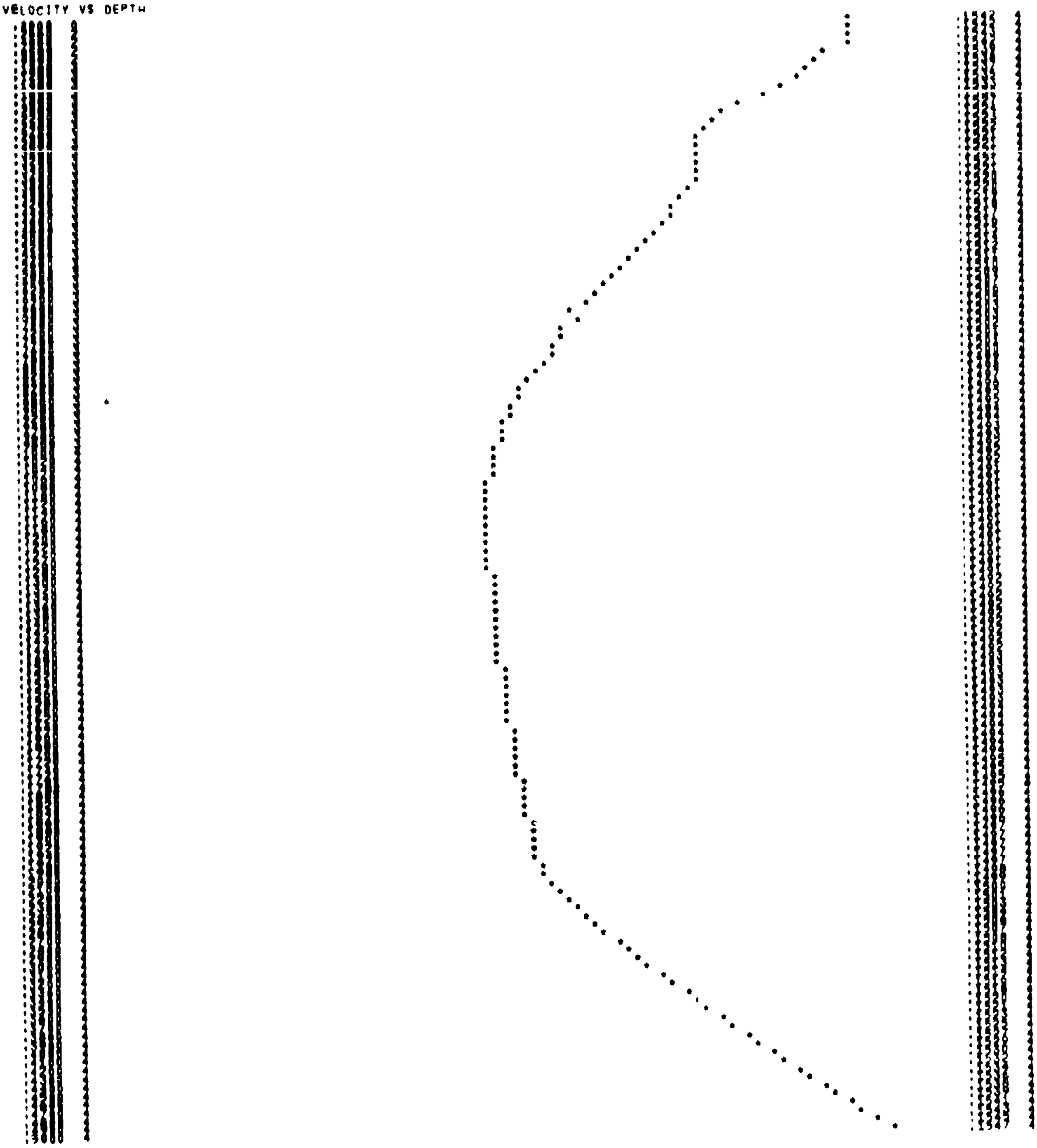

Fig. 52.

SHALLOW PROFILE AT RANGE 270.000 MILES

VELOCITY VS DEPTH

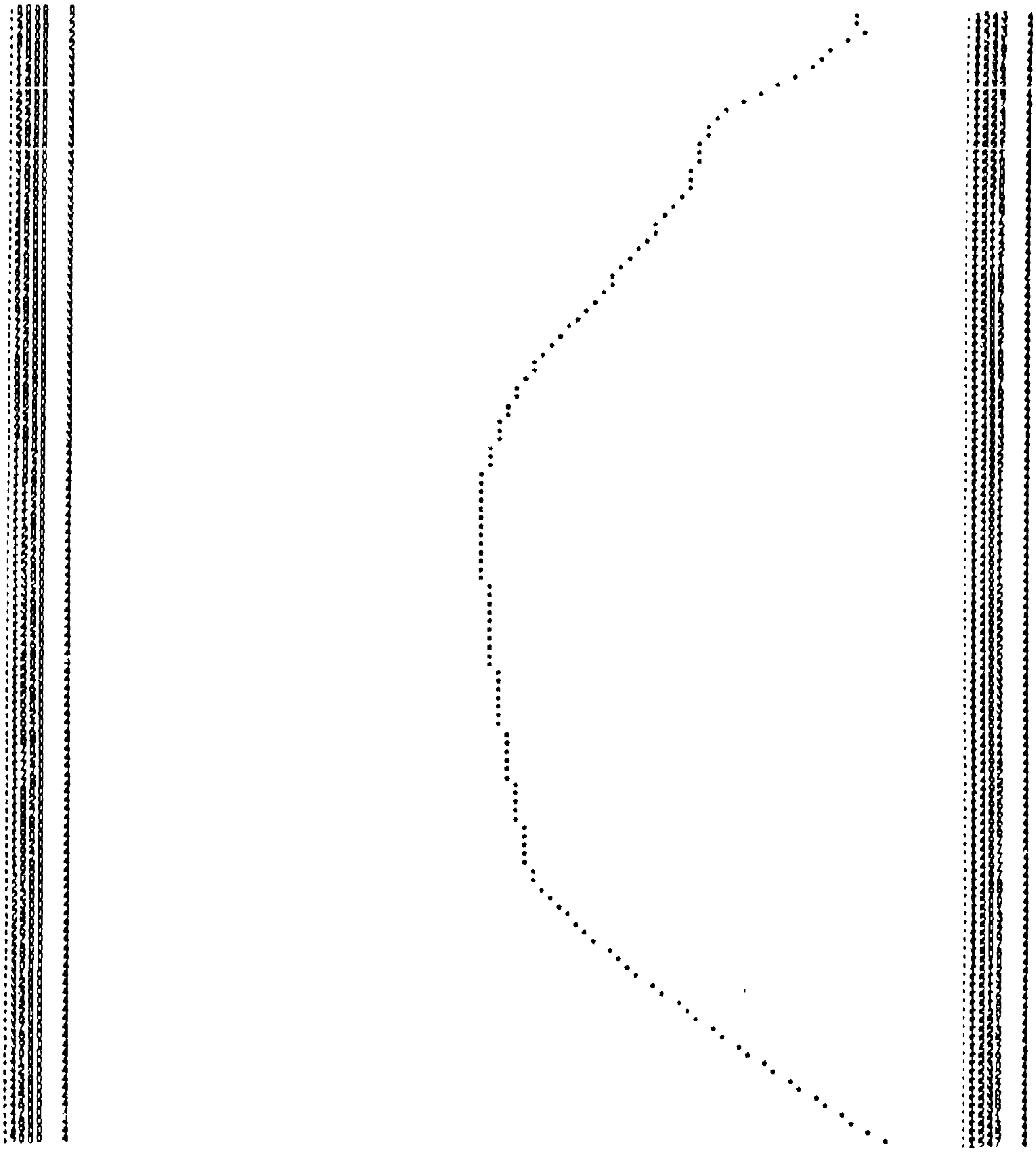

Fig. 53.

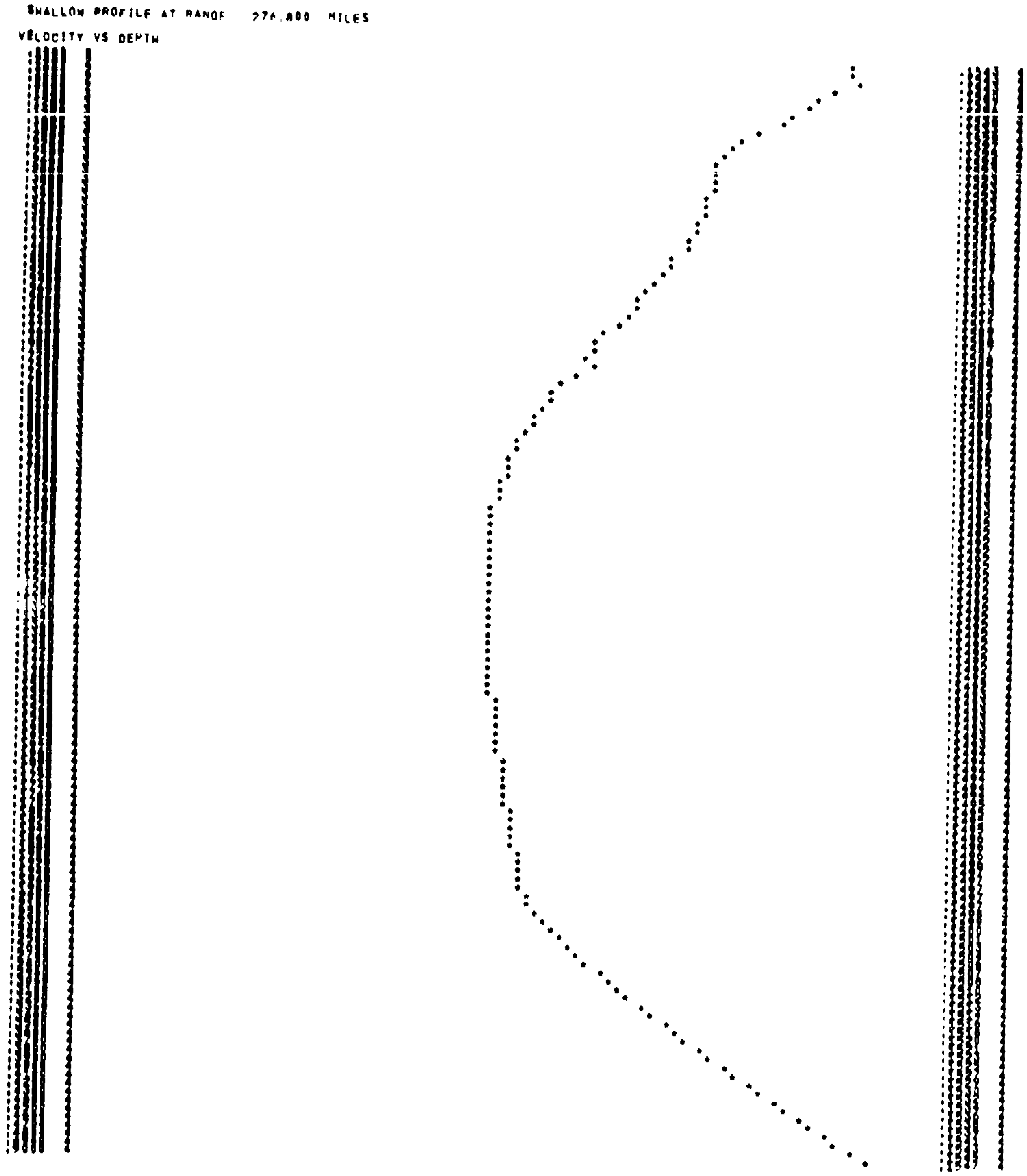

Fig. 54.

SHALLOW PROFILE AT RANGE 281.900 MILES

VELOCITY VS DEPTH

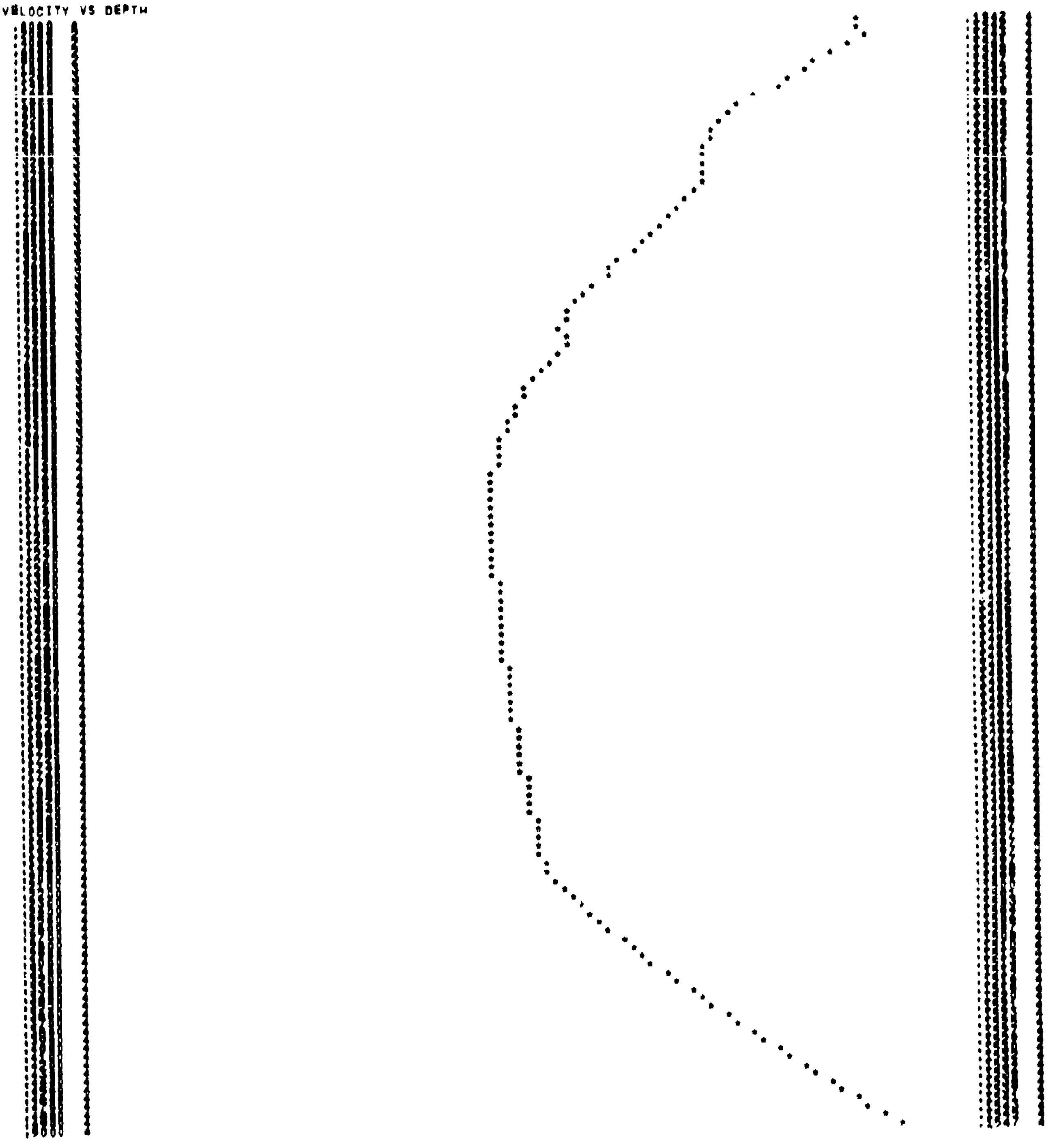

Fig. 55.

SHALLOW PROFILE AT RANGE 288.400 MILES

VELOCITY VS DEPTH

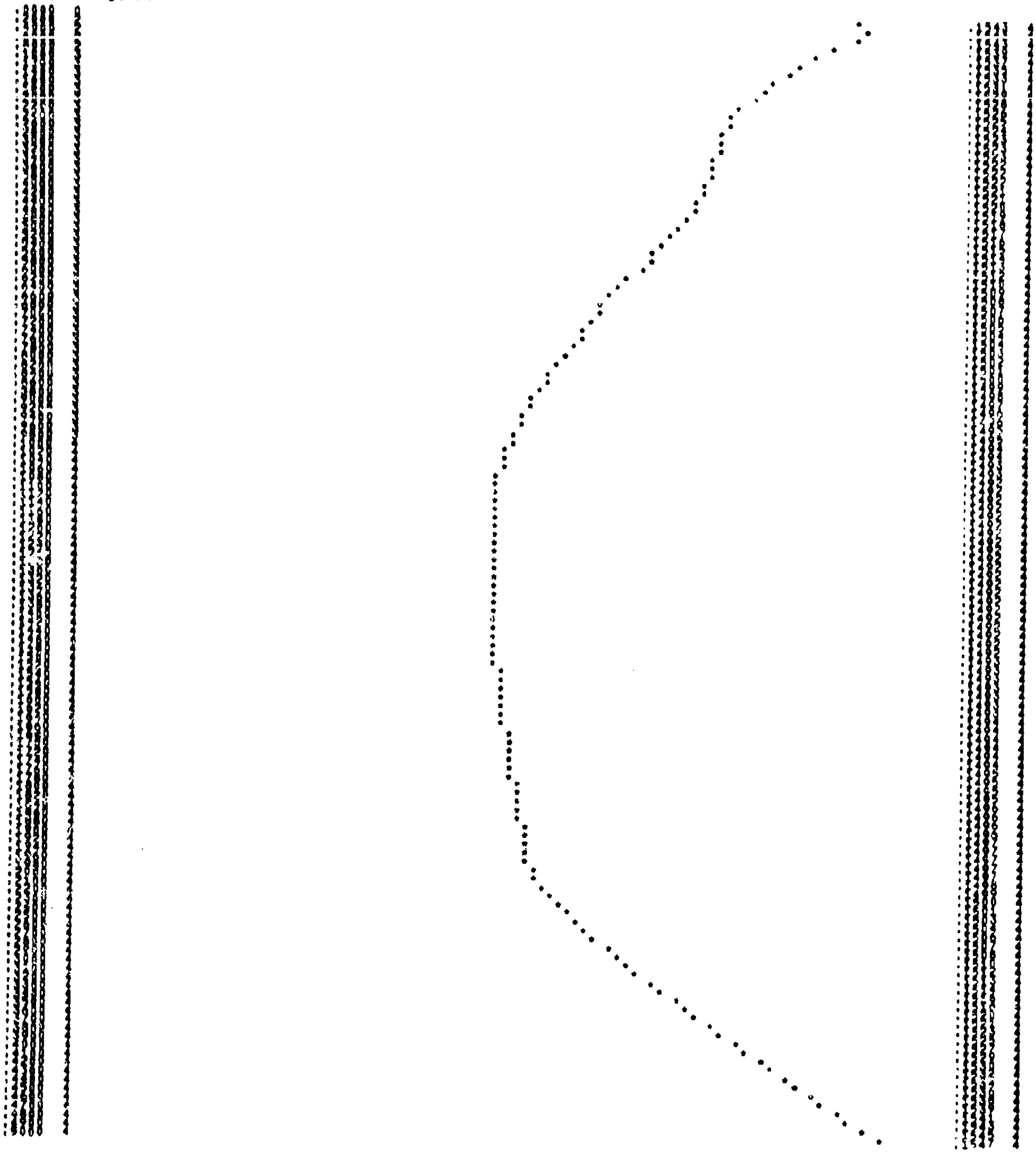

Fig. 56.

DEEP PROFILE AT RANGE 305.700 MILES TEMP AT OBSERVED MAXIMUM DEPTH= 2,209 DEG CENTIGRADE

VELOCITY VS DEPTH

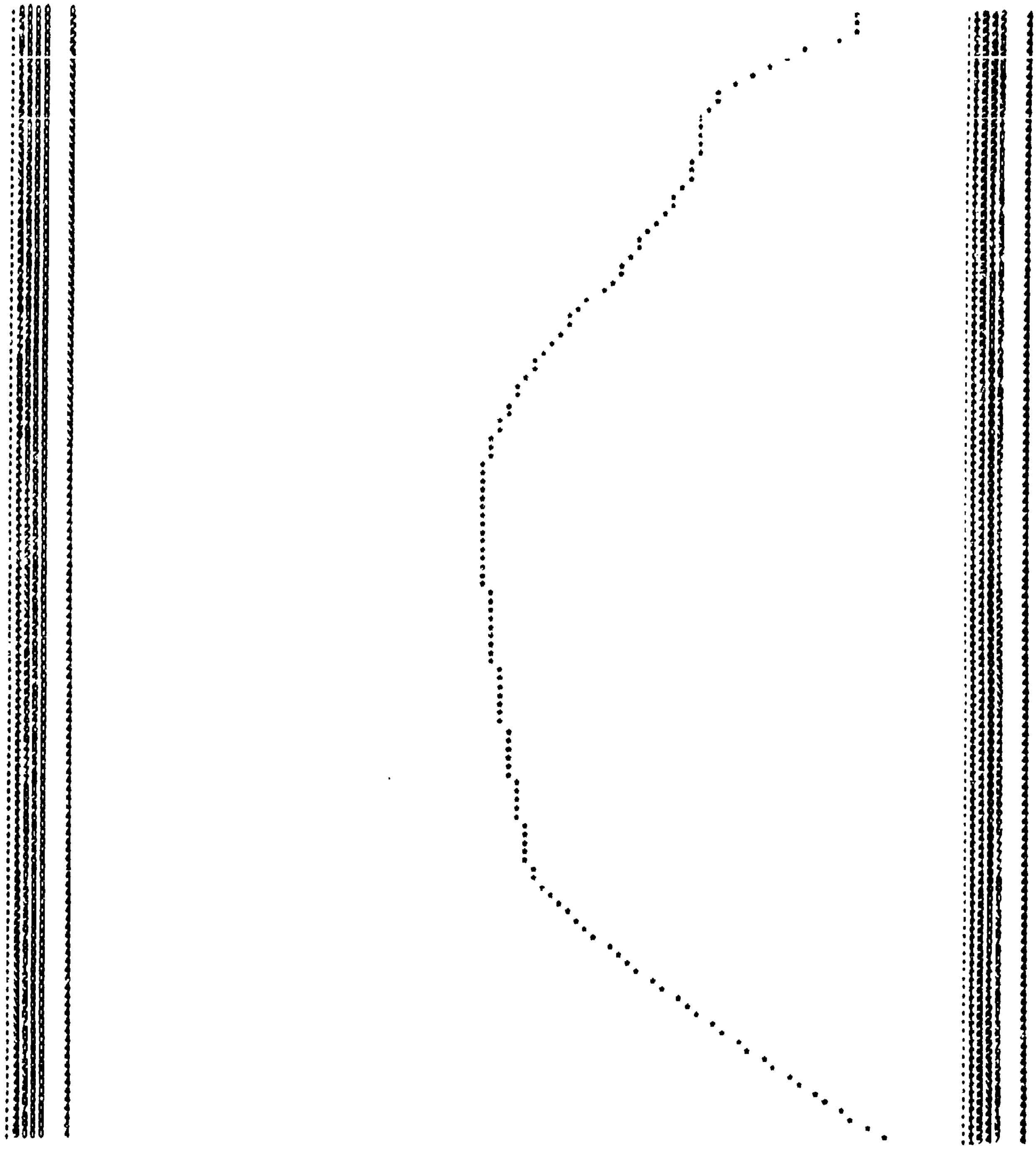

Fig. 57.

DEEP PROFILE AT RANGE 390.000 MILES TEMP AT OBSERVED MAXIMUM DEPTH= 2,209 DEG CENTIGRADE

VELOCITY VS DEPTH

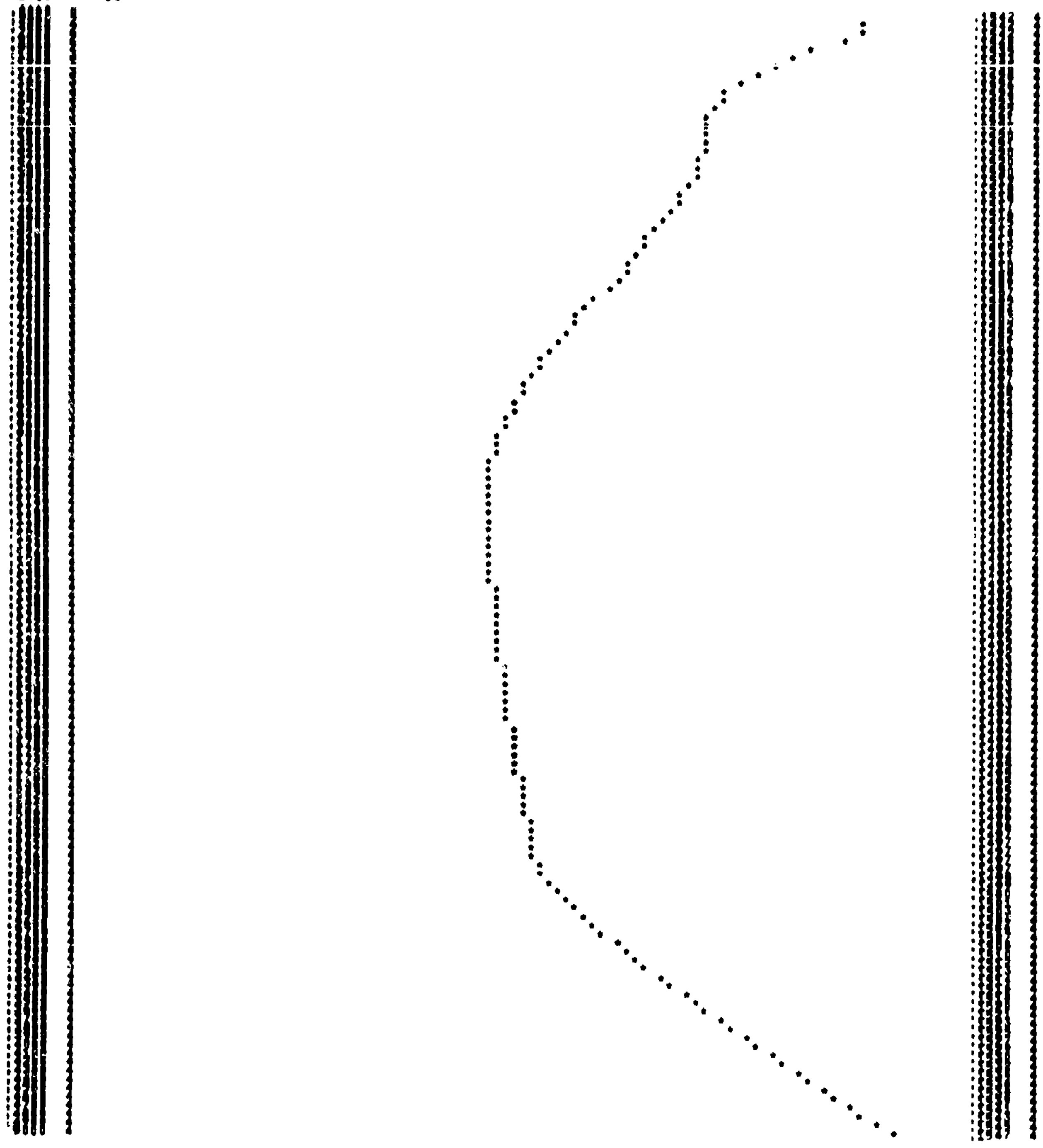

Fig. 58.

DATE 10 4 1968 ID NUMBER 165 SET 1

DEEP PROFILE AT RANGE .000 MILES TEMP AT OBSERVED MAXIMUM DEPTH 2.289 DEG CENTIGRADE

TABLE OF VALUES OF OBSERVED POINTS

DEPTH-METERS	VELOCITY-M/SEC	COEFFICIENT Z	COEFFICIENT D
.000	1541.0500	.15741444 -1	.10004044 -3
10.000	1541.2424	.14741048 -1	.10004044 -3
20.000	1541.3040	.12694264 0	.71000117 -1
30.000	1543.7373	.10494271 0	-.26200104 -1
40.000	1543.4697	-.10379043 0	-.15400124 -1
50.000	1541.6021	-.34062767 0	-.33733724 -1
55.000	1539.4033	-.32370137 0	.44000244 -1
60.000	1538.4245	-.20742734 0	.29333059 -2
70.000	1536.4760	-.17376070 0	.41990626 -2
80.000	1534.9493	-.15376091 0	-.20000498 -3
90.000	1533.4017	-.13176098 0	.45990900 -2
100.000	1532.3141	-.13926102 0	-.53001595 -2
110.000	1530.6064	-.13796215 0	.49000931 -2
120.000	1529.5600	-.20274337 0	-.10000334 -1
125.000	1528.3300	-.21743056 0	.12133450 -1
140.000	1526.4335	-.56420134 -1	.93335317 -2
150.000	1526.3359	-.36941305 -1	-.54491659 -2
175.000	1523.7119	-.58300776 -1	.37250003 -2
185.000	1523.3142	-.70429560 -1	-.61335653 -2
200.000	1521.5670	-.58929698 -1	.76660003 -2
205.000	1521.3690	.74241447 -1	.45601570 -1
210.000	1522.3102	-.41762543 -1	-.92003174 -1
215.000	1520.9513	-.19910117 0	.30667725 -1
225.000	1520.9337	-.35133063 -1	.13257359 -2
250.000	1520.0697	-.24542378 -1	-.40001709 -3
275.000	1519.3056	-.10642250 -1	.92002734 -3
300.000	1519.1215	-.15495707 -1	-.65070394 -3
350.000	1517.5334	-.41644162 -1	-.39603424 -3
400.000	1514.9551	-.49365273 -1	.07909007 -4
450.000	1512.5060	-.20097308 -1	.10467200 -2
460.000	1512.4392	-.43099149 -1	-.94670970 -2
480.000	1510.4838	-.65517807 -1	.32252312 -2
500.000	1509.0105	-.42192083 -1	-.00065000 -3
550.000	1506.6001	-.49826061 -1	.50169969 -3
560.000	1505.3671	-.64658525 -1	-.15705306 -2
575.000	1504.2205	-.16444640 0	-.11734530 -1
600.000	1503.2916	-.15894610 0	.13934682 -1
615.000	1502.4350	-.54750424 -1	-.41929339 -4
650.000	1500.4931	-.59061301 -1	-.20441046 -3
700.000	1497.2045	-.61571732 -1	.10399322 -3
750.000	1494.3359	-.46579662 -1	.49560954 -3
857.200	1492.1900	-.16737239 -1	.81072085 -4
942.900	1490.9807	-.93359875 -2	.11160190 -3
1028.700	1490.5907	-.21542056 -2	.55734412 -4
1114.400	1490.6107	.14466392 -2	.20301173 -4
1200.700	1490.8410	.26259389 -2	-.97093787 -6
1285.800	1491.0609	.61818181 -2	.04540366 -4
1371.500	1491.9011	.72397077 -2	-.59949509 -4
1457.300	1492.3013	.52506190 -2	.13673045 -4
1543.000	1492.8019	.75289639 -2	.30497196 -4
1628.700	1493.5916	.95133409 -2	.68126525 -5
1714.400	1494.4321	.97470189 -2	-.13592942 -5
1800.100	1495.2624	.12130257 -1	.56977421 -4
1885.900	1496.5129	.12130547 -1	-.56570673 -4
1971.600	1497.3433	.12140686 -1	.57207289 -4
2057.300	1498.5038	.14316589 -1	-.64277489 -5
2131.000	1499.6315	.21737909 -2	-.32309187 -3
2143.000	1499.6343	.14100854 -2	.19594095 -3
2228.700	1500.4748	.10966746 -1	.27066314 -4
2314.500	1501.5154	.13302985 -1	.27391449 -4
2400.200	1502.7560	.14535265 -1	.13665229 -5
2485.900	1504.0067	.14535643 -1	-.13577007 -5
2571.600	1505.2474	.14469356 -1	-.18925453 -6
2657.400	1506.4882	.13360111 -1	-.25667284 -4
2743.100	1507.5389	.14516812 -1	.53128216 -4
2828.800	1508.9798	.16930312 -1	.27294249 -5
2914.500	1510.4408	.15763346 -1	-.29963157 -4
3000.200	1511.6816	.13305932 -1	-.27386062 -4
3086.000	1512.7225	.13306289 -1	.27394367 -4
3171.700	1513.9634	.15744548 -1	.29974584 -4
3257.400	1515.4245	.14212222 -1	-.66701566 -4
3288.300	1515.8321	.14242811 -1	.69475918 -4

TABLE OF VALUES OF EXTRAPOLATED POINTS

DEPTH-METERS	VELOCITY-M/SEC	Z COEFFICIENT	D COEFFICIENT
3388.300	1517.6058	.17752647 -1	.32601604 -6
3488.300	1519.3826	.17785101 -1	.32625470 -6
3588.300	1521.1625	.17817802 -1	.32577515 -6
3688.300	1522.9462	.17850389 -1	.32596588 -6
3788.300	1524.7328	.17882891 -1	.32405853 -6
3888.300	1526.5228	.17915287 -1	.32386780 -6
3988.300	1528.3159	.17947578 -1	.32196045 -6
4088.300	1530.1123	.17979727 -1	.32101347 -6
4188.300	1531.9119	.18011723 -1	.31690203 -6
4288.300	1533.7144	.18043566 -1	.31709502 -6
4388.300	1535.5206	.18075237 -1	.31547546 -6
4488.300	1537.3297	.18106718 -1	.31414032 -6
4588.300	1539.1419	.18138037 -1	.31223297 -6
4688.300	1540.9573	.18169136 -1	.30975342 -6
4788.300	1542.7757	.18200016 -1	.30784607 -6
4888.300	1544.5973	.18230696 -1	.30574799 -6
4988.300	1546.4219	.18261137 -1	.30307770 -6
5088.300	1548.2495	.18291349 -1	.30097961 -6
5188.300	1550.0801	.18321266 -1	.29754639 -6
5288.300	1551.9138	.18350964 -1	.29640198 -6
5388.300	1553.7503	.18380375 -1	.29182434 -6
5488.300	1555.5898	.18409443 -1	.28953552 -6
5588.300	1557.4322	.18438244 -1	.28648376 -6
5688.300	1559.2775	.18466759 -1	.28381348 -6
5788.300	1561.1258	.18495140 -1	.28381348 -6

Table 5.5.1.1

DATA 10 4 1966 ID NUMBER 165 SET 1

SHALLOW PROFILE AT RANGE 50.200 MILES

TABLE OF VALUES OF OBSERVED POINTS

DEPTH-METERS	VELOCITY-M/SEC	COEFFICIENT Z	COEFFICIENT D
.000	1541.0900	.15741444 -1	.10004044 -3
10.000	1541.2124	.16741040 -1	.10004044 -3
20.000	1541.3440	.16975495 -1	-.13331005 -2
25.000	1541.4460	.21374291 0	.70000278 -1
30.000	1543.5173	.27034321 0	-.92400157 -1
40.000	1543.6497	-.70250141 -1	-.17900114 -1
50.000	1542.1121	-.17125031 0	-.27001190 -2
60.000	1540.2649	-.29609413 0	-.22064046 -1
65.000	1538.5057	-.21370057 0	.55200272 -1
70.000	1538.1260	-.10009345 0	-.12933420 -1
80.000	1536.3993	-.13026046 0	.69000244 -2
90.000	1535.3617	-.10470046 0	-.20002369 -3
100.000	1534.3041	-.90674733 -1	.30171603 -2
125.000	1532.9801	-.85072240 -1	-.25600609 -2
14 .000	1530.7648	-.45119480 -1	.67042441 -2

TABLE OF VALUES OF EXTRAPOLATED POINTS

DEPTH-METERS	VELOCITY-M/SEC	Z COEFFICIENT	D COEFFICIENT
150.000	1530.6338	-.40429026 -1	-.56008595 -2
175.000	1527.8456	-.65912777 -1	.36013594 -2
185.000	1527.3745	-.71124509 -1	-.40037059 -2
200.000	1525.7672	-.59575685 -1	.63435491 -2
205.000	1525.5408	.51772145 -1	.30175583 -1
210.000	1526.2844	-.44900142 -1	-.76027698 -1
215.000	1525.0095	-.17271436 0	.25709210 -1
225.000	1524.6577	-.38273479 -1	.11029660 -2
250.000	1524.0705	-.27581749 -1	-.32762756 -3
275.000	1523.2706	-.20043793 -1	.03066404 -3
300.000	1523.0603	-.16204936 -1	-.62355550 -3
350.000	1521.4708	-.41506127 -1	-.39200213 -3
400.000	1518.9087	-.50151119 -1	.49892425 -4
450.000	1518.4635	-.28497753 -1	.81024222 -3
460.000	1516.2193	-.47544407 -1	-.46339729 -2
480.000	1514.3409	-.86759157 -1	.27160978 -2
500.000	1513.5490	-.46505795 -1	-.69076157 -3
550.000	1510.3602	-.51584317 -1	.40762067 -3
580.000	1509.0121	-.64373334 -1	-.12402210 -2
595.000	1507.9158	-.14892416 0	-.98798079 -2
600.000	1507.0498	-.14403060 0	.11677310 -1
615.000	1506.2029	-.57477212 -1	-.13685753 -3
650.000	1504.1073	-.68324547 -1	-.40299022 -3
670.000	1502.6443	-.70426814 -1	.27274357 -3
700.000	1500.6542	-.62546517 -1	.26458952 -3
730.000	1498.9023	-.57777004 -1	.41378021 -4
750.000	1497.7550	-.52671657 -1	.46915673 -3
857.200	1494.8043	-.23519346 -1	.74729659 -4
942.900	1493.0632	-.15326415 -1	.11647059 -3
1028.700	1492.1769	-.73509943 -2	.69226969 -4
1114.400	1491.8003	-.24123730 -2	.46236876 -4
1200.700	1491.7643	-.45013616 -3	-.97066766 -6
1285.800	1491.7217	.30047487 -2	.44548230 -4
1371.500	1492.2978	.41500408 -2	-.50945316 -4
1457.300	1492.4131	.29399708 -2	.31724560 -4
1543.000	1492.8015	.67603936 -2	.57433491 -4
1628.700	1493.5918	.95133409 -2	.60126525 -5
1714.400	1494.4121	.97470109 -2	-.13592562 -5
1800.100	1495.2624	.12130257 -1	.96977021 -4
1885.900	1496.5129	.12110547 -1	-.56970673 -4
1971.600	1497.3433	.12140086 -1	.57207209 -4
2057.300	1498.5938	.14316589 -1	-.64277489 -5
2131.000	1499.6315	.21737909 -2	-.32309187 -3
2143.000	1499.6343	.14108854 -2	.19594095 -3
2228.700	1500.4748	.10986746 -1	.27066314 -4
2314.500	1501.5154	.13362985 -1	.27391469 -4
2400.200	1502.7560	.14415265 -1	.13665229 -5
2485.900	1504.0067	.14535643 -1	-.13577007 -5
2571.600	1505.2474	.14347139 -1	-.30414566 -5
2657.400	1506.4472	.13360396 -1	-.19959592 -4
2743.100	1507.5189	.14659243 -1	.50271020 -4
2828.600	1508.9798	.18010312 -1	.27294249 -5
2914.500	1510.4408	.15763366 -1	-.29963157 -4
3000.200	1511.6818	.13365932 -1	-.27386062 -4
3086.000	1512.7225	.13806289 -1	.27394367 -4
3171.700	1513.9434	.15744548 -1	.29974584 -4
3257.400	1515.4245	.14212227 -1	-.66201566 -4
3288.300	1515.8121	.14262811 -1	.69479918 -4
3388.300	1517.6657	.17752647 -1	.32081604 -6
3488.300	1519.3428	.17745101 -1	.32629470 -6
3588.300	1521.1428	.17817802 -1	.32577515 -6
3688.300	1522.9467	.17840399 -1	.32615662 -6
3788.300	1524.7128	.17862881 -1	.32348633 -6
3888.300	1526.5228	.17015277 -1	.32444000 -6
3988.300	1529.3159	.17047588 -1	.32176971 -6
4088.300	1530.1123	.17079727 -1	.32101347 -6
4188.300	1531.9118	.18011713 -1	.31671150 -6
4288.300	1533.7148	.18043566 -1	.31633649 -6
4388.300	1535.5208	.18075247 -1	.31524473 -6
4488.300	1537.1297	.18106719 -1	.31414032 -6
4588.300	1539.1419	.18138037 -1	.31225297 -6
4688.300	1540.9573	.18149136 -1	.30975342 -6
4788.300	1542.7757	.18200016 -1	.30784407 -6
4888.300	1544.5073	.18215705 -1	.30593872 -6
4988.300	1545.4219	.18251127 -1	.30250549 -6
5088.300	1548.2496	.18291130 -1	.30155182 -6
5186.300	1550.0801	.18321285 -1	.29754639 -6
5288.300	1551.9138	.18350964 -1	.29602051 -6
5388.300	1553.7593	.18380365 -1	.29201508 -6
5488.300	1555.5896	.18409443 -1	.28953552 -6
5588.300	1557.4122	.18438244 -1	.28648376 -6
5648.300	1559.2275	.18438244 -1	.28648376 -6

Table 5.5.1..

DATE 19 4 1968 ID NUMBER 165 SET 1

SHALLOW PROFILE AT RANGE 74,400 MILES

TABLE OF VALUES OF OBSERVED POINTS

DEPTH-METERS	VELOCITY-M/SEC	COEFFICIENT Z		COEFFICIENT D	
.000	1541.4000	.17742394	-1	-.09949060	-4
10.000	1541.6024	.18741943	-1	-.09949060	-4
20.000	1541.8248	.27942105	-1	.22499954	-2
30.000	1542.2173	.13000949	0	.20333464	-1
[illegible]	[illegible]	[illegible]	-1	[illegible]	-1
40.000	1542.5097	-.14409211	0	-.12133458	-1
50.000	1540.5521	-.18925963	0	.38900557	-2
60.000	1538.0849	-.10826010	0	-.90C04959	-3
70.000	1537.1864	-.19726095	0	-.93C01213	-2
80.000	1534.9493	-.95740282	-1	.75E00255	-1
85.000	1534.7009	-.10970038	0	-.29C00298	-1
90.000	1533.9017	-.14942756	0	.12533428	-1
100.000	1533.0641	-.11042773	0	-.55734600	-2
115.000	1530.7774	-.10242840	0	.66E67040	-2
120.000	1530.3408	-.18576309	0	-.32C00580	-1
125.000	1529.1200	-.22318421	0	.89001339	-2
150.000	1526.3359	-.15756432	0	-.36001431	-2
160.000	1524.5783	-.12856393	0	.94402211	-2
175.000	1523.7110	-.59942438	-1	-.24002202	-3
200.000	1522.1478	-.51042624	-1	.84E00720	-3
225.000	1521.1137	-.29742230	-1	.92E02429	-3
250.000	1520.6597	-.12941798	-1	.44E01025	-3
275.000	1520.4856	-.12781917	-1	-.48401970	-3
300.000	1520.0218	-.16828817	-1	.13666781	-3
350.000	1519.3535	-.31883403	-1	-.74C05127	-3
400.000	1516.8352	-.48244947	-1	.83980715	-4
450.000	1514.5270	-.14573451	-1	.12636669	-2
465.000	1514.4509	-.20840034	-1	-.20729476	-2
500.000	1512.4587	-.55803781	-1	.17747826	-3
550.000	1509.9904	-.57326249	-1	-.31E37465	-3
580.000	1508.1273	-.54201795	-1	.39333852	-3
600.000	1507.0819	-.91086565	-1	-.30718156	-2
615.000	1505.2553	-.18245279	-1	.13E01370	-1
620.000	1505.3365	-.12951601	-1	-.11E67849	-1
635.000	1503.8299	-.05437063	-1	.46E71210	-2
650.000	1503.3734	-.26833599	-1	.21334076	-3
675.000	1502.7192	-.77372589	-1	-.40964600	-2
700.000	1499.5048	-.38848431	-1	.72407926	-2
715.000	1499.7483	-.80948566	-2	-.32448493	-2
730.000	1499.2618	-.11341340	-1	.28098515	-2
750.000	1499.5965	.91632588	-2	-.75732161	-3

TABLE OF VALUES OF EXTRAPOLATED POINTS

DEPTH-METERS	VELOCITY-M/SEC	Z COEFFICIENT		D COEFFICIENT	
857.200	1496.2274	-.27664231	-1	.81422553	-4
942.900	1494.2070	-.18493556	-1	.11E82655	-3
1028.700	1493.0989	-.10132393	-1	.79830272	-4
1114.400	1492.4686	-.45248146	-2	.55026024	-4
1200.700	1492.2831	-.21023308	-2	-.97077950	-6
1285.800	1492.0930	.13835517	-2	.84540286	-4
1371.500	1492.5203	.24174448	-2	-.59945350	-4
1457.300	1492.5071	.16418459	-2	.41E66121	-4
1543.000	1492.8015	.63246140	-2	.67510029	-4
1628.700	1493.5918	.95153409	-2	.48126525	-5
1714.400	1494.4321	.97470189	-2	-.13592562	-5
1800.100	1495.2624	.12110257	-1	.56977421	-4
1885.900	1496.5129	.12130547	-1	-.56970073	-4
1971.600	1497.3433	.12140686	-1	.57207289	-4
2057.300	1498.5938	.14316589	-1	-.44277489	-5
2131.000	1499.6315	.21737909	-2	-.32309187	-3
2143.000	1499.6343	.14108854	-2	.19594095	-3
2228.700	1500.4748	.10946746	-1	.27066314	-4
2314.500	1501.5154	.13302985	-1	.27391469	-4
2400.200	1502.7560	.14535265	-1	.13E65229	-5
2485.900	1504.0067	.14535643	-1	-.13577007	-5
2571.600	1505.2474	.14287242	-1	-.44393002	-5
2657.400	1506.4569	.13340536	-1	-.17162234	-4
2743.100	1507.5389	.14719245	-1	.48E70729	-4
2828.800	1508.9798	.16910312	-1	.27294249	-5
2914.500	1510.4408	.15743346	-1	-.29963157	-4
3000.200	1511.6818	.13305932	-1	-.27384062	-4
3086.000	1512.7225	.13306789	-1	.27394367	-4
3171.700	1513.9834	.15744548	-1	.29974584	-4
3257.400	1515.4245	.14212222	-1	-.66201546	-4
3288.300	1515.8321	.14242811	-1	.89475918	-4
3388.300	1517.6057	.17752647	-1	.32081604	-6
3488.300	1519.3826	.17745101	-1	.32E29470	-6
3588.300	1521.1628	.17817802	-1	.32577515	-6
3688.300	1522.9462	.17850399	-1	.32E15662	-6
3788.300	1524.7328	.17882881	-1	.32348833	-6
3888.300	1526.5228	.17915277	-1	.32444000	-6
3988.300	1528.3159	.17947588	-1	.32176971	-6
4088.300	1530.1123	.17979727	-1	.32101347	-6
4188.300	1531.9118	.18011713	-1	.31E71130	-6
4288.300	1533.7146	.18043566	-1	.31E33649	-6
4388.300	1535.5206	.18075247	-1	.31528473	-6
4488.300	1537.3297	.18106718	-1	.31414032	-6
4588.300	1539.1419	.18138032	-1	.31223292	-6
4688.300	1540.9573	.18169136	-1	.30975342	-6
4788.300	1542.7757	.18200018	-1	.30784607	-6
4888.300	1544.5973	.18230705	-1	.30593672	-6
4988.300	1546.4219	.18261127	-1	.30250549	-6
5088.300	1548.2498	.18291330	-1	.30155162	-6
5188.300	1550.0801	.18321285	-1	.29754639	-6
5288.300	1551.9138	.18350964	-1	.29E02051	-6
5388.300	1553.7503	.18380363	-1	.29E01500	-6
5478.300	1555.5498	.18409441	-1	.28953552	-6
5588.300	1557.4322	.18436244	-1	.28E48376	-6
5688.300	1559.2778	.18436244	-1	.28E48376	-6

Table 5.5.1.3

DATE 19 4 1968 ID NUMBER 165 SET 1

SHALLOW PROFILE AT RANGE 100,000 MILES

TABLE OF VALUES OF OBSERVED POINTS

DEPTH-METERS	VELOCITY-M/SEC	COEFFICIENT Z	COEFFICIENT D
.000	1541.0500	.47414700 -2	.23000336 -8
10.000	1541.2124	.27741914 -1	.23000330 -8
20.000	1541.6046	.93742466 -1	.10980097 -1
30.000	1543.0073	.38742351 -1	-.21900120 -1
40.000	1542.3797	-.71290259 -1	-.10000329 -3
50.000	1541.6621	-.11725912 0	-.91001701 -8
60.000	1540.6349	-.25019371 0	-.19006747 -1
65.000	1530.5057	-.10076023 0	.46000137 -1
70.000	1538.1269	-.11609357 0	-.10133474 -1
80.000	1536.1573	-.19026120 0	-.50006067 -3
90.000	1534.1417	-.10796141 0	.69000439 -8
100.000	1532.8141	-.18826111 0	.49000168 -8
110.000	1531.9704	-.14096224 0	-.13180243 -1
120.000	1529.6700	-.60740689 -1	.30000998 -1
125.000	1529.9100	-.61781093 -1	-.31803714 -1
130.000	1529.2112	-.13916209 0	.10400110 -8
150.000	1526.0759	-.18618490 0	.10977740 -8
175.000	1524.5519	-.77542714 -1	.12320060 -8
200.000	1522.9070	-.62042913 -1	-.64022087 -4
225.000	1521.4037	-.40742772 -1	.13000342 -8
250.000	1520.6597	-.30162460 -1	-.22009000 -4
275.000	1519.8096	-.24742497 -1	.46000707 -3
300.000	1519.4216	-.23142677 -1	-.33008193 -3
350.000	1517.8434	-.41464180 -1	-.39603900 -3
400.000	1515.2751	-.49949213 -1	.03900478 -4
450.000	1512.9169	-.51160172 -1	-.16002004 -3
500.000	1511.1569	-.07741396 -1	-.13020709 -8
525.000	1509.1431	-.81036440 -1	.19734700 -8
550.000	1506.6001	-.52092677 -1	-.41232409 -4
575.000	1505.2059	-.31946993 -1	.16401304 -8
600.000	1505.0017	-.23912740 -1	-.04942339 -3
650.000	1502.6533	-.67242772 -1	-.01176790 -3
680.000	1500.2701	-.54737020 -1	.16460179 -8
700.000	1499.5040	-.75039623 -1	-.37670771 -8
710.000	1499.5570	-.69039045 -1	.49071920 -8
725.000	1498.0709	-.42006350 -1	-.12060334 -8
750.000	1496.6167	-.52843497 -1	.44820172 -3

TABLE OF VALUES OF EXTRAPOLATED POINTS

DEPTH-METERS	VELOCITY-M/SEC	Z COEFFICIENT	D COEFFICIENT
857.200	1493.5140	-.24280530 -1	.00278712 -4
942.900	1491.7637	-.15228617 -1	.12124003 -3
1028.700	1490.9033	-.44833461 -2	.02011639 -4
1114.400	1490.6511	-.19973077 -3	.64030490 -4
1200.700	1490.8723	.25912601 -2	-.07141910 -6
1285.800	1491.0833	.60771371 -2	.04840009 -4
1371.500	1491.9146	.71316315 -2	-.99949642 -4
1457.300	1492.3050	.51722204 -2	.14209707 -4
1543.000	1492.8015	.75070900 -2	.40109000 -4
1628.700	1493.5910	.95133409 -2	.60126929 -5
1714.400	1494.4321	.97470109 -2	-.13009942 -5
1800.100	1495.2624	.12130257 -1	.96977421 -4
1885.900	1496.5129	.12130947 -1	-.96070673 -4
1971.600	1497.3433	.12140006 -1	.57707209 -4
2057.300	1498.5930	.14316509 -1	-.64277409 -5
2131.000	1499.6315	.21737909 -2	-.32309107 -3
2143.000	1499.6343	.14108054 -2	.19594095 -3
2228.700	1500.4740	.10060746 -1	.27066314 -4
2314.500	1501.9154	.13382905 -1	.27391469 -4
2400.200	1502.7560	.14535269 -1	.13069229 -5
2485.900	1504.0067	.14935643 -1	-.13977007 -5
2571.600	1505.2474	.14725870 -1	-.98713040 -5
2657.400	1506.4464	.13340679 -1	-.14290439 -4
2743.100	1507.5309	.14780717 -1	.47436150 -4
2828.000	1508.9790	.16070312 -1	.27204249 -5
2914.500	1510.4408	.15743346 -1	-.29903197 -4
3000.200	1511.6816	.13305932 -1	-.27386062 -4
3086.000	1512.7229	.13306209 -1	.27304367 -4
3171.700	1513.9634	.15764548 -1	.29574904 -4
3257.400	1515.4249	.14212222 -1	-.60281566 -4
3288.300	1515.8321	.14242011 -1	.69475910 -4
3388.300	1517.6057	.17782647 -1	.32081604 -6
3488.300	1519.3924	.17745101 -1	.32029470 -6
3588.300	1521.1620	.17817802 -1	.32977915 -6
3688.300	1522.9462	.17850399 -1	.32019062 -6
3788.300	1524.7328	.17882881 -1	.32340033 -6
3888.300	1526.5220	.17915277 -1	.32444000 -6
3988.300	1528.3159	.17947500 -1	.32176971 -6
4088.300	1530.1123	.17979727 -1	.32101347 -6
4188.300	1531.9118	.18011713 -1	.31871130 -6
4288.300	1533.7146	.18043566 -1	.31033649 -6
4388.300	1535.5206	.18075247 -1	.31528473 -6
4488.300	1537.3297	.19106718 -1	.31414032 -6
4588.300	1539.1419	.18138037 -1	.31223297 -6
4688.300	1540.9573	.18169136 -1	.30979342 -6
4788.300	1542.7757	.19200016 -1	.30784007 -6
4888.300	1544.5973	.19230705 -1	.30593872 -6
4988.300	1546.4219	.18261127 -1	.30250540 -6
5088.300	1548.2495	.18291330 -1	.30155102 -6
5188.300	1550.0801	.18321285 -1	.29754639 -6
5288.300	1551.9138	.18350964 -1	.29602051 -6
5388.300	1553.7503	.18380365 -1	.29201500 -6
5488.300	1555.5898	.18409443 -1	.28953552 -6
5588.300	1557.4322	.18438244 -1	.28648376 -6
5688.300	1559.2775	.18438244 -1	.28648376 -6

Table 5.5.1.4

DATE 10 4 1968 ID NUMBER 165 SET 1

SHALLOW PROFILE AT RANGE 121.000 MILES

TABLE OF VALUES OF OBSERVED POINTS

DEPTH-METERS	VELOCITY-M/SEC	COEFFICIENT Z	COEFFICIENT D
.000	1541.0900	-.17298644 -1	.47090500 -2
10.000	1541.2124	.49741936 -1	.47000500 -2
20.000	1542.0440	.61942199 -1	-.44000093 -2
30.000	1542.4373	.11097625 0	.14266815 -1
35.000	1543.1605	.10242409 -1	-.54000351 -1
40.000	1542.5097	-.99425062 -1	.57333020 -2
50.000	1541.8021	-.94950785 -1	-.47001076 -2
60.000	1540.7149	-.11075935 0	-.20000490 -3
70.000	1539.9169	-.15020001 0	-.73001209 -2
80.000	1537.5093	-.17124064 0	.43000030 -2
90.000	1536.0917	-.15176104 0	-.40000545 -3
100.000	1534.5941	-.12781020 0	.51086400 -2
125.000	1532.9001	-.14096506 0	-.05602221 -2
135.000	1530.0524	-.10776313 0	.10000209 -1
150.000	1529.5350	-.10496240 0	-.22401225 -2
160.000	1528.3784	-.84070800 -1	.63460424 -2
175.000	1527.0320	-.70329035 -1	-.55060632 -2
200.000	1524.1270	-.99763710 -1	.30720006 -2
225.000	1522.0430	-.51062776 -1	-.40013306 -4
250.000	1521.5297	-.41162720 -1	.91201702 -3
275.000	1520.7056	-.24362335 -1	.43201294 -3
300.000	1520.3116	-.19020910 -1	-.93309909 -5
350.000	1519.3939	-.28643158 -1	-.30003006 -3
400.000	1517.4493	-.41964474 -1	-.15202255 -3
450.000	1515.1570	-.43365212 -1	.05993042 -4
500.000	1513.1000	-.63634300 -1	-.96675900 -3
515.000	1512.0522	-.54290085 -1	.21525502 -2
535.000	1511.3960	-.67679686 -1	-.34860393 -2
550.000	1509.9904	-.72435951 -1	.20446706 -2
565.000	1509.2230	-.61401949 -1	-.13734703 -2
590.000	1507.2590	-.10135640 -1	.94747750 -2
600.000	1507.4320	.43702741 -2	-.29735919 -2
650.000	1504.4339	-.34217215 -1	.10300022 -2
680.000	1503.0785	-.42090096 -1	-.16150044 -2
695.000	1503.0440	-.14711532 0	-.14260292 -1
700.000	1502.0550	-.10011610 0	.11307909 -1
725.000	1501.3009	-.17265094 0	-.11694698 -1
730.000	1500.3710	-.14144707 0	.24136047 -1
740.000	1500.1643	-.94975665 -1	-.14701767 -1
750.000	1498.4864	-.15474033 0	.23040344 -2

TABLE OF VALUES OF EXTRAPOLATED POINTS

DEPTH-METERS	VELOCITY-M/SEC	Z COEFFICIENT	D COEFFICIENT
857.200	1494.9787	-.27670079 -1	.04237442 -4
942.900	1492.9934	-.10346976 -1	.12333791 -3
1028.700	1491.8332	-.95902060 -2	.08490212 -4
1114.400	1491.3647	-.23800770 -2	.71054094 -4
1200.100	1491.4262	.67096153 -3	-.97099301 -6
1285.900	1491.4798	.42264395 -2	.04540395 -4
1371.600	1492.1984	.52063139 -2	-.99049093 -4
1457.300	1492.3840	.37060693 -2	.25115816 -4
1543.000	1492.0019	.70418333 -2	.50065472 -4
1628.700	1493.9910	.95133409 -2	.60126525 -5
1714.400	1494.4321	.97470109 -2	-.13592962 -8
1800.100	1495.2624	.12130857 -1	.56977421 -4
1885.900	1496.5129	.12130547 -1	-.96970673 -4
1971.600	1497.3432	.12140664 -1	.97207209 -4
2057.300	1498.9930	.14310509 -1	-.64277489 -5
2131.900	1499.6315	.21737909 -2	-.32309187 -3
2143.000	1499.6343	.14100094 -2	.10594095 -3
2228.700	1500.4748	.10960746 -1	.27060314 -4
2314.400	1501.5154	.13362985 -1	.27391449 -4
2400.200	1502.7500	.14939265 -1	.13669229 -5
2485.900	1504.0067	.14535643 -1	-.13977007 -5
2571.600	1505.2474	.14172597 -1	-.71157358 -5
2657.400	1506.4378	.13360084 -1	-.11800241 -4
2743.100	1507.5380	.14034131 -1	.44109600 -6
2828.800	1508.9790	.16930312 -1	.27294349 -5
2914.500	1510.4400	.15763346 -1	-.29963157 -4
3000.200	1511.6016	.13309932 -1	-.27306062 -4
3086.000	1512.7225	.13364259 -1	.27394367 -4
3171.700	1513.9634	.15764548 -1	.29974504 -4
3257.400	1515.4245	.14212222 -1	-.66201966 -4
3200.300	1515.0321	.14942011 -1	.69479918 -4
3300.300	1517.6057	.17792047 -1	.32001604 -6
3400.300	1519.3026	.17705101 -1	.32029470 -6
3500.300	1521.1620	.17017002 -1	.32577515 -6
3600.300	1522.9462	.17090399 -1	.32619062 -6
3700.300	1524.7320	.17002001 -1	.32340033 -6
3800.300	1526.5220	.17915277 -1	.32444000 -6
3900.300	1528.3159	.17047508 -1	.32176971 -6
4000.300	1530.1123	.17079727 -1	.32101347 -6
4100.300	1531.9110	.18011713 -1	.31071130 -6
4200.300	1533.7146	.18043966 -1	.31033649 -6
4300.300	1535.5206	.18075247 -1	.31520473 -6
4400.300	1537.3297	.18106718 -1	.31414032 -6
4500.300	1539.1419	.18130037 -1	.31223297 -6
4600.300	1540.9573	.18169136 -1	.30975342 -6
4700.300	1542.7757	.18260016 -1	.30704607 -6
4800.300	1544.5973	.18230705 -1	.30593072 -6
4900.300	1546.4219	.18241127 -1	.30250540 -6
5000.300	1548.2495	.18301330 -1	.30155182 -6
5100.300	1550.0801	.18321205 -1	.29754639 -6
5200.300	1551.9138	.18320964 -1	.29602951 -6
5300.300	1553.7503	.18380365 -1	.29201508 -6
5400.300	1555.5898	.18409443 -1	.28953552 -6
5500.300	1557.4322	.18432244 -1	.28648374 -6
5600.300	1559.2775	.18438244 -1	.28648374 -6

Table 5.5.1.5

DATE 19 4 1956 10 1

SHALLOW PROFILE AT RANGE 144,400 MILES

TABLE OF VALUES OF OBSERVED POINTS

DEPTH-METERS	VELOCITY-M/SEC	COEFFICIENT Z	COEFFICIENT D
.000	1540.1600	.18229129 0	-.10999997 -1
10.000	1541.4324	.77241783 -1	-.10599947 -1
20.000	1541.6644	.28942207 -1	.22000313 -2
30.000	1541.9073	.02975671 -1	.86866616 -2
35.000	1542.5185	-.27758026 -1	-.52800140 -1
40.000	1541.7197	-.16075878 0	-.40016176 -3
45.000	1540.9109	-.25375996 0	-.36800308 -1
50.000	1539.1621	-.24009348 0	.10046900 -1
60.000	1538.6945	-.70259327 -1	-.47000694 -2
70.000	1537.6569	-.11275980 0	-.26000404 -2
80.000	1536.3093	-.13876047 0	-.26000736 -2
90.000	1534.8817	-.20376205 0	-.10400238 -1
95.000	1533.7329	-.10876079 0	.49200745 -1
100.000	1533.8141	-.59093666 -1	-.30133896 -1
110.000	1531.7164	-.18096272 0	.97600860 -2
125.000	1529.6900	-.11981203 0	.24200098 -2
150.000	1527.4100	-.10190266 0	-.10080566 -2
175.000	1524.5519	-.93943203 -1	.16480133 -2
200.000	1522.7178	-.57182705 -1	.12960266 -2
225.000	1521.6037	-.35382320 -1	.44800415 -3
250.000	1520.9497	-.24182216 -1	.44800415 -3
275.000	1520.4856	-.12781879 -1	.46402203 -3
300.000	1520.3116	-.11028531 -1	-.12539502 -3
350.000	1519.3539	-.42330851 -2	.59717287 -3
370.000	1519.3802	-.16505872 -1	-.10334516 -2
400.000	1518.0653	-.46073055 -1	-.19160394 -3
450.000	1515.4770	-.71410032 -1	-.78578513 -3
470.000	1513.8917	-.62400182 -1	.16867701 -2
500.000	1512.7787	-.41624208 -1	-.30170504 -3
550.000	1510.3204	-.32292348 -1	.67737935 -3
575.000	1509.7263	-.10210506 0	-.62871967 -2
580.000	1509.1374	-.16784450 -1	.40403442 -1
585.000	1509.5583	-.84771156 -1	-.47606125 -1
590.000	1508.2897	-.18644702 0	.26939781 -1
600.000	1507.7720	-.33653194 -1	.36260836 -2
615.000	1507.6759	-.17289020 -1	-.14477604 -2
650.000	1506.1837	-.49398456 -1	-.38706445 -3
670.000	1505.1183	-.27016544 -1	.26252556 -2
690.000	1505.1030	-.60103703 -1	-.59339714 -2
700.000	1504.2053	-.75714903 -1	.20117193 -2
725.000	1503.1911	-.48149594 -1	-.60800411 -3
750.000	1501.7968	-.52497012 -1	.26109063 -3

TABLE OF VALUES OF EXTRAPOLATED POINTS

DEPTH-METERS	VELOCITY-M/SEC	Z COEFFICIENT	D COEFFICIENT
897.200	1497.6739	-.33040454 -1	.10039860 -3
942.900	1495.2075	-.23402681 -1	.12349376 -3
1028.700	1493.6614	-.13942993 -1	.94545590 -4
1114.400	1492.8120	-.64882830 -2	.79093372 -4
1200.700	1492.5496	-.30897756 -2	-.07083635 -6
1285.800	1492.2837	.47310580 -3	.84540315 -4
1371.500	1492.6347	.15270077 -2	-.99945173 -4
1457.300	1492.5451	.97492362 -3	.47076080 -4
1543.000	1492.8015	.61047762 -2	.72687107 -4
1628.700	1493.5918	.95113409 -2	.68126525 -5
1714.400	1494.4321	.97470189 -2	-.13592562 -5
1800.100	1495.2624	.12130257 -1	.56977421 -4
1885.900	1496.5129	.12130547 -1	-.56970673 -4
1971.600.	1497.3433	.12140686 -1	.57207289 -4
2057.300	1498.5938	.14516589 -1	-.64277489 -5
2131.000	1499.6319	.21737969 -2	-.32309187 -3
2143.909	1499.6343	.14108854 -2	.19594095 -3
2228.700	1500.4748	.10966746 -1	.27066314 -4
2314.500	1501.5154	.13302985 -1	.27391469 -4
2400.200	1502.7566	.14535265 -1	.13665229 -5
2485.900	1504.0067	.14535643 -1	-.13577007 -5
2571.600	1505.2474	.14117780 -1	-.03940670 -5
2657.400	1506.4278	.13360932 -1	-.92480893 -5
2743.100	1507.5389	.14089004 -1	.44909038 -4
2828.000	1508.9796	.16930312 -1	.27294249 -5
2914.500	1510.4400	.15743346 -1	-.29963197 -4
3000.200	1511.6816	.13305932 -1	-.27306062 -4
3086.000	1512.7229	.13306289 -1	.27304367 -4
3171.700	1513.9634	.15746948 -1	.29574504 -4
3257.400	1515.4249	.14212222 -1	-.66201566 -4
3200.300	1515.8321	.14782811 -1	.69475918 -4
3300.300	1517.6057	.17752647 -1	.32081604 -6
3400.300	1519.3026	.17745101 -1	.32029470 -6
3500.300	1521.1620	.17817802 -1	.32577515 -6
3600.300	1522.9462	.17850399 -1	.32619662 -6
3700.300	1524.7524	.17892081 -1	.32340833 -6
3800.300	1526.5228	.17915277 -1	.32444000 -6
3900.300	1528.3159	.17967588 -1	.32174971 -6
4000.300	1530.1123	.17979727 -1	.32101347 -6
4100.300	1531.9118	.18011713 -1	.31871130 -6
4200.300	1533.7146	.18043566 -1	.31633449 -6
4300.300	1535.5206	.18075247 -1	.31528473 -6
4400.300	1537.3297	.18106718 -1	.31414032 -6
4500.300	1539.1419	.18138037 -1	.31223297 -6
4600.300	1540.9573	.18169136 -1	.30979342 -6
4700.300	1542.7757	.18200016 -1	.30784607 -6
4800.300	1544.5973	.18230705 -1	.30593072 -6
4900.300	1546.4219	.18261127 -1	.30250549 -6
5000.300	1548.2495	.18291330 -1	.30155182 -6
5100.300	1550.0801	.18321285 -1	.29754639 -6
5200.300	1551.9138	.18350964 -1	.29602051 -6
5300.300	1553.7503	.18380365 -1	.29201508 -6
5400.300	1555.5898	.18409443 -1	.28993552 -6
5500.300	1557.4322	.18438244 -1	.28648376 -6
5600.300	1559.2775	.18438244 -1	.28648376 -6

Table 5.5.1.6

[illegible]

[illegible]

TABLE OF VALUES OF [illegible] POINTS

DEPTH—METERS	VELOCITY—M/SEC	Z COEFFICIENT	D COEFFICIENT
.000	[illegible]	[illegible]	[illegible]
10.000	1541.2924	.57[illegible]21 -2	.3[illegible]9336 -2
20.000	1541.1[illegible]	.1[illegible]224 [illegible]	.31[illegible]5 -1
25.000	1542.34[illegible]	.1[illegible]6215 [illegible]	-.34[illegible]6 -1
30.000	1542.417[illegible]	.1[illegible]42137 -1	.54[illegible]91227 -2
40.000	[illegible]	[illegible]	[illegible]
50.000	1542.2721	-.1[illegible]5944 0	-.29[illegible]7 -1
60.000	151[illegible].5845	-.3147512[illegible] 0	.2959224 -1
70.000	1516.4160	-.2[illegible] 0	.2[illegible]0150 -1
80.000	1515.4[illegible]	-.1[illegible]4 0	-.51[illegible]0077 -2
90.000	1533.4[illegible]	-.17276166 0	-.38[illegible]01[illegible]6 -2
95.000	1532.9829	-.8[illegible]2422 -1	.3[illegible]00[illegible]1 -1
100.000	1533.0[illegible]41	-.1[illegible]9283[illegible] -1	-.1123[illegible]4 -1
115.000	1531.547[illegible]	-.2[illegible]59666 0	-.13[illegible]6665 -1
120.000	1530.3488	-.111[illegible]6[illegible] 0	.51[illegible]00343 -1
125.000	1530.4300	-.1[illegible]2630[illegible] -1	-.12[illegible]00779 -1
140.000	1528.8436	-.4[illegible]141[illegible]11 -1	.76[illegible]01[illegible]53 -2
150.000	1528.7460	-.7[illegible]28552 -1	-.12[illegible]13054 -1
165.000	1526.[illegible]098	-.12863[illegible]15 0	.55734455 -2
175.000	1525.3819	-.1[illegible]32055 0	-.209[illegible]5[illegible]0 -2
200.000	1522.1478	-.7[illegible]6[illegible]3331 -1	.39[illegible]40[illegible]3 -2
225.000	1521.4037	-.23[illegible]41981 -1	.46401062 -3
250.000	1520.9497	-.1[illegible]3[illegible]2007 -1	-.16112573 -4
275.000	1520.4958	-.1[illegible]741979 -1	.46402283 -3
300.000	1520.311[illegible]	-.[illegible]284220 -2	-.16534627 -3
350.000	1519.6636	-.1[illegible]3868[illegible] -1	-.66715076 -5
380.000	1517.2506	-.31010167 -1	-.12334150 -2
400.000	1518.[illegible]653	-.3[illegible]1852[illegible] -2	.4110[illegible]4[illegible]4 -2
410.000	1518.5377	.47[illegible]5406 -2	-.25101678 -2
450.000	1510.7271	-.4[illegible] -1	-.1[illegible]1[illegible]19 -3
500.000	1514.0780	-.54666620 -1	-.44[illegible]216[illegible]7 -4
550.000	1511.1[illegible]05	-.5[illegible]647[illegible]36 -1	.91592950 -4
600.000	1509.7021	-.44147294 -1	.24[illegible]00873 -3
650.000	1506.8837	-.4[illegible]367859 -1	-.16[illegible]0[illegible]111 -3
700.000	1504.5553	-.8[illegible]40061 -1	-.17191[illegible]70 -2
715.000	1503.0187	-.66771444 -1	.47560628 -2
730.000	1502.5522	-.4[illegible]601276 -1	-.24[illegible]69738 -2
750.000	1501.[illegible]	-.6[illegible]66[illegible]2 -1	.55[illegible]69220 -3

TABLE OF VALUES OF EXTRAPOLATED POINTS

DEPTH—METERS	VELOCITY—M/SEC	Z COEFFICIENT	D COEFFICIENT
857.200	1496.9138	-.33090363 -1	.10615349 -3
942.900	1494.4712	-.23036861 -1	.12753366 -3
1028.700	1492.9540	-.13244050 -1	.10127061 -3
1114.400	1492.1955	-.52129209 -2	.87503688 -4
1200.700	1492.0711	-.14840189 -2	-.97061569 -6
1285.800	1491.9413	.20718616 -2	.84540073 -4
1371.500	1492.4293	.31257440 -2	-.59945345 -4
1457.300	1492.4768	.21723487 -2	.13721718 -4
1543.000	1492.8015	.65050715 -2	.63392060 -4
1628.700	1493.5018	.95113409 -2	.68126575 -5
1714.400	1494.4321	.97470189 -2	-.13592562 -5
1800.100	1495.2624	.12110257 -1	.56977421 -4
1885.900	1496.5129	.12130547 -1	-.56970673 -4
1971.600	1497.3433	.12140686 -1	.57707289 -4
2057.300	1498.5038	.14316589 -1	-.64777489 -5
2131.000	1499.6315	.21717909 -2	-.32309187 -3
2143.000	1499.6343	.14108854 -2	.19594095 -3
2228.700	1500.4748	.10966746 -1	.27166314 -4
2314.500	1501.5154	.13362985 -1	.27391469 -4
2400.200	1502.7560	.14595265 -1	.13165229 -5
2485.900	1504.0067	.14515643 -1	-.13577007 -5
2571.600	1505.2474	.14065914 -1	-.96044772 -5
2657.400	1506.4189	.13341053 -1	-.68258527 -5
2743.100	1507.5389	.14940961 -1	.43196508 -4
2828.800	1508.9798	.16930312 -1	.27294249 -5
2914.500	1510.4408	.15763346 -1	-.29963157 -4
3000.200	1511.6916	.13305932 -1	-.27386062 -4
3086.000	1512.7225	.13306289 -1	.27394367 -4
3171.700	1513.9634	.15744548 -1	.29974584 -4
3257.400	1515.4245	.14212222 -1	-.66201566 -4
3288.300	1515.8321	.14262811 -1	.69475918 -4
3388.300	1517.6057	.17752647 -1	.32081604 -6
3488.300	1519.3826	.17745101 -1	.32625470 -6
3588.300	1521.1626	.17817802 -1	.32577515 -6
3688.300	1522.9462	.17850391 -1	.32615662 -6
3788.300	1524.7328	.17882891 -1	.32367716 -6
3888.300	1526.5228	.17915277 -1	.32405853 -6
3988.300	1528.3159	.17947578 -1	.32196045 -6
4088.300	1530.1123	.17979727 -1	.32101347 -6
4188.300	1531.9118	.18011723 -1	.31690203 -6
4288.300	1533.7146	.18043566 -1	.31795502 -6
4388.300	1535.5206	.18075237 -1	.31547546 -6
4488.300	1537.3297	.18106718 -1	.31414032 -6
4588.300	1539.1419	.18138037 -1	.31223297 -6
4688.300	1540.9573	.18169136 -1	.30975342 -6
4788.300	1542.7757	.18200016 -1	.30784607 -6
4888.300	1544.5973	.18230705 -1	.30593872 -6
4988.300	1546.4219	.18261137 -1	.30269623 -6
5088.300	1548.2495	.18291330 -1	.30117035 -6
5188.300	1550.0801	.18321276 -1	.29773712 -6
5288.300	1551.9138	.18350964 -1	.29602051 -6
5388.300	1553.7503	.18380365 -1	.29201508 -6
5488.300	1555.5898	.18419443 -1	.28553552 -6
5588.300	1557.4322	.18438244 -1	.28648376 -6
5688.300	1559.2775	.18438244 -1	.28648376 -6

Table 5.5.1.7

[illegible] PROFILE AT RANGE [illegible] MILES

TABLE OF VALUES OF OBSERVED POINTS

DEPTH-METERS	VELOCITY-M/SEC	Z COEFFICIENT	D COEFFICIENT
.500	1541.2700	-.19246574 -1	.82100940 -2
10.000	1541.3124	.27742204 -1	.82 09290 -2
20.000	[illegible]	[illegible]	[illegible]
30.000	1542.4173	.34742254 -1	-.84490695 -2
40.000	1542.5997	.52432838 -2	-.21005490 -2
50.000	1542.5921	-.24946594 -1	-.14805115 -1
55.000	1541.9731	-.71298492 -1	.17800098 -1
60.000	1541.8545	-.23678019 0	-.81600714 -1
65.000	1537.6657	-.10670121 1	.53800402 -1
70.000	1538.9209	-.94254603 -1	.27700403 -1
75.000	1538.8781	-.14676037 0	-.44600766 -1
82.500	1537.1591	-.21669481 0	.21464480 -1
90.000	1536.1117	-.11576042 0	-.26000977 -2
100.000	1535.0441	-.15203265 0	-.83435751 -1
125.000	1531.4400	-.15864454 0	-.12220306 -2
135.000	1529.8124	-.12229586 0	.74534794 -2
150.000	1528.7460	-.80741910 -1	-.12809573 -2
165.000	1527.3494	-.13163038 0	-.99339139 -2
170.000	1526.6607	-.61741982 -1	.32700903 -1
175.000	1526.7519	-.37627964 -1	-.22667329 -1
185.000	1525.2641	-.17763081 0	.43467740 -2
200.000	1523.8478	-.95610465 -1	-.18170654 -1
210.000	1522.5607	-.54282829 -1	.85002527 -2
220.000	1522.3626	-.10776475 0	-.19700617 -1
225.000	1521.9038	-.10776463 0	.19600600 -1
235.000	1521.8861	-.16628228 -1	-.85330847 -1
250.000	1521.5597	-.25178836 -1	-.50609206 -1
275.000	1520.7854	-.19542045 -1	.91703813 -3
300.000	1520.8116	-.73283127 -2	-.93379244 -3
350.000	1520.2539	-.16342343 -1	-.36802368 -3
400.000	1518.9756	-.45730907 -1	-.60171070 -3
410.000	1518.5177	-.12641862 0	-.16534474 -1
415.000	1517.6909	-.55633915 0	.24534918 -1
425.000	1517.8613	-.47049750 -2	-.42208846 -2
450.000	1516.4171	-.67140725 -1	-.75159319 -3
480.000	1514.0441	-.59412969 -1	.18667971 -2
510.000	1513.4288	-.32880861 -1	-.10859628 -3
550.000	1511.4505	-.39540193 -1	-.16002502 -1
600.000	1509.4722	-.49467719 -1	-.24083601 -1
610.000	1508.9445	-.34246177 -1	.33003044 -2
620.000	1508.7464	-.11110958 0	-.22869940 -1
625.000	1507.8479	-.85771561 -1	.40804130 -1
630.000	1507.9591	-.13698195 -1	-.13734702 -1
640.000	1507.3614	-.15698450 -1	.13734741 -1
645.000	1507.1428	-.47772560 -1	-.41604345 -1
650.000	1506.1437	-.81772560 -1	.41604345 -1
655.000	1506.2440	-.14412145 -1	-.13868179 -1
665.000	1505.1471	-.82564154 -1	.10811575 -2
720.000	1503.1352	-.53541781 -1	.28572518 -3
725.000	1501.7409	-.16267880 -2	.41718953 -2
735.000	1501.9133	.16871236 -1	-.13328592 -3
740.000	1501.9949	-.17027043 0	-.98604982 -1
745.000	1500.6159	-.16578407 0	.44009127 -1
750.000	1500.3166	-.54000429 -1	.31231097 -1

TABLE OF VALUES OF EXTRAPOLATED POINTS

DEPTH-METERS	VELOCITY-M/SEC	Z COEFFICIENT	D COEFFICIENT
897.200	1488.2161	-.32440081 -1	.10838487 -3
942.900	1483.8542	-.22947338 -1	.12831858 -3
1028.700	1492.4134	-.12304279 -1	.10247333 -3
1114.400	1491.7971	-.41301363 -2	.90433484 -4
1250.700	1491.7877	-.26904840 -3	-.97142348 -6
1285.800	1491.8817	.32860208 -2	.84540812 -4
1371.500	1492.2735	.43309188 -2	-.59945555 -4
1457.300	1492.4250	.30817378 -2	.30817323 -4
1543.000	1492.8015	.68075543 -2	.96332091 -4
1628.700	1493.5018	.95113409 -2	.60126529 -5
1714.400	1494.4321	.97470109 -2	-.13592562 -5
1800.100	1495.2624	.12110257 -1	.56977421 -4
1885.900	1496.5129	.12130547 -1	-.56970673 -4
1971.603	1497.3633	.12140888 -1	.57287280 -4
2057.300	1498.5638	.14316589 -1	-.64277489 -5
2131.000	1499.6115	.21737909 -2	-.32309187 -3
2133.000	1499.6345	.14108854 -2	.19924098 -3
2228.700	1500.4748	.10966746 -1	.27066314 -4
2314.500	1501.5154	.13302985 -1	.27391449 -4
2400.200	1502.7560	.14515269 -1	.13665229 -5
2485.900	1504.0067	.14915643 -1	-.13577007 -5
2571.600	1505.2474	.14043952 -1	-.10070338 -4
2657.400	1506.4155	.13561100 -1	-.58939043 -5
2743.100	1507.5189	.14040958 -1	.43220831 -4
2828.803	1508.8798	.16010312 -1	.27294249 -5
2914.500	1510.4408	.15743146 -1	-.29963157 -4
3000.200	1511.6816	.11365937 -1	-.27308062 -4
3086.000	1512.7225	.13306780 -1	.27394367 -4
3171.700	1513.9634	.15744548 -1	.20974584 -4
3257.400	1515.4245	.14212222 -1	-.66701566 -4
3288.300	1515.9571	.14242811 -1	.69479918 -4
3388.300	1517.6057	.17742647 -1	.32001604 -6
3488.300	1519.3626	.17785101 -1	.32025470 -6
3588.300	1521.1628	.17817802 -1	.32577519 -6
3688.300	1522.9487	.17890394 -1	.32619662 -6
3788.300	1524.7328	.17882891 -1	.32367706 -6
3888.300	1526.5728	.17915277 -1	.32409053 -6
3988.300	1528.3159	.17942578 -1	.32196045 -6
4088.300	1530.1123	.17979727 -1	.32101347 -6
4188.300	1531.9118	.18011723 -1	.31890203 -6
4288.300	1533.7148	.18043586 -1	.31795502 -6
4388.300	1535.5206	.18075237 -1	.31547546 -6
4488.300	1537.3297	.18106718 -1	.31414032 -6
4588.300	1539.1419	.18118037 -1	.31221297 -6
4688.300	1540.9573	.18149136 -1	.30979342 -6
4788.300	1542.7757	.18200515 -1	.30784607 -6
4888.300	1544.5973	.18210709 -1	.30593872 -6
4988.300	1546.4219	.18241137 -1	.30269823 -6
5088.300	1548.2495	.18291330 -1	.30117339 -6
5188.300	1550.0801	.18321278 -1	.29773712 -6
5288.300	1551.9138	.18350864 -1	.29802351 -6
5388.300	1553.7503	.18382185 -1	.29231598 -6
5488.300	1555.5898	.18404443 -1	.28953552 -6
5588.300	1557.4322	.18418244 -1	.28644376 -6
5688.300	1559.2775	.18418244 -1	.28644376 -6

Table 5.5.1.8

DATE 19 4 1968 ID NUMBER 1A8 SET 1

SHALLOW PROFILE AT RANGE 201.000 MILES

TABLE OF VALUES OF OBSERVED POINTS

DEPTH-METERS	VELOCITY-M/SEC	COEFFICIENT Z	COEFFICIENT D
.000	1541.9300	-.17258549 -1	.23000526 -2
10.000	1541.8724	.57419777 -2	.23000526 -2
20.000	1542.0448	.60742474 -1	.87000465 -2
30.000	1543.0873	.71242618 -1	-.86000176 -2
40.000	1543.4697	-.47577858 -2	-.86000633 -2
50.000	1542.9921	-.10425882 0	-.11300144 -1
60.000	1541.3849	-.18525991 0	-.49000740 -2
70.000	1539.2869	-.18976030 0	.39999962 -2
80.000	1537.5893	-.13576021 0	.68000221 -2
90.000	1536.5717	-.28176320 0	-.36000621 -1
95.000	1534.7129	-.12876091 0	.07201538 -1
100.000	1535.2841	.44575055 -1	-.27867152 -1
115.000	1532.8177	-.86027476 -1	.10453481 -1
125.000	1532.4801	-.54674879 -1	-.41829616 -2
150.000	1529.8060	-.56104028 -1	.40686297 -2
160.000	1529.4484	-.71761856 -1	-.72001953 -2
175.000	1527.5620	-.11791339 0	.10999908 -2
200.000	1524.9679	-.94363556 -1	.75199585 -3
225.000	1522.8438	-.62943104 -1	.17600403 -2
250.000	1521.8197	-.23741978 -1	.13760498 -2
275.000	1521.6557	-.12541679 -1	-.46402588 -3
300.000	1521.2016	-.14428533 -1	.29867757 -3
350.000	1520.8536	-.10161858 -1	-.12801056 -3
400.000	1520.1854	-.31943939 -1	-.74405870 -3
450.000	1517.6577	-.54665680 -1	-.16402893 -3
500.000	1514.7189	-.60066986 -1	-.52023315 -4
550.000	1511.6509	-.55867500 -1	.22000275 -3
600.000	1509.1321	-.54668312 -1	-.17203522 -3
650.000	1506.1837	-.56469345 -1	.99993896 -4
700.000	1503.4857	-.47177517 -1	.27167924 -3
730.000	1502.1921	-.72906024 -1	-.19869130 -2
750.000	1500.3366	-.84492793 -1	.81223607 -3

TABLE OF VALUES OF EXTRAPOLATED POINTS

DEPTH-METERS	VELOCITY-M/SEC	Z COEFFICIENT	D COEFFICIENT
857.200	1496.0652	-.33640329 -1	.11575766 -3
942.900	1493.6874	-.23070406 -1	.13091501 -3
1028.700	1492.1098	-.12745499 -1	.10975881 -3
1114.400	1491.4206	-.37523807 -2	.10011560 -3
1200.700	1491.4696	.52570762 -3	-.97102874 -6
1285.800	1491.5108	.40816015 -2	.84540803 -4
1371.500	1492.1710	.51354889 -2	-.59945999 -4
1457.300	1492.3910	.36775986 -2	.25962541 -4
1543.000	1492.8015	.70857561 -2	.51707412 -4
1628.700	1493.5918	.95133409 -2	.68126525 -5
1714.400	1494.4321	.97470189 -2	-.13592562 -5
1800.100	1495.2624	.12130257 -1	.56977421 -4
1885.900	1496.5129	.12130547 -1	-.56970673 -4
1971.600	1497.3433	.12140686 -1	.57207289 -4
2057.300	1498.5938	.14316589 -1	-.64877489 -5
2131.000	1499.6315	.21737909 -2	-.32309187 -3
2143.000	1499.6343	.14108854 -2	.19594095 -3
2228.700	1500.4748	.10966746 -1	.27066314 -4
2314.500	1501.5154	.13302985 -1	.27391469 -4
2400.200	1502.7560	.14535265 -1	.13665229 -5
2485.900	1504.0067	.14535643 -1	-.13577007 -5
2571.600	1505.2474	.13979967 -1	-.11610248 -4
2657.400	1506.4042	.13381254 -1	-.28119711 -5
2743.100	1507.5389	.15027058 -1	.41687226 -4
2828.800	1508.9798	.16930312 -1	.27294249 -5
2914.500	1510.4408	.15763346 -1	-.29963157 -4
3000.200	1511.6816	.13305932 -1	-.27388062 -4
3086.000	1512.7225	.13306289 -1	.27394367 -4
3171.700	1513.9634	.15764948 -1	.29974584 -4
3257.400	1515.4245	.14212222 -1	-.66201506 -4
3288.300	1515.8321	.14262811 -1	.69475918 -4
3388.300	1517.6057	.17752647 -1	.32081604 -6
3488.300	1519.3828	.17785101 -1	.32025470 -6
3588.300	1521.1628	.17817602 -1	.32577515 -6
3688.300	1522.9462	.17850399 -1	.32615562 -6
3788.300	1524.7328	.17882891 -1	.32367706 -6
3888.300	1526.5228	.17915277 -1	.32405853 -6
3988.300	1528.3159	.17947578 -1	.32196045 -6
4088.300	1530.1123	.17979727 -1	.32101347 -6
4188.300	1531.9118	.18011723 -1	.31890203 -6
4288.300	1533.7146	.18043566 -1	.31795502 -6
4388.300	1535.5206	.18075237 -1	.31547546 -6
4488.300	1537.3297	.18106718 -1	.31414032 -6
4588.300	1539.1419	.18138037 -1	.31223297 -6
4688.300	1540.9573	.18169136 -1	.30975342 -6
4788.300	1542.7757	.18200016 -1	.30784607 -6
4888.300	1544.5973	.18230705 -1	.30593872 -6
4988.300	1546.4219	.18261137 -1	.30269623 -6
5088.300	1548.2495	.18291330 -1	.30117035 -6
5188.300	1550.0801	.18321276 -1	.29773712 -6
5288.300	1551.9138	.18350964 -1	.29602051 -6
5388.300	1553.7503	.18380365 -1	.29201508 -6
5488.300	1555.5898	.18409443 -1	.28953552 -6
5588.300	1557.4322	.18438244 -1	.28648376 -6
5688.300	1559.2775	.18438244 -1	.28648376 -6

Table 5.5.1.9

[illegible]

SHALLOW PROFILE AT RANGE 219.30? MILES

TABLE OF VALUES OF OBSERVED POINTS

DEPTH-METERS	VELOCITY-M/SEC	COEFFICIENT Z	COEFFICIENT D
.000	1541.9400	.15741736 -1	.10002136 -3
10.000	1542.0924	.16741943 -1	.10002136 -3
20.000	1542.2648	.27742290 -1	.21000481 -2
30.000	1542.6473	.49242592 -1	.22000172 -2
40.000	1543.2497	.67421799 -2	-.10600395 -1
50.000	1542.7771	-.93258762 -1	-.91000939 -2
60.000	1541.3849	-.15125952 0	-.25000272 -2
70.000	1539.7469	-.14275980 0	.42000308 -2
80.000	1538.5293	-.99249567 -1	.45600458 -2
90.000	1537.7617	-.77759547 -1	-.20006180 -3
100.000	1536.9141	-.81902951 -1	-.42659889 -3
125.000	1534.7301	-.96041021 -1	-.97604675 -3
150.000	1532.1261	-.95441714 -1	.68799133 -3
175.000	1529.9520	-.10476276 0	-.14240753 -2
200.000	1526.8879	-.61930700 -1	.38458404 -2
210.000	1526.5103	-.67659331 -1	-.59739667 -2
225.000	1524.8239	-.10228093 0	.13533541 -2
250.000	1522.6898	-.63543380 -1	.17600494 -2
275.000	1521.6557	-.29742383 -1	.02603039 -3
300.000	1521.2016	-.15428642 -1	.13866882 -3
350.000	1520.5539	-.25242795 -1	-.49203491 -3
400.000	1518.5754	-.47644700 -1	-.40404129 -3
450.000	1515.7871	-.40622008 -1	.68574896 -3
485.000	1514.7853	.10631595 -1	.22430254 -2
490.000	1514.8689	-.28430893 -1	-.17648024 -1
500.000	1513.7488	-.86149074 -1	.91203875 -2
525.000	1513.1947	-.29744915 -1	-.52605481 -3
550.000	1512.3106	-.42409720 -1	-.57072957 -3
600.000	1509.4722	-.54268150 -1	.99592370 -4
650.000	1506.8837	-.24245931 -1	.11000964 -2
660.000	1506.6961	-.51148938 -1	-.64606976 -2
675.000	1505.1095	-.65103912 -1	.46227010 -2
690.000	1504.7430	-.87440038 -1	-.76275177 -2
700.000	1503.4857	-.10810912 0	.35337003 -2
730.000	1501.8321	-.55804094 -1	-.46098252 -4
750.000	1500.7067	-.55915321 -1	.23357551 -3

TABLE OF VALUES OF EXTRAPOLATED POINTS

DEPTH-METERS	VELOCITY-M/SEC	Z COEFFICIENT	D COEFFICIENT
857.200	1496.2669	-.34944211 -1	.12073624 -3
942.900	1493.7156	-.24085859 -1	.13266754 -3
1028.700	1492.1273	-.13474739 -1	.11467791 -3
1114.400	1491.4037	-.39006649 -2	.10069404 -3
1200.700	1491.4564	.56096338 -3	-.97087510 -6
1285.800	1491.5014	.31294439 -2	.84540334 -4
1371.500	1492.1454	.51793301 -2	-.59945558 -4
1457.300	1492.3891	.37104389 -2	.25705668 -4
1543.000	1492.8015	.70160727 -2	.51452649 -4
1628.700	1493.5918	.95133409 -2	.68126525 -5
1714.400	1494.4321	.97470189 -2	-.13592562 -5
1800.100	1495.2624	.12110257 -1	.56977421 -4
1885.900	1496.5129	.12130547 -1	-.56970873 -4
1971.600	1497.3433	.12140686 -1	.57207289 [illegible]
2057.300	1498.5938	.14316589 -1	-.64277489 [illegible]
2131.000	1499.6315	.21737909 -2	-.32309187 -3
2143.000	1499.6343	.14108054 -2	.19594095 -3
2228.700	1500.4748	.10086746 -1	.27066314 -4
2314.500	1501.5154	.13302985 -1	.27301469 -4
2400.200	1502.7560	.14515265 -1	.13669229 -5
2485.900	1504.0067	.14535643 -1	-.13577007 -5
2571.600	1505.2474	.13935410 -1	-.12650075 -4
2657.400	1506.3969	.13361358 -1	-.73110241 -6
2743.100	1507.5389	.15071693 -1	.40645577 -4
2828.800	1508.9798	.16930312 -1	.27294209 -5
2914.500	1510.4408	.15763346 -1	-.29963157 -4
3000.200	1511.6816	.13305932 -1	-.27386062 -4
3086.000	1512.7229	.13306289 -1	.27394367 -4
3171.700	1513.9634	.15744548 -1	.29974584 -4
3257.400	1515.4249	.14212722 -1	-.46201566 -4
3288.300	1515.6321	.14242811 -1	.69475918 -4
3388.300	1517.6057	.17742647 -1	.32081004 -6
3488.300	1519.3826	.17785101 -1	.32625470 -6
3588.300	1521.1628	.17817807 -1	.32577515 -6
3688.300	1522.9462	.17850399 -1	.32615662 -6
3788.300	1524.7328	.17882891 -1	.32367706 -6
3888.300	1526.5228	.17915277 -1	.32405853 -6
3988.300	1528.3159	.17947578 -1	.32196045 -6
4088.300	1530.1123	.17979727 -1	.32101347 -6
4188.300	1531.9118	.18011723 -1	.31690203 -6
4288.300	1533.7146	.18043566 -1	.31795502 -6
4388.300	1535.5206	.18075237 -1	.31547546 -6
4488.300	1537.3297	.18106718 -1	.31414032 -6
4588.300	1539.1419	.18138037 -1	.31223297 -6
4688.300	1540.9573	.18169136 -1	.30975342 -6
4788.300	1542.7757	.18200016 -1	.30784607 -6
4888.300	1544.5973	.18230705 -1	.30593872 -6
4988.300	1546.4219	.18261137 -1	.30269623 -6
5088.300	1548.2495	.18291330 -1	.30117035 -6
5188.300	1550.0801	.18321276 -1	.29773712 -6
5288.300	1551.9138	.18350964 -1	.29602051 -6
5388.300	1553.7503	.18380365 -1	.29201508 -6
5488.300	1555.5898	.18409443 -1	.28953552 -6
5588.300	1557.4322	.18438244 -1	.28640376 -6
5688.300	1559.2775	.18438244 -1	.28648376 -6

Table 5.5.1.10

DATE 19 4 1968 ID NUMBER 165 SET 1

SHALLOW PROFILE AT RANGE 234.005 MILES

TABLE OF VALUES OF OBSERVED POINTS

DEPTH-METERS	VELOCITY-M/SEC	COEFFICIENT Z	COEFFICIENT D
.000	1542.5800	.87124733 0	-.17180009 0
5.000	1544.8017	.17241859 -1	-.17080009 0
10.000	1542.7524	-.24275818 0	.96800079 -1
20.000	1542.9148	.57421684 -2	-.21800099 -2
30.000	1542.8473	.16742420 -1	.43000603 -2
40.000	1543.2497	-.37757969 -1	-.15200138 -1
50.000	1542.1121	-.56425158 -1	.11486700 -1
55.000	1541.9733	-.13073345 0	-.44800415 -1
60.000	1540.7145	-.21542689 0	.14533437 -1
70.000	1539.2869	-.86259174 -1	.11303106 -1
80.000	1538.9893	-.41298907 -1	-.23000526 -2
90.000	1538.4817	-.53259182 -1	-.10000229 -3
100.000	1537.9241	-.52816430 -1	.22855268 -3
125.000	1536.6807	-.95580837 -1	-.36641052 -2
150.000	1533.1461	-.11876205 0	.18080078 -2
175.000	1530.7421	-.10876274 0	-.10080627 -2
200.000	1527.7080	-.13796459 0	-.13200849 -2
215.000	1525.5915	-.82383230 -1	.87202857 -2
225.000	1525.1039	-.45447935 -1	-.13372062 -2
250.000	1523.5498	-.57383091 -1	.38399353 -3
275.000	1522.2357	-.79582225 -1	.18400737 -2
300.000	1522.0717	-.12495003 -1	-.47469788 -3
350.000	1520.8538	-.24882652 -1	-.20008087 -4
400.000	1519.5854	-.41264191 -1	-.63605347 -3
450.000	1516.7271	-.55045804 -1	.83988952 -4
500.000	1514.0788	-.47466049 -1	.22000122 -3
550.000	1511.9805	-.47538161 -1	-.22288568 -3
570.000	1510.9852	-.41099733 -1	.86672846 -3
600.000	1510.1427	-.73214467 -1	-.30077108 -2
615.000	1508.7056	-.79270871 -1	.22001902 -2
640.000	1507.4114	-.28194618 -1	.18859100 -2
650.000	1507.2238	-.70270634 -1	-.10301113 -1
660.000	1506.0060	-.10822488 0	.27102842 -2
700.000	1503.8452	-.57909259 -1	-.19448323 -3
750.000	1500.7067	-.56254087 -1	.26069010 -3

TABLE OF VALUES OF EXTRAPOLATED POINTS

DEPTH-METERS	VELOCITY-M/SEC	Z COEFFICIENT	D COEFFICIENT
857.200	1496.1741	-.35595269 -1	.12473560 -3
942.900	1493.5817	-.24505190 -1	.13407605 -3
1028.700	1491.9726	-.13864175 -1	.11862826 -3
1114.400	1491.2373	-.37857591 -2	.11190654 -3
1200.700	1491.3273	.10011093 -2	-.97100565 -6
1285.800	1491.4089	.45569871 -2	.84540599 -4
1371.500	1492.1099	.56108802 -2	-.59945460 -4
1457.300	1492.3707	.40336610 -2	.23180443 -4
1543.000	1492.8015	.71241809 -2	.48943707 -4
1628.700	1493.5918	.95133409 -2	.68126525 -5
1714.400	1494.4321	.97470189 -2	-.13592562 -5
1800.100	1495.2624	.12130257 -1	.56977421 -4
1885.900	1496.9129	.12130547 -1	-.56970673 -4
1971.600	1497.3433	.12140686 -1	.57207289 -4
2057.300	1498.5938	.14316589 -1	-.64277489 -5
2131.000	1499.6319	.21737909 -2	-.32309187 -3
2143.000	1499.6343	.14108854 -2	.19594095 -3
2228.700	1500.4748	.10966746 -1	.27066314 -4
2314.500	1501.3154	.13302985 -1	.27391469 -4
2400.200	1502.7560	.14535265 -1	.13665229 -5
2485.900	1504.0067	.14535643 -1	-.13577007 -5
2571.600	1505.2474	.13899618 -1	-.13485359 -4
2657.400	1506.3904	.13361441 -1	.94044021 -6
2743.100	1507.5389	.15107548 -1	.39808831 -4
2828.800	1508.9798	.16930312 -1	.27294249 -5
2914.500	1510.4408	.15783346 -1	-.29963157 -4
3000.200	1511.6816	.13305932 -1	-.27386062 -4
3086.000	1512.7229	.13306289 -1	.27394367 -4
3171.700	1513.9634	.15744568 -1	.29974584 -4
3257.400	1515.4245	.14212222 -1	-.66201506 -4
3288.300	1515.8321	.14262811 -1	.69479918 -4
3388.300	1517.6057	.17792647 -1	.32081604 -6
3488.300	1519.3826	.17785101 -1	.32825470 -6
3588.300	1521.1628	.17817802 -1	.32577515 -6
3688.300	1522.9462	.17850399 -1	.32615662 -6
3788.300	1524.7328	.17882891 -1	.32367706 -6
3888.300	1526.5228	.17915277 -1	.32405853 -6
3988.300	1528.3159	.17947578 -1	.32196045 -6
4088.300	1530.1125	.17979727 -1	.32101347 -6
4188.300	1531.9118	.18011723 -1	.31890203 -6
4288.300	1533.7144	.18043566 -1	.31795502 -6
4388.300	1535.5206	.18075237 -1	.31547546 -6
4488.300	1537.3297	.18106718 -1	.31414032 -6
4588.300	1539.1419	.18138037 -1	.31223297 -6
4688.300	1540.9573	.18169136 -1	.30975342 -6
4788.300	1542.7757	.18200016 -1	.30784607 -6
4888.300	1544.5973	.18230705 -1	.30593872 -6
4988.300	1546.4219	.18261137 -1	.30269623 -6
5088.300	1548.2495	.18291330 -1	.30117035 -6
5188.300	1550.0801	.18321276 -1	.29773712 -6
5288.300	1551.9138	.18350964 -1	.29602051 -6
5388.300	1553.7503	.18380365 -1	.29201508 -6
5488.300	1555.5898	.18409443 -1	.28953552 -6
5588.300	1557.4322	.18438244 -1	.28648376 -6
5688.300	1559.2775	.18438244 -1	.28648376 -6

Table 5.5.1.11

DATA 19 [illegible]

SHALLOW PROFILE AT RANGE 239.200 MILES

TABLE OF VALUES OF OBSERVED POINTS

DEPTH-METERS	VELOCITY-M/SEC	COEFFICIENT Z	COEFFICIENT D
.000	1541.9100	.15741730 -1	.10062136 -3
10.000	1542.0024	.16741941 -1	.10002136 -3
20.000	[illegible]	[illegible]	.10673486 -2
30.000	1542.4173	.18742325 -1	-.09983215 -4
40.000	1542.5097	-.38957992 -1	-.11000080 -1
50.000	1541.6621	-.12825518 0	-.49101579 -2
60.000	1540.3149	-.22609348 0	-.12686702 -1
65.000	1538.7457	-.12075939 0	.54600339 -1
70.000	1538.8260	-.22425588 -1	-.15466817 -1
80.000	1537.8293	-.65294266 -1	.87000816 -2
95.000	1537.5217	-.67886899 -2	.48000336 -2
100.000	1537.6941	.72606686 -3	-.33029022 -2
125.000	1536.6802	-.96040731 -1	-.40321136 -2
150.000	1533.1461	-.17896395 0	-.29601440 -2
155.000	1532.2173	-.15596351 0	.12080322 -1
175.000	1531.5221	-.10449606 0	-.71735772 -2
200.000	1526.6179	-.12849733 0	.60534757 -2
215.000	1525.4915	-.36495031 -1	.51468302 -2
225.000	1525.3430	-.95784065 -1	-.17000637 -1
235.000	1523.5762	-.13043262 0	.81869252 -2
250.000	1522.3997	-.60190028 -1	.24334208 -2
275.000	1521.6557	-.23042135 -1	.46401062 -3
300.000	1521.2016	-.16428642 -1	.13866082 -1
350.000	1520.5535	-.10141858 -1	.11200258 -3
405.000	1520.1854	-.19662705 -1	-.49203644 -3
450.000	1518.5873	-.20706439 -1	.44660706 -3
480.000	1518.1644	.11908206 -1	.17334893 -2
485.000	1518.2458	-.35784186 -1	-.20801646 -1
495.000	1516.8479	-.35784694 -1	.20801544 -1
500.000	1516.9791	.10137919 -1	-.24404990 -2

TABLE OF VALUES OF EXTRAPOLATED POINTS

DEPTH-METERS	VELOCITY-M/SEC	Z COEFFICIENT	D COEFFICIENT
550.000	1514.3453	-.47519177 -1	.13341522 -3
580.000	1513.0192	-.52614896 -1	-.47312984 -3
595.000	1512.1764	-.77009883 -1	-.28908684 -2
600.000	1511.7507	-.77267025 -1	.31700116 -2
615.000	1510.9501	-.57070805 -1	-.49424889 -3
650.000	1508.6496	-.88181672 -1	-.12734864 -2
670.000	1506.6319	-.84818257 -1	.15048279 -2
700.000	1504.8089	-.46786277 -1	.03197081 -3
730.000	1503.8747	-.48005222 -1	-.10792338 -2
750.000	1502.6290	-.57480104 -1	.23014551 -3
857.200	1497.7888	-.38388625 -1	.12615075 -3
942.900	1494.9622	-.27916575 -1	.13457387 -3
1028.700	1493.1724	-.16794234 -1	.12002817 -3
1114.400	1492.1667	-.62763047 -2	.11376447 -3
1200.700	1492.0487	-.14092833 -2	-.97138967 -6
1285.800	1491.9253	.21445808 -2	.84540464 -4
1371.500	1492.4197	.32084809 -2	-.59945364 -4
1457.300	1492.4736	.22783239 -2	.37284361 -4
1543.600	1492.8019	.65736808 -2	.62957525 -4
1628.700	1493.5918	.95133409 -2	.88126525 -5
1714.400	1494.4321	.97470189 -2	-.13502562 -5
1800.100	1495.2624	.12110257 -1	.56977421 -4
1885.900	1496.5129	.12130547 -1	-.56970673 -4
1971.600	1497.3433	.12140686 -1	.57207289 -4
2057.300	1498.5938	.14316589 -1	-.64277489 -5
2131.000	1499.6315	.21737909 -2	-.32300187 -3
2143.000	1499.6343	.14108854 -2	.19594095 -3
2228.700	1500.4748	.10946745 -1	.27066314 -4
2314.500	1501.5154	.13302985 -1	.27391469 -4
2400.200	1502.7960	.14835265 -1	.13665229 -5
2485.900	1504.0067	.14835643 -1	-.13577007 -5
2571.600	1505.2474	.13896954 -1	-.13780898 -4
2657.400	1506.3882	.13341471 -1	.15318613 -5
2743.100	1507.5389	.15120233 -1	.39512775 -4
2028.600	1508.9798	.16910312 -1	.27294249 -5
2914.500	1510.4408	.15763346 -1	-.29963157 -4
3000.200	1511.6816	.13305932 -1	-.27386062 -4
3086.000	1512.7225	.13306289 -1	.27394367 -4
3171.700	1513.9634	.15784548 -1	.29974564 -4
3257.400	1515.4245	.14712222 -1	-.66201566 -4
3288.300	1515.8321	.14742811 -1	.69475918 -4
3388.300	1517.6057	.17742647 -1	.32081604 -6
3488.300	1519.3826	.17745101 -1	.32825470 -6
3588.300	1521.1620	.17817802 -1	.32577515 -6
3688.300	1522.9462	.17850399 -1	.32615662 -6
3788.300	1524.7328	.17882891 -1	.32367706 -6
3888.300	1526.5228	.17915277 -1	.32405853 -6
3988.300	1528.3159	.17947578 -1	.32196045 -6
4088.300	1530.1123	.17979727 -1	.32101347 -6
4188.300	1531.9118	.18011773 -1	.31890203 -6
4288.300	1533.7146	.18043566 -1	.31795502 -6
4388.300	1535.5206	.18075237 -1	.31547546 -6
4488.300	1537.3297	.18106718 -1	.31414032 -6
4588.300	1539.1419	.18138037 -1	.31223297 -5
4688.300	1540.9373	.18169136 -1	.30975342 -6
4788.300	1542.7757	.18200016 -1	.30784607 -6
4888.300	1544.5973	.18230705 -1	.30593872 -6
4988.300	1546.4219	.18261137 -1	.30269623 -6
5088.300	1548.2495	.18291330 -1	.30117035 -6
5188.300	1550.0801	.18321276 -1	.29773712 -6
5288.300	1551.9138	.18350964 -1	.29602051 -6
5388.300	1553.7503	.18380369 -1	.29201508 -6
5488.300	1555.5898	.18409443 -1	.28953552 -6
5588.300	1557.4322	.18438244 -1	.28648376 -6
5688.300	1559.2775	.18438244 -1	.28648376 -6

Table 5.5.1.12

DATE 19 4 1988 TO S ORDER ... SET 1

SHALLOW PROFILE AT RANGE 248.22? MILES

TABLE OF VALUES OF OBSERVED POINTS

DEPTH-METERS	VELOCITY-M/SEC	COEFFICIENT Z	COEFFICIENT D
.000	1542.1500	.15741634 -1	.10004044 -3
10.000	1542.3174	.15742039 -1	.10004044 -3
20.000	1542.4848	.15742220 -1	-.10000229 -3
[illegible]	1542.4479	.57421684 -2	-.21400099 -2
40.000	1542.5997	-.17798064 -1	-.86000490 -[illegible]
50.000	1541.9921	-.94549785 -1	-.47001976 -2
60.000	1540.7149	-.73298477 -1	.89000093 -2
70.000	1540.4269	-.15675970 0	-.24400251 -1
75.000	1539.1681	-.96759415 -1	.46000346 -1
80.000	1537.4573	[illegible]	-.44600937 -1
85.000	1535.3409	-.12276001 0	.17700470 -1
90.000	1530.2117	-.30692176 -1	-.33359619 -3
100.000	1537.9741	-.30799144 -1	-.47220459 -7
110.000	1537.6169	-.69723365 -1	-.77067871 -2
125.000	1535.7101	-.70443432 -1	.75467729 -2
135.000	1535.3829	-.59933727 -1	-.93067779 -2
150.000	1533.8961	-.11092790 -1	.11739984 -1
155.000	1533.9873	-.41427040 -1	-.23867244 -1
165.000	1532.3797	-.13656289 0	.49000931 -2
175.000	1531.2421	-.15933077 0	-.84536476 -2
190.000	1527.8058	-.17643203 0	.67734985 -2
200.000	1526.3479	-.13365027 0	.16228590 -2
225.000	1523.4138	-.84743756 -1	.26080058 -2
250.000	1522.1097	-.29342144 -1	.18740031 -2
275.000	1521.9497	-.12341479 -1	-.46402588 -3
300.000	1521.4914	-.14428507 -1	.29867961 -3
350.000	1521.1436	-.70416150 -2	-.40030063 -3
400.000	1520.7855	-.31743477 -1	-.98407059 -3
450.000	1517.9672	-.65059435 -1	-.30256772 -3
495.000	1515.4254	-.39852348 -1	.18744013 -2
500.000	1515.0387	-.77368342 -1	-.60805339 -2
510.000	1513.9212	-.69101079 -1	.85339864 -2
525.000	1513.8448	-.48433240 -1	-.57782745 -2
540.000	1512.4687	-.48146415 -1	.50805195 -2
550.000	1512.3108	-.32745562 -1	-.34003067 -2
560.000	1511.8129	-.18177484 0	-.26402384 -1
565.000	1510.5740	-.49767153 -1	.79207077 -1
570.000	1511.3152	.23078899 -1	-.22068872 -1
585.000	1510.2787	-.50130899 -1	.29780324 -2
600.000	1509.8122	-.82370796 -1	-.72808054 -2
610.000	1508.6249	-.51247910 -1	.13501263 -1
620.000	1508.7869	-.34769579 -1	-.10200996 -1
630.000	1507.9291	-.68016690 -1	.33669726 -2
650.000	1507.2238	-.49060744 -1	-.13793772 -2
685.000	1504.8618	-.12178750 -1	.36041768 -2
700.000	1504.9154	-.35744236 -1	-.71531750 -2
720.000	1504.7498	-.18308495 0	-.74608960 -2
725.000	1501.7409	-.17677890 0	.29203313 -1
735.000	1501.9135	-.12232475 -1	-.58940277 -2
750.000	1501.0687	-.54860571 -1	.20948160 -3

TABLE OF VALUES OF EXTRAPOLATED POINTS

DEPTH-METERS	VELOCITY-M/SEC	Z COEFFICIENT	D COEFFICIENT
897.200	1496.3887	-.36935233 -1	.12878963 -3
942.900	1493.7134	-.25410290 -1	.13590318 -3
1028.700	1492.0320	-.14336240 -1	.12263326 -3
1114.400	1491.2537	-.40981109 -2	.11722974 -3
1200.700	1491.3400	.95844675 -3	-.87069940 -6
1285.800	1491.4181	.45143510 -2	.84540246 -4
1371.900	1492.1154	.55682401 -2	-.59945399 -4
1457.300	1492.3725	.40017212 -2	.23420806 -4
1543.000	1492.8015	.71135536 -2	.49191719 -4
1628.700	1493.5918	.95133409 -2	.68126925 -5
1714.400	1494.4321	.97470189 -2	-.13592562 -5
1800.100	1495.2624	.12110297 -1	.56977421 -4
1885.900	1496.5129	.12130547 -1	-.56970473 -4
1971.600	1497.3433	.12140806 -1	.57207289 -4
2057.300	1498.5938	.14316569 -1	-.64277489 -5
2131.000	1497.6319	.21737909 -2	-.32309187 -3
2143.000	1499.6343	.14100854 -2	.19594095 -3
2228.700	1500.4748	.10964748 -1	.27066314 -4
2314.500	1501.5154	.13352985 -1	.27391469 -4
2400.200	1502.7560	.14955265 -1	.13665229 -5
2485.900	1504.0067	.14535643 -1	-.13977007 -5
2571.600	1505.2474	.13863338 -1	.14332050 -4
2657.400	1506.3841	.13361526 -1	.26348098 -5
2743.100	1507.5389	.15143892 -1	.38940657 -4
2828.800	1508.9798	.16930312 -1	.27294249 -5
2914.500	1510.4408	.15743346 -1	-.29963157 -4
3000.200	1511.6816	.13305932 -1	-.27386062 -4
3086.000	1512.7225	.13306289 -1	.27394367 -4
3171.700	1513.9634	.15744548 -1	.29974984 -4
3257.400	1515.4245	.14212222 -1	-.66201966 -4
3288.300	1515.8321	.14242811 -1	.69479918 -4
3388.300	1517.6097	.17742447 -1	.32081604 -6
3488.300	1519.3826	.17785101 -1	.32825470 -6
3588.300	1521.1628	.17817802 -1	.32577515 -6
3688.300	1522.9462	.17850399 -1	.32615462 -6
3788.300	1524.7328	.17882891 -1	.32367706 -6
3888.300	1526.3726	.17915277 -1	.32409853 -6
3988.300	1528.3199	.17947578 -1	.32196045 -6
4088.300	1530.1123	.17979727 -1	.32101347 -6
4188.300	1531.9118	.18011723 -1	.31890203 -6
4288.300	1533.7146	.18043566 -1	.31795502 -6
4388.300	1535.5206	.18075237 -1	.31547546 -6
4488.300	1537.3297	.18106718 -1	.31414032 -6
4588.300	1539.1419	.18138037 -1	.31223297 -6
4688.300	1540.9573	.18169136 -1	.30975342 -6
4788.300	1542.7757	.18200016 -1	.30784607 -6
4888.300	1544.5973	.18230705 -1	.30593872 -6
4988.300	1546.4219	.18261137 -1	.30269623 -6
5088.300	1548.2495	.18291330 -1	.30117035 -6
5188.300	1550.0801	.18321276 -1	.29773712 -6
5288.300	1551.9138	.18350964 -1	.29602051 -6
5388.300	1553.7503	.18380345 -1	.29201508 -6
5488.300	1555.5898	.18409443 -1	.28953552 -6
5588.300	1557.4322	.18438244 -1	.28648376 -6
5688.300	1559.2774	.18438244 -1	.28648376 -6

Table 5.5.1.13

DATE 19 4 1969 ID NUMBER 165 SET 1

SHALLOW PROFILE AT RANGE 263.700 MILES

TABLE OF VALUES OF OBSERVED POINTS

DEPTH-METERS	VELOCITY-M/SEC	COEFFICIENT Z	COEFFICIENT U
.000	1542.3600	.20241634 -1	-.21900550 -2
10.000	1542.5324	.62420845 -2	-.21999550 -2
20.000	1542.4848	.57492630 -2	.20999908 -2
30.000	1542.6473	.107422[illegible] -1	.1006022[illegible] -3
40.000	1542.8197	.17942336 -1	.19073486 -7
50.000	1542.9021	-.40250320 -1	-.13300152 -1
60.000	1541.0349	-.29709415 0	-.36247014 -1
65.000	1539.0097	-.20870026 0	.71600571 -1
70.000	1539.7400	-.52753980 -1	-.92000580 -2
80.000	1538.7593	-.09290567 -1	-.10009951 -3
90.000	1537.7617	-.53290373 -1	.93000984 -2
100.000	1537.6941	-.22816293 -9	-.30514744 -2
125.000	1536.1001	-.80960503 -1	-.16040056 -2
150.000	1533.6461	-.80964375 -1	.10205557 -2
160.000	1532.8685	-.22943144 0	-.27733960 -1
165.000	1531.3497	-.22343159 0	.27333900 -1
175.000	1530.4020	-.10613420 0	-.30744311 -2
200.000	1528.6179	-.16393219 0	-.09340770 -3
215.000	1524.0014	-.91290347 -1	.10293050 -1
225.000	1523.6930	-.46405323 -1	-.13406415 -2
250.000	1522.1097	-.46542043 -1	.13440399 -2
275.000	1521.3457	-.10161920 -1	.02803349 -3
300.000	1521.2016	-.66948700 -2	-.10668945 -4
350.000	1520.0534	-.13182041 -1	-.24801700 -3
400.000	1519.0854	-.38143986 -1	-.79205994 -3
450.000	1517.0372	-.48465252 -1	.34000931 -3
500.000	1515.0389	-.53846539 -1	-.55606079 -3
550.000	1511.4505	-.62448071 -1	.21199951 -3
600.000	1508.7921	-.61669006 -1	-.18003693 -3
650.000	1505.4836	-.31992572 -1	.13686943 -2
670.000	1505.1183	-.46680073 -1	-.28403244 -2
675.000	1504.8494	-.19570457 0	-.56005954 -1
680.000	1503.1604	-.19670497 0	.56405792 -1
685.000	1502.8816	-.31767782 -1	.96010844 -2
700.000	1503.4852	-.30348392 -1	-.10481150 -1
710.000	1502.5775	-.79106267 -1	.23335775 -2
730.000	1501.4620	-.37960690 -1	.10001842 -2
750.000	1501.0667	-.23657195 -1	-.30903873 -3

TABLE OF VALUES OF EXTRAPOLATED POINTS

DEPTH-METERS	VELOCITY-M/SEC	Z COEFFICIENT	D COEFFICIENT
857.200	1496.2953	-.37300714 -1	.13281435 -3
942.900	1493.5706	-.25032480 -1	.13692073 -3
1028.700	1491.8662	-.14926965 -1	.12661108 -3
1114.400	1491.0662	-.30517963 -2	.12291772 -3
1200.700	1491.2100	.13079504 -2	-.97086734 -6
1285.800	1491.3250	.49480311 -2	.84940330 -4
1371.500	1492.0596	.60027153 -2	-.59945601 -4
1457.300	1492.3540	.43271335 -2	.20837750 -4
1543.000	1492.8015	.72817962 -2	.46669637 -4
1628.700	1493.9910	.95133409 -2	.60126925 -5
1714.400	1494.4321	.97470189 -2	-.13592562 -5
1800.100	1495.2424	.12130297 -1	.96977421 -4
1885.900	1496.5189	.12130547 -1	-.96970673 -4
1971.600	1497.3433	.12140606 -1	.97207289 -4
2057.300	1498.5938	.14316989 -1	-.64277409 -5
2131.000	1499.6319	.21737909 -2	-.32300187 -3
2143.000	1499.6343	.14160094 -2	.19594095 -3
2228.700	1500.4740	.10966746 -1	.27066314 -4
2314.900	1501.5154	.13302985 -1	.87891449 -4
2400.200	1502.7500	.14935269 -1	.13665229 -3
2485.900	1504.0067	.14935643 -1	-.13877087 -5
2571.600	1505.2474	.18027301 -1	-.19173030 -4
2657.400	1506.3700	.13361610 -1	.43177000 -5
2743.100	1507.5309	.15179991 -1	.30110197 -4
2828.800	1508.9790	.16930312 -1	.2729424[illegible] -5
2914.500	1510.4408	.15763346 -1	-.29963157 -4
3000.200	1511.6816	.13365932 -1	-.27380062 -4
3086.000	1512.7229	.13306289 -1	.27394367 -4
3171.700	1513.9634	.15744948 -1	.29974584 -4
3257.400	1515.4249	.14212222 -1	-.60281566 -4
3200.300	1515.8821	.14262011 -1	.69475918 -4
3300.300	1517.6097	.17792847 -1	.32081604 -6
3400.300	1519.3024	.17789101 -1	.32829470 -6
3500.300	1521.1620	.17017802 -1	.32977915 -6
3600.300	1522.9467	.17050399 -1	.32619662 -6
3700.300	1524.7320	.17882091 -1	.32367706 -6
3800.300	1526.5228	.17915277 -1	.32405855 -6
3900.300	1528.3159	.17947578 -1	.32196045 -6
4000.300	1530.1123	.17979727 -1	.32101347 -6
4100.300	1531.9110	.18011723 -1	.31890203 -6
4200.300	1533.7140	.18043966 -1	.31795502 -6
4300.300	1535.5206	.18075237 -1	.31547546 -6
4400.300	1537.3297	.18106718 -1	.31414032 -6
4500.300	1539.1419	.18138037 -1	.31223297 -6
4600.300	1540.9573	.18169136 -1	.30975342 -6
4700.300	1542.7757	.18200016 -1	.30704007 -6
4800.300	1544.5973	.18230705 -1	.30593872 -6
4900.300	1546.4219	.18261137 -1	.30269423 -6
5000.300	1548.2495	.18291330 -1	.30117035 -6
5100.300	1550.0801	.18321276 -1	.29773712 -6
5200.300	1551.9130	.18350964 -1	.29602051 -5
5300.300	1553.7503	.18380365 -1	.29201508 -6
5400.300	1555.5898	.18409443 -1	.28953552 -6
5500.300	1557.4322	.18438244 -1	.28648376 -6
5600.300	1559.2775	.18438244 -1	.28648376 -6

Table 5.5.1.14

DATE 19 4 1968 ID NUMBER 168 SET 1

SHALLOW PROFILE AT RANGE 270.400 MILES

TABLE OF VALUES OF OBSERVED POINTS

DEPTH-METERS	VELOCITY-M/SEC	COEFFICIENT Z	COEFFICIENT D
.000	1542.5800	.17741680 -1	-.09964142 -4
10.000	1542.7524	.14742039 -1	-.09964142 -4
20.000	1542.9148	.57471884 -2	-.21600099 -2
30.000	1542.8673	.62422752 -2	.22000313 -2
40.000	1543.0357	-.47577858 -2	-.44000435 -2
50.000	1542.7721	-.91798678 -1	-.13400135 -1
60.000	1541.1649	-.11075935 0	.42000008 -2
70.000	1539.9760	-.20798303 -1	.10000208 -1
75.000	1540.0981	-.12175961 0	-.55200729 -1
80.000	1538.7593	-.19876080 0	.74400253 -1
90.000	1537.9017	-.65299552 -1	.22599994 -2
100.000	1537.4541	-.58531119 -1	-.01430882 -3
125.000	1535.7101	-.86140660 -1	-.13120944 -2
150.000	1533.1461	-.12836221 0	-.14240692 -2
175.000	1529.6920	-.13096343 0	.60797119 -3
200.000	1526.6179	-.14363176 0	-.16534373 -2
205.000	1525.8791	-.69742329 -1	.32801208 -1
210.000	1525.9803	-.12276459 0	-.55607112 -1
215.000	1524.6515	-.20643457 0	.22134120 -1
225.000	1523.6038	-.83192247 -1	.25143454 -2
250.000	1522.3997	-.40762596 -1	.88002824 -3
275.000	1521.6557	-.23062135 -1	.46401062 -3
300.000	1521.2016	-.18428764 -1	-.21348942 -4
350.000	1520.2535	-.15142224 -1	.11200256 -3
400.000	1519.5854	-.35435197 -1	-.88292149 -3
420.000	1518.7001	-.32950438 -1	.11333974 -2
435.000	1518.3537	-.73855377 -1	-.49871226 -2
445.000	1517.2860	-.24763552 -1	.16401087 -1
450.000	1517.3472	-.55624008 -2	-.87206268 -2
470.000	1515.4918	-.70933879 -1	.22534798 -2
500.000	1514.3089	-.41976807 -1	-.36634089 -3
535.000	1512.7070	-.95875495 -1	-.26707270 -2
550.000	1510.9804	-.60101318 -1	.73339505 -2
565.000	1510.9040	-.21649653 -1	-.22087284 -2
600.000	1508.7921	-.22136597 -1	.71830459 -2
615.000	1508.7056	-.40767023 -1	-.46004359 -2
620.000	1508.4468	-.15477048 0	-.41204147 -1
625.000	1507.1579	-.16644650 0	.34536941 -1
635.000	1507.3207	-.11711244 -1	-.54938914 -2
650.000	1506.5537	-.51081565 -1	.18051539 -3
700.000	1504.2053	-.90080924 -1	-.17396898 -2
715.000	1502.6586	-.74891431 -1	.37622088 -2
735.000	1501.9133	-.48772338 -1	-.10955794 -2
750.000	1501.0667	-.55079554 -1	.18828385 -3

TABLE OF VALUES OF EXTRAPOLATED POINTS

DEPTH-METERS	VELOCITY-M/SEC	Z COEFFICIENT	D COEFFICIENT
857.200	1496.2498	-.37789600 -1	.13477560 -3
942.900	1493.5130	-.26037885 -1	.13761040 -3
1028.700	1491.7859	-.14619756 -1	.12854646 -3
1114.400	1491.0047	-.37514231 -2	.12500024 -3
1200.700	1491.1467	.16043278 -2	-.97087072 -6
1285.800	1491.2797	.51601918 -2	.84539941 -4
1371.900	1492.0324	.62140808 -2	-.59845104 -4
1457.300	1492.3449	.44854539 -2	.19650773 -4
1543.000	1492.8015	.72744541 -2	.45436747 -4
1628.700	1493.5918	.95133409 -2	.60126525 -5
1714.400	1494.4321	.97470189 -2	-.13592562 -5
1800.100	1495.2624	.12130257 -1	.56977421 -4
1885.900	1496.5129	.12150547 -1	-.56970673 -4
1971.600	1497.3433	.12140686 -1	.57207289 -4
2057.300	1498.5938	.14516589 -1	-.64277489 -5
2131.000	1499.6315	.21737909 -2	-.32309187 -3
2143.000	1499.6343	.14160894 -2	.19994095 -3
2228.700	1500.4748	.10966746 -1	.27066314 -4
2314.500	1501.5154	.13302985 -1	.27391469 -4
2400.200	1502.7560	.14595265 -1	.13069229 -5
2485.900	1504.0067	.14535643 -1	-.13577007 -5
2571.600	1505.2474	.13809772 -1	-.15502125 -4
2657.400	1506.3749	.13361651 -1	.51364173 -5
2743.100	1507.5380	.15107551 -1	.37708394 -4
2828.800	1508.9798	.16930312 -1	.97294249 -5
2914.500	1510.4408	.15783346 -1	-.29963197 -4
3000.200	1511.6816	.13369932 -1	-.27386062 -4
3086.000	1512.7225	.13306289 -1	.27394367 -4
3171.700	1513.9634	.15784948 -1	.29974584 -4
3297.400	1515.4749	.18212222 -1	-.68201566 -4
3288.300	1515.8321	.18282811 -1	.69479918 -4
3388.300	1517.6057	.17792667 -1	.32081604 -6
3488.300	1519.3826	.17785101 -1	.32829470 -6
3588.300	1521.1628	.17817802 -1	.32577515 -6
3688.300	1522.9462	.17850399 -1	.32615662 -6
3788.300	1524.7328	.17882891 -1	.32367706 -6
3888.300	1526.5228	.17915277 -1	.32405853 -6
3988.300	1528.3150	.17947578 -1	.32196045 -6
4088.300	1530.1123	.17979727 -1	.32101347 -6
4188.300	1531.9118	.18011723 -1	.31890203 -6
4288.300	1533.7146	.18043566 -1	.31795502 -6
4388.300	1535.5206	.18075237 -1	.31547546 -6
4488.300	1537.3297	.18106718 -1	.31414032 -6
4588.300	1539.1419	.18138037 -1	.31223297 -6
4688.300	1540.9573	.18169136 -1	.30979342 -6
4788.300	1542.7757	.18200016 -1	.30784607 -6
4888.300	1544.5973	.18230705 -1	.30593872 -6
4988.300	1546.4219	.18261137 -1	.30260823 -6
5088.300	1548.2495	.18291330 -1	.30117025 -6
5188.300	1550.0801	.18321276 -1	.29773712 -6
5288.300	1551.9138	.18350964 -1	.29602051 -6
5388.300	1553.7503	.18380365 -1	.29201508 -6
5488.300	1555.5898	.18409443 -1	.28953552 -6
5588.300	1557.4322	.18438244 -1	.28648376 -6
5688.300	1559.2775	.18438244 -1	.28648376 -6

Table 5.5.1.15

DATE 19 4 1960 ID NUMBER 165 SET 1

SHALLOW PROFILE AT RANGE 276.063 MILES

TABLE OF VALUES OF OBSERVED POINTS

DEPTH-METERS	VELOCITY-M/SEC	COEFFICIENT Z	COEFFICIENT D
.000	1542.8880	-.47981673 -2	.19073486 -7
10.000	1542.7924	-.47599765 -2	.19073486 -7
20.000	1542.7640	.27942270 -1	.64080320 -2
30.000	1543.2073	.27942470 -1	-.63999039 -2
40.000	1543.2497	-.28976085 0	-.49640519 -1
45.000	1541.1499	-.22479948 0	.70090739 -1
50.000	1541.0821	-.50424950 -1	-.12204922 -1
60.000	1539.0045	-.15999990 0	-.71000672 -2
70.000	1537.8060	-.12999901 0	.13700085 -1
80.000	1537.3993	-.54999300 -1	-.99903215 -4
90.000	1536.0127	-.67949590 -1	-.25000763 -2
100.000	1536.0141	-.09051050 -1	-.12343350 -3
125.000	1533.4401	-.92041844 -1	.07190406 -3
150.000	1531.3641	-.18042139 0	-.76600124 -2
160.000	1529.1704	-.17436434 0	.80002134 -2
175.000	1527.5420	-.10291204 0	.73990400 -3
200.000	1525.2370	-.34247229 -1	.46972700 -2
210.000	1525.1303	-.37080980 -1	-.92539400 -2
225.000	1523.9830	-.62079089 -1	.17933972 -2
250.000	1522.9690	-.23361740 -1	.13760437 -2
275.000	1522.8197	-.63612364 -3	-.10003410 -4
300.000	1522.6917	-.05613047 -2	-.20349092 -6
325.000	1522.3236	-.30946279 -2	.10060911 -3
350.000	1522.2778	-.80040540 -2	-.77336020 -3
375.000	1522.1496	-.15077031 0	-.27601729 -1
380.000	1521.6907	-.11170735 0	.47782911 -1
385.000	1521.1319	.64049257 -2	-.39830014 -2
400.000	1520.7855	-.33319026 -1	-.13038392 -2
430.000	1519.1729	-.34700192 -1	.13037816 -2
445.000	1518.0041	-.13198754 0	-.14334861 -1
450.000	1517.9672	-.13193763 0	.14334323 -1
465.000	1517.4080	-.33059995 -1	-.12309792 -2
500.000	1515.4690	-.52093542 -1	.17940426 -3
550.000	1513.2006	-.40446003 -1	-.30019408 -4
600.000	1510.0723	-.62511570 -1	-.92077991 -3
620.000	1509.4460	-.10937307 0	-.41094930 -2
625.000	1508.0600	-.51740112 -1	.27202750 -1
630.000	1509.9492	-.29009337 -1	-.10139240 -1
640.000	1507.7519	-.60770313 -1	.10801094 -1
650.000	1507.5730	.49041740 -2	.49338440 -2
655.000	1507.4550	-.29740774 -1	-.10002023 -1
665.000	1506.4372	.16069027 -1	.27736202 -1
670.000	1506.0699	.39007459 -1	-.10539309 -1
680.000	1506.3400	-.10965933 -1	.69907111 -2
690.000	1506.5032	-.53769909 -1	-.14001522 -1
700.000	1505.2694	-.71271420 -1	.10901196 -1
710.000	1505.0777	.99347614 -1	.23402051 -1
715.000	1505.0690	.99347519 -1	-.23402409 -1
730.000	1504.7024	-.03344086 -1	-.74200497 -3
750.000	1502.0049	-.04063043 -1	.67714927 -3

TABLE OF VALUES OF EXTRAPOLATED POINTS

DEPTH-METERS	VELOCITY-M/SEC	Z COEFFICIENT	D COEFFICIENT
857.280	1497.7726	-.41397049 -1	.13030047 -3
942.000	1494.0114	-.20633142 -1	.13017912 -3
1028.700	1492.0632	-.17122792 -1	.13013834 -3
1114.400	1491.0737	-.60961315 -2	.12719035 -3
1200.700	1491.0713	-.64042017 -3	-.97111432 -4
1285.000	1491.7629	.29044493 -2	.84540456 -4
1371.900	1492.3220	.39603397 -2	-.59945961 -4
1457.300	1492.4412	.27974368 -2	.32038280 -4
1543.000	1492.8019	.67129801 -2	.50530004 -4
1628.700	1493.5910	.95133409 -2	.60126529 -5
1714.400	1494.4281	.97470189 -2	-.13592562 -5
1800.100	1495.2684	.12130297 -1	.96977421 -4
1885.900	1496.5189	.12130947 -1	-.96970073 -4
1971.600	1497.3433	.12140606 -1	.97007209 -4
2057.300	1498.5938	.14316909 -1	-.64277400 -5
2131.000	1499.6319	.21737909 -2	-.32300107 -3
2143.000	1499.6343	.14160054 -2	.19994095 -3
2200.700	1500.4700	.10966746 -1	.27100314 -4
2314.500	1501.5154	.13502905 -1	.27391460 -4
2400.200	1502.7940	.14555265 -1	.13069229 -5
2485.900	1504.0067	.14935643 -1	-.13977007 -5
2571.600	1505.2474	.13709400 -1	-.15917327 -4
2657.400	1506.3729	.13301609 -1	.58072136 -5
2743.100	1507.5300	.15921940 -1	.37372009 -4
2828.800	1508.9790	.16030312 -1	.27594249 -5
2914.500	1510.4400	.19763346 -1	-.20063157 -4
3000.200	1511.4018	.13309932 -1	-.27300062 -4
3085.900	1512.7229	.13306209 -1	.27304307 -4
3171.700	1513.9634	.15764940 -1	.29974304 -4
3257.400	1515.4740	.14212222 -1	-.60301900 -4
3200.300	1515.0321	.14962011 -1	.69479918 -4
3300.300	1517.4097	.17792047 -1	.32081604 -6
3400.300	1519.3026	.17705101 -1	.32029470 -6
3500.300	1521.1680	.17017002 -1	.32977919 -6
3600.300	1522.9467	.17090399 -1	.32619462 -6
3700.300	1524.7320	.17002091 -1	.32367700 -6
3800.300	1526.9220	.17015277 -1	.32409093 -6
3900.300	1528.3159	.17047970 -1	.32196849 -6
4000.300	1530.1123	.17070727 -1	.32111347 -6
4100.300	1531.9118	.15011723 -1	.31890203 -6
4200.300	1533.7146	.18043566 -1	.31799902 -6
4300.300	1535.5206	.18075237 -1	.31547946 -6
4400.300	1537.3297	.18160718 -1	.31414032 -6
4500.300	1539.1419	.18130037 -1	.31223297 -6
4600.300	1540.9973	.18140136 -1	.30979742 -6
4700.300	1542.7757	.18200816 -1	.30784607 -6
4800.300	1544.5973	.18230729 -1	.30573072 -6
4900.300	1546.4219	.18261137 -1	.30269623 -6
5000.300	1548.2499	.18291330 -1	.30117039 -6
5100.300	1550.0081	.15321276 -1	.29773717 -6
5200.300	1551.9130	.18350964 -1	.29642051 -6
5300.300	1553.7503	.18380369 -1	.29261500 -6
5400.300	1555.5090	.18409443 -1	.28953352 -6
5500.300	1557.4327	.18430244 -1	.28440374 -6
5600.300	1559.2775	.18430244 -1	.28440374 -6

Table 5.5.1.16

DATE 19 4 1966 ID NUMBER 165 SET 1

SHALLOW PROFILE AT RANGE 281.900 MILES

TABLE OF VALUES OF [illegible]

DEPTH-METERS	VELOCITY-M/SEC	COEFFICIENT Z	COEFFICIENT D
.000	1542.3800	.28741434 -1	-.31990550 -2
10.000	1542.9924	.67490845 -2	-.91070550 -2
20.000	1542.4848	.16742229 -1	.42999840 -2
30.000	1542.0875	.40942496 -1	.22000894 -2
40.000	1543.4697	.29089410 -2	-.11466777 -1
45.000	1543.3409	-.15779890 0	-.52000360 -1
50.000	1541.8921	-.23942433 0	.22933400 -1
60.000	1540.7149	-.10795927 0	.21000099 -2
70.000	1539.7469	-.12075956 0	-.40000717 -2
80.000	1538.2993	-.12370002 0	.42999840 -2
90.000	1537.2817	-.78799754 -1	.47000994 -2
100.000	1536.7341	-.67014403 -1	-.14514792 -2
125.000	1534.7301	-.11773305 0	-.30098201 -2
135.000	1533.4025	-.10678163 0	.52001038 -2
150.000	1532.3861	-.98711637 -1	-.30601044 -2
175.000	1529.1620	-.12656341 0	.20796204 -3
200.000	1526.0679	-.10356365 0	.16160187 -2
225.000	1523.9838	-.79143591 -1	.33590938 -3
250.000	1522.1097	-.46942767 -1	.22720734 -2
275.000	1521.6557	-.24142178 -1	-.48002625 -3
300.000	1520.9016	-.24429016 -1	.49067920 -3
350.000	1520.2535	-.13142098 -1	-.80024719 -5
400.000	1519.5054	-.60949443 -1	-.22073313 -2
415.000	1518.3089	-.75765662 -1	.12419600 -2
450.000	1516.4171	-.57191725 -1	-.17717234 -3
475.000	1514.9330	-.96083685 -1	-.20373845 -2
485.000	1513.8252	-.77054823 -1	.67471500 -2
500.000	1513.4700	-.70101404 -1	-.50227115 -2
515.000	1511.7222	-.35169443 -1	.10400050 -1
525.500	1511.8946	-.49260815 -1	-.13301125 -1
535.000	1510.7369	-.27765210 -1	.17601445 -1
540.000	1510.0181	-.20008479 -1	-.17734033 -1
550.000	1509.6583	-.10587282 0	.21801643 -2
600.000	1507.0819	-.84512364 -1	-.52577809 -3
620.000	1505.6865	-.35100333 -1	.34640012 -2
630.000	1505.5080	-.13511060 0	-.23460035 -1
635.000	1504.5400	-.15804439 0	.13934720 -1
650.000	1503.7234	-.16044728 0	-.14134839 -1
655.000	1502.7449	-.13711166 0	.23469986 -1
665.000	1502.5468	-.33061062 -1	-.28280653 -2
680.000	1501.7203	-.24314404 -1	.41051865 -2
700.000	1502.0550	-.19769569 -1	-.36904038 -2
720.000	1500.9296	.13350345 -1	.49026944 -2
735.000	1501.9135	-.29454471 -1	-.12068137 -1
745.000	1500.9855	-.20100212 -1	.14934900 -1
750.000	1501.0667	.13482429 -1	-.11019321 -2

TABLE OF VALUES OF EXTRAPOLATED POINTS

DEPTH-METERS	VELOCITY-M/SEC	Z COEFFICIENT	D COEFFICIENT
857.200	1496.1804	-.30196783 -1	.13776760 -3
942.900	1493.4129	-.24391677 -1	.13066410 -3
1028.700	1491.6623	-.14761968 -1	.13150293 -3
1114.400	1490.8001	-.35900957 -2	.12902011 -3
1200.700	1491.0581	.19872419 -2	-.97056959 -4
1285.800	1491.2106	.54831344 -2	.84940310 -4
1371.500	1491.7909	.85370176 -2	-.50045604 -4
1457.300	1492.3312	.47273091 -2	.17761297 -4
1543.000	1492.8015	.73540988 -2	.43559391 -4
1628.700	1493.5918	.95133409 -2	.60126525 -5
1714.400	1494.4321	.97470189 -2	-.13592562 -5
1800.100	1495.2624	.12130297 -1	.56977481 -4
1885.900	1496.5129	.12130547 -1	-.96970673 -4
1971.600	1497.3433	.12140686 -1	.57207209 -4
2057.300	1498.5938	.14314580 -1	-.64277409 -5
2131.000	1499.6315	.21737009 -2	-.33309187 -3
2143.000	1499.6343	.14100854 -2	.19994195 -3
2228.700	1500.4748	.10066746 -1	.27066314 -4
2314.300	1501.9154	.13362905 -1	.27391469 -4
2400.300	1502.7560	.14559265 -1	.13669229 -5
2485.900	1504.0067	.14535643 -1	-.13577007 -5
2571.600	1505.2474	.13782909 -1	-.16207162 -4
2657.400	1506.3703	.13361714 -1	.63072811 -5
2743.100	1507.5309	.15294381 -1	.37082262 -4
2828.800	1508.9798	.10930312 -1	.27294240 -5
2914.500	1510.4408	.15783346 -1	-.29963197 -4
3000.200	1511.6010	.13305932 -1	-.27306062 -4
3086.000	1512.7229	.13306209 -1	.27394367 -4
3171.700	1513.9634	.15764940 -1	.29974584 -4
3257.400	1515.4249	.14212222 -1	-.46201566 -4
3200.300	1515.8321	.14268011 -1	.69475910 -4
3300.300	1517.6057	.17742647 -1	.32081604 -6
3400.300	1519.3826	.17759101 -1	.32029470 -6
3500.300	1521.1428	.17817002 -1	.32577515 -6
3600.300	1522.9462	.17050399 -1	.32453662 -6
3700.300	1524.7320	.17082091 -1	.32367704 -6
3800.300	1526.5220	.17075277 -1	.32405093 -6
3900.300	1528.3190	.17047578 -1	.32196045 -6
4000.300	1530.1123	.17079727 -1	.32101347 -6
4100.300	1531.9118	.18011723 -1	.31890203 -6
4200.300	1533.7144	.18043566 -1	.31799902 -6
4300.300	1535.5204	.18079237 -1	.31547566 -6
4400.300	1537.3297	.18106718 -1	.31414032 -6
4500.300	1539.1419	.18130037 -1	.31223297 -6
4600.300	1540.9573	.18169136 -1	.30975342 -6
4700.300	1542.7757	.18200016 -1	.30784607 -6
4800.300	1544.5973	.18230705 -1	.30593072 -6
4900.300	1546.4219	.18261137 -1	.30269023 -6
5000.300	1548.2495	.18291330 -1	.30117035 -6
5100.300	1550.0801	.10321276 -1	.29777712 -6
5200.300	1551.9138	.10350964 -1	.29602091 -6
5300.300	1553.7503	.10380365 -1	.29201508 -6
5400.300	1555.5898	.10409443 -1	.28953552 -6
5500.300	1557.4322	.10430244 -1	.28648376 -6
5600.300	1559.2775	.10430244 -1	.28648376 -6

Table 5.5.1.17

DATE 19 4 1968 ID NUMBER 185 SET 1

SHALLOW PROFILE AT RANGE 288.400 MILES

TABLE OF VALUES OF OBSERVED POINTS

DEPTH-METERS	VELOCITY-M/SEC	COEFFICIENT Z	COEFFICIENT D
.000	1542.5800	-.37583351 2	.42000389 -2
10.000	1542.7924	.38242054 -1	.42000389 -2
20.000	1543.3448	.27242279 -1	-.63999939 -2
30.000	1543.2973	-.28287801 -1	-.43000221 -2
40.000	1542.8197	-.91798283 -1	-.88000743 -2
45.000	1542.2509	-.22675953 0	-.45700424 -1
50.000	1540.5521	-.20675983 0	.53700302 -1
55.000	1540.1833	-.14275970 0	-.27000250 -1
60.000	1539.1249	-.19776026 0	.56000264 -2
70.000	1537.4269	-.17425985 0	.91000557 -2
80.000	1536.6393	-.66799491 -1	.24000168 -2
90.000	1536.0917	-.10420044 0	-.99002075 -2
100.000	1534.5541	-.13087549 0	.46171984 -2
125.000	1532.7301	-.16685304 0	-.75702026 -2
130.000	1531.8013	-.14536308 0	.89001898 -2
150.000	1530.3260	-.80917175 -1	-.67559984 -3
175.000	1528.1020	-.85182488 -1	.30397644 -3
200.000	1526.0679	-.71182643 -1	.81800952 -3
225.000	1524.5438	-.50382396 -1	.84801075 -3
250.000	1523.5498	-.34582107 -1	.41800647 -3
275.000	1522.8157	-.17941693 -1	.91203308 -3
300.000	1522.6917	-.84947459 -2	-.15467733 -3
350.000	1522.0136	-.18842186 -1	-.25702026 -3
400.000	1520.7855	-.34483520 -1	-.30003311 -3
450.000	1518.5873	-.44884807 -1	-.36018372 -4
500.000	1516.2990	-.49765949 -1	-.16002731 -3
550.000	1513.6107	-.55711704 -1	-.77802870 -4
590.000	1511.3200	-.10987245 0	-.24202347 -2
600.000	1510.1422	-.27098910 -1	.18134944 -1
605.000	1510.2334	-.50787899 -1	-.27002539 -1
610.000	1509.6345	-.11084013 0	.36538458 -2
635.000	1508.0103	-.28382768 -1	.29269435 -2
650.000	1507.9138	-.75637767 -1	-.92276103 -2
660.000	1506.6981	-.87195688 -1	.89340281 -2
680.000	1506.3408	-.35787508 -1	-.18002081 -2
700.000	1505.2654	-.49940695 -1	.38288934 -3
750.000	1503.2470	-.43035324 -1	-.10667449 -3

TABLE OF VALUES OF EXTRAPOLATED POINTS

DEPTH-METERS	VELOCITY-M/SEC	Z COEFFICIENT	D COEFFICIENT
857.200	1498.0206	-.41303087 -1	.13890234 -3
942.900	1494.9914	-.29387053 -1	.13909481 -3
1028.700	1492.9820	-.17726513 -1	.13271264 -3
1114.400	1491.9501	-.64423683 -2	.13062796 -3
1200.700	1491.8806	-.84760115 -3	-.97078154 -6
1285.800	1491.8050	.27082103 -2	.84540027 -4
1371.500	1492.3479	.37621089 -2	-.59944960 -4
1457.300	1492.4498	.28489774 -2	.33997840 -4
1543.000	1492.8015	.66636018 -2	.59692344 -4
1628.700	1493.5918	.95133409 -2	.68126525 -5
1714.400	1494.4321	.97470189 -2	-.13592962 -5
1800.100	1495.2624	.12130257 -1	.96977421 -4
1885.900	1496.5129	.12130547 -1	-.96970673 -4
1971.600	1497.3433	.12140686 -1	.97207209 -4
2057.300	1498.5938	.14316589 -1	-.64277489 -5
2131.000	1499.6315	.21737909 -2	-.32309187 -3
2143.000	1499.6145	.14108854 -2	.19594095 -3
2228.700	1500.4748	.10946746 -1	.27066314 -4
2314.500	1501.5154	.13802985 -1	.27391469 -4
2400.200	1502.7560	.14535265 -1	.13669229 -5
2485.900	1504.0067	.14535643 -1	-.13577007 -5
2571.600	1505.2474	.13772036 -1	-.16462776 -4
2657.400	1506.3689	.13361739 -1	.68987485 -5
2743.100	1507.5389	.15235353 -1	.36626200 -4
2828.800	1508.9798	.16930512 -1	.27294249 -5
2914.500	1510.4408	.15763346 -1	-.29963157 -4
3030.200	1511.6816	.13305932 -1	-.27386062 -4
3086.000	1512.7225	.13306789 -1	.27394367 -4
3171.700	1513.9634	.15784548 -1	.29974584 -4
3257.400	1515.4269	.14212222 -1	-.66201566 -4
3288.300	1515.8321	.14262811 -1	.69475918 -4
3388.300	1517.6057	.17752647 -1	.32081604 -6
3488.300	1519.3826	.17783101 -1	.32825470 -6
3588.300	1521.1628	.17817802 -1	.32577515 -6
3688.300	1522.9467	.17890399 -1	.32615662 -6
3788.300	1524.7328	.17882891 -1	.32367706 -6
3888.300	1526.5228	.17915277 -1	.32405853 -6
3988.300	1528.3159	.17947578 -1	.32196045 -6
4088.300	1530.1123	.17979727 -1	.32101547 -6
4188.300	1531.9118	.18011723 -1	.31890203 -6
4288.300	1533.7146	.18043566 -1	.31795502 -6
4388.300	1535.5208	.18073237 -1	.31547546 -6
4488.300	1537.3297	.18106718 -1	.31414032 -6
4588.300	1539.1419	.18138037 -1	.31223297 -6
4688.300	1540.9573	.18149136 -1	.30975342 -6
4788.300	1542.7757	.18200016 -1	.30784607 -6
4888.300	1544.5973	.18230705 -1	.30593872 -6
4988.300	1546.4219	.18261137 -1	.30269623 -6
5088.300	1548.2495	.18291330 -1	.30117035 -6
5188.300	1550.0801	.18321276 -1	.29773712 -6
5288.300	1551.9138	.18350964 -1	.29602051 -6
5388.300	1553.7503	.18380365 -1	.29201508 -6
5488.300	1555.5898	.18409443 -1	.28953552 -6
5588.300	1557.4322	.18438244 -1	.28648376 -6
5688.300	1559.2275	.18438244 -1	.28648376 -6

Table 5.5.1.18

DATE 19 4 1968 ID NUMBER 365 SET 1

DEEP PROFILE AT RANGE 305.760 MILES TEMP AT OBSERVE MAXIMUM DEPTH= 2.209 DEG CENTIGRADE

TABLE OF VALUES OF OBSERVED POINTS

DEPTH-METERS	VELOCITY-M/SEC	COEFFICIENT Z	COEFFICIENT D
.000	1542.1500	-.17258453 -1	.23100336 -2
10.000	1542.0924	.57418823 -2	.23100336 -2
20.000	1542.2648	.17242146 -1	.19173486 -2
30.000	1542.4173	.57422638 -2	-.22599954 -2
40.000	1542.3797	.57422638 -2	.22590954 -2
50.000	1542.5521	-.10575995 0	-.24600239 -1
60.000	1540.2645	-.28026104 0	-.10300179 -1
70.000	1536.9469	-.26576157 0	.13200073 -1
80.000	1534.9493	-.16526098 0	.69600435 -2
90.000	1533.6412	-.31426175 -1	.19666918 -1
95.000	1533.7329	-.10776081 0	-.50400772 -1
100.000	1532.5641	-.21249587 0	.85667495 -2
125.000	1529.9100	-.10836197 0	-.17603760 -3
150.000	1527.1460	-.11836311 0	-.62405396 -3
175.000	1523.9919	-.88563080 -1	.30080566 -2
200.000	1522.7178	-.45962372 -1	.40000000 -3
225.000	1521.6937	-.35342320 -1	.44600415 -3
250.000	1520.9497	-.24162216 -1	.44600415 -3
275.000	1520.4856	-.67615891 -2	.94104602 -3
300.000	1520.6116	-.10280228 -2	-.48536072 -3
350.000	1519.9535	-.22442730 -1	-.37202759 -3
400.000	1518.3653	-.35363922 -1	-.14402008 -3
450.000	1516.4171	-.46165295 -1	-.28603482 -3
500.000	1513.7488	-.47646111 -1	.22600217 -3
550.000	1511.6505	-.42766438 -1	-.32115228 -4
600.000	1509.4722	-.51147946 -1	-.30404511 -3
650.000	1506.5337	-.92701596 -1	-.13573009 -2
670.000	1504.4082	-.85539411 -1	.20735194 -2
700.000	1502.7751	-.36934821 -1	.11667866 -2
730.000	1502.1921	-.41535740 -1	-.14735146 -2
750.000	1501.0367	-.54836068 -1	.14348169 -3
1114.400	1490.6107	-.33372702 -2	.13516814 -3
1200.700	1490.6410	.26259389 -2	-.97193787 -6
1285.800	1491.0609	.61318181 -2	.84540366 -4
1371.500	1491.9011	.72357077 -2	-.59945509 -4
1457.300	1492.3013	.52506190 -2	.13673045 -4
1543.000	1492.8015	.75289639 -2	.39497196 -4
1628.700	1493.5918	.95133409 -2	.68126525 -5
1714.400	1494.4321	.97470189 -2	-.13592562 -5
1800.100	1495.2624	.12130257 -1	.56977421 -4
1885.900	1496.5129	.12130547 -1	-.56970673 -4
1971.600	1497.3433	.12140686 -1	.57207289 -4
2057.300	1498.5938	.14316589 -1	-.64277489 -5
2131.000	1499.6315	.21737909 -2	-.32309187 -3
2143.000	1499.6343	.41108854 -2	.19594095 -3
2228.700	1500.4748	.10966746 -1	.27068314 -4
2314.500	1501.5154	.13302985 -1	.27391469 -4
2400.200	1502.7560	.14535265 -1	.13165229 -5
2485.900	1504.0067	.14535643 -1	-.13577007 -5
2571.600	1505.2474	.14105587 -1	-.86786290 -5
2743.100	1507.5389	.15663149 -1	.26642626 -4
2828.600	1508.9798	.16930312 -1	.27294249 -5
2914.500	1510.4408	.15763346 -1	-.29963157 -4
3000.200	1511.6816	.13305932 -1	-.27386062 -4
3086.000	1512.[illegible]725	.13306289 -1	.27394367 -4
3171.700	1513.9634	.15744548 -1	.29974584 -4
3257.400	1515.4245	.14212222 -1	-.66201566 -4
3288.300	1515.8321	.14262811 -1	.69475918 -4

TABLE OF VALUES OF EXTRAPOLATED POINTS

DEPTH-METERS	VELOCITY-M/SEC	Z COEFFICIENT	D COEFFICIENT
3388.300	1517.6058	.17752647 -1	.32081604 -6
3488.300	1519.3826	.17785101 -1	.32625470 -6
3588.300	1521.1628	.17817802 -1	.32577515 -6
3688.300	1522.9462	.17850389 -1	.32596588 -6
3788.300	1524.7328	.17882891 -1	.32405853 -6
3888.300	1526.5228	.17915287 -1	.32386780 -6
3988.300	1528.3159	.17947578 -1	.32196045 -6
4088.300	1530.1123	.17979727 -1	.32101347 -6
4188.300	1531.9119	.18011723 -1	.31690203 -6
4288.300	1533.7146	.18043566 -1	.31795502 -6
4388.300	1535.5206	.18075237 -1	.31547546 -6
4488.300	1537.3297	.18106718 -1	.31414032 -6
4588.300	1539.1419	.18138037 -1	.31223297 -6
4688.300	1540.9573	.18169136 -1	.30975342 -6
4788.300	1542.7757	.18200016 -1	.30784607 -6
4888.300	1544.5973	.18230696 -1	.30574799 -6
4988.300	1546.4219	.18261137 -1	.30307770 -6
5088.300	1548.2495	.18291340 -1	.30097961 -6
5188.300	1550.0801	.18321265 -1	.29754639 -6
5288.300	1551.9138	.18350964 -1	.29640198 -6
5388.300	1553.7503	.18380375 -1	.29182434 -6
5488.300	1555.[illegible]898	.18409443 -1	.28953552 -6
5588.300	1557.4122	.18438244 -1	.28648376 -6
5688.300	1559.2775	.18466759 -1	.28381348 -6
5788.300	1561.1256	.18495140 -1	.28381348 -6

Table 3.5.1.1

DATE 19 4 1968 ID NUMBER 165 SET 1

DEEP PROFILE AT RANGE 350 000 MILES TEMP AT OBSERVED MAXIMUM DEPTH 2,209 DEG CENTIGRADE

TABLE OF VALUES OF OBSERVED POINTS

DEPTH-METERS	VELOCITY-M/SEC	COEFFICIENT Z	COEFFICIENT [illegible]
.000	1542.1500	-.17258453 -1	.23600336 -7
10.000	1542.0924	.57418823 -2	.23600336 -7
20.000	1542.2448	[illegible]	.49673486 -7
30.000	1542.4373	.57422638 -2	-.22999954 -7
40.000	1542.5797	.57422638 -2	.22599954 -7
50.000	1542.5521	-.10575895 0	-.24600239 -1
60.000	1540.2645	-.28020104 0	-.10300179 -1
70.000	1536.9469	-.26576157 0	.13700073 -1
80.000	1534.9493	-.15526098 0	.69600439 -2
90.000	1533.6417	-.31426175 -1	.19868918 -1
95.000	1533.7329	-.10776081 0	-.50400772 -1
100.000	1532.5641	-.21249587 0	.85067495 -2
125.000	1529.9100	-.15836197 0	-.17603760 -3
150.000	1527.1460	-.11836311 0	-.62405396 -3
175.000	1523.9019	-.88543080 -1	.30080286 -2
200.000	1522.7178	-.45942372 -1	.40000000 -3
225.000	1521.6937	-.35342320 -1	.44600415 -3
250.000	1520.9497	-.24162216 -1	.44600415 -3
275.000	1520.4856	-.67615891 -2	.94404602 -3
300.000	1520.6116	-.10280228 -2	-.48536072 -3
350.000	1519.9535	-.22442730 -1	-.37292759 -3
400.000	1518.3653	-.35343922 -1	-.14402008 -3
450.000	1516.4171	-.45165295 -1	-.28603462 -3
500.000	1513.7488	-.47666111 -1	.22600217 -3
550.000	1511.6505	-.42746438 -1	-.32015228 -4
600.000	1509.4727	-.51167946 -1	-.30404511 -3
650.000	1506.5337	-.92701596 -1	-.13573009 -2
670.000	1504.4087	-.85539411 -1	.20735194 -2
700.000	1502.7751	-.36934821 -1	.11667866 -2
730.000	1502.1921	-.41535740 -1	-.14735146 -2
750.000	1501.0867	-.54836068 -1	.14348169 -3
1114.400	1490.6107	-.31372702 -2	.13916814 -3
1200.700	1490.8410	.28259389 -2	-.97693787 -6
1285.800	1491.0609	.61815181 -2	.84540366 -4
1371.500	1491.9011	.72357077 -2	-.59945509 -6
1457.300	1492.3013	.52506190 -2	.13673045 -4
1543.000	1492.8015	.75289639 -2	.39497196 -4
1628.700	1493.5918	.95133409 -2	.68126525 -5
1714.400	1494.4321	.97470189 -2	-.13592562 -5
1800.100	1495.2624	.12130257 -1	.56977421 -4
1885.900	1496.5129	.12130547 -1	-.56970673 -4
1971.600	1497.3433	.12140686 -1	.57207289 -4
2057.300	1498.5938	.14316589 -1	-.64277489 -5
2131.000	1499.6315	.21737909 -2	-.32309187 -3
2143.000	1499.6343	.14108854 -2	.19594095 -3
2228.700	1500.4748	.10966746 -1	.27066314 -4
2314.500	1501.5154	.13302985 -1	.27391469 -4
2400.200	1502.7560	.14555265 -1	.13665229 -5
2485.900	1504.0067	.14535643 -1	-.13577007 -5
2571.600	1505.2474	.14105587 -1	-.86786290 -5
2743.100	1507.5389	.15643149 -1	.26642626 -4
2828.800	1508.9798	.16930312 -1	.27294249 -5
2914.500	1510.4408	.15743346 -1	-.29963157 -4
3000.200	1511.6816	.13305932 -1	-.27386062 -4
3086.000	1512.7225	.13306789 -1	.27394367 -4
3171.700	1513.9634	.15744548 -1	.29974584 -6
3257.400	1515.4245	.14212222 -1	-.66201566 -4
3288.300	1515.8321	.14262811 -1	.69475918 -4

TABLE OF VALUES OF EXTRAPOLATED POINTS

DEPTH-METERS	VELOCITY-M/SEC	Z COEFFICIENT	D COEFFICIENT
3388.300	1517.6058	.17752647 -1	.32081604 -6
3488.300	1519.3826	.17785101 -1	.32625470 -6
3588.300	1521.1628	.17817802 -1	.32577515 -6
3688.300	1522.9462	.17850389 -1	.32596588 -6
3788.300	1524.7328	.17882891 -1	.32405853 -6
3888.300	1526.5228	.17915287 -1	.32386780 -6
3988.300	1528.3159	.17947578 -1	.32196045 -6
4088.300	1530.1123	.17979727 -1	.32101347 -6
4188.300	1531.9119	.18011723 -1	.31690203 -6
4288.300	1533.7146	.18043566 -1	.31795502 -6
4388.300	1535.5206	.18075237 -1	.31547546 -6
4488.300	1537.3297	.18106718 -1	.31414032 -6
4588.300	1539.1419	.18138037 -1	.31223297 -6
4688.300	1540.9573	.18169136 -1	.30975342 -6
4788.300	1542.7757	.18200016 -1	.30784607 -6
4888.300	1544.5973	.18230696 -1	.30574799 -6
4988.300	1546.4219	.18261137 -1	.30307770 -6
5088.300	1548.2495	.18291340 -1	.30097961 -6
5188.300	1550.0801	.18321266 -1	.29754639 -6
5288.300	1551.9138	.18350964 -1	.29640198 -6
5388.300	1553.7503	.18380375 -1	.29182434 6
5488.300	1555.5898	.18409443 -1	.28953552 -6
5588.300	1557.4322	.18438244 -1	.28648376 -6
5688.300	1559.2775	.18446759 -1	.28381348 -6
5788.300	1561.1256	.18405140 -1	.28381348 -6

Table 5.5.1.20

1.5363 sec/mile TOTAL TIME: 6:25 REAL DATA

RAY TRACE ANALYSIS PROGRAM- R D MININGHAM - [A-201-U1]
RAY NUMBER= 2 INITIAL ANGLE= 14.800 DEGREES

LIST OF TURNING POINTS

NUMBER	RANGE NM	DEPTH M	SINE	SECONDS
1	42,0365	5330,0164	,01000000	51,9442
2	76,4735	5319,6074	,00000000	94,4787
3	110,7732	5300,5859	,00000000	136,8568
4	211,2336	5320,6432	,00000000	261,0543
5	245,8375	5327,2179	,00000000	303,7818

LIST OF BOTTOM HITS

NUMBER	RANGE NM	DEPTH M	SINE	SECONDS
1	9,6509	5231,3682	,04940010	11,8527
2	144,6268	5303,5306	,01223719	178,6956
3	177,6907	5297,6438	,01939190	219,5898
4	250,6628	4854,2592	,43183014	309,5590

LIST OF SURFACE HITS

NUMBER	RANGE NM	DEPTH M	SINE	SECONDS
1	24,8445	,0000	-,12042871	30,7058
2	59,2619	,0000	-,12022631	73,2196
3	93,6401	,0000	-,11975456	115,6874
4	127,9680	,0000	-,12173470	158,0063
5	161,2821	,0000	-,12035611	199,2898
6	193,9753	,0000	-,11669018	239,7412
7	228,5325	,0000	-,11449216	282,4145

DEPTH M=2331,7246 EPSILON= ,4000 DELTA= 250 MIN DELTA= 25 SIN TEST= ,020

Table 5.5.2.1

1.1372 sec/mile TOTAL TIME: 4145 REAL DATA

RAY TRACE ANALYSIS PROGRAM- R D MININGHAM - (A-201-U1)
RAY NUMBER= 4 INITIAL ANGLE= 14,800 DEGREES

LIST OF TURNING POINTS

NUMBER	RANGE NM	DEPTH M	SINE	SECONDS
1	42,0446	5329,5941	,00000000	51,9537
2	76,4912	5318,3160	,00000000	94,4896
3	110,7887	5299,0879	,00000000	136,8748
4	211,3011	5319,3012	,00000000	261,1343
5	245,9018	5326,4147	,00000000	303,8580

LIST OF BOTTOM HITS

NUMBER	RANGE NM	DEPTH M	SINE	SECONDS
1	9,6513	5231,3729	,04939935	11,8532
2	144,6574	5303,5305	,01188210	178,7315
3	177,7442	5297,4712	,01908254	219,6532
4	250,6504	4868,3945	,43348186	309,5427

LIST OF SURFACE HITS

NUMBER	RANGE NM	DEPTH M	SINE	SECONDS
1	24,8516	,0000	-,12064716	30,7141
2	59,2727	,0000	-,12035742	73,2325
3	93,6588	,0000	-,11957685	115,7094
4	127,9814	,0000	-,12085987	158,1117
5	161,3277	,0000	-,12028807	199,3437
6	194,0436	,0000	-,11713184	239,8223
7	228,5976	,0000	-,11435945	282,4916

DEPTH M=2331,7246 EPSILON= ,4000 DELTA= 500 MIN DELTA= 25 SIN TEST= ,020

Table 5.5.2.2

1.0375 sec/mile TOTAL TIME: 4:20 REAL DATA

RAY TRACE ANALYSIS PROGRAM- R D MININGHAM - (A-201-01)
RAY NUMBER= 6 INITIAL ANGLE= 14,800 DEGREES

LIST OF TURNING POINTS

NUMBER	RANGE NM	DEPTH M	SINE	SECONDS
1	42,0416	5329,5420	,00000000	51,9503
2	76.4852	5318,0826	,00000000	94,4930
3	110,7706	5298,9006	,00000000	136,8542
4	211,5049	5318,0771	,00000000	261,3791
5	246,1231	5325,9340	,00000000	304,1239

LIST OF BOTTOM HITS

NUMBER	RANGE NM	DEPTH M	SINE	SECONDS
1	9,6517	5231,3778	,04939857	11,8536
2	144,7297	5303,5304	,00983707	178,8189
3	177,9301	5296,8711	,01865054	219,8761
4	250,6071	4917,5981	,43891237	309,4898

LIST OF SURFACE HITS

NUMBER	RANGE NM	DEPTH M	SINE	SECONDS
1	24,8489	,0000	-,12116200	30,7111
2	59,2705	,0000	-,12075283	73,2300
3	93,6454	,0000	-,11611114	115,6938
4	127,9670	,0000	-,12083045	158,0952
5	161,4950	,0000	-,12007135	199,5444
6	194,2570	,0000	-,11692902	240,0778
7	228,8217	,0000	-,11411035	282,7607

DEPTH M=2331,7246 EPSILON= ,4000 DELTA=1000 MIN DELTA= 25 SIN TEST= ,020

Table 5.5.2.3

1.4166 sec/mile   TOTAL TIME: 5:55   REAL DATA

RAY TRACE ANALYSIS PROGRAM= R D MININGHAM - (A-201-U1)
RAY NUMBER= 8 INITIAL ANGLE= 14,800 DEGREES

LIST OF TURNING POINTS

NUMBER	RANGE NM	DEPTH M	SINE	SECONDS
1	42,0405	5329,7029	,00000000	51,9489
2	76,4635	5318,8268	,00000000	94,4670
3	110,7569	5299,5013	,00000000	136,8376
4	211,2698	5319,6343	,00000000	261,0982
5	245,8691	5325,7106	,00000000	303,8203

LIST OF BOTTOM HITS

NUMBER	RANGE NM	DEPTH M	SINE	SECONDS
1	9,6509	5231,3682	,04940010	11,8527
2	144,6266	5303,5306	,01170549	178,6958
3	177,7286	5297,5215	,01897265	219,6355
4	250,6578	4859,9059	,43254495	309,5534

LIST OF SURFACE HITS

NUMBER	RANGE NM	DEPTH M	SINE	SECONDS
1	24,8480	,0000	-,12123664	30,7099
2	59,2578	,0000	-,12621877	73,2148
3	93,6253	,0000	-,11967721	115,6701
4	127,9527	,0000	-,12094519	158,0781
5	161,3051	,0000	-,12068439	199,3178
6	194,0297	,0000	-,11900038	239,8065
7	228,5671	,0000	-,11440839	282,4564

DEPTH M=2331,7246 EPSILON= ,4000 DELTA= 250 MIN DELTA=100 SIN TEST= ,020

Table 5.5.2.4

0.9976 sec/mile TOTAL TIME: 4:10 REAL DATA

RAY TRACE ANALYSIS PROGRAM. R D MININGHAM - (A-201-U1)
RAY NUMBER= 10 INITIAL ANGLE= 14.800 DEGREES

LIST OF TURNING POINTS

NUMBER	RANGE NM	DEPTH M	SINE	SECONDS
1	42.0370	5329.4830	.00000000	51.9446
2	76.4790	5319.3832	.00000000	94.4848
3	110.7759	5300.3869	.00000000	136.8895
4	211.1696	5320.3438	.00000000	260.9772
5	245.7714	5328.9850	.00000000	303.7023

LIST OF BOTTOM HITS

NUMBER	RANGE NM	DEPTH M	SINE	SECONDS
1	9.6513	5231.3729	.04939935	11.8532
2	144.6002	5303.5306	.01249403	178.6637
3	177.6388	5297.8114	.01964366	219.5276
4	250.6747	4840.5686	.43046548	309.5735

LIST OF SURFACE HITS

NUMBER	RANGE NM	DEPTH M	SINE	SECONDS
1	24.8407	.0000	-.12113836	30.7013
2	59.2658	.0000	-.12553072	73.2240
3	93.6452	.0000	-.11968959	115.6930
4	127.9640	.0000	-.12097709	158.0910
5	161.2452	.0000	-.12098903	199.2495
6	193.9141	.0000	-.11803983	239.6677
7	228.4672	.0000	-.10513665	282.3358

DEPTH M=2331.7246 EPSILON= .4000 DELTA= 500 MIN DELTA=100 SIN TEST= .020

Table 5.5.2.5

0.8379 sec/mile TOTAL TIME: 3:30

REAL DATA

RAY TRACE ANALYSIS PROGRAM- R D MININGHAM - (A-201-U1)
RAY NUMBER= 12 INITIAL ANGLE= 14.800 DEGREES

LIST OF TURNING POINTS

NUMBER	RANGE NM	DEPTH M	SINE	SECONDS
1	42,0337	5329,6545	,00000000	51,9410
2	76,4458	5318,6603	,00000000	94,4464
3	110,7463	5298,4071	,00000000	139,8251
4	211,4721	5316,1953	,00000000	261,3398
5	246.0347	5323,8121	,00000000	304,0184

LIST OF BOTTOM HITS

NUMBER	RANGE NM	DEPTH M	SINE	SECONDS
1	9,6517	5231,3778	,04939857	11,8536
2	144,6506	5303,5305	,01078931	178,7249
3	177,8585	5297,1021	,01746278	219,7808
4	250,6264	4895,6020	,43682691	309,5142

LIST OF SURFACE HITS

NUMBER	RANGE NM	DEPTH M	SINE	SECONDS
1	24,8481	,0000	-,12125373	30,7100
2	59,2364	,0000	-,12572846	73,1897
3	93,6148	,0000	-,11966235	115,6577
4	127,9364	,0000	-,12082098	158,0592
5	161,3660	,0000	-,12030509	199,3910
6	194,2284	,0000	-,11732424	240,0439
7	228,7490	,0000	-,10125341	282,6740

DEPTH M=2331,7246 EPSILON= ,4000 DELTA=1000 MIN DELTA=100 SIN TEST= ,020

Table 5.5.2.6

1.5363 sec/mile TOTAL TIME: 6:25

REAL DATA

RAY TRACE ANALYSIS PROGRAM- R D MININGHAM - (A-201-U1)
RAY NUMBER= 14 INITIAL ANGLE= 14.000 DEGREES

LIST OF TURNING POINTS

NUMBER	RANGE NM	DEPTH M	SINE	SECONDS
1	42.0455	5329.6878	.00000000	51.9548
2	76.4870	5319.7470	.00000000	94.4947
3	110.7848	5300.2167	.00000000	136.8706
4	211.1763	5321.3377	.00000000	260.9860
5	245.7749	5329.1059	.00000000	303.7074

LIST OF BOTTOM HITS

NUMBER	RANGE NM	DEPTH M	SINE	SECONDS
1	9.6509	5231.3682	.04940010	11.8527
2	144.6044	5303.5306	.01288874	178.6691
3	177.6318	5297.8339	.01950774	219.5198
4	250.6739	4841.5465	.43038896	309.5735

LIST OF SURFACE HITS

NUMBER	RANGE NM	DEPTH M	SINE	SECONDS
1	24.8542	.0000	-.12116547	30.7173
2	59.2754	.0000	-.11963882	73.2356
3	93.6535	.0000	-.11970842	115.7034
4	127.9753	.0000	-.12219315	158.1050
5	161.2301	.0000	-.12041577	199.2281
6	193.9167	.0000	-.11732194	239.6715
7	228.4733	.0000	-.11462670	282.3440

DEPTH M=2331.7246 EPSILON= .4000 DELTA= 250 MIN DELTA= 25 SIN TEST= .100

Table 5.5.2.7

1.1771 sec/mile TOTAL TIME: 4:55 REAL DATA

RAY TRACE ANALYSIS PROGRAM, R D MININGHAM - (A-201-01)
RAY NUMBER= 16 INITIAL ANGLE= 14,800 DEGREES

LIST OF TURNING POINTS

NUMBER	RANGE NM	DEPTH M	SINE	SECONDS
1	42.0289	5329,4214	,00000000	51,9351
2	76,4727	5318,1571	,00000000	94,4778
3	110,7683	5299,3746	,00000000	136,8510
4	211,4513	5317,3756	,00000000	261,3146
5	246,0548	5324,7354	,00000000	304,0414

LIST OF BOTTOM HITS

NUMBER	RANGE NM	DEPTH M	SINE	SECONDS
1	9,6513	5231,3729	,04939935	11,8532
2	144,6852	5303,5306	,01062735	178,7657
3	177,8551	5297,1134	,01840020	219,7867
4	250,6216	4901,1608	,43702034	309,5072

LIST OF SURFACE HITS

NUMBER	RANGE NM	DEPTH M	SINE	SECONDS
1	24,8338	,0000	-,12074029	30,6931
2	59,2561	,0000	-,12070138	73,2128
3	93,6365	,0000	-,11906981	115,6833
4	127,9568	,0000	-,12127232	158,0830
5	161,4037	,0000	-,12009471	199,4357
6	194,1872	,0000	-,11698222	239,9948
7	228,7484	,0000	-,11407567	282,6725

DEPTH M=2331,7246 EPSILON= ,4000 DELTA= 500 MIN DELTA= 25 SIN TEST= ,100

Table 5.5.2.8

1.1572 sec/mile TOTAL TIME: 4:50 REAL DATA

RAY TRACE ANALYSIS PROGRAM- R D MININGHAM - (A-201-U1)
RAY NUMBER= 18 INITIAL ANGLE= 14.800 DEGREES

LIST OF TURNING POINTS

NUMBER	RANGE NM	DEPTH M	SINE	SECONDS
1	42.0381	5329.5289	.00000000	51.9463
2	76.4797	5319.2813	.00000000	94.4863
3	110.7870	5302.1588	.00000000	136.8736
4	210.8398	5326.0975	.00000000	260.5856
5	245.4453	5334.5697	.00000000	303.3153

LIST OF BOTTOM HITS

NUMBER	RANGE NM	DEPTH M	SINE	SECONDS
1	9.6517	5231.3778	.04939857	11.8536
2	144.5002	5303.5306	.01537830	178.5458
3	177.3465	5298.7543	.02085441	219.1809
4	250.7414	4764.6356	.42246072	309.6604
5	254.2508	5357.3188	.83156412	317.6036

LIST OF SURFACE HITS

NUMBER	RANGE NM	DEPTH M	SINE	SECONDS
1	24.8442	.0000	-.12116544	30.7656
2	59.2648	.0000	-.12077400	73.2233
3	93.6445	.0000	-.11972851	115.6031
4	127.9839	.0000	-.12185027	158.1156
5	161.0158	.0000	-.12080315	196.9736
6	193.5735	.0000	-.11772833	239.2634
7	228.1410	.0000	-.11509068	281.9484
8	252.3901	.0000	-.83506663	313.4023

DEPTH M=2331.7246 EPSILON= .4000 DELTA=1000 MIN DELTA= 25 SIN TEST= .100

Table 5.5.2.9

0.7781 sec/mile TOTAL TIME: 3:15 REAL DATA

RAY TRACE ANALYSIS PROGRAM- R D MININGHAM - (A-201-01)
RAY NUMBER= 20 INITIAL ANGLE= 14,800 DEGREES

LIST OF TURNING POINTS

NUMBER	RANGE NM	DEPTH M	SINE	SECONDS
1	42,0468	5329,5295	,00000000	51,9562
2	76,5007	5319,7365	,00000000	94,5108
3	110,8008	5300,4930	,00000000	136,8888
4	211,5932	5317,1658	,00000000	261,4820
5	246,1875	5326,2505	,00000000	304,1984

LIST OF BOTTOM HITS

NUMBER	RANGE NM	DEPTH M	SINE	SECONDS
1	9,6519	5231,3803	,04939794	11,8539
2	144,7633	5303,5303	,00979560	178,8576
3	177,9936	5296,6658	,01803322	219,9500
4	250,5947	4931,8084	,44040136	309,4718

LIST OF SURFACE HITS

NUMBER	RANGE NM	DEPTH M	SINE	SECONDS
1	24,8522	,0000	-,12114329	30,7151
2	59,2774	,0000	-,12011252	73,2381
3	93,6607	,0000	-,11966140	115,7118
4	127,9876	,0000	-,12095391	158,1190
5	161,5311	,0000	-,12004149	199,5856
6	194,3369	,0000	-,11691224	240,1713
7	228,8890	,0000	-,11424799	282,8383

DEPTH M=2331,7246 EPSILON=1,0000 DELTA=1000 MIN DELTA= 25 SIN TEST= ,020

Table 5.5.2.10

0.7382 sec/mile TOTAL TIME: 3:05

REAL DATA

RAY TRACE ANALYSIS PROGRAM- R D MININGHAM - (A-201-U1)
RAY NUMBER= 22 INITIAL ANGLE= 14,800 DEGREES

LIST OF TURNING POINTS

NUMBER	RANGE NM	DEPTH M	SINE	SECONDS
1	42,0446	5329,6439	,00000000	51,9537
2	76,4625	5318,4882	,00000000	94,4660
3	110,7513	5298,2679	,00000000	130,8312
4	211,7912	5315,0929	,00000000	261,7196
5	246,3625	5322,9604	,00000000	304,4061

LIST OF BOTTOM HITS

NUMBER	RANGE NM	DEPTH M	SINE	SECONDS
1	9,6519	5231,3803	,04939704	11,8539
2	144,8202	5303,5302	,00730819	170,9262
3	178,1765	5296,0761	,01752368	220,1693
4	250,5663	4964,1233	,44434381	309,4369

LIST OF SURFACE HITS

NUMBER	RANGE NM	DEPTH M	SINE	SECONDS
1	24,8473	,0000	-,12121006	30,7092
2	59,2477	,0000	-,11993616	73,2036
3	93,6169	,0000	-,12709655	115,6606
4	127,9404	,0000	-,12078162	150,0638
5	161,7009	,0000	-,11992336	199,7892
6	194,5337	,0000	-,11436507	240,4078
7	229,0745	,0000	-,11376782	283,0610

DEPTH M=2331,7246 EPSILON=1,0000 DELTA=1000 MIN DELTA=100 SIN TEST= ,020

Table 5.5.2.11

1.4142 sec/mile TOTAL TIME: 8:15 REAL DATA

RAY TRACE ANALYSIS PROGRAM- R D MININGHAM - (A-201-U1)
RAY NUMBER= 13 INITIAL ANGLE= 12.800 DEGREES

LIST OF TURNING POINTS

NUMBER	RANGE NM	DEPTH M	SINE	SECONDS
1	10,6914	4636,8062	,00000000	13,0886
2	27,3065	56,0691	,00000000	33,6340
3	43,9612	4661,7441	,00000000	54,2266
4	60,5835	58,6136	,00000000	74,7774
5	77,2256	4646,1412	,00000000	95,3522
6	93,7580	59,5792	,00000000	115,7990
7	110,2344	4625,4456	,00000000	136,1792
8	126,9466	63,4847	,00000000	156,8385
9	143,6946	4633,8019	,00000000	177,5402
10	160,3327	57,6701	,00000000	198,1091
11	176,9653	4633,6488	,00000000	218,6714
12	193,6527	65,5746	,00000000	239,2985
13	210,3562	4638,8054	,00000000	259,9449
14	227,3088	65,1093	,00000000	280,8886
15	244,2782	4648,4786	,00000000	301,8926
16	261,3155	64,4044	,00000000	322,8981
17	261,5947	67,7178	,00000000	323,2338
18	261,9443	66,5572	,00000000	323,6544
19	262,2404	67,5114	,00000000	324,0106
20	262.5587	66,6480	,00000000	324,3939
21	262,8330	67,3708	,00000000	324,7235
22	263,1413	66,7344	,00000000	325,0943
23	263,4028	67,2826	,00000000	325,4090
24	263,6868	66,7907	,00000000	325,7506
25	263,9723	67,2401	,00000000	326,0940
26	264,2347	66,9948	,00000000	326,4097
27	264,5808	67,4055	,00000000	326,8261
28	264,8435	67,2746	,00000000	327,1421
29	265,4524	67,7972	,00000000	327,8746
30	265,4995	67,7961	,00000000	327,9312
31	283,2255	4640,7667	,00000000	349,8056
32	299,8845	60,8308	,00000000	370,3989
33	316,4664	4597,2013	,00000000	390,9007
34	332,9613	63,8783	,00000000	411,2989
35	349,4576	4597,2014	,00000000	431,6989

LIST OF BOTTOM HITS

NO BOTTOM HITS

LIST OF SURFACE HITS

NO SURFACE HITS

DEPTH M=2331,7246 EPSILON= ,4000 DELTA= 250 MIN DELTA= 25 SIN TEST= ,100

Table 5.5.3.[1]

1.0285 sec/mile TOTAL TIME: 6:00 REAL DATA

RAY TRACE ANALYSIS PROGRAM- R D MININGHAM - (A-201-U1)
RAY NUMBER= 3 INITIAL ANGLE= 12,800 DEGREES

LIST OF TURNING POINTS

NUMBER	RANGE NM	DEPTH M	SINE	SECONDS
1	10,6907	4636,8044	,00000000	13,0878
2	27,3036	56,1211	,00000000	33,6306
3	43,9552	4661,9209	,00000000	54,2196
4	60,5957	58,7826	,00000000	74,7924
5	77,2364	4647,2377	,00000000	95,3695
6	93,7702	59,3993	,00000000	115,8139
7	110,2481	4627,0526	,00000000	136,1960
8	126,9740	63,1653	,00000000	156,8715
9	143,7364	4634,1481	,00000000	177,5903
10	160,3909	57,3289	,00000000	198,1738
11	177,0383	4634,6345	,00000000	218,7509
12	193,7278	65,5456	,00000000	239,3085
13	210,4404	4639,7244	,00000000	260,0457
14	227,3826	65,3084	,00000000	280,9770
15	244.3490	4648,2251	,00000000	301,9375
16	261,6297	65,9928	,00000000	323,2760
17	278,8663	4638,0370	,00000000	344,5614
18	295,5877	60,0790	,00000000	365,2286
19	312,2357	4593,5493	,00000000	385,8084
20	328,7465	63,4772	,00000000	406,2258
21	345,2652	4593,5491	,00000000	426,6827

LIST OF BOTTOM HITS

NO BOTTOM HITS

LIST OF SURFACE HITS

NO SURFACE HITS

DEPTH M=2331,7246 EPSILON= ,4000 DELTA= 500 MIN DELTA= 25 SIN TEST= .020

Table 5.5.3.2

0.9571 sec/mile TOTAL TIME: 5:35 REAL DATA

RAY TRACE ANALYSIS PROGRAM. R D MININGHAM . (A-201-U1)
RAY NUMBER= 5 INITIAL ANGLE= 12,000 DEGREES

LIST OF TURNING POINTS

NUMBER	RANGE NM	DEPTH M	SINE	SECONDS
1	10,6913	4636,8050	,00000000	13,0884
2	27,3046	56,1166	,00000000	33,6318
3	43,9504	4661,9858	,00000000	54,2140
4	60,6487	56,8267	,00000000	74,8564
5	77,3345	4646,0186	,00000000	95,4838
6	93,8466	59,9596	,00000000	115,9062
7	110,3254	4626,2976	,00000000	136,2896
8	127,0383	63,3897	,00000000	156,9498
9	143,7909	4632,7654	,00000000	177,6568
10	160,4298	57,8472	,00000000	198,2260
11	177,0613	4630,7369	,00000000	218,7868
12	193,7536	66,0643	,00000000	239,4196
13	210,4548	4635,6622	,00000000	260,0633
14	227,4096	65,3854	,00000000	281,0098
15	244,3856	4644,4134	,00000000	301,9817
16	261,4341	64,7589	,00000000	323,0405
17	278,6611	4634,7534	,00000000	344,3386
18	295,4165	60,0433	,00000000	365,0224
19	312,0702	4590,1552	,00000000	385,6089
20	328,5788	63,2596	,00000000	406,0236
21	345,1010	4590,1552	,00000000	426,4546

LIST OF BOTTOM HITS

NO BOTTOM HITS

LIST OF SURFACE HITS

NO SURFACE HITS

DEPTH M=2331,7246 EPSILON= ,4000 DELTA=1000 MIN DELTA= 25 SIN TEST= ,020

Table 5.5.3.3

1.3714 sec/mile TOTAL TIME: 8:00

REAL DATA

RAY TRACE ANALYSIS PROGRAM- R D MININGHAM - (A-201-U1)
RAY NUMBER= 7 INITIAL ANGLE= 12,800 DEGREES

LIST OF TURNING POINTS

NUMBER	RANGE NM	DEPTH M	SINE	SECONDS
1	10,6914	4636,8062	,00000000	13,0886
2	27,3017	56,1523	,00000000	33,6284
3	43,9577	4661,8168	,00000000	54,2223
4	60,6553	56,8423	,00000000	74,8636
5	77,3362	4645,3990	,00000000	95,4850
6	93,8970	58,7015	,00000000	115,9660
7	110,4220	4624,2656	,00000000	136,4847
8	127,1403	63,4974	,00000000	157,0712
9	143,8874	4632,1829	,00000000	177,7718
10	160,5217	57,8238	,00000000	198,3360
11	177,1528	4632,2899	,00000000	218,8965
12	193,8421	65,7586	,00000000	239,5257
13	210,5454	4637,3438	,00000000	260,1718
14	227,4930	65,0827	,00000000	281,1097
15	244,4728	4647,6013	,00000000	302,0861
16	261,5769	64,4407	,00000000	323,2120
17	278,6670	4638,8072	,00000000	344,3211
18	295,3900	60,0678	,00000000	364,9902
19	312,0395	4594,5429	,00000000	385,5718
20	328,5551	63,1064	,00000000	405,9951
21	345,0763	4594,5431	,00000000	426,4250

LIST OF BOTTOM HITS

NO BOTTOM HITS

LIST OF SURFACE HITS

NO SURFACE HITS

DEPTH M=2331,7246 EPSILON= ,4000 DELTA= 250 MIN DELTA=100 SIN TEST= ,020

Table 5.5.3.4

0.9971 sec/mile TOTAL TIME: 5:35 REAL DATA

RAY TRACE ANALYSIS PROGRAM- R D MINIMGHAM - IA-204-US;
RAY NUMBER= 9 INITIAL ANGLE= 12,800 DEGREES

LIST OF TURNING POINTS

NUMBER	RANGE NM	DEPTH M	SINE	SECONDS
1	10,6907	4636,8044	,00000000	13,0878
2	27,2966	56,1725	,00000000	33,6222
3	43,9318	4661,6038	,00000000	54,1914
4	60,6270	56,4987	,00000000	74,8300
5	77,3239	4645,0561	,00000000	95,4704
6	93,8393	60,1172	,00000000	115,8908
7	110,3167	4625,0062	,00000000	136,2780
8	127,0440	63,5148	,00000000	156,9554
9	143,7936	4631,9109	,00000000	177,6891
10	160,4257	57,8058	,00000000	198,2806
11	177,0621	4632,1211	,00000000	218,7874
12	193,7650	65,7179	,00000000	239,4328
13	210,4798	4637,4071	,00000000	260,0927
14	227,4255	64,9886	,00000000	281,0282
15	244,3940	4647,5254	,00000000	301,9910
16	261,3888	64,5162	,00000000	322,9853
17	278,5314	4638,2639	,00000000	344,1880
18	295,2519	60,0506	,00000000	364,8841
19	311,9052	4593,3034	,00000000	385,4101
20	328,4158	63,0558	,00000000	405,8273
21	344,9436	4593,3033	,00000000	426,2691

LIST OF BOTTOM HITS

NO BOTTOM HITS

LIST OF SURFACE HITS

NO SURFACE HITS

DEPTH M=2331,7246 EPSILON= ,4000 DELTA= 500 MIN DELTA=100 SIN TEST= ,020

Table 5.5.3.5

0.8428 sec/mile TOTAL TIME: 4:55

REAL DATA

RAY TRACE ANALYSIS PROGRAM= R D MININGHAM - [A-201-U1]
RAY NUMBER= 11 INITIAL ANGLE= 12.800 DEGREES

LIST OF TURNING POINTS

NUMBER	RANGE NM	DEPTH M	SINE	SECONDS
1	10,6913	4636,8050	,00000000	13,0884
2	27,2995	56,1725	,00000000	33,6256
3	43,9556	4662,0056	,00000000	54,2197
4	60,6478	56,8965	,00000000	74,8548
5	77,3280	4645,3537	,00000000	95,4752
6	93,8796	58,8807	,00000000	115,9452
7	110,3971	4625,1129	,00000000	136,3750
8	127,1151	63,5049	,00000000	157,0411
9	143,8620	4631,8439	,00000000	177,7417
10	160,4931	57,7409	,00000000	198,3820
11	177,1238	4632,3869	,00000000	218,8620
12	193,8154	65,7293	,00000000	239,4941
13	210,5303	4637,7235	,00000000	260,1540
14	227,4887	65,4181	,00000000	281,1047
15	244,4557	4648,3810	,00000000	302,0655
16	261,6114	65,8070	,00000000	323,2537
17	278,7237	4639,9515	,00000000	344,3902
18	295,4405	59,8483	,00000000	365,0516
19	312,0876	4596,3665	,00000000	385,6304
20	328,6163	63,0559	,00000000	406,0693
21	345,1212	4596,3662	,00000000	426,4807

LIST OF BOTTOM HITS

NO BOTTOM HITS

LIST OF SURFACE HITS

NO SURFACE HITS

DEPTH M=2331,7246 EPSILON= ,4000 DELTA=1000 MIN DELTA=100 SIN TEST= ,020

Table 5.5.3.6

1.4142 sec/mile TOTAL TIME: 8:15

REAL DATA

RAY TRACE ANALYSIS PROGRAM= R D MININGHAM - (A-201-U1)
RAY NUMBER= 1 INITIAL ANGLE= 12,800 DEGREES

LIST OF TURNING POINTS

NUMBER	RANGE NM	DEPTH M	SINE	SECONDS
1	10,6914	4636,8062	,00000000	13,0886
2	27,3103	56,1248	,00000000	33,6386
3	43,9638	4661,7430	,00000000	54,2296
4	60,6487	56,9917	,00000000	74,8558
5	77,3220	4645,9849	,00000000	95,4682
6	93,8757	58,9457	,00000000	115,9406
7	110,3853	4625,1242	,00000000	136,3608
8	127.1047	63,2749	,00000000	157,0287
9	143,8547	4633,0407	,00000000	177,7328
10	160,4911	57,7543	,00000000	198,2996
11	177,1219	4633,2844	,00000000	218,8597
12	193,8077	65,6781	,00000000	239,4848
13	210,5176	4638,3765	,00000000	260,1388
14	227,4623	65,0646	,00000000	281.0732
15	244,4385	4648,3111	,00000000	302,0453
16	261,4483	64,3531	,00000000	323,0578
17	278,5465	4639,9808	,00000000	344,1768
18	295,2831	59,8875	,00000000	364,8620
19	311,9376	4595,7191	,00000000	385,4498
20	328,4561	63,0793	,00000000	405,8764
21	344,9815	4595,7192	,00000000	426,3114

LIST OF BOTTOM HITS

NO BOTTOM HITS

LIST OF SURFACE HITS

NO SURFACE HITS

DEPTH M=2331,7246 EPSILON= ,4000 DELTA= 250 MIN DELTA= 25 SIN TEST= ,020

Table 5.5.3.7

1.0857 sec/mile TOTAL TIME: 6:20 REAL DATA

RAY TRACE ANALYSIS PROGRAM= R D MININGHAM = (A-201-U1)
RAY NUMBER= 15 INITIAL ANGLE= 12,800 DEGREES

LIST OF TURNING POINTS

NUMBER	RANGE NM	DEPTH M	SINE	SECONDS
1	10,6907	4636,8044	,00000000	13,0878
2	27,2121	59,3028	,00000000	33,5205
3	43,8122	4660,9987	,00000000	54,0474
4	60,4318	57,9067	,00000000	74,5950
5	77,0846	4644,7097	,00000000	95,1822
6	93,5987	58,5366	,00000000	115,6070
7	110,1091	4623,2235	,00000000	136,0280
8	126,7755	63,3483	,00000000	156,6322
9	143,5324	4632,4670	,00000000	177,3446
10	160,1184	58,3837	,00000000	197,8507
11	176,7542	4631,7805	,00000000	218,4165
12	193,3297	70,0813	,00000000	238,9089
13	209,9772	4635,6417	,00000000	259,4872
14	226,9135	65,3198	,00000000	280,4115
15	243,8874	4646,8911	,00000000	301,3811
16	260,9238	66,4761	,00000000	322,4295
17	261,0603	67,1786	,00000000	322,5897
18	261,3865	64,0827	,00000000	322,9819
19	261,5361	68,0006	,00000000	323,1619
20	261,8037	63,8295	,00000000	323,4837
21	261,9565	68,0460	,00000000	323,6674
22	262,2166	64,6864	,00000000	323,9803
23	279,3651	4636,2463	,00000000	345,1598
24	296,0705	59,9378	,00000000	365,8076
25	312,7273	4590,2854	,00000000	386,3981
26	329,2483	62,2445	,00000000	406,8277
27	345,8016	4590,2854	,00000000	427.2962

LIST OF BOTTOM HITS

NO BOTTOM HITS

LIST OF SURFACE HITS

NO SURFACE HITS

DEPTH M=2331,7246 EPSILON= ,4000 DELTA= 500 MIN DELTA= 25 SIN TEST= ,100

Table 5.5.3.8

0.9857 sec/mile TOTAL TIME: 5:45 REAL DATA

RAY TRACE ANALYSIS PROGRAM- R D MININGHAM - (A-201-U1)
RAY NUMBER= 17 INITIAL ANGLE= 12,800 DEGREES

LIST OF TURNING POINTS

NUMBER	RANGE NM	DEPTH M	SINE	SECONDS
1	10,6913	4636,8050	,00000000	13,0884
2	27,3220	55,9852	,00000000	33,6525
3	44,0020	4662,5671	,00000000	54,2751
4	60,6486	58,6305	,00000000	74,8591
5	77,2973	4646,6479	,00000000	95,4379
6	93,7917	59,7763	,00000000	115,8388
7	110,2801	4627,4540	,00000000	136,2334
8	127,0120	61,9869	,00000000	156,9161
9	143,7606	4632,5523	,00000000	177,6188
10	160,3810	57,2477	,00000000	198,1663
11	177,0098	4632,2882	,00000000	218,7248
12	193,6216	68,9703	,00000000	239,2608
13	210,3042	4637,3472	,00000000	259,8812
14	227,2941	65,1325	,00000000	280,8701
15	244,2557	4648,3104	,00000000	301,8251
16	261,0361	72,0140	,00000000	322,5615
17	277,8818	4641,7828	,00000000	343,3777
18	294,6449	59,5030	,00000000	364,0939
19	311,2956	4598,3941	,00000000	384,6770
20	327,8082	64,9141	,00000000	405,0959
21	344,2577	4598,3942	,00000000	425,4406

LIST OF BOTTOM HITS

NO BOTTOM HITS

LIST OF SURFACE HITS

NO SURFACE HITS

DEPTH M=2331,7246 EPSILON= ,4000 DELTA=1000 MIN DELTA= 25 SIN TEST= ,100

Table 5.5.3.9

0.7428 sec/mile   TOTAL TIME: 4:20   REAL DATA

RAY TRACE ANALYSIS PROGRAM. R D MININGHAM - (A-201-U1)
RAY NUMBER= 19 INITIAL ANGLE= 12,800 DEGREES

LIST OF TURNING POINTS

NUMBER	RANGE NM	DEPTH M	SINE	SECONDS
1	10,6868	4636,8003	,00000000	13,0832
2	27,3011	56,1495	,00000000	33,6281
3	43,9439	4661,6838	,00000000	54,2071
4	60,6462	56,8716	,00000000	74,8542
5	77,3132	4645,0817	,00000000	95,4596
6	93,8454	59,6193	,00000000	115,9062
7	110,3444	4623,5956	,00000000	136,3136
8	127,0344	63,8618	,00000000	156,9458
9	143,7752	4632,5952	,00000000	177,6390
10	160,3966	57,7460	,00000000	198,1081
11	177,0276	4632,1833	,00000000	218,7485
12	193,7437	65,6991	,00000000	239,4096
13	210.4508	4637,8585	,00000000	260,0602
14	227,3672	65,3788	,00000000	280,9606
15	244,3499	4648,2443	,00000000	301,9396
16	261,3937	66,4442	,00000000	322,9932
17	261,6688	67,5553	,00000000	323,3242
18	261,9230	66,6093	,00000000	323,6300
19	262,2022	67,5221	,00000000	323,9658
20	262,5201	66,5614	,00000000	324,3482
21	262,6898	67,2134	,00000000	324,5924
22	262,9665	65,7569	,00000000	324,8852
23	263,1910	68,3954	,00000000	325,1553
24	263,4203	64,5388	,00000000	325,4311
25	280,4882	4632,3086	,00000000	346,5138
26	297,1717	60,6601	,00000000	367,1358
27	313,7951	4588,5859	,00000000	387,6867
28	330,2932	63,3749	,00000000	408,0891
29	346,8065	4588,5858	,00000000	428,5099

LIST OF BOTTOM HITS

NO BOTTOM HITS

LIST OF SURFACE HITS

NO SURFACE HITS

DEPTH M=2331,7246 EPSILON=1,0000 DELTA=1000 MIN DELTA= 25 SIN TEST= .020

Table 5.5.3.10

0.7142 sec/mile TOTAL TIME: 4:10 REAL DATA

RAY TRACE ANALYSIS PROGRAM. R D MININGHAM - (A-201-01)
RAY NUMBER= 21 INITIAL ANGLE= 12.800 DEGREES

LIST OF TURNING POINTS

NUMBER	RANGE NM	DEPTH M	SINE	SECONDS
1	10.6868	4636,8003	,00000000	13,0832
2	27,2949	56,1776	,00000000	33,6206
3	43,9470	4661,5574	,00000000	54,2100
4	60,6399	56,8786	,00000000	74,8461
5	77,3031	4644,0669	,00000000	95,4471
6	93,8538	59,0409	,00000000	115,9161
7	110,3793	4622,1036	,00000000	136,3946
8	127,0868	64,1649	,00000000	157,0079
9	143,8231	4629,3606	,00000000	177,6957
10	160,4318	58,3767	,00000000	198,2296
11	177,0500	4628,9777	,00000000	218,7743
12	193,7418	66,1322	,00000000	239,4065
13	210,4440	4633,7247	,00000000	260,0510
14	227,3592	65,9033	,00000000	280,9619
15	244,3411	4642,8283	,00000000	301,9290
16	261,2806	69,7308	,00000000	322,8568
17	278,2095	4635,5884	,00000000	343,7724
18	294,9371	60,0448	,00000000	364,4462
19	311,5802	4589,6187	,00000000	385,0203
20	328,0742	63,3533	,00000000	405,4181
21	344,5871	4589,6187	,00000000	425,8384

LIST OF BOTTOM HITS

NO BOTTOM HITS

LIST OF SURFACE HITS

NO SURFACE HITS

DEPTH M=2331,7246 EPSILON=1,0000 DELTA=1000 MIN DELTA=100 SIN TEST= ,020

Table 5.5.3.11

5.6. Reversibility Test in Real Velocity Field

A further test of the ray tracing program was made to determine the ability of the program to calculate the reversed ray path and to compare this path with the path determined by a prior calculation. Theoretically, and as a property of the basic ray equation (III. 1), any ray should be exactly reversible. The solution by incremented iterations and the general method of the present program, however, guarantee that the iterations in one direction will be entirely independent of those in the other direction. Thus, the degree to which the ray is returned to its origin by the reversed ray tracing becomes an excellent criterion of the overall accuracy of the program.

The steps followed in these tests were:

i) A forward ray tracing was made to determine the depth and ray angle of the ray at a given range. For these the most accurate control parameters were chosen, corresponding to those in Table 5.5.2.1 for the 14.80° ray and in Table 5.5.3.1 for the 12.80° ray. Actual values were a depth of 4975.40 meters and an angle of 5.22° for the 14.80° ray at the range of 250 miles and a depth of 4085.93 meters and an angle of 6.27° for the 12.80° ray at a range of 350 miles.

ii) The bottom profile and the velocity profiles of the velocity field were reversed in their range sequences by preparing new input data decks for which the given ranges were subtracted from the maximum range of the program.

iii) The final positions of the rays traced in the forward direction were used as origins for a new ray trace in the program with reversed data inputs, but the final angle of the ray in the forward direction was reversed in sign to become the initial angle for the new ray trace.

iv) For convenience in comparing the data results, the printouts of the reversed ray trace were again reversed and are presented in Table 5.6.1 for the 14.80° ray and in Table 5.6.2 for the 12.80° ray. This technique allows the initial depths and angles of these tables to be compared directly with those of Tables 5.5.2.1 and 5.5.3.1 as measures of the overall accuracy of the reversibility test. It also follows that the data printouts of the tables at the largest ranges represent ray path comparisons over the shortest relative range intervals.

The data comparisons speak for themselves - the variations are, in fact, less than the deviations found for the ray tracings in the forward direction only but with different values of the control parameters.

Reference for Chapter V

1. I. Tolstoy and C. S. Clay, Ocean Acoustics, McGraw Hill Book Co., N.Y. (1966).

RAY TRACE ANALYSIS PROGRAM- R D MININGHAM - (A-201-01)
RAY NUMBER= 2 INITIAL ANGLE= -14.827 DEGREES

LIST OF TURNING POINTS

REVERSE

NUMBER	RANGE NM	DEPTH M	SINE	SECONDS
1	42.0606	5330.1087	.00000000	51.9754
2	76.5027	5320.0638	.00000000	94.5191
3	110.8029	5300.9118	.00000000	130.8951
4	211.2359	5320.5766	.00000000	261.0599
5	245.8375	5327.2197	.00000000	303.7848

LIST OF BOTTOM HITS

NUMBER	RANGE NM	DEPTH M	SINE	SECONDS
1	9.6760	5231.6639	.04945235	11.8849
2	144.6398	5303.5306	.01259448	176.7140
3	177.6861	5297.6586	.01939231	219.5873

LIST OF SURFACE HITS

NUMBER	RANGE NM	DEPTH M	SINE	SECONDS
1	24.8634	.0000	-.12124714	30.7307
2	59.2831	.0000	-.12024948	73.2476
3	93.6729	.0000	-.12265150	115.7292
4	127.9989	.0000	-.12197731	158.1359
5	161.2794	.0000	-.12030825	199.2895
6	193.9744	.0000	-.11727685	239.7430
7	228.5317	.0000	-.11430850	282.4165

EPSILON= .4000 DELTA= 250 MIN DELTA= 25 SIN TEST= .020

Table 5.6.1

RAY TRACE ANALYSIS PROGRAM- R D MININGHAM - (A-201-01)
RAY NUMBER= 1 INITIAL ANGLE= -12,808 DEGREES

LIST OF TURNING POINTS REVERSE

NUMBER	RANGE NM	DEPTH M	SINE	SECONDS
1	10,6988	4637,3478	,00000000	13,0979
2	27,3093	55,9885	,00000000	33,6380
3	43,9744	4662,3625	,00000000	54,2430
4	60,6789	56,7735	,00000000	74,8929
5	77,3476	4646,2945	,00000000	95,4996
6	93,9117	58,8693	,00000000	115,9844
7	110,4189	4625,4963	,00000000	136,4017
8	127,1369	63,2249	,00000000	157,0602
9	143,8897	4633,4937	,00000000	177,7756
10	160,5216	57,7453	,00000000	198,3371
11	177,1456	4633,1682	,00000000	218,8892
12	193,8441	65,6737	,00000000	239,5295
13	210,5382	4638,4417	,00000000	260,1645
14	227,4924	65,1435	,00000000	281,1102
15	244,4577	4647,7688	,00000000	302,0693
16	261,5268	64,4545	,00000000	323,1530
17	278,5655	4640,1722	,00000000	344,2005
18	295,2972	59,9395	,00000000	364,8798
19	311,9450	4595,7226	,00000000	385,4594
20	328,4679	63,0808	,00000000	405,8912
21	344,9815	4595,7223	,00000000	426,3121

LIST OF BOTTOM HITS

NO BOTTOM HITS

LIST OF SURFACE HITS

NO SURFACE HITS

EPSILON= ,4000 DELTA= 250 MIN DELTA= 25 SIN TEST= ,020

Table 5.6.2

CHAPTER VI

BATHYMETRY

6.1 Introduction

The present ray tracing program is limited to two-dimensional cylindrical spreading, i.e., propagation along a given bearing. This is not regarded as a serious limitation for the treatment of ray paths that travel entirely through water, since in long-range propagation the possible effects of azimuthal refraction in the water would not be significant in the calculation of transmission loss using the averaged sound distributions described in Chapter IV. Similarly, and recognizing that surface wave scattering can in principle be non-isotropic in its dependence on wave and swell directions, the very small attenuation of such scattering (IV.17) in the low-frequency limit and for prevailing sea states of the ocean shows that there would be no more than a formal advantage in accepting the complexity of a three-dimensional ray tracing program for the sake of including these physical effects.

As discussed in Chapter I, however, bottom-reflected sound energy can make a significant, and at times major, contribution to the acoustical field and must be included in a general-purpose predictive model. The total sound field is made up of numerous and usually unidentifiable arrivals in long-range propagation studies. In applying the present program toward identifying the arrival structure due to explosive sources we have had good success in predicting the arrivals that travel through the water by refraction alone, but have found it more difficult to identify the bottom-reflected arrivals, especially in ocean regions with complex bathymetry.

Chapter I lists the dominant bathymetric interactions as arising from:

i) terrain local to the origin,

ii) intervening obstructions over the ray path, e.g., rises and seamounts, and

iii) distant slopes which alter the vertical sound distribution.

Formally, the use of the cylindrical spreading model demands that the bottom contours taken about the origin of the ray tracing be close approximations to concentric circles about the origin or, at least, that the tangent planes adopted to represent the bottom be not only tangent to the bottom profile used in the program but be also normal to the particular azimuthal plane of the ray tracing. Frequently these conditions will be adequately met and can be used satisfactorily in some geographical locations. However, it may happen that the bathymetry is so poorly defined that this first approximation must be made on a provisional basis in making an initial estimate of the transmission loss. In the latter event the present program provides an estimate of the effect of the bottom reflections through, for example, the ray depth distribution plots. Such initial studies can determine the intervals at which bathymetric measurements are needed as part of an experiment in acoustical propagation.

The general problem of determining the bottom reflectivity coefficients for use in the ray tracing program either experimentally or theoretically is far beyond the scope of the present report. As already noted in Chapter IV, it must be emphasized that scant data exist as a guide for even representative models of the low-frequency, low grazing angle reflections that can be expected to dominate in long-range propagation. The nature of the information that is required can be summarized in three categories that are further discussed below:

1. the emphasis on specular reflection coefficients,
2. the treatment of highly contoured bottoms that do not possess cylindrical symmetry, and
3. the reliability and accuracy of the bottom contours themselves in terms of oceanographic practice and "standard," e.g., BC , charts.

6.2. Specular Reflection

General treatments of boundary layer scattering from a moderately rough surface show that the reflected waves can be resolved into a specular (and coherent) wave and an incoherent wave. Resolution into these classes will be possible whether the boundary may be treated as a simple surface or must be analyzed in terms of subplanes such as those representing sedimented layers. It is to be noted that when bottom penetration exists into a multiply layered boundary, the impulse response may show a long apparent reverberation resulting from the time delays and dispersions that will be associated with the primary and secondary reflections from the individual layers - the presence of such a tail does not, therefore, provide of itself a discrimination of the reflection as specular or incoherent.[1]

The direction of the specular reflection, however, can be treated directly by the ray theory, and the calculation of the spreading loss that is applied to individual arrivals is unaltered by the reflections that occur at plane or nearly plane boundaries. It is necessary, of course, that the changes of the slopes of the boundary planes be small compared with a wavelength as a condition for the application of ray theory - otherwise, there will be additional losses due to diffraction.

The incoherent reflection cannot be treated by continuation of the ray paths after the reflection. The intensity of the incident wave must be evaluated at the boundary and there be used as a source intensity for the wavelets scattered in all the non-specular directions. As a consequence, the energy scattered into any differential solid angle becomes negligible with respect to the energy in the solid angle that is specularly reflected. As a further consequence, the attenuation of the incoherently scattered waves is much greater than that of the specularly reflected wave in the far field when a moderate to strong specularly reflected component can exist, and this can be expected in the region of long wavelengths and low grazing angles that dominate long-range propagation.

The above emphasizes that the bottom scattering attenuations (Chapter IV-4.2.1) that are introduced into the ray tracing program as part of the weighting functions that modify each ray are to apply to specular reflection, at least for the rays that subsequently propagate to long ranges. If, on the other hand, the reflectivity is measured locally, the total incoherently reflected energy contributes as an integral comprised of all of the contributions from the local bottom surface. The net incoherent reflection comes from a large effective solid angle and can be considerably larger than that due to the specularly reflected wave; also, such local measurements will require detailed experimental design and analysis to separate the two types of reflectivity contributions from the scattered intensity. However, the incoherent scattering remains a secondary process, and as the range from the scatterers increases, the effective solid angle from the scattering area decreases so that in the limit of long ranges (and excepting specialized bottom contours) the incoherent scattering becomes negligible.

Strong empiric evidence can be cited for the use of the specular reflection coefficients for the reflections from both the surface and bottom ocean boundaries. In 1962 Berman noted[2] that the arrival structure from long-range explosive shots can be interpreted as an indication of the angular spread of ray arrivals and concluded that over ranges as large as 2000 miles the angular spread was of the order of 0.2°! Such a result cannot be understood unless the reflections were specular.

Berman's arguments for this conclusion require assumptions and simplifications that are unrealistic, e.g., no dispersion and no bottom penetration, and his data analysis makes no distinctions between boundary-reflected arrivals and arrivals that have traveled solely through the water. Nonetheless, applications of the present ray tracing program to shot structure analysis do require conclusions that are similar to Berman's (although we would be considerably more conservative in our own conclusions). It is certainly true that with increasing range resolvable and identifiable bottom-reflected arrivals from explosive shots show far less time spread in their structure than is found in single bottom reflections in local measurements. This is in agreement with the greater attenuation with range of the incoherent components of the reflection, as discussed previously. There are, of course, an increasing number of arrivals with increasing range - it is significant that the time spread of the dominant arrivals is in good agreement with the ray tracing model results for the rays, and this is one basis for the assertion that the energy carried by the bottom reflection arrivals cannot be neglected in long-range propagation.

6.3. Bathymetry with Non-Cylindrical Symmetry

The foregoing remarks constitute a good approximation for the treatment of the bottom reflections when the bottom is approximately flat over an acoustical path and provided that strong reflectors outside the bearing of the acoustical path do not provide special alternative paths that can selectively couple sound energy from the source to the receiver. The calculation of transmission loss that is presented in Chapter IV requires a large number of rays in the azimuthal bearing plane for the purpose of sampling the resultant field distribution and is especially suitable as an averaging process for the bottom reflections over a gently undulating, moderately rough bottom. Specifically, it is expected that the rays that are canted off a given bearing in a reflection will be partially offset by rays that are initially propagating on an adjacent bearing and which by reflection are canted toward the receiver. The presence of such "cross-bearing coupling" that averages to a value independent of the bearing is not inconsistent with the assumption of cylindrical spreading and, in first approximation, would not alter the vertical distribution of channeled sound energy.

In the presence of more complex bathymetry, however, the simplifications of a model based on cylindrical symmetry cannot be justified. In some experiments involving towed low-frequency cw projectors Hudson Laboratories has detected energy which, by its Doppler shift, can be identified as propagating at bearing angles of 30° to 40° from the direct path and which could have been detected only after reflection from adjacent terrain. This experience is anomalous, but is cited as one example that the total sound field results from many contributions. Indeed, if the present ray tracing program were to be extended for greater physical application, and apart from technical improvements that might lead to increased computational efficiency, the direction of the effort would be toward a more realistic inclusion of the contributions from bottom reflections. The following comments are provided not toward discussion of such a revision but in appraisal of the limitations of the cylindrical spreading model. The comments are given in terms of the three principal bottom interactions that affect long-range propagation.

6.3.1. Terrain Local to the Origin

When the origin of the rays occurs at or near a slope or embankment there is a strong possibility that slope-reflected rays will be converted to ray directions that can propagate to long ranges in the sound channel or in an RSR mode, e.g., Figs. 9 and 17. It will be a rare geological structure, however, that does not show troughs or rises and other features which will act to make the coupling of the sound energy to the far field dependent on specific bearing angles.

A realistic model for this type of boundary would consist of small-scale roughness over an averaged bottom that is described by contours taken many wavelengths apart. The roughness leads to incoherent scattering, but if the bottom is smooth on average there will also be a specular reflection that can be described through an attenuation function. The ray tracing from a given origin yields the direction of the wavefronts that are incident against the bottom, and from these data the orientation of facets which will reflect to a given bearing can be determined. The effective cross section for each facet will be proportional to its Gaussian curvature, and the inclination of the reflected ray will determine how the ray is subsequently propagated - the facets that reflect steep rays that require further bottom reflections can be disregarded.

The description in terms of facets is the extension to three dimensions of the two-dimensional profile used for cylindrical spreading. However, the simple two-dimensional profile implies that the specular reflection remains on or close to the bearing angle because the bottom planes are assumed normal to the given bearing; in three dimensions there may be very few or no facets with an orientation that permits coupling to a given bearing or, on the other hand, certain bearings may be very strongly illuminated by extensive, favorably oriented slopes. If an acoustic source and its adjacent terrain were viewed in a manner that corrected for the refraction of the rays in subsequent propagation, three characteristic types of illumination would be clearly visible:

1) direct rays which were not reflected from the bottom,
2) localized images of the source that are reflected from the bottom facets, and
3) a uniform illumination of the entire slope due to incoherent scattering.

The fact that the slope, viewed from the far field, would appear uniformly illuminated by the incoherent scattering is deduced by assuming that the scattering would roughly obey Lambert's Law. This is analogous to the uniform radiance from the surface of the moon produced by reflected sunlight. Unlike the optical analogy, however, it would be expected that for low-frequency acoustical waves a typical slope under water would or could show significant specular reflection from certain facets, and that the specularly reflected energy from these would have much greater brightness than that scattered diffusely. The degree with which each type of illumination contributes to the net far acoustical field will depend on the position of the source in the region of the slope, the nature of the slope itself, and the structure of the velocity profiles which govern both the coupling of the direct rays and the angles of incidence of the rays reflected against the bottom, including those rays which are first reflected from the sea surface.

More importantly, the refraction of the spreading energy of the field propagating from the source and slope will produce modulations of each of the three types of contributions that will depend on the position in the far field. For example, it will be characteristic of shadow zone reception that the major contributions will come from the bottom reflections although the total energy spreading from the source may contain only a small percentage of bottom-reflected energy.

A principal direction of the present program has been toward the inclusion of all significant modes of propagation even though the description and evaluation of such modes is (initially) handled by highly empiric, even ad hoc, procedures. One reason for the inclusion of such effects is to increase the facility with which the predicted transmission loss can be compared with experimental data. Evidently, the bottom-reflected arrival contributions will not only affect the magnitude of the measured transmission loss but will be important also in a description of the transmission loss spectrum and in the shape of the transmission loss taken as a function of range and position in the ocean. Although the present two-dimensional program cannot treat the bottom reflections from complex bathymetry on a quantitative basis it can, at least, contribute toward distinguishing the direct, purely refracted or RSR arrivals from those that do interact with the bottom.

6.3.2. Seamounts and Slopes at Intermediate Ranges

It has already been indicated, e.g., in Fig. 17, that an intervening obstruction can radically modify the vertical distribution of the spreading sound energy, acting as a filter that both attenuates and truncates selected ray bundles. The interaction will not only depend on the bathymetry of the obstruction itself but will be sensitive to the illumination against the obstruction that is determined by the propagation paths between the source for the ray tracing and the interposed bottom. A detailed treatment of this problem, therefore, will be conditional upon a relatively complete, accurate treatment of the incident acoustical field. Further, all the problems raised in the preceding discussions will again apply to this type of blockage, including the question as to whether a cylindrical spreading model that is two dimensional will be applicable.

The model is probably satisfactory if the obstruction is a uniform rise that lies approximately normal to the acoustical path, but it will be obviously inadequate for the treatment of seamounts, many of which have widths that are considerably narrower than a convergence zone. Weston treated the three-dimensional scattering from a round island and concluded that the "radar cross-section" for scattering from this type of feature would increase with deflection angle for source and receiver at angles with respect to the island that approach twice the bottom critical angle.[3] Weston's arguments are highly simplified and he deals only with the specular reflection; also, the fall-off of the specular reflection coefficient with increasing deflection angle will limit such side-of-slope scattering to a smaller value than that estimated by him.

If the seamount obstruction is regarded as being gradually translated across an otherwise unobstructed acoustical path, it would be expected that the rising base of the structure would initially obstruct the propagating field. Later, it may well be possible that reflections from the sides add energy and produce a redistribution of the ray bundles to increase the efficiency of the transmission. Finally, it would be expected that the central core of the seamount would produce maximum occultation in a manner that depends on the depth of the peak and the vertical distribution of the sound field in its location. The most important simple criterion for these effects will be the proportion of the acoustical field that travels directly through the water as compared to the field that arrives from the bottom reflections.

6.3.3. Distant Slopes

When the ray paths are followed across entire ocean basins the field can be regarded as broadly illuminating the far slopes of the basin and will produce a vertical redistribution of the spreading energy as discussed previously and indicated in Fig. 17. Because of the reciprocity theorem (Chapter IV-4.1.3) the comments that apply to the treatment of the local slope near the origin of the ray tracing will also apply to the far-field bottom reflections. There is, of course, the important practical distinction that the origin for the rays will represent a specific choice for which every attempt will be made to define the local bathymetry. The sound field map from this origin can be expected to cover tens of thousands of square miles and it must be expected that detailed bathymetric knowledge will be available for only isolated areas of the total field of illumination.

6.4. Bathymetric Data

The preceding remarks summarize the limitations of the present program for dealing with the acoustical field that has been bottom reflected as well as with extensions to the program that could be formulated so as to provide a more realistic treatment of the effects of the bottom. Over-all, however, such work demands that the bathymetric data must be known with a precision that is at least comparable to that of the velocity profile data. Also, in terms of long-range propagation over paths of several hundred miles range or more, it is necessary that much of the data will come from standard bathymetric charts.

This chapter includes background for readers who are not familiar with the methods used toconstruct such charts. It also discusses the procedures adopted in connection with the present program to obtain the bottom profile that is used in the ray tracing program.

6.4.1. Standard Bathymetric Charts

In recent years the knowledge of deep-sea bathymetry has been greatly increased through oceanographic research and military surveys while at the same time various events have dramatized the need for still more extensive and detailed knowledge in the field. Institutions from which Hudson Laboratories has acquired significant amounts of data for use in the ray trace program include the British Hydrographic Office, National Institute of Oceanography (England), Deutsches Hydrographisches Institut (Germany), Lamont Geological Observatory, Woods Hole Oceanographic Institution, Scripps Institution of Oceanography, Bedford Institute of Oceanography (Canada), and finally the U.S. Naval Oceanographic Office (NAVOCEANO) with the largest bathymetric data-gathering program of all these. This latter office is the official repository of all sounding data obtained by ships under control of the U.S. Navy, but it also receives extensive data from other Government agencies, commercial ships, oceanographic institutions, and foreign hydrographic bureaus. Of all sounding data collected by NAVOCEANO over the past 18 years, 78% was obtained by Navy and Coast Guard vessels, 11% on special surveys, and less than 11% was collected by merchant ships. NAVOCEANO is also responsible for the Department of Defense Bathymetric Data Bank, and is the world's largest producer of bathymetric charts.

The Bathymetry Division, Hydrographic Surveys Department, of NAVOCEANO receives approximately 700 sounding reports annually representing about 1.5 million miles of soundings. Most of the sounding tracks are plotted on the 3000 series plotting sheets (4 inches to a degree of longitude). Soundings are usually entered from echograms at time intervals of every 15 min.[4] However, an automated program developed by Lamont Geological Observatory under the direction of Dr. B. C. Heezen plots soundings at every peak, low, and change of slope.[5] Only in recent years has a program been initiated by NAVOCEANO to inspect the echograms for correctness of interpretation, positional accuracy, and for grading according to the quality of the sounding equipment used.

The soundings are compiled on "collection sheets" which are overlays to specific plotting sheets. There may be two sets of collection sheets (with and without security classification), and also several plotting sheets for each collection sheet. Classified bathymetric data are any data collected with a line spacing of 5 n.m. or less that have been obtained with a high-precision navigation system (e.g., Loran C) on a survey conducted by a Naval vessel. The Navy has no security classification control over a similar sounding density in the same area taken by an independent oceanographic organization.

The Bathymetry Division has the responsibility to provide charts for navigation and for the charting of shallow areas from surveys and merchant ship reports. The discussion in this report is limited to unclassified bathymetry.

Only about 4% of the world oceans has been surveyed by trained personnel operating from specially equipped oceanographic research vessels. Therefore, bathymetric charts are constructed primarily from random data tracks, which are sounding tracks from ships in transit from port to port or to and from operating areas. The sounding and navigation accuracy of these tracks is often open to question as the data may have been obtained or reduced by untrained personnel. A general statement concerning the bathymetric charts of the Atlantic Ocean is that those west of 60°W longitude have reasonably good accuracy, and those from 50° to 60° W longitude have only fair accuracy. The charts over the Mid-Atlantic Ridge delineate the ridge but fail, in most cases, to point out fracture zones and detailed topographical features. Charts along the coast of Europe range from good to fair. There are no BC charts of the South Atlantic, and generally charts north of 50° latitude are poor.

Many reported shallow features are unconfirmed because research and survey vessels have been unable to locate them. A similar situation exists in deep waters. For example, the reports of "phantom" seamounts come, for the most part, from merchant ship observers who operate low-powered sounding equipment that is used only occasionally while the ship is in transit. This results in a discontinuous sounding track that causes operator confusion as to what is the recording phase of the returning echo.[5]

Extensive phantom banks have been reported which display two dominant characteristics: (1) they have depths between 125 and 375 fathoms, and (2) they are always located in the daytime, never at night. Such recordings are not the ocean bottom, but the "Deep Scattering Layer" (DSL). The DSL has been found in most of the world oceans. It descends from the surface at sunrise to depths between 125 and 375 fathoms during the day.

Backus and Worthington[6] have found the DSL in the area of the "American Scout" seamount (46° 22' N, 37° 04' W) reported in July 1948 by the S. S. American Scout and two other merchant vessels the following month, and again in July 1964. Five research vessels have been in the area since 1958, and have failed to detect the mount. Soundings in the area show an average depth of 2420 fathoms.

Another example is Milne Bank shown on current charts at 43° 37' N, 38° 42' W. This was first reported to the British Admiralty in 1864 by Sir Alexander Milne at 43° 35' N, 38° 50' W as a bottom of fine sand and ooze at 92 and 81 fathoms. In 1868 the H. M. S. Gannet obtained 2280 fathoms in Admiral Milne's position. In 1894, the Bank was removed from the Admiralty charts. The S. S. Innaco in 1921 obtained a sounding of 63 fathoms and rocky bottom at 43° 37' N, 38° 42' W, and 75 fathoms about 2 miles southwest of this position. On October 14, 1936, the S. S. Camito ran its Marconi Eckometer sounding gear for 25 min and reported depths from 56 to 160 fathoms during a 5-min period. It reported that the ship was running on Eckometer soundings at 13.8 knots from 43° 39'.5" N, 38° 38'.5" W to 43° 40' N, 38° 37' W. In 1937, the H. M. S. Challenger obtained depths at the original Milne position of 2200 fathoms. In 1957-8, the German research vessels Gauss and Anton Dohrn ran over 350 n. m. of track in the area making continuous soundings. In 1965, Backus and Worthington[7] ran track lines through the area. Neither the 56-fathom peak nor any other seamount feature has been observed by a modern oceanographic vessel.

We are convinced that Milne Bank does not exist in its charted position. However, the lead line soundings of 1864 and 1921 cannot be ignored until a systematic survey of the area is undertaken.

There is no complete up-to-date source combining the presentation of all available data for any single BC area. The data is found at NAVOCEANO in the following forms:

(1) Documents - originals and/or copies of log books, track plots, echograms, sounding listings, charts, publications;

(2) Rolls of 35-mm film;

(3) Micromaster slides;

(4) Punch card data file;

(5) Miscellaneous unplotted data:

(6) Composite charts;

(7) BC charts (need revision, updating).

New programs in 1954 were given priority over routine up-dating of the BC charts. In March 1964 there were 23,438 document units not plotted on BC charts. A document unit consists of soundings crossing one plotting sheet. The backlog is increasing because of the number of sounding reports coming into the division. There are occasional data requests that reduce the backlog, but not to any great degree.

The indexing of the report documents starts with a cursory examination to see that the data reports conform to H. O. Pub. 606b.[8] In this examination many discrepancies with the publication are found, e.g., echograms but no ship navigation logs received, no correlation of navigation with echograms, etc. The data are given a general rating (1 to 4) based on the type of navigation control and completeness of the document. A rating of 1 is the highest rating and has navigational control obtained by Loran A or better with fixes every four hours or less. The data are collected by a survey on an oceanographic vessel using a precision depth recorder and the echogram accompanies the navigation data to NAVOCEANO. A rating of 2 meets all the requirements of 1 except that the navigation is poorer than Loran A. A classification of 3 is given to a document that contains a sounding track with no navigation aids but does contain an echogram. A rating of 4 is the same as a 3 rating without the echogram, and the sounding data may be only a listing of depths and position.

It is at this point that a master chart is prepared on which all the soundings are plotted. The final manuscript contour chart for publication is then drafted by a bathymetrist who must analyze the soundings and select different weights for the reliability of the data so as to fit the soundings to a consistent bathymetric representation. Needless to say, the quality of the BC's differs because not only do different people make varying judgments as to the quality of the data, but also the lack of data in some areas may force the bathymetrist to use poor data that would be omitted in areas where there is good control - e.g , west of 60 W longitude, the poorer data can be omitted completely. The bathymetrist also plots data from foreign nautical charts. The contours are drafted as 100-fathom isobaths that represent the geomorphology of the area. A BC log is kept for each bottom contour chart, consisting of the following: 1) the scientific literature referred to, 2) surveys used, 3) the domestic and foreign charts used, 4) the data of completion of the various steps in construction, and 5) names of personnel performing the work. This work is done by geologists, not cartographers, as the charting of the sea floor differs greatly from contouring aerial topographic maps.

A great deal of practical navigation experience is needed. Knowledge of sounding equipment and the correct delineation of bottom topography depends on the bathymetrist's knowledge of geology and sedimentology. Because the hydrographic chart is made up from only spot soundings, sounding lines, and profiles, placement of the contours on the charts necessarily becomes subjective. It is apparent that the chart quality depends on the bathymetrist's care and expertise in marine geomorphology. A chart must be constructed and reconstructed until the best possible interpretation is developed.

The use of the published Bathymetric Charts in underwater acoustics is limited for two important reasons: 1) the charts have been primarily designed for surface navigation and therefore do not include the positions at which soundings were made, and 2) much of the data used in constructing the chart is of unknown or poor accuracy. Therefore, it is necessary to obtain the "collection sheets," when possible, in order to determine the best profile for the ray tracing program in the area of interest. The published BC charts would be much more usable in acoustical investigations if the actual locations of the sounding data (control lines) were to be routinely incorporated in the construction of the charts. Also, the control lines should preferably be coded (e.g., by color or pattern) as to the reliability in terms of quality of navigation controls, sounding equipment, and other characteristics of the data presented.

6.4.2. Applications of Acoustics to Bathymetry

Essentially all of the data used in the preparation of the bathymetric charts (BC's) comes from echo sounding with greater weight assigned for the type of apparatus found on oceanographic research vessels. Where the contours change rapidly, the older wide-beam (60°) transducer can give ambiguous results arising from apparent multiple bottom structures unless exceptional care is taken in "migrating" the contours to form continuous lines; this problem is reduced when data are taken using narrow-beam (6°) transducers. All such devices have the defect, however, that bottom structure is greatly averaged by the returning echos in transits over the deep ocean and the data are confined to the contours taken over the track lines.

High-powered, deep-sea lateral echo sounders are far more useful for bathymetric determinations, for they determine not only a local bottom depth but also a profile transverse to the ship's track that may be extended to a range of several miles. In consequence, data are obtained that reveal the degree of modulation or roughness of the bottom. Present research programs are concentrating on the extent to which the topography determined by these techniques agrees with that mapped by the insitu observations of a trained geological observer operating from a deep submersible.

Coarser mapping of large-scale bathymetric features such as seamounts or slopes can be obtained by long-range propagation studies. Although these do not provide detail, they can provide surveys over large geographical areas to identify prominent reflectors or occultors of the sound. In reflection, large explosive charges are used as sources and the reflectors are located by comparison of the sound travel times for echoes that are monitored by widely spaced hydrophones. An example of occultation is shown in Fig. 17; if a continuous surface source such as a towed projector were to transit behind the seamount shown in the figure there would be a pronounced attenuation of the detected energy for the bearings that intercept the seamount.

These techniques do not, of course, replace detailed surveys, but they are of immense value in revising the locations of mis-positioned seamounts, in detecting seamounts or windows in unsurveyed areas, and for broad exploration of an area in terms of its reverberation background.

Such work at Hudson Laboratories has, for example, identified a number of acoustic windows in the Mid-Atlantic Ridge and these correspond to prominent fracture zones across the Ridge.

6.4.3. Bathymetric Data Required for Acoustical Applications

The 100-fathom contours of the present bathymetric charts are primarily adapted toward surface vessel navigation using standard echo-sounding apparatus. If the contours are regular and widely spaced, and supplemental information is available as to the physical nature of the bottom, e.g., smooth and sandy, or rocky and rough, such data can be used with some reliability to construct the bottom profiles and approximate reflectivities that are needed for the ray tracing. A special and optimum example would be the Hatteras Abyssal Plain, which is known to be not only flat but to possess a large specular, coherent reflectivity.[1]

Such regions, however, are either exceptional in long-range propagation or they occur at deep depths intermediate between highly contoured slopes and seamounts. For the latter, the contours of bathymetric charts drafted on the basis of a few track lines in the area cannot be considered to provide reliable estimates of the bottom features that will be effective as acoustical reflectors. It must be expected that a major number of applications of the ray tracing program as a predictive model will have no better bottom data than that available from the present bathymetric charts, but it must also be expected that with time, or as a result of special intensive experiments, more precise knowledge of many bottom regions will be accumulated. Such data should be not only bathymetric but geomorphic, including bottom composition and structure, properties of subbottom planes, and other data that can be utilized to refine the predictive model.

At present, it is strongly recommended that the bottom profiles that are generated for a program be drawn from inspection of the original collection sheets (Chapter VI-4.1). At the very least, such inspection will indicate the reliability that can be placed on the treatment of the bottom-reflected energy - it may also indicate regions with smooth slopes, or bearings that intersect smooth slopes which will be favorable as acoustic reflectors.

In using the present ray trace program at Hudson Laboratories the bottom profile is constructed by calculating and plotting the great circle path across the bathymetric chart, and recording the 100-fathom isobaths and positions of slope changes with an accuracy of at least 0.1 mile with respect to the source or receiver. As required, either as a matter of judgment or if additional data are available, entries on a finer scale may be added to represent changing slopes or curved features.

References for Chapter VI

1. Clay, C. S., J. Geophys. Res., 71, 2037 (1966).
2. Berman, A., J. Acoust. Soc. Am., 34, 298 (1962).
3. Weston, D., Proc. Phys. Soc., 78, 46 (1961).
4. Bathymetry, Basis of Inner Space. SP-98, U. S. Naval Oceanographic Office, Washington, D. C. (April 1967).
5. Heezen, B. C., personal communication.
6. Gilg, J. G., McConnell, J. J., "Non-Existent Seamounts, A Case Study," Informal Manuscript No. 66-28, U. S. Naval Oceanographic Office, Washington, D. C. (September 1960).
7. Backus, R. H. and Worthington, L. V., "On the Existence of the Seamount Known as 'American Scout'," Deep-Sea Res., 12, pp. 457-460 (1965).
8. Oceanographic Office Observers Manual, Sonic Soundings Pub. No. 606b, published by the U. S. Naval Oceanographic Office, Washington, D. C. (revised July 1963).

CHAPTER VII

PROGRAMMING

This chapter contains the source listings of 19 major programs in the ray trace data flow system. These are numbered in Fig. 59 in the order of their presentation. The programs have been grouped by general function into three sections: 1) data input programs, 2) ray trace and documentation programs, and 3) ray trace analysis programs. These listings should provide the reader with a greater insight into the technical programming aspects of the ray trace program.

The Hudson Laboratories number of each program (Fig. 59) designates by the second letter the language in which it is written: F for FORTRAN-II, F IV for FORTRAN-IV, G for GAP, and U for Klerer-May USER language. Most of the programs are written in USER language, which is self-documenting without supplementary flow charts. The USER reference manual, Table 7.1, is included in this chapter to give the reader the proper interpretation of statements used in the programs. It should be noted that superscripts that are red in the original source listings form new characters and are not to be interpreted as exponents; in this report these appear as black characters, and the reader must alert himself to distinguish the superscripts used as exponents from those added merely to form a new variable.

The following program source listings constitute the balance of this chapter.

DATA INPUT PROGRAMS

1. A-173-F1 Velocity Data Search Program.
2. A-177-F1 Velocity Profile Punch Program.
3. A-192-F1 Read FNWF Cards.
4. A-186-U1 Velocity Calculations by Wilson's Equation.
5. A-198-U1 Velocity Profile Data Selection Program.
6. A-147-U1 Velocity Profile Interpolation Program.
7. A-197-U1 Comparison of Velocity Profiles.

RAY TRACE AND DOCUMENTATION PROGRAMS

8. A-180-U1 Velocity and Bottom Data Input Program.
9. A-181-U1 Extrapolation and Interpolation of Velocity Profiles.

10. A-199-U1 Profile Plot Program.

11. A-182-U1 Ray Trace Program.

RAY TRACE ANALYSIS PROGRAMS

12. A-187-U1 Ray Depth Distribution Program - Pass 1.

13. A-183-U1 Ray Depth Distribution Program - Pass 3.

14. A-195-U1 Type III Intensity Program - Pass 1.

15. A-185-U1 Type III Intensity Calculation - Pass 3.

16. A-196-U1 Multiplot - Pass 1.

17. A-189-U1 Type II Intensity Calculation - Pass 1.

18. A-184-U1 Type II Intensity Calculation - Pass 3.

19. A-200-U1 Type II Intensity Plot - Pass 4.

RAY TRACE DATA FLOW

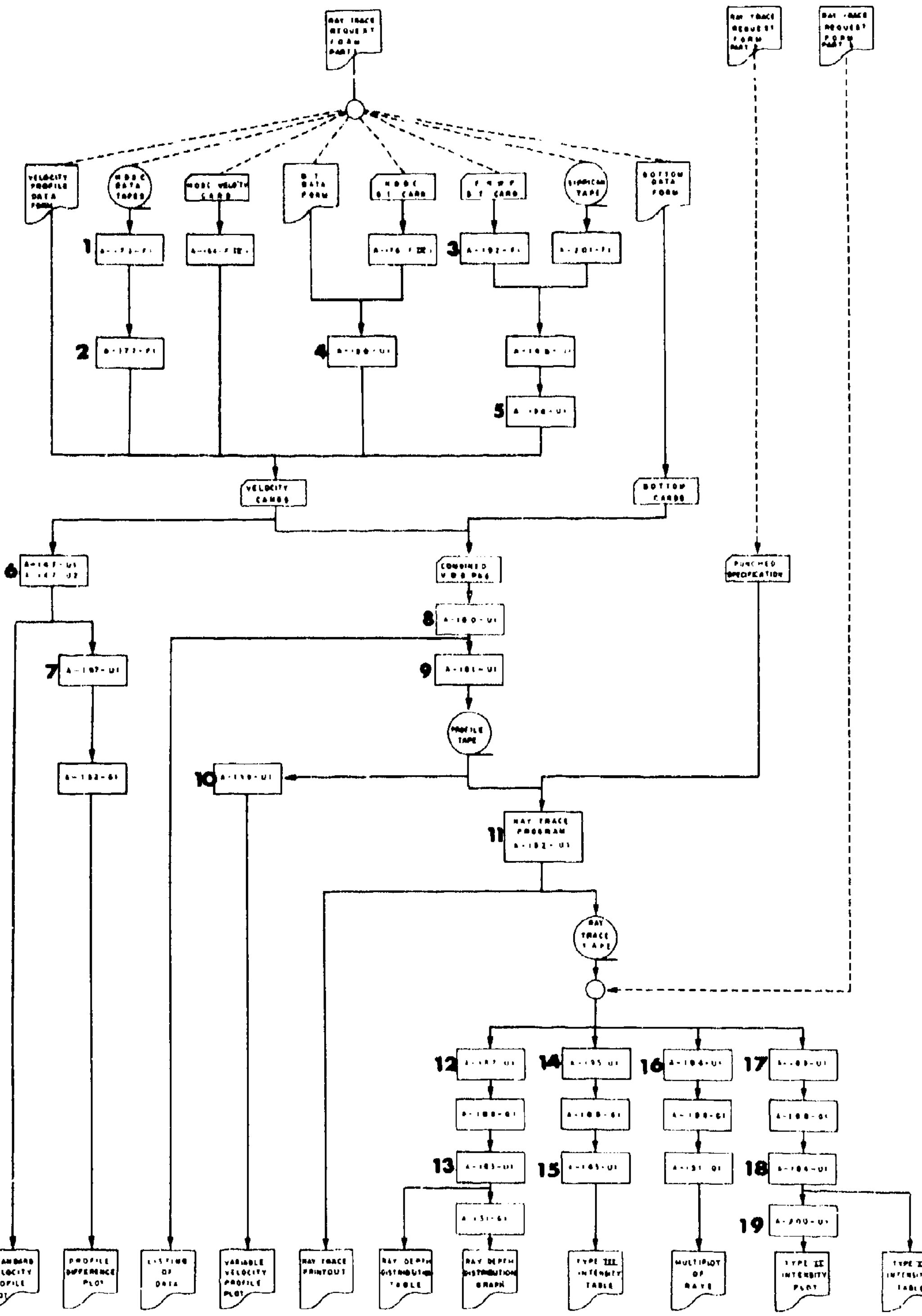

Fig. 59. Ray trace data flow diagram identifying program source listings in Chapter VII.

Vocabulary List

ABS	CARD	END	LN	READ	TANGENT
ABSOLUTE	CARDS	EOF	LOG	RETURN	TANH
AND	COMPUTE	EQUALS	LOOP	REWIND	TAPE
ARC	CONTINUE	EXP	MAXIMUM	ROUND	THE
ARCCOS	COS	FILE	MESSAGE	SEC	THEN
ARCCOSH	COSECANT	FINISH	MINUS	SECANT	TIMES
ARCCOT	COSH	FOR	OF	SECH	TO
ARCCOTH	COSINE	FORMAT	OR	SIN	TOP
ARCCSC	COT	FORMULA	OTHERWISE	SINE	TRUNCATE
ARCCSCH	COTANGENT	FRACTIONAL	PART	SINH	TYPE
ARCSEC	COTH	FROM	PAUSE	SLEW	UNTIL
ARCSECH	CSC	GO	PERFORM	SPECIAL	UPPER
ARCSIN	CSCH	HEADING	PLOT	SQRT	VARIABLE
ARCSINH	CYCLE	IF	PLUS	STATEMENT	VARIABLES
ARCTAN	DIMENSION	INFINITY	PRINT	STOP	WITHIN
ARCTANH	DIVIDED	LABEL	PROCEDURE	SUBROUTINE	WRITE
BY	DO	LINE	PROGRAM	SWITCH	
CALL	ELSE	LINES	PUNCH	TAN	

A period denotes the end of a statement or the end of an implied loop.

Corrections can be made by overtyping or by pressing the control key ERASE when positioned over the error.

Each program must be terminated by the statement END OF PROGRAM or FINISH.

More than one statement per typing line is acceptable.

To continue a statement beyond the maximum typing length for one line, press the carriage return as many times as desired.

Names of variables with more than one character should be defined by a SPECIAL VARIABLES statement before use.

A comma or the word AND may be used to separate computable statements.

FROM i = 1 TO 10 COMPUTE $A_i = B_i + C_{i+1}$, $C_i = A_{i+1}X$ AND $D = SIN\,\theta_i$.

Superscripts and subscripts must be in straight line form but forms such as $(A^a)^2$ are permissible.

Examples of Acceptable Forms

The letters E, F, G denote an arithmetic expression, e.g., F may denote the expression A + 2B + 1, otherwise a single variable is meant. Braces { } denote a choice of forms. Square Brackets [ ] denote those forms that are optional.

$$\sum_{i=E}^{F} \qquad \sum_{i,j=E}^{F}$$

Note: The horizontal extension of the lower limit equation and upper limit expression should not exceed the corresponding arms of the sum symbol. The operand of the sum should be outside the symbol.

$$A_1 \quad A_E \quad A_{1j} \quad A_{E,F} \qquad \prod_{1,j=E}^{F} \qquad \sqrt{E}$$

DIMENSION A = (N, M).

This indicates that A is an (N + 1) by (M + 1) array.

DIMENSION B = 40, Z = 30, Q = (10, 50).

SPECIAL VARIABLE(S) = DIMENSION

SPECIAL VARIABLES TEMPERATURE, HUMIDITY, PRESSURE, COUNT, LBJ = (14, 200), αy = 10.

UPPER is used in the same manner as DIMENSION and SPECIAL VARIABLES except that the indicated arrays are stored in upper memory.

UPPER C, WEIGHT = 56, K = (20, 30).

Subscripted variables need not be dimensioned when used in forms such as

(1) A_{ik} = $B_i Q_{ik}$ FOR k = 0(2)20 AND i = 1 TO 5

or

(2) MAXIMUM n = 10, J = 15

. . . .

A_{ik} = $B_i Q_{ik}$ FOR k = 4, 5, . . . , J WITHIN i = 0 BY 3 UNTIL n.

or

(3) $A = \sum_{i=1}^{40} B_i$, $P = \prod_{i,j=0}^{30} C_{ij}$

or

(4) READ TAPE C, 2, 2, 10.

FROM i = E [BY F] { TO / UNTIL } { [k / etc.] } G

FROM i = E TO G (Unit steps assumed)

FROM i = N BY 2.34 UNTIL A = B

FROM A = B + 5 BY 2 UNTIL Q = 20

FROM i = E TO INFINITY

FOR i = 1, 2, . . . , 5

FOR j = 5(10)55

FOR i = 0, .5, . . . , 7.5

Note: Any number of dots permissible but no extra spaces before terminating comma. The difference between the first two numbers specifies the increment in the first FOR form.

FROM or FOR forms can be used either to begin or end a statement.

C, A, = B, FROM i = 1 TO 10.

FROM i = 1 TO 10 COMPUTE A_i = B_i.

DO [TO / UNTIL] LOOP[ ] CYCLE[ ]

DO STATEMENT 5 FROM J = 1 TO 10.

This indicates that all statements up to but not including 5 will be executed. (No two LOOP statements should terminate at the same statement number. Otherwise, any number of LOOP procedures within or external to other LOOP procedures is permitted.)

FROM WITHIN AND

FOR ϕ = 0, 5, . . . , 90 WITHIN r = 1 TO 10 AND α = 1 TO 5 LOOP TO FORMULA 6.

The loop to be performed most often is the first one; the least often is the last.

READ = READ CARD READ CARDS

READ A, FROM i = 1 TO A_i = 15.

Card Format is free field; number of data points may vary from card to card and may be in either fixed or floating point form.

READ X.

READ A_i, B_{i+1} FROM i = E UNTIL A_i = 93.643.

Data may be punched into cards in the following forms:

2 −2 1.596 +3.213 −4.60 2.78E2 (2.78×10^2)

2.78E−2 (2.78×10^{-2}) 2.78E−3 (2.78×10^{-3})

Each datum should be separated by at least one blank space and the value should be within $\pm 10^{\pm 76}$ and not exceed nine significant digits.

Example

```
C=-1. D=15. E=3. F=4. G=2. M=1.
FROM n=1 UNTIL 4 COMPUTE B_n=5-n.
PERFORM H_r=r FOR r=1 UNTIL r=5.
```

$$A = \sum_{i=1}^{4}\left[i\,\frac{\sum_{j=1}^{n} iB_j \sum_{k=1}^{4} H_k}{C + \frac{D}{E + \frac{F}{G}}} + M \right].$$

```
PRINT A.
FINISH.
```

Three Alternate Formulations Of The Same Problem

```
MAXIMUM n=20.
READ n.
READ A_i, B_i FROM i=0 TO n.
```

$$x = \sum_{i=0}^{n}\left[A_i \prod_{j=1}^{n} B_j A_j\right].$$

```
PRINT x.   FINISH.
```

```
DIMENSION x=20, y=20.
α=0, READ w.
FORMULA 1.  READ x_α, y_α.
α=α+1, IF α≤w GO TO FORMULA 1.
S=α=0, STATEMENT 1. β=α, P=1.
STATEMENT 2, P=Px_β y_β, β=β+1.
IF β≤w THEN GO TO STATEMENT 2.
S=S+Px_α AND α=α+1.
IF α≥w GO TO STATEMENT 1.
PRINT S.   END OF PROGRAM.
```

```
MAXIMUM W=20.
READ W.  p=0.
FROM x=0 TO W READ u_x, v_x.
DO FORMULA 3 FROM x=0 TO W,
α=1,
FROM y=x TO W COMPUTE α=αu_y v_y.
p=p+u_x α.
FORMULA 3.  PRINT p.
END OF PROGRAM.
```

Table 7.1

PRINT X, 1A1,Y,1A.B1,Z. SIN θ, Y) FOR i 1, 2, ..., N.
PRINT E, F 1A.B1, X G1A).
PUNCH E F 1A.B1, X G1A).

A and B are integers between 0 and 9 but their sum may not exceed 9. E and Y will be printed (or card punched) with A places to the left of the decimal point and B places to the right. The value of G and i will be printed (or card punched) as an integer of A places. G will be stored in X. E, and Z, will be printed (or card punched) in floating point form.

PRINT Y E 1A.B.C1.

Same as above except that E is first divided by 10^C to change its range.

In the print statement a maximum of 8 expressions (including a blank between commas) are allowed. Each is centered in a 15 position field.

PRINT LABEL A, COUNT, X-Y, SIGMA (J).
PRINT LABEL LABEL HEADING PRINT HEADING

Each label, separated by commas, in a PRINT LABEL statement may be up to 15 characters in length and will be printed in a 15 position field. A maximum of 8 labels per statement is permitted and should contain only those characters used on the high-speed printer.

The PRINT FORMAT statement may be used when it is desired to mix literals and answers or to have more than 8 answers per line.

PRINT FORMAT n, E, F, X G.
FORMAT n LLL...L xxxx LLL...L x.xx y.

n is an integer of up to four places, LLL stands for any literals that are printable on the high-speed printer. Small x's are used to denote the actual position and number of digits of fixed point quantities while one small y is used for each floating point quantity. The first set of x's denotes the first expression equation variable mentioned in the PRINT FORMAT statement, the second set of x's denotes the second expression...etc. FORMAT statements may be located anywhere in a program.

PRINT FORMAT 12, θ_i, SIN θ_i, $\phi_i = \frac{180\theta_i}{\pi}$ FROM i 1 TO N.

FORMAT 12 ANGLE (RADIANS) y SIN THETA x.xxxx AND THE ANGLE IS xxx DEGREES.

If θ_i $3\pi/4$ then the following would be printed on the high speed printer:

"ANGLE (RADIANS) .23561945 1 SIN THETA .7071 AND THE ANGLE IS 135 DEGREES."

SLEW N (Printer paper spaced N lines)
SLEW [[TO]TOP] (Paper will advance to top of page)

Messages on the typewriter or printer are printed using the following forms:

TYPE NEGATIVE SQUARE ROOT.
PRINT MESSAGE (END OF PROGRAM) AND SLEW.

IF F G THEN GO TO STATEMENT 1.
IF F G GO TO STATEMENT 1.
IF F G THEN B C+E.
IF F G THEN READ... .
IF F G THEN CONTINUE.

IF F G THEN... [{ELSE / OTHERWISE} {E / GO TO / COMPUTE ...}]

Examples of multiple conditions:

IF r 5 OR G H OR SIN θ, β' THEN {COMPUTE... / READ n / C+D / GO TO FORMULA 3 / CONTINUE} OTHERWISE

IF P G AND H r 2 AND. .
IF U O OR (G r SIN θ AND H C_m)...
IF E F≥G THEN...

1) COMPUTE A B+2, (IF i j THEN (IF m n THEN T r SIN θ) OTHERWISE T r COS θ) and PRINT T, A.
2) COMPUTE A B+2, (IF i j THEN (IF m n THEN T r SIN θ OTHERWISE T r COS θ) and PRINT T, A.

In case 1 T = r sin θ if i = j *and* m = n
T = r cos θ when i ≠ j
T is not computed when i = j *and* m ≠ n.
In case 2 T = r sin θ when i = j *and* m = n
T = r cos θ when i = j *and* m ≠ n
T is not computed when i ≠ j.

GO GO[TO]
GO TO STATEMENT 20

PAUSE will cause the object program to go into a loop. Exit out of the loop will occur if console switch No. 0 is toggled.

Comments (non-computable statements) are entered between [ ] symbols.

FROM i 1 TO 10 READ X, [READ VALUES].
$Y_1 [i, j] = i + 12]$.

Use of the next forms eliminates the necessity of using "DO" or "LOOP" statements. Computable sub statements within an implied loop are separated by a comma or AND.

FOR i 1(1)50 AND k 0 BY 2 UNTIL Y 2000 READ $X_{i,k}$, COMPUTE Y $2X_{i,k}$ AND PRINT Y.

FROM i 1 TO INFINITY READ X_i, IF X_i ≠ 10 COMPUTE Y Y + X_i, n n + 2 OTHERWISE GO TO STATEMENT 1.

Superscripts that are *red* are used to form new characters rather than being interpreted as exponents. The following is a short program to determine the maximum absolute value of a set of positive numbers X

FROM i 1 TO 100 IF X_i X^{MAX} THEN X^{MAX} X_i. (red)

In the following magnetic tape commands L is the number of elements in the array V, T is the tape number and P is the controller (plug) number

READ TAPE V_0, T, P, L. The first L elements of the tape record is read into locations V_0 to V_{L-1}.
WRITE TAPE V_2, T, P, 5. (Locations V_2 - V_6 are written on tape)
REWIND T, P. RWD T, P.
WRITE END OF FILE T, P. EOF T, P.
IF END OF FILE P THEN... IF EOF P GO TO...

In the following example Y is the variable to be plotted, X is the "independent index" (i.e. Y = f(X)), A = the minimum value of Y and B = the maximum value of Y.

PLOT Y, X, A, B. PLOT Z_i, i, 0, 1 FROM i 1 TO 565π.

EXAMPLES

READ A_i, COMPUTE $Y = \frac{A_i}{A^{MAX}}$ AND PLOT Y, I, -1, 1 FROM I=1 UNTIL Y>1.

IF α>k COMPUTE $x = \sqrt{(\alpha-k)\Delta}$, $Y = B_{ij}x + C_0 T$ AND PRINT Y, α, T, k, OTHERWISE COMPUTE x=2αk, $Y = B_{ij}x + C_0 T\Delta$ AND PRINT Y, α, T, k FROM α=1 TO n WITHIN T=2 BY .01 UNTIL 3 AND FOR k=0(5)90.

FROM i=1 TO 10 AND j=1 TO 10 READ A_{ij}, COMPUTE $B_{ij} = A_{ij} + X_i + Y_j$ AND PRINT A_{ij}, B_{ij}, X_i, Y_j, i, j.

FOR r=1, 2, ..., 10 AND FOR θ=-π(.01)π COMPUTE $S_r = r\,SIN^2\theta$,

$C_r = \sqrt{r\,COS^{-1}\theta}$, $AM1_r = \sum_{\phi=1}^{30} TAN(.1\pi\phi\theta)$,

$V_r = \prod_{\phi=1}^{25} \frac{LOG_2\phi}{A + \frac{r}{\alpha + \frac{DEF}{G}}}$ AND PRINT r, θ, V_r, A.

IF (X≥Y AND Y>0) OR | 42−Y/ε | > $(X-Y)^2$ THEN COMPUTE $T_{XY} = Y(\epsilon - \frac{X}{Y})^2$ AND $W = (YT_{XY})^{YF}$ AND PRINT W, T_{XY}, X, Y FROM Y=2k+3 BY .01π UNTIL W>5800 AND FROM X=1 TO 100 OTHERWISE GO TO STATEMENT 2.

To define a procedure within a program:

... {SUBROUTINE / PROCEDURE} (Name). ....

.... RETURN ....

RETURN .... [END [(Name)] [SUBROUTINE / PROCEDURE]].

The name of a subroutine can be an alphanumeric string of any length but must begin with an alphabetic character and cannot be identical to any item in the vocabulary list. As many RETURN's as desired may be inserted to branch out of the subroutine back to the main program. The END statement is optional. A STOP or GO TO should precede subroutines.

To call a procedure:

... CALL (Name) [SUBROUTINE / PROCEDURE]

Relative Positions of Special Characters

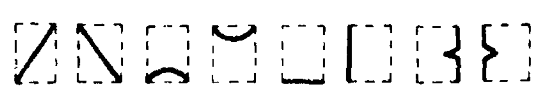

Suggested Reference Citation:
M. KLERER and J. MAY, REFERENCE MANUAL
Columbia University, Hudson Laboratories
Dobbs Ferry, New York
Revised Edition July, 1965

This work has been supported by the Office of Naval Research and the Advanced Research Projects Agency under Contract Nonr-266(84)

Table 7.1 (contd)

1) <u>A-173-F1 Velocity Data Search Program:</u>

Searches NODC master file tape for velocity data along ray path.

Sample printouts: Figs. 18, 23, and 24 in Chapter II.

```
      KOMMON MAR(2000)
      KOMMON T(305), MON(13),MAA(12)
      KOMMON DSAR(50),DSOR(50),DSAL(50),DSOL(50),DFAR(50),DFOR(50)
      KOMMON DFAL(50),DFOL(50)
      DIMENSION MA(21)
      KOMMON BDA(1),BMA(1),BSA(1),BDO(1),BMO(1),BSO(1),EDA(1),EMA(1),
     *ESA(1),EDO(1),EMO(1),ESO(1)
      G = 3.141592/180.
      M = 0
      SM=3443.956
      SH=3432.281
      C = SH/SM
74    READ 10,DIN,MA
30    K=1
      L=1
      N=1
75    READ 11, (BDA(I), BMA(I), BSA(I), BDO(I), BMO(I), BSO(I), I=1, K),
     *(EDA(J), EMA(J), ESA(J), EDO(J), EMO(J), ESO(J), J = 1, L)
      DO 60 I = 1, K
      M = 0
98    ID = BDA(I)
      IM = BMA(I)
      WS = BSA(I)
      JD = BDO(I)
      JM = BMO(I)
      XS = BSO(I)
      BMI = BMA(I)
      BSI = BSA(I)
      BMJ = BMO(I)
      BSJ = BSO(I)
      IF (BDA(I)) 31, 32, 32
31    BMI = -BMA(I)
      BSI = -BSA(I)
32    IF (BDO(I)) 33, 34, 34
33    BMJ = -BMO(I)
      BSJ = -BSO(I)
34    SA  = (BDA(I) + BMI/60. + BSI/3600.) * G
      SO  = (BDO(I) + BMJ/60. + BSJ/3600.) * G
61    DO 60 J = 1, L
      KD = EDA(J)
      KM = EMA(J)
      YS = ESA(J)
      LD = EDO(J)
      LM = EMO(J)
      ZS = ESO(J)
      EMI = EMA(J)
      ESI = ESA(J)
      EMJ = EMO(J)
      ESJ = ESO(J)
      IF (EDA(J)) 35, 36, 36
      ESI = -ESA(J)
35    EMI = -EMA(J)
36    IF (EDO(J)) 37, 38, 38
37    EMJ = -EMO(J)
      ESJ = -ESO(J)
```

```
   38  FA = (FDA(J) + FMI/60. + FSI/3600.) * G
       FO = (FDO(J) + FMJ/60. + FSJ/3600.) * G
  100  SAM = F  - SA
       AM = ABSF (SAM)
       IF (AM) 42, 39, 42
   39  IF (SA - FO) 42, 41, 42
  41   IF(IDUM)541,541,43
  541  IF (  - 25) 44, 43, 43
   43  PRINT  20, LA, SM, SB
       PRINT 23, MA
       M = 0
   44  PRINT 21, ID, IM, FS, JD, JM, XS, KD, KM, YS, LD, LM, ZS
       M = M +1
       ISU = ISU + 1
       GO TO 60
C
C  DISTANCE CALCULATION
C
   42  IF (ABSF(SA) -  89.95 * G) 108, 109, 109
  108  IF (ABSF(FA) - 89.95 * G ) 110, 109, 109
 110   CONTINUE
       DSA=SA/G
       DSO=SO/G
       DFA=FA/G
       DFO=FO/G
       TDSA=DSA
       TDSO=DSO
       TDFA=DFA
       TDFO=DFO
       CALL DR (DSA,DSO,DFA,DFO,SM,SB,DIST,CBR)
       CBS=CBR
       SD=DIST
       IF (ABSF(SA)   .05 * G ) 203, 203, 202
 202     CONTINUE
C
C  PRINT RESULTS OF DISTANCE AND BEARING CALCULATIONS
C
 54    IF (IDF) 58, 56, 73
   58  IF (  - 25) 40, 73, 73
 73    PRINT 20,SM,SB
       PRINT 23, MA
       M = 0
   40  PRINT 22, ID, IM, FS, JD, JM, XS, KD, KM, YS, LD, LM, ZS, SD, CBR
C
C  INCREMENT ALONG A GREAT CIRCLE
C
       IF (DIN) 311,311,308
 308   DIN=0
       DSA=SA/G
       DSO=SO/G
       DFA=FA/G
       DFO=FO/G
       PRINT 314
 309   CONTINUE
       PIN=PIN+DIO
```

```
              CALL DR (DSA,DSO,DFA,DFO,SM,SB,DIST,CBR)
              CALL INC (CBR,DSA,DSO,DIN,DXA,DXO,IXA,IXAM,XAS,IXO,IXOM,XOS)
C
C   PRINT ANSWERS TO INCREMENT CALCULATIONS
C
              DSA=DXA
              DSO=DXO
              IF(PIN-DIN)402,402,401
     401      PRINT 310,PIN2,IXA2,IXAM2,XAS2,IXO2,IXOM2,XOS2,CBR
     402      PIN2=PIN
              IXA2=IXA
              IXAM2=XABSF(IXAM)
              XAS2=ABSF(XAS)
              IXO2=IXO
              IXOM2=XABSF(IXOM)
              XOS2=ABSF(XOS)
              IF (IXA)321,319,321
     319      IXAM2=IXAM
     321      IF(IXO)322,323,322
     323      IXOM2=IXOM
     322      CONTINUE
              IF (DIST-DIN) 311,311,300
C
C   END OF INCREMENTING
C
     311      M = M + 1
        60    CONTINUE
              GO TO 99
     109      IF(DIN)509,509,201
       509 IF (M - 25) 200, 201, 201
       201 PRINT 20, SM, SB
              PRINT 23, MA
              M = 0
       200 PRINT 24, ID, IM, WS, JD, JM, XS, KD, KM, YS, LD, LM, ZS
              GO TO 60
     203      IF(DIN)503,503,205
       503 IF (M- 25) 204, 205, 205
       205 PRINT 20, SM, SB
              PRINT 23, MA
              M = 0
       204 PRINT 25, ID, IM, WS, JD, JM, XS, KD, KM, YS, LD, LM, ZS, SD
              GO TO 60
V 52A    SPB        TYPE,1
V        BCI        8,SOMETHING IS WRONG HERE
V        OCT        2000000
        99    CONTINUE
C   CBS=COURSE BEARING START
C   CBF=COURSE BEARING FINISH
C
C        SBR= START BEARING RIGHT
C        SBL= START BEARING LEFT
C        FBR= FINISH BEARING RIGHT
C        FBL= FINISH BEARING LEFT
C
C   CALCULATION OF CBF
```

```
      DSA=TDFA
      DSO=TDFO
      DFA=TDSA
      DFO=TDSO
      CALL DP (DSA,DSO,DFA,DFO,SM,SB,DIST,CBF)
      CBF=CBR
      DSA=TDSA
      DSO=TDSO
      DFA=TDFA
      DFO=TDFO
C
C  CALCULATION OF MARSDEN SQUARES ALONG THE RAY PATH
C
      DO 906 I=1,2000
  906 MAR(I)=0
      PRINT 1194,MA
      DIN =10.
  801 CALL DP (DSA,DSO,DFA,DFO,SM,SB,DIST,CBR)
      CALL INC (CBR,DSA,DSO,DIN,DXA,DXO,IXA,IXAM,XAS,IXO,IXOM,XOS)
      CALL MARQ (IXA,IXO)
      DSA=DXA
      DSO=DXO
       IF (DIST-DIN)901,901,801
  901 CONTINUE
C
C  CALCULATION OF STARTING AND ENDING POINTS
C
       DSA=TDSA
      DSO=TDSO
      DFA=TDFA
      DFO=TDFO
      READ 905,WID
      TOP=WID/15.
      JOP=TOP+1.
      TOP=JOP
C
      SBR=CBS+90.
      IF(SBR-360.)2,2,1
    1 SBR=SBR-360.
    2 SBL=CBS-90.
      IF(SBL)3,4,4
    3 SBL=SBL+360.
    4 FBR=CBF+90.
      IF(FBR-360.)6,6,5
    5 FBR=FBR-360.
    6 FBL=CBF-90.
      IF(FBL)7,8,8
    7 FBL=FBL+360.
    8 CONTINUE
C
      TSA=DSA
      TSO=DSO
      DO 812 I=1,JOP
      DSA=TSA
      DSO=TSO
```

```
809    FI=I
       DIN=12.*FI
811    CHR=SBR
       CALL INC (CBR,DSA,DSO,DIN,DXA,DXO,IXA,IXAM,XAS,IXO,IXOM,XOS)
       CALL MARO (IXA,IXO)
       DSAR(I)=DXA
       DSOR(I)=DXO
       CHR=SBL
       CALL INC (CBR,DSA,DSO,DIN,DXA,DXO,IXA,IXAM,XAS,IXO,IXOM,XOS)
       CALL MARO (IXA,IXO)
       DSAL(I)=DXA
       DSOL(I)=DXO
       DSA=DFA
       DSO=DFO
       CHR=FBR
       CALL INC (CBR,DSA,DSO,DIN,DXA,DXO,IXA,IXAM,XAS,IXO,IXOM,XOS)
       CALL MARO (IXA,IXO)
       DFAR(I)=DXA
       DFOR(I)=DXO
       CHR=FBL
       CALL INC (CBR,DSA,DSO,DIN,DXA,DXO,IXA,IXAM,XAS,IXO,IXOM,XOS)
       CALL MARO (IXA,IXO)
       DFAL(I)=DXA
       DFOL(I)=DXO
812    CONTINUE
C
C  CALCULATION OF MARSDEN SQUARES ALONG THE GREAT C ROLES
C
       DIN=10.
       DO 1003  I=1,JOP
       DSA=DSAR(I)
       DSO=DSOR(I)
       DFA=DFAL(I)
       DFO=DFOL(I)
1002   CALL DR (DSA,DSO,DFA,DFO,SM,SB,DIST,CBR)
       CALL INC (CBR,DSA,DSO,DIN,DXA,DXO,IXA,IXAM,XAS,IXO,IXOM,XOS)
       CALL MARO (IXA,IXO)
       DSA=DXA
       DSO=DXO
       IF (DIST-DIN)1001,1001,1002
1001   DSA=DSAL(I)
       DSO=DSOL(I)
       DFA=DFAR(I)
       DFO=DFOR(I)
1004   CALL DR (DSA,DSO,DFA,DFO,SM,SB,DIST,CBR)
       CALL INC (CBR,DSA,DSO,DIN,DXA,DXO,IXA,IXAM,XAS,IXO,IXOM,XOS)
       CALL MARO (IXA,IXO)
       DSA=DXA
       DSO=DXO
       IF (DIST-DIN)1003,1003,1004
1003   CONTINUE
       DO 1021 I=1,2000
       IF (MAR(I))1021,1022,1021
1021    PRINT 1024, MAR(I)
1024    FORMAT (I6)
```

```
      1022  CONTINUE
C
C     SEARCH NODC REFERENCE TAPE
C
            REWIND 7
            READ 1191,(MON(I),I=1,12),MAA
            READ 1192, MDO
            PRINT 1131,MDO,MAA,WID,MA
            MDO=MDO/100
            I=1
      1101  CALL REED (T,1,2,300,IFF)
      1102  DO 1110  J=1,301,5
            IF (J-301) 1103,1101,1101
      1103  FAR=MAR(I)
            IF (FAR-T(J)) 1104,1120,1110
      1104  I=I+1
            IF (MAR(I)) 1111,1111,1103
C     TEST FOR DEPTH
      1120  K=J+1
            ID=T(K)/10000.
            IF (ID-MDO) 1110,1105,1105
C     TEST FOR MONTH
      1105  D=ID
            M=(T(K)-D*10000.)/100.
            IF (MON(M)-1) 1110,1106,1110
      1106  L=K+1
            LL=L+1
            LLL=LL+1
C
C     CALCULATE DISTANCE TO PROFILE -PDIST
C
            DSA=TDSA
            DSO=TDSO
            DFA=T(L)
            DFO=T(LL)
            CALL DR (DSA,DSO,DFA,DFO,SM,SB,DIST,CBF)
            PDIST=DIST
C
C     CALCULATE DISTANCE FROM RAY PATH
            IF (CBR-CBS)1201,1201,1202
      1201  A=-1.
            GO TO 1203
      1202  A=1.
      1203  CONTINUE
      1108  CBR=CBS
            DIN=DIST
            CALL INC (CBR,DSA,DSO,DIN,DXA,DXO,IXA,IXAM,XAS,IXO,IXOM,XOS)
            DSA=DXA
            DSO=DXO
            CALL DR (DSA,DSO,DFA,DFO,SM,SB,DIST,CBF)
            IF (PDIST-DIST) 1501,1501,1502
      1501  DIST=PDIST
      1502  CONTINUE
      1109  IF(DIST-WID)1401,1401,1110
      1401  DIST=DIST*A
```

```
C     PREPARE TO PRINT
                 IT1=T(J)
                 ID=ID*100
                 ITK=T(K)
                 IY=ITK-(100*(ID+M))
                 ITL=T(L)
                 ATL=ITL
                 ATL=(T(L)-ATL)*60.
                 ATL=ABSF(ATL)
                 IL=T(LL)
                 AL=IL
                 AL=(T(LL)-AL)*60.
                 AL =ABSF(AL)
                 PRINT 1130,IT1,T(LLL),ID,M,IY,ITL,ATL,IL,AL,PDIST,DIST
                 PUNCH  1193,T(J),T(K),T(L),T(LL),T(LLL)
          1110   CONTINUE
          1111   CONTINUE
C PROGRAM TERMINATION
V        SPB       TYPE,1
V        BCI       5,END OF PROGRAM
V        OCT       2000000
                 CALL EXIT
C TYPEWRITER ROUTINE
V TYPE   INX       1,1
V        LDA       ,1
V        BMI       1,1
V        BNN
V        BRU       *-1
V        SAN       18
V        TYP
V        LDA       ,1
V        BNN
V        BRU       *-1
V        SAN       12
V        TYP
V        LDA       ,1
V        BNN
V        BRU       *-1
V        SAN       6
V        TYP
V        BRU       TYPE
            10   FORMAT ( F8.2, 7(3A3))
            11   FORMAT (F4.0, F3.0, F7.4, 1X, F4.0, F3.0, F7.4)
              13 FORMAT (7(3A3))
          20     FORMAT (1H1,28HVELOCITY DATA SEARCH PROGRAM,/10X, 35HGREAT CIRCLE
                *BEARINGS AND DISTANCES,17H - R.D. MININGHAM, 5X, 10H(A-173-F1) ,//
                *20X,51HCOMPUTED ON CLARK 1866 SPHEROID - DISTANCE IN N. M.,
                *// 20X, 15HMAJOR RADIUS = , F15.6,
                *1/H  MINOR RADIUS = , F15.6//)
            21   FORMAT (1H0, 4(4X, 2I4, F7.3),10X, 18HS A M E  P O I N T)
            22   FORMAT ( 1H0, 4(4X, 2I4, F7.3), 2F15.4)
             23  FORMAT (20X,7(3A3)//6X, 13HFROM LATITUDE, 8X, 9HLONGITUDE, 9X,
                *11HTO LATITUDE, 9X, 9HLONGITUDE,10X, 8HDISTANCE, 8X, 7HBEARING  )
            24   FORMAT ( 1H0, 4(4X, 2I4, F7.3),       6X, 9H* * * * *,6X, 9H* * *
                ** *)
```

```
   25 FORMAT ( 1H0, 4(4X, 2I4, F7.3),F15.4, 6X, 9H* * * * *)
  310 FORMAT (1X, F7.1, 2(2X, 2I4, F6.2),1X, F10.4)
  314 FORMAT(//2X,5HRANGE, 6X,8HLATITUDE,9X,9HLONGITUDE,4X10HBEARING TO/
     *43X,11HFINAL POINT)
  905 FORMAT (F10.5)
 1130 FORMAT (I8,F12.0,I9,3I5,F5.1,I5,F5.1,F12.2,F16.2)
 1131 FORMAT (1H1,56HVELOCITY DATA SEARCH PROGRAM - R.D. MIRINGHAM (A-17
     *3-F1),/23H   SPECIFICATIONS- MOO=,  I5,/19X,7HMONTHS=,4(3A3),/19X,
     *28HMAXIMUM RANGE FROM RAY PATH=,F6.1,//7(3A3),//1X,
     *              88HMARSDEN IDENTIFICATION DEPTH MONTH YEAR LATITUDE LO
     *NGITUDE  DISTANCE FROM  DISTANCE FROM/  1X,
     *86H  SQ                          METERS            DEG MIN   DEG MIN   ORI
     *GIN (NM)        RAY PATH//)
 1191 FORMAT (12I1,4(3A3))
 1192 FORMAT (I5)
 1193 FORMAT (2F10.0,2F10.4,F10.0)
 1194 FORMAT (17H1MARSDEN SQUARES ,7(3A3))
      END
```

2) A-177-F1 Velocity Profile Punch Program (3 pp.):

Punches velocity cards from NODC data tapes calling subroutine A-179-VF1 (1 p.). No sample printouts shown, but see flow chart in Chapter II, Fig. 22.

```
                DIMENSION IA(400),IDC(50,8),IOT(10),M10(50),MLA(50),MLO(50)
                DIMENSION IR(100)
C    SET UP PROGRAM
                MINY=134192
                MINN=199726
                MAX10=0
                MIN10=9999999
                MAX=0
                DO 13 I=1,400
        13      IA(I)=0
                DO 20 N=1,50
                READ 100,M10(N),MLA(N),MLO(N),(IDC(N,J),J=1,8)
                MAX=MAX+1
                IF (M10(N)-MINN)21,39,21
        21      IF (MIN10-M10(N))41,41,40
        40      MIN10=M10(N)
        41      IF (MAX10-M10(N))42,20,20
        42      MAX10=M10(N)
        20      CONTINUE
C
        39      DO 44  I=1,9999999
                CALL REED (IA,1,2,7,IOF)
                IF (IA(6)-MIN10)22,48,48
V 22A   LDZ
V       RCS
V       BPL
V       BRU        44A
                PRINT 102,IA(6),MIN10,MAX10
        44      CONTINUE
C
C   READ TAPE BACKWARDS
V 48A   CTN        2
V       BRU        *-1
V       SEL        2
V       RBD        1,IA,0
V       CTN        2
V       BRU        *-1
C
C    TEST 10 DEGREE SQ,
        6       CALL REED (IA,1,2,400,IOF)
        45      DO 3 I=1,361,40
                DO 3 N=1,MAX
        4       J=I+5
                IF (IA(J)-MAX10)46,46,47
        46      IF (M10(N)-IA(J))3,2,3
C   TEST 1 DEGREE SQUARES
        2       J=2+I
V       STX        ST2,2
V       LDX        J,2
V       LDA        IA,2
V       SLA        13
V       SRA        13
V       STA        M1
V       LDX        ST2,2
                IF (M1-MLA(N))3,5,3
```

```
      5     J=2*I+4
V        STX      ST2,2
V        LDX      J,2
V        LDA      IA,2
V        SLA      13
V        SRA      13
V        STA      M1
V        LDX      ST2,2
            IF (M1-MLO(N))3,9,3
C  TEST IDENTIFICATION NO.
      9     CONTINUE
            K=1
            DO 11 M=24,26
            L=I+M
            DO 11 J=1,3
            K=K+1
            CALL CHAR (IA(L),J,IDT(K))
     11     CONTINUE
            DO 30 J=2,8
            IF (IDC(N,J))31,30,31
     31     IF (IDT(J)-IDC(N,J))3,30,3
     30     CONTINUE
            L=0
            IND=I+27
            DO 50 J=I,IND
            DO 50 K=1,3
            L=L+1
            CALL CHAR (IA(J),K,IB(L))
     50     CONTINUE
C
            MIN=MINN
            IB(4)=MINN
            IF (IB(81)-1)60,61,60
     61     IB(4)=MINY
     60     IF (IB(82)-1)62,63,62
     63     MIN =MINY
     62     CONTINUE
V        LDA      IB+142
V        SLA      12
V        STA      IB+142
V        LDA      IB+16
V        SLA      12
V        STA      IB+16
V        LDA      IB+28
V        SLA      12
V        STA      IB+28
V        LDA      IB+62
V        SLA      12
V        STA      IB+62
C
            IF (IB(80)-3)52,51,3
     52     PRINT 103,IB(16),IB(17),IB(18),IB(6),IB(12),(IB(J),J=4,9),
           * MIN,(IB(J),J=10,15),IB(21),
           *IB(22),IB(19),IB(20),(IB(K),K=72,79)
            GO TO 3
```

```
C  READ NODC DATA TAPE RD MINI†CHAM (A-177-F1)
      51    IF ((IB(47)-6)53,53,3
      53    PRINT 104,((IB(J),J=28,32),((IB(J),J=47,50),IB(16),IB(17),IB(18),
           2 IB(6),IB(12),((IB(J),J=72,79)
V         LDZ
V         RCS
V         BMI
V         BRU       3A
            PUNCH 104,((IB(J),J=28,32),((IB(J),J=47,50),IB(16),IB(17),IB(18),
           2 IB(6),IB(12),((IB(J),J=72,79)
       3    CONTINUE
            GO TO 6
      47    REWIND 7
C
C  FORMATS
     100    FORMAT (4X,A3,2I1,32X,A1,7I1)
     102    FORMAT (3A10)
     103    FORMAT (1H1,59HNODC VELOCITY DATA TAPE PROGRAM - R.D. MININGHAM (A
           2-177-F1)//10HMARSDEN SQ, 2X, 8HLATITUDE, 2X, 9HLONGITUDE, 2X,
           32HMO,2X,2HYR,3X,14HIDENTIFICATION,/12X,3HDEG,1X,3HMIN,4X,3HDEG,
           41X,3HMIN,/3X,5I1,4X,A1,2I1,1X,2I1,1H,,A1,2X,A1,3I1,1X,2I1,1H,,A1,
           * 2X,2I1,
           52X,2I1,4X,A1,7I1//  5X,5HDEPTH,8X,8HVELOCITY,6X,10HMARSDEN SQ,
           6 10X,2HID)
     104    FORMAT (5X,4I1,1H,,A1,8X,1H1,3I1,1H,,I1,10X,5I1,9X,A1,/I1)
     107    FORMAT (A3)
V ST2  BSS      1
            END
```

```
                SUBROUTINE CHAR (I,J,K)
                IN=I
                N=J
V         STX     ST2,2
V         LDX     N,2
V         LDA     IN
V         SRD     12
V         BXL     2,2
V         BRU     1A
V         LDZ
V         SLD     6
V         BXL     3,2
V         BRU     1A
V         LDZ
V         SLD     6
V   1A    STA     IK
V         LDX     ST2,2
                K=IK
V  ST2    BSS     1
                RETURN
                END
```

A-179-VF!

3) A-192-F1 Read FNWF Cards:

Reads depth vs. temperature cards punched by the Fleet Numerical Weather Facility. These cards are then re-formated and written on tape for A-186-U1. No sample printouts shown.

```
C       READ FNWF CARDS (A-192-F4) R. D. MININGHAM
        DIMENSION ID(50),IT(50),ITD(50),A(3)
        REWIND 3
        READ 103,ITS,ITS2
        PRINT 103,ITS,ITS2
     21 PRINT 104
        A(1)=1.
        A(2)=1.
        A(3)=1.
        WRITE TAPE 3,A(1),A(2),A(3)
        DO 20 I=1,100
        IF (I-1) 11,11,12
  11    IL=0
        READ 100, (ID(J),IT(J),ITD(J),J=1,7)
        DO 9 J=1,7
        IF (ITS2-IT(J)) 6,22,6
   6    IF (ITS-IT(J)) 8,7,8
   7    IL=ITD(J)
        GO TO  9
   8    PRINT 101,IL,ID(J),IT(J),ITD(J)
        CALL CHAR (IL,1,I1)
        CALL CHAR (ID(J),1,I2)
        CALL CHAR (ID(J),2,I3)
        A(1)=(100*I1)+(10*I2)+I3
        CALL CHAR (IT(J),1,I1)
        CALL CHAR (IT(J),2,I2)
        CALL CHAR (ITD(J),1,I3)
        AI3=I3
        AI3=AI3/10.
        A(2)=(10*I1)+(I2)
        A(2)=A(2)+AI3
        A(3)=35.
        WRITE TAPE 3,A(1),A(2),A(3)
   9    CONTINUE
        GO TO 20
  12    READ 102, (ID(J),IT(J),ITD(J),J=1,13)
        DO 10 J=1,13
        IF (ITS2-IT(J))3,21,3
   3    IF(ITS-IT(J)) 5,4,5
   4    IL=ITD(J)
        GO TO 10
   5    PRINT 101,IL,ID(J),IT(J),ITD(J)
        CALL CHAR (IL,1,I1)
        CALL CHAR (ID(J),1,I2)
        CALL CHAR (ID(J),2,I3)
        A(1)=(100*I1)+(10*I2)+I3
        CALL CHAR (IT(J),1,I1)
        CALL CHAR (IT(J),2,I2)
        CALL CHAR (ITD(J),1,I3)
        AI3=I3
        AI3=AI3/10.
        A(2)=(10*I1)+(I2)
        A(2)=A(2)+AI3
        A(3)=35.
        WRITE TAPE 3,A(1),A(2),A(3)
  10    CONTINUE
```

```
   20     CONTINUE
          GO TO 21
       22 END FILE 3
          REWIND 3
C     FORMATS
      100 FORMAT (36X,7(A2,A2,A1,1X))
      101 FORMAT (6X,A1,A2,6X,A2,1H,,A1,8X,2H35)
  102     FORMAT(13(A2,A2,A1,1X))
  103     FORMAT(1X,2A2)
      104 FORMAT (8X,1H1,7X,1H1,8X,1H1)
          END
```

4) <u>A-186-U1 Velocity Calculations by Wilson's Equation:</u>
Reads depth vs. temperature and salinity data and computes velocity with Wilson's Equation. No sample printouts shown.

```
SPECIAL VARIABLES ΔVT,ΔVP,ΔVS,ΔVSTP.  SLEW TOP.

DIMENSION A=4,B=5.

STATEMENT 3. READ K,S,M^AR,I^D.  B3=M^AR.  B4=I^D.  SLEW TOP. PRINT S □ ,K □ .

PRINT MESSAGE VELOCITY CALCULATIONS BY WILSONS EQUATIONS - PROGRAMMER R D MININGHAM.
PRINT MESSAGE  ANALYSIS FILE NO (A-186-U2).  SLEW 2.
PRINT FORMAT 10,S.  FORMAT 10 PROFILE NUMBER xxxx. SLEW 2.

PRINT LABEL DEPTH(M),VELOCITY(M-S),TEMPERATURE(C),SALINITY(0-00),MARSDEN SQ,ID.

STATEMENT 1. READ TAPE A1,3,1,3.  P=A1. T=A2. S=A3.
IF EOF 1 THEN GO TO STATEMENT 2.
IF P=1 AND T=1 AND S=1 THEN PRINT P □ ,T □ ,M^AR □ ,I^D □  AND B1=1 AND B2=1 AND WRITE TAPE B1,4,1,4 AND GO TO STATEMENT 3.

IF K=1 THEN D=P(.3048006).
IF K=2 THEN D=P.
IF K=3 THEN D=P(1.8288333).

IF K=1 THEN T=(T-32)(5/9).    P=P/2.25.   P=(P(.0703))+1.0332.

ΔVT=4.6233T-5.4585(10^-2)T^2+2.822(10^-4)T^3-5.07(10^-7)T^4.

ΔVP=1.60518(10^-1)P+1.0279(10^-5)P^2+3.451(10^-9)P^3-3.503(10^-12)P^4.

ΔVS=1.391(S-35)-7.8(10^-2)(S-35)^2.

ΔVSTP=(S-35)(-1.197(10^-2)T+2.61(10^-4)P-1.96(10^-7)P^2-2.09(10^-6)PT)+
      P(-2.796(10^-4)T+1.3302(10^-5)T^2-6.644(10^-8)T^3)+P^2(-2.391(10^-7)T+
      9.286(10^-10)T^2)-1.745(10^-10)P^3T.

V=1449.22+ΔVT+ΔVP+ΔVS+ΔVSTP.

PRINT D(6.1),V(4.2),T(3.2),S(3.2),M^AR □ ,I^D □ . B1=0. B2=V.  WRITE TAPE B1,4,1,4.

GO TO STATEMENT 1.

STATEMENT 2. TYPE END OF PROGRAM. FINISH.
```

5) A-198-U1 Velocity Profile Data Selection Program:

Reduces to a minimum the number of points needed to define a velocity profile while meeting a specified curve fitting tolerance.

DIMENSION z=300, V=300, Z=300, D=300.

UPPER D=2000, V=2000.

RWD 4,1. READ L,T,P. K=0.

READ TAPE A_1,4,1,4.

STATEMENT 1. SLEW TOP. K=K+1. PRINT MESSAGE VELOCITY PROFILE DATA SELECTION PROGRAM (A-198-U1) R D MININGHAM.

PRINT FORMAT 1,L,K. FORMAT 1 PROFILE NUMBER xxxxx xxxxxx. SLEW 2. IF P=1 THEN PUNCH L 4, K 4.

PRINT LABEL DEPTH (M), VELOCITY (M/S), MARSDEN SQ, 10.

FROM j=1 TO INFINITY READ TAPE A_1,4,1,4 AND (IF EOF 1 THEN GO TO STATEMENT 99) AND (IF A_1=1 AND A_2=1 THEN GO TO STATEMENT 2) AND $D_j=A_1$ AND $V_j=A_2$ AND M=j.

STATEMENT 2.

I=10. C=0. i=0.

FROM j=1 TO M COMPUTE (IF D_j=C THEN i=i+1 AND $z_i=D_j$ AND $V_i=V_j$ AND C=C+I) AND (IF C=100 THEN I=25) AND (IF C=300 THEN I=50) AND (IF C= 1000 THEN I=100).

N=i. IF $D_M \neq z_N$ THEN N=N+1 AND $z_N=D_M$ AND $V_N=V_M$.

STATEMENT 5.

FROM i=1 TO N CALL SUBROUTINE ZD.

M^V=0. X=0.

FROM j=1 TO M COMPUTE $z_0=D_j$ AND CALL SUBROUTINE INT AND $D^V=|V_0-V_j|$ AND (IF D^V>T THEN (IF $D^V>M^V$ THEN $M^V=D^V$ AND $z^S=D_j$ AND $V^S=V_j$ AND X=1)).

IF X=0 THEN GO TO STATEMENT 6.

STATEMENT 3.

FROM i=1 TO N COMPUTE (IF $z^S \le z_i$ THEN (FROM l=N BY -1 TO l<i COMPUTE $z_{l+1}=z_l$ AND $V_{l+1}=V_l$ AND $Z_{l+1}=Z_l$ AND $D_{l+1}=D_l$) AND $z_i=z^S$ AND $V_i=V^S$ AND N=N+1 AND GO TO STATEMENT 5).

STATEMENT 6.

FROM i=1 TO N PRINT z_i 5.1, V_i 4.2, A_3 4, A_4 4 AND (IF P=1 THEN PUNCH z_i 5.1, V_i 4.2, A_3 4, A_4 4).

IF P=1 THEN PUNCH A_1 5.1, A_2 4.2, A_3 4, A_4 4. PRINT A_1 5.1, A_2 4.2, A_3 4, A_4 4.

GO TO STATEMENT 1. STATEMENT 99. TYPE END OF PROGRAM. STOP.

SUBROUTINE ZD.

X=0. IF i=1 THEN i=2 AND X=1.

IF i=N THEN $Z_N=Z_{N-1}+D_{N-1}(z_N-z_{N-1})$ AND $D_N=D_{N-1}$ AND RETURN.

$$Z_i = \frac{(V_{i+1}-V_i)(z_{i-1}-z_i)^2-(V_{i-1}-V_i)(z_{i+1}-z_i)^2}{-(z_{i+1}-z_i)(z_{i-1}-z_i)(z_{i+1}-z_{i-1})} .$$

$$D_i = 2\,\frac{(V_{i+1}-V_i)(z_{i-1}-z_i)-(V_{i-1}-V_i)(z_{i+1}-z_i)}{(z_{i+1}-z_i)(z_{i-1}-z_i)(z_{i+1}-z_{i-1})} .$$

IF X=1 THEN $Z_1=Z_i+D_i(z_1-z_2)$ AND $D_1=D_i$ AND i=1. RETURN.

SUBROUTINE INT.

FROM i=1 TO N COMPUTE IF $z_i > z_0$ THEN GO TO STATEMENT 100.

STATEMENT 100. IF $z_0=z_i$ THEN $V_0=V_i$ AND RETURN.

i=i-1.

$$V^1 = V_i+Z_i(z_0-z_i)+D_i\frac{(z_0-z_i)^2}{2} .$$

$$V^2 = V_{i+1}+Z_{i+1}(z_0-z_{i+1})+D_{i+1}\frac{(z_0-z_{i+1})^2}{2} .$$

$$V_0 = \frac{z_0-z_i}{z_{i+1}-z_i}\,V^2 + \frac{z_{i+1}-z_0}{z_{i+1}-z_i}\,V^1 .$$

6) A-147-U1 Velocity Profile Interpolation Program:
Plots velocity data cards in a standard format. Sample printout: Chapter I, Fig. 5.

```
OPEN Q=1 ??, V=1???, E=400, F=10.
TYPE (CHANGE PRINTER TO LINES TO INCH AND PUT TAPE ON 1,  TOGGLE 0). PAUSE.
READ 1,?.

Z=0.
READ L, M, N, P.
STATEMENT 5. IF Z≠0 WRITE TAPE E_1,1,2,365.
Q=0.
A=435, B=555, C=20.
READ X,Y AND IF X=0 GO TO STATEMENT 12.
Z=Z+1.
FROM n=1 TO INFINITY READ D_n, V_n, M^AR, I^D AND IF V_n=1 THEN GO TO STATEMENT 4.
STATEMENT 4.
K=n-1.
SLEW TOP.
PRINT MESSAGE (VELOCITY PROFILE INTERPOLATION PROGRAM (A-147-U1)).
SLEW 1.
PRINT FORMAT 32 , Z, X, Y, L, M, N. F_1=Z, F_2=X, F_3=Y, F_4=L, F_5=M, F_6=N, F_7=M^AR, F_8=I^D.  WRITE TAPE F_1,1,2,8.

SLEW 1.  PRINT FORMAT 33, M^AR, I^D.
SLEW 1.
FORMAT 32  PROFILE xxxx   DRN xxxx - xxxx    DATE xx-xx-xxxx  .
FORMAT 33  PROFILE IN MARSDEN SQUARE xxxxx   IDENTIFICATION NUMBER xxxxxxxxx  .
FROM n=1 TO V_(n+1)=1 (IF D_n>D_(n+1) THEN PRINT FORMAT 29, n+1, D_(n+1), V_(n+1) AND Q=1 AND SLEW 1),

(IF D_n=D_(n+1) THEN PRINT FORMAT 30, n+1, D_(n+1), V_(n+1) AND Q=1 AND SLEW 1),

(IF V_n<1400 OR V_n>1600 THEN PRINT FORMAT 31, n+1, D_(n+1), V_(n+1) AND Q=1 AND SLEW 1).

FORMAT 29 ERROR — DEPTH ORDER —— N=xxxx  D=xxxx.xx  V=xxxx.xx .
FORMAT 30 ERROR — SAME DEPTH —— N=xxxx  D=xxxx.xx  V=xxxx.xx .
FORMAT 31 ERROR -- VELOCITY LIMIT EXCEEDED — N=xxxx  D=xxxx.xx  V=xxxx.xx .
IF Q=1 GO TO  STATEMENT 5.
SLEW 2.
PRINT MESSAGE (DEPTH                                                    VELOCITY(-1000)).
SLEW 1.
PRINT MESSAGE ((METERS)                                                 (METER-SEC)).
IF P=1 THEN PUNCH D_1 (5.1), V_1 (4.2), M^AR (4), I^D (4).   FROM a=1 TO 365  COMPUTE E_a=1.  a=1. E_a=D_1. E_(a+1)=V_1.
SLEW 1.
V_1=V_1-1000.

PLOT V_1, D_1, A, B.

V_1=V_1+1000.

D_0=0.
n=1.
STATEMENT 10.
IF D_0>2000 THEN C=100.

D_0=D_0+C.

STATEMENT 3.
IF D_0=D_K THEN V_0=V_K AND GO TO STATEMENT 1.

IF D_0>D_K THEN GO TO STATEMENT 5.

IF D_0=D_n THEN  V_0=V_n AND GO TO STATEMENT 1.

IF D_0=D_(n+1) THEN  V_0=V_(n+1) AND GO TO STATEMENT 1.

IF D_0=D_(n+2) THEN  V_0=V_(n+2) AND GO TO STATEMENT 1.

IF D_0=D_(n+3) AND V_(n+3)≠1 THEN  V_0=V_(n+3) AND GO TO STATEMENT 1.

IF D_0<D_n  GO TO STATEMENT 10.

IF D_0>D_(n+3) AND V_(n+3)≠1  THEN n=n+1 AND GO TO STATEMENT 3.

IF D_n<D_0 AND D_0<D_(n+1)  AND D_(n+1)<D_(n+2) AND D_(n+2)<D_(n+3) AND V_(n+3)≠6 AND n=1 GO TO STATEMENT 2.

IF D_n<D_0 AND D_0<D_(n+1)  AND D_(n+1)<D_(n+2) AND D_(n+2)<D_(n+3) AND V_(n+3)≠1  AND n≠1  THEN  n=n-1 AND GO TO STATEMENT 3.

IF D_n<D_(n+1) AND  D_(n+1)<D_0 AND D_0<D_(n+2) AND D_(n+2)<D_(n+3) AND V_(n+3)≠1   GO TO STATEMENT 9.

n=n+1 AND IF D_n<D_(n+1) AND D_(n+1)<D_0 AND D_0<D_(n+2) AND D_(n+2)<D_(n+3) AND V_(n+3)≠1 THEN GO TO STATEMENT 9 ELSE n=n-1.

GO TO STATEMENT 6.

STATEMENT 1. IF P=1 THEN PUNCH D_0 (5.1), V_0 (4.2), M^AR (4), I^D (4). a=a+2. E_a=D_0. E_(a+1)=V_0. IF D_0>2000 AND V_0>1555 THEN A=530 AND B=650.  V_0=V_0-1000.  PLOT V_0,
 D_0, A, B.

GO TO STATEMENT 10.
```

STATEMENT 2.

1a) $$V^{P1} = \frac{(D_0-D_{n+1})(D_0-D_{n+2})}{(D_n-D_{n+1})(D_n-D_{n+2})} V_n + \frac{(D_0-D_n)(D_0-D_{n+2})}{(D_{n+1}-D_n)(D_{n+1}-D_{n+2})} V_{n+1} + \frac{(D_0-D_n)(D_0-D_{n+1})}{(D_{n+2}-D_n)(D_{n+2}-D_{n+1})} V_{n+2}.$$

2a) $$V^{P2} = \frac{(D_0-D_{n+1})(D_0-D_{n+3})}{(D_n-D_{n+1})(D_n-D_{n+3})} V_n + \frac{(D_0-D_n)(D_0-D_{n+3})}{(D_{n+1}-D_n)(D_{n+1}-D_{n+3})} V_{n+1} + \frac{(D_0-D_n)(D_0-D_{n+1})}{(D_{n+3}-D_n)(D_{n+3}-D_{n+1})} V_{n+3}.$$

3a) $$V^A = \frac{(V_{n+1}-V_n)(D_0-D_n)}{(D_{n+1}-D_n)} + V_n.$$

4a) $$V^B = \frac{(V_{n+2}-V_n)(D_0-D_n)}{(D_{n+2}-D_n)} + V_n.$$

5a) $$V^C = \frac{(V_{n+2}-V_{n+1})(D_0-D_{n+1})}{(D_{n+2}-D_{n+1})} + V_{n+1}.$$

IF $V^A = V^B$ AND $V^B = V^C$ THEN $V^R = V^A$ AND GO TO STATEMENT 100.

6a) $$V^R = .5\left(V^A + \frac{(V^A-V^B)^2 V^C + (V^A-V^C)^2 V^B}{(V^A-V^B)^2 + (V^A-V^C)^2}\right).$$

STATEMENT 100.

IF $V^R = V^{P1}$ AND $V^{P1} = V^{P2}$ THEN $V_0 = V^R$ AND GO TO STATEMENT 1.

7a) $$V_0 = \frac{|V^R-V^{P1}|\,V^{P2} + |V^R-V^{P2}|\,V^{P1}}{|V^R-V^{P1}| + |V^R-V^{P2}|}.$$

GO TO STATEMENT 1.

(1) $V^{P1} = $ [illegible]

(2) $V^{P2} = \frac{(D_0-D_{n+2})(D_0-D_{n+3})}{(D_{n+1}-D_{n+2})(D_{n+1}-D_{n+3})} V_{n+1} + \frac{(D_0-D_{n+1})(D_0-D_{n+3})}{(D_{n+2}-D_{n+1})(D_{n+2}-D_{n+3})} V_{n+2} + \frac{(D_0-D_{n+1})(D_0-D_{n+2})}{(D_{n+3}-D_{n+1})(D_{n+3}-D_{n+2})} V_{n+3}$.

(3) $V^A = \frac{(V_{n+1}-V_{n+2})(D_0-D_{n+1})}{(D_{n+1}-D_{n+2})} + V_{n+1}$.

(4) $V^B = \frac{(V_{n+1}-V_n)(D_0-D_{n+1})}{(D_{n+1}-D_n)} + V_{n+1}$.

(5) $V^C = \frac{(V_{n+3}-V_{n+2})(D_0-D_{n+2})}{(D_{n+3}-D_{n+2})} + V_{n+2}$.

IF $V^A=V^B$ AND $V^B=V^C$ THEN $V^R=V^A$ AND GO TO STATEMENT 101.

(6) $V^R = .5\ (V^A + \frac{(V^A-V^B)^2V^C + (V^A-V^C)^2V^B}{(V^A-V^B)^2 + (V^A-V^C)^2})$.

STATEMENT 101.

IF $V^R=V^{P1}$ AND $V^{P1}=V^{P2}$ THEN $V_0=V^R$ AND GO TO STATEMENT 1.

(7) $V_0 = \frac{|V^R-V^{P1}|\,V^{P2} + |V^R-V^{P2}|\,V^{P1}}{|V^R-V^{P1}| + |V^R-V^{P2}|}$.

GO TO STATEMENT 1.

STATEMENT 6.

(1a) $V^{P1} = \frac{(D_0-D_{n+2})(D_0-D_{n+1})}{(D_{n+3}-D_{n+2})(D_{n+3}-D_{n+1})} V_{n+3} + \frac{(D_0-D_{n+3})(D_0-D_{n+1})}{(D_{n+2}-D_{n+3})(D_{n+2}-D_{n+1})} V_{n+2} + \frac{(D_0-D_{n+3})(D_0-D_{n+2})}{(D_{n+1}-D_{n+3})(D_{n+1}-D_{n+2})} V_{n+1}$.

(2a) $V^{P2} = \frac{(D_0-D_{n+2})(D_0-D_n)}{(D_{n+3}-D_{n+2})(D_{n+3}-D_n)} V_{n+3} + \frac{(D_0-D_{n+3})(D_0-D_n)}{(D_{n+2}-D_{n+3})(D_{n+2}-D_n)} V_{n+2} + \frac{(D_0-D_{n+3})(D_0-D_{n+2})}{(D_n-D_{n+3})(D_n-D_{n+2})} V_n$.

(3a) $V^A = \frac{(V_{n+2}-V_{n+3})(D_0-D_{n+3})}{(D_{n+2}-D_{n+3})} + V_{n+3}$.

(4a) $V^B = \frac{(V_{n+1}-V_{n+3})(D_0-D_{n+3})}{(D_{n+1}-D_{n+3})} + V_{n+3}$.

(5a) $V^C = \frac{(V_{n+1}-V_{n+2})(D_0-D_{n+2})}{(D_{n+1}-D_{n+2})} + V_{n+2}$.

IF $V^A=V^B$ AND $V^B=V^C$ THEN $V^R=V^A$ AND GO TO STATEMENT 102.

(6a) $V^R = .5\ (V^A + \frac{(V^A-V^B)^2V^C + (V^A-V^C)^2V^B}{(V^A-V^B)^2 + (V^A-V^C)^2})$.

STATEMENT 102.
IF $V^R=V^{P1}$ AND $V^{P1}=V^{P2}$ THEN $V_0=V^R$ AND GO TO STATEMENT 1.

(7a) $V_0 = \frac{|V^R-V^{P1}|\,V^{P2} + |V^R-V^{P2}|\,V^{P1}}{|V^R-V^{P1}| + |V^R-V^{P2}|}$.

GO TO STATEMENT 1.

STATEMENT 12. TYPE (END OF PROGRAM). EOF 1,2. RWD 1,2. FINISH.

7) A-197-U1 Comparison of Velocity Profiles:

Calculates differences between velocity profiles with reference to one profile. A plot of the velocity differences of a set of profiles is shown in Chapter I, Fig. 6.

```
DIMENSION R=400,C=400,C'=10,D=200. RWD 1,2.  RWD 2,2.
READ N.  N=2N.  FROM i=1 TO N READ TAPE R0,1,2,365.  RWD 1,2.
FROM j=0 TO 365 COMPUTE (IF Rj=Rj+1 THEN M=j AND GO TO STATEMENT 1).
STATEMENT 1.  READ TAPE C'0,1,2,8.
IF EOF 2 THEN GO TO STATEMENT 2.  SLEW TOP.
PRINT MESSAGE COMPARSION OF VELOCITY PROFILES PROGRAM (A-197-U1).
SLEW 1.
PRINT  FORMAT  1,C'0,C'1,C'2.  FORMAT 1 PROFILE NUMBER xxxx DATA REDUCTION xxxxxxxx xxxxxxxx.
SLEW 2.  PRINT LABEL DEPTH,DIFFERENCE,REFERENCE,COMPARE.  SLEW 1.

FROM j=1 TO 181 COMPUTE Dj=0.
READ TAPE C0,1,2,365.  J=0.
FROM i=1 BY 2 TO M COMPUTE J=J+1 AND (IF Ci-1=Ci THEN GO TO STATEMENT 3) AND DJ=Ri-Ci AND (IF Ri-1≠Ci-1 THEN PRINT MESSAGE (ORDER ERROR) AND GO TO STATEMENT 1) AND
PRINT Ri-1 (5.1),DJ (3.2),Ri (4.3),Ci (4.3).  STATEMENT 3.  WRITE TAPE D1,2,2,181.  GO TO STATEMENT 1.
STATEMENT 2.  RWD 1,2.  EOF 2,2.  RWD 2,2.
SLEW TOP. PRINT MESSAGE MULTI-PLOT OF VELOCITY PROFILES  (A-197-U[illegible]). SLEW 1.
PRINT FORMAT  1,C'0,C'1,C'2. SLEW 2. FINISH.
```

8) A-180-U1 Velocity and Bottom Data Input Program:

Reads data input package, checks for errors, and writes data on tape. No sample printouts shown.

(A - 180 - U1)

UPPER A=50, R=1000, B=1000, D=500, V=500, C=2. DIMENSION R^R=5, F^R=5, α=5.

TYPE PUT SW 1 AND SW 2 DOWN.

TYPE PUT BLANK TAPE ON 2 2 THEN TOGGLE 0. PAUSE.

TYPE THANKS.
READ A_3, A_4, A_1, A_0, A_2. SLEW TOP. PRINT MESSAGE VELOCITY AND BOTTOM DATA INPUT PROGRAM (A-180-U1). SLEW 1.

RWD 2,2.

PRINT FORMAT 1, A_3, A_4, A_1, A_0, A_2. FORMAT 1 RAY TRACE NUMBER xxxxxxxx xxxxxxxx DATE xx xx xxxx.

IF A_1>12 OR A_0>31 THEN PRINT MESSAGE ERROR-- DATE.

READ A_9, A_{12}. IF A_9=1 THEN PRINT FORMAT 2, A_{12}. IF A_9=0 THEN PRINT FORMAT 3, A_{12}.

IF $A_9 \neq 0$ AND $A_9 \neq 1$ THEN Z=1 AND PRINT MESSAGE ERROR-- INDICATION OR EARTHS CURVATURE CORRECTION- 0=YES 1=NO.

N=0. Z=0.

FORMAT 2 EARTHS CURVATURE CORRECTION NOT USED -- BETA= xxxxx.x METERS.
FORMAT 3 EARTHS CURVATURE CORRECTION USED -- BETA=xxxxx.x METERS.

SLEW 2. PRINT MESSAGE (LIST OF BOTTOM POINTS). SLEW 1.

PRINT LABEL RANGE (NM), BOTTOM (FMS), DRN, BEARING.

READ R_0, B_0, D^{RS}, B^{RS}. PRINT R_0 5.4, B_0 5.4, D^{RS} 4, B^{RS} 5.4. $A_{10} = B_0$. IF $R_0 \neq 0$ THEN Z=1 AND PRINT MESSAGE ERROR-- FIRST RANGE NOT EQUAL TO ZERO.

FROM I=1 TO INFINITY READ R_I, B_I AND (IF R_I=0 GO TO STATEMENT 5) AND READ D^R, B^R AND

(IF $D^{RS} \neq D^R$ OR $B^{RS} \neq B^R$ THEN Z=1 AND PRINT MESSAGE (ERROR-- IDENTIFICATION FOR THE ABOVE BOTTOM POINT IS WRONG)) AND

PRINT R_I 5.4, B_I 5.4, D^R 4, B^R 5.4 AND,

(IF $R_I \leq R_{I-1}$ THEN Z=1 AND PRINT MESSAGE (ERROR-- RANGE OUT OF ORDER)) AND (IF 1.8288037B_I+100 >A_{10} THEN A_{10}=1.8288037B_I+100), AND

(IF B_I<0 OR B_I>6000 THEN Z=1 AND PRINT MESSAGE (ERROR-- DEPTH BEYOND PHYSICAL LIMITS)).

STATEMENT 5. $M^{BR}=R_{I-1}$. $R^P=R_I$. $B=B_I$. $R_I=R_{I-1}+1$. $B_I=B_{I-1}$. I=I+1. $A_{13}=1$. $A_{11}=0$. STATEMENT 25. WRITE TAPE A_0,2,2,14.

IF B≠1 THEN Z=1 AND PRINT MESSAGE ERROR-- FIRST PROFILE MUST BE DEEP.

I=I-1. FROM J=0 TO I COMPUTE $C_0=R_J$ AND $C_1=B_J$ AND WRITE TAPE C_0,2,2,2.

READ M^{AR}, I^{D}.

STATEMENT 7. N=N+1.

FROM K=1 TO 4 COMPUTE α_K=180. α_0=540.

SLEW TOP. PRINT MESSAGE VELOCITY AND BOTTOM DATA INPUT PROGRAM (A-180-U1). SLEW 1.

PRINT FORMAT 1,A_3,A_4,A_1,A_0,A_2. IF A_9=1 THEN PRINT FORMAT 2,A_{12}. IF A_9=0 THEN PRINT FORMAT 3,A_{12}.

IF $A_9 \neq 0$ AND $A_9 \neq 1$ THEN Z=1 AND PRINT MESSAGE ERROR-- INDICATION FOR EARTHS CURVATURE CORRECTION- 0=YES 1=NO.

IF B=1 THEN PRINT FORMAT 4,N,R^P. IF B=0 PRINT FORMAT 5,N,R.

IF B≠0 AND B≠1 THEN Z=1 AND PRINT MESSAGE ERROR-- INDICATION FOR TYPE OF PROFILE- 0=SHALLOW 1=DEEP.

SLEW 2.

```
FORMAT 4 PROFILE NUMBER xxxxx  RANGE xxxxx.xxNM   DEEP PROFILE.
FORMAT 5 PROFILE NUMBER xxxxx  RANGE xxxxx.xxNM   SHALLOW PROFILE.
```

PRINT LABEL DEPTH (M), VELOCITY (M-S),MARSDEN SQ,ID.

READ D_0,V_0,M^{AR},I^D. IF $D_0 \neq 0$ THEN Z=1 AND PRINT MESSAGE ERROR-- PROFILE DOES NOT START AT ZERO DEPTH.

PRINT D_0 (5.1) ,V_0 (4.2) ,M^{AR} (4) ,I^D (4) . IF $1400<V_0<1600$ CONTINUE OTHERWISE Z=1 AND PRINT MESSAGE ERROR-- VELOCITY BEYOND PHYSICAL LIMITS.

$R^R{}_4=D_0$. $F^R{}_4=V_0$.

I=0. DO STATEMENT 6 FROM J=5 BY 2 TO INFINITY. I=I+1.

READ D_I,V_I,M^{AR},I^D.

STATEMENT 51.

IF $D_I \leq D_{I-1}$ THEN GO TO STATEMENT 52.

$R^R{}_5=D_I$. $F^R{}_5=V_I$. IF $R^R{}_5=1$ AND I<3 THEN GO TO STATEMENT 52.

IF $R^R{}_5 \neq 1$ COMPUTE (FROM K=1 TO 4 COMPUTE $R^R{}_K=R^R{}_{K+1}$ AND $F^R{}_K=F^R{}_{K+1}$).

IF I=3 COMPUTE I^I=1 AND $R^R{}_0=R^R{}_2-1$ AND CALL SUBROUTINE FOUR AND CALL SUBROUTINE ALPHA1.

IF I<3 THEN GO TO STATEMENT 52.

IF $R^R{}_5=1$ COMPUTE $R^R{}_0=R^R{}_3+1$ AND CALL SUBROUTINE FOUR AND CALL SUBROUTINE ALPHA2 AND GO TO STATEMENT 52.

$R^R{}_0=R^R{}_2+1$. CALL SUBROUTINE FOUR. CALL SUBROUTINE ALPHA2.

$R^R{}_0=R^R{}_3-1$. CALL SUBROUTINE FOUR. CALL SUBROUTINE ALPHA1.

GO TO STATEMENT 52.

SUBROUTINE ALPHA1.

$A^X=R^R{}_0-R^R{}_3$. $A^Y=F^R{}_0-F^R{}_3$. IF I=3 AND I^I=1 COMPUTE $A^X=R^R{}_0-R^R{}_2$ AND $A^Y=F^R{}_0-F^R{}_2$ AND I^I=0. RETURN.

SUBROUTINE ALPHA2.

$B^X=R^R{}_0-R^R{}_2$. $B^Y=F^R{}_0-F^R{}_2$. IF $R^R{}_5=1$ COMPUTE $B^X=R^R{}_0-R^R{}_3$ AND $B^Y=F^R{}_0-F^R{}_3$. $A=(A^{X2}+A^{Y2})^{1/2}$. $B=(B^{X2}+B^{Y2})^{1/2}$.

$T=((A^XB^X+A^YB^Y)/(AB))$. IF $T<-1$ COMPUTE T=-1. α_3=ARCCOS T. $\alpha_3=(180/\pi)\alpha_3$.

$\alpha_0=\alpha_1+\alpha_2+\alpha_3$. $\alpha_1=\alpha_2$. $\alpha_2=\alpha_3$.

IF $D_I<1000$ THEN (IF $\alpha_0<440$ THEN GO TO STATEMENT 53 OTHERWISE RETURN).

IF $D_I<1500$ THEN (IF $\alpha_0<500$ THEN GO TO STATEMENT 53 OTHERWISE RETURN).

IF $D_I<2000$ THEN (IF $\alpha_0<530$ THEN GO TO STATEMENT 53 OTHERWISE RETURN).

IF $D_I\geq 2000$ THEN (IF $\alpha_0<537$ THEN GO TO STATEMENT 53 OTHERWISE RETURN).

STATEMENT 53. PRINT MESSAGE ERROR-- SHARP GRADIENT CAUSED BY ONE POINT.

Z=1.

RETURN.

SUBROUTINE FOUR.

$$F^R_0 = \sum_{I=1}^{4} \left(F^R_I \left(\prod_{J=1}^{I-1} \frac{(R^R_0 - R^R_J)}{(R^R_I - R^R_J)} \prod_{J=I+1}^{4} \frac{(R^R_0 - R^R_J)}{(R^R_I - R^R_J)} \right)\right). \text{ RETURN.}$$

STATEMENT 52. IF $V_I=1$ AND $D_I=1$ THEN SLEW 2. PRINT D_I (5.1), V_I (4.2), M^{AR} (3), I^D (3).

IF $V_I=1$ AND $D_I=1$ THEN GO TO STTEMENT 8.

IF $D_I<D_{I-1}$ THEN Z=1 AND PRINT MESSAGE ERROR-- DEPTH ORDER.

IF $D_I=D_{I-1}$ THEN Z=1 AND PRINT MESSAGE ERROR-- SAME DEPTH.

IF $M^{ARS}\neq M^{AR}$ THEN Z=1 AND PRINT MESSAGE ERROR-- MARSDEN SQUARE NOT CORRECT.

IF $I^{DS}\neq I^D$ THEN Z=1 AND PRINT MESSAGE ERROR-- IDENTIFICATION NOT CORRECT.

IF $V_I>1600$ THEN $Z\neq 1$ AND PRINT MESSAGE ERROR-- VELOCITY GREATER THAN 1600.

IF $V_I<1400$ THEN Z=1 AND PRINT MESSAGE ERROR-- VELOCITY LESS THAN 1400.

$B_J=D_I$. $B_{J+1}=V_I$.
STATEMENT 6.
STATEMENT 8.

IF I<3 THEN Z=1 AND PRINT MESSAGE ERROR-- 3 OR MORE ROFILE POINTS ARE NEEDED.

$M^{PR}=R^P$. $B_0=1$. $B_1=\beta$. $B_2=1852R^P$. $B_3=D_0$. $B_4=V_0$. K=21. STATEMENT 30. WRITE TAPE B_0,2,2,3. STATEMENT 31. WRITE TAPE B_3,2,2,K.

$R^S=R^P$. $B^{ET}=\beta$. READ R^P,β. IF $R^P=0$ GO TO STATEMENT 10 OTHERWISE READ M^{ARS}, I^{DS} AND
(IF $R^S>R^P$ THEN Z=1 AND PRINT MESSAGE (ERROR-- RANGE ORDER)) AND GO TO STATEMENT 7.

STATEMENT 10. IF $B^{ET}\neq 1$ THEN Z=1 AND PRINT MESSAGE ERROR-- LAST PROFILE MUST BE DEEP.

IF N=1 PRINT MESSAGE (ERROR-- PROGRAM NEEDS TWO PROFILES) AND Z=1.

$B_2=B_2+1852$. STATEMENT 41. WRITE TAPE B_0,2,2,3. STATEMENT 42. WRITE TAPE B_3,2,2,K.

SLEW TOP. IF Z=1 PRINT MESSAGE (THERE ARE ERRORS IN THE ABOVE DATA -- UNLESS THIS DATA IS FOR A THEORETICAL)AND
PRINT MESSAGE (MODEL IT SHOULD BE CORRECTED) AND TYPE (READ PRINTER--TOGGLE 0 TO CONTINUE) AND SLEW TOP AND PAUSE.

IF Z=0 PRINT MESSAGE(ALL DATA WITHIN PHYSICAL LIMITS - HOWEVER THE ABOVE PRINTOUT SHOULD NOT BE LEFT UNCHECKED).

IF $M^{PR}<M^{BR}$ THEN $M=M^{PR}$ OTHERWISE $M=M^{BR}$.

PRINT FORMAT 12,M. FORMAT 12 THE ABOVE DATA CAN NOT BE USED IN RAY TRACES EXCEEDING xxxxx.x NAUTICAL MILES.

SLEW TOP. EOF 2,2. RWD 2,2. FINISH.

9) <u>A-181-U1 Extrapolation and Interpolation of Velocity Profiles:</u> Extrapolates all profiles to a depth greater than the deepest bottom point. See Table 5.5.1.1, Chapter V.

{ R-181-U1 - PROGRAM EXTRAPOLATION AND INTERPOLATION OF VELOCITY PROFILES }

{INITIALIZATION OF PROGRAM}

$T^1=10^{-1}, T^2=T^{12}, T^4=T^{22}, T^5=T^4T^1, T^6=T^5T^1, T^7=T^6T^1, T^8=T^7T^1, T^9=T^8T^1, T^{10}=T^9T^1, T^{12}=T^{10}T^2$. $H^H=0$.

UPPER $z=375, z=375, z^1=375, V=375, V=375, V^1=375, Z=375, Z^1=375, D^D=375, D^{D'}=375$. DIMENSION A=400. REWIND 2,2.

REWIND 1,2. REWIND 3,1. READ TAPE A,2,2,14. FROM i=0 TO 8 COMPUTE $I_i=A_i$. $\epsilon=A_9$, $M^D=A_{10}$, $B=A_{12}$, $M=A_{13}$.

WRITE TAPE I,1,2,5. WRITE TAPE M,1,2,1. FROM i=0 TO M-1 READ TAPE A,2,2,2 AND WRITE TAPE A,1,2,2.

{ PREPARATION OF DEEP PROFILE TAPE}

{SEARCH FOR DEEP PROFILES}

STATEMENT 1. STATEMENT 2. READ TAPE A,2,2,3.

IF EOF 2 GO TO STATEMENT 50. $M=A_0, H=A_1, R=A_2, M^1=2M$.

READ TAPE A,2,2,M^1 AND IF H=0 GO TO STATEMENT 2. K=0.

FROM i=0 BY 2 UNTIL M^1-2 COMPUTE $z_K=A_i, V_K=A_{i+1}, K=K+1$. $P^{MDO}=z_{M-1}, V^{MDO}=V_{M-1}$. S=35.

{EXTRAPOLATION OF DEEP PROFILES - IF NECESSARY CALCULATION OF TEMPERATURE - }

{ EARTH CORRECTION FACTORS - 20 COEFFICIENTS OF FIT}

W=0. CALL SUBROUTINE WILSON. STATEMENT 3. W=1. FROM r=M UNTIL $z_{r-1}>M^D$ DO STATEMENT 300.

COMPUTE $z_r=P^{MDO}+100(r-M+1)$. CALL SUBROUTINE WILSON. STATEMENT 300.

G=P=r-1. IF $\epsilon=1$ GO TO STATEMENT 46. CALL SUBROUTINE CORRECTION. STATEMENT 46. $A_0=R, A_1=P+1, A_2=M, A_3=T^{MDO}$.

WRITE TAPE A,3,1,4. r=1. CALL SUBROUTINE ZD. $Z=Z+D(z_0-z_1)$. $A_0=z_0, A_1=V_0, A_2=Z, A_3=D$. WRITE TAPE A,3,1,4.

FROM r=1 TO P-1 DO STATEMENT 21. CALL SUBROUTINE ZD. $A_0=z_r, A_1=V_r, A_2=Z, A_3=D$. WRITE TAPE A,3,1,4.

STATEMENT 21. r=P. $Z=Z+D(z_r-z_{r-1})$. $A_0=z_r, A_1=V_r, A_2=Z$. WRITE TAPE A,3,1,4. GO TO STATEMENT 2.

{SHALLOW EXTRAPOLATION AND INTERPOLATION }

{SET UP TAPES}

STATEMENT 50. WRITE EOF 3,1 AND REWIND 3,1 AND REWIND 2,2 . $S^N=0$.

READ TAPE A,2,2,14. FROM i=0 TO $A_{13}-1$ READ TAPE A,2,2,2.

{ READ VELOCITY PROFILE T2P2 AND DEEP PROFILE T3P1 }

STATEMENT 6. READ TAPE A,2,2,3. IF EOF 2 GO TO STATEMENT 5 . $M=A_0$, $H=A_1$, $R=A_2$, $M^1=2M$.

IF H=1 READ TAPE A,2,2,M^1 AND GO TO STATEMENT 6. $S^N=1$. READ TAPE A,2,2,M^1. K=0.

FROM i=0 BY 2 UNTIL M^1-2 COMPUTE $z_K=A_i, V_K=A_{i+1}$, K=K+1. STATEMENT 8. READ TAPE A,3,1,4. $R=A_0, P=A_1, M=A_2, T^{MDO}=A_3$.

{ SEARCH FOR BRACKETING DEEP RANGES FOR SHALLOW RANGE - WRITE D-S TAPE T1P2 }

IF R>R GO TO STATEMENT 7. $R^T=R, P^T=P, M^T=M$. $T^{TMDO}=T^{MDO}$. $A_4=1$. WRITE TAPE A,1,2,5.

FROM i=0 TO P-1 READ TAPE A,3,1,4 AND COMPUTE $z_1=A_0$, $V_1=A_1$, $Z_1=A_2$, $D^D{}_1=A_3$ AND WRITE TAPE A,1,2,4.

GO TO STATEMENT 8.

{WRITE D-S TAPE FOR OBSERVED SHALLOW POINTS}

STATEMENT 7. $R^1=R, T^{1MDO}=T^{MDO}, P^1=P$, $M^1=M$. $R=R^T, T^{MDO}=T^{TMDO}, P=P^T, M=M^T$. STATEMENT 43. $A_0=R, A_1=0$,

$A_2=M, A_3=999999, A_4=0$. WRITE TAPE A,1,2,5. G=M-1. IF $\epsilon=1$ GO TO STATEMENT 61. CALL SUBROUTINE CORRECTION.

STATEMENT 61. r=1. CALL SUBROUTINE ZD. $Z=Z+D(z_0-z_1)$. $A_0=z_0, A_1=V_0, A_2=Z, A_3=D$. WRITE TAPE A,1,2,4. .

FROM r=1 TO M-2 LOOP STATEMENT 31. CALL SUBROUTINE ZD. $A_0=z_r, A_1=V_r, A_2=Z, A_3=D$. WRITE TAPE A,1,2,4.

STATEMENT 31. $z_0=z_{M-2}, V_0=V_{M-2}, z_1=z_{M-1}, V_1=V_{M-1}$.

IF $H^H=9$ THEN $H^H=0$ AND GO TO STATEMENT 47.

{PREPARE FOR VERTICAL INTERPOLATION}

FROM I=0 TO P^1-1 READ TAPE A,3,1,4 AND COMPUTE $z^1_i=A_0$, $V^1_i=A_1$, $Z^1_i=A_2$, $D^{D1}_i=A_3$. STATEMENT 47.
IF $P>P^1$ THEN U=P OTHERWISE $U=P^1$. FROM K=0 TO U IF $z_K>z_{M-1}$ THEN J=K AND GO TO STATEMENT 41. STATEMENT 41.
COMPUTE $r=z_{M-1}, \rho=z_J, \rho^1=z_{J-1}, t=V_J, t^1=V_{J-1}, S=Z_J, S^1=Z_{J-1}, T=D^D_J, T^1=D^D_{J-1}$. CALL SUBROUTINE INTERPOLATION. $F=n^1$.
FROM K=0 TO U IF $z^1_K>z_{M-1}$ THEN k=K AND GO TO STATEMENT 9. STATEMENT 9. COMPUTE $r=z_{M-1}, \rho=z^1_k, \rho^1=z^1_{k-1}, t=V^1_k,$
$t^1=V^1_{k-1}, S=Z^1_k, S^1=Z^1_{k-1}, T=D^{D1}_k, T^1=D^{D1}_{k-1}$. CALL SUBROUTINE INTERPOLATION. $G=n^1$. STATEMENT 10.
IF $z^1_k=z_J$ THEN J=J+1. IF J>P-1 THEN $J=1, r=z_{J-1}, n=V_{J-1}, n^1=V^1_k$ AND GO TO STATEMENT 51.
IF $z^1_k>z_J$ THEN GO TO STATEMENT 11 . COMPUTE J=2, $r=z^1_k$, $\rho=z_J$, $n=V^1_k$, $\rho^1=z_{J-1}$, $t=V_J$, $t^1=V_{J-1}$, $S=Z_J$,
$S^1=Z_{J-1}$, $T=D^D_J$, $T^1=D^D_{J-1}$. GO TO STATEMENT 12. STATEMENT 11. COMPUTE J=1, $r=z_J$, $n=V_J$, $\rho=z^1_k$, $\rho^1=z^1_{k-1}$,
$t=V^1_k$, $t^1=V^1_{k-1}$, $S=Z^1_k$, $S^1=Z^1_{k-1}$, $T=D^{D1}_k$, $T^1=D^{D1}_{k-1}$. STATEMENT 12.
CALL SUBROUTINE INTERPOLATION. STATEMENT 51.

{PREPARE FOR RANGE INTERPOLATION}

IF J=1 THEN $V^{D1}=n$, $V^{D2}=n^1$ OTHERWISE $V^{D1}=n^1$ AND $V^{D2}=n$. CALL SUBROUTINE RANGEINT.

{FIND SHALLOW COEFFICIENTS FOR EXTRAPOLATED POINTS}

IF J=1 THEN J=J+1 OTHERWISE k=k+1. $z_2=r, V_2=V^{SP}$. r=1. CALL SUBROUTINE ZD. $A_0=z_1, A_1=V_1, A_2=Z, A_3=D$.
WRITE TAPE A,1,2,4. $z_0=z_1, V_0=V_1, z_1=z_2, V_1=V_2$. IF J>P-1 OR $k>P^1-1$ THEN GO TO STATEMENT 13. GO TO STATEMENT 10.
STATEMENT 13. $A_0=r, A_1=V^{SP}, A_2=Z+D(z_2-z_1), A_3=D$. WRITE TAPE A,1,2,4. $A_0=A_1=A_2=A_3=999999$. WRITE TAPE A,1,2,4.
STATEMENT 42. READ TAPE A,2,2,3. IF EOF 2 GO TO STATEMENT 5. $M=A_0, H=A_1, R=A_2, M^1=2M$. READ TAPE A,2,2,$M^1$.
IF H=1 GO TO STATEMENT 42. K=0. FROM I=0 BY 2 UNTIL M^1-2 COMPUTE $z_K=A_I, V_K=A_{I+1}$, K=K+1.

{WRITES SHALLOW EXTRAPOLATED RECORDS ONTO D-S TAPE}

IF $R<R^1$ THEN $H^H=9$ AND GO TO STATEMENT 43. $A_0=R^1, A_1=P^1, A_2=M^1, A_3=T^{1MOD}, A_4=1$ AND WRITE APE A,1,2,5.
FROM I=0 TO P^1-1 COMPUTE $A_0=z^1_i$, $A_1=V^1_i$, $A_2=Z^1_i$, $A_3=D^{D1}_i$ AND WRITE TAPE A,1,2,4.
$P^T=P^1, T^{TMOD}=T^{1MOD}, M^T=M^1, R^T=R^1$. FROM I=0 TO P^1-1 COMPUTE $z_i=z^1_i$, $V_i=V^1_i$, $Z_i=Z^1_i$, $D^D_i=D^{D1}_i$.
GO TO STATEMENT 8.

{END OF PROGRAM}

{WRITES ALL DEEP RECORDS, FROM DEEP TAPE, FOLLOWING LAST SHALLOW RECORD ONTO D-S TAPE}

STATEMENT 5. IF $S^N \neq 0$ GO TO STATEMENT 48. STATEMENT 49. READ TAPE A,3,1,4.
IF EOF 1 GO TO STATEMENT 60. STATEMENT 37. $A_4=1, P=A_1$. WRITE TAPE A,1,2,5. FROM I=0 TO P-1 READ TAPE A,
3,1,4 AND WRITE TAPE A,1,2,4. GO TO STATEMENT 49. STATEMENT 48.
$A_0=R^1, A_1=P^1, A_2=M^1, A_3=T^{1MOD}, A_4=1$. WRITE TAPE A,1,2,5. FROM I=0 TO P^1-1 COMPUTE $A_0=z^1_i, A_1=V^1_i,$
$A_2=Z^1_i, A_3=D^{D1}_i$ AND WRITE TAPE A,1,2,4. READ TAPE A,3,1,4.
IF EOF 1 GO TO STATEMENT 60 OTHERWISE GO TO STATEMENT 37. STATEMENT 60. WRITE EOF 1,2.
REWIND 2,2. REWIND 1,2. REWIND 3,1. STOP.

{SUBROUTINES}

{ SUBROUTINE CORRECTION}

SUBROUTINE CORRECTION. FROM r=0 TO G COMPUTE $V_r = V_r(1 + \frac{z_r}{6.37(10)^6})$. RETURN .

{SUBROUTINE ZD}

SUBROUTINE ZD. COMPUTE $Z = \frac{(V_{r+1}-V_r)(z_{r-1}-z_r)^2-(V_{r-1}-V_r)(z_{r+1}-z_r)^2}{-(z_{r+1}-z_r)(z_{r-1}-z_r)(z_{r+1}-z_{r-1})}$,

$$D = \frac{2((V_{r+1}-V_r)(z_{r-1}-z_r)-(V_{r-1}-V_r)(z_{r+1}-z_r))}{(z_{r+1}-z_r)(z_{r-1}-z_r)(z_{r+1}-z_{r-1})}$$. RETURN.

{SUBROUTINE WILSONS EQUATIONS TO FIND VELOCITY FROM TEMPERATURE OR

TEMPERATURE FROM VELOCITY }

SUBROUTINE WILSON. IF W=0 THEN T=10 AND $D=P^{MDO}$ OTHERWISE $D=z_r$ AND $T=T^{MDO}$. STATEMENT 100. IF D>200 GO TO STATEMENT 101. $\alpha=-3.54428T^{12}$, $\beta=9.961477T^{4}$, D=-D, $P^{SI}=((-\beta+(\beta^2-4\alpha D)^{.5})/(2\alpha))/689.47$. GO TO STATEMENT 102. STATEMENT 101. $\alpha=-2.62085T^{12}$, $\beta=9.94765T^{4}$, $\eta=2.40443T^{1}$, D=-D, $P^{SI}=((-\beta+(\beta^2-4\alpha(\eta+D))^{.5})/(2\alpha))/689.47$. STATEMENT 102. D=-D. $P=.0703P^{SI}+1.0332$. $\Delta^{VT}=4.6233T-5.4585T^{2}T^{2}+2.822T^{4}T^{3}-5.07T^{7}T^{4}$. $\Delta^{VP}=1.60518T^{1}P+1.0279T^{5}P^{2}+3.451T^{9}P^{3}-3.503T^{12}P^{4}$. $\Delta^{VS}=1.391(S-35)-7.8T^{2}(S-35)^{2}$. $\Delta^{VSTP}=(S-35)(-1.197T^{2}T+2.61T^{4}P-1.96T^{7}P^{2}-2.09T^{6}PT)+P(-2.796T^{4}+1.3302T^{5}T^{2}-6.644T^{8}T^{3})+P^{2}(-2.391T^{7}T+9.286T^{10}T^{2})-1.744T^{10}P^{3}T$. $V^{T}=1449.22+\Delta^{VT}+\Delta^{VP}+\Delta^{VS}+\Delta^{VSTP}$.

IF W=1 THEN $V_r=V^{T}$ AND RETURN . IF $|V^{1}-V^{MDO}|<.0001$ THEN $T^{MDO}=T$ AND GO TO STATEMENT 103. $\Delta^{V}=V^{MDO}-V^{T}$, $\Delta^{T}=\Delta^{V}/4$, $T=T+\Delta^{T}$ AND GO TO STATEMENT 100. STATEMENT 103. RETURN.

{SUBROUTINE INTERPOLATION}

SUBROUTINE INTERPOLATION. $K=t^{1}+S^{1}(r-\rho^{1})+T^{1}(r-\rho^{1})^{2}/2$. $L=t+S(r-\rho)+T(r-\rho)^{2}/2$.

$$n^{1} = \frac{(r-\rho^{1})L}{(\rho-\rho^{1})} + \frac{(\rho-r)K}{(\rho-\rho^{1})}$$. RETURN.

{SUBROUTINE RANGEINT}

SUBROUTINE RANGEINT. IF $r<z_{M-1}$ OR $B<z_{M-1}$ THEN TYPE (RANGE INTERPOLATION VALUES INCORRECT) AND STOP.

IF $r \leq B$ THEN $V^{SP}=V^{D1}+\frac{(R-R)(V^{D2}-V^{D1})}{(R^{1}-R)}-\frac{(B-r)(R-R)(G-F)}{(B-z_{M-1})(R^{1}-R)}+\frac{(B-r)(V_{M-1}-F)}{(B-z_{M-1})}$ OTHERWISE

$V^{SP}=V^{D1}+\frac{(R-R)(V^{D2}-V^{D1})}{(R^{1}-R)}$. RETURN.

10) A-199-U1 Profile Plot Program:

Plots velocity profiles used by Ray Trace Program. Sample printout: Fig. 39 in Chapter V.

DIMENSION A=750, I=10. UPPER z=750, V=750, Z=750, D=750. REWIND 2,2. READ TAPE I_1,2,2,5.

READ TAPE B,2,2,1. FROM 1=1 TO 3 READ TAPE A,2,2,2. READ B, $\Delta^1, \Delta^2, M^1, M^2, P^1, P^2, P^3, P^4$.

STATEMENT 20. SLEW TOP. PRINT FORMAT 10, I_1, I_2, I_3, I_4, I_5.

SLEW 2. STATEMENT 1. READ TAPE A,2,2,5. IF EOF 2 THEN GO TO STATEMENT 9. $R=A_0/1852, P=A_1-1, V=A_2-1, T^{MDO}=A_3, H=A_4$. IF H=0 THEN PRINT FORMAT 20,R OTHERWISE

PRINT FORMAT 30,R,T^{MDO}. SLEW 2. IF H=1 GO TO STATEMENT 2. 1=0. STATEMENT 3. READ TAPE A,2,2,4. IF EOF 2 THEN TYPE (TAPE READ ERROR) AND STOP.

IF A_0=999999 GO TO STATEMENT 5. $z_1=A_0, V_1=A_1, Z_1=A_2, D_1=A_3$, 1=1+1. GO TO STATEMENT 3. STATEMENT 5. P=1-1. GO TO STATEMENT 7. STATEMENT 2.

FROM 1=0 TO P READ TAPE A,2,2,4 AND (IF EOF 2 TYPE (TAPE ERROR) AND STOP) AND COMPUTE $z_i=A_0, V_i=A_1, Z_i=A_2, D_1=A_3$. STATEMENT 7.

PRINT MESSAGE TABLE OF VALUES OF OBSERVED POINTS. SLEW 1.

LABEL DEPTH-METERS, VELOCITY-M/SEC, COEFFICIENT Z, COEFFICIENT D. SLEW 1. FROM 1=0 TO M PRINT z_1 {5.3}, V_1 {4.1}, Z_1, D_1. SLEW 2.

PRINT MESSAGE TABLE OF VALUES OF EXTRAPOLATED POINTS. SLEW 1. LABEL DEPTH-METERS, VELOCITY-M/SEC, Z COEFFICIENT, D COEFFICIENT. SLEW 1.

FROM 1=M+1 TO P PRINT z_1 {5.3}, V_1 {4.4}, Z_1, D_1. SLEW TOP. IF H=0 PRINT FORMAT 20,R OTHERWISE PRINT FORMAT 30,R,T^{MDO}. SLEW 2.

PRINT MESSAGE VELOCITY VS DEPTH . SLEW 1. $P^I=P^1, P^A=P^2$, A=0, $M^{AX}=M^1, \Delta=\Delta^1$. O=B. STATEMENT 68. FROM t=0 BY Δ UNTIL M^{AX} DO STATEMENT 70.

FROM 1=A TO INFINITY (IF 1>P TYPE (MAX DEPTH EXCEEDED)), IF $z_1 \le t \le z_{1+1}$ THEN $V^S=V_i+Z_1(t-z_1)+D_1(t-z_1)^2/2$, $V^{S1}=V_{1+1}+Z_{1+1}(t-z_{1+1})+D_{1+1}(t-z_{1+1})^2/2$,

$V^{SS}= V^{S1}\dfrac{t-z_1}{z_{1+1}-z_1} + \dfrac{z_{1+1}-t}{z_{1+1}-z_1} V^S$, (IF $V^{SS}>P^A$ THEN $P^I=P^3, P^A=P^4$), PLOT V^{SS}, t, P^I, P^A AND A=1 AND GO TO STATEMENT 69. STATEMENT 69. STATEMENT 70.

IF $M^1=M^2$ GO TO STATEMENT 20. IF $M^{AX}=M^1$ THEN $M^{AX}=M^2$, $O=M^1+\Delta^2$, $\Delta=\Delta^2$ AND GO TO STATEMENT 68. GO TO STATEMENT 20. STATEMENT 9. REWIND 2,2. STOP.

FORMAT 10 DATE xx xx xxxx ID NUMBER xxxxx SET xx.

FORMAT 20 SHALLOW PROFILE AT RANGE xxxxx.xxx MILES.

FORMAT 30 DEEP PROFILE AT RANGE xxxxx.xxx MILES TEMP AT OBSERVED MAXIMUM DEPTH= xx.xxx DEG CENTIGRADE. FINISH.

11) A-182-U1 Ray Trace Program:

Traces rays through velocity field. Sample printout: Chapter I, Fig. 9.

```
{INPUT PROCEDURES - SET UP FOR CORRECT PROFILE AND DEPTH}

{ INITIAL RANGE NM, FINAL RANGE NM, INITIAL DEPTH M, MAX ITERATION, MIN ITERATION, EPSILON, MAX SINL CHANGE, }
{ MAX SURFACE HITS, MAX BOTTOM HITS, MAX GRAZING ANGLE, PRINTOUT INCREMENT, SURFACE DELTA }

DIMENSION F=4 .  UPPER z=375,V=375,Z=375,D=375,z=375,V=375,Z=375,D=375,X=375,Y=375.

STATEMENT 100.
Q=0.  E^OF=0.

 READ K,E,I,Δ^M,F_3,ε,S^S,F,F,H,S,Δ.

S=1852S,E=1852E,K=1852K.

 STATEMENT 10.
IF E^OF=1 THEN WRITE EOF 2,2 AND E^OF=0. REWIND 1,2. SLEW TOP. READ TAPE A,1,2,5. G=K. D^1=Q=w=t=α=H=N=R=M=0.
READ θ.  IF θ= 999 GO TO STATEMENT 100.  PRINT FORMAT 1,A_1,A_0,A_2,A_3,A_4.  SLEW 2.
PRINT FORMAT 2,I,θ,ε,Δ^M,F_3,S^S. S^IN=SIN (πθ/180),r=K,y=I,Δ=Δ^M. SLEW 2. PRINT FORMAT 4.

 { READS BOTTOM  PROFILE OFF TAPE - STORE IN RANGE X, DEPTH Y }

READ TAPE A,1,2,1. M=A_0. FROM i=0 TO M-1 READ TAPE A,1,2,2 AND COMPUTE X_i=1852A_0,Y_i=1.82880366A_1.
FROM i=0 TO X_{i+1}>K COMPUTE i=i.  t=((Y_{i+1}-Y_i)/(X_{i+1}-X_i)) (K-X_i) +Y_i.  IF I>t THEN y=t.  t=0.


 {THE 2 BRACKETING PROFILES ARE SELECTED AND STORED IN R,z,V,Z,D AND R,z,V,Z,D}

 STATEMENT 3.
Q=0.  READ TAPE A,1,2,5. R=A_0,T=A_3.

 STATEMENT 9.
{IF Q=1 SEARCH ONLY FOR THE RIGHT BRACKETING PROFILE AND STORE IN R,z,V,Z,D}
IF R>r GO TO STATEMENT 4.  IF Q≠1 GO TO STATEMENT 1.
FROM i=0 TO G-1 COMPUTE z_i=z_i,V_i=V_i,Z_i=Z_i,D_i=D_i. P=G,R=R AND GO TO STATEMENT 3. STATEMENT 1. R=R.

IF T=999999 THEN (FROM i=0 TO INFINITY READ TAPE A,1,2,4 AND (IF A_0=999999 THEN P=i AND
GO TO STATEMENT 3) AND COMPUTE z_i=A_0,V_i=A_1,Z_i=A_2,D_i=A_3)  OTHERWISE P=A_1 AND (FROM i=0 TO P-1 READ TAPE A,1,2,4 AND
COMPUTE z_i=A_0,V_i=A_1,Z_i=A_2,D_i=A_3) AND GO TO STATEMENT 3.

 STATEMENT 4.
IF Q=1 GO TO STATEMENT 5.

IF T=999999 THEN (FROM i=0 TO INFINITY READ TAPE A,1,2,4 AND
(IF A_0=999999 THEN G=i AND GO TO STATEMENT 5) AND COMPUTE z_i=A_0,V_i=A_1,Z_i=A_2,D_i=A_3) OTHERWISE G=A_1 AND
(FROM i=0 TO G-1 READ TAPE A,1,2,4 AND COMPUTE z_i=A_0,V_i=A_1,Z_i=A_2,D_i=A_3).
```

{A NEW BOTTOM POINT IS SELECTED}

STATEMENT 5.

FROM $i=0$ TO INFINITY IF $y \le z_{i+1}$ GO TO STATEMENT 6. STATEMENT 6.

FROM $j=0$ TO INFINITY IF $y \le z_{j+1}$ GO TO STATEMENT 7. STATEMENT 7. IF $Q \ne 0$ GO TO STATEMENT 11.

FROM $k=M$ TO $M-1$ IF $r < X_{k+1}$ THEN GO TO STATEMENT 8. STATEMENT 8. $M=k$.

STATEMENT 11. $L=0$.

{INTERPOLATION – WITH GIVEN r,y – BRACKETING PROFILES}

{THE POINT IS FOUND WITH COEFFICIENTS – STORED IN r,y,V^R,Z^R,D^R,G^R}

$I=V_i, K=Z_i, L=z_i, N=D_i$. $S^U=1$. GO TO STATEMENT 25. STATEMENT 21.

$V^K=V^T, Z^K=Z^T, I=V_{i+1}, L=z_{i+1}, K=Z_{i+1}, N=D_{i+1}$. $S^U=2$. GO TO STATEMENT 25. STATEMENT 22.

$V^{K1}=V^T, Z^{K1}=Z^T, J=z_i, U=D_i$. $S^V=1$. GO TO STATEMENT 27. STATEMENT 28. $V^J=V^T, Z^J=Z^T, D^J=D^T$.

$I=V_j, K=Z_j, L=z_j, N=D_j$. $S^U=3$. GO TO STATEMENT 25. STATEMENT 23. $V^K=V^T, Z^K=Z^T$. $I=V_{j+1}$.

$K=Z_{j+1}, L=z_{j+1}, N=D_{j+1}$. $S^U=4$. GO TO STATEMENT 25. STATEMENT 24. $V^{K1}=V^T, Z^{K1}=Z^T$.

$J=z_j, U=D_j$. $S^V=2$. GO TO STATEMENT 27.

STATEMENT 29.

$V^{J1}=V^T, Z^{J1}=Z^T, D^{J1}=D^T$. $R^1=(R-r)/(R-R), R^2=(r-R)/(R-R)$.

IF $Q \ne 0$ THEN $V^Q=R^1V^J+R^2V^{J1}$ AND (IF $Q=1$ GO TO STATEMENT 30 OTHERWISE GO TO STATEMENT 32).

$V^R=R^1V^J+R^2V^{J1}, Z^R=R^1Z^J+R^2Z^{J1}, D^R=R^1D^J+R^2D^{J1}, G^R=(V^{J1}-V^J)/(R-R)$. IF $r=K$ THEN $C=\cos(\pi\theta/180)/V^R$.

$C^{OS}=V^RC$. IF $|S^{IN}|>.01$ THEN $S^{IN}=\left(\left(|1-C^{OS2}|\right)/S^{IN}+S^{IN}\right)/2$.

IF $\alpha=2$ THEN $S^{IN}=\mu C^{OS}-\omega S^{IN}$, $C=\omega C+\mu S^{IN1}/V^R$, $\alpha=0$, $C^{OS}=V^RC$. $T^{AN}=S^{IN}/C^{OS}$.

$S^T=|C^2V^R(Z^R-G^RT^{AN})\Delta+C^2(Z^{R2}S^{IN}+Z^RG^RC^{OS}+V^RD^RS^{IN})\Delta^2/2+C^2(3Z^RD^RS^{IN2}-CZ^RC^{OS}(Z^{R2}+V^RD^R))\Delta^3/6|$.

IF $S^T>S^S$ THEN $\Delta=(S^S/S^T)^{.5}\Delta$. $S^T=|C^2Z^RD^R\Delta^3|$. IF $S^T>S^S$ THEN $\Delta=((S^S/S^T)^{.5})\Delta$. GO TO STATEMENT 26

STATEMENT 25.

$V^T=I+K(y-L)+N(L-y)^2/2, Z^T=K+N(y-L)$. IF $S^U=1$ GO TO STATEMENT 21. IF $S^U=2$ GO TO STATEMENT 22.

IF $S^U=3$ GO TO STATEMENT 23. IF $S^U=4$ GO TO STATEMENT 24.

STATEMENT 27.

$S=y-J, T=L-J, W=S/T, Y=L-y, U=Y/T, V^T=WV^{K1}+UV^K, Z^T=WZ^{K1}+UZ^K+(V^{K1}-V^K)/T$, $D^T=2(Z^{K1}-Z^K)/T+WN+UU$.

IF $S^V=1$ GO TO STATEMENT 28. IF $S^V=2$ GO TO STATEMENT 29.

STATEMENT 26.

{THE PAST POINT IS DEFINED - IN THIS CASE INITIALIZATION - r, y, V^R, Z^R, D^R, G^R}

IF $r=K$ THEN $V^R=V^R, Z^R=Z^R, D^R=D^R, G^R=G^R, y=y, r=r, C=C, S^{IN}=S^{IN}$.

{TESTING FOR Δ CHANGE BECAUSE OF NEW VELOCITY FIELD}

IF $\Delta \leq (R-r)/C^{OS}$ THEN $F_1 = \Delta$ AND CALL SUBROUTINE VQ, $R^M=r$, $y^M=y$, $y=y+\delta^Z$, $r=r+\delta^R$, $Q=1$ AND GO TO STATEMENT 5.
GO TO STATEMENT 31.

STATEMENT 30.

$r=R^M, y=y^M, Q=0$. IF $|V^\Delta - V^Q| < \epsilon$ GO TO STATEMENT 40. $\Delta = \epsilon\Delta / |V^\Delta - V^Q|$. IF $\Delta < F_3$ THEN $\Delta = F_3$.
GO TO STATEMENT 40.

STATEMENT 31.

$\Delta^R = (R-r)/C^{OS}$, $F_1 = \Delta^R$. CALL SUBROUTINE VQ .
$Q=2$, $R^M=r$, $y^M=y$, $y=y+\delta^Z$, $r=r+\delta^R$. GO TO STATEMENT 5.

STATEMENT 32.

$Q=0, r=R^M, y=y^M$. IF $|V^\Delta - V^Q| < \epsilon$ THEN $\Delta = \Delta^R$ OTHERWISE $\Delta = \epsilon\Delta^R / |V^\Delta - V^Q|$ AND (IF $\Delta < F_3$ THEN $\Delta = F_3$), GO TO STATEMENT 40.
FROM $v=0$ TO $G-1$ COMPUTE $z_v=z_v, V_v=V_v, Z_v=Z_v, D_v=D_v$. $R=R, P=G$. READ TAPE A,1,2,5. $R=A_0$.
IF $A_3=999999$ THEN (FROM $v=0$ TO INFINITY READ TAPE A,1,2,4 AND (IF $A_0=999999$ THEN $G=v$ AND GO TO STATEMENT 40),
$z_v=A_0, V_v=A_1, Z_v=A_2, D_v=A_3$) OTHERWISE $G=A_1$ AND (FROM $v=0$ TO $G-1$ READ TAPE A,1,2,4 AND
COMPUTE $z_v=A_0, V_v=A_1, Z_v=A_2, D_v=A_3$).

STATEMENT 40.

IF $|V^Q q| > 1$ THEN $\Delta = F_3$.

{TESTING FOR SURFACE HITS}

IF $y > \Delta |S^{IN}| + \Delta$ THEN GO TO STATEMENT 50. IF $y > 0$ GO TO STATEMENT 41.
$\alpha=1$. $Z^X = Z^R - yD^R/2$. IF $|Z^X| < .0001$ THEN $\Delta = -y/(S^{IN})$ OTHERWISE

$$\Delta = \frac{S^{IN} + \sqrt{|S^{IN2} + 2yC^2V^RZ^X|}}{C^2V^RZ^X}$$. $Z^R=Z^R, V^R=V^R, D^R=D^R, G^R=G^R, y=y, r=r, S^{IN}=S^{IN}, C=C, C^{OS}=V^RC, T^{AN}=S^{IN}/C^{OS}$.

CALL SUBROUTINE ITRAT. $y^1=0$. GO TO STATEMENT 60.

STATEMENT 41.

$Z^X = Z^R - yD^R/2$. IF $S^{IN2} + 2yC^2V^RZ^X \leq 0$ GO TO STATEMENT 60. IF $|Z^X| < .0001$ THEN $n = -y/(S^{IN})$ OTHERWISE

$$n = \frac{S^{IN} + \sqrt{|S^{IN2} + 2yC^2V^RZ^X|}}{C^2V^RZ^X}$$. IF $n \leq 0$ OR $n > \Delta$ GO TO STATEMENT 60.

$\Delta = n$. $\alpha=1$. CALL SUBROUTINE ITRAT. $y^1=0$. GO TO STATEMENT 60.

{TESTING FOR BOTTOM HITS}

STATEMENT 50.

FROM $k=M$ TO $M-1$ (IF $r<X_{k+1}$ THEN GO TO STATEMENT 51). STATEMENT 51.

IF $r+\Delta C^{OS}+CZ^{R}S^{IN}\Delta^{2}/2\leq X_{k+1}$ THEN GO TO STATEMENT 52. $\Delta=(X_{k+1}-r)/C^{OS}$, $M=M+1$. STATEMENT 52.

IF $y\leq Y_{k}-\Delta$ AND $y\leq Y_{k+1}-\Delta$ GO TO STATEMENT 60.

$$\beta=\frac{Y_{k+1}-Y_{k}}{X_{k+1}-X_{k}},\quad \sigma=(\beta C^{OS}-S^{IN})^{2}-2C^{2}V^{R}Z^{R}(Y_{k}-y+\beta(r-X_{k})).$$

IF $\sigma\leq 0$ GO TO STATEMENT 60. IF $|Z^{R}|<.0001$ THEN (IF $Y_{k}-y+\beta(r-X_{k})<0$ THEN GO TO STATEMENT 60 OTHERWISE

$$n=\frac{Y_{k}-y+\beta(r-X_{k})}{S^{IN}-\beta C^{OS}}\text{) OTHERWISE }\quad n=\frac{S^{IN}-\beta C^{OS}-\sigma^{.5}}{C^{2}V^{R}Z^{R}}.$$

IF $n\leq 0$ GO TO STATEMENT 60. IF $n>\Delta$ GO TO STATEMENT 60. $\Delta=n$. $\alpha=2$. CALL SUBROUTINE ITRAT.
$\sigma=2\beta/(1-\beta^{2})$, $\omega=1/(1+\sigma^{2})^{.5}$, $\mu=\sigma\omega$. GO TO STATEMENT 60.

{PROCEDURES FOR EXIT OR RETURN}

STATEMENT 60.

IF L = 0 THEN CALL SUBROUTINE ITRAT. L=0. CALL SUBROUTINE PRINT. CALL SUBROUTINE TIME.
Q=1. $t=t+\theta$. $y=y^{1}$, $r=r^{1}$, $C=C^{1}$, $C=C^{T}$, $r=r^{T}$, $V^{R}=V^{R}$, $Z^{R}=Z^{R}$, $D^{R}=D^{R}$, $G^{R}=G^{R}$, $S^{IN}=S^{IN1}$, $S^{IN}=S^{INT}$, $\Delta=\Delta^{M}$, $y=y^{T}$.

IF $r>E$ PRINT MESSAGE (MAX RANGE), $E^{OF}=1$ AND GO TO STATEMENT 10 .

IF $\alpha=1$ THEN $H=H+1$ AND $S^{IN}=-S^{IN}$, $r=r^{1}$, $y=y^{1}$, $C=C^{1}$, $S^{IN}=S^{IN}$. IF $H>F$ THEN PRINT MESSAGE (MAX SURFACE HITS), $E^{OF}=1$ AND GO TO STATEMENT 10 . IF $\alpha=2$ THEN $N=N+1$ AND GO TO STATEMENT 9.

IF $N>F$ THEN PRINT MESSAGE (MAX BOTTOM HITS), $E^{OF}=1$ AND GO TO STATEMENT 10 .
$\alpha=0$. GO TO STATEMENT 9.

{ITRAT SUBROUTINE}

SUBROUTINE ITRAT.

STATEMENT 90.

L=1. $C^{1}=C-C^{2}G^{R}(1+T^{AN2})\Delta+C^{3}G^{R}Z^{R}T^{AN}(1+T^{AN2})\Delta^{2}$,

$r^{1}=r+C^{OS}\Delta+C(Z^{R}S^{IN}-G^{R}S^{IN}T^{AN})\Delta^{2}/2+C(D^{R}S^{IN2}-C^{2}V^{R}Z^{R}(Z^{R}-G^{R}T^{AN}))\Delta^{3}/6-C^{3}Z^{R}(4V^{R}D^{R}S^{IN}+Z^{R}G^{R}C^{OS}+Z^{R2}S^{IN})\Delta^{4}/24$.

$y^{1}=y+S^{IN}\Delta-C^{2}V^{R}(Z^{R}-G^{R}T^{AN})\Delta^{2}/2-C^{2}(Z^{R2}S^{IN}+Z^{R}G^{R}C^{OS}+V^{R}D^{R}S^{IN})\Delta^{3}/6-C^{2}(3Z^{R}D^{R}S^{IN2}-CZ^{R}C^{OS}(Z^{R2}+V^{R}D^{R}))\Delta^{4}/24$,

$S^{IN1}=S^{IN}-C^{2}V^{R}(Z^{R}-G^{R}T^{AN})\Delta-C^{2}(Z^{R2}S^{IN}+Z^{R}G^{R}C^{OS}+V^{R}D^{R}S^{IN})\Delta^{2}/2-C^{2}(3Z^{R}D^{R}S^{IN2}-CZ^{R}C^{OS}(Z^{R2}+V^{R}D^{R}))\Delta^{3}/6$.

IF $D^{1}\neq 0$ GO TO STATEMENT 81. RETURN.

TESTING FOR PRINTING CONDITIONS - INTERVAL, INFLECTION, BOTTOM OR SURFACE HIT - PRINT SUBROUTINE

SUBROUTINE PRINT.

IF $S^{IN}S^{IN1} \le 0$ AND $\alpha = 0$ THEN $\alpha = 3$. FROM $v = 1$ TO 2 DO STATEMENT 89.

IF $v=1$ AND $\alpha=3$ AND $Q > r^1$ THEN $\alpha=4$.
$C^{T1}=C^1, S^{INT1}=S^{IN1}$. $r^T=r, y^T=y, \Delta^T=\Delta, S^{INT}=S^{IN}, C^T=C$.
IF $\alpha=4$ THEN $\Delta=\Delta^T S^{IN}/(S^{IN}-S^{IN1})$ AND $w=1$ AND GO TO STATEMENT 90.
IF $v=1$ AND $Q > r^1$ THEN GO TO STATEMENT 83. $D^1=1, r^{T1}=r^1, y^{T1}=y^1$,
IF $\alpha<3$ THEN $\Delta=\Delta^T(Q-r)/(r^1-r)$, $Q=Q+S$ AND GO TO STATEMENT 90.
IF $\Delta^T S^{IN}/(S^{IN}-S^{IN1}) < \Delta^T(Q-r)/(r^1-r)$ THEN

(IF $v=1$ THEN $\Delta=\Delta^T S^{IN}/(S^{IN}-S^{IN1})$ AND $w=1$ OTHERWISE $\Delta=\Delta^T(Q-r)/(r^1-r)$ AND $Q=Q+S$)
OTHERWISE (IF $v=1$ THEN $\Delta=\Delta^T(Q-r)/(r^1-r)$ OTHERWISE $Q=Q+S$ AND $w=1$ AND $\Delta=\Delta^T S^{IN}/(S^{IN}-S^{IN1})$). GO TO STATEMENT 90.

STATEMENT 81.
$F_2=1$. GO TO STATEMENT 103.

STATEMENT 104.
$F_2=0$. $t=t+B$. $D^1=0, S^{IN}=S^{IN1}, y=y^1, r=r^1$.
FROM $k=0$ TO $M-1$ IF $r<X_{k+1}$ THEN $M=k$ AND GO TO STATEMENT 84.

STATEMENT 84.
$W=Y_M+(r-X_M)(Y_{M+1}-Y_M)/(X_{M+1}-X_M)-y$. IF $\alpha=2$ AND $v=2$ THEN $S^{IN1}=(S^{IN1}-\beta C^{OS})/(1+\beta^2)^{.5}$ AND $w=0$.
IF $w=1$ THEN $S^{IN1}=0$ AND $w=0$. $\theta_1=W$.

PRINT FORMAT 3, $r/1852, y, S^{IN1}, t, W$.

$\rho_0=r/1852, \rho_1=y, \rho_2=S^{IN1}, \rho_3=t, \rho_4=W$. WRITE TAPE ρ,2,2,5. IF $\alpha=2$ AND $v=2$ THEN
(IF $|S^{IN1}|>H$ THEN PRINT MESSAGE (CRITICAL SINE) AND COMPUTE $E^{OF}=1$ AND GO TO STATEMENT 10), $S^{IN1}=S^{IN}$.

$t=t-B$. IF $v=2$ AND (IF $\alpha=1$ OR $\alpha=2$ GO TO SYATEMENT 89).
$r^1=r^{T1}, y^1=y^{T1}, C^1=C^{T1}, S^{IN1}=S^{INT1}$. $r=r^T, y=y^T, \Delta=\Delta^T, S^{IN}=S^{INT}, C=C^T$.

STATEMENT 83.
IF $v=1$ AND $\alpha<3$ AND $Q>r^1$ THEN $S^{INT}=S^{IN}, r^T=r, y^T=y, C^T=C$.
IF $v=1$ AND $\alpha=0$ THEN RETURN.
IF $v=1$ AND $\alpha \ge 3$ GO TO STATEMENT 88.
IF $v=1$ THEN $v=v+1$ AND GO TO STATEMENT 81.

STATEMENT 88.
STATEMENT 89. RETURN.

SUBROUTINE VQ.

$\delta^Z=S^{IN}F_1-C^2V^R(Z^R-Q^RT^{AN})F_1{}^2/2-C^2(Z^{R2}S^{IN}+Z^RQ^RC^{OS}+V^RD^RS^{IN})F_1{}^3/6-C^2(3Z^RD^RS^{IN2}-CZ^RC^{OS}(Z^{R2}+V^RD^R))F_1{}^4/24$.

$\delta^R=F_1C^{OS}+C(Z^RS^{IN}-Q^RS^{IN}T^{AN})F_1{}^2/2+C(D^RS^{IN2}-C^2V^RZ^{R2})F_1{}^3/6-C^3Z^RV^RD^RS^{IN}F_1{}^4/6$.

$V^\Delta= V^R+Z^R\delta^Z+D^R\delta^{Z2}/2+Q^R\delta^R$.

RETURN.

SUBROUTINE TIME.
STATEMENT 103.
$B=\Delta(1-C(Z^RT^{AN}+Q^R)\Delta/2+C^2(Z^{R2}-V^RD^RT^{AN2}+2Z^{R2}T^{AN2}+2Z^RQ^RT^{AN}+2Q^{R2})\Delta^2/6)/V^R$. IF $F_2=1$ GO TO STATEMENT 104.
RETURN.

FORMAT 1 DATE= xx xx xxxx RUN=xxxx xxxx.

FORMAT 2 DEPTH=M=xxxx.xxxx ANGLE DEG=xxx.xxx EPSILON=x.xxxx DELTA=xxxx MIN DELTA=xxx SIN TEST= .xxx .
FORMAT 3 xxxx.xxxx xxxx.xxxx x.xxxxxxx xxxx.xxxx xxxx.xxxx .

FORMAT 4 RANGE NM DEPTH M SINE SEC BOT DIF M.
FINISH.

12) A-187-U1 Ray Depth Distribution Program - Pass 1:
Selects plotting information from ray trace output tape, and writes a tape for the sort program (A-188-G1).

```
{ RAY TRACE DEPTH DISTRIBUTION}
{PROGRAM NUMBER 531   PASS 1}
{PROGRAMMER HOWARD L DAVIS FOR DR W A HARDY}


FUNCTION H(A,U,C)= (A/1.38 )^2 +18.364(CSIN A)^2/(U).
O=0.  FUNCTION BH(A,U,C)=1/(e^H(A,U,C)).


TYPE RAY DEPTH DSSTRIBUTION / INPUT T 1,2/HARDY.
TYPE ( GE 531  ( A 187 U1)).
STATEMENT 5002.  RWD 1,2 AND RWD 2,2.
READ CARD λ.

UPPER  R^R=150, R^γ=100, γ=100, R^β=100, β=100, R^FOUND=25. Z^F=25, ω^F=25, T^F=25, B^F=25, A^F=25.

DIMENSION W=16.
 N^R=150, N^β=100, N^γ=100, M=25.
SPECIAL VARIABLE  ATT  .

{ READ ATTENUATION LOWER LIMIT, EPSILON ANGE METERS, EPSILON ANGLE RADIANS,DUMMY,MAXIMUM
}NUMBER OF RECORDS, NUMBER OF CONSECUTIVE RAYS TO BE PROCESSED}


READ CARD A^TT, E^R,E^θ,D^U,M^AX,N^θ.
STATEMENT 300.    { READ PRINTOUT RANGES}
SLEW 2 AND PRINT MESSAGE ( RANGE).
 FROM  L=O TO INFINITY IF L>N^R GO STATEMENT 350 ELSE  READ CARD R^R_L AND
IF R^R_L=9999992 THEN (  N^R=L AND ( FROM P=O TO L-2  IF R^R_P>R^R_P+1 PRINT FORMAT 100, P+1) AND
GO TO STATEMENT 302) ELSE PRINT R^R_L.


STATEMENT 302. { READ BOTTOM RANGE AND ASSOCIATED ATTENUATION COEFFICIENT }
SLEW 2 AND PRINT MESSAGE ( BOTTOM RANGE   ATTENUATION).
FROM  L=O TO INFINITY IF L>N^β GO STATEMENT 350 ELSE  READ CARD R^β_L  AND  IF R^β_L=9999993 THEN
( N^β=L,   AND ( FROM P=O TO L-2  IF R^β_P>R^β_P+1 PRINT FORMAT 400, P+1) AND GO STATEMENT 303)
ELSE READ CARD β_L AND PRINT R^β_L,β_L.


STATEMENT 303. { READ SURFACE ATTENUATION RANGE AND ASSOCIATED COEFFICIENT}
SLEW 2 AND PRINE MESSAGE ( SURFACE RANGE ATTENUATION).
 FROM L=O TO INFINITY IF L>N^γ GO STATEMENT 50 ELSE  READ CARD R^γ_L  AND  IF R^γ_L=9999994 THEN
( N^γ=L, ( FROM P=O TO L-2  IF R^γ_P>R^γ_P+1 THEN PRINT FORMAT 300,P+1) AND GO TO STATEMENT 304)
ELSE READ γ_L  AND PRINT R^γ_L,γ_L.

STATEMENT 350. TYPE CARD INPUT ERROR TOO MANY CARDS , TERMINATE .


STATEMENT 304. TYPE CARD INPUT COMPLETED.
```

```
SLEW 1.  LABEL ( WAVELENGTH ).  PRINT λ.
SLEW 1. PRINT FORMAT 500, N^θ,N^U,N^Y,N^R.
SLEW 2. PRINT FORMAT 600, A^TT, E^R, E^T, D^U. SLEW 1. PRINT FORMAT 601, M^AX,N.
FORMAT 100 RANGE INPUT ERROR, RANGE CARD NO y.
FORMAT 200 INITIAL ANGLE INPUT ERROR, ANGLE CARD NO y.
FORMAT 300 SURFACE ATTENUATION ERROR, SURFACE ATTENUATION CARD NO y.
FORMAT 400 BOTTOM ATTENUATION ERROR, BOTTOM ATTENUATION CARD NO y.
FORMAT 500  y INITIAL ANGS y RANGES  y SURFACE AND y BOTTOM ATTENUATIONS.

FORMAT 600 ATT LIMIT y EPSR y EPSTHETA y DUMMY y.
FORMAT 601 MAXIMUM NUMBER OF RECORDS y  MAX RANGES IN CYCLE y .
{ END OF CARD READING SEQUENCE }
{ INITIAL ANGLE SEARCH  INITIAL ANGLE (ω) WHICH IS  T_2 OF FIRST RECORD }

STATEMENT 1000.  N^UMBER=0  . { FILE COUNT }

STATEMENT 1. E=0, C^REC=0. { CREC IS ASCENDING COUNT OF RECORD READ FOR EACH FILE }

STATEMENT 3. READ TAPE T_0,1,2,5  IF EOF 2 GO TO STATEMENT 1
OTHERWISE   R=T_0, Z=T_1 , ω=(180/π)ARCSIN T_2,  B=T_4.

θ=ω.

{ INITIALIZATION EACH TIME NEW RAY IS EXAMINED }
STATEMENT 2.  N^UMBER=N^UMBER+1,S^H=0, S^B=0, ATT=1,Z^MIN=Z,Z^MAX=Z,Z^CRIT=Z, J^R=0,
 C^CRIT=1,D=0,C^REC=1, E=0, T^EST=0, O^K=0, T^APE=0.

{ ATTENUATION AND RANGE ANAYSIS }
STATEMENT 100.    CALL  ( ATTENUATION ) .
STATEMENT 201. IF ATT<A^TT THEN TYPE ( ATT LIMIT ) IF O^K=0 THEN GO STATEMENT 151.

STATEMENT 15A. CALL ( RANGE ANALYSIS).

{ TERMINATION CONDITIONS WHEN A RANGE IS NOT BEING PROCESSED }
IF O^K=0 THEN ( IF EOF 2 GO STATEMENT 151 ELSE IF E=1 OR ATT<A^TT OR  T^EST>N^R
 OR T_0<0 OR C^REC>M^AX GO STATEMENT 151 ).

STATEMENT 10.  READ TAPE T_0,1,2,5  AND C^REC=C^REC+ 1 AND
IF T_0<0 OR C^REC>M^AX THEN ( IF O^K=1 GO TO STATEMENT 15A
OTHERWISE GO TO STATEMENT 151 ).
IF EOF 2 THEN E=1 AND (IF O^K=1 GO STATEMENT 15A ELSE GO STATEMENT 151).  GO TO STATEMENT 100.

{ TERMINATION ROUTINE }
STATEMENT 151.  IF T^EST<N^R  THEN  (  FROM L=T^EST+1 TO N^R COMPUTE
W_0=R^R_L-1, ( FOR P=1(1)13 COMPUTE W_P=O^U),
W_14=θ, W_15=(W_0+θ/360),WRITE TAPE W_0,2,2,16  ).
STATEMENT 153. IF N^UMBER<N^θ THEN (IF E=1 GO STATEMENT 1 ELSE (FROM L=0 TO INFINITY
READ TAPE T_0, 1, 2, 5 AND IF EOF 2 GO STATEMENT 1)).
EOF 2,2  AND TYPE END OF RUN / USE SORT PROGRAM / SORT ON 16TH WORD OF EACH RECORD.

TYPE SORT CODE 32  32 31   32.

STOP.

SUBROUTINE ( RANGE ANAYSIS).  { FINDS DESIGNATED RANGES KEEPING TRACK OF TURNING POINTS }

{ CONDITIONS INDICATING TAPE WRITE WHEN RANGE IS BEING PROCESSED }

IF C^REC>M^AX OR T_0<0 OR ATT<A^TT  THEN (  IF O^K=1 THEN Z^OCRIT=T_1 AND GO TO STATEMENT 200).
IF EOF 2 THEN (IF O^K=1 THEN Z^OCRIT=T_1 AND GO STATEMENT 200).
R=T_0, Z=T_1, ω=T_2,  B=T_4.
```

```
STATEMENT 101. J=J^R. STATEMENT 102.
{ SEARCH FOR RANGE }

IF R>(R^R_J-E^R) AND R<(R^R_J+E^R) THEN O^K=1 AND GO TO STATEMENT 205.
{ O^K=1 MEANS RANGE FOUND [illegible] WRITTEN}


{ TAPE RANGE TOO SMALL GO CONTINUE SEARCHING }

IF R<(R^R_J-E^R) THEN GO STATEMENT 10C.

{ TAPE RANGE TO LARGE ASSUME CURRENT TAPE RECORD IS PROPER RANGE }
IF O^K=O THEN ( PRINT FORMAT 201, R^R_J,θ AND ( FOR L=1(1)4 COMPUTE T_L=D^U ) AND TYPE (RANGE ERROR CONTINUE), O^K=1,

AND GO TO STATEMENT 205 ) ELSE GO TO STATEMENT 10C.


{ BUFFER FOR RANGES BETWEEN COMMON TURNING POINTS, UP TO A MAXIMUM OF 25 }

STATEMENT 205. J^R=J+1 , T^EST=T^EST+1, T^APE=T^APE+1,
IF T^APE>25    THEN TYPE MORE THAN 25 RANGES IN CYCLE, TERMINATE.
STATEMENT 104. W=T^APE-1 , R^FOUND_W=R^R_J, Z^F_W=T_1, ω^F_W=T_2, τ^F_W=T_3, θ^F_W=T_4, A^F_W=ATT.


{ TEST FOR TURNING POINT }

STATEMENT 106.  IF |ω| SE^θ OR BSE^R OR ZSE^R  THEN Z^OCRIT=Z^CRIT, Z^CRIT=Z, C^CRIT=C^REC
AND GO TO STATEMENT 200 ELSE RETURN.



FORMAT 201 RANGE y NOT ON TRACE OF INITIAL ANGLE y .
STATEMENT 200. IF O^K=O  THEN RETURN.   IF Z^OCRIT<Z^CRIT THEN Z^MAX=Z^OCRIT,
Z^MIN=Z^CRIT  OTHERWISE Z^MAX=Z^CRIT, Z^MIN= Z^OCRIT.

{ WRITING  ON TAPE FROM BUFFER WHEN TURNING  POINTS FOUND }
FROM K=O TO T^APE-1 LOOP STATEMENT 401.
W_0=R^FOUND_K, W_1=Z^F_K, W_14=θ, W_15=(W_0+θ/360) AND  W_2=Z^MIN, W_3=Z^MAX, W_4=A^F_K, W_5=τ^F_K, W_6=ω^F_K, W_7=θ^F_K.

( FOR L=8(1)13 COMPUTE W_L=D^U) AND  WRITE TAPE W_0,2,2,16.


STATEMENT 401.

 T^APE=O, O^K=O . RETURN.


{ CALCULATION OF ATTENUATION }

SUBROUTINE (ATTENUATION).

R=T_0, Z=T_1, B=T_4.
IF ZSE^R GO TO STATEMENT 130.
IF BSE^R GO TO STATEMENT 131. RETURN.


STATEMENT 130. S^H=S^H+1  , GO TO STATEMENT 132.
 STATEMENT 131 . S^B=S^B+1  , GO TO STATEMENT 15.

STATEMENT 132. FROM Q=O TO N^Y-1  IF R^Y_Q>R  THEN S=Q  AND GO TO STATEMENT 17.
  TYPE  ATTENUATION CONSTANT ERROR(SURFACE), TERMINATE. STOP.

STATEMENT 15.  FROM K=O TO N^B-1 IF R^B_K>R THEN μ=K AND  GO TO STATEMENT 16 .
TYPE  ATTENUATION ERROR HERE (BOTTOM),TERMINATE. STOP.

STATEMENT 16. Δ=ARCSIN T_2.


 ATT=ATTXBH(Δ,λ,B_μ).

 RETURN.
 STATEMENT 17.  ATT=ATTXT_S.  RETURN.
    [illegible]SH.
```

13) A-183-U1 Ray Depth Distribution Program - Pass 3:
Reads sort output, prints Ray Depth Distribution Table and writes tape for plot program. Sample printout: Chapter I, Fig. 11.

{ PASS 3 RAY DEPTH DISTRIBUTION GE 532, A 183 U1 }

{ PROGRAMMED BY HOWARD L. DAVIS FOR DR. W.A. HARDY }

TYPE RAY DEPTH DISTRIBUTION.
TYPE (GE 532 (A 183 U1)).

RWD 1,2 AND RWD 2,2.

READ CARD N,M,B. { NUMBER OF RAYS OR INITIAL ANGLES SAME AS FOR PASS 1}
{ DECIMAL FRACTION OF PAPER TO BE USED FOR TIME PLOT, MAXIMUM BOTTOM DPETH TO BE FOUND }
UPPER C=225 , W=3600. FROM Q=0 TO INFINITY LOOP STATEMENT 100.
G=-1.

FROM L=0 BY 16 TO 16(N-1) READ TAPE W_L,1,2,16 AND IF EOF 2 GO STATEMENT 101
ELSE IF $W_{L+5} \leq 28$ THEN G=(G+1), $C_G = W_{L+5}$. $T^{MIN} = T^{MAX} = C_0$.

FROM P=0 TO G IF $T^{MIN} > C_P$ THEN $T^{MIN} = C_P$ ELSE IF $T^{MAX} < C_P$ THEN $T^{MAX} = C_P$.
$P = (T^{MAX} - T^{MIN})/(120M)$.
SLEW TOP.

FORMAT 300 y y ELIMINATED.
FORMAT 200 y y RANGE NOT FOUND.
FORMAT 400 y y y y y y.

PRINT MESSAGE (RAY DEPTH DISTRIBUTION).

SLEW 2. FROM G=0 BY 16 TO 16(N-1) IF $(W_{G+1} + W_{G+7}) \leq 28$ THEN $D = W_{G+1} + W_{G+7}$ AND GO STATEMENT 401.
STATEMENT 401.
PRINT FORMAT 100, W_0, D, P, Q+1.
FORMAT 100 RANGE y BOTTOM DEPTH y TIME SCALE y COUNT xxx.

SLEW 2. PRINT LABEL (COUNT, INITIAL ANGLE, DEPTH, ATTENUATION, TIME, ANGLE).

FROM G= 0 BY 16 TO 16(N-1) LOOP STATEMENT 99.
IF $W_{G+1} > 28$ THEN (IF $W_{G+2} < 28$ THEN PRINT FORMAT 200,(G+16)/16,W_{G+14} ELSE PRINT FORMAT 300,(G+16)/16,
AND (FROM L=G TO G+15 COMPUTE $W_L = 28$), AND GO TO STATEMENT 50.

PRINT FORMAT 400, (G+16)/16, W_{G+14}, W_{G+1}, W_{G+4}, W_{G+5}, ARCSIN W_{G+6} .

$W_{G+11} = D$, $W_{G+12} = -(MB(W_{G+5} - T^{MIN})/(T^{MAX} - T^{MIN}) + P(M+1.5)/120)$, $W_{G+13} = 0$.

FOR L=0(1)15 COMPUTE $W_{L+G} = -W_{G+L}$.

STATEMENT 50. WRITE TAPE W_G,2,2,16.

STATEMENT 99. CONTINUE.
EOF 2,2.
STATEMENT 100. CONTINUE. STATEMENT 101.
FROM L=0 TO 10 COMPUTE EOF 2,2.
TYPE (EOF MULTIPLEX PLOT , RWD 1,2 AND RWD 2,2. TYPE (END OF PROGRAM) AND STOP.
[illegible]

14) A-195-U1 Type III Intensity Program - Pass 1:
Reads ray trace output tape, calculates transmission loss for specified ranges, and writes tape for sort program (A-188-G1).

```
{ PROGRAM NUMBER 547 BY HOWARD DAVIS FOR DR. W.A. HARDY}
TYPE INTENSITY 111   ( A 195 U1).
SPECIAL  VARIABLES RFOUND,ATT, EOF.
```

```
{ PROGRAM NUMBER 547 BY HOWARD DAVIS FOR DR. W.A. HARDY}
TYPE INTENSITY 111  ROBERT MININGHAM RAY TRACE SYSTEM NUMBER   ( A 195 U1).
SPECIAL  VARIABLES RFOUND,ATT, EOF.
DIMENSION T=16, W=16, Z=3, ATT=5, λ=5.
UPPER  R^β=200, β=200,  T=(3,15), Q=500, R=500,  R=501, Δ^J=500, α=500, Z^F=500.

{ M=NUMBER OF INTERVALS, N^θ=NUMBER OR RAYS TO BE PROCESSED, σ=SURFACE ATTENUATION COEFFICIENT }
{ E^R=ALLOWABLE VARIANCE IN RANGE IDENTIFICATION, E^θ=ALLOWABLE VARIANCE IN ANGLE IDENTIFICATION }

READ CARD M,N^θ,σ,  E^R,E^θ.  O=0.   IF M>500 TYPE ( TOO MANY INTERVALS TERMINATE), STOP.
SLEW TOP, LABEL ( NUM INTERVALS,NUM ANGLES,EPSILON R,EPSILON THETA,SUR ATT COEFF)  ,
AND PRINT M,N^θ, E^R,E^θ,σ.
SLEW 2,   LABEL ( RANGES).
{ READ IN RANGES AT WHICH CALCULATIONS ARE TO BE MADE }
FROM L=0 TO 500 READ CARD R_L   IF R_L=9999991 THEN ( N^R=L, (FROM P=0 TO L-2  IF R_P+1≤R_P  THEN
TYPE ( RANGE INPUT ERROR) , STOP),GO STATEMENT 301) ELSE
PRINT R_L.
TYPE ( MORE THAN 501   INPUT RANGES TERMINATE ) , STOP.
STATEMENT 301.
SLEW 2.
      LABEL ( RANGE, BOTTOM ATT).
{ READ IN RANGE AND ASSOCIATED BOTTOM ATTENUATION COEFFICIENT }
FROM L=0 TO 200 READ CARD R^β_L   AND     IF R^β_L=9999992 THEN ( N^β=L, (FROM P=0 TO L-2 IF R^β_P+1≤R^β_P THEN
TYPE (ATTENUATION RANGE INPUT ERROR), STOP),
GO STATEMENT 302  ) ELSE READ CARD β_L  AND      PRINT R^β_L,β_L.
TYPE ( MORE THAN 201 ATTENUATION INPUT RANGES TERMINATE ), STOP.
STATEMENT 302. SLEW 2.
```

{ READ IN WAVELENGTHS ON CARDS }

LABEL (WAVELENGTHS). FROM L=0 TO 5 READ CARD λ_L IF λ_L=9999993 THEN (N^λ=L , GO STATEMENT 303) ELSE PRINT λ_L AND ATT_L=1.

TYPE (MORE THAN 5 WAVELENGTHS TERMINATE), STOP. STATEMENT 303.

RWD 1,2 AND RWD 2,2 AND RWD 3,1 AND R^{31}=0.

{ R^{31}=0 MEANS TAPE 3,1 IS IN REWOUND CONDITION , R^{31}=1 MEANS TAPE 3,1 IS NOT REWOUND }

LABEL (RANGES, BOTT ATTEN, WAVE LENGTHS), PRINT N^R,N^θ,N^λ.

IF MN^RN^θ>25000 THEN TYPE (OUTPUT TAPE 2,2 WILL BE OVERLOADED, TERMINATE), STOP.

READ A^{AA}. PRINT LABEL BT SCATTERING. PRINT A^{AA}.

TYPE (CARD INPUT COMPLETED).

C^{OUNT}=0.

{ Δ=1 MEANS MINIMAX FOUND EOF=1 MEANS EOF FOUND }

{ KEEP READING TAPE UNTIL A TURNING POINT IS FOUND THEN TEST FOR RANGE STATUS }

{ THE BEGINING AND ENS OF EACH FILE IS TREATED AS A TURNING POINT }

STATEMENT 3.

READ TAPE T_0,1,2,5 AND IF EOF 2 THEN GO STATEMENT 3 ELSE α^C=T_2, Z^{CRIT}=T_1, R^C=T_0, θ=(180/π)ARCSIN(T_2), Z^{BI}=T_1, Δ=0, EOF=0, J=0.

{ Z^{BI} IS THE INITIAL DEPTH AT ORIGIN }

FROM L=1 TO N^λ COMPUTE ATT_{L-1}=1 AND T_{L+6}=1. WRITE TAPE T_0,3,1,16 AND R^{31}=1.

{ RFOUND FROM ZERO EACH NEW TIME THROUGH}

STATEMENT 4. RFOUND =0.

STATEMENT 5.

READ TAPE T_0,1,2,5 AND IF EOF 2 THEN Δ=1, EOF=1 , GO STATEMENT 206 ELSE CALL (ATTENUATION), Δ=0 , WRITE TAPE T_0,3,1,16 AND R^{31}=1.

{ TURNING POINT FOUND } IF $|T_2| \leq E^{\theta}$ OR $T_1 \leq E^R$ OR $T_4 \leq E^R$ THEN Δ=1. { TEST FOR RANGE} STATEMENT 205.

IF $T_0 \leq R_J - E^R$ THEN GO STATEMENT 206.

IF $T_0 > R_J + E^R$ TYPE (RANGE SKIPPED TERMINATE MAYBY ER IS TOO SMALL), LABEL (R SKIPPED) , PRINT T_0, J, R_J, E^R, RFOUND AND STOP.

{ RANGE FOUND}

J=J+1, $Z^F_{RFOUND} = T_1 + T_4$, RFOUND=RFOUND+1, IF RFOUND > 500 THEN
TYPE (FOUND RANGES BETWEEN MINIMAX OVERSTORED TERMINATE), STOP.

STATEMENT 206.
{ IF Δ=0 THEN CONTINUE SEARCH }

IF Δ=0 THEN GO STATEMENT 5.
IF EOF=0 AND RFOUND=0 THEN (IF R^{31}=1 THEN RWD 3,1 AND R^{31}=0) AND $Z^{CRIT} = T_1$, $R^C = T_0$, $\alpha^C = T_2$,

WRITE TAPE T_0,3,1,16 AND R^{31}=1 AND GO STATEMENT 5.

$Z^{NCRIT} = T_1$, $\alpha^{CN} = T_2$, $R^{CN} = T_0$, EOF 3,1.

{ ALL INFORMATION BETWEEN MINIMAX NOW ON TAPE NUMBER OF RANGES FOUND IS RFOUND}

{ MONOTONIC INCREASING Δ=1 ELSE Δ=0 MONOTONIC DECREASING}
IF $Z^{CRIT} > Z^{NCRIT}$ THEN $Z^{MAX} = Z^{CRIT}$, $Z^{MIN} = Z^{NCRIT}$, Δ=1 ELSE $Z^{MAX} = Z^{NCRIT}$, $Z^{MIN} = Z^{CRIT}$, Δ=0.
STATEMENT 10. FROM S=0 TO RFOUND-1 LOOP STATEMENT 19.

(IF R^{31}=1 THEN RWD 3,1 AND R^{31}=0), $\Delta^Z = Z^F_S/M$, P=1, $\Delta^J_p = \Delta M \Delta^Z$, $F^{LAG1} = F^{LAG2} = E^{31} = 0^K = 0$.

STATEMENT 110. $Z = \lfloor (P - \Delta M) \Delta^{Z} \rfloor$.

IF $Z^{MIN} < Z < Z^{MAX}$ THEN $Q_{P+1} = 1$, GO STATEMENT 111.

IF $Z^{MIN} \geq Z$ THEN $S^{MIN} = 0$ ELSE $S^{MIN} = 1$. IF $Z^{MAX} \leq Z$ THEN $S^{MAX} = 0$ ELSE $S^{MAX} = 1$.

$\alpha_{P+1} = R_{P+1} = P$, $\Delta^{J}_{P+1} = Z$, $Q_{P+1} = 0$.

IF ($\Delta = 0$ AND $S^{MAX} = 0$ AND $F^{LAG2} = 0$) OR ($\Delta = 1$ AND $S^{MIN} = 0$ AND $F^{LAG2} = 0$) THEN $Q_{P+1} = 1, R_{P+1} = R^{CN}, \alpha_{P+1} = \alpha^{CN}, \Delta^{J}_{P+1} = Z^{NCRIT}$, $F^{LAG2} = 1$.
GO STATEMENT 18.

STATEMENT 111.
IF $F^{LAG1} = 0$ THEN $\alpha_P = \alpha^{C}$, $R_P = R^{C}$, $\Delta^{J}_{P} = Z^{CRIT}$, $F^{LAG1} = 1$.

READ TAPE W_0,3,1,16 AND $R^{31} = 1$, IF EOF 1 THEN TYPE (EOF ERROR TERMINATE),
LABEL (P,W(O),THETA,DELTA), PRINT P,W_0,θ,Δ,S AND STOP.

FROM Y=0 TO 15 COMPUTE $T_{0,Y} = T_{1,Y}$, $T_{1,Y} = T_{2,Y}$, $T_{2,Y} = W_Y$.
STATEMENT 120. { CROSS OVER Z}

IF $\Delta = 0$ THEN (IF $W_1 < Z$ THEN GO STATEMENT 111 ELSE GO STATEMENT 112).
IF $W_1 > Z$ THEN GO STATEMENT 111.

STATEMENT 112.

READ TAPE W_0,3,1,16 AND $R^{31} = 1$, IF EOF 1 GO STATEMENT 207 ELSE (FROM Y=0 TO 15 COMPUTE $T_{3,Y} = W_Y$).
GO STATEMENT 150.

STATEMENT 207. FROM Y=0 TO 15 COMPUTE $T_{3,Y} = T_{0,Y}$.
$E^{31} = 1$. { MEANS EOF ON 31 HAS BEEN HIT }

STATEMENT 150. FROM Y=1 TO 3 COMPUTE $Z_Y = T_{Y,1}$.

```
CALL ( INTERPOLATION). { RETURNS INTERPOLATED RANGE AND ANGLE }

IF P≥M THEN GO STATEMENT 18.

IF Δ=0 THEN ( IF |(P+1-ΔM)Δ^Z| >Z^MAX THEN GO STATEMENT 18 ELSE O^K=0).
IF Δ=1 THEN ( IF |(P+1-ΔM)Δ^Z| <Z^MIN THEN GO STATEMENT 18 ELSE O^K=0) .
IF E^31=1 THEN O^K=1, GO STATEMENT 600.

IF Δ=0 THEN ( IF T_3,1 ≯ |(P+1-ΔM)Δ^Z| THEN O^K=1) , GO STATEMENT 600.
IF T_3,1 ≮ |(P+1-ΔM)Δ^Z| THEN O^K=1.

STATEMENT 600.

IF O^K=1 THEN P=P+1 , Q_P+1=1, Z=|(P-ΔM)Δ^Z| , GO STATEMENT 150.

STATEMENT 18. IF P<M THEN ( FROM Y=0 TO 15 COMPUTE T_1,Y=T_2,Y, T_2,Y=T_3,Y), P=P+1, GO STATEMENT 110.

FROM L=2 TO M+1 LOOP STATEMENT 666.

W_0=R_J+S-RFOUND, { INPUT RANGE VALUE }
W_1=(Δ^J_L-Δ^J_L-1), { DEPTH DIFFERENCES USING REAL END POINTS }
W_2=(π/180)θ, { INITIAL ANGLE OF RAY IN RADIANS }
W_3=α_L, { INTERPLOATED TANGENT ANGLE }
W_4=Q_L, { 0 OR 1 }
W_5=Δ^J_L, { DEPTHS INCLUDING REAL END POINTS }
W_6=R_L-R_L-1, { INTERPOLATED RANGE DIFFERENCES }
(FROM Y=0 TO 4 COMPUTE W_Y+7=T_2,Y+7),
W_12=|( L-2-Δ(M-1))Δ^Z| +Δ^Z,
W_13=Z^F_S, { BOTTOM DEPTH AT INPUT RANGE }
W_14= R^CN-R^C, { LOCAL RANGE INTERVAL }
W_15= W_0+ |( L-2-Δ(M-1))| /10000 , { SORT VARIABLE } .

WRITE TAPE W_0,2,2,16.

STATEMENT 666.

CONTINUE.
```

STATEMENT 19.

(IF $R^{31}=1$ THEN RWD 3,1 AND $R^{31}=0$), $R^{C}=R^{CN}$, $Z^{CRIT}=Z^{NCRIT}$, $\alpha^{C}=\alpha^{CN}$.

IF $J<N^{R}$ THEN GO STATEMENT 81 ELSE (IF EOF=0 THEN

(FROM L=0 TO INFINITY READ TAPE T_0,1,2,5 AND IF EOF 2 THEN GO STATEMENT 405) ELSE GO STATEMENT 405).

STATEMENT 81. IF EOF=1 THEN GO STATEMENT 91 ELSE $\Delta=0$, EOF=0, GO STATEMENT 4.

STATEMENT 91. FROM 1=J TO $N^{R}-1$ LOOP STATEMENT 667.

FROM L=2 TO M+1 LOOP STATEMENT 668.

$W_0=R_1$, $W_2=\theta(\pi/180)$, $W_4=0, W_1=W_3=W_5=W_6=9999999$, $W_{15}=W_0+|(L-2)|/10000$, (FROM j=0 TO 4 COMPUTE $W_{j+7}=0$), WRITE TAPE W_0,2,2,16.

STATEMENT 668.

STATEMENT 667.

} J GREATER THAN N RED R

STATEMENT 405. $C^{OUNT}=C^{OUNT}+1$.

IF $N^{\theta}\leq C^{OUNT}$ THEN EOF 2,2 AND TYPE (PROGRAM FINISHED), RWD 2,2 AND RWD 1,2 AND

(IF $R^{31}=1$ THEN RWD 3,1 AND $R^{31}=0$), STOP, ELSE GO STATEMENT 3.

STOP. SUBROUTINE (ATTENUATION).

FUNCTION $BE(A,U,C)=(A/1.38)^2+128.55(CSIN\ A)^2/(7U)$. FUNCTION $BH(A,U,C)=A^{AAA}/(e^{BE(A,U,C)})$.

IF $T_1\leq E^{R}$ THEN (FROM L=0 TO $N^{\lambda}-1$ COMPUTE $ATT_L=\sigma ATT_L$), GO STATEMENT 512.

IF $T_4\leq E^{R}$ THEN (FROM Y=0 TO $N^{\beta}-1$ IF $T_0\leq R^{\beta}{}_{Y}$ THEN (FROM L=0 TO $N^{\lambda}-1$ COMPUTE

$ATT_L=ATT_L BH(ARCSIN(T_2),\lambda_L,\beta_Y)$), GO STATEMENT 512) TYPE (ATTENUATION RANGE FOR BOTTOM HIT NOT FOUND TERMINATE), STOP ELSE RETURN.

STATEMENT 512.

FROM P=0 TO 4 COMPUTE T_{P+7}=ATT_P. RETURN.

STOP. SUBROUTINE (INTERPOLATION).

IF $Z=T_{2,1}$ THEN $\alpha_{P+1}=T_{2,2}$, $R_{P+1}=T_{2,0}$, GO STATEMENT 352.

$$R_{P+1}=\frac{(Z-Z_2)(Z-Z_3)T_{1,0}}{(Z_1-Z_2)(Z_1-Z_3)}+\frac{(Z-Z_1)(Z-Z_3)T_{2,0}}{(Z_2-Z_1)(Z_2-Z_3)}+\frac{(Z-Z_1)(Z-Z_2)T_{3,0}}{(Z_3-Z_1)(Z_3-Z_2)}.$$

$$\alpha_{P+1}=T_{1,2}+\frac{(Z-Z_1)(T_{2,2}-T_{1,2})}{(Z_2-Z_1)}.$$

STATEMENT 352. $\Delta^J_{P+1}=Z$.

RETURN.

FINISH.

15) <u>A-185-U1 Type III Intensity Calculation - Pass 3:</u>
Reads sort output and prints table. Sample printout: Chapter I, Fig. 15.

```
{ TYPE 111 INTENSITY CALCULATION FOR DR. W.HARDY BY H.DAVIS }

{ PROGRAM 549 MININGHAM NUMBER A 185 U1 }
TYPE (A 185 U1 ) .
O=0.
DIMENSION W=16,  λ=5 .
UPPER ATT=250, F=250, Q=250, Δ^1=250, α=250, θ=250, Δ^J=250 .
FUNCTION D(E)=9.5x10^-3/(E)^2 .  FUNCTION G(A,B,C)=4(SIN(6.28A/BSIN(C)))^2 .
SLEW TOP AND PRINT MESSAGE (TYPE 111 INTENSITY CALCULATION (A 185 U1 ) PASS 3).
READ CARD N^TP,N^P,N,N^R,Z^I,r .
SLEW 1 AND LABEL ( TOT NUM ANGLES, NUM ANGLES, NUM INTERVALS, NUM RANGES, INITIAL DEPTH, SMALL R),
  PRINT N^TP,N^P,N,N^R,Z^I,r .
SLEW 1 AND LABEL (WAVELENGTHS) .
FROM L=0  TO 5 READ CARD λ_L  AND IF λ_L=9999991 THEN N^λ=L, GO STATEMENT 2 ELSE PRINT λ_L .
TYPE (MORE THAN 5 WAVELENGTHS TERMINATE),  STOP.
STATEMENT 2.
FROM M=0 TO N^λ-1   { NUMBER OF WAVELENGTHS }  LOOP STATEMENT 26.
RWD 1,2.

TYPE ( NEW WAVELENGTH ) .
IF Z^I≤λ_M r THEN μ=1 ELSE μ=0 .
FROM Y^OU=1 TO N^R  { NUMBER OF  INPUT RANGES }  LOOP STATEMENT 25.
O^K=1.
FROM Y=1 TO N  { NUMBER OF  INTERVALS }  LOOP STATEMENT 24.
D^UM=1.
CALL ( TAPEOREAD).

IF O^K=1 THEN CALL ( SET UP),O^K=0.

CALL ( INTENSITY CAL ).

PRINT FORMAT 40, Y,Z,T^L.

STATEMENT 24.  STATEMENT 25.  STATEMENT 26.
 TYPE (END  OF PROGRAM ).  STOP .
```

```
SUBROUTINE ( TAPEOREAD ) .
Z^CI=0.
FROM L=1 TO  N^P LOOP STATEMENT 10.  READ TAPE W_0,1,2,15.  R=W_0 ,  { INPUT RANGES }

θ_L=W_2 ,  { INITIAL ANGLES }
α_L=W_3 ,  { TANGENT ANGLES }                Q_L=W_4 , { EITHER 0 OR 1 }
Δ^1_L=W_6 ,  { RANGE INTERVAL FOR DEPTH INTERVALS }        ATT_L=W_M+7,   { ATTENUATION FOR THE M^TH WAVELENGTH }
( IF W_3<10000 THEN Z=W_12, Z^CI=Z^CI+1) ,  { DEPTH FOR CALCULATION }        Z^A=W_13 ,  { BOTTOM DEPTH AT RANGE }  .

Δ^J_L=W_14,  { LOCAL RANGE INTERVAL }  .
IF W_3>10000 THEN D^UM=D^UM+1.
IF Z^CI=0 THEN Z=0.

STATEMENT 10.  RETURN .  STOP .

SUBROUTINE (SET UP).  SLEW TOP ,
PRINT MESSAGE ( TYPE 111 INTENSITY CALCULATION ), SLEW 1, PRINT FORMAT 10, R, Y^OU, M+1 .
PRINT FORMAT 20, Z^A,N AND SLEW 1 AND PRINT MESSAGE ( NUMBER OF ANGLES ), PRINT N^P,
SLEW 1 AND PRINT FORMAT 30, λ_M .
SLEW 3 AND PRINT MESSAGE (  COUNT    DEPTH        TRANSMISSION  LOSS  ).
               FORMAT 40    xxx    y    y  .
SLEW 1.

FORMAT 10 RANGE xxxxxxx.x  NAUTICAL MILES                    xxx RANGE OF xxx WAVELENGTH .
FORMAT 20 BOTTOM DEPTH xxxxxx.x METERS       DEPTH INTERVALS M=xxx.
FORMAT 30 WAVELENGTH xxxxxx.x METERS.

RETURN.  STOP.

SUBROUTINE (INTENSITY CAL).
σ=λ_M.  IF Z≤λ_M r THEN F=1 ELSE F=0.
```

$$T^L = 10LOG \left[\frac{\pi N e^{-RD(\sigma)}}{2215 Z^A N^{TP}_R} \sum_{j=1}^{N^P} \left(ATT_j (G(Z,\lambda_M,\alpha_j)F+1-F)\,(G(Z^I,\lambda_M,\theta_j)\mu+1-\mu)\,\frac{\Delta^1{}_j COS(\theta_j)}{\Delta^J{}_j COS(\alpha_j)}\; Q_j\right) \right] .$$

16) A-196-U1 Multiplot - Pass 1:

Selects ranges to be plotted from ray trace output tape and writes tape for sort program (A-188-U1). Sample multiplot: Chapter I, Fig. 10.

REWIND 2,2. READ A,B,D. I=0. STATEMENT 33. READ TAPE C,1,2,5. IF EOF 2 THEN WRITE EOF 2,2 AND I=I+1 AND GO TO STATEMENT 4.
WRITE TAPE C,2,2,5. GO TO STATEMENT 33. STATEMENT 4. IF A=B GO TO STATEMENT 6. IF I=A THEN TYPE (CHANGE INPUT TAPE THEN TOGGLE 0) AND PAUSE. STATEMENT 6.
IF I=B THEN (IF B>D GO TO STATEMENT 5),(FROM I=B+1 TO D COMPUTE (FROM 1=0 TO 4 COMPUTE C_1=0), WRITE TAPE C,2,2,4 AND WRITE EOF 2,2) AND GO TO STATEMENT 5.
GO TO STATEMENT 1. STATEMENT 5. WRITE EOF 2,2. TYPE (PROGRAM IS NOT FINISHED). REWIND 1,2. REWIND 2,2.
TYPE (PUT BLANK TAPE ON T1P2 AND SAVE INPUT TAPE THEN TOGGLE 0). PAUSE.

(IF THERE ARE TAPE FORMAT ERRORS ON RAY TRACE TAPE T2 P2 A NEW TAPE IS WRITTEN ON T1 P2)
DIMENSION D=100,E=100,F=100. READ N. FROM 1=1 TO N READ F_1. J=1,K=1,E_0=-1. SLEW TOP.
PRINT MESSAGE MORE THAN ONE ANGLE IN THE FOLLOWING FILE. LABEL INDEX-LAST REC,FILE.
STATEMENT 1. 1=1,B=-1. STATEMENT 2. READ TAPE A,2,2,5. IF J>F_N GO TO STATEMENT 10. IF EOF 2 THEN J=J+1 AND GO TO STATEMENT 1.
IF A_0>B THEN 1=1+1,B=A_0 AND GO TO STATEMENT 2. IF E_{K-1}=J THEN K=K-1. D_K=1-1, E_K=J. B=A_0. PRINT D_K ,E_K . K=K+1. GO TO STATEMENT 2. STATEMENT 10.
IF K=1 THEN T=2,S=1 AND PRINT MESSAGE (TAPE IS GOOD) AND GO TO STATEMENT 14 OTHERWISE S=2,T=1. M=K-1.
TYPE (PROGRAM IS STILL NOT FINISHED). REWIND 2,2. REWIND 1,2. K=1,J=1. STATEMENT 13.
IF E_K≠J GO TO STATEMENT 11. G=D_K. FROM 1=1 TO G READ TAPE A,2,2,5 AND WRITE TAPE A,1,2,5. WRITE EOF 1,2. K=K+1. STATEMENT 11.
READ TAPE A,2,2,5. IF EOF 2 GO TO STATEMENT 12. WRITE TAPE A,1,2,5. GO TO STATEMENT 11. STATEMENT 12.
WRITE EOF 1,2. J=J+1. IF K>M THEN K=1. IF J>F_N GO TO STATEMENT 14. GO TO STATEMENT 13. STATEMENT 14. IF T=1 WRITE EOF 1,2.
TYPE (PROGRAM IS STILL IN PROCESS). REWIND 1,2. REWIND 2,2.
IF S=1 TYPE (OUTPUT TAPE WILL BE T1P2) OTHERWISE TYPE (OUTPUT TAPE WILL BE T2P2 - PUT BLANK ON T2P2 - THEN TOGGLE 0) AND PAUSE.

(WRITE NEW RAY TRACE TAPE TO BE USED FOR MULTIPLEX PLOT)
READ Δ,ε,M^R,D. J=1,1=1. STATEMENT 20. IF J=F_1 THEN GO TO STATEMENT 21. STATEMENT 22. READ TAPE A,T,2,5.
IF EOF 2 THEN J=J+1 AND GO TO STATEMENT 20. GO TO STATEMENT 22. STATEMENT 21. FROM n=0 BY Δ UNTIL M^R LOOP STATEMENT 24. READ TAPE A,T,2,5.
IF EOF 2 GO TO STATEMENT 25. STATEMENT 26.
IF $|A_0-n|<\epsilon$ THEN $A_2=A_1+A_4$,A_0=n, A_1=-A_1,A_2=-A_2,A_3=0 AND WRITE TAPE A,S,2,4 AND GO TO STATEMENT 23. READ TAPE A,T,2,5. IF EOF 2 GO TO STATEMENT 25.
GO TO STATEMENT 26. STATEMENT 23. STATEMENT 24. READ TAPE A,T,2,5. IF EOF 2 CONTINUE OTHERWISE TYPE (RANGE GREATER THAN GIVEN MAXIMUM) AND STOP.
STATEMENT 25. L=n. FROM n=L BY Δ UNTIL M^R COMPUTE A_0=n AND (FROM r=1 TO 3 COMPUTE A_r=0) AND WRITE TAPE A,S,2,4.
1=1+1,J=J+1. IF 1>N GO TO STATEMENT 30. GO TO STATEMENT 20. STATEMENT 30. WRITE EOF S,2. TYPE (END OF PROGRAM). REWIND T,2. REWIND S,2. FINISH.

17) <u>A-189-U1 Type II Intensity Calculation - Pass 1:</u>
Reads ray trace output tape, calculates transmission loss for specified ranges, and writes tape for plot program (A-200-U1).

```
{ PASS 1 TYPE 11 INTENSITY CALCULATION GE 541  ( A 189 U1 ) }
{ PROGRAMMED BY HOWARD L DAVIS FOR W A HARDY }

FUNCTION BE(A,U,C)=(A/1.38)^2+128.55(CSIN A)^2/(7U).
FUNCTION BH(A,U,C)=1/(e^BE(A,U,C)).

O=0.
TYPE INTENSITY  TYPE 11 .
TYPE ( GE 541 ( A 189 U1)).

SPECIAL VARIABLES ATF=(9,18), ATT=10.
DIMENSION W=16,λ=10,R^F=18, 7=18, ω=18,  T^F=18. B=18.
UPPER R=1000,R^β=500, β=500.
SLEW TOP.
{ READ IN EPSILON RANGE, DIFFERENCE BETWEEN ADJOINING RANGES, NUMBER OF  RAYS TO BE PROCESSED }
{ SURFACE HIT ATTENUATION COEFFICIENT }
READ CARD E^R,Δ,D^U,N^θ,γ.
LABEL (  RANGE DIFFENCE). PRINT Δ. SLEW 1.
LABEL (  DUMMY). PRINT D^U.  SLEW 1. LABEL (EPSION RANGE , NUM OF ANGLES, SURFACE COEFF ).
PRINT E^R,N^θ,γ.  SLEW 2.
LABEL ( RANGES).   { READ IN CENTER RANGES }
FROM L=0 TO 1000 READ R_L AND IF R_L=9999991 THEN
( N^R=L AND ( FROM P=0 TO N^R-2 IF R_P+1≤R_P THEN TYPE ( RANGES NOT IN ASCENDING ORDER TERMINATE))
AND GO STATEMENT 75)  ELSE PRINT R_L.
TYPE ( MORE THAN 1000  RANGES IN INPUT BY CARD ).  STATEMENT 75.
SLEW 2.
PRINT MESSAGE ( MINIMUM RANGE  BOTTOM ATTENUATION).
{ READ IN RANGE AND BOTTOM COEFFICIENT UP TO THAT RANGE }
FROM L=0 TO 500 READ R^β_L AND IF R^β_L=9999992 THEN ( N^β=L AND ( FROM P=0 TO N^β-2 IF R^β_P+1≤R^β_P  THEN
TYPE ( BOTTOM ATTENUATION RANGES AND COEFFICIENTS NOT IN ASCENDING ORDER)) AND GO STATEMENT 76)  ELSE
READ β_L AND PRINT R^β_L,β_L.
TYPE ( MORE THAN 501  BOTTOM ATTENUATIONS FOUND CONTINUE).
STATEMENT 76. LABEL ( WAVE LENGTHS). FROM L=0 TO 9  READ λ_L  AND
IF λ_L=9999993 THEN ( N^λ=L AND ( GO STATEMENT 85) ) ELSE PRINT λ_L.
TYPE ( OVER 10  WAVELENGTHS CONTINUE).
STATEMENT 85 ,  TYPE ( CARD INPUT COMPLETED).
SLEW 2.  LABEL ( NUMBER RANGES, NUM BOTT ATT , NUM WAVELENGTHS). PRINT N^R,N^β,N^λ.
RWD 2,2 AND RWD 1,2.
```

```
{ PROCESSING OF FIRST 18 RAY TRACE RANGES }
N^LM=0.
STATEMENT 100. H=1,J=0,C^TRD=18, C^ΔRG=-18.
FROM L=0 TO 5 COMPUTE ATT_L=1 AND ( FROM P=0 TO 18 COMPUTE ATF_L,P=0).

STATEMENT 101.
READ TAPE T_0,1,2,5 IF EOF 2 GO STATEMENT 101 ELSE N^LM=N^LM+1, ω=ARCSIN T_2, CALL ( ATTENUATION).
FROM G=0 TO 18 READ TAPE T_0,1,2,5 IF EOF 2 TYPE ( EOF IN FIRST 18 RANGES), AND STOP ELSE CALL ( ATTENUATION).

{ TEST RANGE 18 TO BE SURE IT IS NOT TO LARGE }
IF T_0>R_0 THEN TYPE ( FIRST RANGE LOWER THAN 18 TH RANGE ON RAY TERMINATE ) AND STOP.

{ NORMAL PROCESSING BEGINS }

FORMAT 102 RANGE y ON TRACE LARGER THAN y INPUT RANGE y DELTA y.

STATEMENT 102.
READ TAPE T_0,1,2,5 AND IF EOF 2 GO STATEMENT 200 ELSE
C^TRD=C^TRD+1 AND IF T_0<0 GO STATEMENT 200 ELSE CALL ( ATTENUATION).
IF T_0>R_J+ΔC^ΔRG +E^R THEN PRINT FORMAT 102,T_0,R_J+C^ΔRG..., R_J,C^ΔRG.
IF T_0≤R_J +ΔC^ΔRG-E^R GO STATEMENT 102.
{ WHEN RANGE IF FOUND }

L=C^ΔRG/2 +9.
R^F_L=R_J+ΔC^ΔRG, Z_L=T_1, ω_L=ARCSIN T_2,T^F_L=T_3,R_L=T_4, ( FROM P=0 TO N^λ-1 COMPUTE ATT_P,L=ATT_P).
C^ΔRG=C^ΔRG+2 . IF L=18 THEN C^ΔRG=-18 , J=J+1 AND
GO STATEMENT 103 ELSE GO STATEMENT 102.

STATEMENT 103. FROM G=0 TO 18 LOOP STATEMENT 109.
W_0=R^F_G,W_1=Z_G,W_2=ω_G, W_3=T^F_G, W_4=R_G, W_5=θ, ( FROM P=0 TO N^λ-1 COMPUTE W_6+P=ATT_P,G ).

WRITE TAPE W_0,2,2,10 .
STATEMENT 109. IF H=0 GO STATEMENT 200. IF J<N^R THEN GO STATEMENT 102. IF N^LM<N^R GO STATEMENT 100.
EOF 2,2 AND TYPE ( END OF PROGRAM [illegible] PROGRAM ).

{ TERMINATIONS }

STATEMENT 200. H=0.

L=C^ΔRG/2 + 9.
IF J<N^R THEN ( FROM G=L TO 18 COMPUTE R^F_G=R_J+C^ΔRG, Z_G [illegible] , [illegible] ( FROM P=0 TO N^λ-1 COMPUTE ATT_P,G=0).
C^ΔRG=C^ΔRG+2), C^ΔRG=-18, J=J+1, GO STATEMENT 103. IF N^LM<N^R GO STATEMENT 100.
EOF 2,2 AND TYPE ( END OF PROGRAM [illegible] TERMINATED ).

[illegible]TINE ( ATTENUATION).
IF T_1≤E^R THEN [illegible]+1 AND ( [illegible] ATT [illegible] AND RETURN.

IF T_1≤E^R THEN [illegible]
FROM [illegible] IF [illegible] THEN GO STATEMENT [illegible]
TYPE ( [illegible] ATTENUATION [illegible] NOT [illegible] TERMINATE )
AND [illegible] STATEMENT [illegible].
ω=ARCSIN T_2 AND ( FROM [illegible] N^λ-1 [illegible]

RETURN.
END.
```

18) A-184-U1 Type II Intensity Calculation - Pass 3:

Reads sort output, prints table, and writes tape for plot program (A-200-U1). Sample printout: Chapter I, Fig. 13.

```
{ TYPE 11 INTENSITY CALCULATION PASS 2 }
{ PROGRAM NUMBER 542 , PROGRAMMED BY HOWARD L. DAVIS FOR DR. W.A. HARLY }

TYPE ( TYPE 11 INTENSITY CALCULATION NUMBER 542 ).
TYPE ( GE 542 ( A 184 U1)).

SPECIAL VARIABLES ATT,TL.
Q=0.

DIMENSION Z^P=9, W=16, α=250, Z^A=250.
UPPER TL=(250,9), Z=250, ATT=250, θ=250.
FUNCTION G(A,B,C)=4(SIN(6.28A/BSIN C))^2.
FUNCTION Y(A^1,B^2,C^3) = (P(A^1-B^2)/(C^3))^2.
FUNCTION D(E)=9.5x10^-3/(E)^2.

{ DIMENSION OF DEPTHS AND BOTTOM DIFFERENCE AND INITIAL BOTTOM IN METERS NO CONVERSIONS MADE }

{ INITIAL DEPTH, NUMBER OF RAYS, TOTAL NUMBER OF RAYS, }
{ SMOOTHING FACTOR, RECEIVER AND SOURCE FUNCTION CONSTANT }
READ CARD Z^BI,N^θ, N^Tθ,P,r.

PRINT MESSAGE ( DEPTHS).
FROM L=0 TO 250 READ Z_L IF Z_L=9999990 THEN N^Z=L AND ( FROM L=0 TO N^Z-2 IF Z_L+1≤Z_L THEN
TYPE ( DEPTH INPUT NOT IN ASCENDING ORDER)) , GO STATEMENT 103 ELSE PRINT Z_L.
STATEMENT 103.

IF N^Z>252 THEN TYPE ( MORE THAN 251 DEPTHS TO MANY).
LABEL (WAVELENGTHS).
FROM L=0 TO 9 READ CARD λ_L AND IF λ_L=9999991 THEN ( N^λ=L AND GO STATEMENT 85) ELSE PRINT λ_L.

TYPE ( MORE THAN 10 WAVELENGTHS CONTINUE).

STATEMENT 85.

PRINT LABEL ( NUM WAVE LENGTH, NO ANGLES, TOTAL NU ANGS,NO DEPTHS , SMOOTHING FACT, INIT DEPTH , SMALL R ).
PRINT N^λ,N^θ, N^Tθ,N^Z,P,Z^BI, r. SLEW TOP.

N^R=0, N^P=0.
STATEMENT 107.
 FORMAT 5 TYPE 11 INTENSITY CALCULATION    (A 184 U1)                    XXXX.
FORMAT 10 CENTER RANGE y NAUTICAL MILES.
FORMAT 20 BOTTOM DEPTH y METERS.

FORMAT 30 WAVELENGTH y  SMOOTHING FACTOR y  NO ANGLES y.
```

```
{ READ FOR ONE ANGLE ONCE FIRST Q≠9 THEN Q=8

N=N^Z.

M=-1, Q=9.

STATEMENT 500.

RWD 1,2.
M=M+1 IF M≥N^λ THEN TYPE ( PROGRAM COMPLETED) AND STOP.  N^R=0.
IF Z^B'≤λ_M' THEN F=1 ELSE F=0. STATEMENT 600.

FROM L=0  TO Q LOOP STATEMENT 10.
K=0.

FROM S=0  TO N^θ-1  LOOP STATEMENT 63.
 READ TAPE W_0,1,2,16 AND IF EOF 2 GO STATEMENT 201 .

Z^A_S=W_1, α_S=W_2, θ_S=W_5, ATT_S=W_6+M.
IF ATT_S=0  THEN K=K+1  ELSE  R=W_0,  Z^B_L=W_1+W_4.

STATEMENT 63.
IF  K≥N^θ  THEN GO STATEMENT 202.

CALL ( INTENSITY CALCULATION ).
STATEMENT 53.   CONTINUE.

STATEMENT 10.
IF Q=8 GO STATEMENT 11.  STATEMENT 12.   N^R=N^R+1.
 SLEW TOP .  PRINT FORMAT 5, N^R.  PRINT FORMAT 10, R.

PRINT FORMAT 30, λ_M,P,N^θ. Q=8 .  SLEW 2.   PRINT FORMAT 11.

PRINT FORMAT 21, Z^B_0, Z^B_1, Z^B_2, Z^B_3, Z^B_4, Z^B_5, Z^B_6, Z^B_7, Z^B_8, Z^B_9.

SLEW 2.  FROM L=0 TO N-1 PRINT FORMAT 1 , Z_L,TL_L,0,TL_L,1,TL_L,2,TL_L,3,TL_L,4,TL_L,5,TL_L,6,TL_L,7,TL_L,8,TL_L,9.
GO STATEMENT 600.
```

STATEMENT 11.

SLEW 3. PRINT FORMAT 12. $G=9$. $N^P=N^P+1$.

PRINT FORMAT 22, Z^B_0, Z^B_1, Z^B_2, Z^B_3, Z^B_4, Z^B_5, Z^B_6, Z^B_7, Z^B_8.

SLEW 2. FROM L=0 TO N-1 PRINT FORMAT 2, Z_L, $TL_{L,0}$, $TL_{L,1}$, $TL_{L,2}$, $TL_{L,3}$, $TL_{L,4}$, $TL_{L,5}$, $TL_{L,6}$, $TL_{L,7}$, $TL_{L,8}$.

GO STATEMENT 600.

STATEMENT 201. IF L=0 AND S=1 THEN TYPE (EOF OK CONTINUE) AND GO STATEMENT 500 ELSE PRINT FORMAT 25, S, N^R.

FORMAT 25 EOF ERROR AT HEAD y OF ANGLE y.

STATEMENT 203. TYPE (IMPROPER EOF) AND STOP.

SUBROUTINE (INTENSITY CALCULATION).

$\mu=\lambda_M$.

STATEMENT 19.

FROM i=0 TO N-1 LOOP STATEMENT 9.

IF $Z_i > Z^B_L$ THEN $Z^S=Z_i$, $Z_i=Z^B_L$, $\Delta=0$ ELSE $\Delta=1$.

{ CONSTANT CONVERTED FOR METERS}

IF $Z_i \le \lambda_M$, THEN H=1 ELSE H=0.

$$TL_{i,L}=10LOG\left[\frac{Pe^{-RD(\mu)}}{1250 Z^B_L N^T \theta_R}\sum_{j=0}^{N^\theta-1}(ATT_j(1+(Y=Y(Z_i,Z^A_j,Z^B_L))-Y)(G(Z^{B'},\lambda_M,\theta_j)F+1-F)(G(Z_i,\lambda_M,\alpha_j)H+1-H)(\cos\theta_j)(e^{-Y})/(\cos\alpha_j))\right]$$

IF $\Delta=0$ THEN (FROM $\Delta=i+1$ TO N-1 COMPUTE $TL_{\Delta,L}=0$), $Z_i=Z^S$, GO STATEMENT 9.

STATEMENT 9.

RETURN.

{ ZERO ATTENUATIONS }

STATEMENT 202. FROM i=0 TO N-1 COMPUTE $TL_{i,L}=0$. $Z^B_L=0$. GO STATEMENT 53.

```
FORMAT 1 xxxxx    xxxx.xxx  xxxx.xxx  xxxx.xxx  xxxx.xxx  xxxx.xxx  xxxx.xxx  xxxx.xxx  xxxx.xxx  xxxx.xxx  xxxx.xxx.
FORMAT 21 BOTTOM  xxxxxx.x  xxxxxx.x  xxxxxx.x  xxxxxx.x  xxxxxxxx  xxxxxx.x  xxxxxx.x  xxxxxx.x  xxxxxx.x  xxxxxx.x .
FORMAT 11 RANGE     R-18      R-16      R-14      R-12      R-10      R-8       R-6       R-4       R-2       R .

FORMAT 2 xxxxx              xxxx.xxx  xxxx.xxx  xxxx.xxx  xxxx.xxx  xxxx.xxx  xxxx.xxx  xxxx.xxx  xxxx.xxx  xxxx.xxx.

FORMAT 22 BOTTOM            xxxxxx.x  xxxxxx.x  xxxxxx.x  xxxxxx.x  xxxxxx.x  xxxxxx.x  xxxxxx.x  xxxxxx.x  xxxxxx.x .

FORMAT 12 RANGE               R+2       R+4       R+6       R+8       R+10      R+12      R+14      R+16      R+18 .
```

19) <u>A-200-Ul Type II Intensity Plot - Pass 4:</u>

Plots transmission loss. Sample printout: Chapter I, Fig. 14.

CHAPTER VIII

CONCLUSIONS AND RECOMMENDATIONS

The present program must be regarded as an initial step, a prototype program directed toward a comprehensive model of long-range, low-frequency acoustical propagation in the deep ocean. Many of the factors that influence the propagation are introduced in an admittedly ad hoc manner, e.g., bottom and surface reflectivity. Other problems are avoided by the introduction of special restrictions - the chief example is the smoothing of the effects of multipath interference structure by the demand that the transmission loss calculation be interpreted as a spatial and frequency average in comparison with experimental data. Finally, the effects of diffraction, as they arise in boundary reflections and wavefront aberrations, have been included only indirectly, and the degree to which they will change the calculated average distributions of the acoustical field has not even been estimated.

Despite these evident limitations, the program does provide a structure for appraising the effects of known and dominant environmental factors on the distribution, arrival structure, and intensity of the acoustical field. Indeed, at present the accuracy of the program is undoubtedly limited far more by the inherent imprecision in the data inputs of the sound velocity field and the sea bottom shape and reflection properties than by lack of formal treatment of factors such as those given in the previous paragraph. Also, as the environmental data become more refined, the treatment of these effects can be developed more precisely and used to upgrade and extend the present program in a straightforward manner.

A potential user for the program should refer to the several Data Specification Forms given in Chapter I of this report. What specification can he give to the bottom or surface reflectivity functions that are required, or to the appropriate source and/or receiver directivity functions appropriate to his application? Similarly, how is the velocity accuracy test parameter, ϵ , selected and what determines the density of initial ray angles to be traced or the number of bottom hits allowed before a ray is considered terminated? The questions demand,

```
{  PLOT OF DAVIS TYPE 2  OUTPUT  HARDY  J TRANTUM  2/1/68 }
{  INPUT = OUTPUT OF DAVIS PASS 3      TAPE ON 2,2 }

SPECIAL VARIABLES MIN,MAX,RO,RMAX,ΔR  .
DIMENSION D=50 , T=50 , λ=10  .
READ N,L  .  { NUMBER OF DEPTHS , NUMBER OF WAVELENGTHS }
READ MIN,MAX  .  { PLOT SCALE }
READ RO,RMAX,ΔR  .  { RANGE VALUES }

FROM I=1 TO N READ D_I .  FROM I= 1  TO L READ λ_I .
STATEMENT 1 .
 READ I .  {DEPTH ARGUEMENT}   IF I=99 STOP .
 FROM J=1 TO L LOOP TO STATEMENT 3 . SLEW TOP . PRINT FORMAT 1 , λ_J,D_I .
 FORMAT 1                              WAVELENGTH = xxxxx          DEPTH = xxxxx  .
 PRINT FORMAT 2 ,MIN , MAX .
 FORMAT 2  xxxxx --------------------------------------------- SCALE -------------------------------------------- xxxxxx  .
 SLEW 1 .
 FROM R =RO BY ΔR TO RMAX LOOP TO STATEMENT 2 .
 READ TAPE T_1,2,2,N . IF EOF 2 REWIND 2,2 AND GO TO STATEMENT 1 .
 PLOT T_1,R , MIN,MAX .
STATEMENT 2 .
STATEMENT 3 .
 REWIND 2,2 . GO TO STATEMENT 1 .  FINISH .
```

of course, familiarity with the structure of the present program; more broadly interpreted, the questions become open-ended.

Central not only to the application of the program but to its development and evaluation there must be an experimental program that is sufficiently comprehensive to include a detailed description of the environment in parallel with precise measurements of the acoustical field. It is to be expected that the process of comparing predicted and experimental results will be highly adaptive in the sense that initial calculations will show which factors most strongly influence the acoustical propagation and, in turn, the experimental results will demonstrate whether such factors have been under- or over-estimated. For example, if the ray tracing shows that the dominant acoustical energy is propagated by paths that involve bottom interactions then the experimental data can be used to determine bottom loss parameters. A second calculation using these parameters can then be compared with independent experimental data and would be expected to provide improved agreement.

Over-all, and from the experience of Hudson Laboratories in using the ray tracing program and in applying it to experimental data, continuation of the program would be directed in three categories which are listed below and are discussed in greater detail in subsequent sections:

i) Technical improvements in the present program.

ii) Extension toward more complex environments than can be presently treated.

iii) Experimental programs which either supplement the ray tracing program or provide specific tests of its predictions.

8.1. Technical Improvements

In Chapter VII we recognized that during the growth of the program a number of procedures were followed which have been shown on subsequent analysis to be inefficient in computer utilization. They were not corrected during several revisions of the program because of the expectation that it would later be entirely re-programmed for a larger computer than the presently used GE-235, and that such technical improvements could be accomplished most efficiently during this process. Apart from this type of specific programming for machine efficiency it is believed that substantial improvements could be effected by changes in the structure of the program itself, and these are outlined below.

8.1.1. N-Parameter Representation of Velocity Profiles

The solution of the ray equation by iteration demands a technique for expressing the change in the velocity field as a function of displacement from a given position. In the present program this was achieved by a Taylor expansion that also identifies the derivatives of the velocity field at a given point, i.e., considering only the depth dependence,

$$v(z) = v(z_o) + \frac{\partial v}{\partial z}\bigg]_{z_o} (z-z_o) + \ldots + \frac{1}{n!} \frac{\partial^n v}{\partial z^n}\bigg]_{z_o} (z-z_o)^n + \ldots \qquad \text{(VIII. 1)}$$

Only the quadratic terms are included in the present program (Chapter III).

If the expansion (VIII. 1) is carried to the n-th order, the coefficients of the expansion must be evaluated in terms of $(n+1)$ or more data inputs points from a velocity profile. There is no unique form or method for achieving this expansion except that the result must be gauged with respect to its ability to represent the properties of the actual velocity profiles in the real ocean. For example, it has been noted in Chapter II, Fig. 29, that the 4-point Lagrangian representation can produce unrealistically large curvatures in the neighborhood of individual data points. In general, however, the range of validity of (VIII. 1) will be increased for large values of n and, if the iterated solutions of the ray equation are expressed in terms of the coefficients of (VIII. 1), the length of the iteration increments can be increased correspondingly. It follows that over-all computer running time can be reduced at the cost of deriving more complex iteration equations.

The above conclusion assumes that the velocity profile data that are entered to construct the velocity field are pre-edited such that the input data contain not only the velocity value but also the coefficients of (VIII. 1) that are needed for the expansion. The method is most useful when many rays are to be traced because the input data are processed once and then are repeated for each trace. Indeed, if the range of the expansion (VIII. 1) can be made large enough, the velocity accuracy test, i. e., ϵ-test, is no longer required and this would save the time required in the present program for i) making a test iteration, ii) determining the velocity by means of a field expansion over the test iteration, iii) computing the velocity given by the velocity field construction program at the terminus of the test iteration, and iv) comparing these results to determine the accuracy of the projected iteration and the truncation required if this is necessary. Also, the higher order representation of the field expansion would smooth the intermediate coefficients of (VIII. 1) so that, for example, the curvature would not fluctuate as erratically as is evidenced in the real data values of Tables 5. 3. 1.

8. 1. 2. Direct Calculation of Spreading Loss

In Chapters III and IV the spreading loss, or magnification function, was determined as the change of depth for rays with differentially incremented initial angles. It is well known that this change can be also expressed in terms of the local field derivatives of individual rays; Born and Wolf,[1] for example, give the ray intensity $I(\vec{r})$ at position $\vec{r}$ as a function of an initial intensity $I_o(\vec{r}_o)$ at position $\vec{r}_o$ by

$$I(\vec{r}) = \frac{v(\vec{r}_o)}{v(\vec{r})} I_o(\vec{r}_o) \exp\left\{ - \int_{\vec{r}_o}^{\vec{r}} v(\vec{r}) \left[\operatorname{div}\left(\frac{\hat{t}}{v(\vec{r})}\right)\right] ds \right\} \qquad \text{(VIII. 2)}$$

where $\hat{t}$ is the vector ray direction and ds is taken over the ray path. (VIII. 2) is readily expressed as an iteration equation similar to those used in the program for computing the ray positions or the travel time. Also, the intensity distributions, calculated in Chapter IV, can be re-expressed in terms of the "local" spreading losses derived through (VIII. 2)

This approach was not followed in the present program because the formulation of Chapter IV, oriented toward the estimation of ray densities, is more general and does not require the detail expressed by (VIII. 2). This decision has been regretted, however, and the tabulation of (VIII. 2) in the Ray Depth Distribution Plot tables would have been helpful in many applications.

8.1.3. Additional Distribution Plots

The Ray Depth Distribution Plot provides a summary of the manner in which the set of rays with differing initial angles combine to form a field distribution at a given range. The plot, with its associated table, lists:

i) the ray depth

ii) the ray angle

iii) the travel time

iv) an attenuation factor based on bottom losses only.

By following the methods given in Chapter IV, further compilations of these data can be obtained as weighted distribution functions taken with respect to travel time or arrival angle, and these can be plotted individually. Such plots would be valuable in making direct comparisons with experimental data.

It is evident that the distribution routines that are based on data from the ray tracing outputs, i.e., the plot routines mentioned above as well as the various intensity calculations, are similar in type and depend on common input data. In terms of computer utilization it is efficient to prepare all of these outputs in one pass, provided that the computer has sufficient capacity to store the data range needed for the computations in active memory and to compute all of the independent outputs. This has not been possible with our present computer nor has sufficient attention been given, in view of the fact that the output routines were developed and programmed independently, to a more optimum program organization. Considerations of this type are mandatory for the development of a flexible, integrated program.

8.2. <u>Program Extension</u>

Future extensions of the program have been studied and planned to provide capabilities for the inclusion of more complex environmental data or for more detailed physical predictions than are possible with the present program, but programming in these directions has been delayed pending extensive evaluation of the predicted results of this program with experimental data. Additionally, many of the extensions not only would require increased computer capacity, but also they involve modification of the basic ray tracing program and the methods by which data are introduced and used in it. The examples given below, therefore, represent both re-programming requirements as well as theoretical extensions. They may also be cited to summarize some of the limitations of the present approach toward acoustical prediction.

8.2.1. Three-Dimensional Modeling

An appraisal of the two-dimensional restriction of the present program has been presented in Chapter VI. One conclusion was that the bending of rays in the azimuthal plane by refraction would not be important for the prediction of sound intensities as averages, but there are other applications in which it would be useful to have quantitative estimates of the magnitude of such bending. Formally, the extension of the iteration equations to include an azimuthal spreading would be elementary - the real problem is the specification of the velocity field to include transverse gradients as well as the prescription which is used to determine these gradients from velocity profile data. For the most part, it is the opinion of the present authors that in long-range propagation involving many multipath contributions the deviations from a great circle bearing that are sometimes observed in azimuthal arrival angle most probably represent bottom scattering rather than azimuthal refraction.

8.2.2. Treatment of Bottom Facets

The acoustical scattering from a contoured bottom slope, especially an extensive slope near the origin of the ray tracing, has been discussed schematically in Chapter VI. One approach toward this problem was outlined in Chapter VI and consisted of a method for compiling the available bottom contours to determine the location and curvature of bottom facets that would provide specular reflection of rays from the ray tracing origin into a given bearing. The ray tracing is then carried through in a standard manner for the rays that are purely refracted, but the bottom-reflected rays are summed over the facets that have been identified and are assigned weights that depend on the curvature of the facets. This treatment is especially appropriate for long wavelength sound and for bottom contours that change slowly compared with a wavelength. Finally, the results of such a program would be valuable for estimating not only the number of arrivals that occur in the vertical plane at the origin, but also the number and intensity of the arrivals with different azimuthal angles at the origin. Indeed, and because the illumination against the slope will depend on the position of a source in the far field, an estimate is also obtained of the fluctuations of the azimuthal arrivals as a function of the range of the source from a given receiver.

8.2.3. Wavefront Calculations

It has been emphasized in this report that ray tracing in real velocity fields using a dense set of initial angles shows significant wavefront aberration and this aberration grows with the range of the ray tracing to the point where distinctions can no longer be made between a normal arrival and arrivals which are sub-structures of an aberrant wavefront. This is clearly evidenced in the fluctuations of the magnification functions, i.e., the slopes, of the Ray Depth Distribution Plots.

Such distortions can be traced to specific features of the input velocity field data and are related to the fluctuating curvatures of the velocity profiles as these are shown, for example, in Table 5.3.1. It is to be noted, however, that the curvature fluctuations arise from the particular representation of the velocity profile that is used in the present program and that this is an intermediate step toward achieving formally correct solutions of the ray equation. Because the ray tracing program uses other controls, such as the ε-test and that of the semi-invariant, the computer solutions have averaged the curvature fluctuations and, as shown in Chapter V, the solutions can be accepted as accurate formal solutions with a precision that is determined by selection of the program control parameters. Since the fluctuations of the magnification functions that are found in calculations based on real data inputs are much greater than the variations that occur for different but nominal ranges of the control parameters, it must be concluded that the resultant wavefront aberration that is calculated represents a physical property of underwater sound transmission.

It would be useful to explore these properties further by means of ray-diffraction calculations such as those indicated in the Appendix. For this purpose it would be desirable to generate the wavefronts themselves from the computer program using the travel time of the set of rays, the ray positions and directions, the phase changes of the rays, and the spreading loss of (VIII.2) of this chapter. From these data, and using methods derived from the discussion of the Appendix, the interference structure of the aberration can be predicted except, of course, in the immediate regions of caustics or foci.

8.2.4. Surface Ducts and Surface Scattering

The present program uses a flat sea surface. This is an excellent approximation for low frequencies and for the specular, surface-reflected wave. However, if a surface sound channel exists at the sea surface, non-specularly reflected energy can excite this duct and can propagate in it. Two regimes must be distinguished depending on whether the ray tracing origin is in or below the surface duct. If the origin is in the duct, the present program can easily handle transmission in the duct but does not predict leakage from the duct as this may be due either to diffraction or to scattering from a modulated sea surface. If the origin is well below the duct, the converse applies.

Neglect of such surface-duct transmission is often permissable in low-frequency, long-range propagation both because the leakage from the duct attenuates this mode of transmission more rapidly than modes due to alternative paths in deeper water, and because the mixed velocity profiles found in long-range propagation will tend to interrupt and destroy the surface channel. However, this will not always be true, and it becomes useful to include such modes as part of an extension of the program to short to intermediate ranges.

Various techniques can be used to estimate the contribution of the surface-duct transmission to the total sound field, but they will not be discussed here. Instead, it is recommended that the program be extended to include a modulation of the shape of the sea surface. This capability would, in turn, be used for research-oriented investigations of the surface-scattered wavefronts due to reflection of sound from a point source.[2]

8.2.5. Noise Distributions

It would be expected that noise that originates at the sea surface can be described, statistically, in terms of a directivity function and an amplitude that depends on the local sea state. In turn, the net noise field at any point in the ocean depends on the integrated contributions of the entire surface, but with modifications that are introduced by the sound velocity field and bottom structure. The Type III intensity distribution that is an option of the present program is well adapted to such calculations - the averaging over the range positions of a ray can be interpreted as an average over the possible range positions of the source. In turn, the summation of a number of Type III intensity calculations, weighted by an appropriate surface area, would be a calculation of the surface-generated noise field. This result demands the specification of the noise distribution function but, if this is given, the amplitude of the function for a given sea state can be determined by comparison of the calculated results with experimental data.

8.2.6. Arrival Interference Statistics

The subject of this report is the application of ray tracing techniques to the prediction of acoustical transmission in the ocean, and comparisons with the alternative mode theory have been avoided. This is unfortunate in the sense that any model that attempts to be comprehensive should be free to assimilate the most useful treatments and to combine these as necessary for predictive purposes. Many authors have commented on the equivalence of the two theories when each is carried through toward the determination of a net acoustical field. Indeed, it may be noted that some of the discussion of this report has been guided by interpreting the results of mode theory in terms of ray theory.

For example, the discussion of arrival structure in Chapter IV and the summation of arrival structure to determine the spatially averaged field given by Eq. (IV.36) can be regarded as a summation of weighted mode functions. The difference is that the functions of Eq. (IV.36) are determined by operations on the ray tracing solutions for a set of initial angles rather than by the process of determining the mode solutions of the wave equation in the given velocity field. It is obvious that the ray tracing derived functions do not include diffraction effects except as these are assimilated in the averaging processes specified for the intensity calculations. It is also believed that the functions derived from the ray tracing solutions are far more accurate representations of the field distributions in a complex ocean environment than are the functions derived from mode theory for a simplified stratified medium with only weakly interacting boundary planes. It is clear that the selection of specific tools will depend on the nature of the application as well as being influenced by what tool is available.

Attention is called to the work of C. S. Clay.[2, 3] This can be summarized as a specification of measurements that can be made on the sound field to distinguish signals that originate from local or point sound sources with respect to the properties of fields that originate in extended sources. Clay's use of mode theory for his derivations should not obscure the importance of these objectives nor be interpreted as a prohibition against a fully equivalent derivation in terms of local plane waves, i.e., ray theory.

These analyses, based on intensity interferometry, regard the intensity fluctuations as originating in the summation of interfering arrivals. The power spectrum of the fluctuations taken over a suitable time interval, or range interval for a moving source, is independent of the phase relationships of individual arrivals and becomes a unique signature of the sound field. By extension of the Type II intensity calculations and by using the variable of arrival angle rather than mode vector, these spectra can be computed from the ray tracing calculation and be used to compare with experimental data. Incidentally, and as computed by ray theory, the spectra can be used to distinguish wavefront aberrations from independently interfering arrivals. In short, this extension of the ray tracing program would be of great value for testing the predictive model and for the analysis of the effects of the environment on the structure of the sound propagation.

8.3. Experimental Programs

The objective of any associated experimental program is, of course, to obtain data on the properties of sound transmission in the ocean. However, insofar, as the model of propagation that can be calculated for the experiment becomes even first-order reliable, it becomes a framework for interpreting the experiment and for identifying the environmental factors that have influenced the measurements. The types of experiments listed below can be recommended partly because the data they would provide would be independently useful as characteristic of acoustical propagation in the ocean, and they are also recommended for comparison with the predictions that can be computed through, for example, the methods of this report. It is understood that environmental data taken during the experimental program must be of a precision and quantity adequate to serve as data inputs into the predictive program.

8.3.1. Determination of Acoustical Flux

Basic to the concept of cylindrical spreading is the prediction that the net, outwardly radiating acoustical flux will fall off inversely with the range while experiencing an additional attenuation due to bulk absorption, scattering, and bottom losses. If small angular factors are neglected the acoustical flux, F, is the integral of the vertical intensity distribution $I(z)$,

$$F = \int_{0}^{z_B} I(z)\, dz \quad . \qquad \text{(VIII. 3)}$$

It is recommended that the flux be determined as a function of the range between source and receiver and, using broadband sources, as a function of the acoustical frequency. The experiment should be repeated for various types of bottoms and, in particular, for bottom obstructions such as those indicated in Fig. 17. Basically, this experiment determines the transmission anomaly of the sonar equation.

8.3.2. Vertical Intensity Distribution

Incidental to the data of the above experiment would be the measurement of $I(z)$ itself, and the modulation of this with range that reveals convergence zone structure as well as the damping of this structure due to the specific form of the velocity field and the relative contribution of bottom-reflected energy. It would be of especial interest if the sources used to excite these fields consisted of both point sources, to excite the full field, and directional sources to provide selective illumination of initial angles. Again, the experiment should be repeated for differing forms of bottom topography to determine, for example, the effect of seamount obstructions as filters of ducted sound energy.

8.3.3. Vertical Arrival Structure

Impulse sources, e.g., shots, are commonly detected as a train of resolved arrivals. For the quantitative analysis of long-range propagation, far more attention must be given to the structure of these arrivals for acoustical paths that propagate by refraction only, concentrating on the phase changes produced by the refractive paths and on the effects of wave-front aberrations on the structure of the waveforms. The analysis can also be greatly assisted by resolution in the vertical plane of the arrival directions of the signals, using vertical arrays, both to identify the arrival paths and to evaluate the magnitudes in terms of a spreading loss. It is important to establish relationships between the loss of time resolution of the impulse signal with range and the spread of the signal in the vertical arrival directions. At the higher angles, the vertical array can distinguish the bottom-reflected contributions and be used to determine bottom reflectivity losses and, by correlation, to distinguish the coherent reflectivity from the incoherent components.

8.3.4. Noise Distributions and Directivity

Associated with the above programs would be measurements of similar properties for the acoustical noise field. These can be used with the predictive model, vide 8.2.5 above, to determine the amplitudes and directivities of the noise excitation functions for surface-generated noise, if this can be isolated from other noise sources of biological, machine, or seismic origin.

8.3.5. Signal Statistics

Section 8.2.6 outlines the role of intensity spectra in the interpretation of acoustical propagation. These measurements become part of a statistical analysis program to determine, for example, the extent of the spatial intervals required for averaging multipath spectra, the fluctuations that occur about such averages, the degree of correlation of signals that can be achieved in practice in the presence of wavefront aberration, the "higher frequency" components of the intensity spectra that represent bottom interactions, and the degree of discrimination that the statistical analyses provide with reference to similar ocean noise spectra.

8.3.6. Specific Environmental Interactions

When, either by experimental control or by the ray tracing analysis, signals can be isolated as having had specific interactions with the environmental structure, the data can be used to determine the interaction parameters that are required in the predictive model. Experiments in these directions should emphasize the frequency dependence of the effect, the time dependence of the interaction that is responsible for frequency spreading, and the dependence on interaction angle. Examples of such experiments include:

i) Boundary scattering from either the sea surface or bottom to include isolation of the coherent and incoherent reflectivities, the effect of the scattering on the directivity functions used in the present program, 4.2.4, and the Doppler shifting of the moving sea surface.

ii) The use of the Doppler shift to analyze the angular directivity of the sound propagated from a moving source.

iii) Analysis of scattered signals in terms of roughness coefficients and, for the sea bottom, layer structures and acoustical penetration into these.

References for Chapter VIII

1. M. Born and E. Wolf, Principals of Optics, Pergamon Press, N.Y. (1959).
2. I. Tolstoy and C. S. Clay, Ocean Acoustics, McGraw-Hill Book Co., N.Y. (1966).
3. C. S. Clay, Revs. of Geophysics 4 (4), 475-507 (1966).

CHAPTER IX

ACKNOWLEDGMENTS

Many individuals, both within and without Hudson Laboratories, have provided material assistance in the preparation and execution of these programs, and the authors gratefully acknowledge all such support. We wish particularly to thank LCDR James C. Froid of the Office of Naval Research for his efforts in providing us with data inputs for the program, for his administrative help in conducting a number of experiments that have been carried out as part of the present program, and for his continued encouragement.

A Workshop on Ray Tracing was arranged by the Office of Naval Research in August 1967, and was held at Monterey, California, under the direction of Captain Paul Woolf of the Fleet Numerical Weather Facility; the authors wish to acknowledge the comments that were received during the Workshop from all the participants and particularly those from Captain Woolf and his staff. Mr. Donald Atkocius of the Naval Oceanographic Office has given continued support to the program, especially in making available extensive bathymetric data for use in the construction of bottom profiles.

Within Hudson Laboratories, discussions with Drs. C. S. Clay and I. Tolstoy have contributed toward an appraisal of theoretical problems in underwater sound propagation. Dr. Norman Lord kindly reviewed an initial draft of this report and further suggested the form of the bottom scattering function used in preliminary intensity calculations. Dr. A. N. Guthrie and Mr. J. D. Shaffer permitted us to use their data for the calculations reported in Chapters I and IV. Over all, Dr. Winston L. Hole has given continued advice and assistance in the preparation of this report.

The staff of the Hudson Laboratories Computing Department have been especially helpful both in running the programs and in the solution of many programming difficulties. We wish to recognize explicitly the assistance received from Mr. John Trantum and Mr. Fred Grossman. Mr. John Seney prepared a preliminary program which demonstrated the advantages of the iteration method, and which was subsequently developed into the present program.

Finally, Mrs. Catherine Gerow prepared many of the figures and data compilations used in this report and contributed considerable editorial assistance. Photographic reproductions of the computer printouts and plots were prepared by Miss Vivian Bruno with skill and attention to detail.

APPENDIX

THE PHASE OF RAY ARRIVALS

This Appendix gives a further discussion of ray theory as applied to the exact determination of the intensity of the acoustic field in a non-homogeneous medium, i.e., the wave intensity that is determined by computing the phase and amplitude of individual arrivals and adding these algebraically to form the net field amplitude. The material is relegated to an appendix because it differs in emphasis from the principal concern of the main report which is the estimation of transmission loss for long-range acoustical propagation in the real ocean. For the latter it would be a rare physical situation for which the exact velocity field would be known with sufficient accuracy to justify any connection between a computed travel time and the total phase change of a ray over its path. In the main report it is recommended that the far field intensity be determined as a probability that represents the averaging of the intensities of individual arrivals. This is to be achieved by averaging spatially over an interval that is large enough to allow for those acoustical field fluctuations which are due to the wave interference of the amplitudes of individual arrivals and may include temporal averaging for changes in the velocity field or for broad frequency bandwidth.

This appendix originated in discussions among the authors and their colleagues at Hudson Laboratories as to the validity of the ray theory and the extent to which it could be applied meaningfully to a wave field. The discussion is included in this report for the following reasons:

1. The ray theory has been severely criticized as inexact and even inapplicable to wave propagation due to, for example, "failure at turning points," "shedding of energy for a curved ray," and "failure to predict phase changes." To the authors such attacks on ray theory seem unjustified and unsupported on theoretical grounds which we present in this appendix. (It is true that a <u>simple</u> ray theory, i.e., a theory applied to extended plane waves rather than "local" plane waves, does not predict the phase change of a wave that is refracted against a velocity gradient, as has been discussed by Tolstoy and Clay, and Tolstoy.[1,2] However, their comments have sometimes been improperly generalized as criticisms of ray theory in general.)

2. The new ray trace program has been used to construct a wave field for a model situation, discussed below, and in presenting these calculations the accuracy and utility of the present program is further demonstrated. Also, we expect to make a number of similar calculations in future research programs and it is convenient to document our methods in the present report.

3. By presenting this discussion we may clarify for some readers the distinctions between the actual wave field, which includes the interference effects of many arrivals, and the averaged field discussed previously.

The material of this appendix is summarized as follows:

1. A review of wave propagation using the Kirchoff development of the wave theory of Huygens and Fresnel.
2. The extension of the Kirchoff theory to inhomogeneous media.
3. The phase change across ray foci.
4. Calculation of the field of a plane wave refracted against a field gradient.
5. Conclusions.

A-1. Review of Kirchoff Theory

The Kirchoff theory is central to the calculation of diffraction fields and is discussed in detail in a number of standard references. In this section the theory is briefly reviewed, following the presentation of Born and Wolf,[3] to lay a formal basis for the subsequent calculations.

Let $U(r)$ and $U'(r)$ be two wave fields which are the space-dependent solutions of monochromatic waves $V(r,t)$ and $V'(r,t)$ each with time dependence t that is periodic with angular frequency ω, i.e.,

$$V(r,t) = U(r)\, e^{-i\omega t} \tag{A.1}$$

$$V'(r,t) = U'(r)\, e^{-i\omega t} \tag{A.2}$$

$U(r)$ and $U'(r)$ are to satisfy the wave equations

$$(\nabla^2 + k^2)\, U = (\nabla^2 + k^2)\, U' = 0 \quad . \tag{A.3}$$

k is the usual wave vector for which

$$k = \frac{\omega}{c(r)} = \frac{2\pi}{\lambda(r)} \tag{A.4}$$

where $c(r)$ is the sound velocity written as a function of space in an inhomogeneous medium and $\lambda(r)$ is the wavelength. If $U'(r)$ also possesses a singularity at a point P of the form

$$U'(r) \rightarrow \frac{e^{ikr}}{r} \quad \text{as} \quad r \rightarrow 0 \tag{A.5}$$

then U(P) can be determined from a Green's theorem if $U(r)$, $U'(r)$ and their derivatives are known on a bounding surface S that surrounds P :

$$U(P) = \frac{1}{4\pi} \oiint_S \left\{ U \frac{\partial U'}{\partial n} - U' \frac{\partial U}{\partial n} \right\} ds \quad . \tag{A.6}$$

The differentiation with respect to n is along the inward normal from S (Fig. A-1). Equation (A.6) expresses the solution U (P) in terms of an interference between the functions U and U′ and their normal derivatives on the surface S .

In homogeneous space the particular $U'(r)$ of (A.5) is everywhere an exact solution of (A.3), and the limit of application of (A.6) is determined solely by the precision to which $U(r)$ is known on the boundary surface S .

If an arbitrary function of time, $V(r,t)$, is expressed as a Fourier series

$$V(r,t) = \frac{1}{\sqrt{2\pi}} \int_{-\infty}^{\infty} U_{\omega}(r)\, e^{-i\omega t}\, d\omega \tag{A.7}$$

then it is straightforward to use this in (A.6) and recombine the series to show that $V(r,t)$ is given by

$$V(P,t) = \frac{1}{4\pi} \oiint_S \left\{ [V]_{t-T} \frac{\partial U'}{\partial n} - U' \left[\frac{\partial V}{\partial n}\right]_{t-T} \right\} ds \qquad (A.8)$$

where the functions in square brackets are defined on S at the retarded times (t-T) and T is the travel time from P to points on S. Again, the differentiation is defined with respect to the inward normal to S.

The classical test of Eq. (A.8) is the determination of the scalar wave field in the neighborhood of a diffraction focus. Using the coordinates of Fig. A-2, (A.8) becomes

$$U(P) = \frac{ik}{4\pi} \frac{e^{-ikf}}{f} \oiint_S \frac{e^{iks}}{s} (\hat{s} \cdot \hat{n} - 1)\, ds \qquad (A.9)$$

The accuracy of (A.9) for prediction of the detailed wave field to the right of surface S in Fig. A-2 is well established. In particular, (A.9) leads to the well-known "phase anomaly" of value π that exists[4] between wave surfaces that lie on opposite sides of the origin O of Fig. A-2.

A-2. Extension to Inhomogeneous Media

Equations (A.6) through (A.8) of the preceding section are also valid in an inhomogeneous medium provided that the "test" function $U'(r)$ satisfies the wave equation (A.3) and possesses the $(1/r)$ singularity of (A.5) at the point P at which the field $U(r)$ is to be evaluated. Thus the application of the Kirchoff development in an inhomogeneous medium requires not only that the field $U(r)$ be known on a boundary surface S but also that a suitable test function $U'(r)$ can be found for use in Eqs. (A.6) through (A.8).

For this purpose a wave function $U'(r)$ that is derived from ray theory will be satisfactory except in certain special regions that are discussed below. By $U'(r)$ is meant the function[5]

$$U'(r) \to \frac{e^{ikr}}{r} \quad \text{for} \quad r \to 0 \qquad (A.5)$$

$$= A(r)\, e^{i\omega T} \quad \text{for} \quad r \gg \lambda \qquad (A.10)$$

where $A(r)$, the amplitude of the ray, is to be real and positive and the travel time T is calculated from position P along the ray path to a point on the surface S by

$$T = \int_P^S \frac{dr}{c(r)} \quad . \tag{A.11}$$

General discussions of the validity of this solution are given in the standard references - it is certainly a valid solution of the wave equation in the asymptotic limit of short wavelengths.[5]

The collection of rays emanating from P represent the directions along which the intensity is directed, and the orthogonal surfaces to these rays are wave surfaces defined by a constant travel time T. If $U'(r)$ of (A.10) is an acoustic pressure, the associated particle velocity is given by

$$\vec{u}' = \frac{-i}{\omega\rho} \text{ grad } U'(r) \tag{A.12}$$

where ρ is the density of the medium, or, using (A.10) and (A.11)

$$\vec{u}' = \frac{-i}{\omega\rho} \left(\frac{\text{grad } A(r)}{A(r)} + i \frac{\omega}{c(r)} \hat{r} \right) A(r)\, e^{i\omega T} \quad . \tag{A.13}$$

The time-averaged intensity vector has the direction of the ray for

$$2\rho c \langle \vec{I} \rangle = \rho c \text{ real } (U' \vec{u}') = [A(r)]^2 \hat{r} \quad , \tag{A.14}$$

where $\hat{r}$ gives the ray direction. In the asymptotic limit of small wavelengths (or large k with $k = 2\pi/\lambda$) the condition

$$\left| \frac{\text{grad } A(r)}{A(r)} \right| \ll \frac{\omega}{c} = \frac{2\pi}{\lambda} = k \tag{A.15}$$

will be valid everywhere except where the gradient of the amplitude diverges. This is also one condition for the validity of the ray theory.

Straightforward application of flux conservation using (A.14) can be used to determine the amplitudes $A(r)$ from the ray tracing solutions. The rays emitted into a differential solid angle $\delta\Omega$ from P form a ray tube. In propagating through the inhomogeneous medium these tubes may expand or contract in cross section as they follow the curving ray. If the tube intersects surface S with cross section dS and orientation $\hat{n}$ the amplitude on S is given by

$$A(r) = \sqrt{\frac{1}{\hat{r} \cdot \hat{n}} \frac{c_S}{c_P} \frac{d\Omega}{dS}} \tag{A.16}$$

where c_S is the sound velocity on S and c_P is the sound velocity at P.

If the cross section of the ray tube shrinks to zero, as it will if the rays cross or focus, the condition (A.15) cannot be maintained and the ray solution (A.10) cannot be extrapolated through a ray crossing point. Note, however, that the energy carried by such a ray tube can be carried through a ray crossing in view of (A.14), i.e., a ray crossing point is not a scattering point. The amplitudes $A(r)$ in a region where the rays cross are determined by diffraction and the wave field must be extrapolated through the region by use of a wave theory. In the following section the principal concern will be toward the modification of ray theory when ray solutions are projected through such geometrical divergences.

The use of the test function $U'(r)$ of (A.10) and (A.11) and the condition (A.15) modify Eq. (A.8) to

$$V(P,t) = \frac{1}{4\pi} \oiint_S \left\{ [V]_{t-T} (ik\hat{r} \cdot \hat{n}) - \left[\frac{\partial V}{\partial n}\right]_{t-T} \right\} A(r)\, dS \quad . \tag{A.17}$$

Preferably the surface S will be chosen such that on it $V(r,t)$ will either vanish or can be defined as a local plane wave with direction $\hat{s}$ and amplitude $B(r)$. That is, the harmonic component of $V(r,t)$, $U(r)$, can be expressed as a local plane wave on S of the form

$$U(r) = B(r)\, e^{ikr\hat{s} \cdot \hat{r}} \tag{A.18}$$

and (A.17) further simplifies to

$$U(r) = \frac{i}{4\pi} \oiint_S k\,(\hat{r} \cdot \hat{n} - \hat{s} \cdot \hat{n})\, A(r)\, B(r)\, e^{i\omega T}\, dS \tag{A.19}$$

where T, from (A.11), is a function of r on S.

A-3. Phase Change Across Ray Crossings

The above is used to investigate the typical ray crossing situation in an inhomogeneous medium that is sketched in Fig. A-3. The set of rays that radiate spherically from P are represented by a center ray 0 and an adjacent pair of rays, +1 and -1, which will be required to determine the amplitude of ray 0 through use of (A.16). The rays cross to form a caustic or focus in the general region of C and subsequently diverge from this region. While the amplitudes of the diverging rays can still be estimated by the use of (A.16), it is desired that an indication be given as to:

i) the calculation of the diffraction field in the region of C.

ii) the determination of a phase change of the ray bundle on transit through the ray crossing region C.

The surface S_1 is to be the wave front representing the waves from P advancing towards C, but is constructed well before C so that the amplitude of the wave front on S_1 is given by (A.16) without violation of the condition (A.15). In the asymptotic limit of small wavelengths S_1 will be normal to the rays and will also represent equal travel time T for the ray bundle. Similarly, S_2 is the wave front of the waves diverging from C and S_2 is constructed well behind C as measured along ray 0.

Although the physical field, represented by the rays from P, has ray crossings in the region C, it is possible to construct an entirely new ray field solution from points on S_2 to those on S_1 for which none of the rays will cross one another. In fact, if the surfaces S_1 and S_2 are not too far apart and the velocity field gradients are not exceptionally large in the region of C, the ray (or wave) field $U''(r)$ will be very nearly

$$U''(r) \approx \frac{e^{iks}}{s} \qquad \text{(A.20)}$$

in which s is the distance along a ray path from a point O_2' on S_2 to a point O_1'' on S_1. The field on the surface S_1 is given by the ray solution (A.10), (A.11), and (A.16) for the rays from P The field due to this is found on the surface S_2 by the use of the test function $U''(r)$ in (A.8). For a harmonic wave this is formally expressed by

$$U(r) = \frac{ie^{\omega T}}{4\pi} \oiint_{S_1} k\,(\hat{s}\cdot\hat{n} - \hat{r}\cdot\hat{n})\,A(r)\,U''(r)\,e^{i\omega T''}\,dS \qquad (A.21)$$

giving the continuation of the field from S_1 to S_2. T'' is the travel time computed for the rays of $U''(r)$.

Although the amplitudes $A(r)$ of (A.10) will diverge in the region C , this is not reflected in any anomalous behavior of the ray trajectories themselves as determined by the ray Eq. (III.1) of the main report. Thus the travel time T'' between the wave surfaces is still, by Fermat's principle, an extremum for those ray paths that coincide with the ray paths originally followed from point P and which are normal to the two surfaces. In going from the general point O_2' on S_2 to points O_1'' on surface S_1 there will, of course, be many new paths that must be computed for the integral (A.21) which are not normal to S_2 and are not, therefore, normal to S_1. It is a consequence of this that T'' in (A.21) can be expanded in terms of coordinates that lie on the surface of S_1 and that the expansion will be stationary about a point O_1' which lies on the ray path $P\,O_1'\,O_2'$.

A specific example of the integration of an integral of the type of (A.21) will be given in a later section. Here, the magnitude of the integral is neglected to give the phase contribution. The general form of the integral will be

$$W = \oiint_s g(x,y)\,e^{ikf(x,y)}\,dx\,dy \qquad (A.22)$$

where $f(x,y)$ can be expanded in the form

$$f(x,y) = f(x_o,y_o) + \frac{\beta}{2}(x-x_o)^2 + \frac{\gamma}{2}(y-y_o)^2 + \eta(x-x_o)(y-y_o) + \ldots \qquad (A.23)$$

the result is given by[6]

$$W = \frac{2\pi i\sigma}{\sqrt{|\beta\gamma - \eta^2|}}\; g(x_0, y_0)\; \frac{e^{ikf(x_0, y_0)}}{k} \qquad \text{(A. 24)}$$

where the positive square root is taken and

$$\sigma = +1 \quad \text{for} \quad \beta\gamma > \eta^2 \;,\quad \beta > 0 \qquad \text{(A. 24a)}$$

$$= -1 \quad \text{for} \quad \beta\gamma > \eta^2 \;,\quad \beta < 0 \qquad \text{(A. 24b)}$$

$$= -i \quad \text{for} \quad \beta\gamma < \eta^2 \qquad \text{(A. 24c)}$$

The physical origin of the phase factors (i) in (A. 24) and (-i) in (A. 24c) that multiply the exponential of (A. 24) can be simply explained. The expansion (A. 23) represents a surface for which there will be constant phase contours centered about a point of stationary phase at the position (x_o, y_o) . If a wavefront satisfying the condition (A. 24a) is advancing toward an observer, the wavefront will appear convex to him. Similarly, the wavefront of the solution for (A. 24b) will be concave, but the wavefront represented by (A. 24c) will be warped and possess two curvatures of differing algebraic sign, i. e., a saddlepoint, as seen by the observer. At large distances from the origin, for which $x - x_o$ and $y - y_o$ become large, the exponential of (A. 22) oscillates so rapidly that such source points make a vanishing contribution to W – the major contribution comes from the area about the central point of stationary phase.

If the equal phase contours represented by (A. 23) are spaced one-half wavelength apart, the areas between the contours correspond to Fresnel Zones. The integral (A. 23) is continuous across such zones and each zone, starting from the center point of stationary phase, contributes an average value with a phase of $\pi/2$ if the surface is convex. Although the successive zones tend to cancel each other, the contribution of each diminishes for increasing zones from the center to leave the net phase value $\pi/2$ which is given by the factor (i) in (A. 24). If the surface is concave, which is the solution (A. 24b), the average phase of the central zone is $-\pi/2$. If the surface is a saddlepoint with the solution (A. 24c) the contribution from the central zone tends to vanish, and it is the higher-order zones that make the principal contribution to the integral. For each zone, however, the average phase is zero and, if $g(x_0, y_0)$ is real, the integral W for the solution (A.24c) is also real and shows no phase change.

Equation (A.21) is readily cast into the form of Eq. (A.22) and all the functions except the exponential become real and are evaluated at the point of stationary phase. This, as noted before, lies on the normal ray path from P that connects the two surfaces S_1 and S_2. The choice of the solutions (A.24a, b, c) will depend on the type of curvature of the wave field. For underwater acoustics the dominant situation will consist of cylindrical spreading in one dimension and, for the example of Fig. A-3, a convergent wavefront for S_1 in the plane of Fig. A-3. The radii of curvature have, therefore, differing algebraic signs and the solution (A.24c) will apply. The product of the imaginary factors and the signs in (A.21), (A.24), and (A.24c) leave a net phase shift of $-\pi/2$ such that the phase of the wave at S_2 is given by

$$\Phi = \text{phase} = \omega \int_P^{S_2} \frac{ds}{c(r)} - \frac{\pi}{2} = \omega T - \frac{\pi}{2} \quad . \tag{A.25}$$

In applying the above to the use of ray theory in underwater acoustics to calculate the amplitude and phase of wave fields, the solutions of (A.10) and (A.11) are to be augmented by the prescription that a phase of $\pi/2$ is to be subtracted for each ray crossing undergone by a differential ray bundle; also, the solution will not apply in the immediate region of the ray crossing. The field must there be calculated by detailed evaluation of integrals of the form of (A.21) to express the diffraction spreading.

A-4. Ray Calculation of a Plane Wave Refracted Against a Stratified Velocity Gradient

One of the few exact calculations that can be made for wave propagation in an inhomogeneous medium demonstrates that a plane wave refracted against a stratified velocity gradient is reflected with an additional phase change of $-\pi/2$ with respect to ωT, where T is the travel time along the ray paths. The conventional ray diagram for this reflection is indicated in Fig. A-4 which shows the normal rays from plane surface S that propagate into the gradient region. They are turned by the gradient at a common depth z_t and return to the homogeneous medium to form a new wave front that passes through point P. The surface that is formed by the turning points of all the rays at depth z_t is a caustic surface in Fig. A-4, and the $\pi/2$ phase shift that is not predicted for the rays is usually ascribed to a breakdown of the ray theory at the turning point at depth z_t.

We have investigated this physical situation to test whether the ray solution of (A. 10) and (A. 11) can be used in (A. 19), with the modification indicated by (A. 25), to calculate the field at P due to the reflected wavefront S. The test also measures the ability of the ray solution to predict the wavefield from a source at point P that propagates onto the surface S. Figure A-5 shows the construction, and it is clear that the individual rays from P no longer have turning points at a common depth z_t.

For the parameters given in Fig. A-5, the ray tracing program was used to compute the travel time of the ray, T, the position of the ray on plane S, and the angle of inclination α of the ray to plane S. Calculations were made for a range of initial angles from P and also for sets of rays that propagate in planes with differing azimuthal angles with respect to the plane normal to S that also contains points P and O. The latter calculations provided data to give the ray parameters for the intersection of the rays over the entire surface of S. The results are given graphically in Figs. A-6 through A-9. No calculations were made for rays from P that would arrive at S without being refracted by the velocity gradient as this would represent only the direct arrival and is of no interest to the present problem.

The smoothness of the data shown in the figures indicates the consistency of the calculation. The ray paths are readily given by elementary calculations for the particular model that was chosen, and checks indicated that the calculational accuracy was precise in time to several microseconds and in positions to fractions of a millimeter. The calculation is difficult for the ray trace program because no program modification was made to indicate to the computer that the velocity field would change slope at depth $z = 0$. However, it was required that during any iteration the predicted velocity at the terminus of an iteration should match the given velocity field within 0.01 meter/sec. Printouts of the ray data on surface S were obtained by treating the surface as a bottom together with a demand that the rays terminate after the first bottom hit.

From the figures it is clear that there are two types of arrivals on surface S . As indicated in Fig. A-9 the arrivals with initial angle $\theta \le \theta_c$ have crossed one another, and contrarily. The caustic of such intersections reaches surface S for angle θ_c at position y_c below O on S . From the data given in the figures the field V (P, t) may be evaluated using equation (A. 19).

At the region about O on surface S and for $\theta \le \theta_c$, (A. 19) together with (A. 16) are readily placed in the forms (A. 22) and (A. 23). The appropriate curvatures were evaluated from Figs. A-6 and A-8. For an incident wave on S of the form

$$V(r,t) = e^{-i(\omega t - kn)} , \qquad \text{(A.26)}$$

(A. 24) and (A. 24a), corrected for the phase shift due to the ray crossings, give

$$V(P,t) = 0.999\ e^{-i\omega(t-T_o) - i\frac{\pi}{2}} . \qquad \text{(A.27)}$$

The result was obtained by a simple numerical estimate of the curvatures of Figs. A-6 and A-8 about the point O from the graphical constructions; the result could be refined by numerical curve-fitting techniques, but this has not been thought to be necessary. Equation (A. 27) is the result predicted by theory.[7]

From Fig. A-6 it is seen that with respect to the initial angle θ there is also a point of stationary phase for T about the angle θ_c and this could make an additional contribution to the result of (A. 27), above. However, the integral that is required by (A. 19) is over the surface S , and Fig. A-7 indicates that y_c is not a point of stationary phase for T . Also, and although the amplitude A(r) of (A. 16) diverges about $y = y_c$, this divergence makes no contribution to the integral (A. 19). Thus, for the expansion of y about θ_c ,

$$y = y_c + \frac{\varepsilon}{2} (\theta - \theta_c)^2 \tag{A.28}$$

$$dy = \varepsilon (\theta - \theta_c) d\theta \quad . \tag{A.29}$$

The amplitude at $y = y_c$ diverges as

$$A(r) \approx \sqrt{\frac{d\theta}{dy}} \tag{A.30}$$

and

$$V(P,t) \approx g' (x_c, y_c) \oiint_S e^{-i\omega(t-T)} dx \sqrt{dy\, d\theta}$$

$$\approx g' (x_c, y_c) \oiint_S e^{-i\omega(t-T)} dx\, d\theta \sqrt{\varepsilon (\theta - \theta_c)} \quad . \tag{A.31}$$

In (A.31) $g' (x_c, y_c)$ represents the slowly varying functions for the stationary phase integral that are evaluated at (x_c, y_c). It follows that when T is expanded to form a stationary phase integral about θ_c the term in the square root following the differentials in (A.31) causes the net contribution from the region of θ_c to vanish. Finally, if the caustic on S were to make a contribution to the field at P its phase would depend on T_c and on the specific details of the velocity gradient - this is contrary to the known theoretical solutions of the wave equation applicable to this problem.

The vanishing of (A.31) at θ_c demonstrates that the $\pi/2$ phase shift is not due to a focussing to P of secondary waves from S, i.e., Huygen's wavelets that propagate away from the normal to plane S, especially as these would originate from S at the position of the caustic at y_c.

The foregoing has used the ray tracing solution from a point, P, to form a "test" solution to the wave equation that can be used in the Kirchoff theory for inhomogeneous media to calculate the complete field, including diffraction, at point P. The solution (A.27) is similar to that which would be obtained by using only the normal rays from surface S, as in Fig. A-4, but the detailed development has shown that the field at P is due entirely to the Huygen's wavelets radiated from the area of S where the ray from P is normal to surface S . Also, the $\pi/2$ phase shift of the field at P after reflection from the velocity gradient is due to the ray crossings by the wavelets as they spread cylindrically but are refocussed due to refraction in the stratified medium.

The solution can also be used to determine the field on a plane surface S due to a point source at P provided the field is not extended into regions where the field amplitude of (A. 16) diverges. For simplicity, the method is illustrated here by the simpler calculation of the field on a conical shell with cone axis through P and for which the plane S of Fig. A-5 is a tangent plane. The amplitude of (A. 16) is directly determined from the inverse slope $d\theta/dy$ obtained from Fig. A-6. As a rough approximation both y and T were expressed in terms of θ through

$$y = c_1 + c_2\theta + c_3\theta^2 + c_4\theta^3 \qquad \text{(A. 32)}$$

$$T_1 = d_1 + d_2\theta + d_3\theta^2 + d_4\theta^3 \qquad \text{(A. 33)}$$

where the subscripted constants were determined to emphasize the region of θ_c .

The net field on the conical surface S will consist of two arrivals. Due to the ray crossings of the rays with $\theta \le \theta_c$ these will have a $\pi/2$ phase lag with respect to the larger initial angles from P , and this must be included in computing the interference pattern of the two arrivals. If the amplitudes are A_1 and A_2 , respectively, the intensity on S is given by

$$I = \frac{1}{\rho c}\left[A_1^2 + A_2^2 + 2A_1A_2 \sin 2\pi f\,(T_1 - T_2)\right] \qquad \text{(A. 34)}$$

with $T_2 = T_1\,(2\theta_c - \theta)$. The solution (A. 34) cannot be continued to the position of the caustic at y_c on surface S because the amplitudes will diverge. Using the constants in (A. 32) and (A. 33) that were derived from Fig. A-6, (A. 34) has been plotted as a function of position on S in Fig. A-10 for a frequency of 20 Hz. The dashed line in Fig. A-10 indicates the nature of the effect of diffraction to spread the geometrical divergence of the amplitudes over a finite spatial interval.

A-5. Conclusions

Based on the interpretation of ray theory given in this appendix, we conclude:

1. The phase change does not occur at the "turning point" at which the rays become horizontal but only applies after the region where the rays cross one another.

2. The ray solutions for propagation from a point source that utilize (A. 10), (A. 11), and (A. 16) cannot give the wave field in the region of shadow zones or foci or caustics; however, these solutions can describe the field at surfaces that bound such points and solutions of the form of (A. 19) can then be attempted. If the contributions from caustics or foci that may occur on such bounding surfaces can be shown to be negligible, the method can be used to compute the wave field at individual points within the surface.

3. If the medium is not horizontally stratified but possesses gradients in two dimensions, greater care must be used at ray crossing points. Specifically, it must be determined whether solution (A. 24b) or solution (A. 24c) applies to the stationary phase integral. The former will give a phase shift of $-\pi$ while the latter gives only one-half that phase shift.

4. It is incorrect to automatically apply corrections of $-\pi/2$ to a ray that goes through a turning point. For example, in Fig. A-9, the correction is appropriate to rays that reach the plane S with initial angles less than θ_c, but is incorrect for the steeper rays that leave the source at angles greater than θ_c. Note also that in the example of Fig. A-9, and provided that the velocity gradient region is thick enough, the first arrival will have no phase change but the second arrival will.

5. If high reflectivity surfaces bound the velocity gradient region from above in such a manner that the steeper rays from P are surface reflected and do not reach the plane S in the region of point O in Fig. A-4 but the rays refracted about the initial angle θ_o are permitted,

the phase change correction will still be applicable even though the other field contributions are eliminated.

6. While it must be determined that the frequencies for which these results are applied are high enough so that ray theory is valid as an asymptotic limit, the criteria for the existence of the phase shift depend solely on the ray crossings prior to an arrival point unless, of course, this point is taken so close to a focus or caustic that the full wave field must be evaluated.

7. When multiple arrivals are present, and provided that the observation point is not near a caustic or focus, the total field amplitude may be determined by superposition of the independent ray fields unless the medium is nonlinear.

8. The ray solutions are not adequate for the evaluation of reflection and transmission coefficients at boundaries with discontinuous changes in the sound velocity. Ray theory can be used for these if these coefficients are given independently, including both the real and imaginary components.

9. The caution given in the beginning of this appendix is re-emphasized here; in applying these techniques to a nonhomogeneous medium such as the ocean, it must be established that the velocity field can be known with sufficient accuracy to justify any connection between the computed travel time T for a model velocity field and the actual phase change of the ray over its path. It is most probable - and this will be established in future research - that such investigations will be valuable for adjacent rays that travel over nearly the same ray paths. For this situation, together with the approach of (A.2) above, one wishes to establish procedures for determining, for example, the effective width of convergence zones including diffraction effects.

Appendix References

1. I. Tolstoy and C. S. Clay, Ocean Acoustics, McGraw-Hill Book Co., New York (1966).
2. I. Tolstoy, J. Acoust. Soc. Am. 37, 1153 (1965).
3. M. Born and E. Wolf, Principles of Optics, Chapter 8, Pergamon Press, New York (1959).
4. M. Born and E. Wolf, loc. cit., Section 8.8.4.
5. The Physics of Sound in the Sea, Summary Technical Report of NDRC, Division 6, Volume 8, Chapter 3, Washington, D. C. (1946).
6. M. Born and E. Wolf, loc. cit., Appendix III.
7. A. H. Carter, Multi-Mode Acoustic Propagation in an Inhomogeneous Bounded Medium, Thesis (unpublished), Brown University (1963).

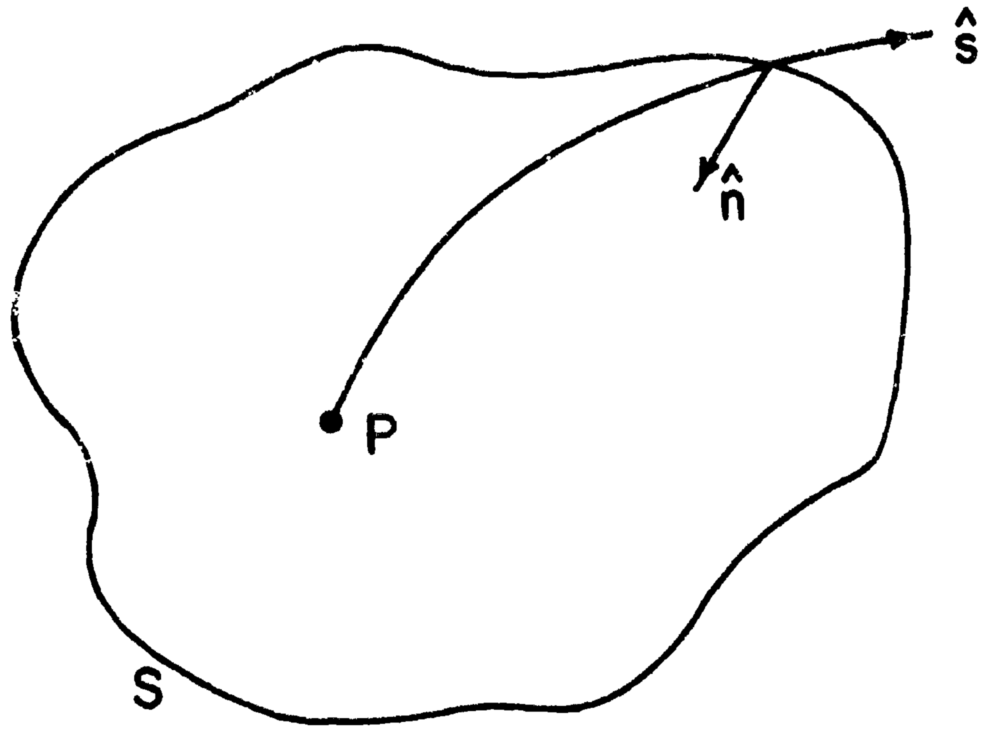

Fig. A-1. Coordinate system used for Eq. (A.6).

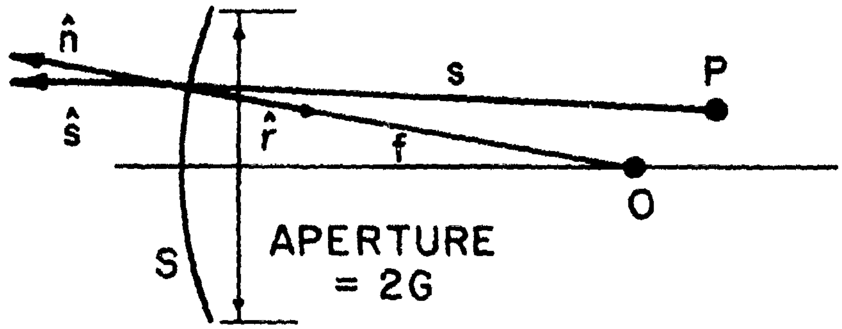

Fig. A-2. Coordinate system used to construct an aperture-limited diffraction field. On the spherical surface S of radius f the wave V(r, t) is constant in phase and magnitude and is given by $\frac{e^{-ikf}}{f}$. The field due to this wave, representing the truncation of the wave by the finite aperture of S, of diameter 2G, is determined at P. O is the focal point of S.

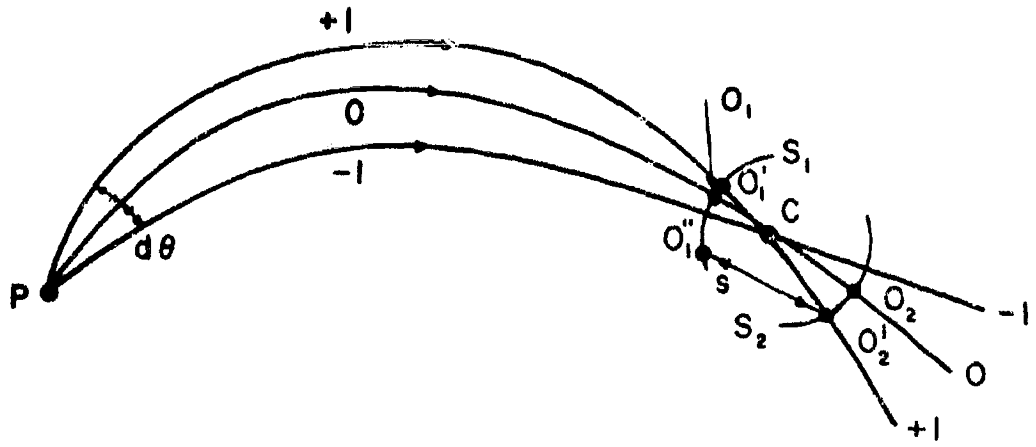

Fig. A-3. Ray geometry used to extend wave solution on surface S_1 through the region of ray crossings, C , to a further surface S_2 Equation (A.21) is used to determine the field on S_2 in terms of the field on S_1 and in terms of ray solutions from points O_2' on S_2 to the points on surface S_1 at O_1'' These are separated by the travel time T''

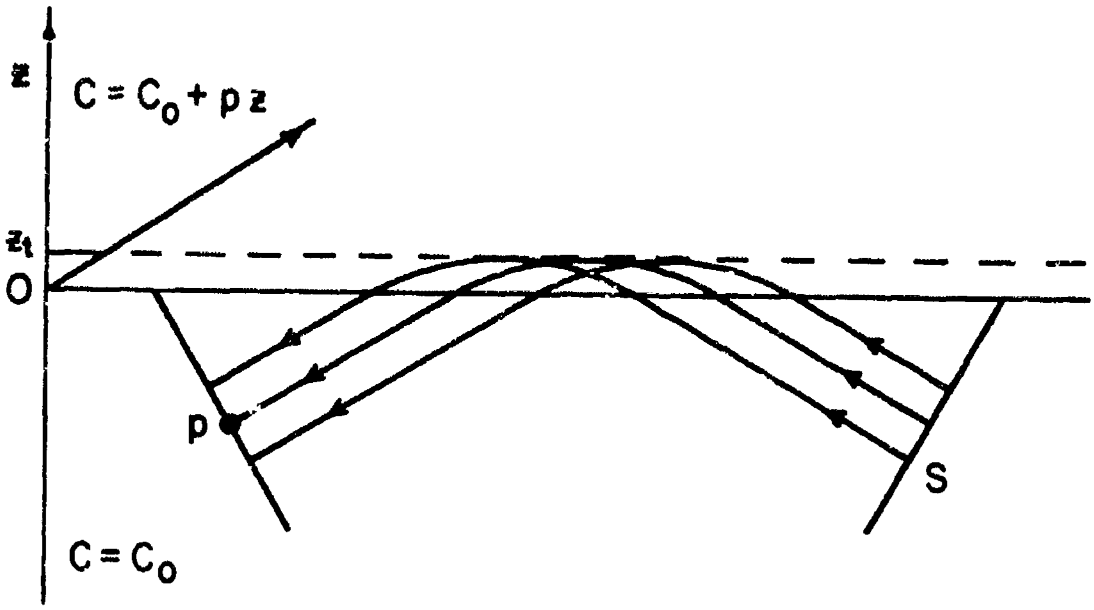

Fig. A-4. Conventional ray diagram for the refraction of an incident plane wave against a velocity gradient. The medium is horizontally stratified with constant sound velocity for negative values of z and with a constant gradient for positive values of z. The gradient is given by p. The normal rays of an incident wavefront at surface S are turned in the gradient region and are refracted back toward negative depths. z_t is the depth at which the rays are turned to be horizontal.

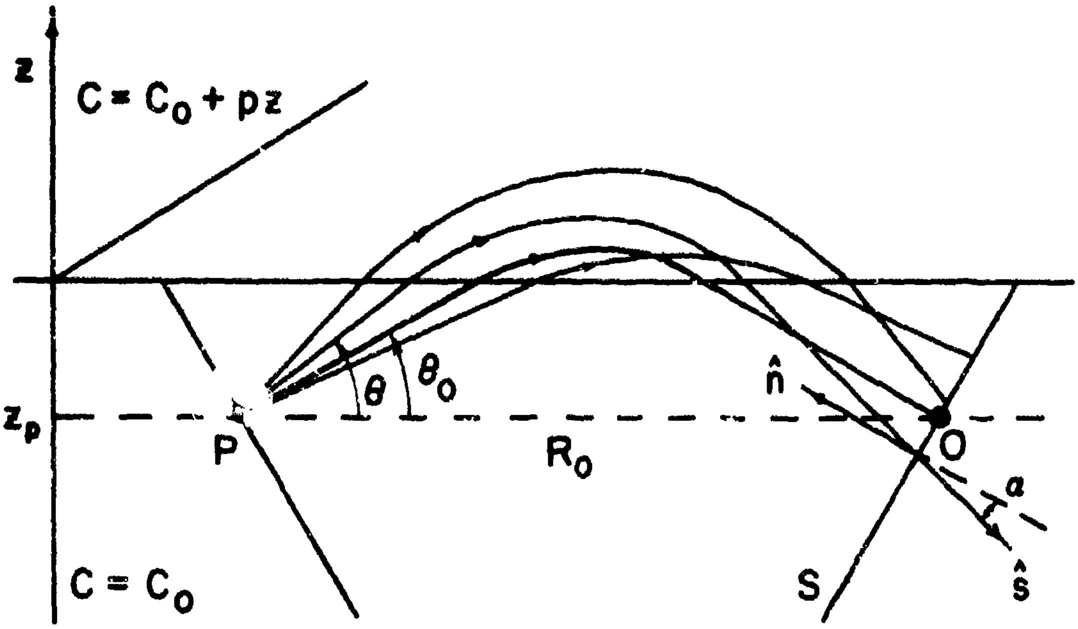

Fig. A-5. Huygen's determination of the field at P due to an incident plane wave at S. The diagram is otherwise analogous to Fig. A-4. The rays from P are specified by their angle with respect to the horizontal, θ. P has been chosen to be on the same level as the normal ray from point O on S, and this ray makes an angle θ_o with the horizontal. On S the ray from P have a ray direction s that is inclined by the angle α with respect to the normal of plane S. Points P and O are separated in range by distance R_o. As specified parameters for the ray tracing program the following values were chosen:

$\theta_o = 30°$ $\qquad$ $p = 0.50/\text{sec}$

$R_o = 17,320.5080$ meters $\qquad$ $c_o = 1500$ m/sec

$z_p = -4000$ meters

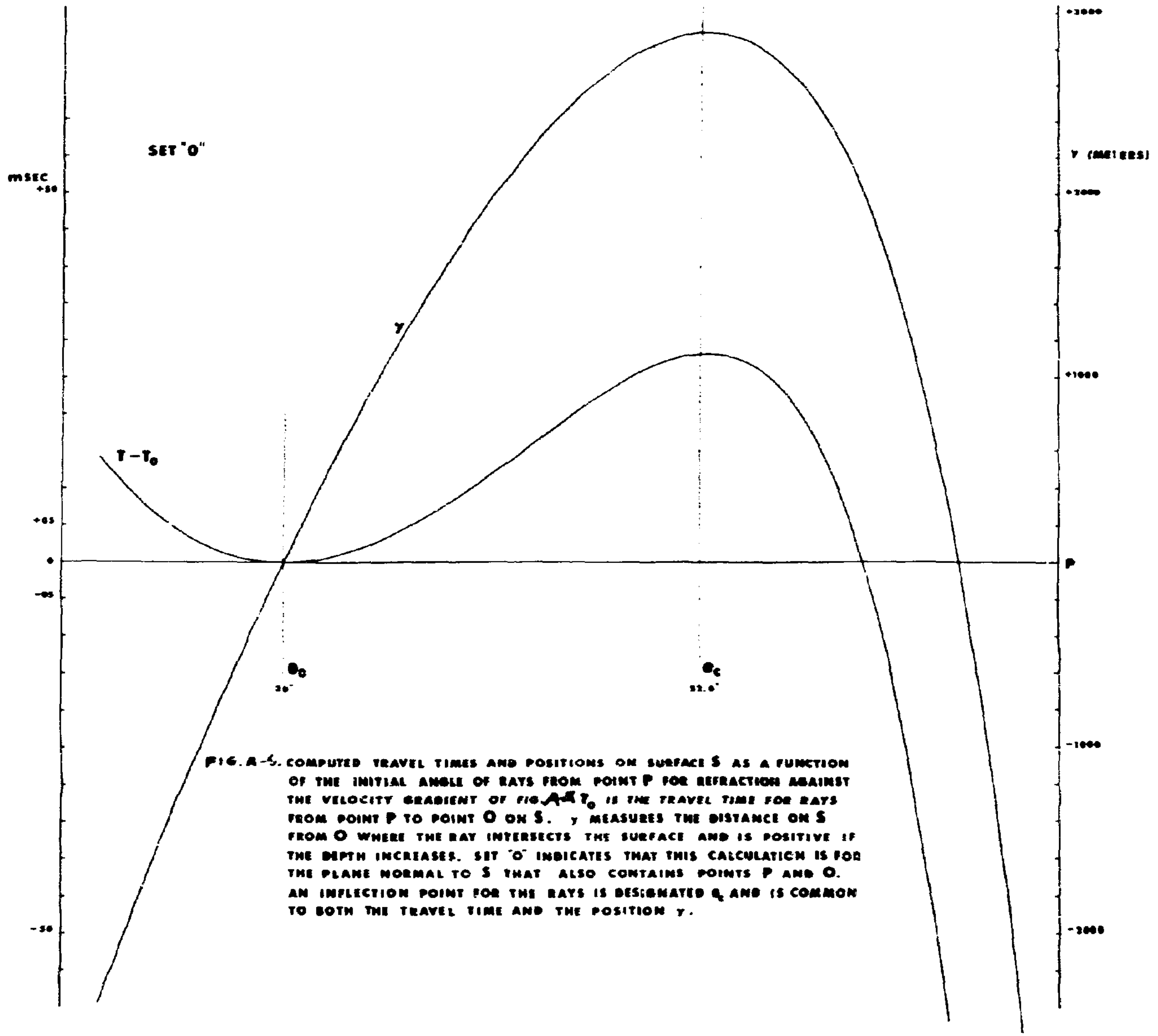

FIG. A-5. COMPUTED TRAVEL TIMES AND POSITIONS ON SURFACE S AS A FUNCTION OF THE INITIAL ANGLE OF RAYS FROM POINT P FOR REFRACTION AGAINST THE VELOCITY GRADIENT OF FIG. A-4. T_0 IS THE TRAVEL TIME FOR RAYS FROM POINT P TO POINT O ON S. y MEASURES THE DISTANCE ON S FROM O WHERE THE RAY INTERSECTS THE SURFACE AND IS POSITIVE IF THE DEPTH INCREASES. SET "O" INDICATES THAT THIS CALCULATION IS FOR THE PLANE NORMAL TO S THAT ALSO CONTAINS POINTS P AND O. AN INFLECTION POINT FOR THE RAYS IS DESIGNATED θ_c AND IS COMMON TO BOTH THE TRAVEL TIME AND THE POSITION y.

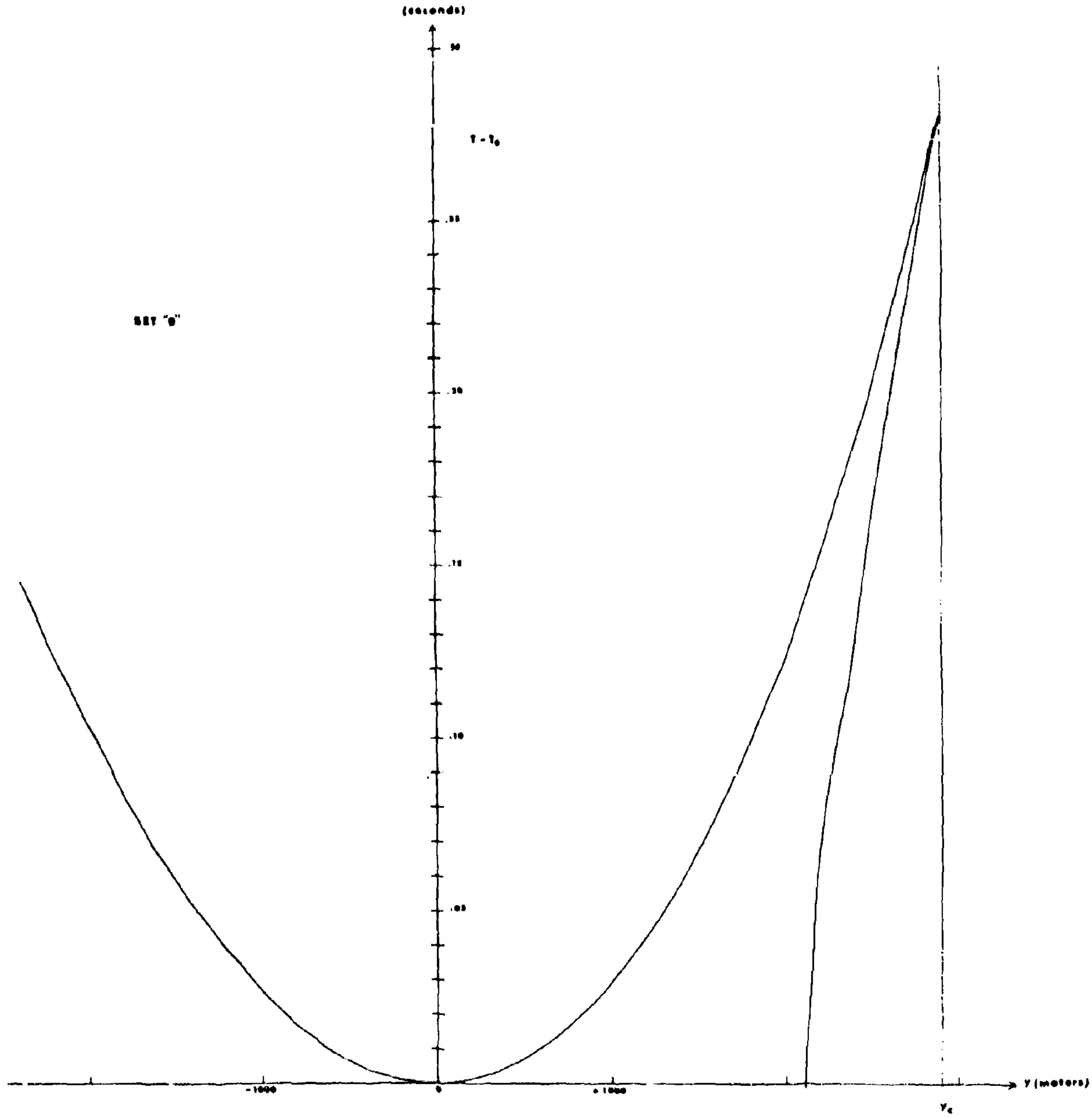

Fig. A-7. The data of Fig. A-6 replotted to show the travel time $T-T_o$ as a function of position on plane S ; also for set "O"

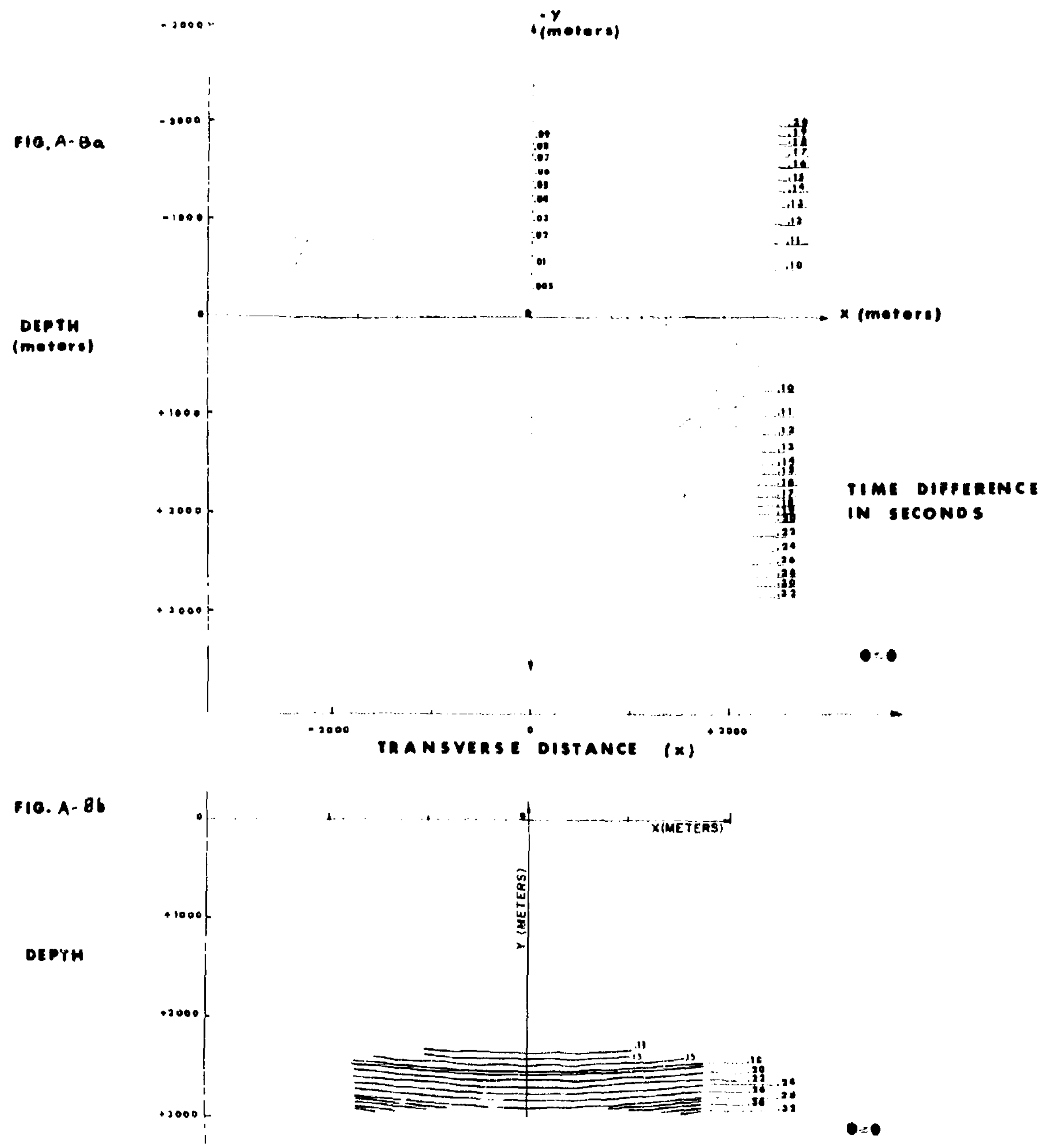

Fig. A-8. Contours of equal travel time for rays from P to the plane surface S measured with respect to point O on S . Fig. A-8a gives the contours for initial angles $\theta \leq \theta_c$ and Fig. A-8b gives the contours for initial angles $\theta \geq \theta_c$.

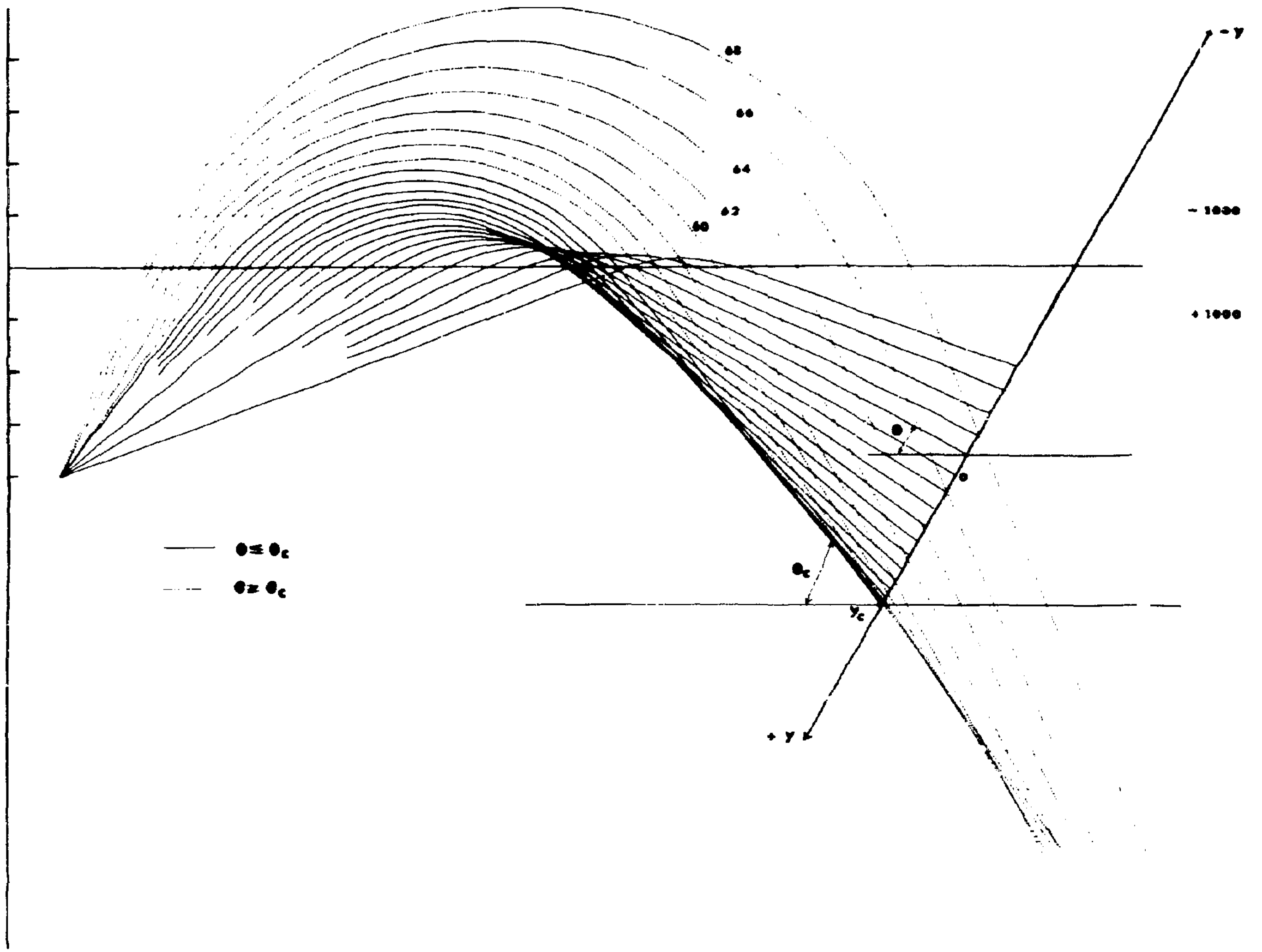

FIG. A-9. DETAILED RAY PATHS FOR SET '0' RAYS SHOWING RAY INTERSECTIONS. SOLID LINES INDICATE RAYS WITH $\theta \leq \theta_c$ AND DASHED LINES INDICATE RAYS WITH $\theta \geq \theta_c$. ADJACENT RAYS WITH $\theta \leq \theta_c$ HAVE MADE ONE INTERSECTION BEFORE MEETING PLANE S BUT THE RAYS WITH $\theta \geq \theta_c$ HAVE NOT INTERSECTED BEFORE MEETING PLANE S.

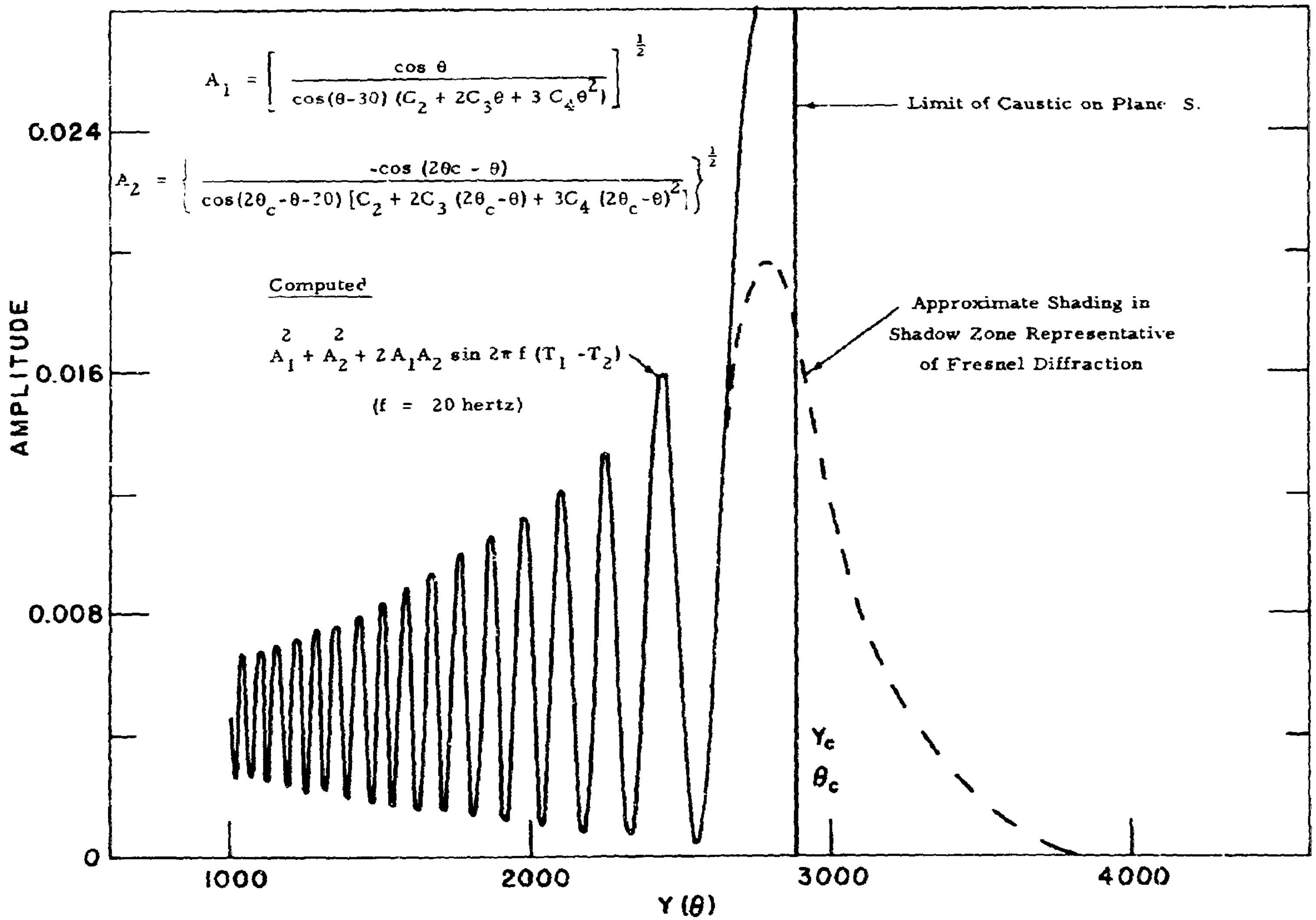

Fig. A-10. Two-arrival interference pattern of field from a point source reflected against a velocity gradient as in Fig. A-5.

UNCLASSIFIED
Security Classification

DOCUMENT CONTROL DATA - R & D

(Security classification of title, body of abstract and indexing annotation must be entered when the overall report is classified)

1. ORIGINATING ACTIVITY (Corporate author)	2a. REPORT SECURITY CLASSIFICATION
Hudson Laboratories of Columbia University 145 Palisade Street Dobbs Ferry, New York 10522	UNCLASSIFIED
	2b. GROUP Not applicable

3. REPORT TITLE

THE HUDSON LABORATORIES RAY TRACING PROGRAM

4. DESCRIPTIVE NOTES (Type of report and inclusive dates)

Technical Report

5. AUTHOR(S) (First name, middle initial, last name)

H. Davis, H. Fleming, W. A. Hardy, R. Miningham, S. Rosenbaum

6. REPORT DATE	7a. TOTAL NO. OF PAGES	7b. NO. OF REFS
June 1968	363	31

8a. CONTRACT OR GRANT NO.	9a. ORIGINATOR'S REPORT NUMBER(S)
Nonr-266(84)	Technical Report No. 150
b. PROJECT NO	
c.	9b. OTHER REPORT NO(S) (Any other numbers that may be assigned this report)
d.	

10. DISTRIBUTION STATEMENT

Document cleared for public release and sale; its distribution is unlimited.

11. SUPPLEMENTARY NOTES	12. SPONSORING MILITARY ACTIVITY
	Office of Naval Research, Code 466

13. ABSTRACT

A series of computer programs has been developed for the calculation of the acoustical field in long-range, low-frequency underwater sound propagation in the deep ocean. The programs involve the extraction of data inputs from available data banks, the calculation of ray trajectories, and intensity calculations that are based on the mapping of ray densities into the far acoustical field. This report outlines the methods used in the calculations and provides incidental commentary on the results of the program and its application to underwater sound propagation.

UNCLASSIFIED
Security Classification

14 KEY WORDS	LINK A		LINK B		LINK C	
	ROLE	WT	ROLE	WT	ROLE	WT
Ray tracing						
Long-range underwater sound propagation						
Terrain shadowing (underwater sound)						
Computer applications - ray tracing						
Vertical distribution of sound intensity (in underwater propagation)						
Multipath interference (underwater sound)						
Transmission loss (underwater sound)						
Bottom reflections (underwater sound)						
Phase changes in ray theory						

DD FORM 1 NOV 65 1473 (BACK)
S/N 0101-807-6821

UNCLASSIFIED
Security Classification

A-31409